

AD635206

A STUDY OF TECHNIQUES AND EQUIPMENT FOR THE EVALUATION OF EXTRAVEHICULAR PROTECTIVE GARMENTS

DAVID G. PARRY
LeROY R. CURRY, JR.
DONALD B. HANSON
GEORGE B. TOWLE

HAMILTON STANDARD
DIVISION OF UNITED AIRCRAFT CORPORATION

FEBRUARY 1966

CLEARINGHOUSE FOR FEDERAL SCIENTIFIC AND TECHNICAL INFORMATION			
Hardcopy	Microfiche	427	pp
\$ 7.25	\$ 2.00		ad
/ ARCHIVE COPY			

Distribution of this document
is unlimited

DDC
JUL 18 1966
A

AEROSPACE MEDICAL RESEARCH LABORATORIES
AEROSPACE MEDICAL DIVISION
AIR FORCE SYSTEMS COMMAND
WRIGHT-PATTERSON AIR FORCE BASE, OHIO

NOTICES

When US Government drawings, specifications, or other data are used for any purpose other than a definitely related Government procurement operation, the Government thereby incurs no responsibility nor any obligation whatsoever, and the fact that the Government may have formulated, furnished, or in any way supplied the said drawings, specifications, or other data, is not to be regarded by implication or otherwise, as in any manner licensing the holder or any other person or corporation, or conveying any rights or permission to manufacture, use, or sell any patented invention that may in any way be related thereto.

Requests for copies of this report should be directed to either of the addressees listed below, as applicable:

Federal Government agencies and their contractors registered with Defense Documentation Center (DDC):

DDC
Cameron Station
Alexandria, Virginia 22314

Non-DDC users (stock quantities are available for sale from):

Chief, Input Section
Clearinghouse for Federal Scientific & Technical Information (CFSTI)
Sills Building
5285 Port Royal Road
Springfield, Virginia 22151

Change of Address

Organizations and individuals receiving reports via the Aerospace Medical Research Laboratories' automatic mailing lists should submit the addressograph plate stamp on the report envelope or refer to the code number when corresponding about change of address or cancellation.

Do not return this copy. Retain or destroy.

ACCESSION for	
CFSTI	WHITE SECTION <input checked="" type="checkbox"/>
DDC 700	DIFF. SECTION <input type="checkbox"/>
UNANNOUNCED	June 1966 773-47-1022
JUSTIFICATION	
BY	
DISTRIBUTION/AVAILABILITY CODES	
DIST.	AVAIL. and/or SPECIAL
1	

**A STUDY OF TECHNIQUES AND EQUIPMENT
FOR THE EVALUATION OF
EXTRAVEHICULAR PROTECTIVE GARMENTS**

*DAVID G. PARRY
LeROY R. CURRY, JR.
DONALD B. HANSON
GEORGE B. TOWLE*

**Distribution of this document
is unlimited**

FOREWORD

The study resulting in this report was conducted by the Hamilton Standard Division of the United Aircraft Corporation in Windsor Locks, Connecticut under Contract AF 33(615)-1780 in support of Project 6301, "Aerospace Systems Personal Protection," Task 630104, "Space Protective Garments." The requirement for this study was recognized by William L. Lee, Major, MC, USAF, who as chief of the Altitude Protection Branch provided the initial effort to start the study. The study was monitored for its duration, August 1964 through June 1965, by the Altitude Protection Branch, Physiology Division, Biomedical Laboratory, Aerospace Medical Research Laboratories, Wright-Patterson Air Force Base, Ohio. The technical monitor was Lt. Darrel L. Haub. The final report was submitted in November 1965 and is on file at Hamilton Standard as HSER 3671.

The authors gratefully acknowledge the contributions of Lt. Darrel L. Haub, J. D. Bowen, and D. Rosenbaum, and other personnel at the Aerospace Medical Research Laboratories and at Hamilton Standard who were helpful in all areas of the study.

The authors further acknowledge indebtedness to representatives of the following organizations for assistance during the study. Some of the general thoughts presented herein are directly or indirectly a result of the willingness of representatives of these organizations to discuss the present state-of-the-art and to express their ideas.

Aircrew Equipment Laboratory, Navy, Philadelphia Navy Yard, Philadelphia, Pennsylvania

Aiderson Research Laboratories, Inc., Long Island City, New York

Arnold Engineering Development Center, USAF, Tullahoma, Tennessee

Cornell Aeronautical Laboratories, Inc., Buffalo, New York

Illinois Institute of Technology Research Institute, Chicago, Illinois

Manned Spacecraft Center, NASA, Houston, Texas

Natick Laboratories, USA/QMC, Natick, Massachusetts

Norden, Division of United Aircraft Corporation, Norwalk, Connecticut

Sanders Associates, Inc., Nashua, New Hampshire

Springfield College, Springfield, Massachusetts

This technical report has been reviewed and is approved.

WAYNE H. McCANDLESS
Technical Director
Biomedical Laboratory
Aerospace Medical Research Laboratories

ABSTRACT

The purpose of this study was to establish a test methodology and a test system for objective, quantitative, and accurate evaluation of extravehicular space protective garments. Areas of testing studied include functional performance, life support, and environmental protection. Emphasis is placed on the problem of suit torque restraints, i.e., mobility. Concepts for appropriate evaluation criteria are discussed. The information presented and conclusions reached are the results of experience in suit testing, technical analysis, search of the literature, and discussions with experts. The nature and causes of suit torque restraint are discussed and a pin jointed model is developed for precise description of suit torques and body interlink angles. Various techniques for torque vector and body angle measurement are explored and it is concluded that a powered articulated dummy and an intrasuit exoskeletal electrogoniometer with off-line computer coupling are required to produce accurate data and useful figures of merit. Measurement techniques for reach envelope, glove evaluation, and comfort are also discussed. Various approaches to thermal and respiratory system evaluation were studied and steady state manned tests at moderate altitudes with minimum suit-wall heat transfer are recommended. The meteoroid, vacuum, thermal, and radiation hazards of space are reviewed and direction for further study in these fields is suggested. Overall facility requirements for suit evaluation are discussed and a digital data acquisition system for conditioning, editing, recording, and processing of functional and life support data is described.

TABLE OF CONTENTS

	Page
SECTION I	
INTRODUCTION	1
SECTION II	
SUIT EVALUATION REQUIREMENTS	
The Space Mission	3
The Space Environment.	4
Life Support Requirements	5
Space Suit Concepts and Designs	7
Suit Evaluation and Testing.	22
Summary	25
SECTION III	
METHODOLOGY FOR THE EVALUATION OF	
FUNCTIONAL SUIT MECHANICS	
Introduction	27
Torque versus Angle Measurement	
Introduction	29
Definitions	32
Torque in Pressurized Space Suits	40
Torque Evaluation Criteria	51
Torque Measurement Techniques Investigation	64
Hardware Implementation	77
Angle Measurement Techniques	90
Optical Sensing Techniques	96
Inertial Sensing Techniques	104
Exoskeletal Techniques	111
Conclusions on Torque and Angle Measurements	120
Mechanical Load Distribution	
Definitions	122
Load Distribution Criteria.	124
Pressure Distribution Measurement Techniques	125
Conclusions on Load Distribution Measurements	131
Glove Evaluation - Dexterity Testing	134
Reach Envelope Measurement	
Definitions	136
Evaluation Criteria	139
Hardware Implementation	142
Conclusions on Reach Measurements	147
Conclusions on Functional Suit Mechanics	148

SECTION IV

METHODOLOGY FOR LIFE SUPPORT EVALUATION

Introduction	151
Physiological Considerations.	151
Suit System Design Considerations.	161
Suit Evaluation Concepts	169
Cooling System Evaluation.	170
Helmet Flushing Evaluation	181
Metabolic Cost Evaluation	184
Test Conditions	184
Metabolic Measurement in a Pressurized Suit	190
Transduction Techniques	196
An Integrated Life Support Test System	
Description.	206
Operation.	209
Data Reduction.	212
Conclusions on Life Support Evaluation	217

SECTION V

EXTRAVEHICULAR ENVIRONMENTAL HAZARDS

Introduction	219
The Vacuum Environment	219
The Thermal Environment	
Description.	223
Simulation Criteria and Techniques	226
Role of the Thermal Dummy.	233
Special Measurement Techniques	235
The Meteoroid Environment	
Description.	237
Impact Phenomenon	242
Accelerators	245
The Space Radiation Environment	252
Summary	258

SECTION VI

METHODOLOGY FOR THE EVALUATION OF SUIT COMPONENTS

Pressure Garment	261
Fatigue Life	262
Burst Pressure	265
Incremental Inflation.	266
Coolant Flow Distribution	267
Thermal Conductivity	270
Leakage	272

	Page
Helmet, Boots, and Gloves	
Visor Optics and Defogging	273
Helmet Impact	276
Thermal Conductivity of Boots and Gloves	277
Summary	280
 SECTION VII	
TEST PLANNING, PROGRAMS, AND FACILITIES	
Test Planning	281
Facilities Requirements	288
An Ideal Facility	294
Conclusions	296
 SECTION VIII	
DATA ACQUISITION AND PROCESSING SYSTEM	
Introduction	297
System Conceptual Design	298
System Description and Operation	
Functional Suit Mechanics System.	302
Life Support and Medical Monitoring System.	312
Digital/Analog Recording System	326
System Specification.	328
Major Component Description.	331
System Characteristics.	336
Conclusions on Data Acquisition System.	337
 SECTION IX	
CONCLUSIONS AND RECOMMENDATIONS	
Conclusions	339
Recommendations.	341
 APPENDIX I	
Some Mathematics of Pin Jointed Linkage Systems for Application to	
Exoskeletons and Dummies	343
 APPENDIX II	
Mechanical Work and its Relation to Suit Joint Motion.	371
 APPENDIX III	
Calculation Showing Near Equivalence of Torque Testing at Sea Level	
Pressure to Testing at Space Pressure.	375

	Page
APPENDIX IV	
Calculation of the Torque About Any Joint of a Generalized Dummy Linkage System from the Readouts of Force Transducers on the Links and the Interlink Angle Transducers	379
APPENDIX V	
Error Analysis for Suit Torque as Calculated from the Outputs of a Blanket of Force Transducers Completely Covering a Dummy Arm in an Optimal Array	381
APPENDIX VI	
Error Analysis for Suit Torque as Calculated from the Outputs of Force Transducers Supporting a Load Bearing Shell on a Dummy Linkage System	391
APPENDIX VII	
Calculation of Dummy Shoulder Interlink Angles from Exoskeleton Data	397
APPENDIX VIII	
Meteoroid Shielding	403
APPENDIX IX	
Space Suit Reliability Evaluation	405
REFERENCES	411

LIST OF ILLUSTRATIONS

Figure		Page
1	Constant Wear Garment	12
2	Model AX-6H Pressure Garment	13
3	Thermal-Meteoroid Garment and Extravehicular Helmet Assembly	14
4	Liquid Cooled Garment	15
5	Schematic of Typical Gas Cooled Life Support System	18
6	Typical Performance Values for a Gas Cooled Life Support System	20
7	Schematic of a Typical Gas--Liquid Cooling Life Support System .	21
8	Typical Performance Values for a Gas/Liquid Cooled Life Support System	23
9	Basic Functional Characteristics of Space Suit Design.	26
10	Dempster's Link System	30
11	Torque Output and Flexion Angle Reduced by Suit Torque	31
12	Model for Definition of Suit Torque	35
13	Typical Human Torque Output Curves	39
14	Man's Elbow Joint Torque Surface	39
15	Sketch for Definition of Mechanical Work.	41
16	Model for Thermodynamic Work Expression	43
17	Torque Curve for Linear Joint	44
18	Parabolic Volume Dependence for Joint with Linear Torque Curve	45
19	Running Friction.	47
20	Viscous Friction.	47
21	Static Friction.	48
22	Combination of Friction Effects.	48
23	Typical Suit Torque Curves	49
24	Suit Torque versus Internal Pressure	50
25	Suit Elbow Torque Surface	51
26	Elbow Torque Curves from Two Different Suits	52
27	Torque Curve for Joint with Hysteresis and Volume Change. . . .	52
28	Torque Curve for Joint with Hysteresis but without Volume Change	53
29	Task Metabolic Cost.	55
30	Suit Metabolic Cost	56
31	Data Flow for Metabolic Figure of Merit.	57
32	Joint Model for Discussion of Tracking Problem.	62
33	Torque Measurement Concepts	65
34	Manned and Unmanned Suit Torques	66
35	Model for Shell Torque Transduction.	72
36	Model for Distributed Force Transduction	73
37	Section of Dummy Link with Ring Transducer	75
38	Dummy Linkage with Shell Force Transduction	76

Figure		Page
39	Bar Analyzer	79
40	Bridge for Torque Measurement with Bar Analyzer	79
41	Bridge for Force Measurement with Bar Analyzer.	80
42	Notched Bar Analyzer.	80
43	Cruciform and Axial Bar Torque Meters.	81
44	Bridge for Torque Meters of Figure 43.	81
45	Bar Analyzer with Cruciform Torque Meter	81
46	Elbow Bar Analyzer Concept	83
47	Shell Load Measuring System.	85
48	Cross Section of Shell Load Measuring System.	86
49	Gamma-Type Balance.	86
50	Distorted Frame Transducer with Bridge Arrangement	87
51	Tension-Compression Strip Transducer	87
52	Eccentric Blade Type Transducer	88
53	Suited Powered Articulated Dummy Showing Torque Instrumentation Concept.	91
54	Shoulder-Arm Dummy Linkage System.	93
55	Model for Definition of Link Lengths and Angles in Shoulder Complex	94
56	Coordinates for Modified Electro-Optical Technique.	97
57	Coordinates of Light Sources in Link #1	100
58	Coordinates for Cameras	101
59	Location of Gyros on Shoulder Complex	104
60	Problem Considered for Inertial Sensing Technique	105
61	Schematic of a Free Gyro.	106
62	Schematic of a Rate Gyro	108
63	Coordinates for Three-Axis Gyro Problem.	109
64	Block Diagram of Integrating Rate Gyro	111
65	Cornell Aeronautical Laboratories Exoskeleton - Front View. . .	112
66	Cornell Aeronautical Laboratories Exoskeleton - Rear View . . .	113
67	Relation of Generalized Exoskeleton Linkage to Dummy Linkage .	114
68	Time History of Hip, Knee, and Ankle Position During Straight, Level Walking at Normal Walking Rate (Reference 75).	115
69	Elgons on Hand	118
70	Close-Up of Elgon.	119
71	Data Flow for Figures of Merit.	121
72	Surface Coordinates on Arm	122
73	Seating Area Pressure Distribution. Female Control Subject on 1" Foam Rubber, with Feet Supported. 25 yrs, 136.5 lbs. Isobars are in mm Hg	127
74	Ideal Load Distribution Transducer.	129
75	Hand Position for Measurement of Grasping Reach Envelope . . .	137
76	Grasping Reach Envelope at 35" Above Seat Reference Point . . .	138
77	Isometric View of Grasping Reach Envelope	139
78	Automated Reach Envelope Apparatus	144

Figure		Page
79	Pictorial View of Reach Apparatus in Use	145
80	Cross Section of Ventilating Passage	164
81	Multi-Section Dummy, Temperature Controlled (Reference Table III).	172
82	Multi-Section Dummy - Heat Controlled (Reference Table III). . .	173
83	Sectional Heat Loss Variation (From Clifford, Ref. 22).	174
84	Control Concept for Dummy Thermoregulatory Simulation	175
85	Typical Sea Level Test Setup	178
86	Effect of Rebreathing Through Known Dead Space Volumes (Adapted from Comfort, Reference 22).	182
87	Variation of Alveolar Partial Pressure with Inspired Carbon Dioxide (Adapted from Lambertsen, Ref. 65)	183
88	Typical Respiration Rate and Alveolar Carbon Dioxide Concentration	184
89	Closed Circuit Spirometry Schematic.	188
90	Typical Time-Volume Spirometry Trace (Adapted from Hardy and Lang, Ref. 47)	188
91	Open Circuit Spirometry Schematic.	189
92	Spirometry Concepts for Pressurized Suits	191
93	Retractable Helmet Mouthpiece for Spirometry	194
94	Sample Calibration Curves - MSA LIRA 300	202
95	Simple Gas Analysis Sampling System	205
96	Schematic Representation of Integrated Test Facility	207
97	Schematic of Spirometry Setup	208
98	Typical End Tidal $p\text{CO}_2$ vs. Helmet Flow	213
99	Model for Energy Balance.	214
100	Altitude vs. Pressure.	220
101	Effect of Folds on Local Absorptance.	227
102	Spectral Intensity Distribution of Carbon Arc, Tungsten Source, and the Sun.	229
103	Earth, Cislunar, and Near Lunar Meteoroid Environment (Reference 14).	240
104	Light Gas Gun Hypervelocity Accelerators.	248
105	Electron and Proton Flux Densities versus Equatorial Altitude (Reference 45).	254
106	Fatigue Life as a Function of Load	263
107	Elbow or Knee Joint Cycling Fixture	264
108	Cable Tensiometer	268
109	Coolant Flow Distribution Test Setup.	269
110	Garment Thermal Conductivity Test Fixture	271
111	Leakage Rate Test Setup	273
112	Remote Controlled Visual Acuity Projector for Helmet Defog Testing.	275
113	Helmet Impact Test Fixture.	276
114	Boot Thermal Conductivity Test Fixture	278

Figure		Page
115	Environmental Control System Stand	289
116	Space Chamber Oxygen Supply System	293
117	Ideal Space Suit Test Facility	294
118	Space Chamber Operating Cost versus Volume.	295
119	The Data Acquisition System	301
120	Suit Mechanics Test Console	303
121	Load Distribution Display Manikin	304
122	Recording System Digital/Analog.	305
123	Suit Mechanics Data System Block Diagram	306
124	350 Ω Full Bridge Signal Conditioner	309
125	Sample and Hold Device	310
126	Life Support Data System Block Diagram, Part I	314
127	Life Support Data System Block Diagram, Part II	316
128	Thermal Instrumentation	318
129	Medical System Block Diagram	322
130	Medical Monitoring Instrumentation	324
131	Digital/Analog Recording System Block Diagram	327
132	Binary Format - Data Words of 11 Bit Plus Sign.	330
133	Cartesian Coordinates.	343
134	Cylindrical Coordinates.	344
135	Spherical Coordinates.	344
136	Relations Between Coordinates	345
137	Position of an Object	348
138	Direction Angles.	349
139	Rotated Coordinate Systems.	353
140	Rotation of the Space Axes Through Ψ About z to Form the Intermediate Axes (X, Y, Z)	354
141	Rotation of the (X, Y, Z) Axes Through the Angle Θ About Y to Form the Second Set of Intermediate Axes (X', Y', Z')	355
142	Rotation of the (X', Y', Z') Axes Through the Angle Φ About X' to Form the Final or Body-Fixed Axes (x, y, z)	355
143	Hardware Interpretation of Eulerian Angles	356
144	Interpretation with Order of Rotations Interchanged	356
145	Rotated Coordinate System	358
146	Translated Coordinate System	359
147	Translated and Rotated Coordinate System	360
148	Model for Torque Discussion	361
149	The x Axis Rotation	363
150	The z Axis Rotation	364
151	Generalized Model Illustrating Successive Transformations.	367
152	Model for Definition of Mechanical Work.	371
153	Forces and Rotary Motion.	372
154	Model for Discussion of Thermodynamic Work.	375
155	Model for Definition of Notation.	380

Figure		Page
156	Model for Error Analysis	381
157	Sample Pressure Distribution.	387
158	Model for Error Calculation	391
159	Dummy Shoulder Linkage Geometry	397
160	Meteoroid Shielding	403
161	Shielded Area	404
162	Partial Definition of Suit Systems, Assemblies, and Interfaces for Reliability Program	407
163	Lifetime Failure Rate Distribution	408
164	Reliability versus Mission Time	409

LIST OF TABLES

Table		Page
I	Parameters for Error Calculation	103
II	Qualitative Analysis of Transducer Elements	132
III	Sectional Body Heat Transfer	156
IV	Gas Cooled Suit - Approximate Performance Values for Altitude and Sea Level Operations (Reference Figure 6)	166
V	Liquid Cooled Suit - Approximate Performance Values for Altitude and Sea Level Operations (Reference Figure 8)	168
VI	Comparison of Spirometry Concepts	193
VII	Solar Energy Distribution.	224
VIII	Estimated Planetary Albedos	225
IX	Spectral Absorptance of Candidate Materials.	228
X	Spectral Energy Absorbed.	230
XI	Meteoroid Shower Stream Velocities	241
XII	Hypervelocity Accelerators	246
XIII	Broad Test Program Outline	282
XIV	Detailed Test Procedure	284
XV	Classification of Operational Chambers	295
XVI	Values for Calculating Optimal R, S, and E Based on Assumed Pressure Distributions	388

SECTION I

INTRODUCTION

Since the advent of high performance, high altitude aircraft, several generations of protective garments have been developed to provide secondary "backup" protection should an emergency decompression of the primary vehicle occur. With the development of advanced spacecraft these garments are being further developed to provide primary protection permitting the astronaut to leave the space capsule. For secondary protection, functional mobility and comfort can be compromised for lighter weight, simplicity, and lower cost. However, for primary protection, these compromises can no longer be made.

Maximum functional performance demands that man's sensory inputs and physical outputs not be degraded. Adequate comfort and minimum physiological stress require proper temperature and humidity control; points of mechanical pressure or chafing must be minimized; and protection must be provided from the environmental hazards of space: meteoroids, space radiation, near vacuum, and temperature extremes.

For the suit designer to achieve these goals, the performance of his designs must be quantitatively, objectively, and accurately evaluated. Most current suit evaluation techniques are too subjective to meet these demands. The current techniques are useful to assess the performance of a specific design for a specific mission; but, the results cannot be adequately extrapolated to future designs or missions and lack the basic information required to develop improved suits. Thus, new techniques are required to satisfy these needs.

The objectives of this study have been to delineate those critical areas of suit test technology where improved evaluation methods are required; to develop a test methodology for each of these areas; to define and bring into focus vague or misleading concepts in the current methodology of suit testing; to study methods, equipment, facility requirements, and data handling techniques for the implementation of the methodology; and to recommend an overall approach to suit evaluation. Wherever possible, techniques have been established which are sufficiently general in nature to be useful not only for the suit designs of today but also for the suit designs of the future. Every effort has been made to recommend modern instrumentation techniques and facilities which maximize objectivity, accuracy, and convenience.

The study report has been subdivided into eight major sections which define the guide lines and concepts upon which the study is based and describe the suits, missions, and environments considered (Section II); present criteria, a test methodology, and recommended techniques for the evaluation of the mechanical constraints that the suit imposes upon the wearer (Section III); discuss the test concepts, requirements, and a recommended procedure for the evaluation of the life support aspects of the space garments (Section IV); review techniques for the

evaluation of the protective capability of the suit in the earth orbital and lunar space environments (Section V); present techniques for the evaluation of various suit components such as the helmet, visor, boots, and gloves, and for the assessment of fatigue strength, endurance life, and reliability of the overall suit system (Section VI); establish procedures for test programming, test planning, facility selection, and integration of testing within the available facilities (Section VII); and describe the preliminary design of an integrated analog/digital data system for acquiring recording, processing, and displaying the information obtained during the suit tests.

To avoid frequent breaks in the continuity of the main text, many of the mathematical derivations are presented as appendixes.

SECTION II

SUIT EVALUATION REQUIREMENTS

INTRODUCTION

Before a methodology for the testing of extravehicular protective garments can be developed, it is first necessary to consider the probable mission tasks that the astronaut must perform, the environments from which he must be protected, the physiological requirements for his well being, and the probable types of garments that he will wear. It is also necessary to define the purposes for which the evaluation is being made, the philosophy of this evaluation, and the extent to which objectivity, accuracy, and specificity are required. This section is devoted to the discussion of these basic considerations, from which it is possible to delineate those areas which require evaluation and then to develop test criteria, techniques, and equipment to form an integrated test system to accomplish these evaluations.

THE SPACE MISSION

Currently the role of man in space is one of exploration and scientific research. As knowledge increases and new vehicles are developed, added scientific, military, and possibly commercial goals will extend man's role in these programs. His tasks within the vehicle will be as varied as the missions themselves. Outside the vehicle his tasks may include minor vehicle repairs, space station assembly, surveillance of foreign satellites, reconnaissance, and research experimentation.

This study is not concerned with any particular mission; however, the development of a test methodology and, in particular, test criteria require that the limits of performance be established. For the purposes of this study, it was assumed that the activities of the astronaut will include moderately strenuous activities such as walking, climbing, crawling, digging, and operating heavy tools; light activities such as operating scientific instruments, using small tools, and piloting the vehicle; and very light activities such as reporting observations, monitoring the status of other crew members, and resting. For these activities full freedom of body motion, low physiological stress, minimum degradation of sensory stimuli, and maximum comfort are essential if man's full capabilities in the space environment are to be utilized. The duration of these extravehicular missions may range from a few minutes to a few hours. Missions of longer duration will presumably be accomplished with secondary roving or capsule vehicles. For purposes of this study, the hypothetical mission will consist of both intravehicular and extravehicular operation requiring full body mobility and will be of sufficient duration to produce approximately steady state physiological conditions.

THE SPACE ENVIRONMENT

The space environment poses many unique hazards for the extravehicular astronaut. He must be protected from the extremely low pressure of the space atmosphere, thermal radiation from many sources, space nuclear radiation, and meteoroid bombardment. These environmental factors are discussed briefly below and are treated in more detail in Section V. Although the discussion is limited to the space environment, artificially induced environmental factors such as nuclear radiation from on-board power plants, electromagnetic emanations to or from ground-based stations, and thermal radiation or material flux from thrusters must be given due consideration.

The extremely low gas pressure in space presents the most immediate environmental hazard to the astronaut. Pressure decreases rapidly with altitude reaching an estimated 10^{-6} torr at 100 miles and 10^{-13} torr in interplanetary space. In addition to the obvious physiological problems which would result from man's exposure to these pressures, serious problems can also result from the evaporation or sublimation of materials. In the absence of monomolecular surface layers, the emissivity of the suit changes and friction increases causing additional wear and sometimes even cold welding.

Incident thermal radiation is generally of three types -- direct solar radiation, reflected solar radiation, and infrared radiation from the planets, vehicle, etc. For earth-lunar operations the solar flux density is approximately 1.2×10^3 kcal/m²/hr (0.14 watts/cm²) with a peak spectral irradiance at a wave length of 0.5 micron. The intensity of this radiation is sufficient to produce substantial temperature differences on the external surface of the suit and can produce retinal damage unless adequate protection is provided.

Direct thermal emission at far infrared wave lengths from the vehicle and planetary bodies will normally represent a small thermal input to the suit. Other than the heat rejection mechanism of the life support system, the principle thermal loss from the suit is by radiation to deep space.

The intensity of space radiation varies substantially with location and time. The principle known radiation hazard is within the Van Allen radiation belt, a doughnut shaped region in the equatorial plane extending from an altitude of approximately 300 miles to 30,000 miles. Within this belt, geomagnetically trapped electrons and protons reach energies and concentrations sufficient to preclude extravehicular operations. In certain regions the intensity of the Van Allen belt has been substantially increased by the man-made radiation injected into the belts by United States and Russian nuclear explosions. Solar flares generate high energy protons of potentially hazardous intensities. However, observation of solar flare activity makes possible reasonable dosage prediction, and extravehicular operation may be scheduled during periods of minimum flux. Cosmic radiation originating principally from beyond our solar system will be

present during all extravehicular operations irrespective of time and location; however, levels are sufficiently low to pose no serious hazard to either spacecraft or astronaut on missions extending less than one or two years.

The flux density of meteoroids varies approximately inversely with the mass of the particles. Since it is impossible to protect the astronaut from particles of all sizes, suit protection is based on the probability of penetration which depends upon the size and energy density of meteoroid material, the penetration resistance of the protective garment, and the duration of the mission.

Since extravehicular suits normally serve as intravehicular emergency garments, the suit must also provide adequate protection from the environment within the vehicle. Except during launch and recovery, this environment poses no extremes, for the capsule is maintained in a "shirt-sleeve" condition. In the event of certain vehicle failures, however, the intravehicular environment could be significantly altered. Loss of the pressure integrity of the vehicle would require suit full pressure operation during the balance of the mission. In vehicles which depend on rotation to minimize temperature gradients, failure of the vehicle attitude control system could significantly alter wall temperatures within the vehicle. Failure of the vehicle life support system would require remedial action which could alter the internal environment of the suit. It is primarily to these conditions and the extravehicular environmental conditions that this study has been directed.

LIFE SUPPORT REQUIREMENTS

A closed space suit system not only must protect the wearer from the external environment but must also create a habitable and reasonably comfortable environment within the suit. This requires systems which will remove metabolic heat, control pressure, supply oxygen, remove carbon dioxide and noxious odors, evaporate excess moisture, and prevent skin temperature extremes. Very briefly, the physiological requirements for these systems are discussed below. A more complete discussion of the respiratory and inter-related thermophysiological factors is presented in the sections which deal with specific evaluation techniques. Waste management, and feeding and drinking systems are also required for suits, but are not considered here, because techniques for their evaluation are specific to the particular system design.

The metabolic heat production rate during extravehicular operation depends in large measure on suit encumbrance which is not well defined, particularly in view of the little known effects of zero gravity on task performance. Estimates of metabolic energy expenditure rate are, therefore, continually being reappraised. Current estimates range from a resting rate of 100 kcal/hr (400 BTU/hr) to an average working rate of 400 kcal/hr with a peak sustained rate of 500 kcal/hr.

The pressure of the pure oxygen atmosphere in current suit designs is set at approximately 180 mmHg (3.5 psia). This is considered the lowest oxygen pressure that can be tolerated for the duration of the mission without physiological degradation. Higher pressures result in greater suit loading and in decreased mobility. Higher pressure atmospheres of oxygen or oxygen combined with an inert gas such as nitrogen or helium are being investigated actively for extended spacecraft missions. However, the relatively short duration of the extravehicular mission, the need for maximum mobility, and the relatively short pure oxygen purge period required for denitrogenation indicate the continued choice of the current atmosphere for extravehicular operations.

The oxygen supply rate depends upon the rate of oxygen consumption required to satisfy metabolic demands and the rate of suit leakage. At the peak metabolic rate of 500 kcal/hr, oxygen will be consumed at a rate of about 1.73 std liter/min (ref. 70). Suit leakage depends upon the individual suit design, but current design leakage rates are about 200 scc/min; thus, the total oxygen supply requirement is about 1.93 std liter/min.

Carbon dioxide production is directly related to oxygen consumption. For a normal individual on a typical spacecraft diet, approximately 0.8 liters of carbon dioxide are produced for each liter of oxygen consumed. In a recirculating system, expired carbon dioxide must be purged from the oral-nasal region of a sufficient rate to maintain the inspired carbon dioxide concentration at an acceptable level. The carbon dioxide tolerance level for extravehicular operations in a 180 mmHg pure oxygen atmosphere has not been clearly established; however, 8 mmHg is a commonly accepted value which seems to cause no significant physiological changes (ref. 100).

The evaporative water loss that occurs during a specific mission varies widely depending on total metabolic heat production and the mechanism of heat removal. If the metabolic heat can be removed without raising the mean skin temperature above a critical value of about 35°C, then only the water from the respiratory tract and from diffusion through the skin will enter the ventilation stream. Some water loss is desirable to maintain comfort; however, excessive water loss will result in significant physiological stress. If the metabolic heat cannot be removed below the critical skin temperature, then sweating will occur. The rate of water loss will depend on the metabolic rate, the latent capacity of the ventilation system, and the effectiveness of the ventilation system but the net loss should not exceed 2 percent of body weight (ref. 112).

Concurrent with the requirements for heat rejection and water loss control, skin temperature extremes and excessive body heat storage must be avoided. Tolerable skin temperatures range from about 2°C to 45°C, however, for comfort a much narrower range is required. The specific limits depend on many factors such as the mechanism of heat rejection, the rate of metabolic heat production, and the desired degree of comfort. Body heat storage occurs at high work levels

when the heat rejection mechanism is incapable of removing all the metabolic heat produced. The quantity of heat stored per unit body weight is a measure of physiological thermal stress and at about 2.3 kcal/kg, precipitous physiological decline is imminent (ref. 57).

SPACE SUIT CONCEPTS AND DESIGNS

For a successful mission, the garments worn by an astronaut must fulfill three basic functions. They must: (1) provide a satisfactory ecological system for the support of life; (2) offer adequate protection from the hazards of the environment; and (3) allow sufficient mobility and sensory stimuli to permit completion of the mission tasks. The relative difficulty in achieving each of these functions in a particular suit design depends in large measure on the specific mission goals. Until recently, the emphasis in suit design has been on emergency protection from loss of cabin pressure in high altitude aircraft. The demand for life support and functional mobility were the bare minimum required to reach safe breathing altitude quickly. This early "get me down" concept was achieved through the use of both full and partial pressure suits like the AF CSU 4/P Quick Donning Suit. Under most circumstances, the "get me down" concept results in an aborted mission and therefore efforts were directed toward the development of a "mission completion" suit. This suit required greater mobility, particularly in the arms and shoulders, and improved life support to cope with the problems of metabolic heat removal. This suit is typified by the Air Force A/P22S-2 and the Navy Mark IV full pressure suits. It is these suits that led to the intravehicular suits for the Mercury, Dyna-Soar, and early Gemini programs. The increasing scope and duration of the activities of the crewmen on these programs have required the continued development of more mobile protective garments with more complete ecological systems. Throughout these programs, however, the protective garments have not been true space suits but have been worn to provide emergency protection in the event of cabin pressure loss. Functional mobility has been subordinated to pressure and thermal protection and the life support function has been supplied primarily by the vehicle system. The suits for these programs have, therefore, been logical sequels to their aircraft predecessors.

When the astronaut leaves the spacecraft and ventures forth into free or lunar space, a true space suit must protect him from the environment. He must carry a complete life support system to supply oxygen, remove carbon dioxide, control temperature, and remove wastes. He must have sufficient mobility to leave the vehicle, move himself about, perform his mission, operate his suit controls, communicate with the vehicle, return, and re-enter the spacecraft.

Suit Concepts

Many concepts have been proposed for garments for extravehicular operation. In general, these can be classified as follows:

1. Soft anthropomorphic suit
2. Hard anthropomorphic suit
3. Mechanical pressure suit
4. Two pressure suit
5. Liquid filled suit
6. Nonanthropomorphic hard suit

SOFT ANTHROPOMORPHIC SUIT

The soft suit is a gas pressurized, form fitting, fabric garment not unlike a conventional flight suit when unpressurized. Protection from low pressure is provided by a rigid helmet and an impermeable pressure envelope which is constrained from overexpansion by the outer fabric layers. Protection from the thermal, meteoroid, and radiation hazards is provided by the vehicle while intravehicular and by an outer garment when extravehicular. Basic life support provisions include metabolic heat removal by either gas ventilation or liquid circulation, respiratory gas control by oxygen flushing in the helmet, and waste removal. Cooling and breathing fluids are provided through an umbilical connection from either an on-board life support system or a portable back or chest pack. Functional mobility is obtained through the use of composite fabric joints which, with cords, cables, bellows or by other means, seek to prevent volumetric changes in the joint as it is flexed. (Decreasing joint volume during flexing results in increased joint actuating forces.)

The soft suit ensemble normally consists of an undergarment, the pressure garment including integral boots, gloves, and helmet, and an outer thermal and meteoroid garment. It is lightweight, tailored for individual fitting, convenient, and requires little space for storage. It is comfortable and provides a high degree of mobility in the unpressurized state. It is not, however, without disadvantages. When pressurized, it is difficult to control the fit of the suit and to minimize the joint volume changes due to the flexible nature of the material used. Pressure points and chafing are also difficult to control.

The choice between gas cooling and liquid cooling is a trade-off between many physiological and engineering factors. Gas cooling is generally desirable for resting and light work during which most of the metabolic heat is removed sensibly (as opposed to latently) with little body water loss. However, at moderate and high work rates, heat must be removed principally by evaporation resulting in significant dehydration and physiological stress. For typical suit ventilation systems, gas cooling is limited to average metabolic rates of about 350 kcal/hr which represents about 0.6 kg/hr of body water loss. Over a 4 hour extravehicular mission with gas cooling more than 2% loss of body weight will occur with resulting general discomfort.

Liquid cooling prevents excessive water loss by removing heat from the body surface by direct conduction at skin temperatures below the onset of sweating. When used in conjunction with a gas ventilation system, the liquid system is the principal heat removal mechanism while the gas system provides oral-nasal purging and evaporation of respiratory moisture and insensible perspiration. The soft suit concept is exemplified by both the advanced Apollo lunar exploratory suit and by the current Gemini extravehicular suit.

HARD ANTHROPOMORPHIC SUIT

The term hard suit refers to a protective garment which is more or less anthropomorphic, largely of rigid metal construction, and utilizing mechanical joints to provide the required mobility. Pressurization, thermal protection, and meteoroid protection is provided by a single integrated garment. Life support provisions are similar to those for the soft suit, metabolic heat removal being provided by a liquid cooled undergarment and respiration requirements by oxygen flow to the helmet. Since the materials used are rigid, geometry control presents little or no difficulty and the problems of joint mobility due to volumetric change are minimized. When the hard suit is pressurized, its encumbrance may be equal to or perhaps less than the soft suit; however, when unpressurized it is significantly more encumbering and uncomfortable and is, therefore, not generally practical as an intravehicular suit.

Hard and soft suits are about equal in weight, but for many missions the hard suit presents a serious storage problem due to its bulk. The hard suit concept is best exemplified by the current advanced extravehicular suit being developed for NASA by Litton Industries.

MECHANICAL PRESSURE SUIT

In the mechanically pressurized suit, respiratory counter-pressure is supplied to the skin by mechanical means rather than by gas pressure. The counter-pressure could be applied by pneumatic capstans as in the Air Force partial pressure suit, the expansion of closed-cell sponge-like material, or by edema induced by the low pressure. Such a suit must fit the body extremely well to be unencumbering. Metabolic heat could be rejected either by liquid cooling or by direct diffusion through a porous suit surface. Ventilation would be provided only to the helmet. Although this suit is less bulky than either the soft or the hard anthropomorphic suit, mobility and comfort will probably be poor due to stretching of the material and bunching in such areas as the armpits, knees, and elbows. Compression of the capillary beds near the skin surface and the blocking of major veins by the lack of uniform mechanical pressure over the surface of the body may prove to be the limiting physiological factor. Although the mechanically pressurized suit has some attraction as an automatic means for emergency protection, the physiological disadvantages appear overwhelming for extended extravehicular use.

TWO PRESSURE SUIT

Since the joint torque of soft suits is often proportional to suit pressure, it has been proposed that the pressure around the arms and legs be reduced below that required for respiration to achieve greater joint mobility. Between the regions of different pressure a sealing mechanism is required. Since the shoulder and hip joints present the most difficult mobility problems, these joints should be in the low pressure region; however, seals which would permit this without restricting blood flow to and from the extremities would be very difficult to construct. The different surface pressures acting on the skin would distort the normal cardiovascular system pressures resulting in physiological impairment as well as discomfort. Additionally, separate ventilating or cooling systems must be provided, one for the head and torso and the other for the arms and legs. Considering that the basic philosophy of space suit design is to recreate an earth-like environment, this suit concept does not appear desirable, particularly in view of the strides being made in improving the mobility of conventional soft suits.

LIQUID FILLED SUIT

In the liquid filled suit the astronaut is immersed to the neck in a pressurized liquid medium. A breathable atmosphere is supplied to the helmet as in a conventional suit. The liquid transfers heat and liquid waste from the suit, provides some degree of radiation protection and balances the atmospheric pressure in the lungs. Although this concept may hold certain advantages for intravehicular use under severe acceleration or vibration conditions, it holds few advantages for extravehicular use. Sealing the helmet from the torso without cutting off blood and air flow to and from the head is a particularly difficult problem. Also a fluid must be found which will not cause skin irritation during extended use. The logistics problem of handling the liquid filling presents problems in both storage and weight and finally, the mobility is probably less than the gas pressurized suit, particularly if the volumetric changes in the joints are large.

NONANTHROPOMORPHIC SUIT

Many concepts have been proposed for nonanthropomorphic capsule-type suits. One of these consists of a cylinder extending from the upper thighs to above the head. Attached to the cylinder are anthropomorphic legs and arms. These are either manually or power operated by the man within the cylinder. The suit would provide walking capability and might be quite comfortable. The concept could eliminate the mobility problem through powered joints. Due to the rigid construction incorporated in this concept, it is necessarily bulky and difficult to store. In effect, it is a secondary vehicle in itself in which an earth-like environment could be maintained. Due to the specialized nature of this secondary

vehicle, it is assumed that it does not obviate the need for a more mobile, versatile space suit assembly, but merely provides another type of extravehicular mission capability.

Suit Design

The preceding discussion is necessarily qualitative since only limited design and testing have been carried out on some of these concepts. Comparison of the relative merits of the different concepts and their suitability for the extravehicular mission seem to indicate that within the next 5 to 10 year period the principle efforts will continue to be directed toward the development of improved soft and hard anthropomorphic suits. It is, therefore, toward these two basic concepts that this study report has been directed. Naturally, many of the techniques discussed will be applicable or adaptable to the remaining concepts or perhaps to any new concepts not discussed here.

For purposes of the study, the soft suit has been considered in two versions -- gas cooled and combined gas ventilated and liquid cooled -- as exemplified by the Apollo lunar exploratory space suit. The gas cooled version of this suit consists of (1) a constant wear garment, (2) a flexible pressure envelope with integral boots, gloves, and helmet, and (3) a thermal meteoroid garment with extravehicular visor assembly as shown in Figures 1, 2, and 3, respectively. In the liquid cooled version, the constant wear garment is replaced by an undergarment on which is installed a matrix of liquid cooling tubes as shown in Figure 4. The hard anthropomorphic suit has been considered only in the liquid cooled version. The hard suit ensemble is assumed to consist of a liquid cooled undergarment; a rigid pressure envelope with integral boots, helmet and visor; and gloves. Since this study is concerned with the evaluation of the basic protective ensemble, techniques for the evaluation of a portable life support system, emergency oxygen system, locomotion or propulsion system, telemetry system, and communications are not included. For evaluation purposes, the basic modular suit components are assumed to be of the following design.

CONSTANT WEAR GARMENT

The constant wear garment is a loosely woven, hydrophillic, snug fitting, one piece garment for continuous wear which is intended to provide abrasion resistance, minor impact protection, general comfort, and thermal transfer to the ventilating gas stream.

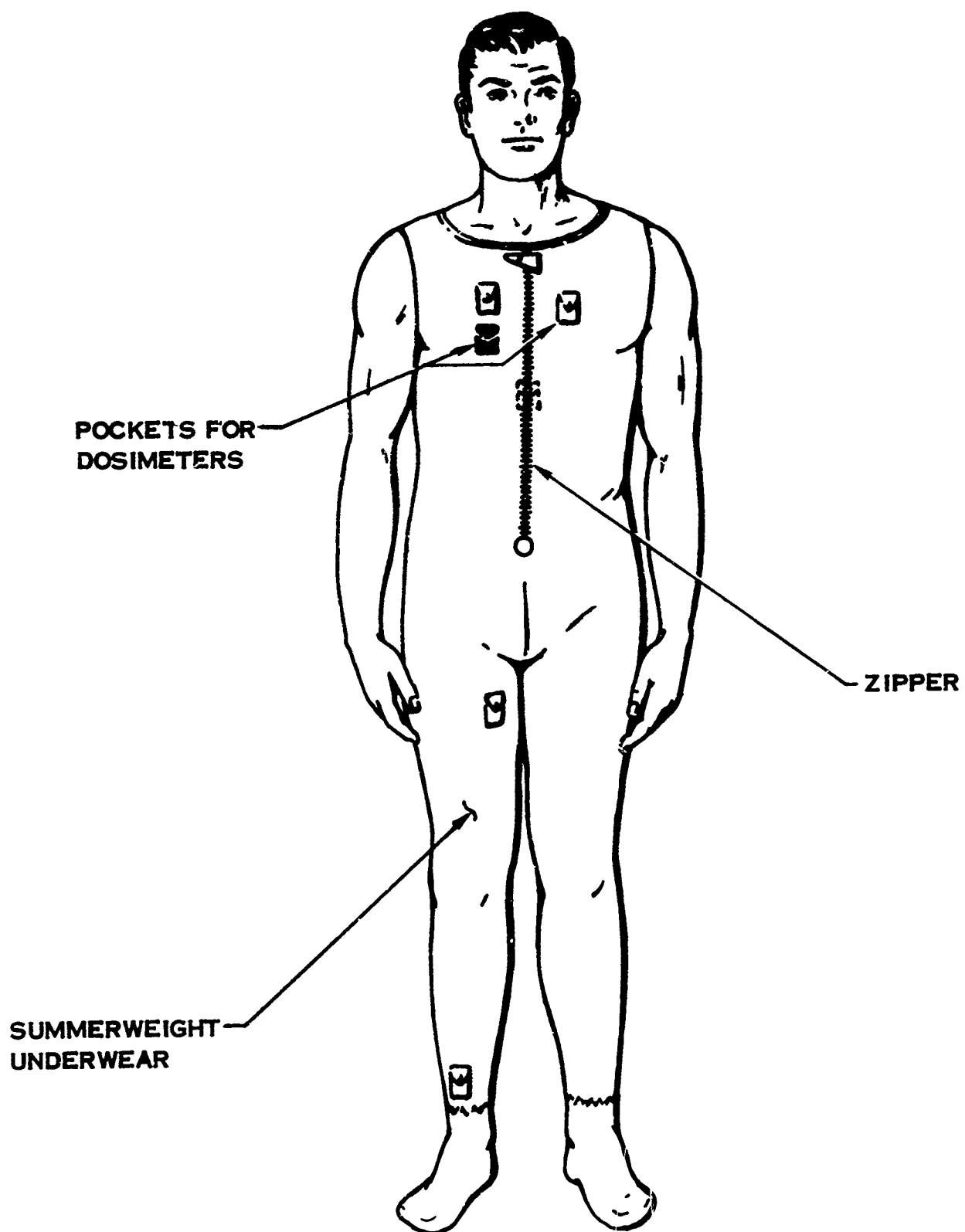


FIGURE 1. CONSTANT WEAR GARMENT

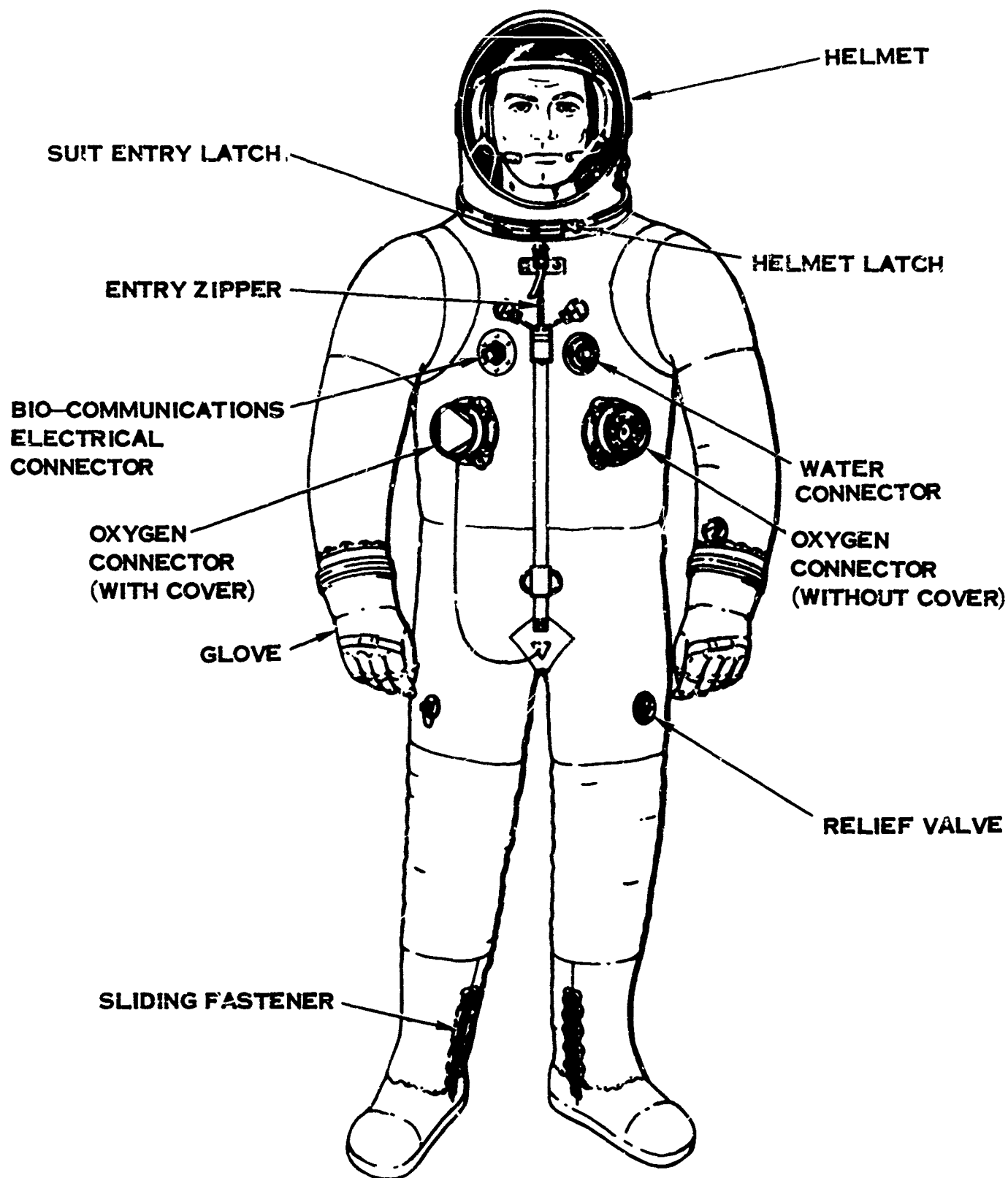


FIGURE 2. MODEL AX-6H PRESSURE GARMENT

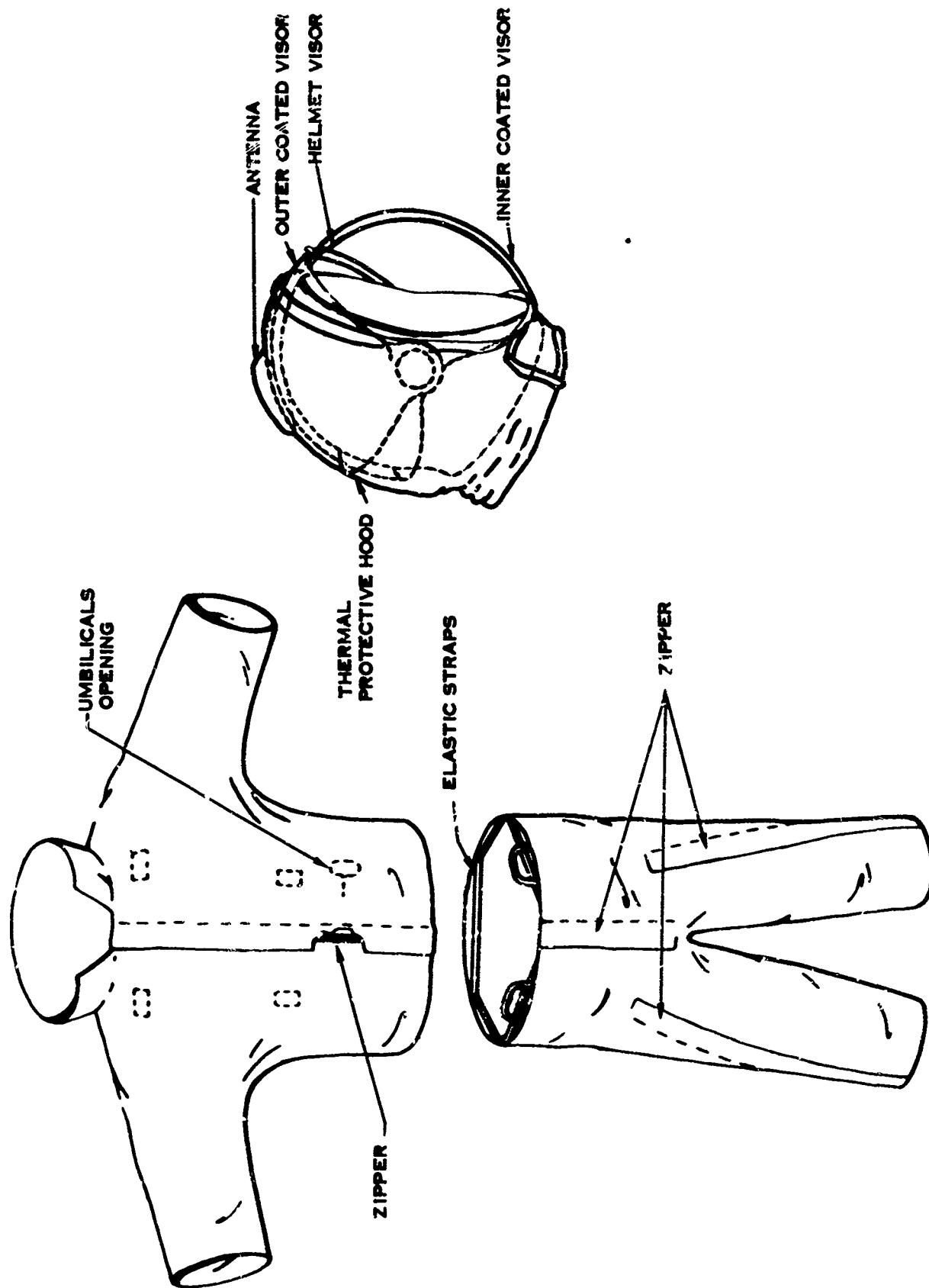


FIGURE 3. THERMAL-METEOROID GARMENT AND EXTRAVEHICULAR HELMET ASSEMBLY

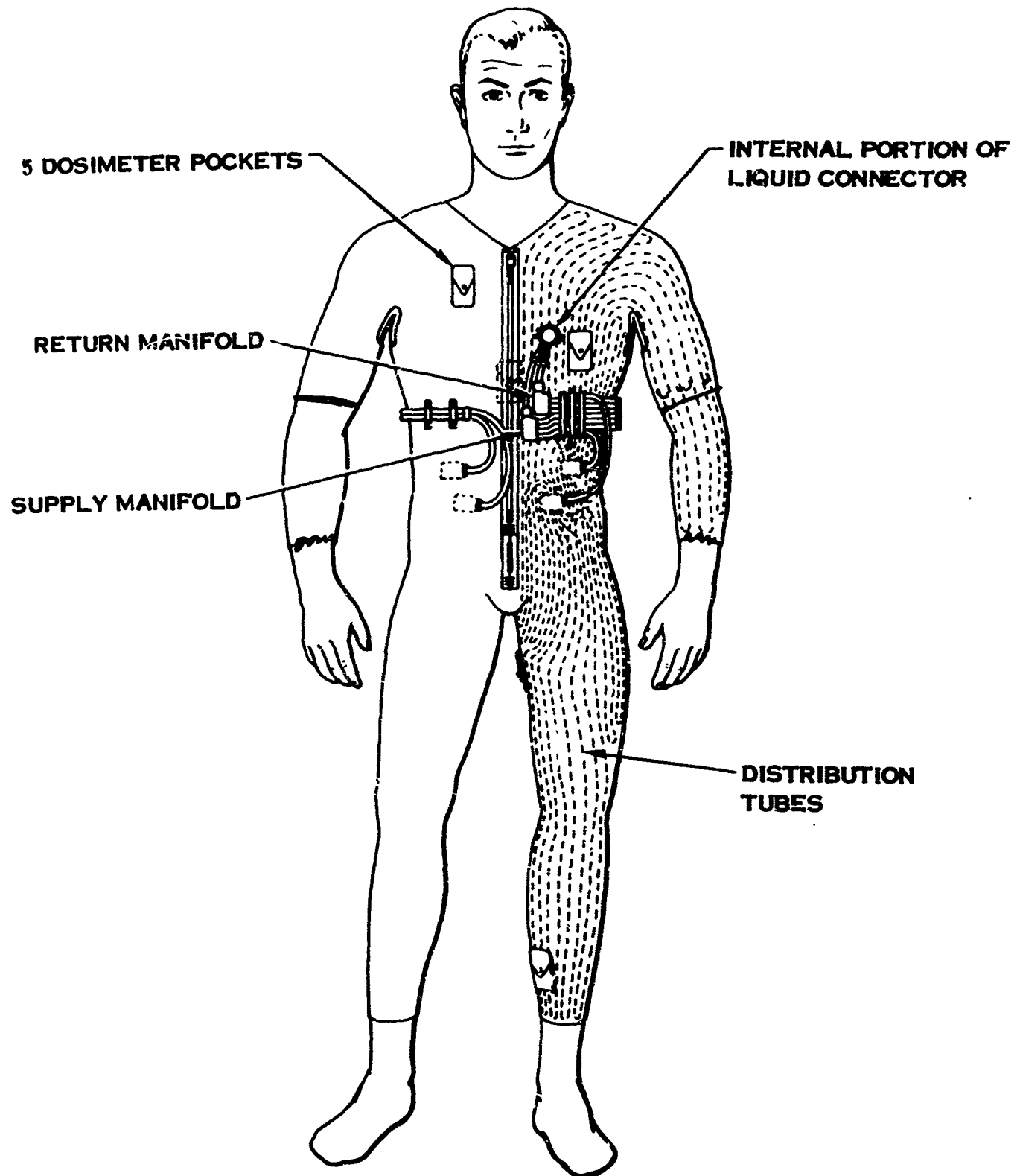


FIGURE 4. LIQUID COOLED GARMENT

LIQUID COOLING GARMENT

The liquid cooling garment is a one piece, snug fitting, fish net weave suit upon which is sewed a matrix of small plastic tubes which bring cool water to the body surface for the removal of metabolic heat by conduction. The tubes fan out from and return to central manifolds with quick connect cooling and return water connections.

FLEXIBLE PRESSURE ENVELOPE

The soft suit flexible pressure envelope is contoured to the limbs and torso with integral boots and detachable helmet, gloves, and waste management components and provides a ventilated, pressured environment for the astronaut. It has an inner liner, a ducted ventilation distribution system, a primary pressure bladder, and a nondistending outer covering. Flexible joints are located at wrists, elbows, shoulders, neck, torso and hips, knees, and ankles. Sizing geometry and pressure distortion are controlled by lacing adjustments. No specific design of a flexible joint is assumed since this is currently an area of intense activity. Details of some of these joint designs are discussed in Section III. Connections are provided on the torso to supply the pressurization, cooling, and flushing flows to the suit. Ventilation ducts carry the vent flow to the helmet and the extremities with free counterflow over the constant wear garment to return ducts in the torso region.

RIGID PRESSURE ENVELOPE

The hard suit rigid pressure envelope is a two piece anthropomorphic assembly consisting of an upper torso-arm-helmet section and a lower torso-leg-boot section locked together into an integral pressure vessel similar in function to the soft suit flexible pressure envelope. Flexible fan-folded, rolling diaphragm, or other joints provide the required freedom of motion. Within the essentially nondistensible pressure shell is a soft liner material, ventilation ducts, super-insulation, cooling and flushing connections, and waste management components.

GLOVES

The gloves consist of a wrist disconnect which permits wrist rotation, a flexible convolute for wrist flexion, a hand and finger cover designed to maximize finger tactility and dexterity, and adjusting straps to minimize ballooning when fully pressurized.

HELMET

The helmet consists of a hard spheroidal shell with a transparent visor of sufficient size to permit normal vision. The helmet is mounted on a convoluted neck joint and rotating neck ring disconnect. Within the helmet are ventilation ducts, earphones and ear protectors, microphone, defogging vent tubes, and load suspension harness. Outside the helmet are head suspension adjustment knobs and a dark supplemental visor for flash protection.

THERMAL-METEOROID GARMENT

The thermal-meteoroid garment is a multi-layer coverall providing protection by a reflective metallized film superinsulation. Protection from meteoroid material is provided by a composite fabric system like ballistic nylon.

Portable Life Support System Design

Although it is not the intention of this study to develop techniques for the evaluation of the portable life support system, which is essential for untethered extravehicular operation, it is necessary to describe this system. The portable life support system may be back or chest mounted or both. It consists of a densely packaged group of components which pressurize, cool, ventilate, revitalize, and dehumidify. It may also contain a telemetry system for communication and for monitoring suit status. Many concepts for life support systems have been proposed. However, only two typical systems will be discussed here; one a gas cooled suit system and the other a combined gas-liquid cooled system.

GAS COOLED SYSTEM

A typical gas cooled portable life support system is shown schematically in Figure 5. Referring to the schematic the operation is as follows: Leaving the pressure suit, the oxygen flow, which is water saturated near the body temperature, passes through a flexible hose to a fitting on the contaminant control canister. This canister contains a debris trap to remove free liquids and large solid particles, a lithium hydroxide bed to remove carbon dioxide, an activated charcoal bed to remove odors and other contaminants, and a filter to remove fine particles and dust. A fan located downstream of the contaminant control canister provides sufficient pressure rise to produce recirculating flow through the system. Immediately downstream of this fan the oxygen flow enters an evaporative water boiler where the temperature is lowered to approximately 8°C (47°F). In lowering this temperature, latent heat is removed resulting in condensation of water in a quantity equal to that evaporated from the astronaut. This water is removed from the oxygen stream by a water separator located immediately downstream of the

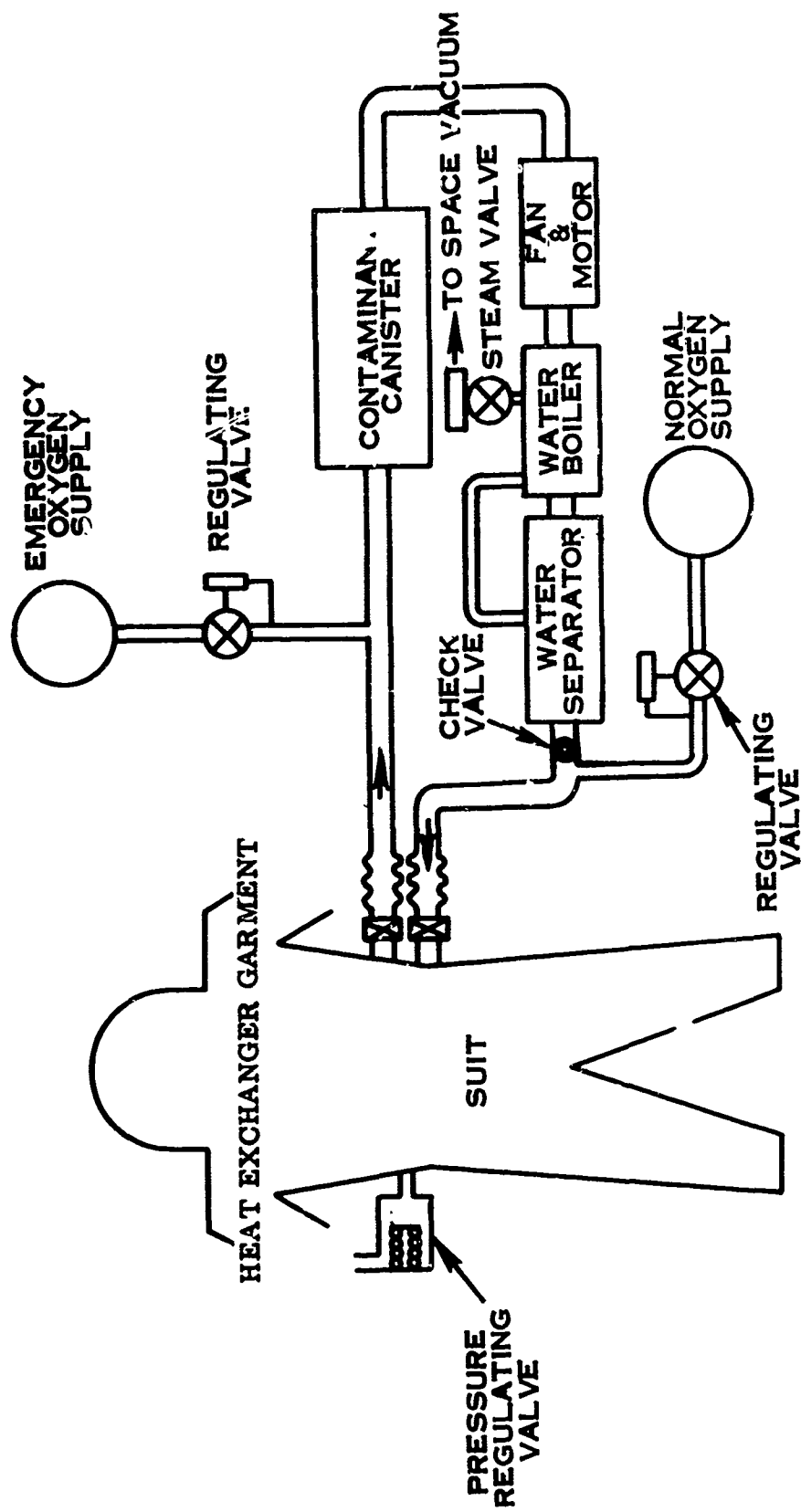


FIGURE 5. SCHEMATIC OF TYPICAL GAS COOLED LIFE SUPPORT SYSTEM

water boiler. The water is then conducted by a transfer device to the water side of the water boiler core. This collected water is then used for additional heat rejection. Oxygen stream temperature is controlled by a simple steam back pressure valve which controls the water boiling rate by sensing core temperature. Leaving the water separator the oxygen passes through a check valve and re-enters the pressure suit. Make-up oxygen from a high pressure storage bottle enters just downstream of this check valve. Pressure reduction valves control the suit pressure to the desired value. The life support system contains a battery which is used to supply electrical energy to the circulating fan, telemetry, communication, and instrumentation systems.

Performance values for a typical gas cooled suit and portable life support system are shown on the performance chart in Figure 6. These values typify operation at a metabolic energy expenditure rate of 350 kcal/hr (1400 BTU/hour). The values are based on the assumption that 30% of the total flow to the suit is directed toward the helmet for carbon dioxide control in the oral-nasal region and for defogging. In these calculations the heat leak from the environment is assumed to be 38 kcal/hr. Note that of the 350 kcal/hr of metabolic heat produced, 346 kcal/hr are removed by latent body cooling, resulting in a body water loss of 0.57 kg/hr. Only 4 kcal/hr are removed by sensible cooling. Downstream of the contaminant control canister both the humidity and temperature have increased due to the heat and water vapor produced in the lithium hydroxide-carbon dioxide reaction.

LIQUID COOLED SYSTEM

A typical combination gas-liquid cooled suit and portable life support system are shown schematically in Figure 7. Operation of the gas loop portion is identical to that described previously for the gas cooled system; however, the gas flow is smaller and much less water is evaporated. Referring to the schematic, operation of the liquid portion of the loop is as follows. Water flow leaving the liquid cooled undergarment flows through a flexible tube to a recirculating pump in the portable pack. This pump provides a pressure rise of about 260 mmHg (5 psi) to maintain the flow through the pack and undergarment circuit. From the pump the water is directed to a water boiler where both the gas and liquid flows are cooled. A bypass around the water boiler is used to control the liquid temperature. Leaving the water boiler, the water continues through a second flexible line to re-enter the liquid cooling garment. Upon entering this garment the water flow splits into a number of flow paths which lead to the extremities of the body. The flow then splits again into a large number of very small equi-resistant flow paths. These smaller flow paths all lead back toward the suit water outlet connector where they recombine and repeat the circuit. The constant flow rate and minimum inlet temperature of the system are sized to maintain the body temperature below the sweat threshold at the maximum anticipated metabolic rate.

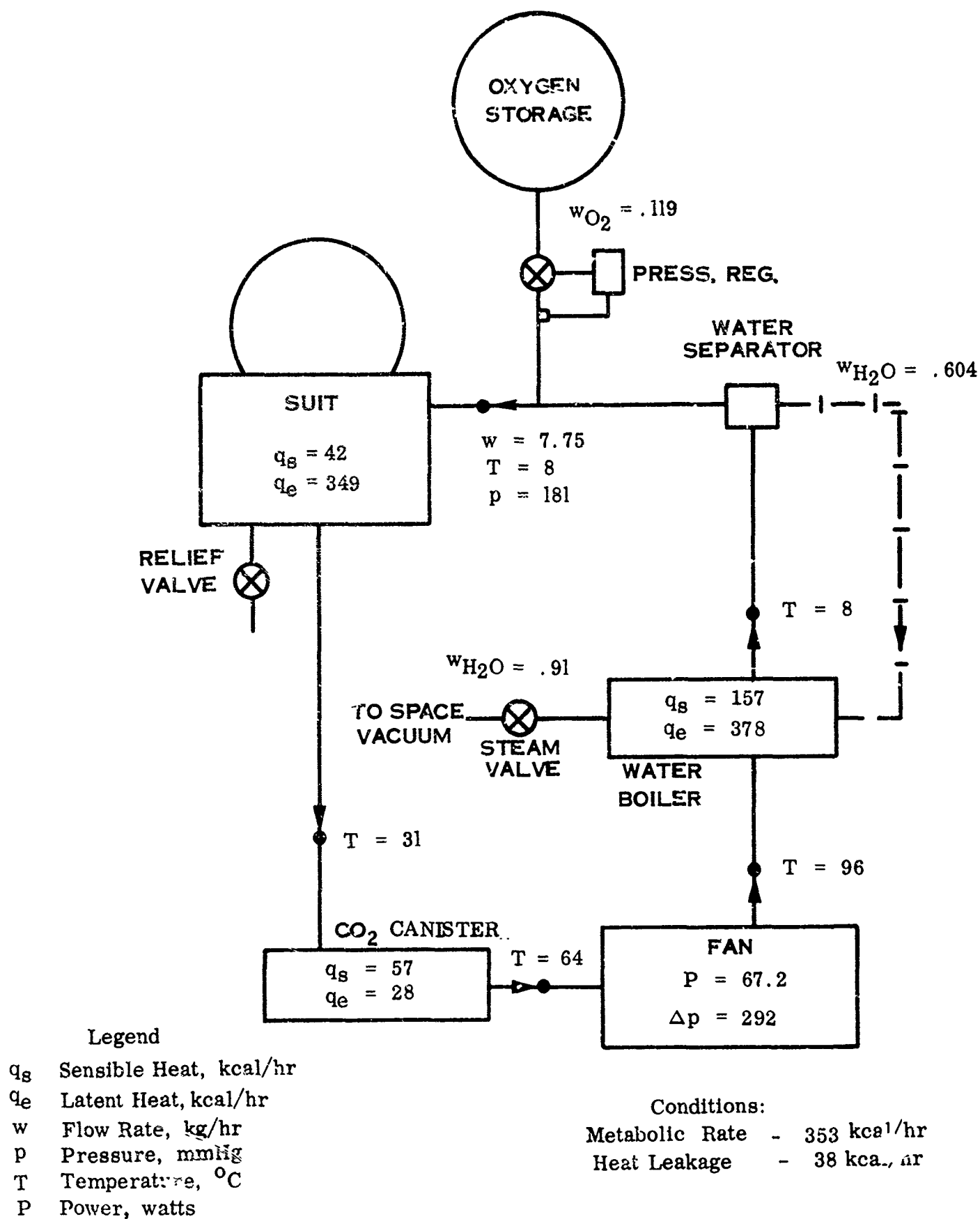


FIGURE 6. TYPICAL PERFORMANCE VALUES FOR A CAS COOLED LIFE SUPPORT SYSTEM

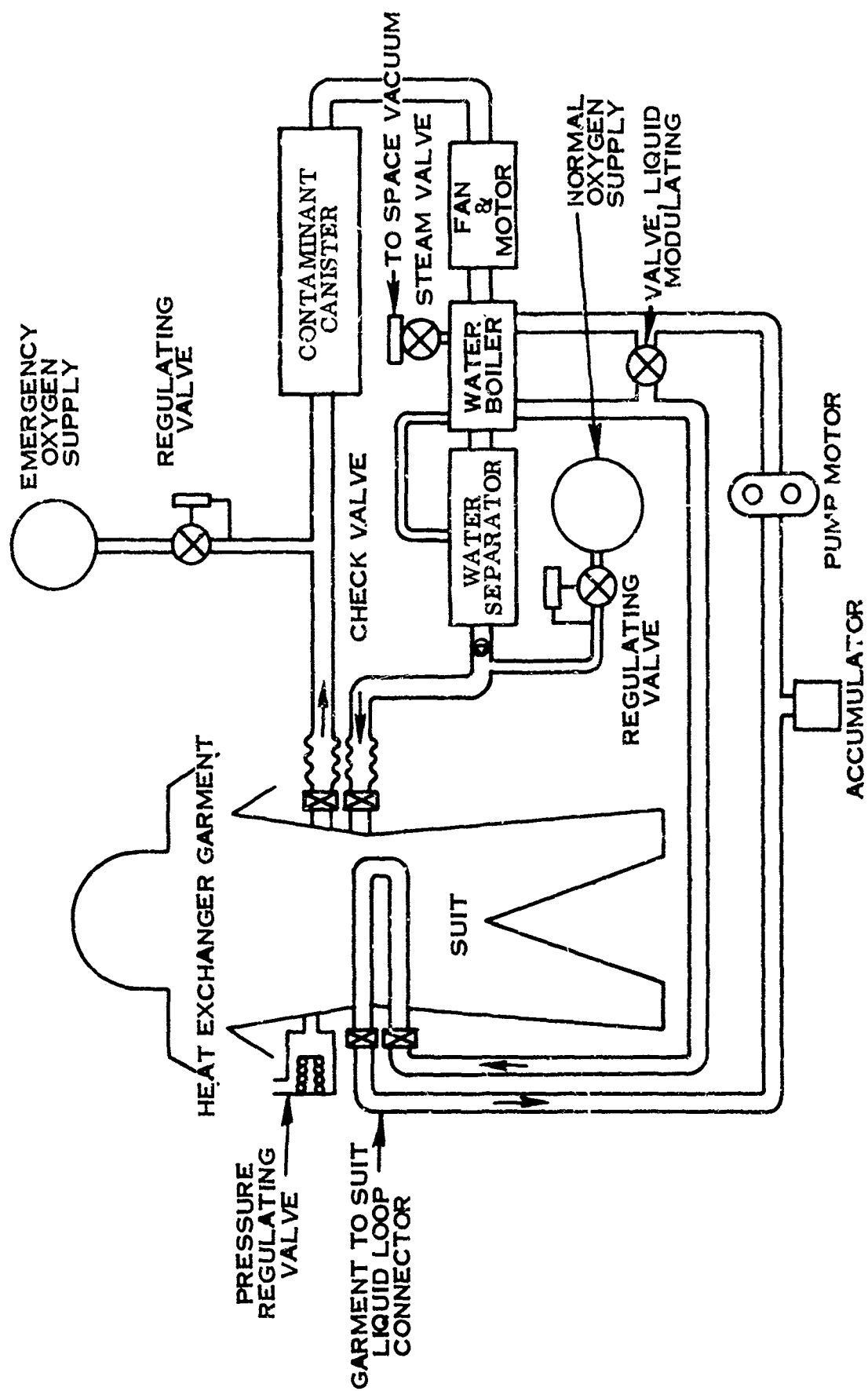


FIGURE 7. SCHEMATIC OF A TYPICAL GAS -- LIQUID COOLING LIFE SUPPORT SYSTEM

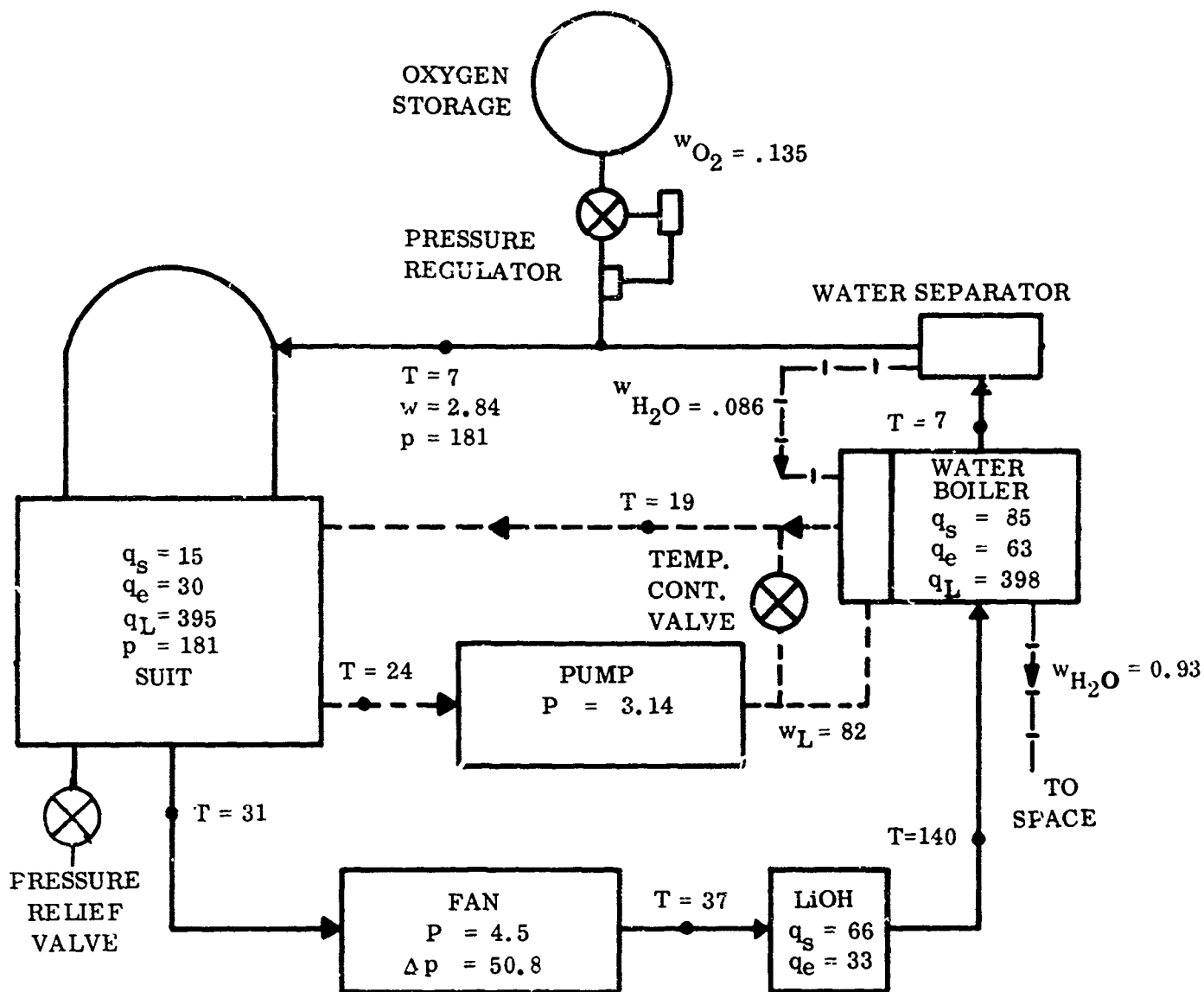
Performance of a typical combination liquid gas cooled suit and portable life support system is shown in the performance chart in Figure 8. Note that for the metabolic energy expenditure of 400 kcal/hr (1600 BTU/hr), 354 kcal/hr are removed sensibly by both the liquid and gas cooling systems. Only 20 kcal/hr are rejected latently corresponding to a water loss of 0.05 kg/hr. This rate of water loss for a four hour extravehicular mission results in less than 0.3 percent loss in body weight.

SUIT EVALUATION AND TESTING

In the preceding sections the basic requirements for the design of extravehicular protective assemblies have been set forth and some of the concepts for implementation have been discussed. The acceptability of the final product, however, rests not with the design concept but with the proof that comes from an extensive test program. These tests range from the determination of the properties of the basic suit materials to the final testing of the man, suit, and mission in a fully duplicated environment. Between these extremes a very large number of tests is conceivable.

Ideally, the goal is to have available a wardrobe of completely defined space garments so that once a mission and a reliability goal are specified, an ensemble of garments can be selected from the wardrobe with full assurance of their compatibility with the mission. More practically, the goal is to have available a full complement of test techniques which make possible the continued development of space garments based on sound physical data and objective, realistic criteria as well as on subjective and necessarily statistical methods.

Traditionally, suit test programs have been directed toward an immediate and specific mission requirement. In the resulting mission oriented testing, "Can the mission tasks be performed?", "Will the suit withstand the environment?", and "Is the physiological stress level tolerable?" have been the principal questions asked. These questions are vital and must be answered; however, they normally provide little quantitative data upon which the engineer can rely to improve the suit design. The fact that the astronaut cannot reach and actuate a given control fast enough is of justifiable concern; but, with most current test techniques it is difficult to determine the cause of unsatisfactory performance. It may have been due to a lack of shoulder mobility, excessive elbow torque, a coordination problem due to the joint geometry, a lack of glove flexibility, or visual disorientation due to distortion in the visor optics. Even if the specific problem can be isolated, in many cases there are no adequate techniques available to quantify the significant parameters. Furthermore, in most cases, the criteria on which to judge improvements in these parameters have not been well developed.



Legend

q - Heat Load, kcal/hr
w - Weight Flow, kg/hr
T - Temperature, °C
p - Pressure, mmHg
P - Power, watts

Subscripts
s Sensible (Gas)
e Latent
L Sensible (Liq.)

Conditions:
Metabolic Rate - 402 kcal/hr
Heat Leakage - 38 kcal/hr

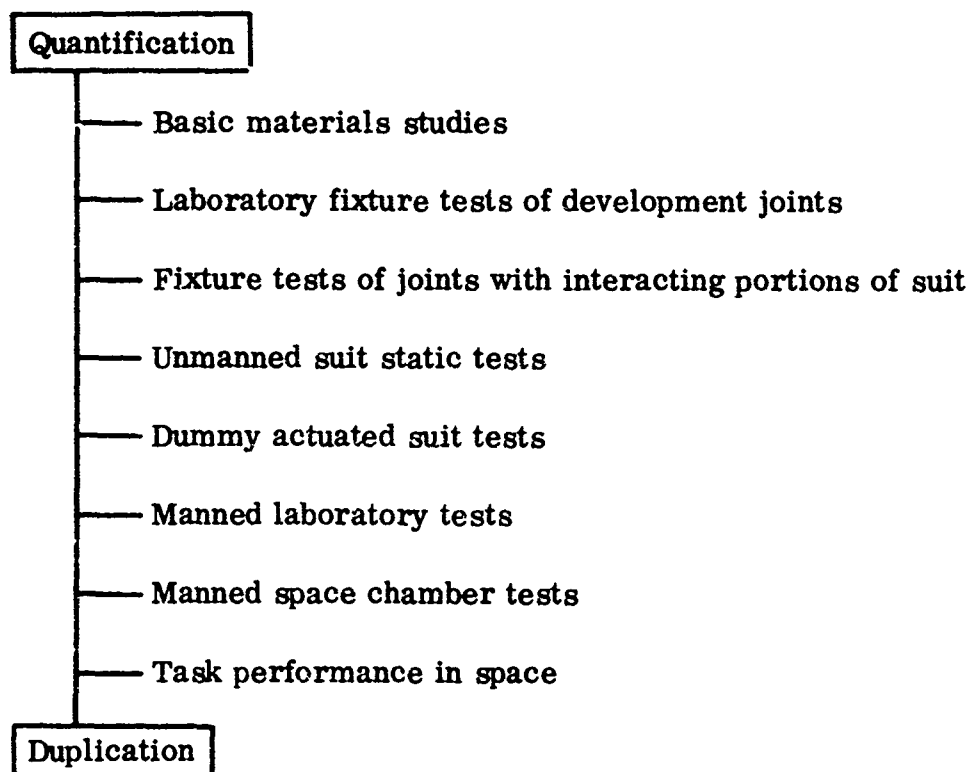
FIGURE 8. TYPICAL PERFORMANCE VALUES FOR A GAS/LIQUID COOLED LIFE SUPPORT SYSTEM

In addition to mission oriented data, the engineer normally has available materials test data and the results of simple, well controlled suit component tests. In general, these are also insufficient to satisfy his requirements for design improvement since they cannot realistically be related to actual suit operating conditions.

This lack of objective, accurate data to quantify the basic functional, life support, and protective characteristics of a suit ensemble is a well recognized problem and is the basic impetus for this study. In no area is this more evident than in the assessment of suit mobility. Many mission oriented studies of reaction time, reach envelope, task performance, and metabolic cost have been conducted to measure the restrictions that a pressurized suit imposes upon the wearer, but these tests lack the vital quantitative measures such as torque, force, pressure distribution, joint velocity, and friction that are needed to define joint performance. Likewise, materials test data on the neoprene, fabrics, cords, and cables of which joints are constructed and even the results of tests of joint performance do little to aid the engineer in the solution of the complex problem of joint volume and geometry control.

For the purpose of discussing suit test philosophy, it is instructive to consider a scale with objectivity, accuracy, simplicity, and quantification on one end and subjectivity, specificity, complexity, and mission duplication at the other end. All suit tests can be placed on this scale roughly as shown in the example of suit torque below.

SCALE OF SUIT TORQUE TESTS



It is neither possible nor desirable to attempt both accurate quantification and mission duplication in the same test. For example, if one needs quantitative data on the ventilation system of a specific suit design, then a test in which temperature, humidity, and flow distributions are measured should be conducted under accurately controlled conditions, independent of the subjective responses of a test subject. If one wants assurance that the ventilation system will perform adequately on a particular mission, then the mission tasks and environment should be accurately duplicated and only a minimum of physical measurements used to supplement the subjective and physiological responses of the subject. Attempting both of these goals in a single test results in serious compromises. Fully instrumenting a test subject while duplicating the environment leads to excessive weight, encumbrance, and extra heat sources which compromise the duplication requirements. Similarly, the duplicate environment is so complex that the detail data from the instrumentation probably defies interpretation.

In many test areas, therefore, a gap exists in measurement and test technology. It is the intent of this study to utilize the latest instrumentation technology to fill this gap that lies between the accurate-objective materials testing, which cannot be related to actual suit experience, and the mission oriented assurance testing, which cannot provide the suit engineer with quantitative data.

Because of the broad range of testing possible and the varied interests of those concerned with suit development, the areas of evaluation cannot be organized into a cohesive pattern of equal benefit to all. Recognizing this difficulty, the areas of evaluation have been rather arbitrarily organized by suit function. The functional organization can be illustrated by considering the following simplified chart representing the basic functional characteristics considered in the design of a space ensemble. (Figure 9)

SUMMARY

The scope of this study has been established on the basis of the space mission, the space environment, life support requirements, and suit concepts and design. The guiding philosophy has been to devise tests with optimum levels of quantification and duplication of the end use for the benefit of suit design engineers and evaluators.

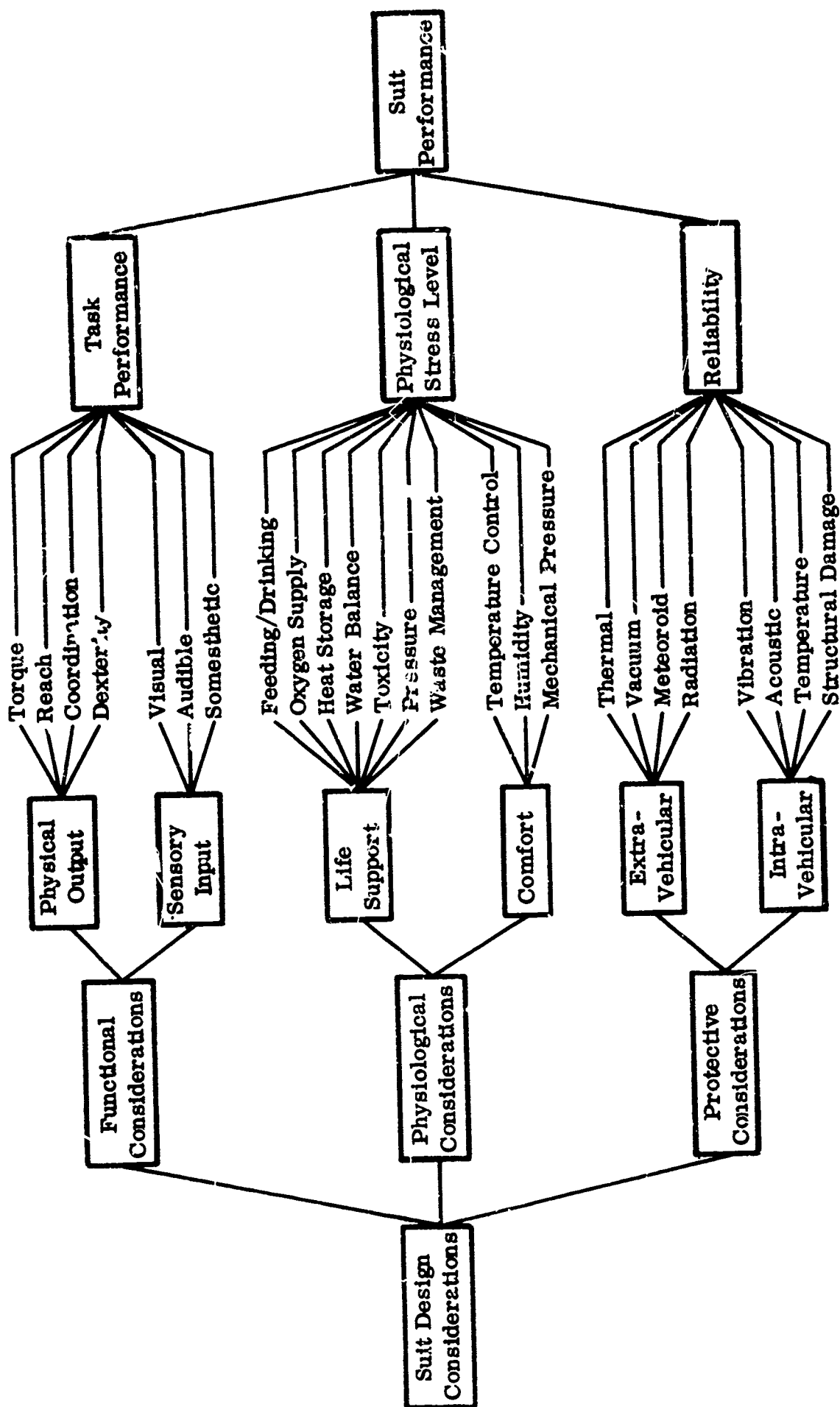


FIGURE 9. BASIC FUNCTIONAL CHARACTERISTICS OF SPACE SUIT DESIGN

SECTION III

METHODOLOGY FOR THE EVALUATION OF FUNCTIONAL SUIT MECHANICS

INTRODUCTION

By providing an adequate thermal and respiratory environment and protection from environmental hazards, the space suit makes a positive contribution to the welfare of the astronaut. In the area of functional suit mechanics, however, the suit's contributions are all negative. Nothing in the space environment intrinsically impairs mobility. Rather, the space suit imposes the mechanical restrictions. This section is devoted to description of the mechanical restrictions of the suit, to discussion of their causes and effects, and to development of a methodology for the testing and evaluation of suit functional performance.

Functional suit mechanics includes all the properties of space garments which impair the normal mechanical functions of the wearer. The mechanical impairment appears as a loss in effective strength, a decrease in the angular ranges of the body joints, a loss in coordination and dexterity, reduction in tactile cues, an increase in discomfort from the mechanical loading, and increased muscular effort and consequent metabolic energy expenditure. As a result, the extravehicular astronaut is effectively weaker, less capable, less efficient, and more highly stressed than in the earth environment.

Thus, functional suit mechanics is an area of vital concern. It is the study of the mechanical interface between the suit and the man and its effect on his performance.

Mechanically, a space suit is a pressure vessel with joints corresponding to those of the wearer so that he can move as well as exist. Several kinds of joints are in current usage and many more are being developed to obtain further improvement in this critical area of suit design. Suit joints, in general, consist of combinations of cords, cables, and fabric layers which restrain bellows, bladder, or convolute pressure vessels. Because this is an area of active development and because many of the designs have security classification, further description is inappropriate.

To keep soft suits from lengthening under pressure, various types of restraint systems and tie-downs are used. These tie-downs normally support large loads and must, therefore, be located so as not to interfere with joint motion.

The three basic causes of suit restriction are volume change, material strain, and friction. A volume decrease when a joint is flexed requires torque, and therefore, mechanical work, even with perfect pressure regulation. If the strain

energy of the fabric or cables is increased during joint flexion, torque is again required. Friction arising from the sliding of material and running gear under tension also requires torque for motion.

The reduction of suit torque is a particularly difficult problem for the suit designer. Truly constant volume soft suit joints have thus far not been realized. Joint centers of rotation seldom are fully compatible with the changing joint centers of the human; thus some motions are restricted or require excessively high torques. A close fit is needed to minimize suit volume in the capsule and to reduce suit limb interference.

The tests required to define the functional performance of the suit must be chosen to cover fully the mechanical interface between man and the suit without overlap or redundancy. Tests are needed to provide specific, quantitative data of value to the suit designer for assessing the performance of suit components. Tests are also needed to establish the overall performance of the suit and the effect of component performance on this performance. The tests must yield physical data such as torque, force, and angle which can be used directly in the evaluation of joint design and in the development of new theoretical concepts.

The measurement of torque alone, however, is not sufficient. Criteria are needed against which to judge the results of torque tests and assess any improvements in suit design. The criteria must be as objective as possible and sufficiently complete to be useful indicators of suit performance.

Ideally, each criterion would yield a single normalized figure of merit from objective mechanical measurements and would be physiologically based on metabolism, coordination, dexterity, or comfort.

Based on these considerations, the testing of functional suit mechanics was broken down into the following areas.

1. Joint torque vector versus angle measurement
2. Mechanical load distribution measurement
3. Dexterity testing
4. Reach envelope measurement

Torque, load distribution, dexterity, and reach testing are discussed individually in separate subsections. In each of these subsections the man's capabilities and the nature and cause of the restrictions are discussed. These lead to discussions of evaluation criteria and concepts for ideal measurement systems which define the quantities to be measured and provide a basis for evaluating the inevitable compromises of measurement hardware. Various possible approaches to the measurement problem then are discussed and, finally, measurement techniques are proposed which fit in with the overall test plan and data system.

JOINT TORQUE VERSUS ANGLE MEASUREMENT

Introduction

Measurement of the torques that a suit imposes on the astronaut as functions of his joint angles is particularly difficult because man's body with its changing joint centers, linear distance changes, and compliant flesh creates geometrical problems which make transduction very complex and because a pressure-sealed, close-fitting space suit leaves little space for instrumentation. For a better understanding of this measurement problem, this section begins with a discussion of the mechanical capabilities of men and suits and the quest for appropriate criteria on which to judge the mechanical encumbrance of a suit. Then the measurement problem is defined thoroughly and several measurement techniques are discussed in detail. One of these techniques is recommended for development and some interim techniques are suggested for use until the more advanced techniques become available.

Because man's skeletal structure is basically a jointed link system, torques about these joints are appropriate to describe his mechanical performance and encumbrance. Although the body joint structures and motion are extremely complex in detail, it is generally sufficient for this study to think of the body in terms of a simplified model, provided its limitations are realized. The model purposely simplifies the problem so that body position can be described analytically in terms of simple parameters such as pin joint angles. One such model which has been valuable to human engineers is W. T. Dempster's (ref. 33) link system. This system describes the body in terms of the basic links illustrated in Figure 10.

It is emphasized that this model is presented as an aid to visualization and discussion and should be applied with extreme care. Although the link system generally corresponds to the human frame, the instantaneous joint centers are fixed instead of changing and the ranges of motion are not limited.

The suit torque about a specified human joint is the torque imposed by the suit on the man. Loosely, the suit torque is the algebraic product of the average normal suit force acting outboard of a joint and the effective distance from the joint at which it acts. Suit torque is a measure of the additional muscular effort needed to produce a given body motion or assume a given position when wearing the suit. Torque will be given a rigorous mathematical definition including a discussion of its vector properties.

Detailed study of suit torques is essential since man is torque-limited. He can produce tremendous forces through toggle action if properly braced, but his torque capabilities are relatively independent of body angles. A suited man's net torque output, T_{net} , as a function of joint angle is equal to his nude torque capability, T_{nude} , minus the suit torque, T_{suit} .

$$T_{net} = T_{nude} - T_{suit} \quad (1)$$

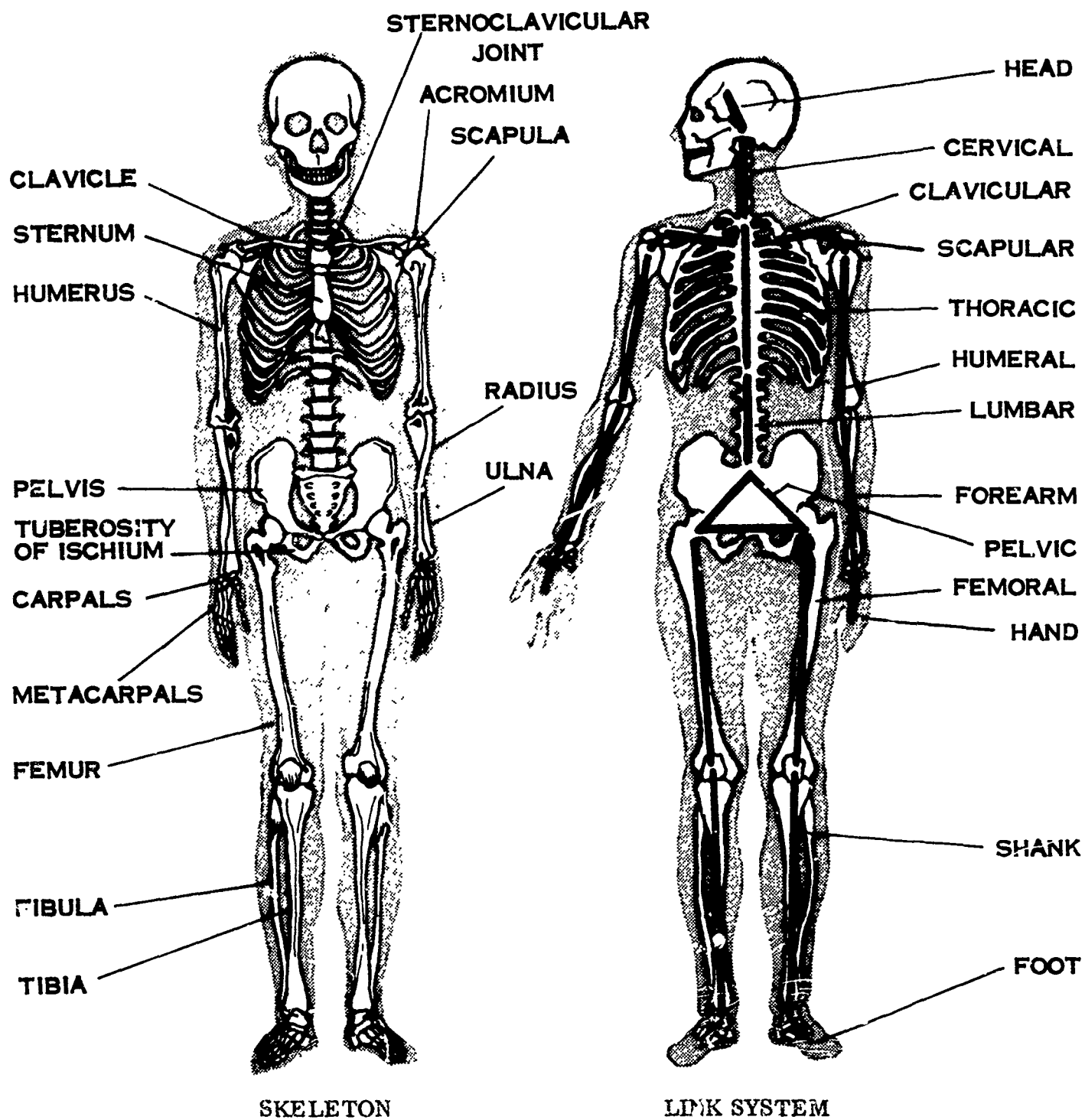


FIGURE 10. DEMPSTER'S LINK SYSTEM

The typical curves of nude and suit torque shown in Figure 11 illustrate how the effective or net torque output of the man-suit system is reduced.

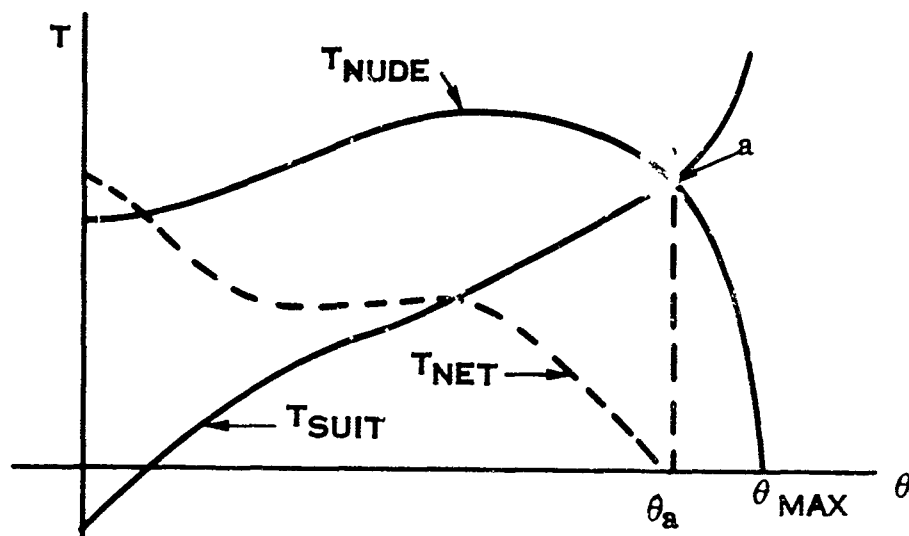


FIGURE 11. TORQUE OUTPUT AND FLEXION ANGLE REDUCED BY SUIT TORQUE

The suit torque also limits the maximum flexion angle from θ_{max} to θ_a , the angle at which the two curves cross. The metabolic cost of performing a task also increases with increasing suit torque. Increased metabolic requirements bring on earlier fatigue, higher physiological stress, and increased load on the portable life support equipment. Thus the duration of an extravehicular mission is closely tied to metabolic cost. Torque, particularly nonlinear torque, can severely affect coordination resulting in slow and awkward task performance. This problem can be partially solved through adequate astronaut training; however, the danger exists that the training may be forgotten in emergency situations. Since maximum joint flexion angles are reduced, equipment design must be modified to compensate for limited reach.

The torque of a particular suit joint depends upon several independent variables including the angle of the joint, its angular velocity, its angular acceleration, the suit pressure, the position of the other suit joints, and the suit fit or adjustment.

The measurement of torque alone, however, is not sufficient--criteria are required to relate the torque to actual performance. It is important, therefore, to consider the various end uses of the torque data. Torque values can be used to evaluate joint designs, to establish specification limits and, in conjunction with physiological and biomechanical information, to determine figures of merit for overall suit performance.

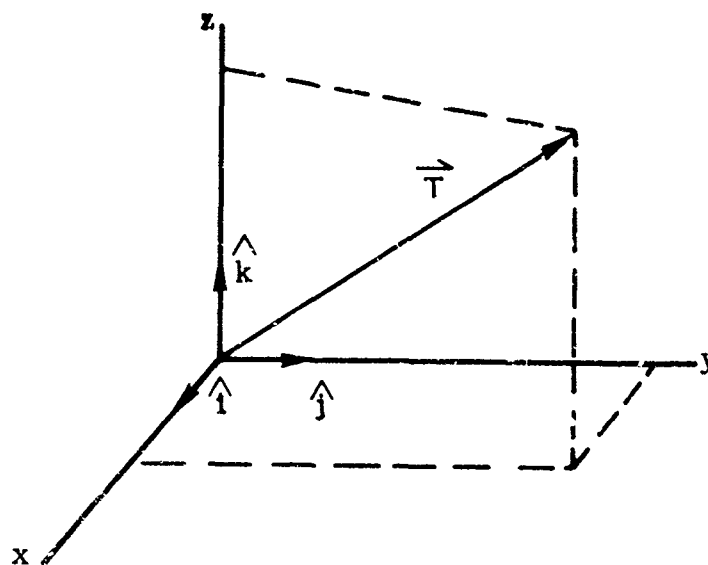
Although the joint with the lowest torque may be best, trade-offs between lowest peak torque, minimum metabolic cost, linearity, and coordination may be required in addition to the usual engineering criteria of cost, reliability, maintainability, etc.

Definitions

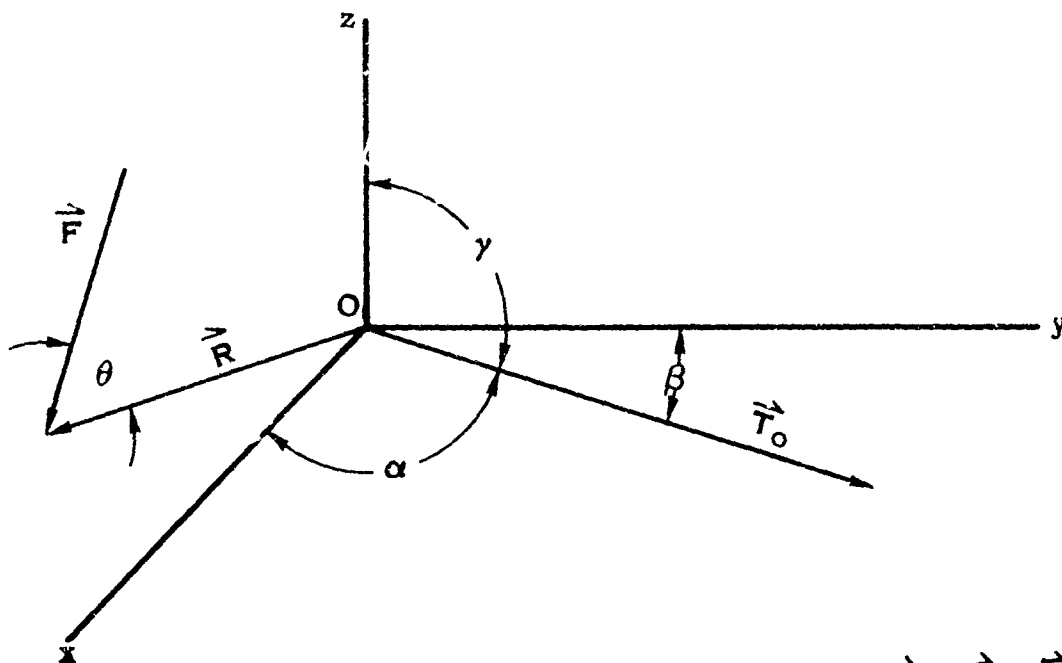
SUIT TORQUE

Torque is a vector quantity. Three numbers are required to express its magnitude and direction. In much of the literature concerned with suit torque, its vector properties are disregarded; yet they are essential to a full understanding of the suit torque problem. To set the stage properly for what follows, a detailed mathematical definition of suit torque is presented here. Although the definition has little direct application operationally, it is valuable as an ideal because every measurement technique must be considered in terms of this definition. The definition which follows is stated in vector notation. This notation and the applicable rules of vector and matrix algebra are presented in considerable detail in Appendix I.

A torque vector \vec{T} can be expressed as the sum of three components in a rectangular coordinate system, $\vec{T} = T_x \hat{i} + T_y \hat{j} + T_z \hat{k}$.



The symbols, \hat{i} , \hat{j} , and \hat{k} represent dimensionless unit vectors which specify the directions of the coordinate axes. Thus, to express a torque (or any vector), a coordinate system must be erected and the three components of the vector in that coordinate system must be given. Similarly, force and position are vector quantities. Consider the force \vec{F} acting at the point \vec{R} as follows:



The torque \vec{T}_O about the origin O due to a force \vec{F} acting at \vec{R} is $\vec{T}_O \equiv \vec{R} \times \vec{F}$.

If

$$\begin{aligned}\vec{T}_O &= T_x \hat{i} + T_y \hat{j} + T_z \hat{k} \\ \vec{R} &= R_x \hat{i} + R_y \hat{j} + R_z \hat{k} \\ \vec{F} &= F_x \hat{i} + F_y \hat{j} + F_z \hat{k}\end{aligned}\quad (2)$$

then the "cross" notation can be defined with equal validity by any of the following expressions.

$$\vec{T}_O \equiv \vec{R} \times \vec{F} = \begin{vmatrix} \hat{i} & \hat{j} & \hat{k} \\ R_x & R_y & R_z \\ F_x & F_y & F_z \end{vmatrix} = (R_y F_z - R_z F_y) \hat{i} + (R_z F_x - R_x F_z) \hat{j} + (R_x F_y - R_y F_x) \hat{k} \quad (3)$$

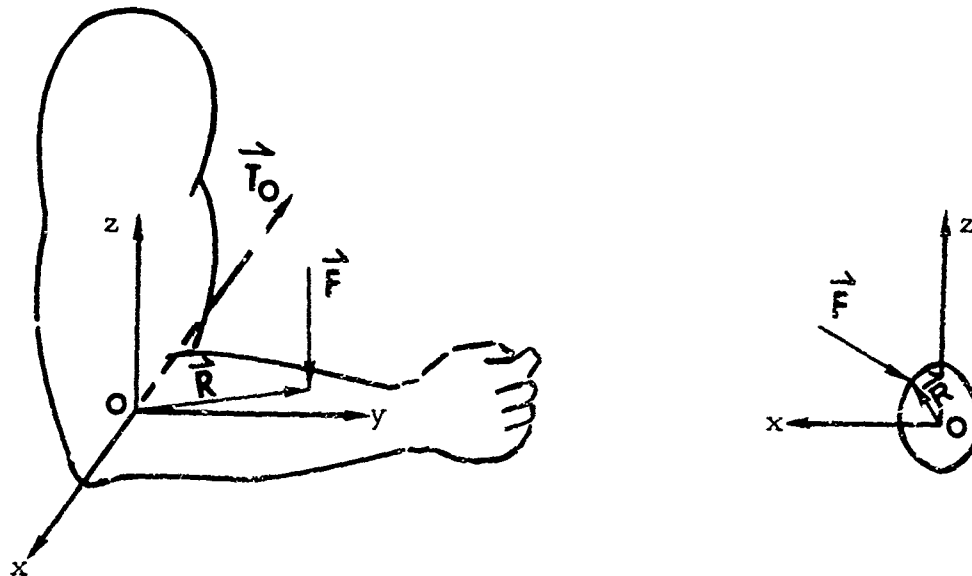
Also

$$\vec{T}_O = T_O (\hat{i} \cos \alpha + \hat{j} \cos \beta + \hat{k} \cos \gamma) \quad (4)$$

where

$$T_O \equiv |\vec{T}_O| \equiv |\vec{R}| |\vec{F}| \sin \theta \quad (5)$$

Normally, the suit elbow torque vector might be expected to be parallel to the elbow joint axis. This is not always true and it is because of this that a vector definition is insisted on. To illustrate this point, consider the following example:



If \vec{F} is parallel to the z axis and if it acts at a point \vec{R} in the y, z plane, then the torque is:

$$\vec{T}_O = \vec{R} \times \vec{F} = (0\hat{i} + R_y\hat{j} + R_z\hat{k}) \times (0\hat{i} + 0\hat{j} + F_z\hat{k}) = R_y F_z \hat{i} + 0\hat{j} + 0\hat{k} = R_y F_z \hat{i} \quad (6)$$

This is indeed a vector parallel to the axis of joint rotation. However, if the problem is just slightly more general, say with \vec{F} not parallel to the z axis as above, then

$$\vec{T}_O = (R_y\hat{j} + R_z\hat{k}) \times (F_x\hat{i} + F_z\hat{k}) = R_y F_z \hat{i} + R_z F_x \hat{j} - R_y F_x \hat{k} \quad (7)$$

This vector has components along all three axes which means that, as the elbow is flexed, the force \vec{F} at \vec{R} not only resists the elbow flexion, but it also tends to rotate the upper arm. Often this problem is called the tracking problem in suit mechanics and is discussed in considerable detail in the criteria section.

To define the suit torque at a joint, the following model is used. Consider a body link such as the forearm and conceptually place an origin of coordinates at the proximal joint center. Since joint centers in humans are not clearly defined, the origin is best placed fixed with respect to one of the link bones near the center of the locus of instant centers of rotation. The coordinate axes can be erected arbitrarily in the link, but it is usually desirable to align one axis with the link and one axis with the axis of rotation if the joint is a single degree of freedom joint like the elbow.

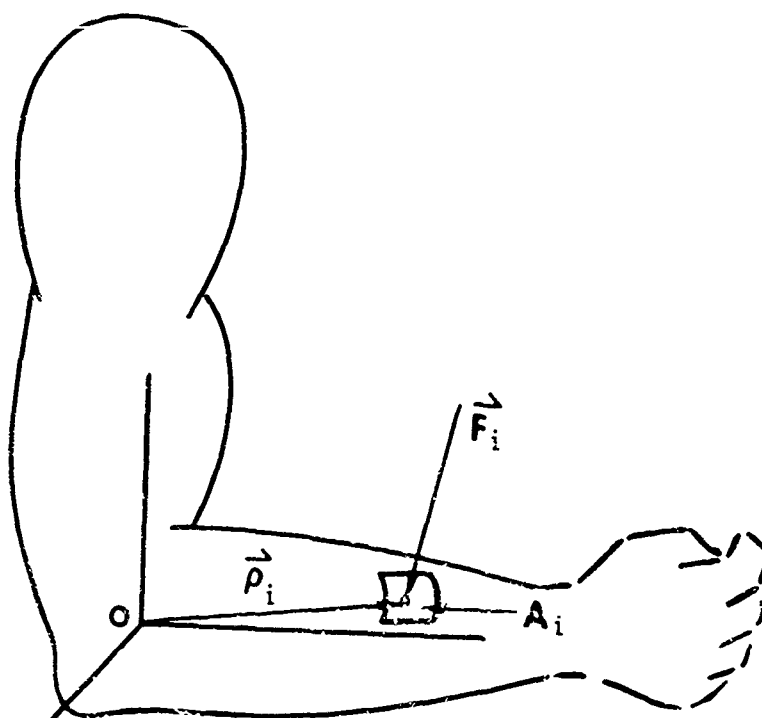


FIGURE 12. MODEL FOR DEFINITION OF SUIT TORQUE

Divide the link surface up into many small areas A_i . \vec{F}_i is the net force due to the suit on the skin area A_i and is considered to be acting at $\vec{\rho}_i$, which is some point on A_i . Now if $\vec{\rho}_i$ is properly chosen within A_i , the suit torque about O due to the force \vec{F}_i on A_i is $\vec{T}_i = \vec{\rho}_i \times \vec{F}_i$. Since torques can be added like any other vectors, the total suit torque about O is

$$\vec{T}_O = \sum_i \vec{T}_i = \sum_i \vec{\rho}_i \times \vec{F}_i \quad (8)$$

The sum is over all of the areas, A_i , which cover the link outboard from O. Now, conceptually divide the surface into smaller and smaller elemental areas A_i the largest of which is A_i^* . As the areas become smaller, so do the forces acting on the A_i 's but, in the limit as A_i approaches zero, the ratio of F_i to A_i approaches a unique value at the point $\vec{\rho}_i$. This ratio is called the mechanical pressure \vec{P}_i and is defined by

$$\vec{P}_i = \lim_{A_i^* \rightarrow 0} \frac{\vec{F}_i}{A_i} \quad (9)$$

Let \hat{u}_i be a unit vector in the direction of \vec{P}_i . This is the direction of the mechanical pressure on the surface at $\vec{\rho}_i$ and is not necessarily parallel to the unit outward normal vector \hat{n}_i at $\vec{\rho}_i$. This illustrates that the skin will support shear stresses due to the coefficient of friction between the skin and the suit.

Introducing this concept into the expression for torque and taking the limit such that all elemental areas approach zero subject to the constraint that $\sum_i A_i = A$, the total area from O outboard, the torque becomes

$$\vec{T} = \lim_{A_i^* \rightarrow 0} \sum_i \vec{\rho}_i \times \frac{\vec{F}_i}{A_i} A_i = \lim_{A_i^* \rightarrow 0} \sum_i A_i P_i \vec{\rho}_i \times \hat{u}_i \quad (10)$$

$$= \iint_{\substack{\text{Body surface} \\ \text{outboard from origin}}} dA P(\vec{\rho}) \vec{\rho} \times \hat{u}(\vec{\rho}) \quad (11)$$

P is defined only on the skin surface, not throughout the volume. Because of this, P and \hat{u} are better written as functions of some generalized surface coordinates ξ and η which locate a point on the skin surface. That is, $P = P(\xi, \eta)$, $\hat{u} = \hat{u}(\xi, \eta)$, and $\hat{n} = \hat{n}(\xi, \eta)$.

Now the suit torque about the joint with origin O is defined to be:

$$\vec{T} = \iint_{\substack{\text{Body surface} \\ \text{outboard from origin}}} P \vec{\rho} \times \hat{u} dA \quad (12)$$

Although this expression defines torque and should be considered when any measurement technique is evaluated, it may never be useful as an operational definition because accurate transduction of $\vec{P}(\xi, \eta)$, a continuous vector function of position on the skin surface, is beyond the state-of-the-art. Also, the position of a point on the skin $\vec{\rho}(\xi, \eta)$ varies because of the compliance of the flesh. If, however, a rigid transducer were constructed which could neither support nor measure shear loads, then the magnitude of the mechanical pressure vector would be the hydrostatic pressure; that is,

$$\vec{P}(\xi, \eta) = -P(\xi, \eta) \hat{n} \quad (13)$$

The expression for torque therefore becomes:

$$\vec{T} = \iint P \vec{\rho} \times \hat{u} dA = - \iint P \vec{\rho} \times \hat{n} dA \quad (14)$$

or

$$\vec{T} = \iint P(\xi, \eta) \vec{B}(\xi, \eta) dA \quad (15)$$

where

$$\vec{B} \equiv -\vec{\rho} \times \hat{n} \quad (16)$$

\vec{B} is a function of the geometry of the transducer and is independent of how it is loaded. In this case, if the magnitude of the normal pressure could be transduced, Equation 15 could be computer integrated to obtain the torque about the origin.

JOINT ANGLE

Since suit torque is usually measured as a function of joint angle, it follows that angle must also be defined as completely as possible. Since man's joint angles and the suit joint angles are not necessarily equal, it is important to state which angle is being considered. Man's joint angles are of prime interest because he is the common factor from suit to suit. Since suit joint designs may be vastly different, the use of suit joint angles as independent variable would prevent valid comparison of torque data. Also because evaluation criteria based on physiological considerations are sought, the man's joint angles are the logical choice.

Man's joint angles have traditionally been described by a medically derived goniometric terminology (flexion-extension, adduction-abduction, etc.). Although adequate for the descriptions of specific positions and motions, this terminology is not adequate for the general description of general motions or the automatic transduction of angles. Body position is defined to be the set (or list) of interlink angles, $\{\theta_i\}$, for the link model used in the measurement system. An operational definition of angle, however, depends on the measurement technique and, therefore, is deferred until later.

Man's Torque Producing Capabilities

THE MECHANISM OF TORQUE PRODUCTION

Before considering how to measure torque and on what criteria to judge the data, the torque producing capabilities of the body should be examined. Oversimplified for discussion, the skeleton is considered to be a system of links joined end-to-end by pin joints and ball joints. To these links are attached muscles which produce tensile forces on contraction. This tension results in a torque. When the torques produced by the agonistic muscles and the antagonistic muscles are unequal, there is a resulting net torque to act on the surroundings or accelerate the link.

If a man applies a torque to his environment, then it will exert an equal and opposite torque on him. Unless he is braced against something, he will rotate.

The torque output capability of a given man's joint in a given state of conditioning and fatigue is a function of several independent variables the most important of which are angle, angular velocity, positions of adjoining limbs, and method of bracing. The angular velocity dependence has the appearance of viscous friction

and has been the subject of study for many years by noted physiologists such as A. V. Hill and others. (These biomechanical concepts are treated in detail in many reference works such as 50, 51, 83, 90, 91.)

SOME DATA ON MAN'S TORQUE OUTPUT

Only a limited body of literature is available concerning the unbraced torque producing capability of man as a function of angle and angular velocity which is specifically applicable to the space suit problem. There is a great deal of literature available, however, on the general subject of torque capability. The inapplicability is due primarily to the complexity of the problem, the fact that the independent variables can take on any number of values, and that too little is known to extrapolate strength values confidently from one body position to another. Frequently, the measuring techniques, mode of bracing, and anthropometric data are inadequately defined. Better instrumentation, standardized test techniques and data presentation, and larger statistical samples are needed to define man's torque producing capabilities adequately. Nevertheless, the typical torque curves in Figure 13 have been compiled from the existing literature for the purpose of illustration. No claims are made for accuracy as much of the data is calculated from force information. However, an attempt is made to show the angular dependences. The joints and angles chosen are the same as those in typical suit torque curves in Figure 23.

TORQUE SURFACE FOR A MAN'S ELBOW JOINT

The curves presented above are for static torque. That is, the measurements were taken at zero angular velocity. But Hill has shown that a man's maximum output torque is a strong function of the angular velocity of the joint. Thus a more complete description of the torque capacity of a joint would include the angular velocity dependence. This function $T(\Theta, \omega)$ can be represented by a surface if torque is plotted along the vertical axis, Θ is plotted along one horizontal axis, and ω plotted along the other horizontal axis.

An approximate $T(\Theta, \omega)$ surface for an elbow has been constructed from Hill's equations (ref. 50). Singh (ref. 103) has measured the "concentric" and "eccentric" elbow torques, which would complete the torque surface in the three remaining octants.

This style of data presentation is a convenient way to visualize the functional dependence of torque. Its further value in developing joint torque criteria is explained in the criteria discussion.

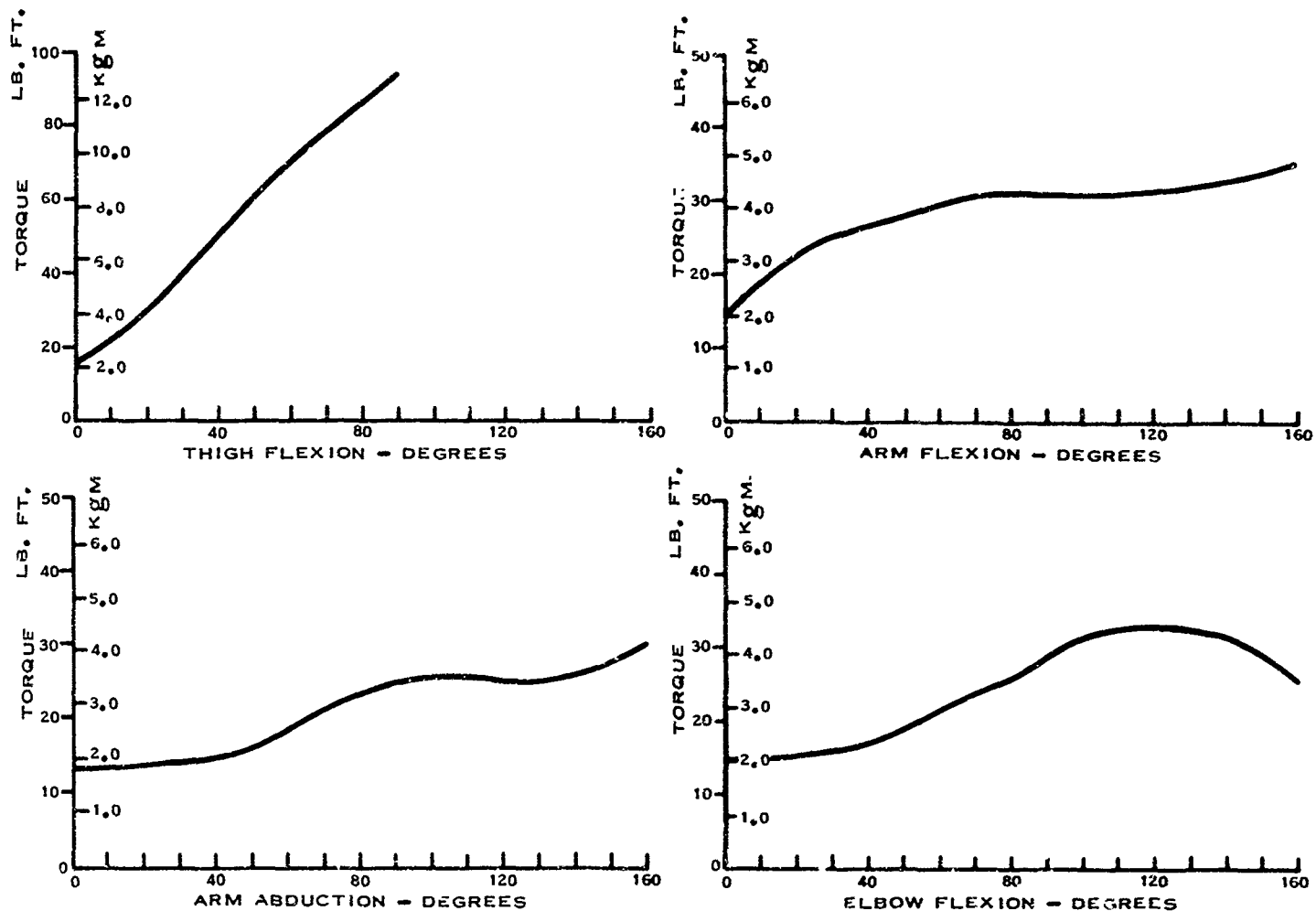


FIGURE 13. TYPICAL HUMAN TORQUE OUTPUT CURVES

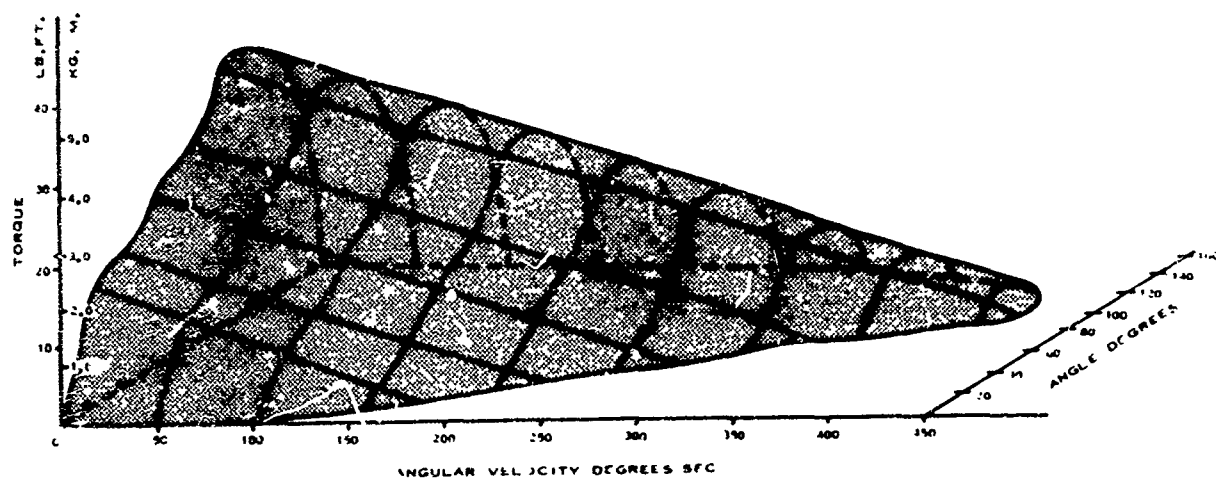


FIGURE 14. MAN'S ELBOW JOINT TORQUE SURFACE

Torque In Pressurized Space Suits

In this section an analytical discussion of the fundamental causes of suit torque is presented as a guide to the measurement and evaluation problem and to dispel some popular misconceptions about the mechanics of flexible pressure vessels. Some experimental torque curves for typical soft suits are given for comparison with man's torque producing capability. Finally, a torque surface, $T(\Theta, \omega)$, for an actual suit joint is plotted from experimental data for comparison with the man's torque surface shown in Figure 14.

GENERALIZED SUIT JOINTS

Suit joints, in general, must provide a pressure environment, allow an adequate range of flexion of the man's joint, offer little impedance to his motion, and should conform to his body to minimize suit bulk. In common space suit terminology, the joint must maintain pressure and provide mobility. In soft suits this is accomplished with various fabric, elastomeric, and metallic materials in combination. Pressure is generally maintained by a neoprene bladder which fills the joint. The bladder is kept from expanding by a surrounding fabric or with loosely interwoven cords or fibers which are arranged in an attempt to maintain constant volume in the joint and to minimize friction. Restraining cables are sometimes used to keep the joints from extending under pressure. The steel or nylon cables used to resist this tension are sometimes attached at both ends and sometimes run over pulleys, over turn-arounds, or through tubes.

Hard suit joints have been designed with rolling diaphragm joints and fan-like joints which, because of their metallic shell, are more simple to design for low unmanned torque than are soft suit joints. However, the fit problem is more critical.

Suit rotary joints, in particular the wrist joint, are normally of conventional sealed ball bearing design. The suits are light in weight but have a significantly larger fraction of their mass in the limbs than does the man.

CAUSES OF SUIT TORQUE

This section treats the mechanical analysis of suit torque. It is valid for suit joints in general and provides a basis for the understanding and analysis of specific suit joints. There are five distinct causes of torque in a suit joint. They are:

1. Volume change
2. Material strain
3. Weight
4. Moment of inertia
5. Friction

These will be treated one at a time and then related to the actual design problem.

Before considering each of the causes of suit torque, it is essential to discuss the concept of work as associated with these torques. Work is a precisely defined physical concept which is of considerable value in biomechanical studies. There is an apparent paradox, however -- when performing isometric exercises or pushing against an immovable wall, metabolism increases and muscles tire but no mechanical work is done. Apparently as a result of this paradox, many authors have expressed their results in terms of various quantities called work which do not obey the fundamental mechanical definition of work. Experience may have shown that these quantities have some empirical value for certain special problems, but their use for other problems must be approached with extreme caution. The fundamental definition of work is presented below and is discussed in greater detail in Appendix II. The apparent paradox of "static work" is left for discussion in a later section.

When a force \vec{F} is applied to a body and that body moves, mechanical work is done on the body. More specifically, when a force \vec{F} acts along a path \vec{r} in space, as in Figure 15, the mechanical work W_{12} in moving the body from \vec{r}_1 to \vec{r}_2 is defined to be

$$W_{12} = \int_{\vec{r}_1}^{\vec{r}_2} \vec{F}(\vec{r}) \cdot d\vec{r} \quad (17)$$

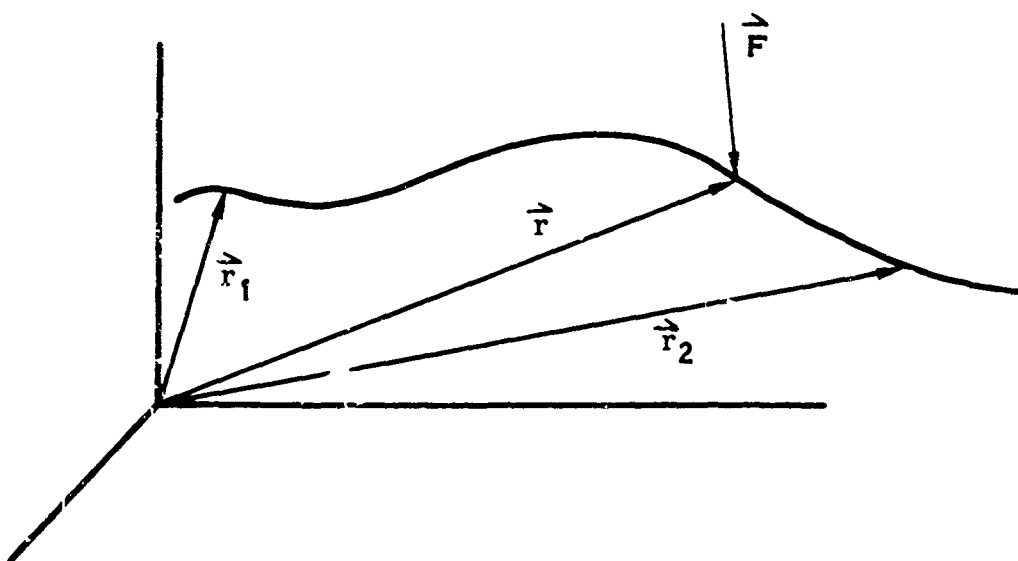


FIGURE 15. SKETCH FOR DEFINITION OF MECHANICAL WORK

Or if Θ is the angle between \vec{F} and the tangent to the path at any instant, then $W_{12} = \int_{\vec{r}_1}^{\vec{r}_2} F \cos \Theta \, dr$. In the special case of one dimensional motion and constant force, the work equals the product of force and the distance moved. Thus, work is done by a force only when it acts through a distance. Although one tires of pushing against an immovable wall, no mechanical work is done if the wall does not move.

In terms of applied torque and angle, the expression for work in moving a body along the path \vec{r} from \vec{r}_1 to \vec{r}_2 is:

$$W = \int_{\vec{r}_1}^{\vec{r}_2} \vec{T} \cdot d\vec{\Theta} \quad (18)$$

The consequences of this are:

1. If there is no motion, i.e., $d\Theta = 0$, then the work is zero.
2. If the force field is conservative, i.e., no friction, then the work in moving a body from \vec{r}_1 to \vec{r}_2 is independent of the path and the time.
3. If the force field is conservative, then the work of moving a body and returning it to its starting point is zero. This means that when a joint in which there is no friction is cycled, the mechanical work done per cycle is zero.

When work is done, energy appears in one or more of three distinct forms: an increase in potential energy, a conservative increase in kinetic energy, or a dissipative increase in kinetic energy, which ultimately appears as heat. Of the five causes of torque listed above, volume changes, material strain, and weight lifting increase potential energy; changes of angular or linear velocity cause changes in kinetic energy through the moment of inertia and mass; and work done against friction appears as heat.

VOLUME CHANGE -- A volume change in a suit joint during flexing requires an external torque. Volume change presents a difficult problem to the designer of suit joints because of the flexibility of the suit material and the complexity of the human geometry. Since this problem is frequently misunderstood, it is discussed in detail here. Consider a child's balloon in the shape of a long sausage. When fully inflated, its pressure is only a fraction of a pound per square inch, yet it is very stiff. The high torque required to bend the balloon is due to the volume decrease that occurs when it is bent. Early attempts at suit design produced results not unlike the child's balloon.

The effect of the volume change is analyzed by considering the thermodynamics of a gas in a closed cylinder with a piston.

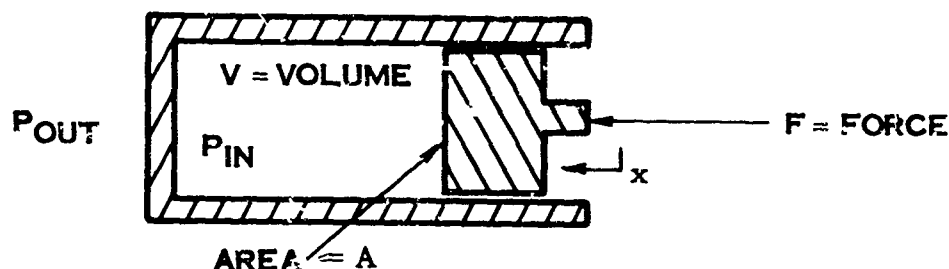


FIGURE 16. MODEL FOR THERMODYNAMIC WORK EXPRESSION

If $P = P_{in} - P_{out}$, then $F = PA$. From the definition of work,

$$dW = F dx = PA dx = P dV \quad (19)$$

so that

$$W_{12} = \int_{V_1}^{V_2} P dV \quad (20)$$

This result is true for a gas volume of any shape and is the basis for the following discussion.

The differential of work for angular motion, can be expressed as:

$$dW = - T d\Theta^* \quad (21)$$

Thus,

$$T_V (\Theta) = - P (\Theta) \frac{dV}{d\Theta} \quad (22)$$

This expression is true for either the suit's or the man's joint angle; however, in this discussion only the man's angle is considered. The minus sign in equation 21 makes T the suit torque rather than the torque applied by the man.

Two points are now obvious. First, for a constant volume joint $\left(\frac{dV}{d\Theta} = 0\right)$, the torque to deflect the joint is zero. Secondly, if the pressure remains constant

* See Appendix II

when a joint is flexed slowly (a pressure regulated suit), then $T_V(\Theta) = -P_0 \frac{dV}{d\Theta}$. Thus, the first task of the joint designer is to minimize $\frac{dV}{d\Theta}$.

For example, consider a joint whose torque curve appears in Figure 17.

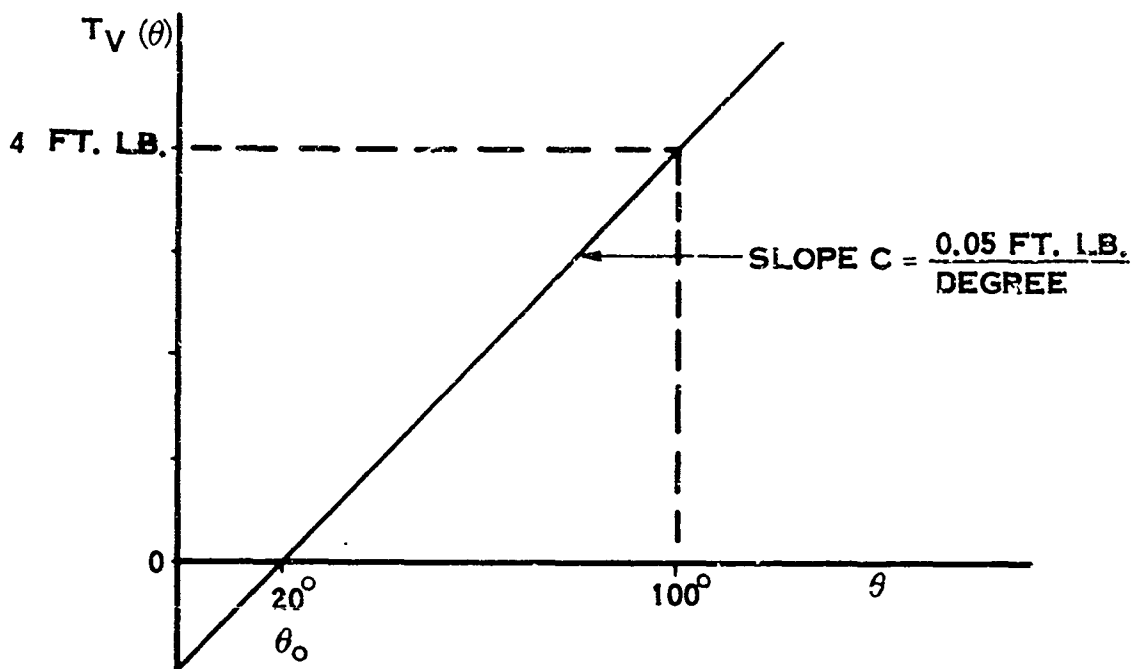


FIGURE 17. TORQUE CURVE FOR LINEAR JOINT

By substituting the linear torque-angle dependence into the differential expression for work and integrating, the volume change becomes:

$$\Delta V = V(\Theta) - V_0 = -\frac{C}{2P_0} (\Theta - \Theta_0)^2 \quad (23)$$

Thus, the suit volume as a function of joint angle for a "linear" joint has a parabolic dependence on angle as in Figure 18.

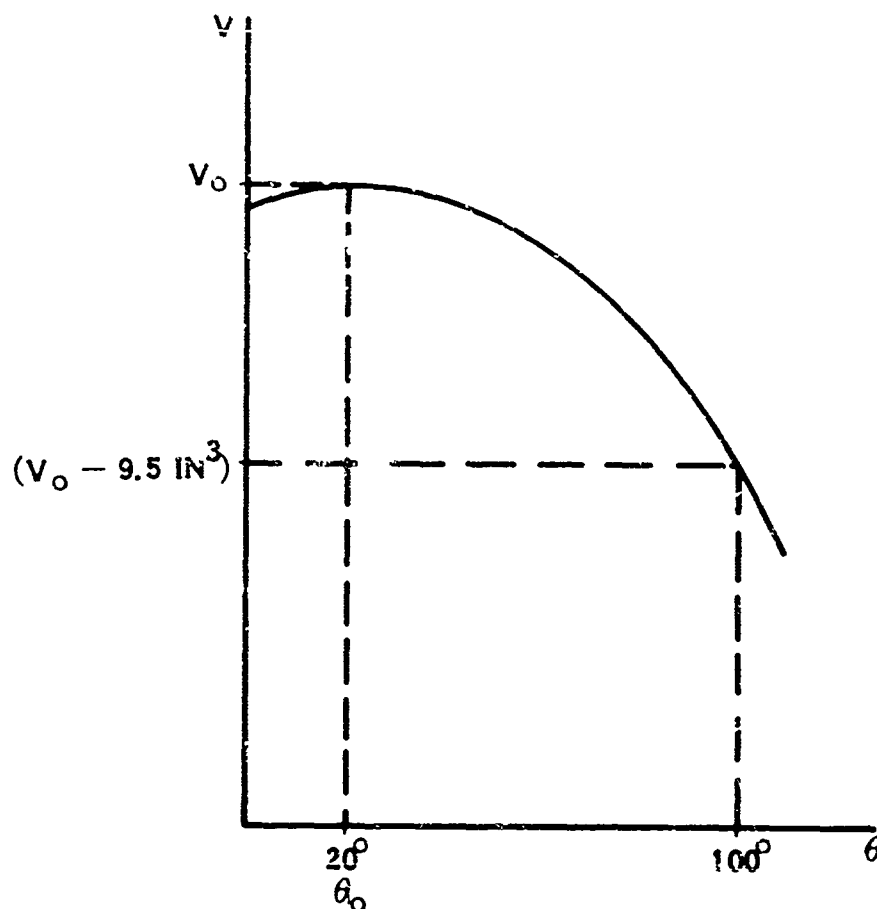


FIGURE 18. PARABOLIC VOLUME DEPENDENCE FOR JOINT WITH LINEAR TORQUE CURVE

Note that for slow flexion ($P = \text{constant}$) the torque is independent of the total volume V_0 of the enclosure.

For joint flexions faster than the pressure regulator can follow, P depends on time and T_V will increase. In this case, the torque also depends slightly on the absolute pressure in the suit; however, the correction for these effects in current suits is less than 1%. These calculations are shown in Appendix III.

MATERIAL STRAIN -- Possibly the suit designer's biggest problem is in creating joints which will follow the man's motion without stretching the material. Human kinesiology is such that, even in normal motions, joint centers are difficult to define and linear distances over the skin can vary tremendously. For instance, the length of a line drawn on the skin from elbow to elbow across the back can easily vary 6 inches. Design of the suit shoulder joint is particularly difficult because of the many degrees of freedom and the large surface area changes involved.

The analysis of material strain energy is a boundary value problem of considerable difficulty because of the variable suit and human geometry. However, the general principle will be explained and a simple example will be given. The work done in increasing the strain potential energy of the suit material is $dW_s = d(P.E.)_s$. As before, the torque due to this effect is $T_s = \frac{dW_s}{d\theta}$, so that

$$T_s = \frac{d(P.E.)_s}{d\theta} \quad (24)$$

This is to say that the torque due to straining the material is equal to the increase in strain energy per unit angle (in radians). In general $\frac{d(P.E.)_s}{d\theta}$ is impossible to compute from geometrical considerations because it depends on how the suit fits the man. However, the expression for T_s can be written if it is due to stretching restraint cables. For a cable, the change in potential energy with length is $d(P.E.)_s = kx dx$ where k is the spring constant and x is the length of the cable. If there are several cables involved in a joint, the torque due to stretching them will be

$$T_{s \text{ cables}} = \sum_i k_i x_i \frac{dx_i}{d\theta} \quad (25)$$

This is the mathematical expression for the obvious fact that the cables should be placed so that the $\frac{dx_i}{d\theta}$ are minimized.

WEIGHT -- Suit weight is not a serious problem; however, it is worthwhile writing down the expression for the joint torque due to this cause. Using the potential energy approach again,

$$T_w = \frac{d(P.E.)_w}{d\theta} \quad (26)$$

But the change in gravitational potential energy is $d(P.E.)_w = mg dh$ where dh is the change in height of the center of gravity of the suit limb in question. g is the local acceleration of gravity. m is the mass of the suit limb. Thus

$$T_w = mg \frac{dh}{d\theta} \quad (27)$$

At lunar gravity, these terms are only 1/6 their terrestrial value and in orbit they are zero. Although this torque presents little problem to the suit designer, it must be considered during accurate torque testing.

INERTIA -- The inertial torque T_I is also small and has usually been neglected in suit torque testing. It can be expressed simply as

$$T_I = I \ddot{\theta} \quad (28)$$

where I is the moment of inertia of the joint in question and $\ddot{\theta}$ is its angular acceleration. This term is independent of the local acceleration of gravity.

FRICITION -- Frictional forces are classified by their functional dependence on velocity into running friction, viscous friction, and static friction. The terminology is defined for forces and linear velocities but may also be applied to torques and angular velocity, ω .

Pure running friction (also known as kinetic and coulomb friction) is dependent only on the sign of the velocity.

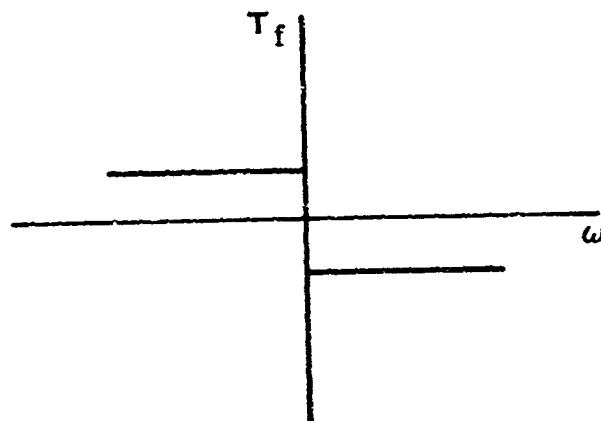


FIGURE 19. RUNNING FRICTION

Viscous friction is proportional to velocity, although higher order dependences are usually called viscous also.

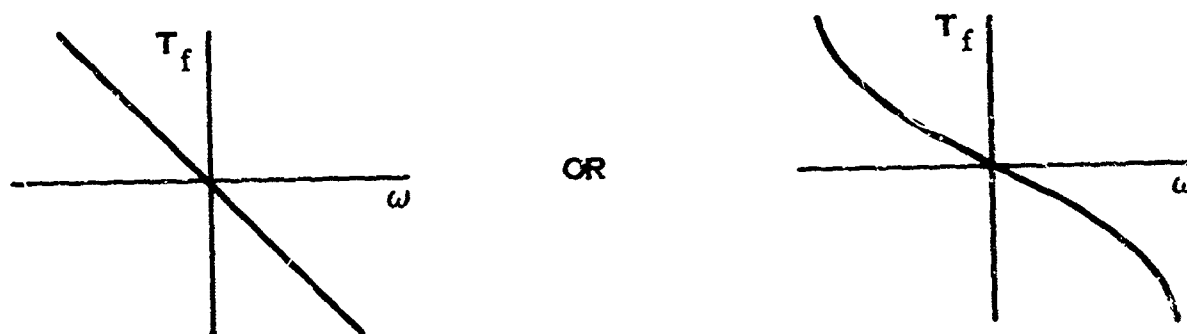


FIGURE 20. VISCOUS FRICTION

Static friction or "stiction" appears when starting a body to move and disappears when it is moving.

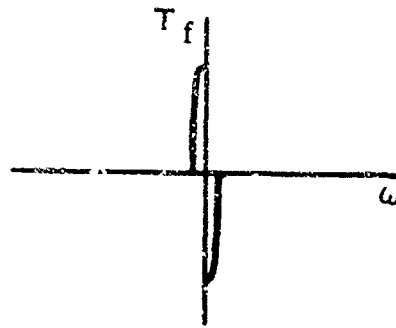


FIGURE 21. STATIC FRICTION

An actual case will be some combination of the three basic types as in Figure 22.

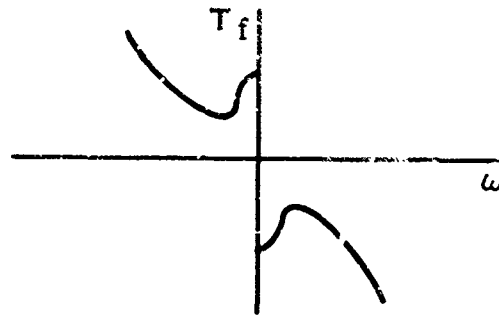


FIGURE 22. COMBINATION OF FRICTION EFFECTS

The sign of the friction force always opposes the motion. Because of its non-linear character, friction is difficult to predict analytically. For instance, when coulomb friction is added to a linear torque curve, a hysteresis band results as in Figure 27.

For single degree of freedom motion, the work done against friction is $W_{12} = \int_{x_1}^{x_2} F_f dx$ or $\int_{\theta_1}^{\theta_2} T_f d\theta$ where F_f and T_f are friction force and torque. F_f and T_f arise when material slides over other material as in sliding cords over fabric and when material is permanently deformed.

THE DESIGN OBJECTIVE

The five causes of suit torque have been enumerated and their theoretical basis explained. Collectively, they are:

$$T = T_v + T_f + T_s + T_w + T_i \quad (29)$$

or

$$T = - P(\Theta) \frac{dv}{d\Theta} + T_f + \frac{d(P.E.)_s}{d\Theta} + mg \frac{dh}{d\Theta} + I \ddot{\Theta} \quad (30)$$

The design objective is to minimize this sum for each of the joints. The joint system must be designed to maintain pressure yet follow the man's joint flexion and skin length changes with minimum fabric strain, minimum volume change, low friction in the running gear, minimum weight, and moment of inertia. This is generally accomplished by making the suit joint centers coincide with the man's joint centers; however, there is no theoretical necessity for this. Despite the simplicity of the problem statement, the solutions are hard to achieve.

SOME TYPICAL VALUES OF SUIT TORQUE

Static torque data for several joints in two different kinds of soft suits are presented in Figure 23 for comparison with the curves for man's capability in Figure 13. These were measured in a horizontal plane (eliminating gravitational effects) with a spring scale and a protractor. During the test the subject was limp within the suit.

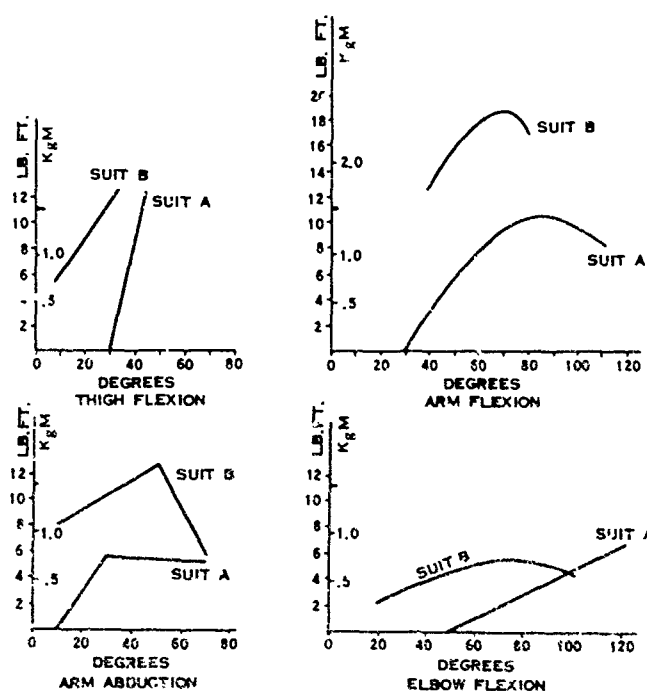


FIGURE 23. TYPICAL SUIT TORQUE CURVES

TORQUE SURFACE FOR A SUIT ELBOW JOINT

The data above for static deflections do not necessarily reflect the dynamic characteristics of the joint. Because joints are used at finite angular velocities,

it is of interest to know the dependence of suit torque on angular velocity. A simple dynamic suit joint tester was built consisting of a reversible variable speed transmission, a reducer gear box, a driving arm with torque and angle instrumentation, and a pressure gage and transducer. A current sliding cord restrained joint was tested by recording deflection torque and angle at four pressures and various angular velocities up to 60 degrees/second. Figure 24 shows that torque increases linearly with pressure as predicted by theory.

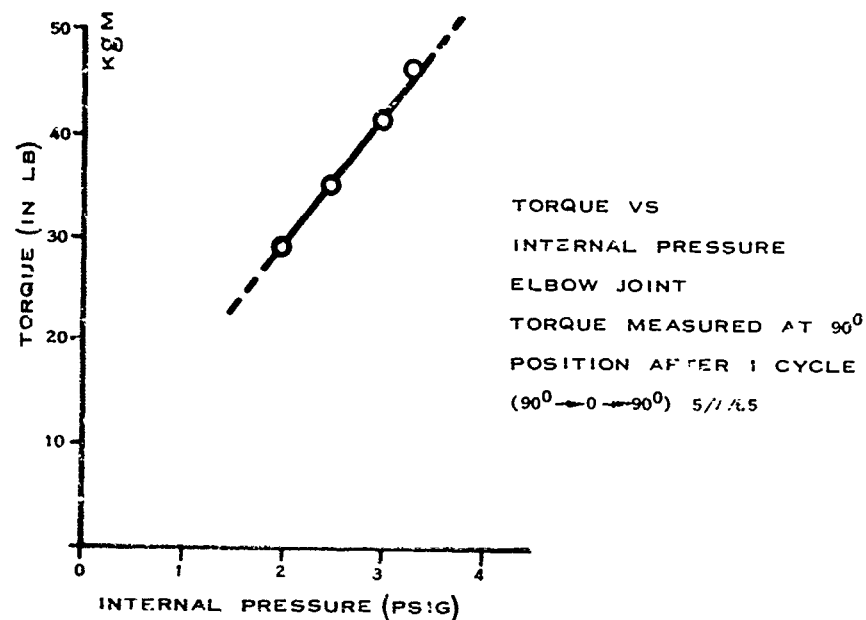


FIGURE 24. SUIT TORQUE VERSUS INTERNAL PRESSURE

The torque surface in Figure 25 was constructed from the dynamic test data after corrections were made from Figure 24 for the increase in pressure due to volume decrease.

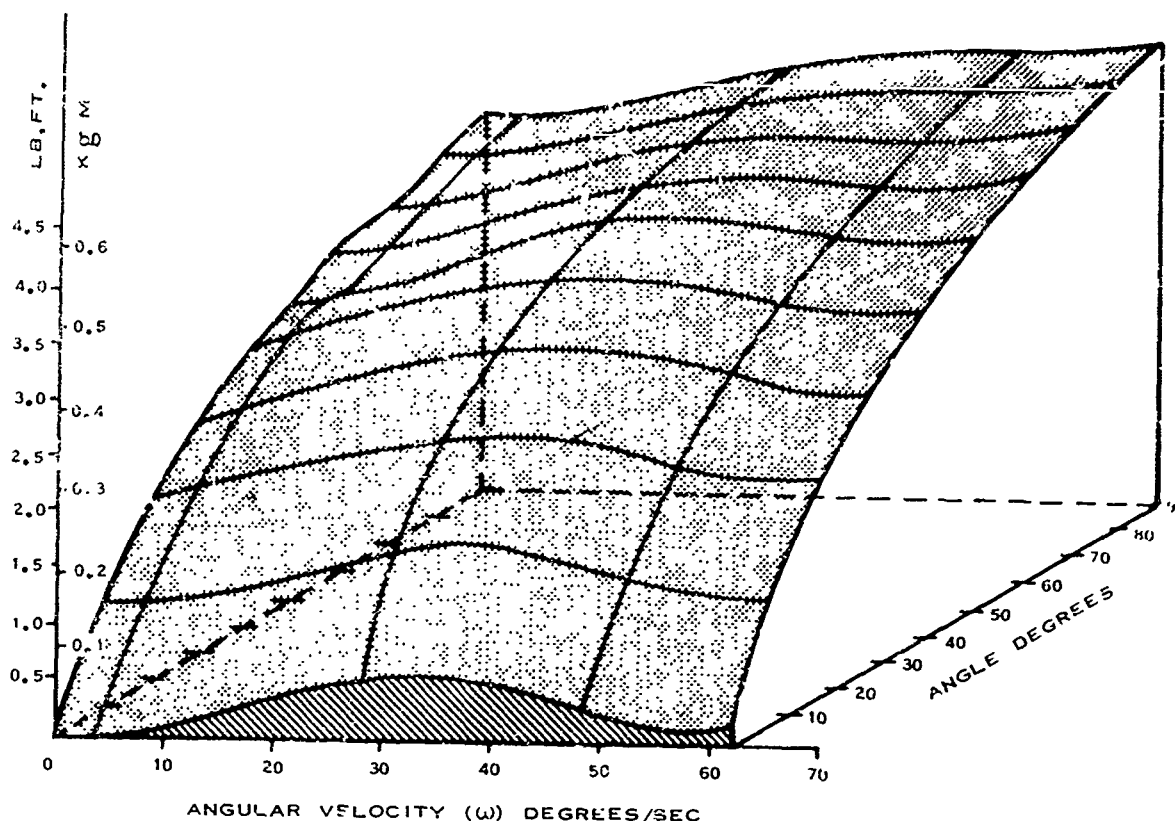


FIGURE 25. SUIT ELBOW TORQUE SURFACE

Torque Evaluation Criteria

In order to make full use of any torque data from suit joint measurement, adequate criteria must be developed on which to judge this data. This section discusses the basic criteria requirements and suggests four possible approaches for appropriate and useful criteria. These approaches are:

1. The use of normalized maximal torque-angle-velocity volumes as a measure of suit joint performance.
2. The use of respiratory measurements of metabolic cost as a measure of overall suit encumbrance.
3. The use of a figure of merit based on muscle metabolism and computed from direct mechanical measurements.
4. The use of average psychomotor performance scores and suit tracking torque.

Like all criteria, their value is measured by the results of their use and only time and experience can reveal this value.

THE NEED FOR TORQUE EVALUATION CRITERIA

The need for torque criteria is graphically illustrated by this example: Two suit joints are being evaluated and compared on the basis of their static torque curves in Figure 26. Which joint is better?

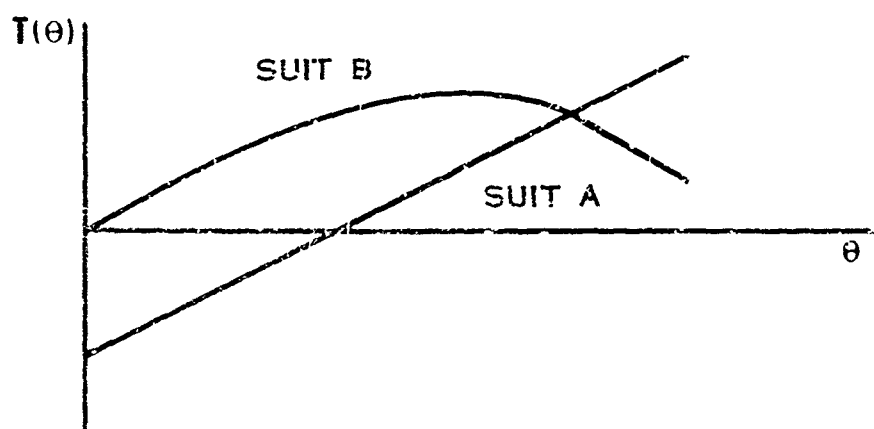


FIGURE 26. ELBOW TORQUE CURVES FROM TWO DIFFERENT SUITS

These are actual experimental curves from a comparative evaluation of prototype suits manufactured by different companies. The evaluation problem is obvious. When the curves cross, which is better? How should negative torque be considered?

Hysteresis is another problem. The torque curve for a joint with both volume change and static friction appears as follows

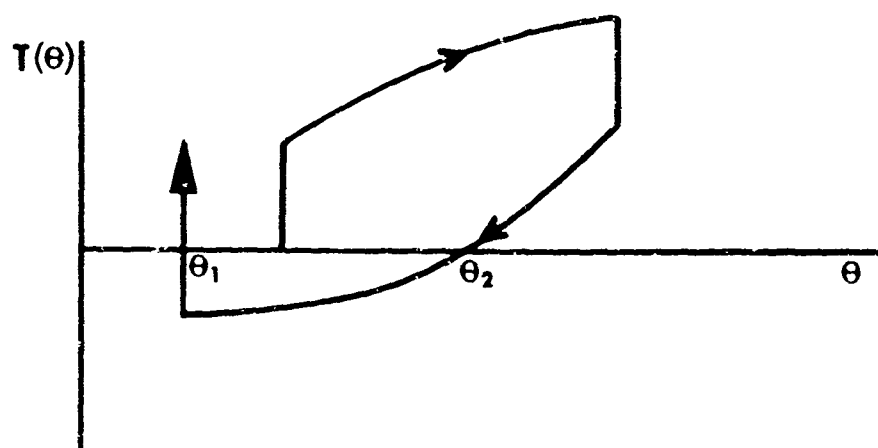


FIGURE 27. TORQUE CURVE FOR JOINT WITH HYSTERESIS AND VOLUME CHANGE

This joint requires relatively high torque to achieve a given angle, yet for angles from θ_1 to θ_2 requires no torque to maintain the flexion angle. Thus, while static friction is not in itself desirable, it can help counteract other effects;

two bad effects produced a more desirable joint. Without the volume change, the torque curve would have appeared as in Figure 28.

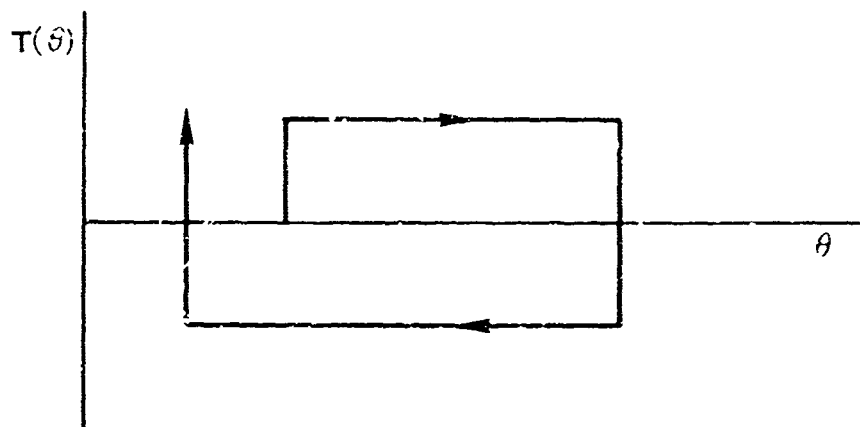


FIGURE 28. TORQUE CURVE FOR JOINT WITH HYSTERESIS BUT WITHOUT VOLUME CHANGE

In this case static friction is clearly undesirable.

Obviously, torque evaluation is by no means straightforward. The two examples chosen were not rare suit joints. Clearly, criteria are needed if optimum joints are to be designed and if effective suit specifications are to be written which permit necessary design trade-offs while achieving the desired goals.

BASIS AND PROPERTIES OF CRITERIA

The basis for evaluating torque data must be fundamentally rooted in physiology since torque affects man's coordination, his metabolism, his effective strength, and the range of motion of his joints. However, the criteria must be objective; they must be specific to the suit joint in question; they must be independent of the test subject; and they must be realistic. As an example of this latter point, if for a particular mission the elbow would never be flexed more than 140° , then the data beyond that point should be excluded from the criteria. Similarly, if most of the operation is between 20° and 90° , then the data should be weighed more heavily in this region. Therefore, if the suit is being evaluated for a particular mission, a profile of that mission should be included in the criteria. If not, a generalized mission should be considered. With these points in mind, the effects of suit-imposed torques on human performance will be discussed.

TORQUE SURFACE CRITERIA

In Figures 14 and 25, approximate torque surfaces were displayed. These plots of human torque output capability and the suit torque as functions of angle θ and angular velocity ω can provide very useful information for the evaluation

of suit joints. The volume enclosed by the torque surface for a man's elbow is a measure of elbow torque capability. The volume enclosed by the suit elbow torque surface represents a degradation of that capability. Consideration of these volumes and their actual shapes could provide evaluation criteria. The volume enclosed by the man's elbow torque surface can be written:

$$V_m = \iint T_m (\Theta, \omega) d\Theta d\omega \quad (31)$$

The "volume" has the units of power and is obviously not a physical volume but a constructed quantity. The torque volume accessible to a man wearing a suit can be calculated from Equation 32.

$$V'_m = \iint \left[T_m (\Theta, \omega) - T_s (\Theta, \omega) \right] d\Theta d\omega \quad (32)$$

$$|T_m| > |T_s|$$

This figure is normalized and the units removed by dividing by V_m giving

$$\frac{V'_m}{V_m} = \frac{\iint \left[T_m (\Theta, \omega) - T_s (\Theta, \omega) \right] d\Theta d\omega}{\iint T_m (\Theta, \omega) d\Theta d\omega} \quad (33)$$

Very likely, some portions of the torque volume will be more important than others so that weighting factor $W(\Theta, \omega)$ would assign relative importance to various parts of the torque volume. The new weighted figure of merit, designated here as M , is calculated from Equation 34.

$$M = \frac{\iint \left[T_m (\Theta, \omega) - T_s (\Theta, \omega) \right] W(\Theta, \omega) d\Theta d\omega}{\iint T_m (\Theta, \omega) W(\Theta, \omega) d\Theta d\omega} \quad (34)$$

where again the integration is over $|T_m| > |T_s|$. M is a number between 0 and 1 which is a measure of joint performance normalized to the test subject. $M = 1$ would imply a perfect joint.

METABOLIC COST CRITERIA

The metabolic rate required to perform a given task increases significantly with suit encumbrance. For example, in the simple task of walking at 2.0 mph on level ground (or a treadmill) at earth gravity, the metabolic rate is increased from an unencumbered rate of 180 kcal/hr to 400 kcal/hr for a typical soft suit at 3.5 psid.

This change in metabolic rate is important for it represents higher physiological stress and earlier fatigue. Since an astronaut must carry with him oxygen, carbon dioxide removal equipment, water, and electrical power, an increased rate also means greater load on the life support equipment, more rapid consumption of vital stores, and/or shorter missions.

In space suit testing, this metabolic increase is commonly referred to as metabolic cost. Metabolic cost has two common usages: the metabolic cost of performing a task and the metabolic cost of a suit. These two definitions do not have the same meanings or even the same physical units.

The metabolic cost of performing a task is the total metabolic energy expenditure during the task plus the energy expended over the normal rest metabolism during the recovery period.

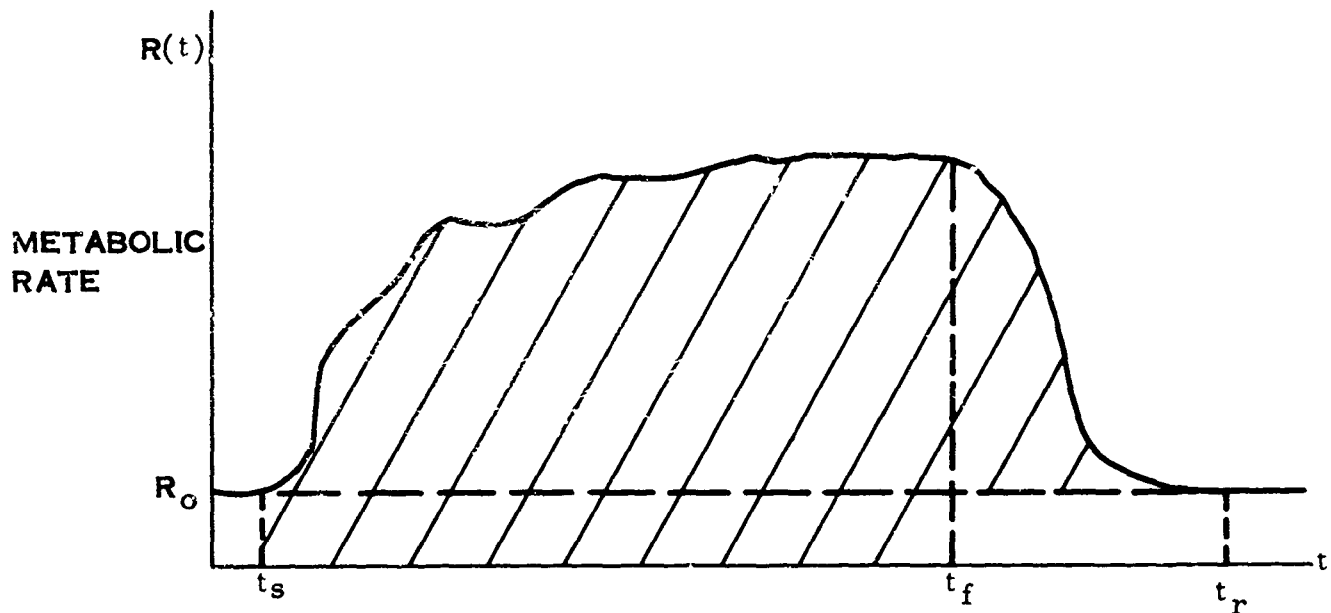


FIGURE 29. TASK METABOLIC COST

The curve in Figure 29 is a typical record of metabolic rate versus time for a certain task. Prior to the start of testing, the subject rests in some defined way with a metabolic rate, R_0 . At the time t_s , he starts the task and completes it at t_f . He returns to the rest condition so that at t_r his rate has returned to the initial rest rate. The metabolic cost of the task is defined to be

$$M.C._{Task} = \int_{t_s}^{t_f} R(t) dt + \int_{t_f}^{t_r} [R(t) - R_0] dt \quad (35)$$

which is the shaded area under the curve. It is an absolute figure which indicates the total metabolic energy produced for the task.

The metabolic cost of wearing a space suit, on the other hand, is the difference between the suited and unsuited metabolic energy production rates while performing a task. Normally, the task is repetitive, as walking, and is performed as nearly as possible the same way suited and unsuited.

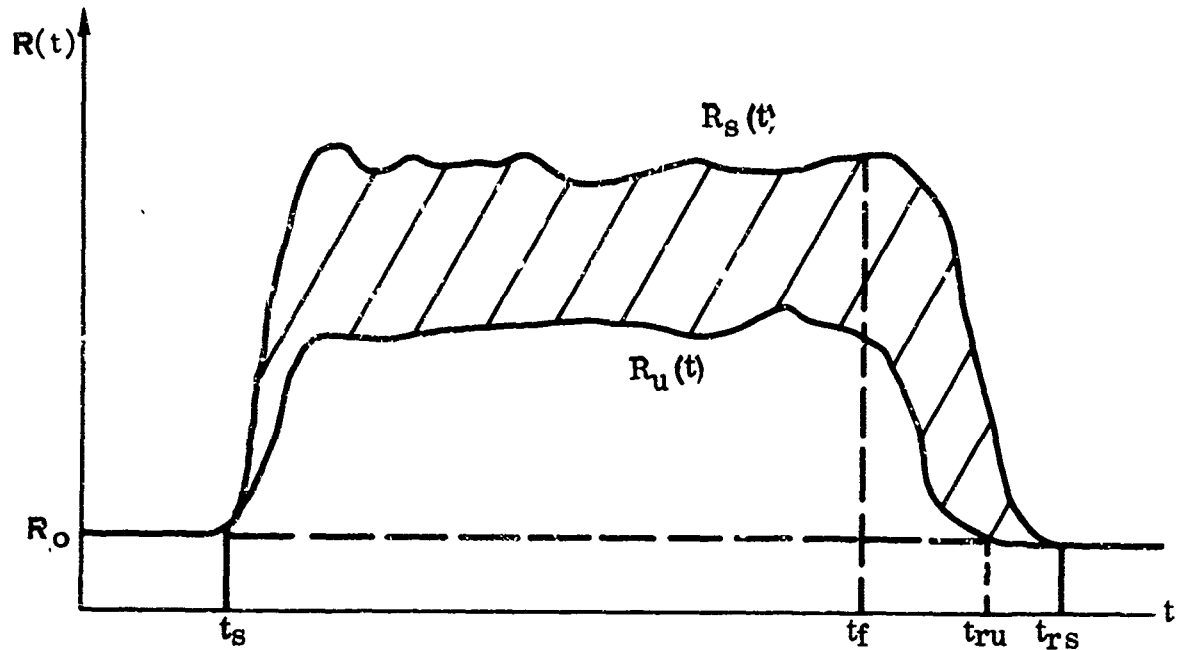


FIGURE 30. SUIT METABOLIC COST

The record of the metabolic rates suited R_s and unencumbered R_u might look like Figure 30. The metabolic cost of the suit for the task which was performed between t_s and t_f is the average difference between the two rates as in Equation 36.

$$\text{M. C. Suit} = \frac{1}{t_f - t_s} \int_{t_s}^{t_{rs}} [R_s(t) - R_u(t)] dt \quad (36)$$

By definition, the test subject is expected to perform the task in the same manner during both tests.

Traditionally, the metabolic cost, by either meaning, has been measured by indirect calorimetry, i.e., pulmonary gas analysis. This provides a rather accurate measure of total task performance; however, it is subject to the motivational and physiological variability of the test subject and more importantly it is not specific to any particular joint. Therefore, metabolic cost cannot provide the suit designer with the specific information required to improve joint designs. As is pointed out in a later section, metabolic measurements must be taken over a significant time interval if statistical variability is to be minimized. Approximately two minutes are required to stabilize the metabolic production rate and at least ten minutes more are required if normal tidal variations are to be minimized. For many joint motions, a strenuous uniform exercise cannot be maintained for the required measurement interval. Reduction in the time interval decreases the total difference in energy expended, further decreasing the accuracy of the

measurement. Lack of repeatability in joint motion, rapid subject fatigue, and/or low measurement sensitivity have frustrated most attempts at metabolic cost measurements of single joints.

Although the basic measurement technique may improve to some extent, it is unlikely that metabolic cost alone will prove very useful as a joint torque criterion. It is, however, and will undoubtedly continue to be an effective criterion of overall suit performance.

MUSCLE METABOLISM "FIGURE OF MERIT" CRITERION

Measurement problems notwithstanding, metabolic energy expenditure remains an ideal criterion of suit joint performance provided it can be specific to a particular joint. What is needed is a more objective and sensitive measure of metabolic cost. Since the muscle tissue is the basic site of the metabolic process and the external torques produced depend on these processes, the possibility was investigated of computing a metabolic figure of merit from measured mechanical properties of the suit joint and the man's joint motion.

Ideally, the figure of merit would be derived as illustrated in Figure 31.

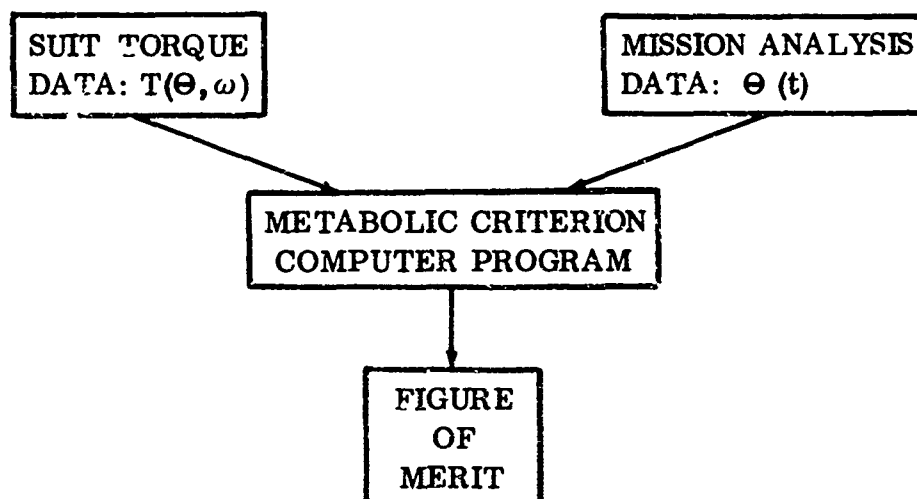


FIGURE 31. DATA FLOW FOR METABOLIC FIGURE OF MERIT

Suit data in the form of torque surfaces for each joint, together with histograms of all the motions required for a mission or task, are entered into a formulation which combines the suit and mission data into a composite description of the total torque-angle-time history for each joint. This composite history is then related mathematically to the metabolism of the associated muscle groups and the total muscle metabolic energy production is computed. One might hope for a relatively simple relationship between the metabolism of a single muscle and the forces and work that it produces. Such, of course, is not the case; however, the

relationships for single muscles, although complex, do appear to be amenable to the calculation of a figure of merit which could be of substantial value for suit studies. The mathematical basis for the approach follows.

To be of value, the metabolic figure of merit must have the following properties:

1. It must be computed from measured mechanical quantities.
2. It must increase with, and preferably be proportional to, metabolic cost.
3. It must be calculable from a general computer program.
4. It must use only joint properties and mission profile data as input variables.
5. It must be independent of the test subject's strength, endurance, and motivation.

There is a considerable body of literature on the heat production in muscles. Of particular note is the work of the physiologists: A. V. Hill, D. R. Wilkie, and W. O. Fenn. This work, both experimental and theoretical, treats the heat production in single muscles due to contraction under electrical stimulation. The muscles most extensively studied are the sartorius muscles of frogs. The variables studied are force, length, velocity, and time. Heat production is measured with a thermopile.

The literature indicates that the rate of metabolic heat production in a particular muscle may be a single-valued function of its length x , its velocity of contraction $v = \dot{x}$, the tension F , and time t . That is, $R = R(x, v, F, t)$ where $R = \frac{dH}{dt}$ and H is the metabolic heat produced in the muscle in contraction. If this is true, then the chain rule for the total differential can be applied.

$$dR = \frac{\partial R}{\partial x}dx + \frac{\partial R}{\partial v}dv + \frac{\partial R}{\partial F}dF + \frac{\partial R}{\partial t}dt \quad (37)$$

In general, the partial derivatives $\frac{\partial R}{\partial x}$, $\frac{\partial R}{\partial v}$, etc. are functions of the four variables which must be determined experimentally. The differentials for any muscle dx , dv , and dF , can be expressed in terms of the differentials of joint angle Θ , angular velocity ω , and the torque T produced by the muscle if the hinge point and points of muscle attachment are known. That is, $x(\Theta)$ must be found from biomechanical and anatomical considerations based on data much of which is available. From these data these quantities could be determined:

$$dx = \frac{dv}{d\Theta} d\Theta$$

$$dv = \frac{\partial v}{\partial \Theta} d\Theta + \frac{\partial v}{\partial \omega} d\omega \quad (38)$$

$$dF = \frac{\partial F}{\partial \Theta} d\Theta + \frac{\partial F}{\partial T} dT$$

The differential of metabolic heat production rate can then be written:

$$dR = \frac{\partial R}{\partial x} \frac{dx}{d\Theta} d\Theta + \frac{\partial R}{\partial v} \left[\frac{\partial v}{\partial \Theta} d\Theta + \frac{\partial v}{\partial \omega} d\omega \right] + \frac{\partial R}{\partial F} \left[\frac{\partial F}{\partial \Theta} d\Theta + \frac{\partial F}{\partial T} dT \right] + \frac{\partial R}{\partial t} dt \quad (39)$$

Or collecting terms,

$$dR = \left[\frac{\partial R}{\partial x} \frac{dx}{d\Theta} + \frac{\partial R}{\partial v} \frac{\partial v}{\partial \Theta} + \frac{\partial R}{\partial F} \frac{\partial F}{\partial \Theta} \right] d\Theta + \frac{\partial R}{\partial v} \frac{\partial v}{\partial \omega} d\omega + \frac{\partial R}{\partial F} \frac{\partial F}{\partial T} dT + \frac{\partial R}{\partial t} dt \quad (40)$$

Since $x(\Theta)$ is known, the partials of R can be written as functions of Θ, ω, T , and t . Then the total differential dR can be written simply:

$$dR = f_1(\Theta, \omega, T, t) d\Theta + f_2(\Theta, \omega, T, t) d\omega + f_3(\Theta, \omega, T, t) dT + f_4(\Theta, \omega, T, t) dt \quad (41)$$

or

$$dR = f_1 d\Theta + f_2 d\omega + f_3 dT + f_4 dt \quad (42)$$

From this, the function $R(\Theta, \omega, T, t)$ could be constructed in analytic or tabular form by integration. This is a mathematical model for the rate of metabolic heat production in a muscle as a function of joint angle, angular velocity, torque produced by the muscle, and time.

Since Θ, ω , and T are measured functions of time, R can be integrated by a computer to yield the net heat production H in the muscle groups controlling the particular joint under consideration.

$$H = \int R[\Theta(t), \omega(t), T(t), t] dt \quad (43)$$

So far, only the heat production in the muscle has been discussed; the desired quantity is the metabolic energy E expended by the muscles in flexing the joint. When a muscle contracts, complex biochemical processes are involved (ref. 83); fortunately, however, these need not be understood to determine the desired energy expenditure. In the most general form, the overall biochemical reactions must appear as follows



In the reaction, the released energy must be the difference in binding (or potential) energies of the reactants and products. This released energy is the metabolic energy expenditure and it can appear in only two forms: heat and mechanical work. Thus:

$$E = \int R dt + \int T d\theta \quad (44)$$

The "metabolic cost" of flexing a joint can therefore be calculated from mechanical measurements by the following steps:

1. Determine experimentally $R_1 (\theta, \omega, T, t)$ for each of the muscle groups involved.
2. Determine analytically and experimentally $R (\theta, \omega, T, t)$ for the joint involved.
3. Formulate an expression and computer program for the figure of merit.
4. Measure the torque, $T_s (\theta, \omega)$, which the suit imposes on the joint.
5. Measure or assume a history of angles, $\theta (t)$, which the subject's joint will experience during a mission.
6. Enter the experimental torque T_s and angle $\theta (t)$ data in the computer program for the figure of merit and integrate.

How feasible is the approach and what are the problems? The possibility of constructing $R_1 (\theta, \omega, T, t)$ from the chain rule depends on the validity of the assumption that $R_1 (x, v, F, t)$ is single valued. From the works of Hill and others, this appears true although the explicit time dependence could cause some difficulty. The partial derivatives of R with respect to x, v, F and t would have to be determined experimentally. Current experimental data (ref. 50) which was obtained for maximal effort contractions will not suffice. The needed submaximal data have proven very difficult to obtain. As suggested by Normann*, several levels of submaximal stimulation can be achieved for muscles with nerve bundles which separate into 2 or 3 roots near the spinal column. This is done by maximal stimulation of the various combinations of roots. The effect of temperature gradients in the muscle tissue presents an as yet unassessed instrumentation problem.

It must be noted that the metabolic cost computed by this method represents by definition the cost due to increased muscular metabolism. When muscle metabolism during exercise increases, other body processes also vary to sustain the

*Normann, N. A., M. D., May, 1965, Personal communication.

additional activity. Cardiac output and tidal volume increase. Blood flow is redistributed to muscles and to the skin surface and some body processes slow down. The overall metabolic cost is, therefore, the sum of the increase in metabolic energy expenditure within the muscles and the increase in metabolic activity of the balance of the system to handle the increased muscle requirements.

There are other points which must also be considered. For instance, there may be extensors as well as flexors acting in a joint flexion, in which case the muscle tension may not be uniquely related to output torque. This problem has been treated by Yves Nubar (ref. 80) on the basis of the "Principle of Least Effort", with some interesting results. Delayed heat production (Hill's after-heat), arm weight, potential energy stored in the stretched tendons, and imperfectly known muscle geometry are also problems; but these are refinements which should not affect the feasibility of the over-all approach.

SUIT TRACKING CRITERIA

As discussed above, the torque vector in a specific suit joint does not necessarily act wholly along the axis of rotation, but may possess components normal to the axis. These normal components can become sufficiently large to prevent the astronaut from performing certain motions. For instance, when the outstretched arm is raised, the hand may follow a skewed path in spite of all efforts to track parallel to the sagittal plane. Even when the normal torque components are relatively low, natural body rhythms are undoubtedly altered and work space time scores will in all probability increase. This effect of torque components normal to the direction of joint rotation axis is called the tracking problem.

The disorienting tracking forces can be partially counteracted by new muscle patterns developed through extensive training. However, since some missions may require more than one type of suit and training is sometimes forgotten in emergency situations, training is not an ideal solution of the tracking problem.

For a mathematical discussion of the problem, first consider the linkage model of a joint in Figure 32. If pins in this joint are close enough together, the system can represent the proximal humerus joint, where Θ_1 represents arm flexion, Θ_2 arm adduction, and Θ_3 arm rotation. The set of angles Θ_1 , Θ_2 and Θ_3 defines a unique position of the joint. Also, say that the torque vector \vec{T} is measured and represented in the x, y, z coordinate system. $\vec{T} = T_x \hat{i} + T_y \hat{j} + T_z \hat{k}$. The desired torque components are those parallel to the three pin joint axes: T_1 , T_2 , and T_3 . The relation between these two sets is

$$\begin{aligned} T_1 &= T_x \sin \Theta_2 + T_z \cos \Theta_2 \\ T_2 &= T_y \\ T_3 &= T_z \end{aligned} \tag{45}$$

or in matrix form

$$\begin{bmatrix} T_1 \\ T_2 \\ T_3 \end{bmatrix} = \begin{bmatrix} \sin \Theta_2 & 0 & \cos \Theta_2 \\ 0 & 1 & 0 \\ 0 & 0 & 1 \end{bmatrix} \begin{bmatrix} T_x \\ T_y \\ T_z \end{bmatrix} \quad (46)$$

It should be noted that although (T_x, T_y, T_z) is a vector, the components T_1, T_2 , and T_3 are not; that is $|\vec{T}| \neq \sqrt{T_1^2 + T_2^2 + T_3^2}$

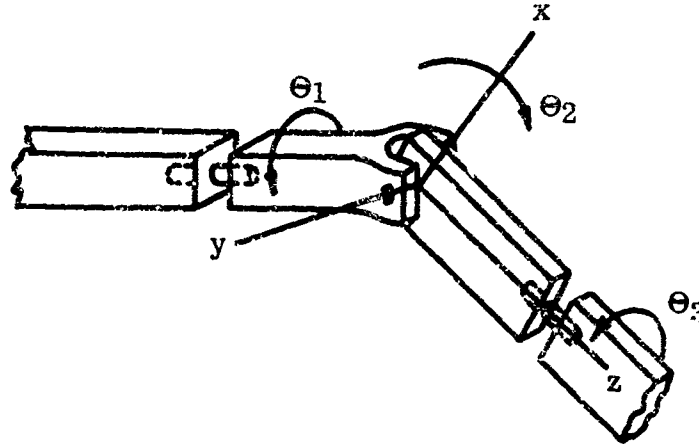


FIGURE 32. JOINT MODEL FOR DISCUSSION OF TRACKING PROBLEM

If, in a particular suit, the torque components about the three joints are independent of the other joint angles; that is, if the joint always moves in the direction it is pushed, then there is no problem with tracking. Mathematically, the torque would be expressed as $dT_1 = k_1(\Theta_1) d\Theta_1$, where k_1 is constant if the joint is linear. Unfortunately, many joints do not have this property; in some positions they tend to track on different axes from the desired axis of motion; i.e., they do not move in the direction in which they are pushed. For a single-valued function $T_1 = T_1(\Theta_1, \Theta_2, \Theta_3)$, the total differential can be written

$$dT_1 = \frac{\partial T_1}{\partial \Theta_1} d\Theta_1 + \frac{\partial T_1}{\partial \Theta_2} d\Theta_2 + \frac{\partial T_1}{\partial \Theta_3} d\Theta_3 \quad (47)$$

$$dT_1 = \sum_{j=1}^3 f_{1j} d\Theta_j \quad (48)$$

If any of the f_{1j} 's with $i \neq j$ are nonzero, then a tracking problem exists. In

matrix form, Equation 48 is written

$$\begin{bmatrix} dT_1 \\ dT_2 \\ dT_3 \end{bmatrix} = \begin{bmatrix} f_{11} & f_{12} & f_{13} \\ f_{21} & f_{22} & f_{23} \\ f_{31} & f_{32} & f_{33} \end{bmatrix} \begin{bmatrix} d\theta_1 \\ d\theta_2 \\ d\theta_3 \end{bmatrix} \quad (49)$$

In this form it can be seen that the problem lies in the off-diagonal terms. It should be noted that this effect can exist even where the man has single degree of freedom joints such as the elbow. $[d\theta_1 = d\theta_3 = 0 \text{ implies } d\vec{T} = (f_{12} \hat{i} + f_{22} \hat{j} + f_{32} \hat{k}) d\theta_2]$. An example of this is wind-up of the forearm during elbow flexion.

As pointed out earlier, if not too severe, the tracking problem can be overcome partially by many hours of practice in training suits. Man is highly adaptive, and can even learn to switch his method of coordination easily from the pressurized to the unpressurized condition. Nevertheless, the off-diagonal terms are undesirable because with them, the man will never fully regain his unencumbered level of coordination, and because of the potential for error during emergency situations.

To date, no known measurements have been made to quantify the effect. Quantification requires the measurement of the torque vector at each suit joint. However, even if suit data were available, there are few known physiological data which could serve as the basis of a criterion.

What are needed are the results of work space performance tests for subjects whose performances have been degraded by the addition of increasingly large torques normal to the direction of motion. That is, a laboratory simulation of the tracking problem evaluated on test devices such as the AMRL Workspace Apparatus (ref. 102). Once such data were available, the average degradation in performance scores could be used as the basic criterion by relating actual measured suit-tracking torques to these scores.

An Ideal Measurement Technique For Torque And Angle

Before investigating practical methods for suit torque and angle measurement, it is advantageous to establish an ideal methodology against which to judge any proposed techniques. Theoretically, the torque imposed on the man by the suit can be calculated from the operational definition (Equation 12) which says that the torque for any suit joint is the cross product of a position vector and the mechanical pressure integrated over the skin surface from the joint to the end of the limb. This definition then forms the basis for an exact measurement system. Skin-mounted, unencumbering, mechanical pressure transducers between the man and the suit would measure the instantaneous mechanical pressure distribution over the entire skin surface. The transducer outputs and their skin surface locations would be continuously entered into a computer to calculate and plot the

magnitude and direction of the torque imposed by the suit. This technique, although impractical, is an exact measure of man's torque output and, in the absence of external torques, is exactly equal to the suit torque about the man's joint center. Since the pressure transducers support the entire load, the man acts as a prime mover only -- he cannot influence the measurement.

Simultaneously, the ideal measurement system would provide a continuous readout of instantaneous body interlink angles against which to relate the torque values. The computer again would provide continuous plots of joint angles, velocities, and accelerations with which torque surface, tracking, and metabolic figures of merit could be calculated for the joint being investigated.

Having defined an ideal measurement system, a frame of reference is available for the assessment of the practical techniques which are discussed in the following sections.

Torque Measurement Techniques Investigation

The measurements of suit torques and body angles are both difficult problems. They are closely inter-related and must be studied together. The ultimate goal is the expression of suit torques as functions of the independent variables, the body angles, and angular velocities. In this section, torque is discussed first because, as will be shown, the solution to the torque measurement problem dictates an operational definition for the body angles.

TORQUE MEASUREMENT CONCEPTS

The study of torque measurement techniques requires first a listing of all the reasonable techniques that could be utilized. These techniques are conveniently thought of in the four categories illustrated in Figure 33. Each of these techniques was systematically investigated to find: (1) what data to take and how to handle it to determine the desired torque information, (2) how accurate the torque determination will be and how closely it approaches the ideal measurement scheme, (3) how convenient and practical the technique will be when developed, (4) what errors are involved, and (5) what it might cost. The investigation of a technique ceased when it was clearly inadequate or inferior to another.

COMPARISON OF A SUBJECT'S NUDE AND SUITED OUTPUT TORQUES -- In this method, which falls into concept D in Figure 33, the subject is asked to exert a torque on an external measuring device while unsuited and while suited. Since he is to provide the same amount of torque each time, he is asked to exert maximum torque because submaximal efforts are not repeatable. The net torque for various practiced motions are measured nude and suited and the pairs of values subtracted. The differences are considered to be the suit torques.

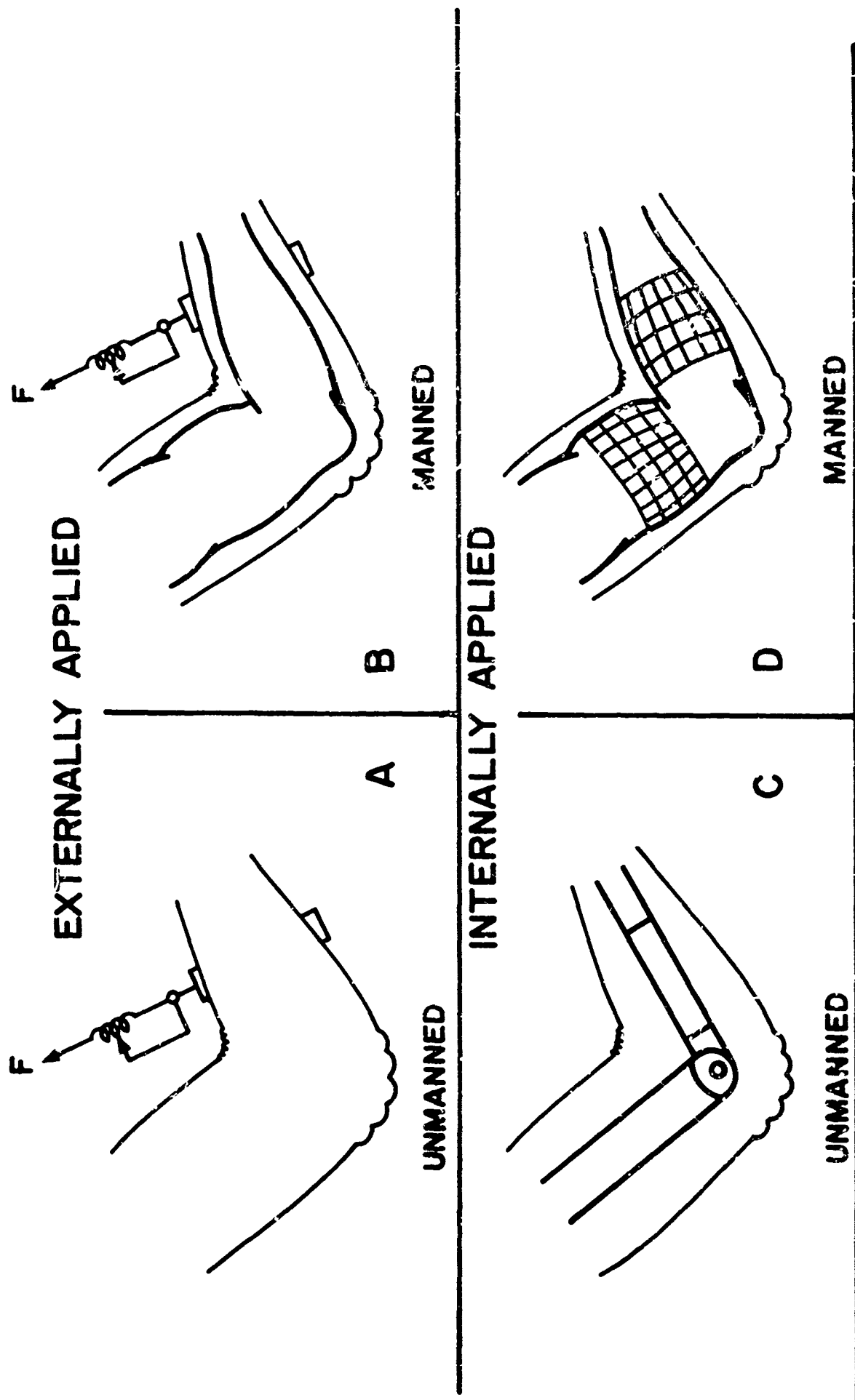


FIGURE 33. TORQUE MEASUREMENT CONCEPTS

This approach has some obvious drawbacks. One is that the percent error in suit torque will be quite large for low values of suit torque. The off-axis components of the torque vector are very difficult to measure with this technique. Subject fatigue and motivation are also serious problems.

Despite these shortcomings, the technique is inexpensive and simple. Because of this it has been used to good advantage by B. F. Pierce (refs. 85, 86) in the evaluation of soft suits.

MEASUREMENT OF THE EXTERNAL TORQUE REQUIRED TO DEFLECT THE SUIT WITH A LIMP SUBJECT -- In this method (concept B in Figure 33), the torque which deflects the suit joint is applied and measured externally. The test subject simply provides the bulk and joints to make the suit bend approximately the same way it does when he supplies the torque. That the test subject is essential is illustrated in Figure 34 by experimental curves from a soft suit test.

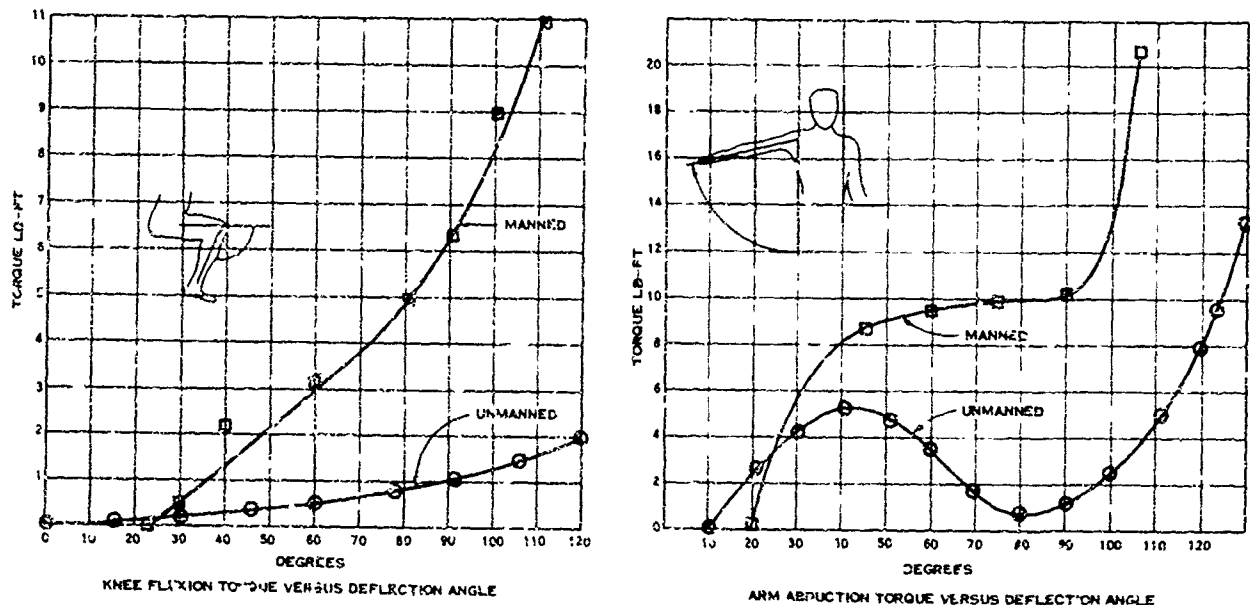


FIGURE 34. MANNED AND UNMANNED SUIT TORQUES

The large discrepancies between the curves for the manned and unmanned joints are due to the presence of the man's links which force the suit joints to assume different volume-angle and strain-angle relationships. Thus concept A is of no value.

The external torque is applied through the force of a spring scale or similar device perpendicular to the limb at a known distance from the joint center. The externally applied torque is the product of this force and distance. This is equal to the suit torque if the joints of the man and suit coincide, if the man applies no torque through muscle tension or weight, and if the load applied at a single external point produces the same suit torque as the man's distributed load would have produced. This technique, with a suitable restraint system, might be used

to measure more than one component of torque at a joint, but probably not all three components. Dynamic measurements are not practical with this technique and the error is high. However, subject fatigue and motivation are no problem.

This technique has been used successfully for testing of the Apollo, Gemini, Goodrich, and other suits. Since the error is probably less than in the difference measurements first discussed, and because the technique is simple and fast, it is recommended as an interim approach until a more sophisticated methodology can be developed. The technique is being standardized and a report should be published within the year (ref. 89).

The "torque box" at AMRL similarly applies and measures torque externally, but it can only be used for development joints because of the pressure seal requirements between the box and the suit.

FORCE TRANSDUCERS BETWEEN THE MAN AND THE SUIT -- In this technique, which also falls under concept D, the suit is totally supported by force transducers at known locations and orientations on the man's skin surface. The transducers would in effect measure the mechanical pressure distribution on the skin surface. The torque would be calculated by summing the torques due to the forces on all of the transducers. To do this, the location and orientation of each transducer with respect to the body joint must be known. If the i th transducer is located at \vec{R}_i (in the link coordinate system) and the force on it is $\vec{F}_i = F_i (\hat{i} \cos \alpha_i + \hat{j} \cos \beta_i + \hat{k} \cos \gamma_i)$ where F_i is the magnitude of the force and α_i , β_i , and γ_i are the direction angles which describe the orientation of the sensing axis of the transducer, then the torque due to the forces on the transducers is

$$\vec{T} = \sum_i \vec{R}_i \times \vec{F}_i \quad (50)$$

The practical calculation of torque from transducer outputs and known geometry is discussed in detail in Appendix IV.

This technique closely approaches the ideal measurement technique described on page 63. By recording the outputs of the transducers as a function of time, a complete description of the time varying torque vector as a function of body angle could be obtained. Aside from the error, the only conceptual problem is the bulk of the transducers which might change the actual values of the suit torques by changing the suit fit.

The error, however, makes this approach hopeless. The sources of error are: (1) transducer errors, (2) an inexact knowledge of the locations and orientations of the transducers due to the compliance of the body surface, and (3) spatial uncertainty of the center of force on each transducer. Because of these errors, the technique has been eliminated. The instrument error and error due to the finite size of each transducer have been treated analytically. This problem was studied in detail and is discussed on page 74. The error calculations are performed in Appendix V.

TRANSDUCERS ON AN ARTICULATED DUMMY -- In this technique, concept C in Figure 33, the suit to be evaluated is worn by a powered, articulated dummy instrumented to measure the suit torque. A detailed study of the various concepts for suit torque transduction and dummy operational problems is presented in the following sections. It will be shown that for accurate and objective dynamic measurements of the torque vector at each joint as a function of angle and angular velocity, one is lead inevitably to the use of a dummy which can perform human-like motions on command. This realization is reached reluctantly because the fabrication of such a dummy is a formidable task. Since the Illinois Institute of Technology Research Institute under NASA contract has demonstrated the feasibility of fabricating such a dummy, this report will consider only the instrumentation and control problems.

A Torque Instrumented Dummy

CONCEPTS FOR TORQUE MEASUREMENT USING DUMMIES

There are several different methods of measuring and calculating suit torque with a dummy. These concepts will be discussed in this section and some will be eliminated on the conceptual level. The hardware implementation of the remaining concepts is discussed later. First, however, it is necessary to define the basic dummy mechanism being considered.

DESCRIPTION OF THE ARTICULATED DUMMY -- In concept, the dummy is similar to the present powered articulated dummy being fabricated for NASA by the Illinois Institute of Technology. The anthropomorphic dummy consists of rigid metal links joined by pin joints each of which is hydraulically actuated, the hydraulic power being supplied through a servovalve from a central hydraulic power supply. Each joint of the dummy has a feedback potentiometer connected through control electronics to provide positional accuracy. The hydraulic servovalves which control the position of each of the individual links of the dummy system are contained within the chest cavity. It is further assumed that there are sufficient numbers of links and rotary actuators to provide all the basic human motions of the extremities except for prehension. In the upper extremity these would include:

- | | |
|-----------------------|----------------------|
| 1. Shoulder elevation | 6. Forearm flexion |
| 2. Shoulder flexion | 7. Forearm pronation |
| 3. Arm flexion | 8. Wrist flexion |
| 4. Arm abduction | 9. Wrist abduction |
| 5. Arm rotation | |

Any motion or combination of motions can be achieved by supplying command voltages from a magnetic program tape to the appropriate servovalves which in turn operate the rotary actuators at the specific joints. Potentiometers feeding back a control voltage maintain a stable, high response system.

To be of value, the measurement system on the dummy must provide data to determine the following quantities

1. The torque vector at each joint
2. Angles of all the joints
3. Angular velocity of the test joint

The vectors are to be measured as functions of joint angle Θ for each of several angular velocities ω_1 . In the measurement of $\vec{T}_{\text{suit}}(\Theta, \omega_1)$, the other suit joint angles must be fully specified. Several basic torque measurement concepts might satisfy these requirements. These concepts are as follows.

1. Actuation Torque Transduction -- Measure the torque required to actuate the dummy.
2. Shell Torque Transduction -- Measure the torques on shells surrounding the central spars of each dummy limb.
3. Distributed Force Transduction -- Measure the force at a very large number of locations over the entire skin surface. Multiply these forces by their perpendicular distances from the joint center and sum.
4. Similar to 3, but reduce the number of force measurements by having several circular rings stacked up along each spar axis.
5. Shell Force Transduction -- Measure the forces imposed on a shell surrounding the central spar.

Each of these five concepts is now considered in turn.

ACTUATION TORQUE TRANSDUCTION -- Consider the use of strain gages to measure the torque reacted against the central shaft of one of the dummy links. When the dummy is suited, this torque, \vec{T}_{suited} , is not only the torque due to the suit loading but includes the torque due to the weight and inertia of the dummy link itself. This is, of course, not the desired torque; however, it could be used to find the desired torque \vec{T}_{suit} by either of two methods. In the first of these methods, the dummy torque is measured when the dummy is suited and pressurized and then measured again nude. Then $\vec{T}_{\text{suit}} = \vec{T}_{\text{suited}} - \vec{T}_{\text{nude}}$, measured. (Since $\vec{T}_{\text{nude}} \approx \vec{T}_{\text{unpressurized}}$ in a soft suit, it may at times be desirable to compare the two suited measurements.)

The other approach is to calculate the nude dummy torque from known dummy dynamics. Then, $\vec{T}_{\text{suit}} = \vec{T}_{\text{suited}} - \vec{T}_{\text{nude, calculated}}$. In both cases, \vec{T}_{suited} is measured by programming the dummy to move at different constant angular velocities ω_1 and measuring the resulting $\vec{T}_{\text{suited}}(\Theta, \omega_1)$. If the dummy has enough torque output to maintain the required constant velocity exactly despite suit loading, then $\vec{T}_{\text{nude}}(\Theta, \omega_1)$ can be calibrated for each joint and it need not be measured for each run. However, because of design limitations and safety considerations, the torque capability of the dummy probably will not exceed that of a strong man and in some cases may not be as large. Consequently, the dummy will not always be able to maintain the commanded constant ω_1 's because of high suit torque and therefore \vec{T}_{nude} must be determined separately for each run from actual angle versus time data recorded during the suited test run. \vec{T}_{nude} , measured would be found by using the actual angle to program the dummy motion for the nude torque measurement.

$\vec{T}_{\text{nude, calculated}}$ would be calculated from the actual values of $\Theta(t)$, $\dot{\Theta}(t)$, and $\ddot{\Theta}(t)$ and the dynamic equations for the dummy. The complex dynamic equations involve the inertia, weight, and friction of each joint and require not only Θ , $\dot{\Theta}$, and $\ddot{\Theta}$ for each joint but also sufficient information to define the local vertical.

The inertia and weight terms for any given joint will vary as functions of positions of the link attached to the joint and all the distal links. The inertial torque, \vec{T}_I , is equal to the time rate of change of angular momentum \vec{L} , and for the general case must be calculated from the measured angular accelerations and the inertia tensor for the dummy links.

The dummy weight torque is the cross product of the vector to the center of gravity \vec{R}_{cg1} and weight vector $m_1 \vec{g}$ where m is the mass of the dummy links outboard of the i th joint.

$$\vec{T}_{w1} = \vec{R}_{cg1} \times (m_1 \vec{g}) \quad (51)$$

\vec{R}_{cg1} is calculated from the interlink angles outboard of Θ_1 . m_1 is constant. The angle of the vertical must be determined in at least one of the links, probably the central torso section. Then \vec{g} can be calculated knowing the angles of the joints inboard of the i th joint.

Naturally, if the actuator has sufficient torque to drive the joint at constant velocity, $\vec{T}_I = 0$; however, \vec{T}_{w1} must always be considered.

Thus, with dummy torque transducers, the main conceptual problem seems to lie in the determination of the torque, \vec{T}_{nude} . Either an extra run must be made to measure \vec{T}_{nude} or it must be calculated by a fairly involved computer program which requires transduction of all interlink angles from the vertical sensor through the i th joint and out to the distal link. Any advantages in using the

calculation procedure seem to be outweighed by the complexity of the approach; therefore, the measurement technique for \vec{T}_{nude} is recommended.

The tare torque $\vec{T}_w + \vec{T}_I$ will cause a serious measurement error if it is much larger than the suit torque because of the subtraction operation in

$$\vec{T}_{suit} = \vec{T}_{suited} - \vec{T}_{nude} \quad (52)$$

For instance, if the absolute error in the x component of \vec{T}_{suit} is $\Delta T_{x suit}$, then from the methods of random error analysis

$$\Delta T_{x suit} = \sqrt{(\Delta T_{x suited})^2 + (\Delta T_{x nude})^2} \quad (53)$$

Since the two measurements, \vec{T}_{suited} and \vec{T}_{nude} , are made at the same dummy positions with the same measuring devices, the absolute errors for both measurements are nearly equal, i.e., $\Delta T_{x suited} \approx \Delta T_{x nude}$. Thus,

$$\Delta T_{x suit} = \sqrt{2} \cdot \Delta T_{x nude} \quad (54)$$

Dividing by the suit torque to find the relative error,

$$\frac{\Delta T_{x suit}}{T_{x suit}} = \sqrt{2} \cdot \frac{\Delta T_{x nude}}{T_{x suit}} = \sqrt{2} \frac{T_{x nude}}{T_{x suit}} \cdot \frac{\Delta T_{x nude}}{T_{x nude}} \quad (55)$$

Thus, although dummy torque can be measured to about one percent accuracy, ($\frac{\Delta T_{x nude}}{T_{x nude}} < 0.01$), the fractional error in the suit torque $\frac{\Delta T_{x suit}}{T_{x suit}}$ grows indefinitely as $T_{x suit}$ becomes small with respect to $T_{x nude}$.

SHELL TORQUE TRANSDUCTION -- A reduction in tare torque or \vec{T}_{nude} in the above equations could eliminate or greatly reduce the error. Tare weight and inertia could be reduced by fabricating lightweight load carrying shells over the heavy dummy links and actuators. The shells could be instrumented to measure torques and, if sufficiently light, their inertias and weights could be neglected. Unfortunately, this technique is conceptually invalid because the desired torques cannot be calculated from the transduced torques. To show this, consider the model for the upper arm and forearm shown in Figure 35. The transduced torques are $\vec{T}_1 = \rho_1 \times \vec{F}_1$ and $\vec{T}_2 = \rho_2 \times \vec{F}_2$, which are the torques at joints 1 and 2 due to the forces \vec{F}_1 and \vec{F}_2 acting at ρ_1 and ρ_2 respectively. The desired torque is \vec{T}_{0a} , the total torque at joint 1 due to \vec{F}_1 and \vec{F}_2 . $\vec{T}_0 = \vec{T}_1 + (\vec{R} + \vec{\rho}) \times \vec{F}_2 = \vec{T}_1 + \vec{R} \times \vec{F}_2 + \vec{\rho} \times \vec{F}_2$ or $\vec{T}_0 = \vec{T}_1 + \vec{T}_2 + \vec{R} \times \vec{F}_2$, which shows that to find the torque at joint 1 due to \vec{F}_2 , transduction of \vec{T}_2 alone is not adequate. \vec{F}_2 must also be transduced.

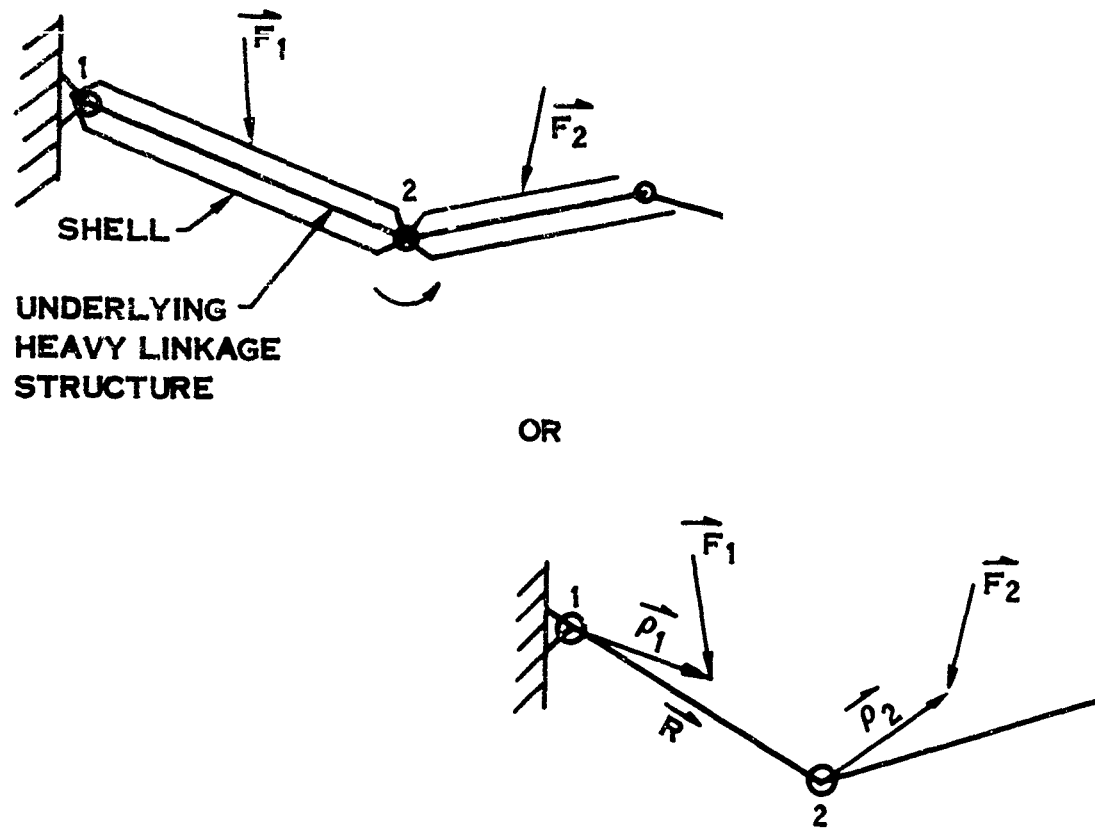


FIGURE 35. MODEL FOR SHELL TORQUE TRANSDUCTION

DISTRIBUTED FORCE TRANSDUCTION -- Since force transducers alone are sufficient to define total torque in a multi-joint system, then torque need not be transduced at all. Consider the dummy covered with force transducers at known locations and orientations which support the entire suit load. The torque about any joint can be calculated by summing the contributions of the forces on all transducers. The general equations for this calculation are derived in Appendix IV. A two link special case is presented in Figure 36 for discussion purposes.

The dummy surface has N_1 transducers on the humerus link and N_2 on the forearm link. The z_2 axis, which is parallel to the z_1 axis, is the elbow axis of rotation. The elbow angle Θ is the angle between the x_1 and x_2 axes. Then

$$\begin{aligned}\vec{T}_{O1} &= \sum_{i=1}^{N_1} \vec{\rho}_{1i} \times \vec{F}_{1i} = \text{torque at } O_1 \text{ due to forces on link 1} \\ \vec{T}_{O2} &= \sum_{i=1}^{N_2} \vec{\rho}_{2i} \times \vec{F}_{2i} = \text{torque at } O_2 \text{ due to forces on link 2}\end{aligned}\tag{56}$$

$$\vec{X}_{12} = x_{12} \hat{i}_1 \text{ vector from } O_1 \text{ to } O_2 \quad (57)$$

\vec{T}_0 = torque at O_1 due to all forces on links 1 and 2

$$\begin{aligned} \vec{T}_0 &= \sum_{i=1}^{N_1} \vec{\rho}_{1i} \times \vec{F}_{1i} + \sum_{i=1}^{N_2} (\vec{X}_{12} + \vec{\rho}_{2i}) \times \vec{F}_{2i} \\ &= \vec{T}_{01} + \vec{T}_{02} + \vec{X}_{12} \times \sum_{i=1}^{N_2} \vec{F}_{2i} \\ \vec{T}_0 &= \vec{T}_{01} + \vec{T}_{02} + \vec{X}_{12} \times \vec{F}_2 \end{aligned} \quad (58)$$

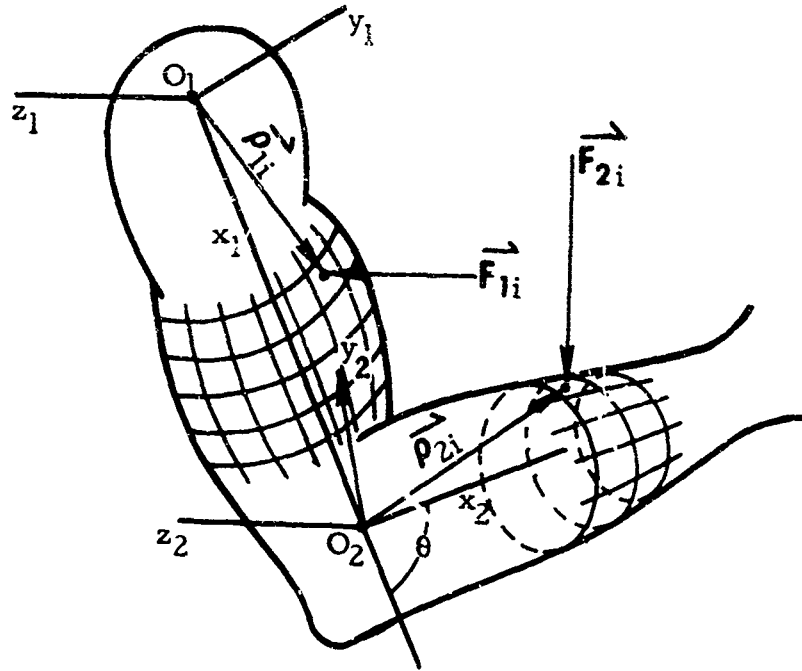


FIGURE 36. MODEL FOR DISTRIBUTED FORCE TRANSDUCTION

\vec{F}_2 is the total force on link 2, but since \vec{F}_{2i} and $\vec{\rho}_{2i}$ are measured in the coordinate system of link 2 they must be transformed so that the addition and crossing operations can be performed. Vectors represented in link 2 are transformed to their representation in link 1 by the rotation operator $D(\Theta)$ which in matrix form is

$$D(\Theta) = \begin{bmatrix} \cos \Theta & -\sin \Theta & 0 \\ \sin \Theta & \cos \Theta & 0 \\ 0 & 0 & 1 \end{bmatrix} = \begin{bmatrix} d_{11} & d_{12} & d_{13} \\ d_{21} & d_{22} & d_{23} \\ d_{31} & d_{32} & d_{33} \end{bmatrix} \quad (59)$$

Then

$$\vec{T}_0 = \vec{T}_{01} + D(\Theta) \vec{T}_{02} + \vec{X}_{12} \times [D(\Theta) \vec{F}_2] \quad (60)$$

The terms on the right would be calculated from transduced quantities as follows

$$\vec{X}_{12} \times [D(\Theta) \vec{F}_2] = X_{12} \sum_{p,m,n=1}^3 \sum_{i=1}^{N_2} \hat{i}_{1p} \epsilon_{p1m} b_{2in} d_{mn}(\Theta) F_{2i} \quad (61)$$

$$\vec{T}_{01} = \sum_{p=1}^3 \sum_{i=1}^{N_1} \hat{i}_{1p} A_{1ip} F_{1i} \quad (62)$$

$$\vec{T}_{02} = \sum_{p,n=1}^3 \sum_{i=1}^{N_2} \hat{i}_{1p} A_{2in} d_{pn}(\Theta) F_{2i} \quad (63)$$

Or, after collecting terms,

$$\vec{T}_1 = \sum_{p=1}^3 \hat{i}_{1p} \left[\sum_{i=1}^{N_1} A_{1ip} F_{1i} + \sum_{i=1}^{N_2} \left(\sum_{n=1}^3 A_{2in} d_{pn}(\Theta) + X_{12} \sum_{m,n=1}^3 \epsilon_{p1m} b_{2in} d_{mn}(\Theta) \right) F_{2i} \right] \quad (64)$$

Where \hat{i}_{1p} are the unit basis vectors in link 1, A_{1ip} , A_{2in} , b_{2in} are calibration constants, ϵ_{p1m} is defined on page 347, and F_{1i} and F_{2i} are the transducer read-outs. Thus the suit torque can be expressed in terms of calibration constants and transduced quantities only.

A detailed error analysis was performed for this method of torque transduction and is presented in Appendix V. The transducer arrangement and total number of transducers selected (60) were optimized to yield minimal error. Nevertheless, it was found that for a single link torque measurement with 5% accuracy, force transducers with an absolute accuracy of 0.05 pounds are required. Since any transducer may be subjected to peak loads as high as 50 pounds, the percentage accuracy of each transducer must be better than 0.1%. For a multi-link system the error with 0.1% transducers would be much greater. Considering the operational complexity and the almost impossible transducer requirements, this technique is considered impractical at this time.

RING FORCE TRANSDUCTION -- The previous error analysis shows that the large number of transducers is the main source of inaccuracy. A reduction in the number of transducers is therefore essential if the technique is to be practical. Consider the use of approximately ten adjacent rings around a typical dummy link to support the suit load. Each ring is supported by two orthogonal force transducers. In cross section the dummy arm would appear as in Figure 37.

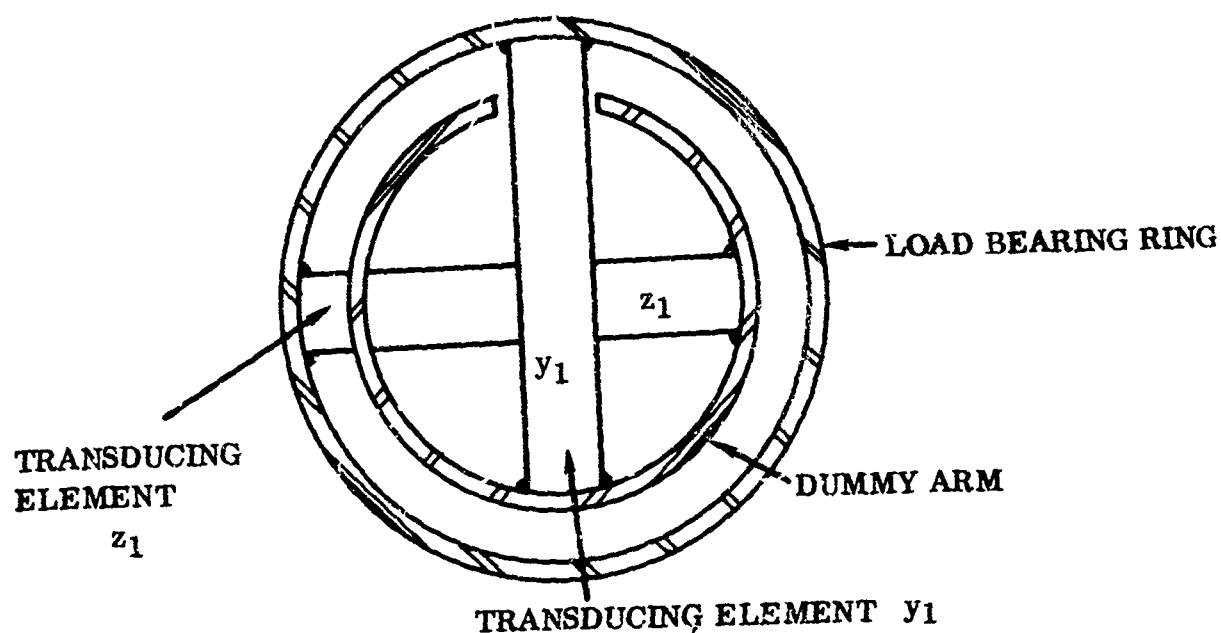


FIGURE 37. SECTION OF DUMMY LINK WITH RING TRANSDUCER

For 5% torque measurement on a single link using the previous analysis procedures, 0.5% force transducers are required. This is possible but is still a difficult transduction requirement.

SHELL FORCE TRANSDUCTION -- A further reduction in the number of force transducers can be achieved by surrounding each of the links with a load supporting shell as was previously considered; however, in this case, the shell is supported by force transducers rather than torque transducers. The model in Figure 38 was considered for analysis of the problem. The linkage is similar to the NASA-IIT dummy forearm and hand. Θ_8 is the wrist pronation-supination angle and Θ_9 is the wrist flexion-extension angle. The F's are the transducer readouts. There are no transducers on link 8 because the shell from link 7 is cantilevered to the wrist. For simplicity, assume $x_{71} = x_{73}$, $x_{72} = x_{74}$, $x_{91} = x_{93}$, and $x_{92} = x_{94}$.

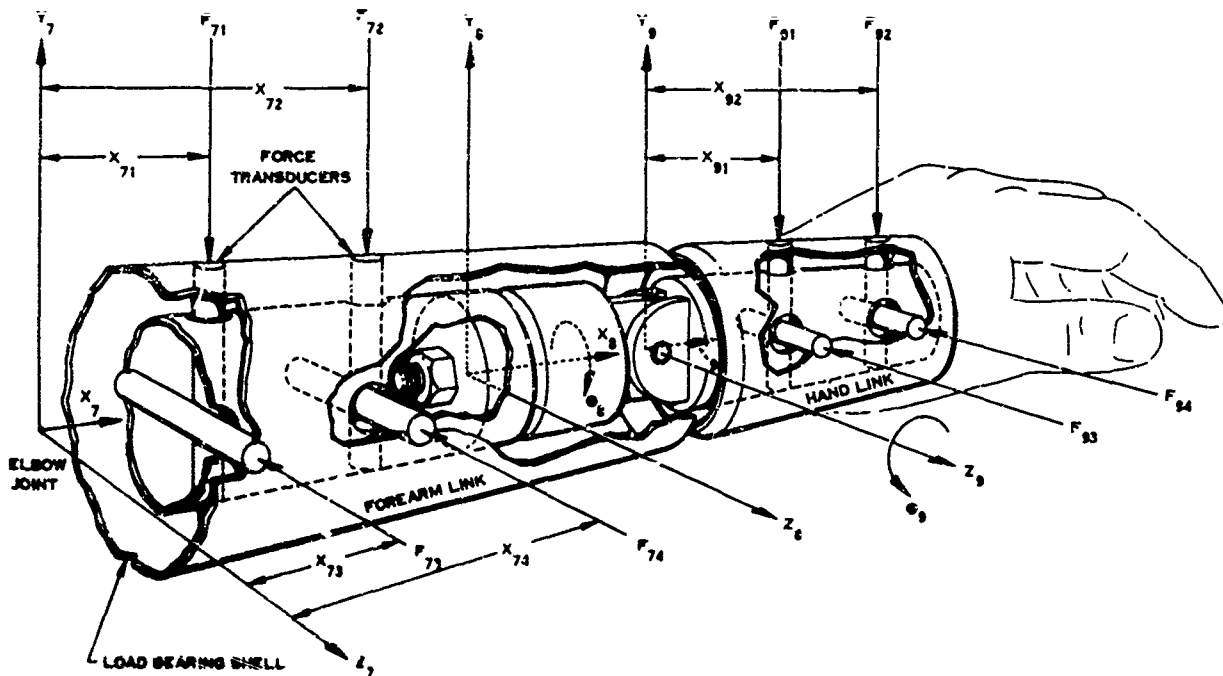


FIGURE 38. DUMMY LINKAGE WITH SHELL FORCE TRANSDUCTION

The z component of the elbow torque is:

$$T_{7z} = -x_{71} F_{71} - x_{72} F_{72} - (X_{70} C_{10} + x_{91}) C_8 F_{91} - (X_{79} C_9 + x_{92}) C_8 F_{92} \\ + (X_{70} + C_{10} x_{91}) S_8 F_{93} + (X_{79} + C_9 x_{92}) S_8 F_{94} \quad (65)$$

where

$$S_8 = \sin \theta_8, C_8 = \cos \theta_8, \text{ etc.} \quad (66)$$

The expression for error in this quantity (ΔT_{7z}) is written as follows if all the x's are uncertain by Δx and all the F's by ΔF .

$$(\Delta T_{7z})^2 = \left[F_{71}^2 + F_{72}^2 + 2(F_{91}^2 + F_{92}^2 + F_{91} F_{92}) \right] (\Delta x)^2 + \\ + \left[x_{71}^2 + x_{72}^2 + x_{91}^2 + x_{92}^2 + 2X_{79}(x_{91} + x_{92} + X_{78}) \right] (\Delta F)^2 + \\ + \left[(X_{79} + x_{91}) F_{93} + (X_{79} + x_{92}) (F_{94}) \right]^2 (\Delta \theta_8)^2 \quad (67)$$

For the derivation of Equation 67 and general expression see Appendix VI. Some typical values for the F's and x's were calculated and used as weighting factors in this expression. The errors used were $\Delta x = 0.002''$, $\frac{\Delta F}{F} = 2\%$, and $\Delta \theta_8 = 0.01$

radians. For these values $\frac{\Delta T_z}{T_z} = 1.5\%$, neglecting the weight of the shells. Thus, by reducing the number of transducers, the error has been significantly reduced.

SUMMARY OF DUMMY TORQUE TRANSDUCTION CONCEPTS -- Of the several techniques considered, three have been eliminated at the conceptual level by theoretical and practical considerations. Only the following techniques appear practical.

1. Measure dummy actuation torques and calculate $\vec{T}_{\text{suit}} = \vec{T}_{\text{suited}} - \vec{T}_{\text{nude}}$.
2. Suit load bearing shells over the dummy limbs supported by force transducers.

The hardware implementation of these two techniques is discussed in the following section.

HARDWARE IMPLEMENTATION FOR SUIT TORQUE MEASUREMENT

The test methodology for the determination of suit torque must ultimately employ a powered articulated dummy with the capability of preprogrammed motions and for accurate measurement of these motions and resultant torques. The goal is to develop a dummy which is not a robot, but a complex instrumentation system. All design decisions must not compromise this goal. The feasibility of this approach has been demonstrated by the dummy developed by the Illinois Institute of Technology under NASA contract, and it was shown above how the dummy would be integrated into an overall test methodology. The basic design requirements for the dummy are as follows

1. The dummy must be anthropomorphic with tissue simulating material over the limb and torso surfaces. It should have limited adjustability within some size range, say medium regular. Test suits would be tailored to fit the dimensions of the dummy which thus would serve as a reproducible standard.
2. The dummy must produce human-like motions through a system of powered actuators, linkages, and pin joints. The dummy should produce the basic human motions with the exception of finger, neck, and toe motion; there is no reason for the dummy to have a head.
3. The dummy should be capable of motions at velocities up to about 50% of the maximum human limb velocities and should be able to accelerate to these velocities at near human acceleration rates. Within this frequency domain, the basic dummy system must be stable without overshoot or significant random noise.

4. The output torque capability of the dummy actuators should be equal to or somewhat greater than the equivalent torque capability of an average astronaut. The final selection of the type of actuator; hydraulic, pneumatic, or electrical, depends upon many design considerations and is not important to the instrumentation system provided the actuators produce sufficient torque and meet the system requirements for dynamic stability.
5. The motions of the dummy must be programmable from an analog tape input and provision must be made for readout of the instantaneous limb position from angular feedback transducers.
6. The dummy must, of course, be compatible with suit testing; that is, the suit must don easily, the operating temperature must be moderate, and the dummy should not contaminate the suit with oil or other materials.
7. A torque measurement system is required to measure the three components of the torque vector at each joint with an accuracy of approximately 2 percent of full scale.

As discussed earlier, the measurement of torques within the dummy is a particularly difficult problem which can best be approached by either measuring dummy actuation torques or by measuring the forces upon shells which support the suit limbs.

ACTUATION TORQUE -- To meet the requirements for system dynamic performance, it is important that each limb of the dummy be non-resonant within the operating frequency domain. To accomplish this with simultaneous measurement of the torque levels produced by the limb, it is important that the torque measuring technique selected result in a maximum limb angular stiffness.

In instrumentation problems of this type, strain gages almost invariably provide the simplest and most direct solution, and in the following discussion, only strain gage techniques will be treated. During the design study which would normally precede dummy development, various other techniques for torque measurement should be considered although their eventual selection in preference to the strain gage is unlikely. There has been a broad experience in strain gage transduction techniques throughout the aerospace industry over the last twenty years; in particular, wind tunnel balances and rocket stand thrust measurements have brought this measurement technology to a high state of development. Through the careful application of this technology, a suitable strain gage based transduction technique for the measurement of the three components of the dummy torque vector can be achieved.

Consider the problem of the measurement of these three torque components for a single limb like the elbow. The problem has many similarities to the problems faced in wind and water tunnel measurements in which the direction of the applied loads on an aerodynamic or hydrodynamic model are of interest. In the most general case, these components are the lift, drag, and side components of thrust and the roll, pitch, and yaw moments. One technique used for the measurement of several of these components is the simple bar analyzer shown in Figure 39. (refs. 2, 92)

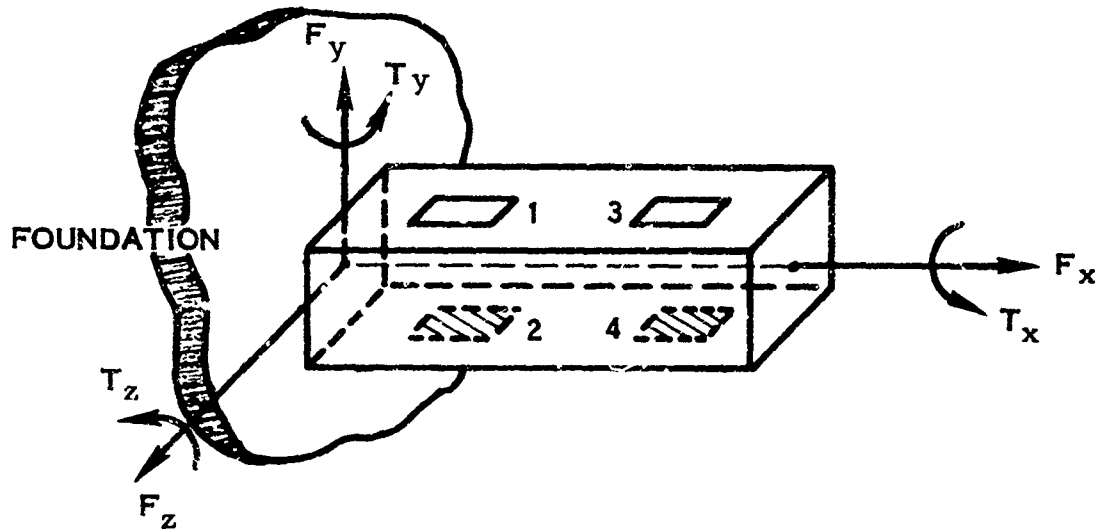


FIGURE 39. BAR ANALYZER

The bar analyzer is essentially a cantilever beam firmly fastened to some foundation; in this case, the elbow joint. Using strain gages on this simple cantilever, the shearing forces F_y and F_z and bending moments T_y and T_z on the bar can be found. If strain gages are installed at positions 1, 2, 3, and 4 as shown, it can be shown that T_z will be proportional to the output of the summing Wheatstone bridge in Figure 40.

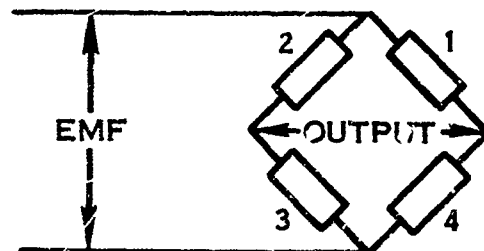


FIGURE 40. BRIDGE FOR TORQUE MEASUREMENT WITH BAR ANALYZER

It can also be shown that the output from these strain gages is independent of the load lever arm and proportional only to the force F_y when the difference circuit in Figure 41 is used.

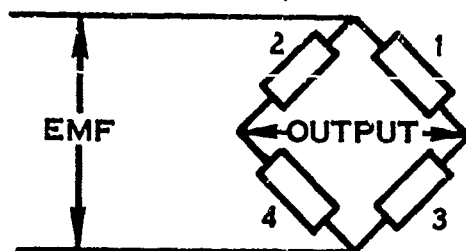


FIGURE 41. BRIDGE FOR FORCE MEASUREMENT
WITH BAR ANALYZER

In similar fashion, if strain gages are bonded to the adjacent faces of this beam, their summing and differential bridge outputs are proportional to the moment T_y and the force F_z , respectively.

In practice, the bar is notched at the gage locations to increase the stresses locally and thereby increase the sensitivity of the strain gages to load. The beam then takes the shape shown in Figure 42.

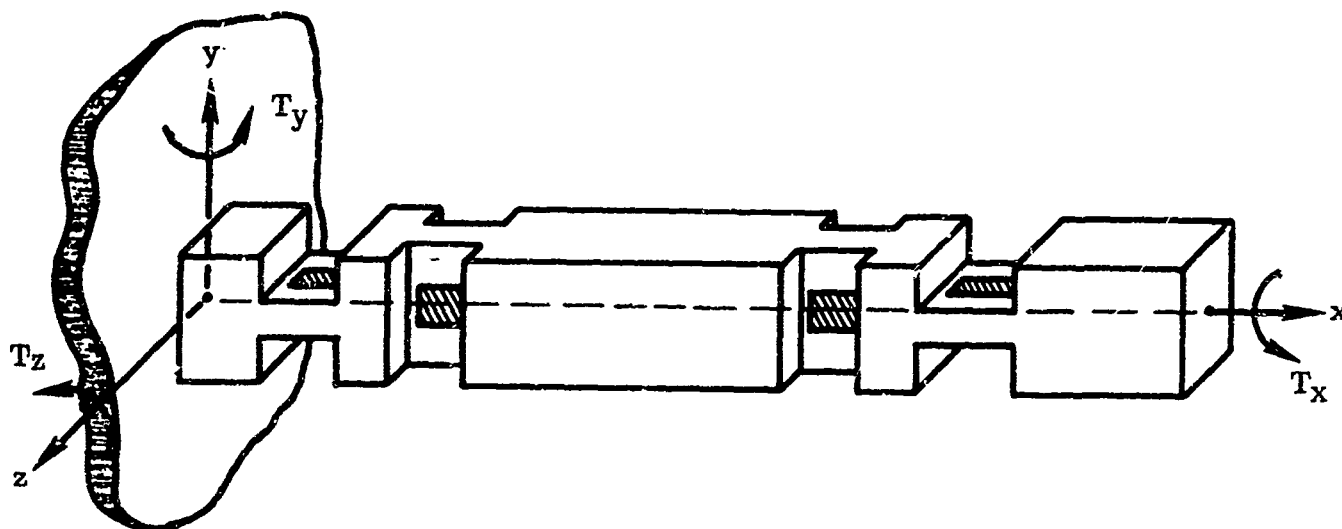


FIGURE 42. NOTCHED BAR ANALYZER

If the device is to be used to indicate the simultaneous values of forces F_y and F_z and moments T_y and T_z , then the number of strain gages is doubled so as to be useful in different circuits at the same time. Usually doubling the number of gages is done by installing them side-by-side in each notch location.

The bar itself is a complete instrument for the sensing of four of the six load components, the remaining being the moment T_x and force F_x . Both of these quantities are difficult to transduce and require the use of more hardware. Consider the moment T_x . This is transduced by a torque meter which can have many forms. Two which have been used successfully in the past are the strain gaged cruciform and the four axial bars as shown in cross section in Figure 43.



FIGURE 43. CRUCIFORM AND AXIAL BAR TORQUE METERS

The strain gages are placed so that they sense the tensile and compressive surface strains in the cruciform when the assembly is loaded in torsion by moment T_x . Notice that the moment T_x not only twists the elements of the structure but bends them as well. The strain gages are wired in the bridge circuit of Figure 44 so that compressive and tensile bending strains add to the bridge output.

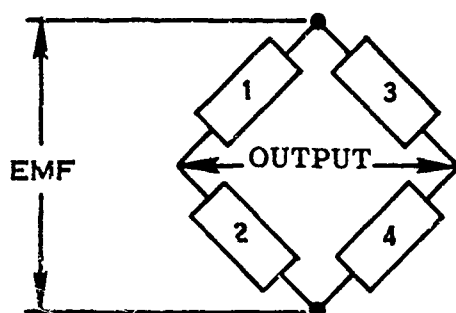


FIGURE 44. BRIDGE FOR TORQUE METERS OF FIGURE 43

It can be shown that this circuit is insensitive to other types of loading. The cruciform torque meter section can be added directly to that of the bar analyzer as depicted in Figure 45.

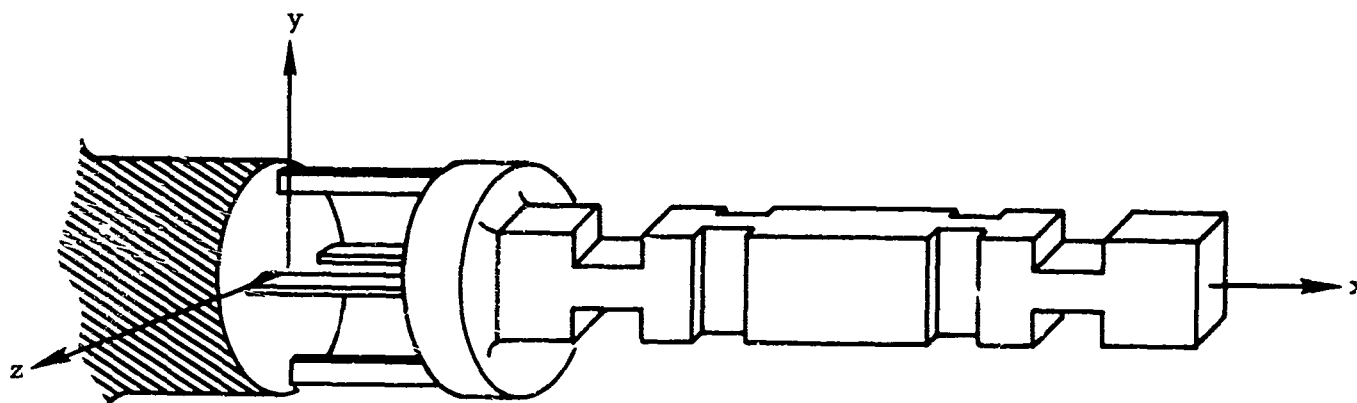


FIGURE 45. BAR ANALYZER WITH CRUCIFORM TORQUE METER

This bar analyzer as illustrated with the cruciform torque meter section is now capable of measuring the forces F_y , F_z , and torques T_x , T_y , and T_z . For the particular problem of the measurement of the elbow torque vector, only the three torques T_x , T_y , and T_z are needed and the last two notched sections are unnecessary.

The bar analyzer is not the only mechanical system which may be employed to measure these torques. The particular choice of the mechanical system depends upon many considerations including the interaction of the various load sensing elements, the mechanical size and strength of the analyzer, the sensitivity of the gages employed, the natural frequency of the system, the geometrical considerations which determine its suitability for placement on any given limb, and the accuracy requirements.

No generalized statements can be made regarding the selection of one system in preference to another without a thorough design study which considers all of the loading and packaging problems. However, it is not essential that the same method of torque transduction be used in all of the dummy joints.

As an example, the bar analyzer is shown in Figure 46. The order of the load elements in the line-up from the point of load application to the joint depends upon the particular loading situation. In general, the stiffest component is located closest to the point of load application thereby reducing component deflection and, as a result, mechanical interactions between the various measurement components are minimized.

The task of building an efficient and accurate load measuring system is formidable and no detail can be neglected. Regardless of the mechanical concept selected, there are certain basic design considerations which must be observed if the system is to provide an optimum method of transduction.

1. One-piece construction of the load elements should be used wherever possible since the fewer the number of pieces, the lower will be the hysteresis, scatter, zero shift, and nonlinearity.
2. High strength, low internal hysteresis materials such as 17-4 PH stainless steel should be used in the fabrication of the load elements since it can be machined without appreciable warpage, welds easily, and has good fatigue properties.
3. The material should be as hard as practical in the finished state to minimize hysteresis. Careful stress relief during machining is also important to avoid locked-in stresses and undue warpage.

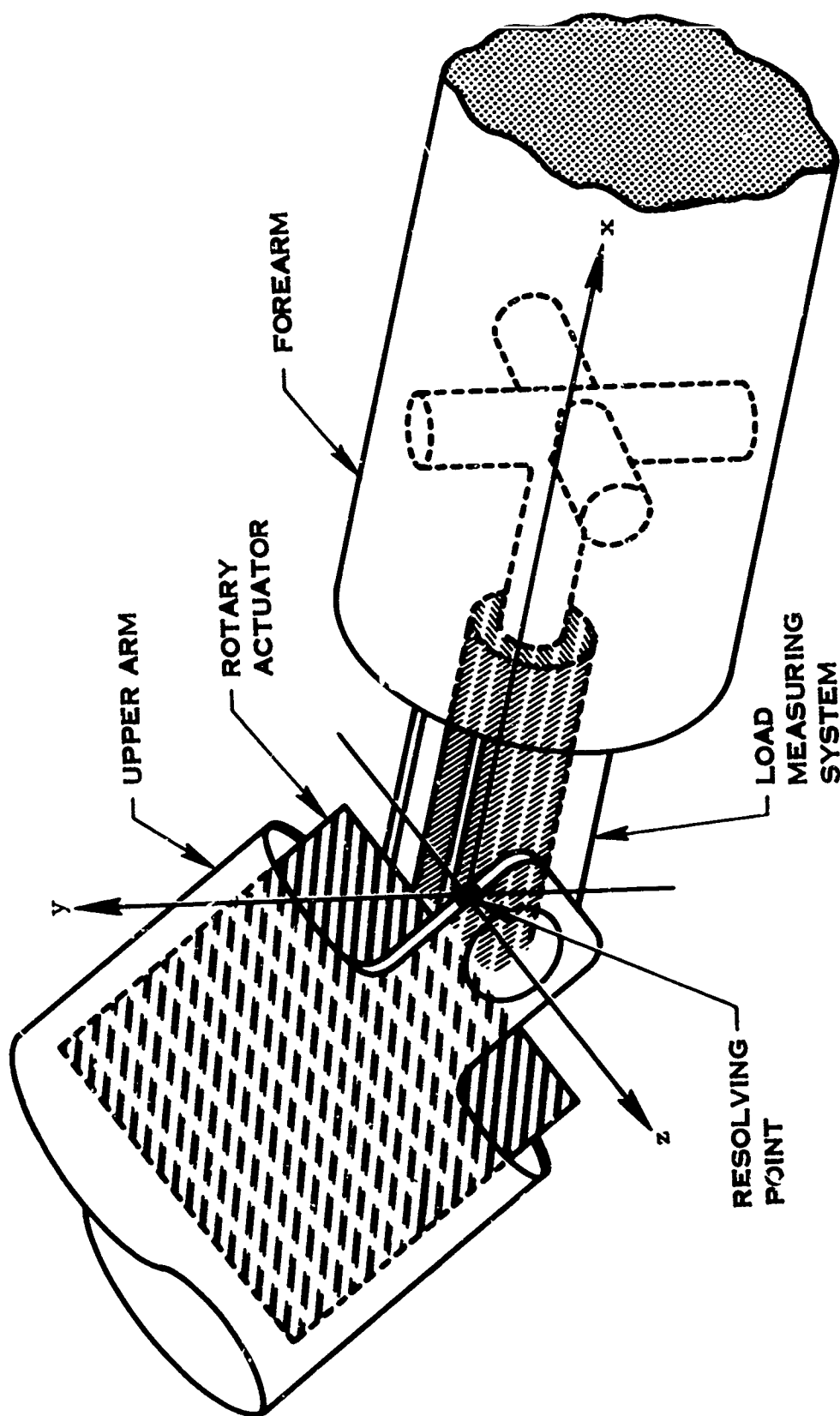


FIGURE 46. ELBOW BAR ANALYZER CONCEPT

4. Throughout the transducer, stress levels should be kept within one-half of the endurance limit of the material, joints should be placed in regions where the shear stress is low, and the material surface strain under the strain gages should not exceed 1,000 micro-inches per inch of strain.
5. Deflection of the entire load measuring system should be kept as low as possible to reduce interaction and maintain a high natural frequency.
6. Strain gages should be located on flat, chemically etched surfaces accessible for repair but protected from abuse during handling and operation.
7. Strain gages must be very carefully aligned on the load elements to prevent reduced sensitivity and increased interaction.
8. In general, foil type strain gages should be used and applied with epoxy adhesives which transmit shear strain more faithfully and are less temperature sensitive than other adhesives.
9. Strain gages should be selected of a material having the same thermal coefficient of expansion as the load element material.
10. The lowest excitation current consistent with circuit sensitivity should be used to minimize self heating effects.

In addition to these basic transducer design considerations, there are many subtle design and experimental techniques that have been applied for further reduction of interactions and sensitivity variations that remain due to thermal deformation, friction, elastic hysteresis, temperature gradients, material modulus changes, and spurious thermal potentials. It is clear that the basic design of the dummy must be dictated by the instrumentation requirements if the dummy is to produce satisfactory results.

FORCE SENSING SHELLS OVER THE DUMMY LIMBS -- In this type of system, rather than measure the actuation torque components, the forces acting upon the limbs of the dummy are measured directly. This is the system described on page 75, which utilizes load-supporting shells having great stiffness, low mass, and little inertia in contrast to the actuation torque measuring system which has relatively large mass and inertia. Accuracy is the principal difficulty with the load-supporting shell concept. The torque at the shoulder, for instance, is not simply the torque in the upper arm shell, but the sum of the torques in the upper arm, lower arm, and wrist shells each computed about the shoulder joint. The calculation is relatively complex, involving many force and angle transductions for each torque component. This is discussed in detail in Appendix VI.

The shell load measuring system has proved to be a very useful device in wind tunnel work having the advantages of good thermal stability, very high efficiency in the separation of mechanical interactions, and high stiffness (ref. 46, 93). On the other hand, this device is more difficult to design, fabricate, and service than the bar analyzer because of its completely shrouded elements. The shell-loading system is illustrated schematically in Figure 47.

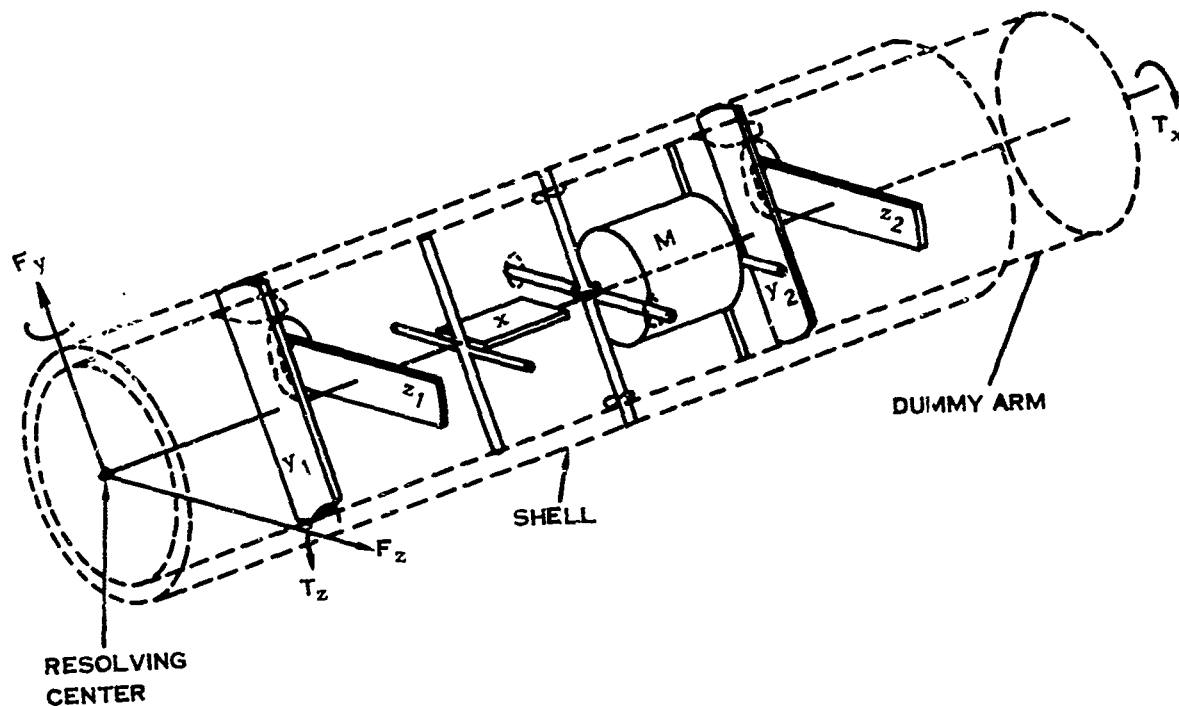


FIGURE 47. SHELL LOAD MEASURING SYSTEM

As shown, the system consists of the load bearing shell attached to the dummy arm through the six load transduction devices. The elements, Y_1 and Y_2 detect forces F_{y1} and F_{y2} which yield the net load F_y and the torque component T_z . To get a clearer understanding of this device and how loads are transmitted through from the shell to the dummy arm, a cross section through the arm viewed in the positive x direction is shown in Figure 48. The elements Z_1 and Z_2 detect forces F_{z1} and F_{z2} which are combined to yield the load component F_z and the moment T_y . The force F_x is measured directly through element X and the moment T_x is detected by the four bar cruciform M .

Consider the problem of designing the load sensing components Y_1 , Y_2 , Z_1 , Z_2 , and X . In the actuator output torque measuring system, this was accomplished by designing a device, the bar analyzer, which sensed the bending loads in the limb. In the shell loading system the devices used must sense axial rather than bending loads.

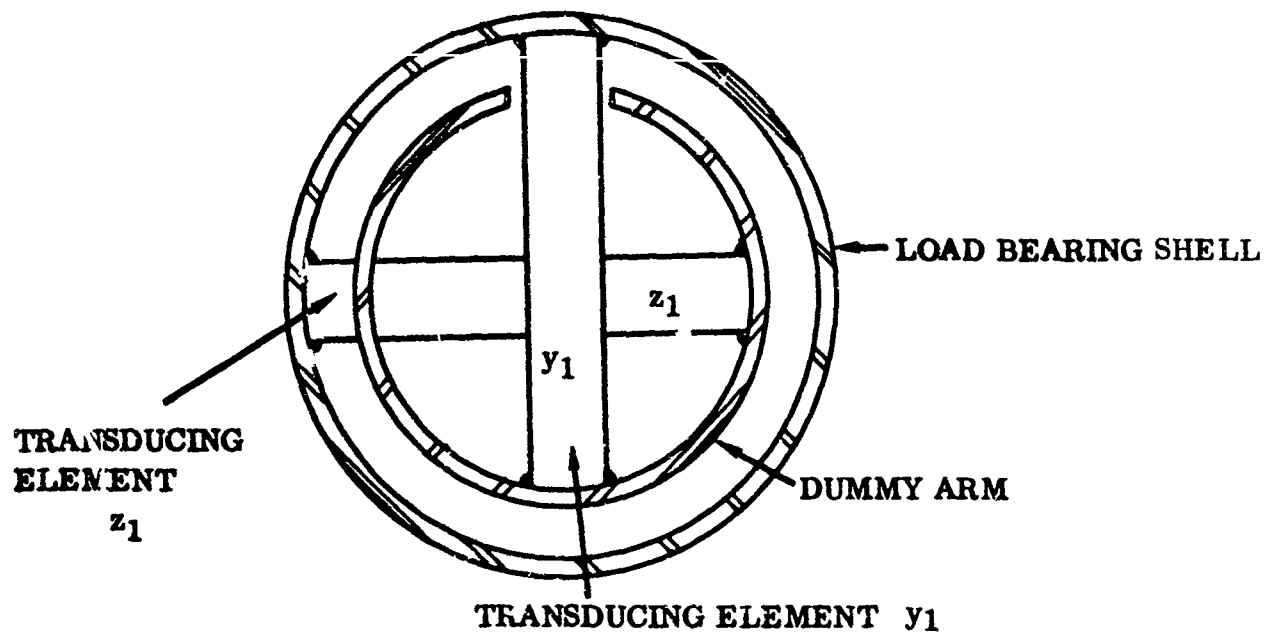


FIGURE 48. CROSS SECTION OF SHELL LOAD MEASURING SYSTEM

One often used type of axial load measuring device is the gamma-type balance shown in Figure 49, so named because of its shape. The axial load causes the strain gaged blade to bend through a circular arc, thereby producing elongation in the strain gage elements. Notice that the sensitivity of the device is readily increased by increasing the lever arm of the applied load.

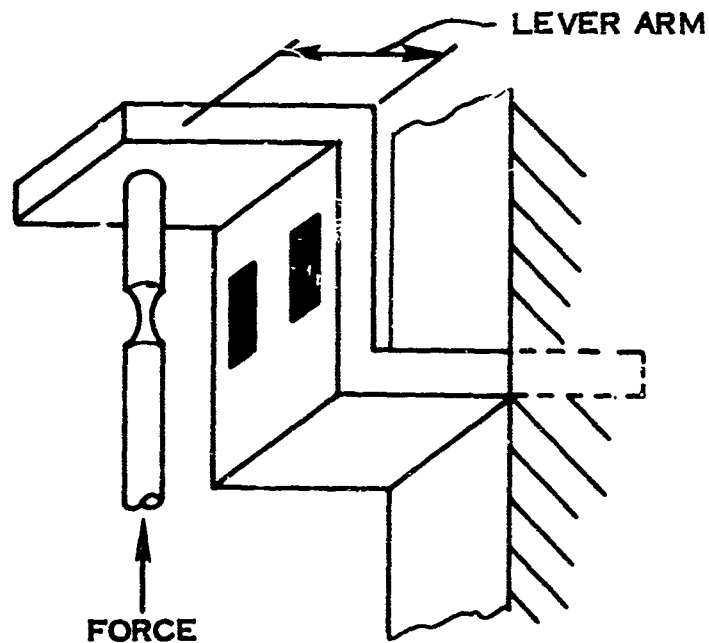


FIGURE 49. GAMMA-TYPE BALANCE

Another type of axial load sensor is the distorted frame shown in Figure 50. This design maintain parallel motion of the frame under the distorting load. The sketch illustrates the distortion of this device when under load and shows the placement of strain gages.

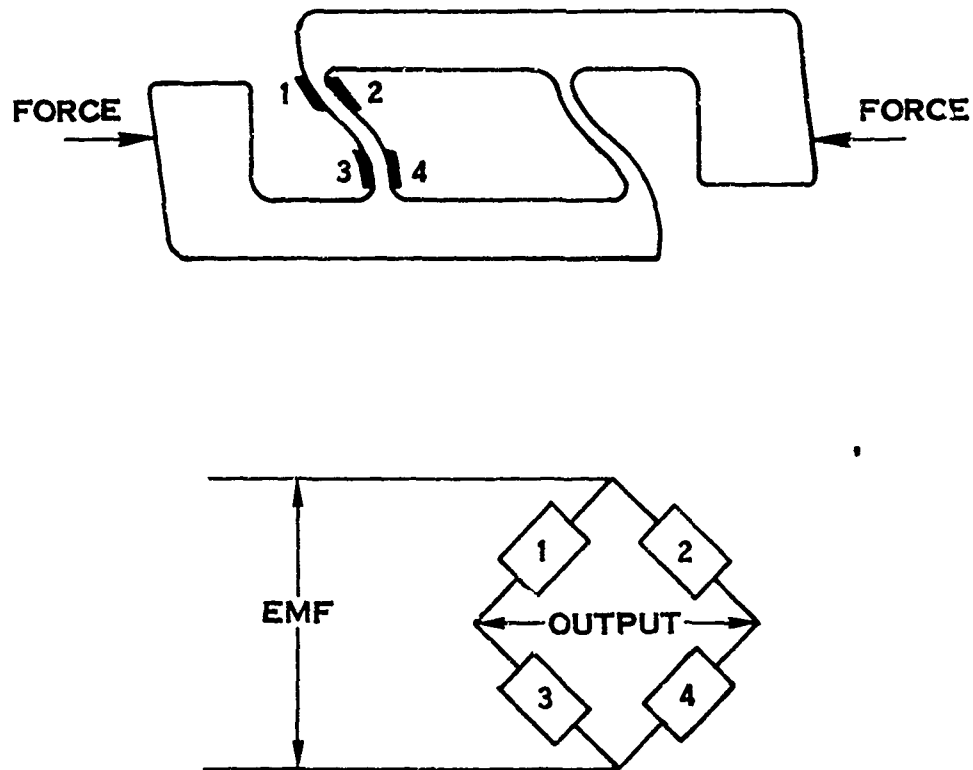


FIGURE 50. DISTORTED FRAME TRANSDUCER WITH BRIDGE ARRANGEMENT

One of the better designs from the standpoint of reduced interactions from other load components is the tension-compression strip depicted in Figure 51. This device is more rigid than most other designs and as such would have a higher natural frequency. It has the disadvantage of being rather complex to fabricate.



FIGURE 51. TENSION-COMPRESSION STRIP TRANSDUCER

An example of an extremely simple design is the eccentric blade type sensor in Figure 52. When strained, this unit has the tendency to moment load the attachment points; however, if the surrounding structure is sturdy enough this is not a disadvantage.

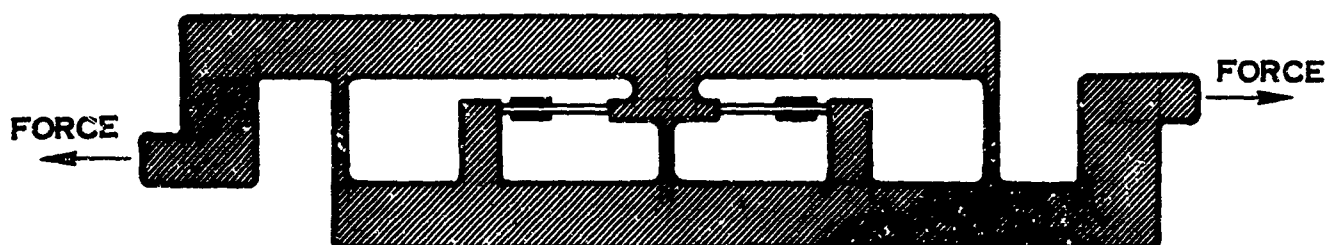


FIGURE 52. ECCENTRIC BLADE TYPE TRANSDUCER

This discussion of the various possibilities for the load measuring components of the shell type load system, while not exhaustive, is a cross section of the type of device employed for the fabrication of multicomponent force and torque measuring systems.

The fabrication of the shell-type transduction system requires the same basic mechanical and electrical considerations as the bar analyzer. Like the bar analyzer, this system must be incorporated into the basic dummy design early in the design study in order to realize the maximum potential of the torque measurement system.

In either the bar analyzer or the shell analyzer, the strain gage circuitry would be powered and the output signals conditioned through the control console for functional suit mechanical testing. This console, together with the analog/digital recording system will acquire, process, and record all of the basic transduction data for the later calculation and display of actual suit torque values. The operation of this system is described in detail in Section VIII.

FORCE SENSOR CALIBRATION -- Regardless of the basic measurement technique chosen, the accuracy of the system can be no better than the calibration of the system. The calibration of the completed load measuring assembly on the dummy is accomplished by loading with precision laboratory dead weights. The calibration force or moment is a known vector. There must be at least as many independent calibration vectors as there are load sensing components in each system. For example, the bar analyzer measures the three components of torque about a joint; hence, there must be at least three independent calibration moments applied to the system for calibration check out. Similarly, the shell-load system determines three components each of force and torque from six force measurements and therefore requires six independent calibration vectors. (Independent calibration vectors are dissimilar in both magnitude and direction.)

Calibration vectors with different magnitudes are required for linearity checks; different directions are required for determination of interactions.

For example, in the shell method the most general system would support the shell on six independent force transducers with voltage outputs V_1 through V_6 . The quantities to be calculated are the three components of the torque vector T_1 , T_2 , and T_3 . (The components of the force vector T_4 , T_5 , T_6 can also be calculated if necessary.) By definition, if the system is linear, any T_i can be written as in Equation 68 where the A_{ij} 's are constants.

$$T_i = \sum_{j=1}^6 A_{ij} V_j \quad (68)$$

For discussion purposes, Equation 68 can be written in operator form as $T = AV$ which stands for the matrix relation in Equation 69.

$$\begin{bmatrix} T_1 \\ T_2 \\ T_3 \\ T_4 \\ T_5 \\ T_6 \end{bmatrix} = \begin{bmatrix} A_{11} & A_{12} & A_{13} & A_{14} & A_{15} & A_{16} \\ A_{21} & A_{22} & A_{23} & A_{24} & A_{25} & A_{26} \\ A_{31} & A_{32} & A_{33} & A_{34} & A_{35} & A_{36} \\ A_{41} & A_{42} & A_{43} & A_{44} & A_{45} & A_{46} \\ A_{51} & A_{52} & A_{53} & A_{54} & A_{55} & A_{56} \\ A_{61} & A_{62} & A_{63} & A_{64} & A_{65} & A_{66} \end{bmatrix} \begin{bmatrix} V_1 \\ V_2 \\ V_3 \\ V_4 \\ V_5 \\ V_6 \end{bmatrix} \quad (69)$$

T and V are loosely called vectors and A is the matrix of influence coefficients A_{ij} . Calibration is the determination of the A_{ij} 's. This is done by applying six independent calibration vectors $T^{(1)}$ through $T^{(6)}$ and measuring the resulting voltage vectors $V^{(1)}$ through $V^{(6)}$. This results in six equations for each row of coefficients in A (Equation 70).

$$T_i^{(M)} = \sum_{j=1}^6 A_{ij} V_j^{(M)} \quad M = 1, 2, \dots, 6 \quad (70)$$

When written out for all six rows ($i = 1, \dots, 6$), there are 36 equations in the 36 A_{ij} 's which are solved by computer.

For redundancy, more than six calibration vectors are used. It is not necessary that any components of the calibration vectors be zero. The advantage of employing the above technique is that the accuracy of calibration is preserved without requiring (1) accurate alignment of the calibration vectors (only accurate knowledge of their alignment) or (2) extremely precise mechanical alignment of the strain gages on the load element during assembly.

GENERAL CONSIDERATIONS IN FORCE SENSING -- The building of a dummy torque measuring system will require a design study to establish an optimum design with minimal error; however, similar systems have been and are being built to accuracies of better than 1% of the full scale load values. Figure 53 illustrates some of the torque measuring concepts discussed above.

In the design, careful consideration must be given to the handling of the dummy. With limbs consisting in part of transducers sensitive to the loads imposed by the space garment, the dummy must be handled carefully to avoid damaging the load measuring system. The designer and test engineer must realize that the dummy is not just a powered manikin but a precise instrumentation system. Because deflection of the load-sensing elements must be minimized to reduce the interaction problem, a system to protect the load-sensing elements would be difficult to design. A more practical approach is to de-rate all the elements by a factor of 10 or 20; for instance, a 5-pound load element should be built to withstand loading of 50 to 100 pounds without damage. Obviously, the less de-rating required the greater will be the accuracy of measurement.

Angle Measurement Techniques

DEFINITION

The definition of body position or of the body link angles has long plagued the anthropologists. Man with his complex skeletal system, and ill-defined joint centers can assume positions and perform motions which are difficult to describe without ambiguity with existing goniometric terminology. In this study, an operational description of body position has been developed which is mathematically unambiguous. Using the Dempster link concept, man can be represented by a finite number of pin-jointed inextensible links each of which is constrained to a limited range of angular movement. Man is then represented by a physical model which has pin rather than human joints and links rather than bone and ligature systems. The accuracy of the description of man's position based on the interlink angles of the physical model depends only on the number of links. The physical model must have at least as many joints as the man has degrees of freedom.

Since an articulated dummy geometrically similar to man has been settled upon for the measurement of suit torque, an operational definition of body angle can be formulated in terms of this hardware rather than in the vagueness of goniometric terminology. To be useful, the dummy angles must be related to the human body angles so that the torques measured will represent actual human torque levels. In fact, it would be useful to program the dummy for human-like motions and to create mission oriented criteria based on actual human motion patterns.

For this part of the study, "body position" is defined to be that set (or list) of dummy angles θ_i which puts the dummy in the same position as the man.

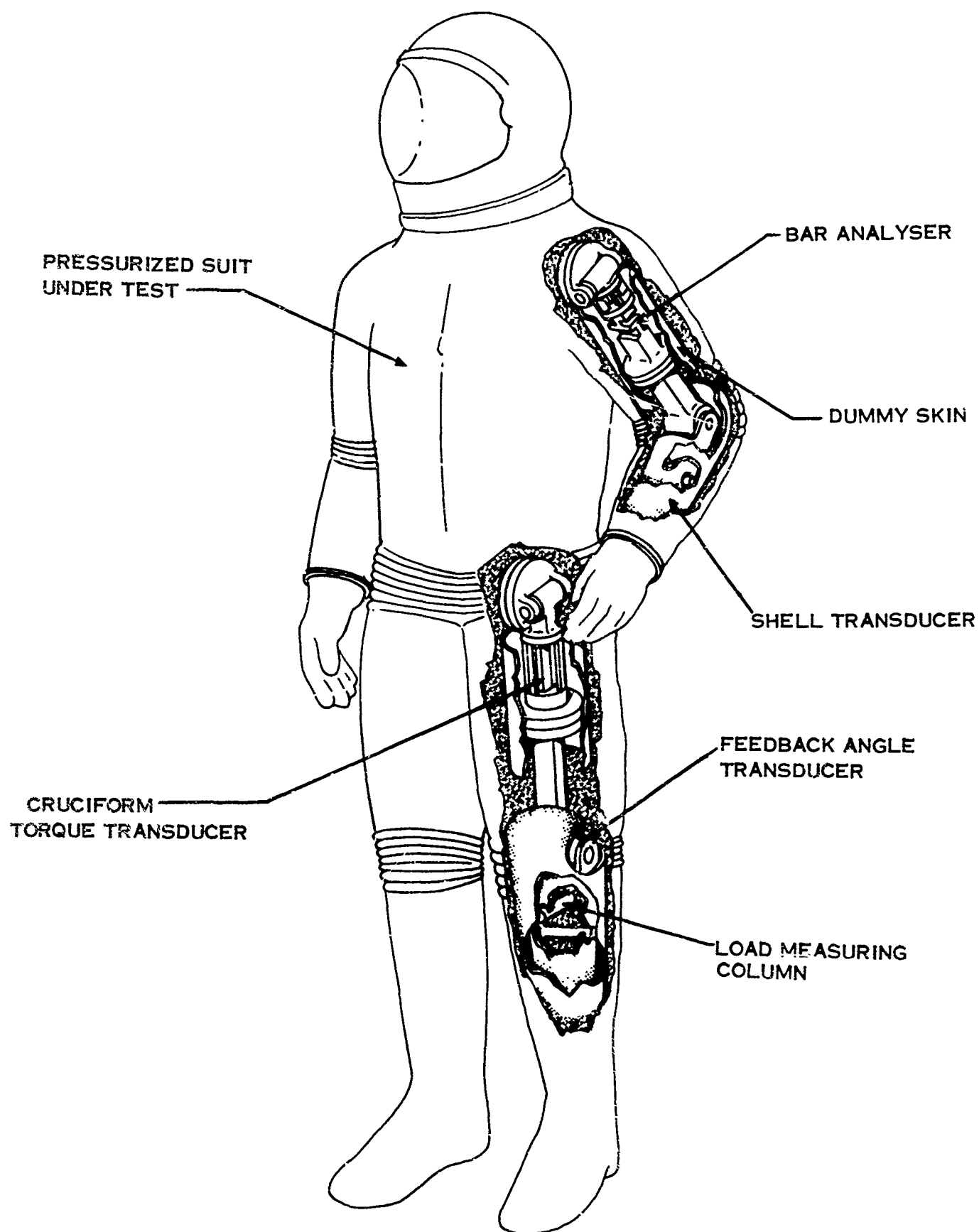


FIGURE 53. SUITED POWERED ARTICULATED DUMMY SHOWING TORQUE INSTRUMENTATION CONCEPT

How the "same position" is achieved will depend on the angle measuring technique used. For the accuracy required here, man's position is defined by a set of about forty dummy angles measured by transducers at each dummy link.

To relate the human body angles to the dummy link angles, a transfer device is needed. When this device, an angle measuring instrument, is worn by a test subject or the dummy, its outputs are the n variables $\{\Phi_j\}$. The device must be such that when it is worn by the dummy, the set of variables $\{\Phi_j\}$ defines a unique set of dummy angles $\{\Theta_i\}$. (The uniqueness does not have to hold in the reverse sense.) Transfer equations $\Theta_i = \Theta_i(\Phi_1, \Phi_2, \dots, \Phi_n)$ relate each dummy angle to the angle measuring instrument readouts. The calibration and operational procedure is as follows.

1. The dummy is adjusted to the size of the test subject as determined from some standard anthropometric procedure.
2. The angle measuring instrument is adjusted to fit both the dummy and the man.
3. The instrument is installed on the dummy which performs a standard set of maneuvers to determine the constants in the transfer equations.
4. The transfer device is installed on the subject who proceeds to execute the test maneuvers while the Φ_j 's are recorded.
5. These outputs are entered into a computer which uses the transfer equations to determine the dummy angles, $\{\Theta_i\}$, required for the dummy to reproduce the same maneuvers, and which prepares a tape recorded program to activate the dummy angle control system.

In the determination of the body angles, the dummy is used only in the calibration of the angle measuring instrument. The body position angles thus obtained are the command angles for the dummy.

The desirability of the above definition is apparent from these two considerations. First, it is a definition in terms of hardware; that is, instead of lines drawn on skin or on invisible bones and joints without defined centers of rotation, angles are defined simply in terms of pin joint angles. Second, since the dummy is used for torque testing, the dummy angles are of prime interest. In fact, there is no need to know the angles between the subject's bones except for their utility in developing more fundamental evaluation criteria.

TRANSDUCTION OF THE SHOULDER-ARM COMPLEX

For the purpose of evaluating various body angle measuring techniques, a specific part of the transduction problem, the arm and shoulder complex, was considered. This narrows the problem to specific essentials. Transduction of the

shoulder is the sine qua non of any technique. Generalization of the technique to total body measurement is straightforward.

For the study, the dummy linkage system shown in Figure 54 was chosen for the shoulder.

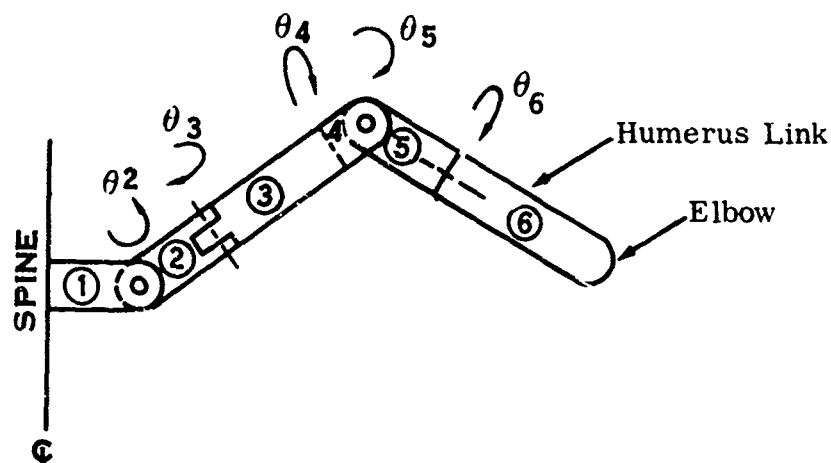


FIGURE 54. SHOULDER-ARM DUMMY LINKAGE SYSTEM

The set of angles $\{\theta_i\}$ for $i = 2, 3, 4, 5, 6$ is called the shoulder position. The correspondence of these angles to goniometric terminology is as follows,

θ_2 = shoulder elevation - depression

θ_3 = shoulder rotation

θ_4 = arm extension - flexion

θ_5 = arm abduction - adduction

θ_6 = arm rotation

(This is believed to be the linkage geometry of the NASA - IIT dummy.)

The human shoulder, because of the flesh covering and the lack of specificity in joint location, presents few good attachment places for transducers. The two best places are the upper arm near the elbow (link 6) and the spine (link 1). The acromion, corresponding to link 3 just inboard of joint 4, is also a possible attachment point.

The problem then is to place instrumentation on the body in such a way as to make the corresponding dummy angles which describe body position calculable.

An analysis of the shoulder linkage model was undertaken to answer the following question: "If the location and orientation of the spine and upper arm are known, can the dummy angles between the six links be calculated?" The analysis

shows that each of the angles Θ_1 can be determined uniquely, except in the degenerate case when $\Theta_5 = 0$, that is, when the Θ_4 and Θ_6 axes coincide. The analysis that led to this conclusion is presented in Appendix VII. The results are presented here.

First the angles and link lengths are defined in Figure 55.

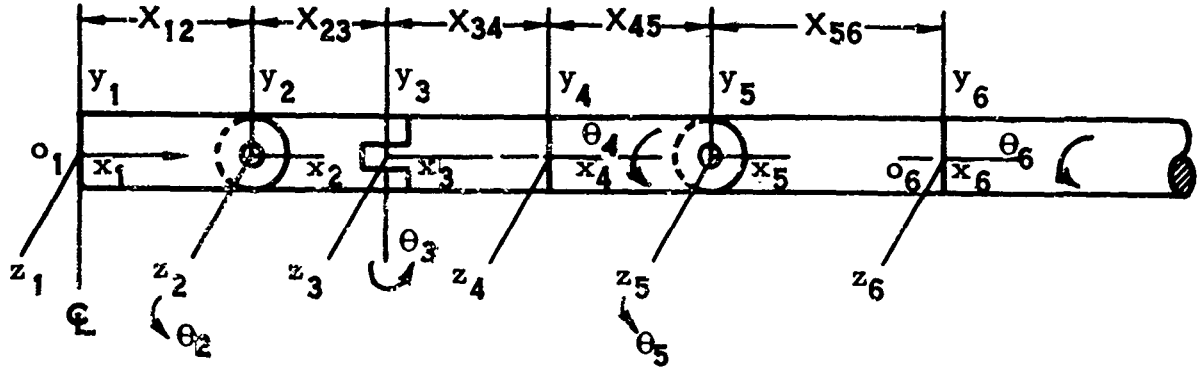


FIGURE 55. MODEL FOR DEFINITION OF LINK LENGTHS AND ANGLES IN SHOULDER COMPLEX

The position of link 6 with respect to link 1 is the vector $\vec{R}_{16} = R_x \hat{i}_1 + R_y \hat{j}_1 + R_z \hat{k}_1$ from o_1 to o_6 (represented here in the coordinate system of link 1) and the orientation of link 6 with respect to link 1 is described by the matrix of direction cosines D with element d_{mn} , the cosine of the angle between the m th axis of link 1 and the n th axis of link 6. The sine and cosine of the angles are abbreviated:

$$\begin{aligned} \sin \Theta_n &= S_n \\ \cos \Theta_n &= C_n \end{aligned} \quad (71)$$

Then the position and orientation of link 6 with respect to link 1 are described by:

$$\begin{aligned} R_x &= X_{12} + X_{23} C_2 + (X_{34} + X_{45}) C_2 C_3 + X_{56} (C_2 C_3 C_5 - S_2 C_4 S_5 + C_2 S_3 S_4 S_5) \\ R_y &= X_{23} S_2 + (X_{34} + X_{45}) S_2 C_3 + X_{56} (S_2 C_3 C_5 + C_2 C_4 S_5 + S_2 S_3 S_4 S_5) \\ R_z &= - (X_{34} + X_{45}) S_3 + X_{56} (-S_3 C_5 + C_3 S_4 S_5) \end{aligned} \quad (72)$$

$$\begin{aligned} d_{11} &= C_2 C_3 C_5 - S_2 C_4 S_5 + C_2 S_3 S_4 S_5 \\ d_{12} &= - C_2 C_3 S_5 C_6 - S_2 C_4 C_5 C_6 + C_2 S_3 S_4 C_5 C_6 + S_2 S_4 S_6 + C_2 S_3 C_4 S_6 \\ d_{13} &= C_2 C_3 S_5 S_6 + S_2 C_4 C_5 S_6 - C_2 S_3 S_4 C_5 S_6 + S_2 S_4 C_6 + C_2 S_3 C_4 C_6 \end{aligned} \quad (73)$$

$$\begin{aligned}
d_{21} &= S_2 C_3 C_5 + C_2 C_4 S_5 + S_2 S_3 S_4 S_5 \\
d_{22} &= -S_2 C_3 S_5 C_6 + C_2 C_4 C_5 C_6 + S_2 S_3 S_4 C_5 C_6 - C_2 S_4 S_6 + S_2 S_3 C_4 S_6 \quad (74) \\
d_{23} &= S_2 C_3 S_5 S_6 - C_2 C_4 C_5 S_6 - S_2 S_3 S_4 C_5 S_6 - C_2 S_4 C_6 + S_2 S_3 C_4 C_6
\end{aligned}$$

$$\begin{aligned}
d_{31} &= -S_3 C_5 + C_3 S_4 S_5 \\
d_{32} &= S_3 S_5 C_6 + C_3 S_4 C_5 C_6 + C_3 C_4 S_6 \quad (75) \\
d_{33} &= -S_3 S_5 S_6 - C_3 S_4 C_5 S_6 + C_3 C_4 C_6
\end{aligned}$$

These are twelve transcendental equations in the five unknown quantities Θ_2 through Θ_6 and have these unique solutions (except at $\Theta_5 = 0$).

$$\begin{aligned}
\Theta_3 &= \arcsin \left(\frac{d_{31} X_{56} - R_z}{X_{35}} \right) \\
\Theta_2 &= \arcsin \left(\frac{R_y - d_{21} X_{56}}{X_{23} + C_3 X_{35}} \right) \\
\Theta_5 &= \arccos \left(d_{31} S_3 + C_3 \sqrt{1 - d_{31}^2 - (d_{21} C_2 - d_{11} S_2)^2} \right) \quad (76) \\
\Theta_4 &= \arccos \left(\frac{d_{21} C_2 - d_{11} S_2}{S_5} \right) \\
\Theta_6 &= \arcsin \left(\frac{S_4 (S_2 d_{23} + C_2 d_{13}) + S_3 C_4 (S_2 d_{13} - C_2 d_{23})}{d_{12} d_{23} - d_{13} d_{22}} \right)
\end{aligned}$$

As written, these equations must be solved in order because the expressions for Θ_4 , Θ_5 , and Θ_6 contain functions of Θ_2 and Θ_3 . Thus if \bar{R}_{16} and D can be found by instrumentation, the shoulder position can be calculated. The fact that only $\Theta_4 + \Theta_6$ can be determined at the instant that Θ_5 passes through zero should cause no problems.

Since in practice the equations for the Θ_i 's would be solved by computer, an estimate of computation time is of interest for economic reasons. To estimate computer time a hypothetical problem was programmed and timed. The actual computational problem considered was the reduction of goniometer data to the dummy shoulder and arm angles $\{\Theta_i\}$. The input was the set of angles $\{\Phi_j\}$ for a five joint exoskeleton with arbitrary geometry. From the Φ_j 's, \bar{R}_{16} and D were calculated. These in turn were used to solve for $\{\Theta_i\}$. One set of arbitrary data was inserted in the program and run repetitively on both an IBM 1620 and an IBM 7094. On the 1620 the computation took one minute per set of input angles $\{\Phi_j\}$. On the 7094 the rate was 100 sets per second. These time estimates are conservative since with more effort a more efficient program could be written. Nevertheless, the figures show that the processing of dynamic data on a large computer is practical.

Techniques for the measurement of body position can be broken down into three broad categories: (1) optical or electro-optical sensing techniques, (2) inertial sensing techniques, and (3) exoskeletal techniques. During the study each showed considerable promise and was therefore studied in depth to determine which technique would yield the position \vec{R}_{16} and orientation D of the humerus with respect to the spine with the greatest accuracy, convenience, and simplicity.

OPTICAL SENSING TECHNIQUES

Optical techniques have been used for many years to study human motion and have formed the basis for the classic studies of Elftman and others. Walking is the motion most extensively studied. Since extensive reviews of these techniques appear in the literature, (refs. 34, 35) they will only be listed here. The techniques can be classified by camera type used, camera array, and target. The cameras used are still, movie, or X-ray cameras or special cameras with the film moving by the lens at constant speed for cyclograms. The array can be a single camera, a stereo pair, or three cameras aligned along orthogonal or other axes. Light bulbs, reflecting tape, painted-on bullseyes, and strapped-on targets have been used to identify the position of the subject's limbs. In the study at the University of California (ref. 27) targets were rigidly attached to underlying bones by drilling through the skin. With this method, errors as low as $\pm 2\%$ in interlink angles were achieved for limited ranges of motion in certain positions.

In general, the optical techniques used to date have been sufficiently accurate but the magnitude of the data reduction problem has prohibited general motion analyses. Computation has been done by high speed computers but a great deal of hand work is required to digitize the data on the film. For this reason, a faster method of data reduction and computer entry was considered worthy of investigation. This portion of the study was performed by Norden, Division of the United Aircraft Corporation, because of their extensive experience in contact analog displays, navigational systems, tracking techniques, and television cameras and displays.

A MODIFIED ELECTRO-OPTICAL TECHNIQUE

The problem considered was to determine the position and orientation of a human limb with respect to a laboratory coordinate system. Each limb to be measured is assumed to contain a system of coordinates fixed with respect to that limb. The problem may be solved if a vector from the origin of the laboratory coordinate system to the origin of the limb coordinate system and the direction cosines of the limb coordinate axes with respect to the laboratory coordinate axes can be determined. In Figure 56, the positions of links 1 and 6 with respect to the lab frame R_{L1} and R_{L6} and the corresponding matrices of direction cosines D^{L1} and D^{L2} are shown. If these can be found, then the desired quantities \vec{R}_{16} and D

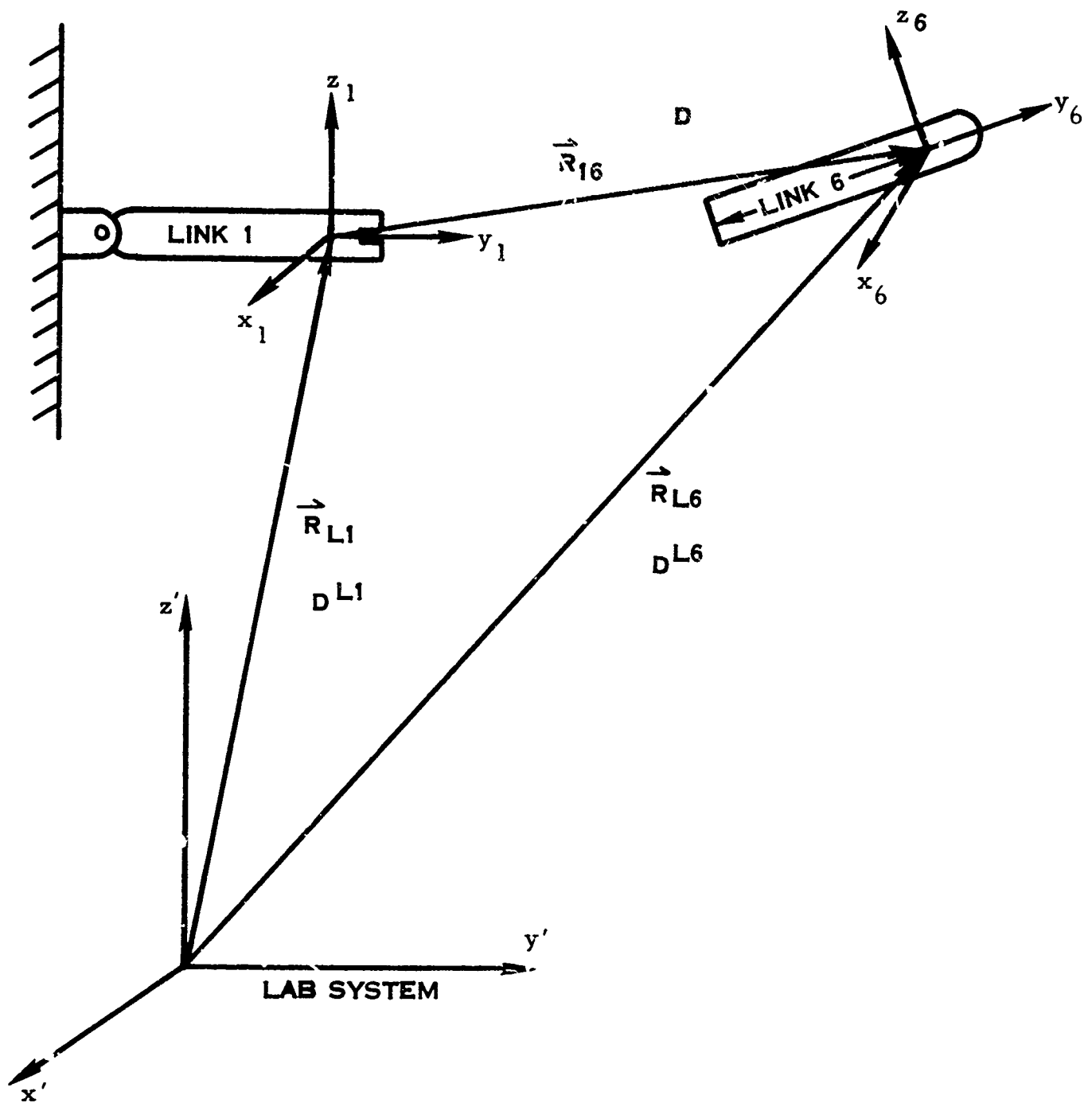


FIGURE 6. COORDINATES FOR MODIFIED ELECTRO-OPTICAL TECHNIQUE

can be calculated as follows. From the figure,

$$\vec{R}_{L1} + \vec{R}_{16} = \vec{R}_{L6} \quad (77)$$

and

$$DL1 \ D = DL6 \quad (78)$$

Then

$$\vec{R}_{16} = \vec{R}_{L6} - \vec{R}_{L1} \quad (79)$$

and

$$D = \tilde{D}^{L1} \ DL6 \quad (80)$$

In order to determine these positions and orientations optically, it is necessary to attach light sources or targets to the man or his clothing which are fixed with respect to some known point in his body. Three possible configurations of targets or lights were considered and one was studied in detail. The first scheme involved placing a target of some geometrical shape such as a square or triangle on the limb. This target would be viewed by a single TV or film camera. Accuracy with this method would be insufficient due to the limited size of rigid targets which could be attached to the limb without limiting the motion of the limb. Ambiguities are possible which create problems in data reduction. For example, the appearance of a rectangle is unaltered when it is rotated in 180° steps about an axis perpendicular to it.

The second method considered would require placement of three small collimated light sources on the limb to be measured. These light sources would be positioned in a cluster with a known angular relationship to one another. Data would be gathered by photographing the intercepts of these light beams on a plane screen placed some distance from the subject. In order to instrument a number of points, light coding or sequencing would be required which would lead to very high TV or motion picture frame rates for good motion definition. This, plus the fact that a multiplicity of screens are required, tend to make this method impractical.

The third method considered shows some promise of success. With this arrangement the subject would wear four spherical non-coplanar light sources on each limb. The position of each of these lights would be accurately known in the limb coordinate system. By photographing these lights from two vantage points, their locations in the laboratory coordinate system may be determined, and calculations may be performed to find the required vector and the direction cosines.

The geometry of the problem is shown in Figure 57. The primed coordinate system is fixed in the laboratory, and the unprimed system is fixed in the limb to be measured. Points P_1 to P_4 represent the light sources and the vectors \vec{B}_1 to \vec{B}_4 define their respective positions in the unprimed system. Vectors \vec{A}_1 to \vec{A}_4 are the measured positions of the light sources in the primed system. The vector \vec{R}_{L1} and the direction cosines of the unprimed axes are to be found. By inspection, $\vec{A}_i = \vec{B}_i + \vec{R}_{L1}$, where i denotes the particular point under consideration. Equating the x' , y' and z' components yields the following set of linear equations:

$$\begin{aligned} x'_i &= x_i d_{11} + y_i d_{12} + z_i d_{13} + X_0 \\ y'_i &= x_i d_{21} + y_i d_{22} + z_i d_{23} + Y_0 \\ z'_i &= x_i d_{31} + y_i d_{32} + z_i d_{33} + Z_0 \end{aligned} \quad (81)$$

The $\vec{B}_i = x_i \hat{i} + y_i \hat{j} + z_i \hat{k}$ are known from light placement. The $\vec{A}_i = x'_i \hat{i}' + y'_i \hat{j}' + z'_i \hat{k}'$ are measured by the camera system.

$$\begin{aligned} x'_i &= A \frac{v(d-p)}{d^2 - vp} \\ y'_i &= A \frac{p(d-v)}{d^2 - vp} \\ z'_i &= A \frac{u(d-v)}{d^2 - vp} = A \frac{w(d-p)}{d^2 - vp} \end{aligned} \quad (82)$$

where p , u , v , and w are read from the films. A and d are from camera geometry and calibration.

If these equations are written for four non-coplanar points, a system of 12 independent equations in 12 unknowns will result. The unknowns are the components of the position vector,

$$\vec{R}_{L1} = X_0 \hat{i}' + Y_0 \hat{j}' + Z_0 \hat{k}' \quad (83)$$

and of the orientation matrix,

$$DL1 = \begin{bmatrix} d_{11} & d_{12} & d_{13} \\ d_{21} & d_{22} & d_{23} \\ d_{31} & d_{32} & d_{33} \end{bmatrix} \quad (84)$$

The remainder of the problem involves finding the coordinates, x_i , y_i , z_i , with respect to the laboratory system. Figure 58 shows the projections of a single light source onto two image planes which are centered on and orthogonal to the x' and y' axes of the laboratory system. The light is viewed from points x_0' and y_0' which are located a distance d behind the image planes. The image planes need

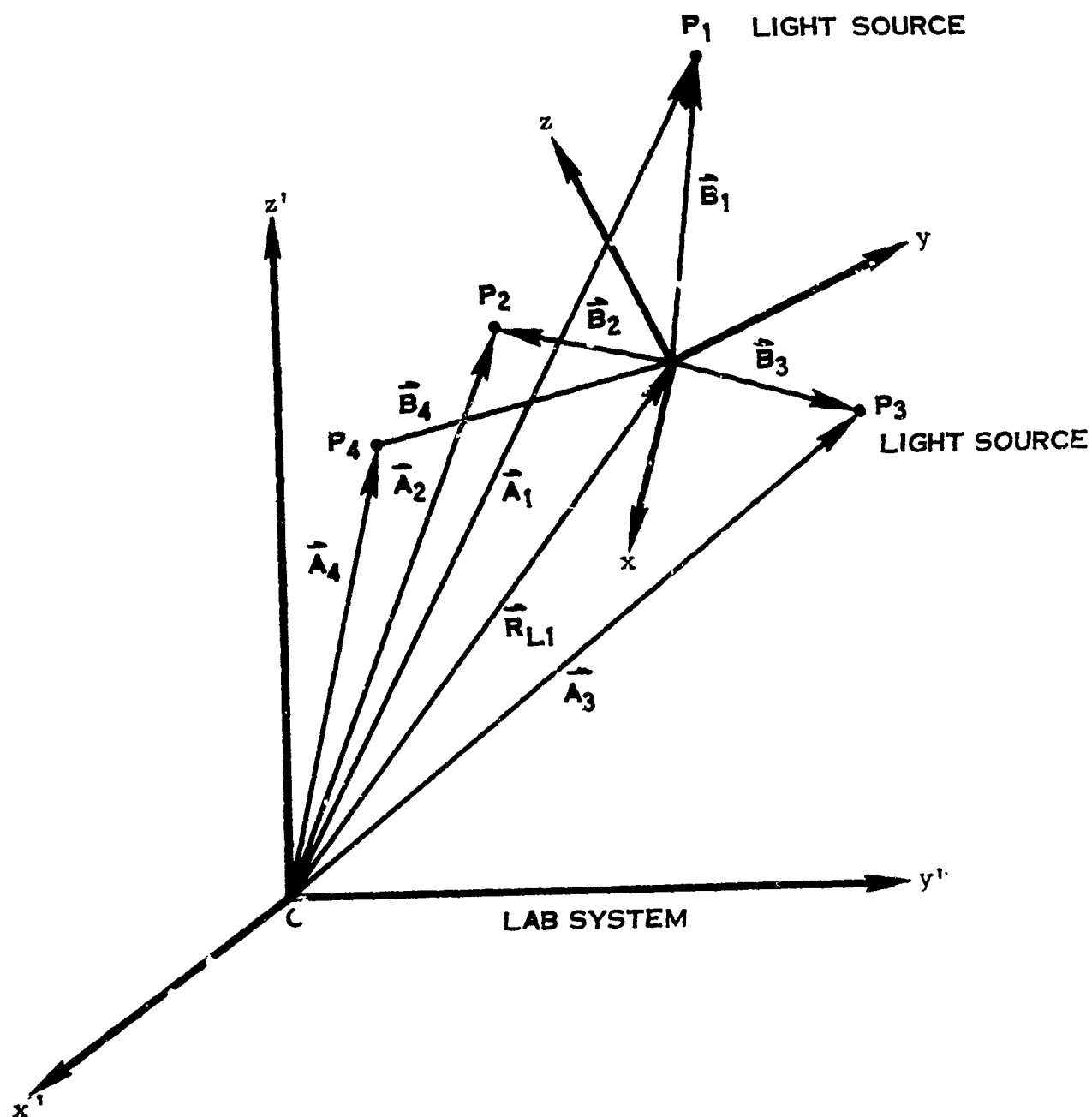


FIGURE 57. COORDINATES OF LIGHT SOURCES IN LINK #1

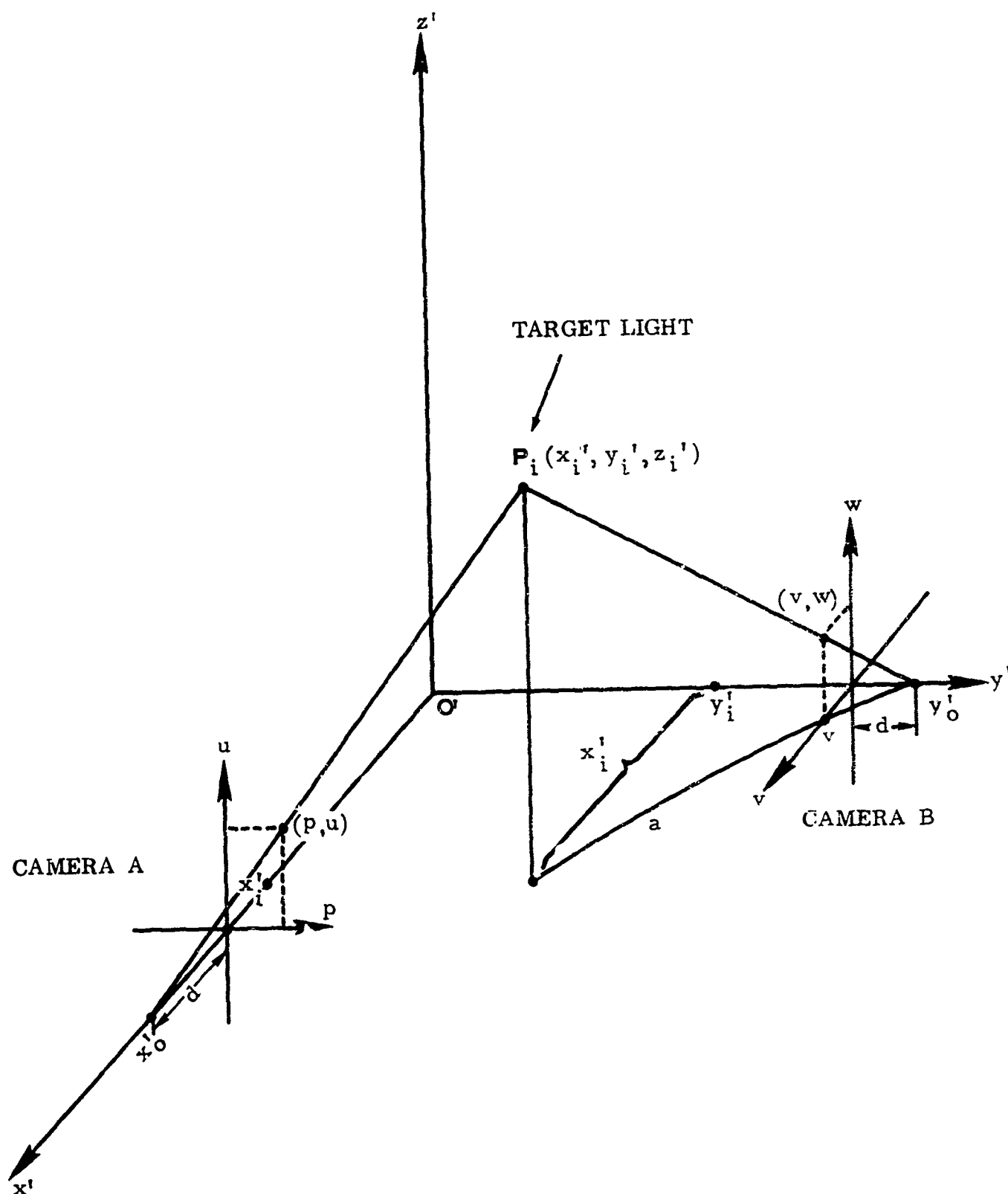


FIGURE 58. COORDINATES FOR CAMERAS

not be orthogonal, but this relationship yields the best accuracy and simplifies the computations. Each image plane will be defined by separate coordinate systems as shown, by which the position of the light image may be measured. With reference to Figure 58, the following equations may be written:

$$\begin{aligned}x_1' &= \frac{y_0' - y_1'}{d} v \\y_1' &= \frac{x_0' - x_1'}{d} p \\z_1' &= \frac{x_0' - x_1'}{d} u = \frac{y_0' - y_1'}{d} w\end{aligned}\tag{85}$$

These equations are solved simultaneously for x_1' , y_1' , and z_1' . To aid interpretation, it is assumed that $x_0' = y_0' = A$.

The errors which can be expected in these calculations and their effect on the results of the matrix inversion will now be considered. The constants A and d may be determined to a high degree of accuracy and therefore will not be considered as having a detrimental effect on overall accuracy. For optimum accuracy, the factor vp/d^2 should be much less than 1. This means that the constant d which corresponds to the focal length of the optical system should be as large as practical. With a given value of d, the range A is chosen to restrict the field of view to the area of interest. With the foregoing assumptions, values of $d = 4$ in. and $A = 200$ in. were selected. The maximum errors obtained, assuming a 1% accuracy in measuring the position of the light in the image plane, were on the order of 0.25 in. in the values of x_1' , y_1' , and z_1' .

In order to assess the effect of this error on the matrix inversions, it was necessary to select four points arbitrarily located in the unprimed coordinate system, arbitrarily select the orientation of the unprimed system with respect to the primed system, calculate values of x_1' , y_1' , z_1' , and then perturb these values, invert the matrix, and observe the errors. The values chosen for the positions of the four points and for the direction cosines of the primed axes with respect to the unprimed axes are listed in Table I.

A worst case situation was simulated by perturbing the x, y, z, parameters 0.25 in. in such a way as to maximize the errors. This was done by inspection. The maximum error obtained in the parameters X_0 , Y_0 , and Z_0 was 0.25 in. while the maximum error in the direction cosines was 0.07. The expected errors, therefore, are within reason. The error in the direction cosine can be minimized by making use of the orthogonality of the coordinate axes.

As presently conceived, this method of position measurement would require off-line data processing. Motion pictures of the subject would be taken from the two vantage points, probably with color film to permit color coding of the various lights in a group. The film would then be projected on a convenient size screen

by means of a TV raster and projection system. The operator would cause positional data to be entered into storage by touching the images of the lights sequentially with a light pencil. The light pencil will detect the passage of the electron beam and gate information out of horizontal and vertical counters to define the position of the pencil. A fixed sequence of colors would be followed by the operator until all data on a frame has been entered. Then the operator will advance the film and repeat the procedure. Careful editing of the film prior to data reduction would be required to permit the readout of all significant data in a reasonable length of time.

TABLE I
PARAMETERS FOR ERROR CALCULATION

	x	y	z
P ₁	-2"	+4"	+3"
P ₂	+1"	+3"	-1"
P ₃	+3"	0"	+1"
P ₄	1"	2"	0"
d ₁₁ , d ₁₂ , d ₁₃	$-\frac{1}{2}$	$+\frac{1}{2}$	$\frac{\sqrt{2}}{2}$
d ₂₁ , d ₂₂ , d ₂₃	$+\frac{1}{2}$	$-\frac{1}{2}$	$\frac{\sqrt{2}}{2}$
d ₃₁ , d ₃₂ , d ₃₃	$\frac{\sqrt{2}}{2}$	$\frac{\sqrt{2}}{2}$	0

From the point of view of time required to digitize data, an automatic readout system would certainly be preferable. However, a number of considerations suggested the method described. First of all, extremely high frame rates would be required if the lights were time sequenced for identification. In addition, short term obscuration of a light could cause an automatic system to read out incorrect data. An operator, on the other hand, can estimate the position of an obscured light or make a decision to discard erroneous data. Extra lights may be located in each coordinate system to be measured so that the operator may select a group of four which will give the best data. This will largely prevent self obscuration from being a problem. The problem of one light passing in front of another is also eliminated.

A readout system involving an operator with a light pencil eliminates the necessity for a complex electronic system. This consideration must be weighed against the time required for an operator to obtain a sufficient amount of data.

In conclusion, the electro-optical technique appears feasible but entails the undesirable necessity of human handling of the data. Also, since the target lights must be mounted on the suit, the desired motion of the body is not transduced directly. It is felt that a more practical technique is necessary.

INERTIAL SENSING TECHNIQUES

Recent advances in the miniaturization of gyroscopic sensors prompted an investigation of their application to the measurement of a man's interlink angles. For the purposes of the initial discussion, the gyro can be considered to be a package which continually reads out its own orientation in the form of direction cosines, which are the cosines of angles between each axis of a coordinate system fixed in the gyro package and each axis of the laboratory coordinate system. The gyros do not intrinsically provide any position information, although if the constraints of their mounting are known, sometimes position can be deduced from orientation. Thus, for definition of shoulder position $\{\Theta_i\}$, $i = 2, 3, 4, 5, 6$, three gyro packages are needed to deduce the 5 shoulder angles. These are located at the spine, acromion, and upper arm.

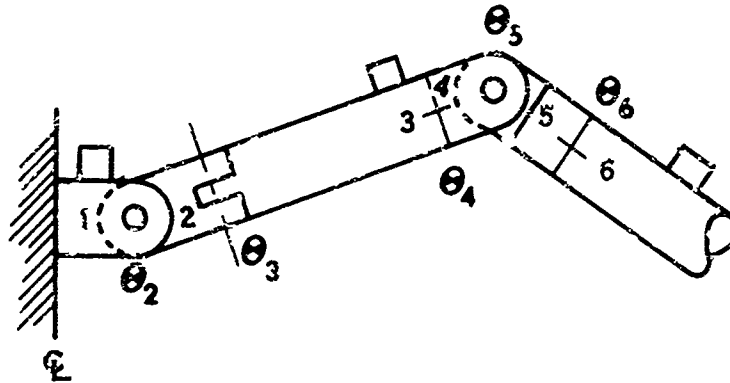


FIGURE 59. LOCATION OF GYRO'S ON SHOULDER COMPLEX

This breaks the problem down into two simpler ones. The more difficult of the two is considered here. The angles Θ_4 , Θ_5 , and Θ_6 are really the Eulerian angles in the roll-pitch-roll convention and can be handled by the techniques of Appendix I. The two gyro packages marked 3 and 6 give the matrices of direction cosines D^{L3} and D^{L6} which describe the orientations of links 3 and 6 with respect to the lab frame. In the notation of Appendix I,

$$D^{L6} = D^{L3} \tilde{D}_x(\Theta_4) \tilde{D}_z(\Theta_5) \tilde{D}_x(\Theta_6) \quad (86)$$

or

$$\tilde{D}^{L3} D^{L6} = \tilde{D}_x(\Theta_4) \tilde{D}_z(\Theta_5) \tilde{D}_x(\Theta_6) = D^{36} \quad (87)$$

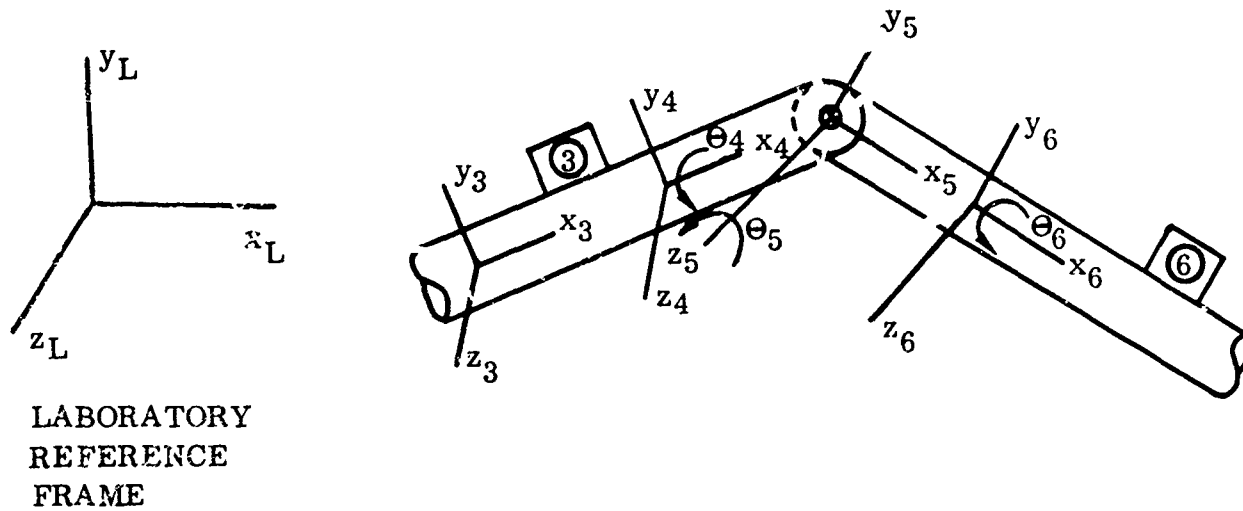


FIGURE 60. PROBLEM CONSIDERED FOR INERTIAL SENSING TECHNIQUE

When written out by components,

$$D^{36} = \begin{bmatrix} d_{11} & d_{12} & d_{13} \\ d_{21} & d_{22} & d_{23} \\ d_{31} & d_{32} & d_{33} \end{bmatrix} = \begin{bmatrix} C_5 & -S_5 & C_6 & S_5 & S_6 \\ C_4 S_5 & C_4 C_5 C_6 - S_4 S_6 & -C_4 C_5 S_6 - S_4 C_6 \\ S_4 S_5 & S_4 C_5 C_6 + C_4 S_6 & -S_4 C_5 S_6 + C_4 C_6 \end{bmatrix} \quad (88)$$

where

$$S_i \equiv \sin \theta_i \quad (89)$$

and

$$C_i \equiv \cos \theta_i \quad (90)$$

This matrix equation is equivalent to nine transcendental equations in the three unknowns θ_4 , θ_5 , and θ_6 . The three angles specify a unique orientation $D^{36}(\theta_4, \theta_5, \theta_6)$. However, D^{36} does not specify a unique set of angles because $D^{36}(\theta_4, \theta_5, \theta_6) = D^{36}[(\theta_4 + 180^\circ), \theta_5, (\theta_6 + 180^\circ)]$. However, if θ_5 is restricted to $-180^\circ < \theta_5 \leq 0$, then the equations can be solved for a unique set $\{\theta_i\}$. This corresponds to the anatomical fact that the arm can be abducted only 90° (to the horizontal) before the shoulder must be elevated (θ_2) to continue the motion. Thus, given the orientations of the gyro packages and the physical limit on the arm abduction angle, the arm position $\{\theta_i\}$, $i = 4, 5, 6$, can be found by

a straightforward (non-iterative) procedure. This technique is subject to errors caused by the compliance of the flesh on which the gyro packages are mounted. The extent of this error could only be determined by experiment.

Thus far the gyro has been treated simply as a black box which continuously reads out its orientation. In this section the transducers available for the inertial technique and their applicability, error, cost, and computational problems are considered individually. The three types of transducers (ref. 97) considered were:

1. Free gyros
2. Rate gyros
3. Rate integrating gyros

These generally come as one or sometimes two axis units which can be combined into the three axis packages needed for transduction of general motion.

THE FREE GYRO -- A free gyro is a constant speed rotating wheel suspended in a set of gimballed rings with orthogonal axes as shown in Figure 61.

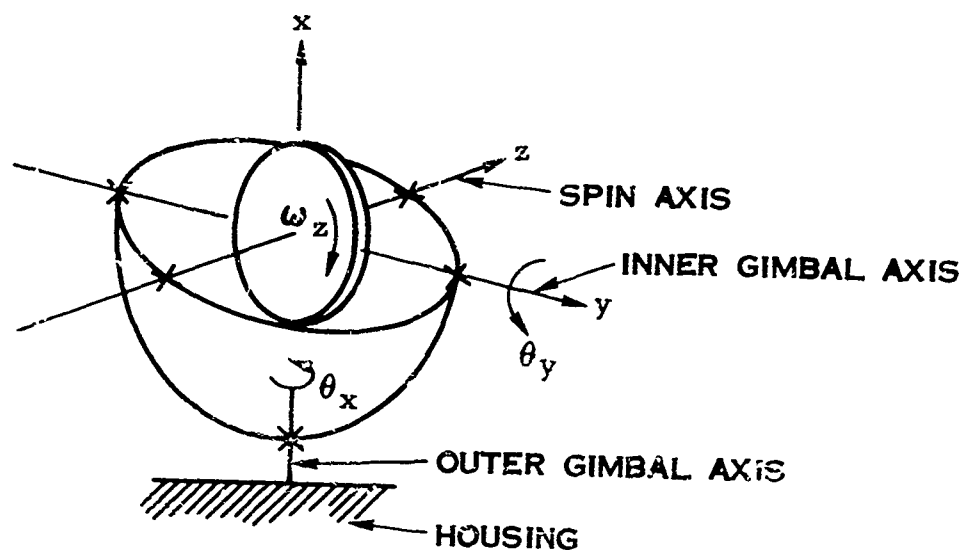


FIGURE 61. SCHEMATIC OF A FREE GYRO

With friction-free bearings on each axis, no torque can be applied to the spinning wheel by motion of the gyro housing. Angle transducers of the microsyn or potentiometer type can be used to measure either or both of the gimbal angles, i.e., the angle between the housing and the outer gimbal, θ_x , and the angle between the inner and outer gimbals, θ_y . These two angles are equivalent to the first two Eulerian angles in either the roll-pitch-roll or the yaw-pitch-roll sequence. For complete definition of orientation, a third angle is needed and must be obtained from another gyro unit. When this has been provided, the direction

cosine orientation matrix can be calculated from the equations in Appendix I or their equivalents. Thus, theoretically the orientation of a package of two or three free gyros can be computed directly from the electrical outputs at any instant of time. No integration or time history is required.

Hardware limitations, however, eliminate the free gyro as a transducer of general body angles. Θ_y must be limited to a travel of less than $\pm 80^\circ$ to prevent the condition known as "gyro lock", which occurs when the spin axis and the outer gimbal axis coincide. When this occurs, the gimbals rotate about the x axis because of spin axis bearing friction and the gyro must be "caged" to regain control.

Although the free gyro is inadequate for general motion studies, it can be useful for limited motion studies. A vacuum driven free gyro of the type used in aircraft has been useful in Apollo suit testing despite its large size (roughly a 3 inch cube). For horizontal motions this device replaces the pendulous flexometer used for motion in vertical planes. A miniaturized single-axis free gyro is typified by the Systron-Donner type PHU. This is a two-axis free gyro with unlimited range of travel about the outer gimbal axis. Θ_x is limited to 75° and is not transduced. The device weighs 9 oz and is 2.00" in diameter by 2.3" high. It drifts at a maximum of $1^\circ/\text{minute}$ and is linear to within 0.5% of full scale.

THE RATE GYRO -- The rate gyro is a "strapped down" device whose voltage output is proportional to the torque required to keep the rotor axis fixed with respect to the housing. Or, more generally, when the housing of the gyro is rotating in space with some angular velocity $\vec{\omega}$, the reaction torque is proportional to the projection of $\vec{\omega}$ onto the input axis, which is one of the body-fixed axes. Consider the stick drawing of a rate gyro in Figure 62. In the rate gyro the outer gimbal is fixed to the housing and the angle between the inner and outer gimbals Θ_y is limited by springs or a torsion bar with effective torsional spring constant k . $T_{yk} = -k \Theta_y$. When the housing is rotated about the input axis, a precessional torque T_{yp} tends to rotate the wheel and inner gimbal about the y axis. At a steady rate, this torque is proportional to the angular momentum of the wheel H_z and to the input axis angular velocity $\omega_x = \dot{\Theta}_x$ as shown by the relation:

$$T_{yp} = A \dot{\omega}_y - H_z \omega_x \quad (91)$$

When the oscillations have damped out so that $\dot{\omega}_y = 0$, the output angle Θ_y will be such that the sum of the precessional and spring torques is zero.

$$T_{yp} + T_{yk} = -k \Theta_y - H_z \omega_x = 0 \quad (92)$$

so that

$$\Theta_y = -\frac{H_z}{k} \omega_x = \text{constant } \omega_x \quad (93)$$

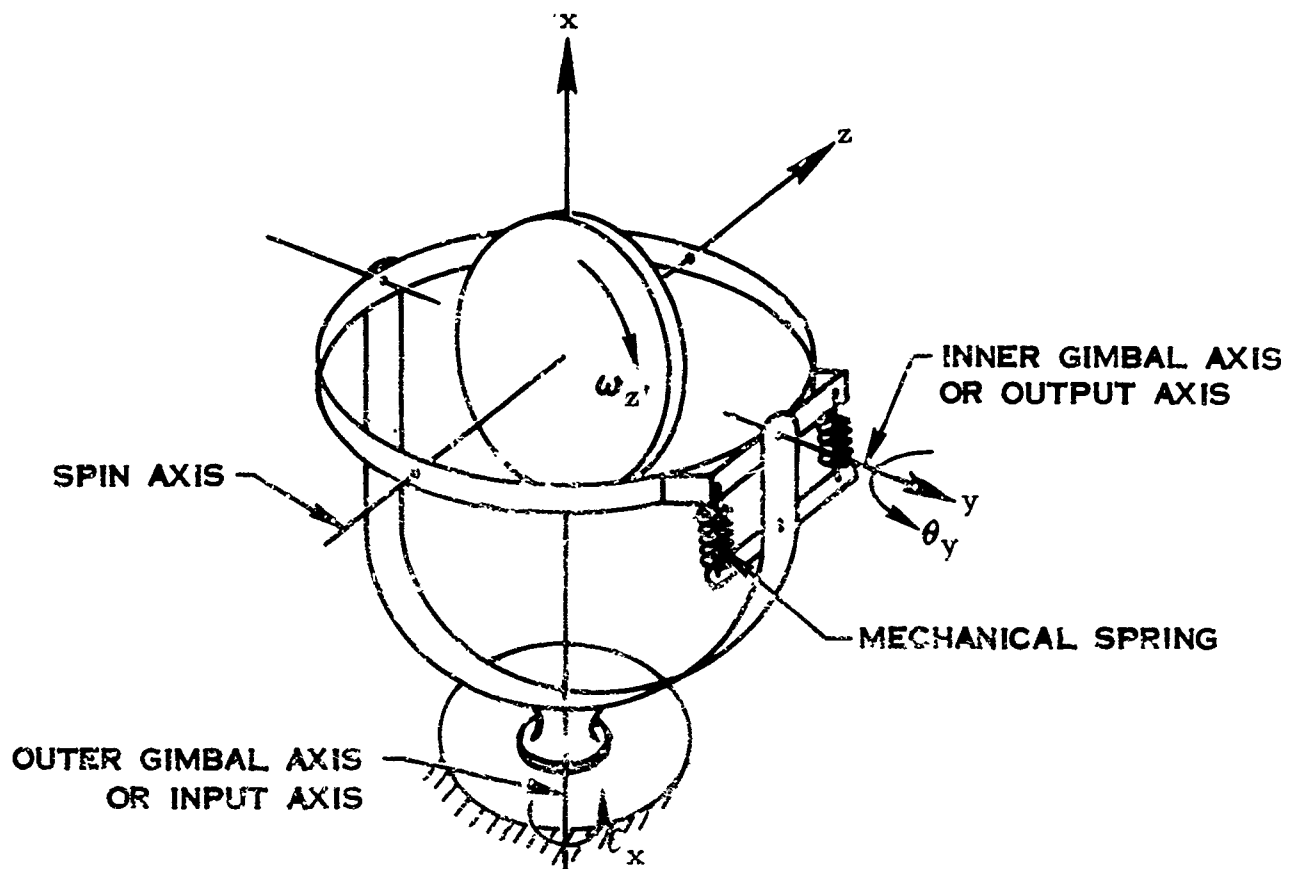


FIGURE 62. SCHEMATIC OF A RATE GYRO

θ_y is transduced with a potentiometer, torsional strain gages, or most frequently a microsyn pick off, and thus the voltage output is proportional to input rate. For single axis motion about the input axis, the input angle θ_x is simply

$$\theta_x = \int \omega_x dt \quad (94)$$

Feasibility of transducing single axis motion with rate gyros has been demonstrated in a controlled laboratory experiment.

For general motion a three-axis package must be provided and the computation of orientation is a great deal more complicated. The working equations and computational problems will be discussed here; the derivations are left to Kolk (ref. 63). Consider the three-axis rate gyro package on the n th link with body fixed axes $x_n, y_n,$ and z_n and the laboratory (inertial) reference frame with axes $x_L, y_L,$ and z_L as in Figure 63. The outputs of the gyro package are voltages (p_n, q_n, r_n) or simply (p, q, r) which are proportional to the projections of its angular velocity vector $\vec{\omega}_n$ onto its body-fixed axes. That is, $\vec{\omega}_n$ or $\vec{\omega} = p\hat{i} + q\hat{j} + r\hat{k}$. The elements of the orientation matrix D^{Ln} are d_{ij}^{Ln} or simply d_{ij} , which are the cosines of the angles between the i th laboratory axis and j th body axis. The Eulerian angles, in the yaw-pitch-roll convention, (see Appendix I),

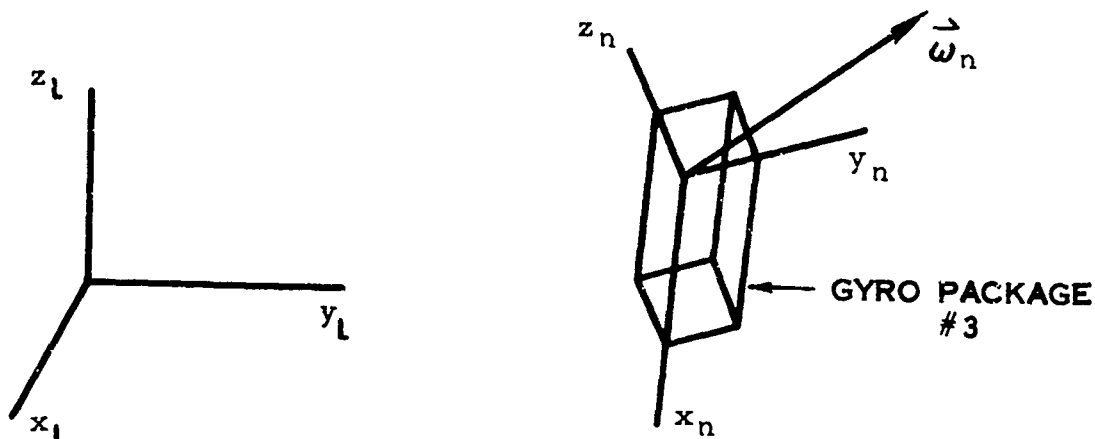


FIGURE 63. COORDINATES FOR THREE-AXIS GYRO PROBLEM

are Ψ , Θ , Φ . The d_{ij} 's or (Ψ, Θ, Φ) can be found as functions of p , q , and r by the integration of either of two sets of equations. For the direction cosines, these nine coupled linear first order differential equations must be integrated:

$$\begin{aligned} \dot{d}_{11} + d_{13} q - d_{12} r &= 0 \\ \dot{d}_{12} + d_{11} r - d_{13} p &= 0 \\ \dot{d}_{13} + d_{12} p - d_{11} q &= 0 \end{aligned} \quad (95)$$

$$\begin{aligned} \dot{d}_{21} + d_{23} q - d_{22} r &= 0 \\ \dot{d}_{22} + d_{21} r - d_{23} p &= 0 \\ \dot{d}_{23} + d_{22} p - d_{21} q &= 0 \end{aligned} \quad (96)$$

$$\begin{aligned} \dot{d}_{31} + d_{33} q - d_{32} r &= 0 \\ \dot{d}_{32} + d_{31} r - d_{33} p &= 0 \\ \dot{d}_{33} + d_{32} p - d_{31} q &= 0 \end{aligned} \quad (97)$$

For the Eulerian angles, these three coupled transcendental differential equations must be integrated:

$$\begin{aligned} \dot{\Psi} &= \frac{1}{\cos \Theta} (r \cos \Phi + q \sin \Phi) \\ \dot{\Theta} &= q \cos \Phi - r \sin \Phi \\ \dot{\Phi} &= p + \tan \Theta (q \sin \Phi + r \cos \Phi) \end{aligned} \quad (98)$$

Neither of these sets of equations can be solved in closed form so that computers and numerical integration techniques must be used. There are various advantages and disadvantages to each of the sets but they both require about the

same computation time and are both capable of about the same computation accuracy. (The discontinuities in $\dot{\psi}$ and $\dot{\phi}$ at $\Theta = 0$ can be handled by sophisticated computer techniques.) The most appropriate computation schemes are either second or fourth order Runge-Kutta integration (ref. 49). For example, sets of transducer readouts p , q , and r , can be converted into sets of direction cosines, d_{ij} by fourth-order Runge-Kutta integration on an IBM 7094 computer at the rate of 4500 sets per minute of computation time.

The number of sets of orientation matrices per unit of real time that are integrated depends on the allowable computation error and the maximum angular velocities. The cumulative computation error appears as a drift rate and is due to round-off of data (word length) and truncation (integration scheme and time interval). For example, if the angular velocities are less than $300^\circ/\text{sec}$ and an error of $0.1^\circ/\text{hour}$ real time can be tolerated, then the data points must be no more than 0.01 second apart in real time. 100 points per second are necessary for adequate definition of human interlink angles and their time derivatives. Thus, in the example chosen, the computation time for the orientation of a single link is roughly equal to the data acquisition time. Transduction of total body motion is thus theoretically possible but would be quite costly in computer time because many 3-axis packages would be required.

The error considered above was only that due to computation. The effect of instrument error must be added, but unfortunately it is difficult to assess. Instrument error, which is the difference between the indicated and actual angular velocities, contributes to system drift in a way that depends on the motion of the gyro. For a practical situation, the error can be determined by experiment.

The instrument error for rate gyros is due to non-linearity and hysteresis. The smallest commercially available rate gyros weigh about 3 oz., have a volume of 1.5 cubic inches, and are relatively expensive. They are linear within about 2% of full scale with a hysteresis of less than 0.1% of full scale.

Although the size and accuracy of current hardware are certainly inadequate for the suit transduction problem, there is a device being developed by the General Electric Company which shows promise. This device, which has been called a "solid state rate gyro", uses film circuitry to achieve a size of approximately $0.5 \times 0.5 \times 1.0$ inch. Its weight, while unknown, will be slight and its theoretical power consumption will be tenths of a watt. Resolution is expected to be of order of $.001^\circ/\text{sec}$. This device is based on the vibrating reed principle and has no rotor. When the device is rotated, Coriolis forces are imparted which drive the reed orthogonally to the direction of induced vibration. This orthogonal component is transduced and the output is proportional to the input angular rate.

THE RATE INTEGRATING GYRO -- The accuracy of rate measurement can be improved greatly with rate integrating gyros. In the rate integrating gyro the spring restraint of the rate gyro is replaced by a torque generator used to keep the wheel from precessing (i.e., to null Θ_y). As with the rate gyro, this restraining

torque T_{yr} is proportional to the input angular velocity. As shown in Figure 64, torque in the generator is developed by a current i_r which passes through a fixed resistor resulting in a voltage V_o proportional to angular rate.

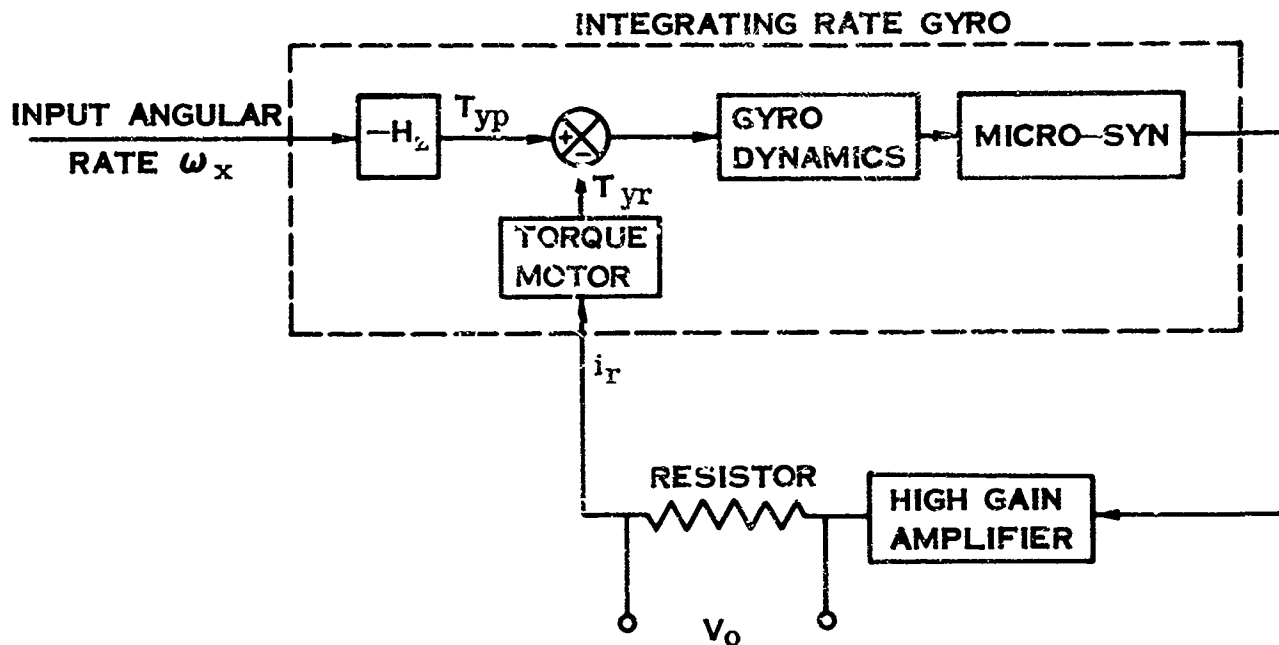


FIGURE 64. BLOCK DIAGRAM OF INTEGRATING RATE GYRO

Because this is a closed-loop nulling device, the errors are reduced by roughly an order of magnitude. Although the gyro can be packaged nearly as compactly as a rate gyro, the cost increases about ten times.

In conclusion, gyroscopic devices may be practical for single axis motion studies. The transduction of completely general motions is theoretically possible with rate or rate integrating devices but at present the hardware is too cumbersome, inaccurate, and costly to acquire and to use.

EXOSKELETAL TECHNIQUES

By far the most promising technique for dynamic measurement of the body interlink angles during general motion is an instrumented exoskeleton. An exoskeleton, as the name implies, is a jointed system of rigid links to be worn by a man which corresponds to and follows the motion of his body. The feasibility of such a structure has been demonstrated by the outstanding work of the Cornell Aeronautical Laboratories in their study of man-amplifiers (ref. 20, 75, 76). See Figures 65 and 66.

The CAL exoskeleton is a system of rigid links, some of which are adjustable in length, joined by 38 pin joints, which are instrumented for angle measurement, and one sliding joint. The linkage is attached to the body with leather

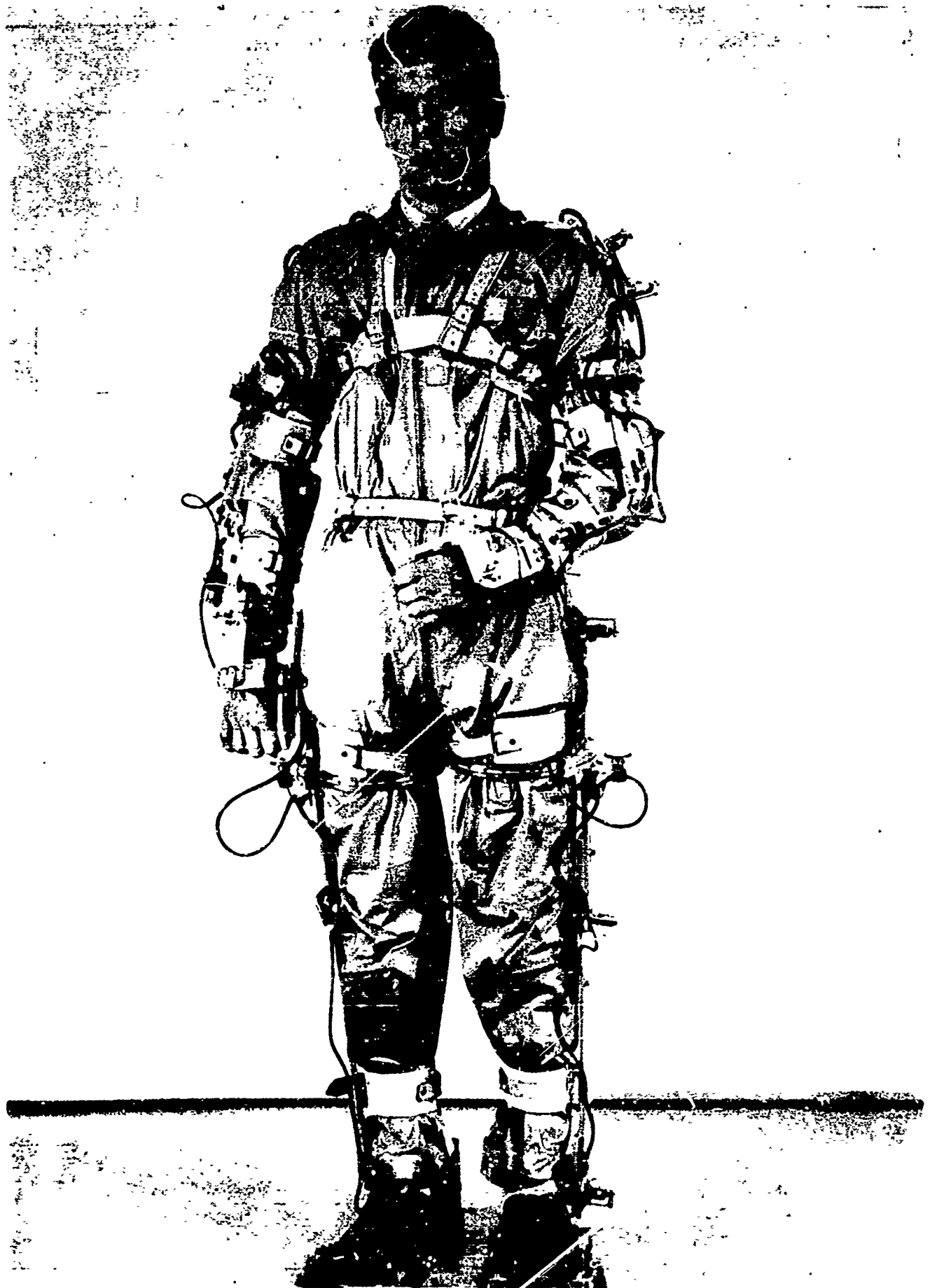


FIGURE 65. CORNELL AERONAUTICAL LABORATORIES
EXOSKELETON - FRONT VIEW



FIGURE 66. CORNELL AERONAUTICAL LABORATORIES
EXCSKELETON - REAR VIEW

harnesses and "Velcro" straps. There are adjustable stops at each joint which limit the subject's range of angular motion. Because of these stops, the device is much stronger and bulkier than would be necessary for a purely geometric application. The encumbrance of the device was evaluated on the AMRL Workspace Apparatus and reach rig and was found to be either satisfactorily low or unmeasurable. Thus the feasibility of a measurable exoskeleton has been established although a device for space suit evaluation may be very much different in appearance. Some typical angle versus time data for walking obtained from the CAL device are shown in Figure 68.

Conceptually, the application of an instrumented exoskeleton to the shoulder measurement problem chosen for study is relatively straightforward. For this discussion the exoskeleton is considered to be made up of m rigid links joined to one another by instrumented single degree-of-freedom joints, i.e., single axis rotating joints and nonrotating sliding joints. Some of the links are strapped firmly to the body. Thus, speaking in terms of the dummy shoulder model in Figure 67, the first link of the exoskeletal linkage would be firmly attached to link 1 of the dummy and the m th to link 6 of the dummy. It is assumed that a linkage geometry has been chosen which does not impede motion of the shoulder and arm. As stated before, the measurement problem is to find R_{16} and D , the position and orientation of link 6 with respect to link 1.

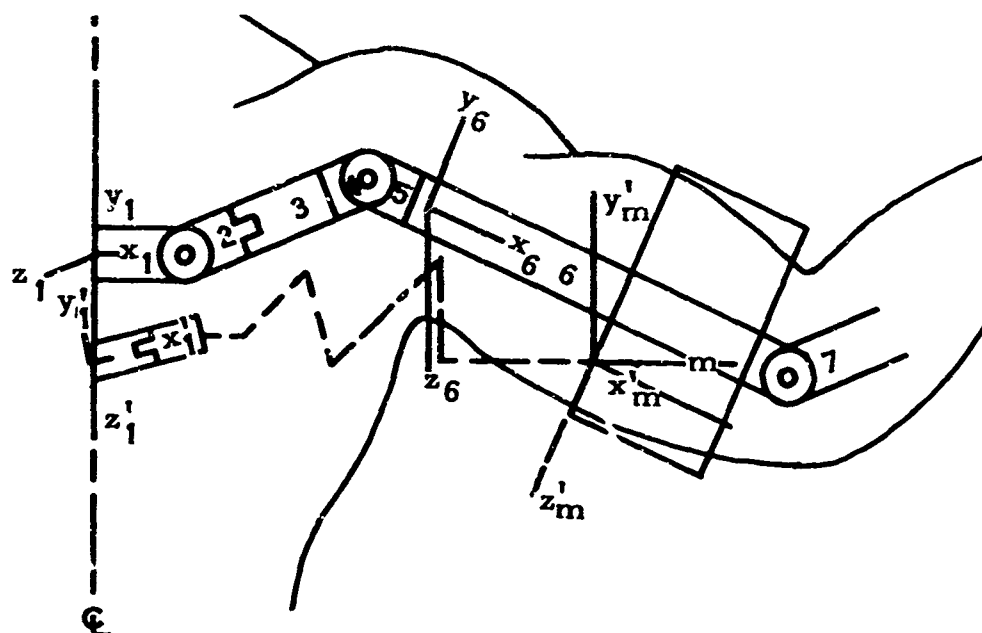


FIGURE 67. RELATION OF GENERALIZED EXOSKELETON LINKAGE TO DUMMY LINKAGE

Let the position and orientation of the first exoskeleton link with respect to the first dummy link be described by the vector \vec{Q}_1 and the matrix M_1 . Similarly let the position and orientation of exoskeleton link m with respect to dummy link 6 be described by \vec{Q}_6 and M_6 . As shown in Appendix VII, the position \vec{R}_{1m} and

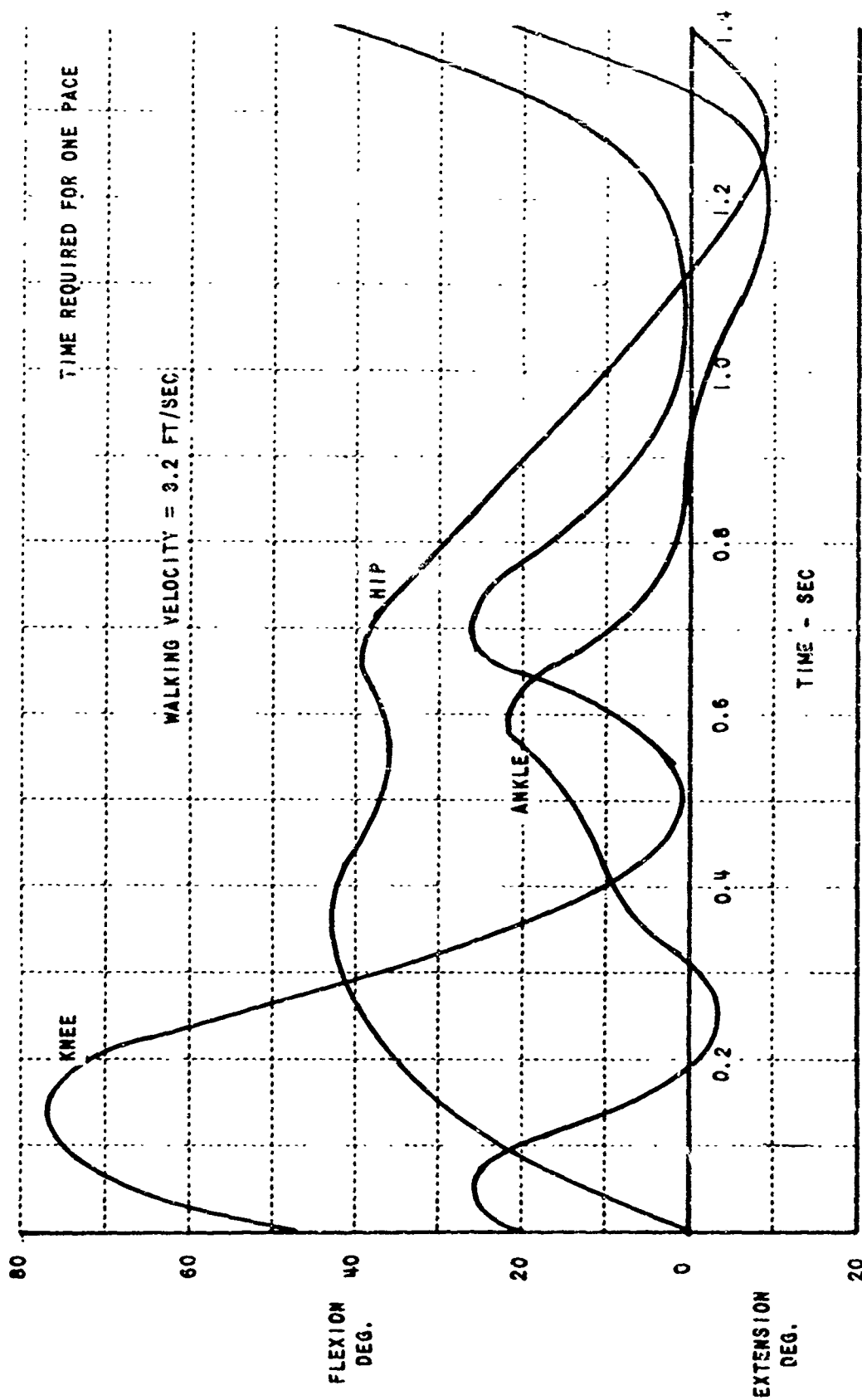


FIGURE 68. TIME HISTORY OF HIP, KNEE, AND ANKLE POSITION DURING STRAIGHT, LEVEL WALKING AT NORMAL WALKING RATE (REFERENCE 75)

orientation D of the m th exoskeleton link with respect to the first can be written as functions of the transduced angles and lengths ϕ_2 through ϕ_m . That is,

$$\vec{R}'_{1m} = \vec{R}'_{1m}(\phi_2, \phi_3, \dots, \phi_m) \quad (99)$$

and

$$D' = D'(\phi_2, \phi_3, \dots, \phi_m) \quad (100)$$

Then from

$$\vec{R}_{16} = \vec{Q}_1 + \vec{R}'_{1m}(\phi_2, \phi_3, \dots, \phi_m) + \vec{Q}_6 \quad (101)$$

and

$$D = M_1 D'(\phi_2, \phi_3, \dots, \phi_m) M_6 \quad (102)$$

the dummy interlink angles $\{\Theta_i\}$ can be found by solution of Equations 76.

The calculations of \vec{R}'_{16} and D' involve only the simple multiplications and additions of the transduced quantities; no integration or iteration is required. The Q 's and the M 's are obtained by calibration with the exoskeleton on the dummy and are assumed constant. The accuracy of the technique depends primarily on this assumption. Physically, this is equivalent to assuming that the first and last exoskeleton links can be rigidly fixed to the subject's spine and humerus bone. This appears to pose no problem since the exoskeleton can be very light and nearly frictionless. Because the method of attachment to the dummy and the human subject is the same, the attachment errors should be partially self-cancelling. Similarly, all other conceivable techniques are subject to the same assumption unless the targets or sensors are pinned through the skin to the bone as discussed in reference 34. The other error source is instrument error in the potentiometers which can be as low as 0.5% of full scale. Transduction of the whole body (less the digits) is just as feasible as the shoulder transduction because the shoulder is the most difficult problem. With the addition of more links and potentiometers, the mathematics increases in quantity but not complexity because a section of linkage between strap-on points is isolated mathematically from the rest of the problem. With the exoskeletal technique, there are no shadowing or field-of-view problems because there is no reference to a laboratory coordinate system. No manual data handling is required except for editing, and there is no drifting or integration involved to cause accumulating error.

HARDWARE IMPLEMENTATION -- The exoskeletal technique is clearly the most practical, accurate, and economical method of obtaining dynamic human position data. Further, it appears possible to devise such an instrument to be worn under a space suit. This would not be strictly an exoskeleton because some of the links might be flexible. The feasibility of this approach has been partially

demonstrated by the work with "Elgons" at the Physiological Research Laboratory of Springfield College in the evaluation of athletic performance (ref. 1). The most recent models of the "Elgon" are shown in Figures 69 and 70.

The "Elgon" employs a very small commercial conductive film trim potentiometer measuring approximately 0.28 inch in diameter by 0.11 inch thick. Fastened to the plastic case and the rotor of the potentiometer are thin, flexible, plastic straps which form the limb links of the exoskeleton. When they are properly fastened to the joint of a human test subject, his interlink angular motion can be transduced directly for simple joints. Springfield College has installed "Elgons" on many test subjects to transduce joint motion. A most difficult task was accomplished in the measurement of angular motion of the big toe while an athlete wore a track shoe and did high jumps. This example should serve to illustrate the small size and relative nonencumbrance of this device.

Insofar as accuracy is concerned, a calibration of one of the Springfield College "Elgons" was made and it was shown to be approximately 1% accurate in the mid-100° region of its 360° total range. The potentiometer, being of the film type, has rather severe distortion of output at the extremes of its overall range because of film thickness and area effects near the film electrical connections; hence, in the actual application, care should be taken to avoid regions of extreme nonlinearity when matching goniometer angle to human joint angle. To make a complete electrogoniometer to be worn under a space suit would probably involve strain gage transducers as well as potentiometers. Repeatable placement of the device on a calibrated test subject could be achieved by locating datum holes in the exoskeleton links or straps over microscopic dots tattooed on the subject. If the device were flexible, then perhaps a more sophisticated mathematical approach than the simple one presented above would be required. Theoretically, the mathematical requirements of an exoskeletal device for shoulder transduction is that each set of transducer outputs corresponds to a unique shoulder position. The uniqueness need not hold in the reverse sense. Mathematically speaking, the mapping of the space of dummy angles onto the space of exoskeleton outputs need only be homomorphic, not isomorphic. The development of an instrumented exoskeleton for use under a suit would require some clever engineering and theoretical work, but it certainly appears feasible at this time.

In use, the outputs of the potentiometers (and strain gage transducers) would be routed to signal conditioners in the control console of the data acquisition system described in Section VIII. The conditioned outputs are fed to "quick-look" editing devices to insure that the test subject (or dummy) is performing the desired maneuvers repeatably. The edited outputs are then continuously recorded for storage on digital magnetic tape in a computer compatible format. The tape, together with the computer program, would be processed and the results displayed in the form of fan-folded data tabulations, control tape for dummy motion programming, and oscillograms of body angles versus time. Other readouts are also possible, if desired.



FIGURE 69. ELGONS ON HAND

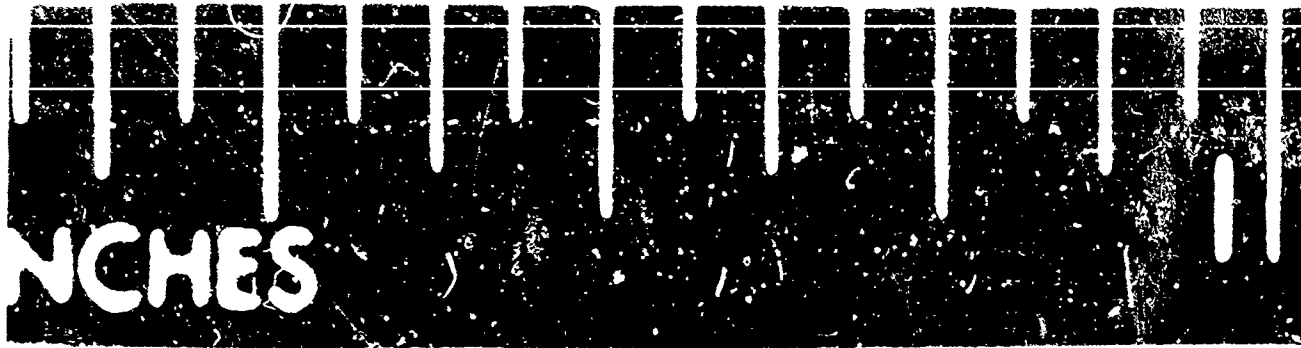


FIGURE 70. CLOSE-UP OF ELGON

Conclusions On Torque And Angle Measurements

Based on the preceeding discussions it is clear that the objective, accurate, and meaningful determination of suit torque requires development of techniques, procedures, equipment, and criteria which do not currently exist. Despite the fact that many of the areas require further study and testing, the general methodology for suit torque evaluation can be defined. The evaluation procedure requires the following steps:

1. Gather data for a statistical definition of the mission in terms of the set of body interlink angles $\{\Theta_i(t)\}$ and angular velocities $\{\dot{\Theta}_i(t)\}$ as functions of time. This would involve a human test subject wearing an exoskeletal electrogoniometer under the space suit. He would simulate the parts of the mission of interest while the electrical outputs $\{\Phi_j\}$ are being recorded on magnetic tape. This step would be omitted if mission data is already available from previous tests or if a standardized mission profile is to be used for a general evaluation.
2. The suit is then put on an articulated, powered anthropomorphic dummy which has been instrumented for determination of the suit torque vector at each joint. Each dummy joint is flexed in turn at several constant angular velocities. The torque and angle data are also entered on magnetic tape; that is, for each joint $\bar{T}_1(\Theta_1, \omega_{11})$, $\bar{T}_1(\Theta_1, \omega_{12})$, etc. would be recorded.
3. After editing, both of the data tape reels and a program reel would be fed into a computer which would compute the actual suit torques and figures of merit for the whole suit or any of its joints based on metabolic and coordination criteria. The computer would also plot out the torque surfaces for any joint of interest so that the trouble areas can be spotted. These steps are summarized in Figure 71.

In spite of its feasibility, nearly all of the hardware and data needed for this approach do not exist today. Thus a long-range development and research program is required to acquire the necessary equipment and know-how. The following necessary items of hardware already exist:

1. The AMRL Workspace Apparatus.
2. Adequate computing facilities.

These items must be developed:

1. An instrumented powered anthropomorphic dummy.
2. An instrumented exoskeleton to be worn under the suit.

3. An analog/digital data system for acquiring, processing, and recording the man/suit motion and torque data.

Concurrently, basic studies of the relationships of measureable mechanical quantities such as torque, angle, and velocity to muscle metabolism and overall metabolic cost are needed. Likewise, studies of the relationship between off-axis torque components and coordination are required to define criteria for the suit tracking problem.

Meanwhile, torque and angle measuring techniques such as those described in a forthcoming Grumman document can be exploited until more accurate and sophisticated techniques become available (ref. 89).

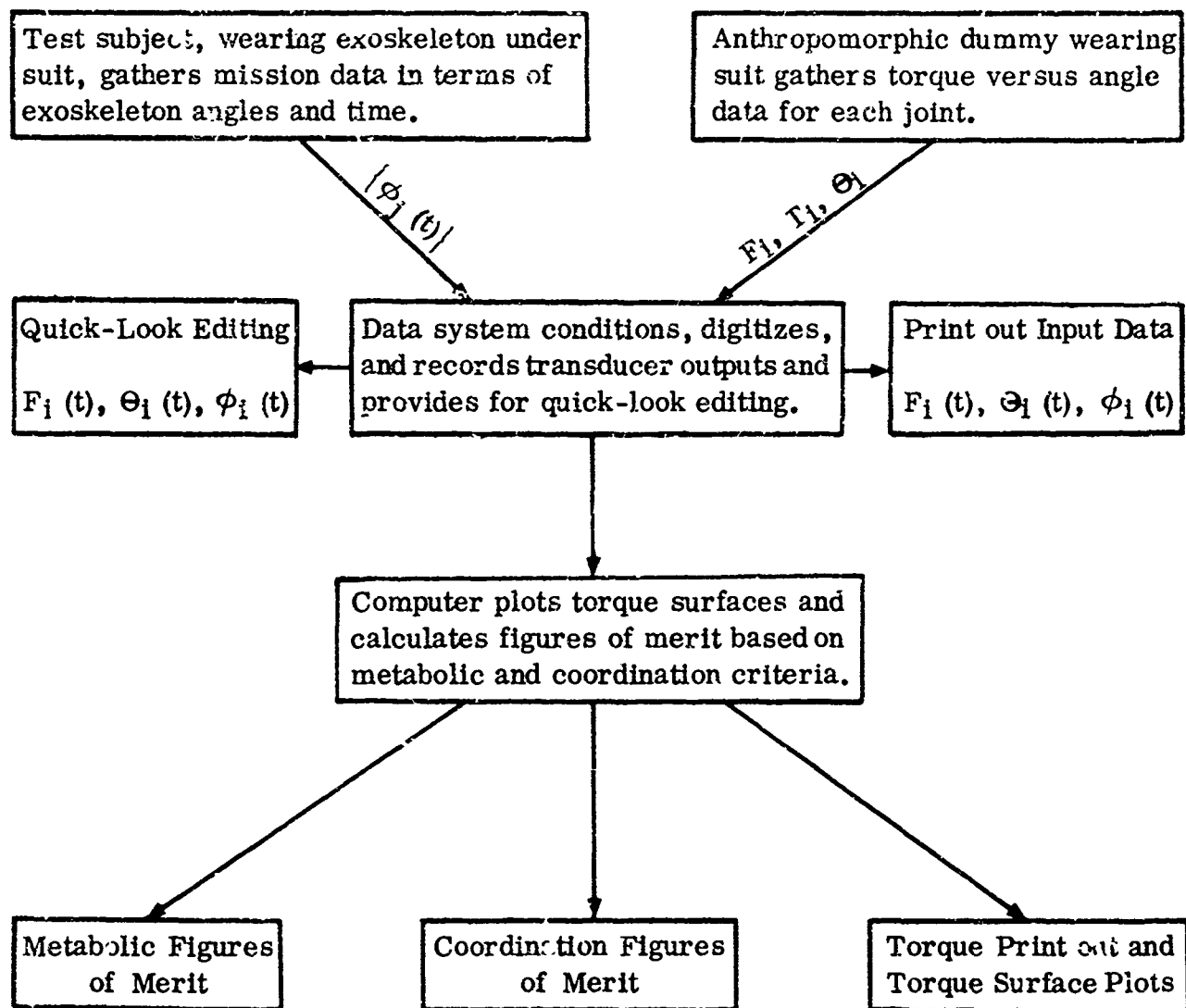


FIGURE 71. DATA FLOW FOR FIGURES OF MERIT

MECHANICAL LOAD DISTRIBUTION

Introduction

Thus far, the causes, effects, and measurement of the torques that a space suit imposes on a man have been treated. It has been shown that torque vector at a joint is a net effect of the mechanical loading of the suit on the limbs and is appropriate for describing the restrictions of the suit on man's angular motions. For the torque measurements, the distribution of the loading was unimportant; however, the distribution of mechanical load is important for other reasons and is considered in this section. Specifically, the quantity of interest is the mechanical pressure imposed by the suit on the man as a function of position on the skin surface and of body interlink angles. A precise definition of mechanical pressure is given later.

The mechanical pressure distribution is of interest in two basic problems: (1) the highly subjective problem of comfort, (2) the description of the forces contributing to the joint torques. In fact, knowledge of the mechanical pressure distribution completely describes the mechanical interface between the suit and the man.

Definitions

The description of pressure distribution necessarily involves also a definition of position on the body surface. Position on any physical surface can be defined by a system of two surface coordinate parameters as in latitude and longitude on the earth's surface. Figure 72 illustrates how the surface coordinates might appear on the arm.

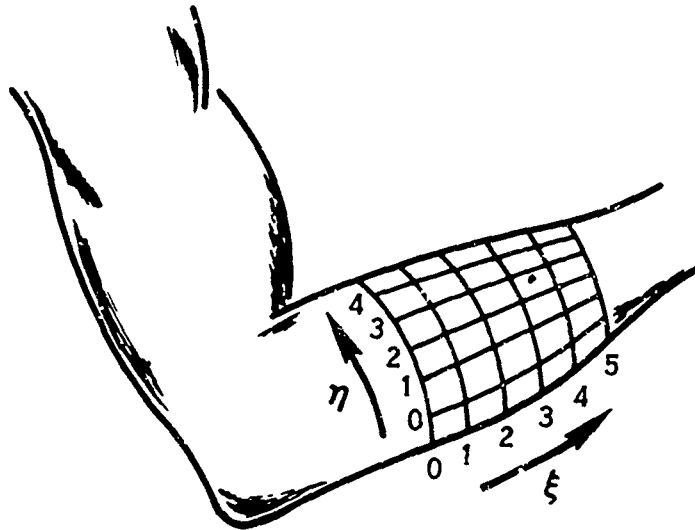


FIGURE 72. SURFACE COORDINATES ON ARM

These are to be considered painted on the skin so that flexibility is not a conceptual problem. A particular point on the skin is designated by giving its coordinates (ξ, η) interpolated between coordinate lines. The point in the figure would be (3.5, 2.8). The lines need not be orthogonal.

To define mechanical pressure, consider an area of the skin A_1 centered at the point (ξ_1, η_1) with a net force vector \vec{F}_1 acting on it. The average mechanical pressure is \vec{F}_1/A_1 . Now as A_1 approaches zero, \vec{F}_1 does also, but the ratio approaches a unique value at the point (ξ_1, η_1) . Thus the mechanical pressure at (ξ_1, η_1) is

$$P(\xi_1, \eta_1) = \lim_{A_1 \rightarrow 0} \frac{\vec{F}_1}{A_1} \quad (103)$$

Since the definition holds at all points, the subscripts can be dropped leaving the vector $\vec{P}(\xi, \eta)$. It is seen that pressure is a point function, whereas a force acting on a mathematical point is physically impossible. Thus, the mechanical load distribution over a surface is the value of \vec{P} at all points on that surface.

The pressure vector can be written $\vec{P} = P\hat{u}$ where \hat{u} is a unit vector defining the direction of the pressure and P is the magnitude of \vec{P} . In the special case where \hat{u} and \hat{n} , the unit inward surface normal, are equal, then \vec{P} is normal to the surface at that point and P is the familiar hydrostatic pressure. In general, however, the magnitude of the normal component is $\vec{P} \cdot \hat{n} = P_n$. The magnitude of the tangential component is $P_T = |\vec{P} \times \hat{n}|$. P_T exists because the skin will support shear stresses applied through friction.

Nature And Cause Of Mechanical Loading

Discomfort due to mechanical loading falls into two basic categories: (1) the low but continuous normal pressure applied over a long period of time and (2) chafing which involves an oscillating tangential component of pressure due usually to the activity of the subject. The short-term high normal loads which cause instant pain are considered beyond the realm of discomfort. They can be handled at the subjective level.

Because friction requires a contact force, there must always be a normal component of pressure where a tangential component exists. Discomfort due to chafing can build up very fast when the subject is performing a repetitive task. For instance, when walking in a pressurized suit, the subject's heel generally lifts off the sole of the boot before the boot leaves the ground. This results in an oscillatory P_T which can soon lead to blisters and bleeding if the foot is not adequately protected.

The long-term problem of discomfort due to continuous normal pressures P_n is considered by some to be the greatest single problem in space suit design. If, for any reason, capsule pressure is lost on a space flight, the astronauts will have to complete the journey with their suits pressurized. For lunar trips, this could amount to five days or more. When the applied pressure P_n is greater than the local systolic blood pressure, local circulation will be interrupted and skin lesions can result. The problem is pathologically similar to the bedsore problem studies by Lindan and Hickman (refs. 3, 49), who measured the pressures and times required for the onset of decubitus ulcers.

The normal loading of the suit is due to the torque required to move it and may be uniformly distributed over a limb surface, or may be localized due to pinching and buckling of the suit. For transducer resolution purposes, the loading is assumed to be primarily local due to creases with minimum radius of 1/8 inch. The undergarments and lining of the suit tend to distribute the mechanical pressure so that the skin surface pressures are moderated. In the liquid cooled suit, however, the cooling tubes lie against the skin and can create local high-pressure areas. Seams, connectors, joint rings, and other prominences of the suit can also cause high local pressure.

Although no data on suit mechanical pressure distributions appear in the literature, transient normal pressures of 1000 mm Hg (20 psi) and continuous values of 100 mm Hg (2 psi) must be commonplace. If the coefficient of static friction between the suit lining and the skin is high, the tangential component of pressure can have similar values.

Load Distribution Criteria

There is little useful quantitative data on the correlation between discomfort and mechanical pressure and, therefore, before criteria for the evaluation of comfort can be established, a great deal of testing must be done. Aside from subjective variations, the correlation will depend on the location of the skin surface (ξ, η), duration of pressure, and area over which pressure is applied.

For short-term loading Fogel (ref. 37) quotes 200 gm/mm² as a typical threshold of pain. This pressure is equivalent to 14,500 mm Hg (280 psi). If this pressure were applied over several square inches, severe tissue damage would result; yet for small areas it is a threshold figure. This points out the need for area as well as pressure considerations.

Generally, for long-term loading, the applied pressure should not exceed the local capillary pressure, about 25 mm Hg (0.5 psi). Pressures much greater than this will eventually cause lesions. Average pressures of 10 mm Hg have proved tolerable for one day or more in tests with earphone cups. (ref. 74).

If the pressure data are used to describe the joint loading which causes the suit torque, then no criteria are appropriate. The data must be displayed so the design engineer may visualize and intuitively or analytically interpret the test results.

In summary, few if any criteria on load distribution exist which are useful for suit testing. This may, in part, be due to the lack of transducers to gather data for correlation with subjective comfort evaluations.

Ideal Measurement And Display Techniques

Consideration of ideal measurement schemes is useful as a philosophical guideline and in weighing the inevitable compromises of measurement hardware. The ideal mechanical pressure transducer would be in the form of a garment so thin that when worn under a space suit it would not change the levels of normal mechanical loading significantly. The garment would have to stretch with the skin during body movement and would have a skin-like texture so that the tangential load components would be unaltered. The transducer would be scanned for P_n and P_T as continuous functions of body surface position.

Because of the varied uses for the data, both on-line and off-line displays are desirable. The on-line display which would show the experimenter at a glance where the trouble spots are and when improvement was being made would be used for suit fitting and development. The display should be anthropomorphic in shape and should have two modes of operation: one for display of $P_n (\xi, \eta)$, and the other for $P_T (\xi, \eta)$. The off-line display which would be used for acceptance testing, comfort evaluations, and joint development would be pressure contour plots like the isobars of weather maps. These displays are well suited for interpretation of the mass of pressure data involved in a scan of the surface. The points of maximum pressure are located immediately and the gradients are indicated by the spacing of the contours.

Pressure Distribution Measurement Techniques

The existing hardware and data for load distribution measurement has come from studies of man's weight distribution over his supporting surface or seating area. Although these techniques are not suitable for the suit measurement problem, they are discussed here briefly to point out the difficulty of this kind of measurement and to illustrate some of the data. In the literature, only the transduction of normal pressure is attempted. Shear loading presents a higher level of difficulty and has not been attempted.

DISTRIBUTION OF BODY WEIGHT OVER SUPPORTING SURFACE

Pressure distribution transducers can be classified into "continuous" or nearly infinite resolution types and discrete types which measure the net force on a known area, thus measuring the average pressure.

The continuous types have been used in the seating comfort studies of Hertzberg (ref. 48) and Swearingen (ref. 106) and led to pressure contour plots. Hertzberg describes "a boxlike structure, about 2 feet cubic, whose top is a sheet of thick transparent plastic. This plastic is edge-lighted by a green fluorescent tube concealed inside the box. Underneath the plastic is a large mirror set at 45° to the horizontal. On top of the plastic lies a very thin sheet of latex rubber. When the subject stands on the latex sheet, he presses it close to the plastic, causing a bright green glow in the regions of high pressure and a duller glow in the zones of lower pressure." This device was modified with adjustable back and foot rests for seating pressure evaluation.

Swearingen's technique used "absorbent paper over inked corduroy cloth. Density of ink transfer was calibrated in lbs/in^2 and the seating pressure prints evaluated using a photometer."

Neither of these techniques is truly infinite in resolution, but the resolution is certainly adequate for seating or space suit studies. However, obvious handling problems make them impractical for suit work.

Several discrete force transducer arrays have been developed for seat pressure study. The "Universal Test Seat" of Lay and Fischer (ref. 67) for automotive studies appears to be the first general study. They measured the deflections of calibrated springs to determine force. The "Filpip" of the Franklin Institute (ref. 38) is an array of thin pressure sensitive capacitors on a flexible blanket. The sensitivity was adequate but the shielding required because of the high impedance and high frequency would be prohibitive for space suit applications. A most interesting study was performed at Case Institute of Technology and Highland View Hospital in Cleveland, Ohio (ref. 68). That study concerned the onset of decubitus ulcers (bedsores) as affected by normal pressure distributions applied for various periods of time. One of the transducers is a rubber-like blanket with an array of 1886 pneumatic cells on one centimeter centers. The inside surfaces of each cell form the contacts of a switch which opens when the supply pressure reaches the average applied pressure on the cell. A ramp pressure is supplied to the blanket and data is recorded automatically by photographing an array of lights which corresponds to the cell matrix. Six runs can be made on a subject in two hours. Figure 73 is the pressure distribution of a 61.9 kg (136.5 lb) female control subject seated on a 2.5 cm foam rubber sheet with feet supported.

This is the type of data sought for suit loading but the technique is too slow for pressure suited subject to remain still during a pressure sweep (6 min). Also, the bulk of the device even if fitted to a man would change the quantities being measured.

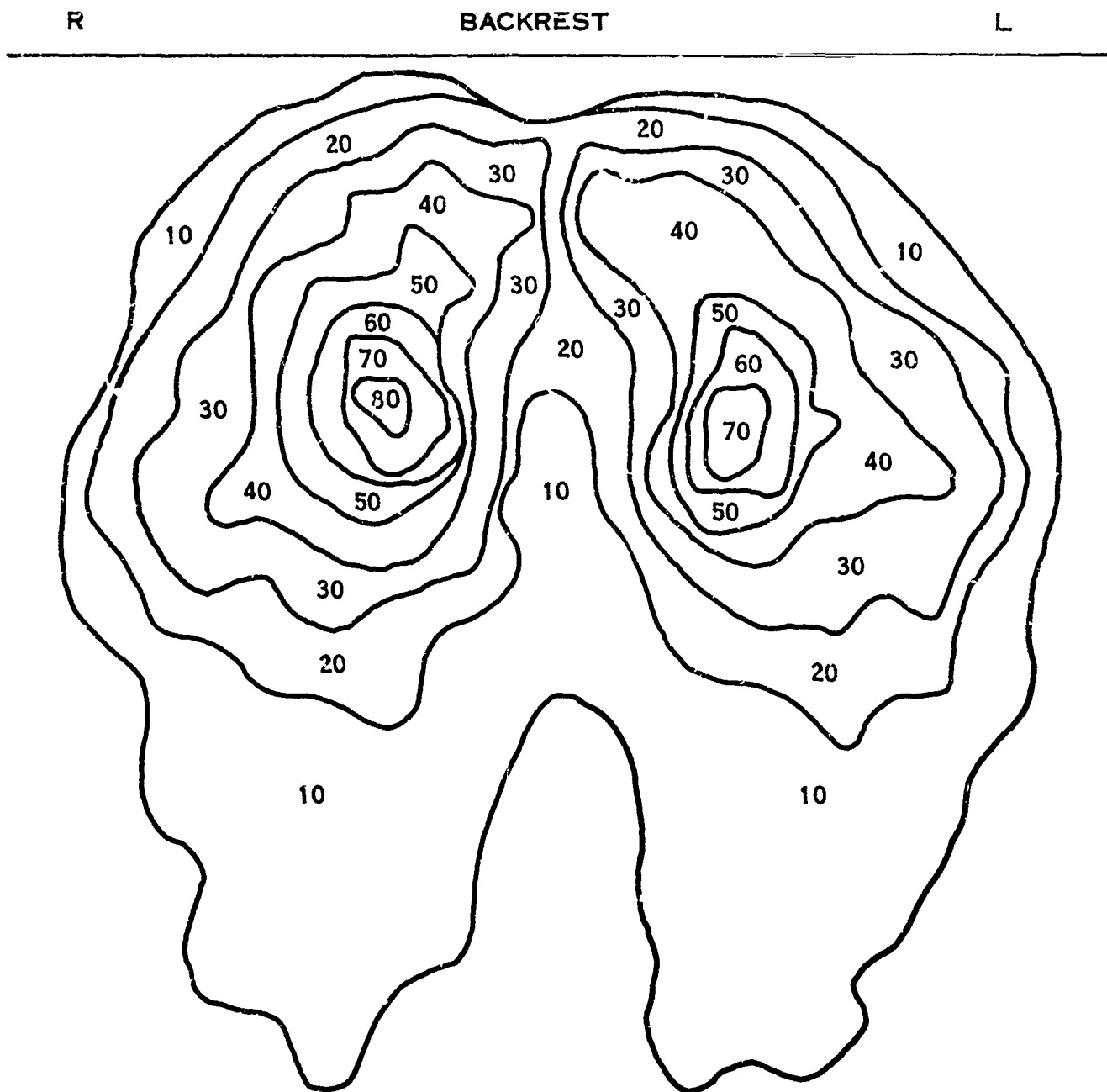


FIGURE 73. SEATING AREA PRESSURE DISTRIBUTION. FEMALE CONTROL SUBJECT ON 1" FOAM RUBBER, WITH FEET SUPPORTED. 25 YRS., 136.5 LBS. ISOBARS ARE IN mm Hg

Transducer Concepts For Suit Application

In the search for applicable transduction techniques, only normal loading was considered. Also, only discrete force transducers were considered because continuous pressure transduction does not appear feasible in an automatic system under a space suit. With the normal force restriction, the transducer must not only be insensitive to but must also be incapable of supporting tangential forces. Collectively, the transducers must support the total suit load including any external loads on the suit surface. Desirable properties would include thinness, flexibility, a variety of shapes, low impedance, high sensitivity, low cost, low temperature sensitivity, moderate accuracy (5% to 10%), and frequency response to 50 cps.

Commercial transducers with all these characteristics are not available. There are miniature (0.25" dia. x 0.020" thick) strain gaged diaphragm pressure transducers available, but these are designed for measurement of fluid pressure and require uniform loading over the sensitive surface. Because of the limited market, the industry shows little interest in developing force transducers with the proper qualifications for the suit pressure distribution problem.

Therefore, a limited feasibility study of transducers was undertaken. The concepts considered included pressure sensitive materials such as carbon and manganese dioxide with various binder and electrode configurations, strain gaged elastomeric devices, and strain gaged metallic structures.

PRESSURE SENSITIVE MATERIALS

This concept holds considerable appeal because of the inherent low cost, thinness, and variety of shape. An inherent low cost is only of value, however, if the output signal is readily compatible with inexpensive electronic circuits. Perhaps the most desirable material would have a conductivity S proportional to stress σ , $S \propto \sigma$. Consider the following simple model.

The sensitive material is spread out as a lamina of thickness h and any outline shape on the x, y plane with electrodes as in Figure 74.

The following assumptions which are reasonable in a first-order calculation are made:

1. The materials are electrically and mechanically isotropic.
2. Deformation of the material is negligible.
3. The upper electrode is such that pressures acting on it are transmitted directly to the sensitive material.

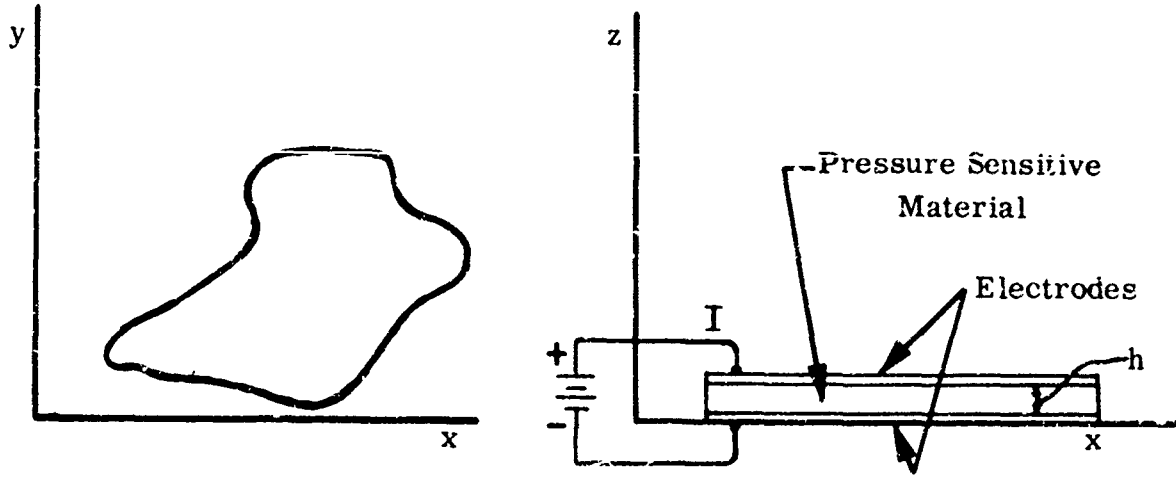


FIGURE 74. IDEAL LOAD DISTRIBUTION TRANSDUCER

4. The conductivity in any direction is proportional to the stress in that direction. (The stress tensor is proportional to the conductivity tensor.)
5. The material is thin enough so that the electric field lines are all parallel to the z axis.

Using these assumptions, the compressive stress in the material σ_{zz} is uniform and equal to the normal mechanical pressure P_n .

$$P_n = \sigma_{zz} = \sigma \quad (104)$$

The conductivity is proportional to stress $S = k \sigma$ so that

$$S = k P_n \quad (105)$$

But the conductivity is defined by the relation between the current density \vec{J} and the electric field \vec{E} .

$$\vec{J} = S \vec{E} \quad (106)$$

The magnitude of the electric field $E = \frac{V}{h}$ where V is the voltage applied to the electrodes. Thus

$$J = \frac{SV}{h} = \frac{kV}{h} P_n \quad (107)$$

The current $I = \int J \, dx \, dy$, so that

$$I = \int \frac{kV}{h} P_n(x, y) \, dx \, dy \quad (108)$$

But the normal force $F_n = \int P_n(x, y) dx dy$, so that

$$I = \frac{kV}{h} F_n \quad (109)$$

where k is a property of the material, h is its thickness, and V is the applied voltage.

Now the desirability of the assumed response law is apparent. The conductance $\frac{kF_n}{h}$ depends only on the force, not on how it is distributed. Also, note that the conductance is independent of the area and shape of the transducer. Thus, to the extent to which the above approximations are valid, a sandwich of pressure sensitive material between two conductors could be made up, then cut to any size and shape, loaded in any way, and the conductance would depend only on normal force. With these highly desirable features in mind, some materials were investigated.

The first material tested was the pressure sensitive paint manufactured by the Clark Electronics Laboratories in Palm Springs, California. This paint appears to contain graphite and silicon dioxide mixed with a solution of neoprene in benzene. When the benzene evaporates, the remaining carbon-filled rubber changes resistance with pressure. From the manufacturer's literature, the paint appeared to obey the desired response law. Several transducers were made following the instructions of the manufacturer (ref. 19) as well as several variations and, as claimed, the conductance varied strongly with pressure. Also for any one test, the conductance was fairly linear with pressure. Unfortunately, the conductance of all prototypes tested also varies strongly with time t (creep) and with the sign of $\frac{\partial F_n}{\partial t}$ (hysteresis). The curves were unrepeatable from run to run.

Because of these other variables, the paint was considered unsuitable for space suit applications. It was subsequently found that several other experimenters (refs. 10, 71, 109, 110) had found similar results as well as aging, temperature effects, and discontinuities in the resistance-force curves.

In further pursuit of this approach, neoprene was filled with carbon black and then pressed into sheets. The resulting transducers had high sensitivity but again had unacceptable creep and hysteresis. It is felt that the major problems lie in the inherent hysteresis and creep of the neoprene binder.

Other pressure sensitive materials, specifically cupric oxide, silicon, and manganese dioxide were tried with various binder and electrode configurations. The results, as above, were similarly discouraging. A summary of the results of the testing of these devices is presented in Table II on page 132.

STRAIN GAGE DEVICES

Tests of spiral foil and rosette gages sandwiched between sheets of rubber showed the same hysteresis and creep problems as with the previous elastomeric devices. Another load cell was fabricated by cementing a small foil gage on the wall of a one-eighth inch diameter nickel ring. The ring was made by plating 0.001 inch of nickel on a wax rod which was later dissolved in xylene.

The resulting device had adequate sensitivity and negligible creep and hysteresis. It was, however, highly sensitive to location of the center of force. This effect persisted when shim stock was cemented on the top and bottom and a load button added on top to localize the force.

In conclusion, the tests have shown that any concept involving elastomers as binders, carriers, or support for pressure or strain sensitive materials is of very limited value for load distribution transducers because of creep and hysteresis. Strain gages on metallic structures have greater potential for success although more complex, expensive, and fragile.

Conclusions On Load Distribution Measurements

The fabrication of a garment which could transduce accurately the load distribution over the body surface is conceptually sound and could be of great value not only for space suit evaluation but in many other areas where the measurement of the mechanical interface between man and his environment is of interest. Current techniques of transduction are unacceptable. A series of tests of pressure sensitive materials and strain gage devices did not yield any acceptable transduction methods; however, the study of techniques was not sufficiently exhaustive to assess feasibility.

TABLE II
QUALITATIVE ANALYSIS OF TRANSDUCER ELEMENTS

MATERIAL	FORM	TREATMENT	ELECTRODE MATERIAL	STATEMENT OF RESULTS	
				POSITIVE	NEGATIVE
Carbon	Carbonized cloth	None	Stainless steel plates	High sensitivity Negligible creep Fair repeatability	Resistance very low ($2\ \Omega$) Material very fragile Material very dirty (dusty)
	Carbonized cloth	None	Conductive silver paste	Lower sensitivity than above. Negligible creep. Fair repeatability. Cleaner material.	Resistance very low ($0.1\ \Omega$) Material very fragile
	Graphite	None	Stainless steel	High sensitivity	Poor repeatability Resistance very low
	Graphite	Mixed with Duco Cement	Stainless steel	High sensitivity	Poor repeatability High creep Low resistance
	Graphite	Mixed with Cu_2O (Cuprous Oxide) and Duco Cement	Stainless steel	High sensitivity when bonded to one electrode, pressure contact with other electrode. Resistance can be varied with mixture proportions.	High creep
	Graphite	Mixed with Silastic	Stainless steel	Fair sensitivity. Resistance can be varied with mixture proportions.	High creep
	Graphite	Polyurethane Sponge impregnated with mixture of Duco Cement & graphite	Stainless steel	Resistance can be varied with mixture proportions	Low sensitivity High creep

TABLE II (continued)

QUALITATIVE ANALYSIS OF TRANSDUCER ELEMENTS

MATERIAL	FORM	TREATMENT	ELECTRODE MATERIAL	STATEMENT OF RESULTS	
				POSITIVE	NEGATIVE
Carbon	Graphite	Polyurethane Sponge impregnated with mixture of Duco Cement, graphite, Cu_2O	Stainless steel	Resistance can be varied by changing mixture proportions High sensitivity	High creep
	Amorphous Carbon	None	Stainless steel	Results are generally the same as with graphite	
Cuprous Oxide	Fine powder	None	Stainless steel	Good resistance value (20,000 Ω)	High hysteresis Fair repeatability
	Fine powder	Mixed with Duco Cement	Stainless steel	High sensitivity Good resistance	High creep
	Fine powder	Mixed with Silastic	Stainless steel		No conductivity
	Fine powder	Mixed with silver paste	Stainless steel	High sensitivity Good resistance	High creep Poor repeatability
	Fine powder	Mixed with Duco Cement	Silver paste coated mylar	High sensitivity Good resistance	High creep Poor repeatability

GLOVE EVALUATION - DEXTERITY TESTING

Functional evaluation of the extravehicular glove is, fundamentally, no different from the functional evaluation of the suit itself. The glove imposes torque restraints upon the fingers and creates a mechanical pressure distribution which can cause discomfort and degrade tactile sensations. Glove torques and pressure distributions could conceivably be measured using the suit techniques already described; however, the fabrication of torque instrumented dummy hands and miniature load transducers highly complicates an already formidable task. Furthermore, the results of such measurements cannot be easily related to human performance as in suit limb testing. Consequently, glove functional performance is best evaluated by dexterity measurements during manned testing. This is not to say that objective testing is useless. Indeed, quantitative glove characteristics such as Bradley's tenacity, suppleness, and snugness can be very valuable for development work in pinpointing the shortcomings of a glove (refs. 12, 13).

The Nature Of The Problem

Space suit gloves impose torques on the wearer due to the same five causes discussed in the section above on torque. In addition, tactile sensation is lost due to the thickness of the material and its growth away from the skin. For this reason, fit, as in other areas of suit mechanics, is highly critical. However, the loss of dexterity is different from other functional suit problems in that the presence of the unpressurized gloves can cause as much loss in dexterity as the subsequent pressurization. Pierce's Purdue Pegboard tests (ref. 85) have shown greater than 50% decreases in dexterity scores when wearing an unpressurized suit. Pressurization dropped the scores only one third more. Eowen's testing of the X-20A suit (ref. 11) showed the same trends but not so dramatically.

Present Dexterity Testing

Dexterity testing to date has been directed primarily toward the evaluation of the task performance of man and suit rather than toward glove evaluation. Current pegboard testing requires motion of the shoulder and elbow because of the location of some of the peg holes with respect to the cups. Also, during some pegboards tests, the inflation of the suit and obstruction of vision by the helmet has forced the body into different positions for the suited and unsuited tests. In testing with the Workspace Apparatus (ref. 102), gross motion of the shoulder and arm is required because the hand must return from the control array to the knee after each actuation. When arm motion is involved, it is difficult to isolate the effect of glove encumbrance even though the time scores are known for several elements of the overall tasks.

Dexterity Measurement Technique

Non-specificity is the principal deficiency in current dexterity measurement techniques. To develop a more specific and objective measure of glove performance, a technique is required which eliminates all motion but that of the glove itself and which can be easily duplicated nude or suited.

This can be accomplished by a modification of current pegboard techniques. In concept, the pegs and washers are contained in a central cup and the holes are located on a turntable or drum which automatically indexes to the next hole each time the peg assembly task is completed. The indexing, obviously, must be sufficiently rapid to move the next hole into position before the next peg is lifted from the cup. Devices for many different operations or tasks appropriate for space suit use (such as elements of motions for the use of small tools, instruments, and controls) could also be designed to apply to glove motion only. For instance, several switches could be located to require a specific glove motion such as wrist flexion or rotation. Randomly sequenced lights would signal the subject to actuate the appropriate switches to extinguish the lights as in the Workspace Apparatus.

During these tests the arm of the working hand must be restrained from motion. Care must be exercised to prevent abnormal restraint or distortion of the wrist ring bearing. An adjustable seating system is needed to insure that the subject can be positioned identically for all conditions of testing, i.e., nude, suited-unpressurized, and suited-pressurized. Obviously, the body position must be chosen so that the subject need not exert himself to maintain his position or see his working area.

Conclusions On Dexterity Testing

Current dexterity testing is not sufficiently specific for objective glove evaluation and new devices are necessary to achieve this objectivity. These devices must be designed to insure glove motion only and to evaluate separately the fundamental wrist-hand motions.

REACH ENVELOPE MEASUREMENT

Introduction And Definitions

Thus far, the test techniques discussed have been directed toward the evaluation of individual suit joints, components, and localized problems. The results of these evaluation tests could be combined into an overall figure of merit for the suit; this artificial figure, although undoubtedly useful, could never give a true measure of the overall performance degradation of the man-suit combination. The measurement of reach envelope integrates the performance of all the suit parts with a human test subject in such a way that a normalized degradation figure can be calculated.

A reach envelope is the surface in space which contains all points accessible to some part of the body under specified conditions of body restraint and orientation of the reaching member. Several types of reach envelope have been defined for different purposes. Among these are the following:

1. The ergosphere, strophosphere, and kinetosphere of Dempster (ref. 33). An ergosphere is the surface enclosing the total work space available to a hand or foot related to some fixed point of reference. The strophosphere and kinetosphere are ergospheres with constraints placed on the orientation of the distal member.
2. The finger tip range limit and working range of the hand as defined by Wright (ref. 116).
3. The grasping reach envelope of Kennedy (ref. 59), in which the distance to a point between the thumb and the middle segment of the forefinger is measured.

In addition, another envelope useful for suit testing can be defined:

4. The boundary on the surface of the suit itself enclosing the area of the suit which can be reached with the fingers.

For any of these concepts to be useful, the test conditions must be defined explicitly including the suit pressure, method of subject restraint, point on the distal member which defines the envelope, and any constraints on the orientation of the member.

The selection of the particular reach envelope best suited for a specific application depends on the end uses of the data. Some possibilities are:

1. Suit evaluation and acceptance testing.
2. Cockpit design data.

3. Auxiliary equipment design and evaluation including couches, seat belts, and harnesses.
4. Determination of accessibility of suit components such as the emergency oxygen supply.
5. Suit fitting and adjustment and development of adjustment procedures.
6. Suit joint development testing.

Three reach envelopes are proposed for suit evaluation. First is the grasping reach envelope (GRE) which is defined to be the locus of extreme points accessible to the tip of the right (or left) thumb when the thumb is pressed against the second phalanx as shown in Figure 75. There are no constraints on the orientation of the hand other than those from suit and human limitations as dictated by the specified body position and harnessing.

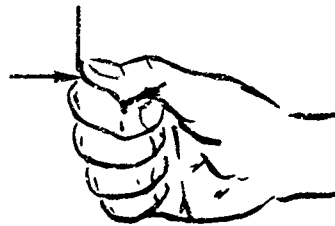


FIGURE 75. HAND POSITION FOR MEASUREMENT OF GRASPING REACH ENVELOPE

Second is the boot tip envelope (BTE) which is defined as the locus of extreme positions of a point on the right (or left) boot tip. The body position would be determined by the same considerations as used in the GRE above. This envelope is valuable for lunar tasks such as walking and also for free space use because man's ultimate capabilities can be realized only through full body mobility.

Third is the suit surface envelope (SSE) which is defined as the boundary on the suit of the area accessible to the fingers of either hand. This envelope shows to what extent the suit controls can be reached and operated.

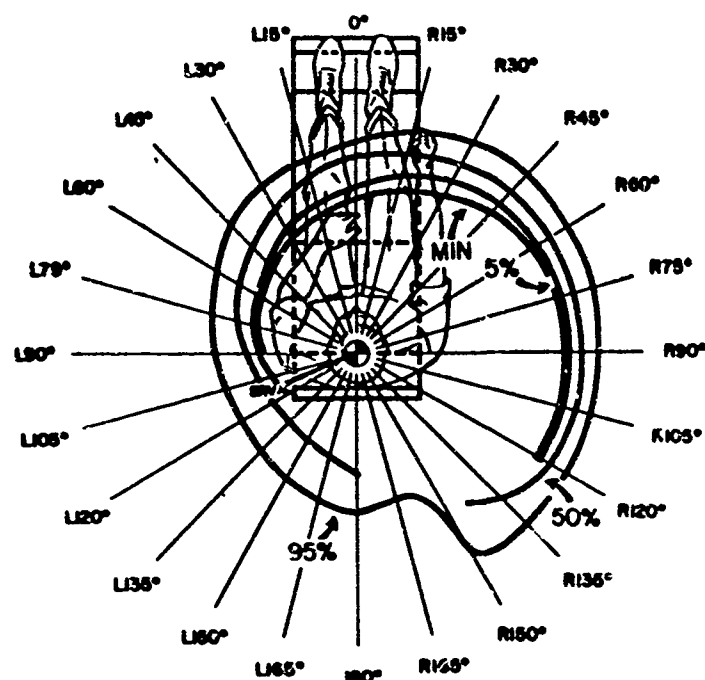
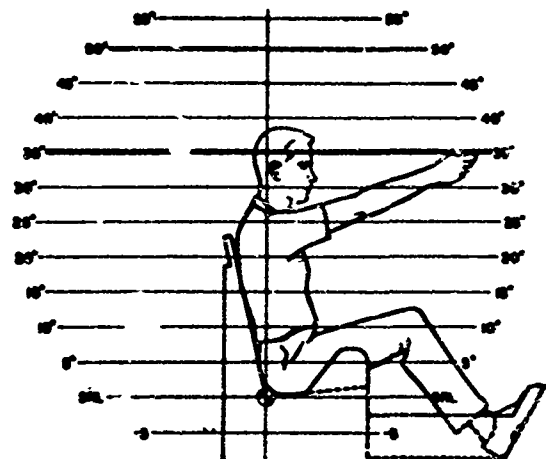
Reach Envelope - Unencumbered

Before considering evaluation criteria and measurement techniques, consider some of the existing reach data for unencumbered subjects. Kennedy reports a study of the GRE of twenty subjects anthropometrically representative of USAF personnel (ref. 59). The data are presented in the form of polar coordinate reach versus angle plots for different heights above a seat reference point as shown in Figure 76, which is a typical data page from Kennedy's report showing the maximum reach at 35 inches above the seat reference point.

Linear Data for Grasping Reach (in inches)

Angle	Percentiles				
	N	Min	5th	50th	95th
L165°	10			14.75	21.00
L150°	12			13.75	20.00
L135°	14			13.25	19.00
L120°	19		10.75	13.25	18.75
L105°	19		12.25	14.00	18.75
L 90°	20	12.75	13.75	15.50	20.00
L 75°	20	14.25	15.00	17.25	21.00
L 60°	20	15.25	16.00	18.75	21.50
L 45°	20	16.25	17.25	20.50	24.75
L 30°	20	18.00	19.25	22.50	26.25
L 15°	20	19.25	21.00	24.75	27.00
0°	20	20.75	22.25	26.50	28.50
R 15°	20	22.75	24.75	27.75	31.00
R 30°	20	24.50	26.75	29.25	32.75
R 45°	20	26.75	28.25	30.50	33.75
R 60°	20	28.00	29.00	31.00	33.75
R 75°	20	28.75	29.50	31.25	34.00
R 90°	20	29.00	29.75	31.25	33.50
R105°	20	29.00	29.75	31.50	33.50
R120°	20	28.50	29.00	31.00	33.50
R135°	15			28.50	33.50
R150°	3				31.50
R165°	5				21.75
180°	10			16.50	22.25

35-Inch Contours



Angular Reach from SRV at
the 35-inch Level

Minimum	L 90° to R121°
5th %ile	L120° to R121°
50th %ile	R178° to R143°
95th %ile	360°

FIGURE 76. GRASPING REACH ENVELOPE AT 35" ABOVE SEAT REFERENCE POINT

In Figure 77 the 50 percentile data has been combined into the isometric drawing of the GRE for easier visualization of the workspace. Other reach envelope data are available in limited amounts in the references.

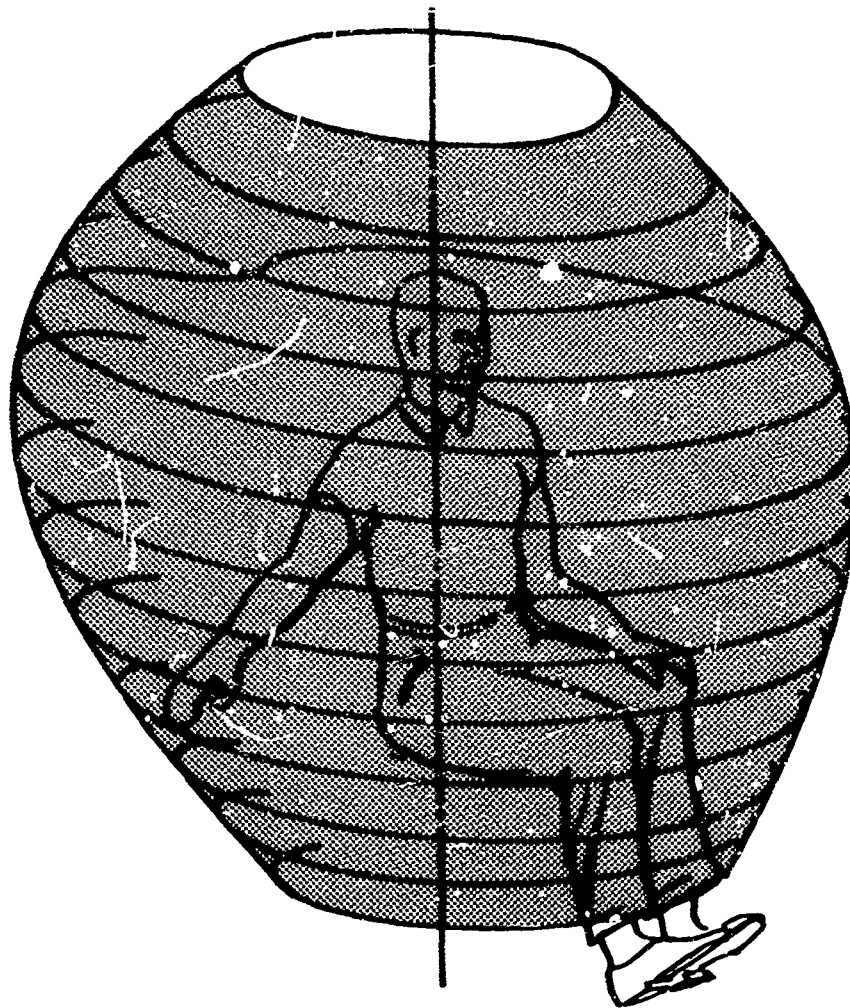


FIGURE 77. ISOMETRIC VIEW OF GRASPING REACH ENVELOPE

Evaluation Criteria

A substantial number of data points are required to define a reach envelope. Consider now how these data can best be used. Figures of merit and evaluation criteria must be developed and a method of data presentation must be evolved so that the trouble spots can be pinpointed.

FIGURE OF MERIT

To be useful, a figure of merit must provide insight to the basic problem being evaluated and should be normalized to the test subject. The simplest single number which describes a reach envelope is the volume it encloses. Thus, a

simple figure of merit would be the ratio of the volumes accessible to the subject when suited and in shirtsleeves.

$$\text{Figure of Merit} = \frac{V_s}{V_n} \quad (110)$$

This is a figure which varies from 0 to 1 with the "perfect suit" having a rating of 1. Here one number is used to describe the functional performance of the suit. Since "grasping reach" is a linear measure and volume increases as the cube of the linear dimensions, the raw ratio V_s/V_n tends to exaggerate the effect of the suit encumbrance. The figure can be linearized by taking the cube root:

$(V_s/V_n)^{1/3}$. For instance, in the evaluation of the X-20 Dyna-Soar prototype suit (ref. 95), the subject's nude reach volume V_n was 31.9 cu.ft. and his reach volume V_s while suited and pressurized to 5 psig was 12.0 cu.ft. Using these figures,

$$\frac{V_s}{V_n} = 0.376 \quad (111)$$

but

$$\left(\frac{V_s}{V_n}\right)^{1/3} = 0.722 \quad (112)$$

The latter number is certainly a more appropriate figure for evaluation purposes. One might say that the suit scored 72% in the GRE evaluation.

So far the discussion of reach figures of merit has not considered the performance of the suit. It is more important that the astronaut be able to reach positions within his field of view than those for which he must grapple behind his back. The console layout may suggest some areas as more critical than others. Based on these considerations a weighting factor $W(\vec{\rho})$ can be assigned to every point in the space surrounding the subject. Then the weighted figure of merit would be:

$$R \equiv \left[\frac{\int_{\text{suited}} W(\vec{\rho}) dV}{\int_{\text{nude}} W(\vec{\rho}) dV} \right]^{1/3} \quad (113)$$

where dV is the differential of volume. Establishing a useful $W(\vec{\rho})$ will require some statistical study and considerable intuition. A similar relation holds for boot tip reach envelope.

A normalized figure of merit for accessible suit area SSE should be based on the total suit area. By arguments similar to those above, an appropriate figure might be the square root of the ratio of the suit area accessible to the finger tips

to the total suit area $(A_s/A)^{1/2}$. Perhaps again a weighting factor W_a as a function of position on the surface could be derived. Then the weighted figure for accessible suit area would be:

$$R_a = \left[\frac{\int_{\text{suited}} W_a \, dV}{\int_{\text{suit}} W_a \, dV} \right]^{1/2} \quad (114)$$

If any of the essential controls, such as the emergency oxygen supply, were inaccessible, then the suit would automatically fail this test.

DATA PRESENTATION

The weighted figures of merit, R and R_a , presented above are useful numbers for comparison purposes. However, since they are single numbers, they do not reveal where a particular suit is deficient. Thus, for suit development the data is best plotted in one or more analog forms depending on the purpose of the evaluation. If the reach envelope is to be compared with the console layout, then polar coordinate plots of the console and the GRE for different elevations could be computer plotted on the same paper. Likewise, polar plots of the suited and nude GRE can be displayed on the same paper.

For the display of SSE, the suit surface area would be mapped on a two dimensional grid showing the locations of controls and other landmarks for the suit being evaluated. The subject would sweep out the boundary of the area accessible to his finger tips in some systematic way. These boundaries would be hand plotted on the suit maps. Areas would be determined with a planimeter.

Coordinate Systems

To speak in concrete terms about data display, coordinate systems for measurement and data presentation should be established. If the same coordinate system can be used for both, then reduction of the data and computation of figures of merit is simplified. For the grasping reach envelope of a standing subject, a cylindrical coordinate system with vertical z axis is the best for data presentation because polar coordinate plots of reach r versus angle θ for various elevations z_1 can be studied individually. Spherical coordinates are unsuitable for two dimensional displays because planar motion can only be achieved by holding the azimuthal angle θ constant. (The different coordinate systems and the relations between them are presented in Appendix I.) When this is done, the data planes all intersect on the polar axis. For data gathering, a device based on cylindrical coordinates is desirable not only for data reduction purposes but also because of the greater versatility allowed in the hardware. The subject can stand or sit or

be supported from above as in a restraint harness. The $z = 0$ plane can be shifted at will with no additional complexity in data handling. Rigs based on spherical coordinates have proved to be simpler to build but the additional data reduction, the consequent loss of accuracy, and the reduced versatility have limited the utility of these devices. Reach measuring devices based on cartesian coordinates are unsuitable for continuous transduction when angle is swept out.

Ideal Measurement Techniques

Before actual measurement hardware is considered, it is always worthwhile to consider an ideal measurement technique. The quantity of interest should be defined and the independent variables enumerated so that they can be varied or at least controlled. The ideal technique is to be kept in mind when the inevitable hardware compromises are weighed.

The desired quantity is reach r versus angle Θ and elevation z . The data in most elementary form are to be plotted for discrete planes as $r(\Theta, z)$. Two of the independent variables are seen to be Θ and z . Another variable which may be of considerable importance is the angular velocity $\dot{\Theta}$ at which the data is gathered. The reasons for this are the viscous-like effects in the human musculature and in the suit joints. The magnitude of the effect appears to be about

$$\frac{\partial T}{\partial \dot{\Theta}} = 1 \text{ in lb /degree/second} \quad (115)$$

Also because of inertial effects in the suit subject's limbs, the angular acceleration $\ddot{\Theta}$ must be considered. Because of these effects, the subject should be constrained to sweep angle at some constant angular velocity so that results will be repeatable and comparable from suit to suit. The many test conditions such as suit pressure, fit, subject size, and subject position must all be noted. The most difficult challenge in controlling variables, however, is in motivation of the subject. The motivational problems which are inevitable with manned testing require clever techniques to prevent their affecting the test results. Since the subject must exert considerable effort to achieve his maximum reach, he should have an analog display which is designed to indicate level of performance but which will not allow comparison with previous tests.

The ideal technique, therefore, consists of a lightweight rigid cylindrical structure around the subject with which reach $r(\Theta, z)$ can be accurately transduced, and Θ can be controlled. The device should produce data with sufficient rapidity to eliminate fatigue and be independent of motivational influence.

Hardware Implementation

The existing measurement hardware and reach data are reviewed in detail by

Kennedy (ref. 59) and thus need not be discussed here. The desired data is reach as a function of angle for fixed angular velocity and discrete elevations, $r(\Theta, z)$. (The optimum angular velocity must be found by experiment.) The test apparatus must accept subjects in any position and any variety of seats, couches, and harnesses. It must transduce and digitize reach data accurately and automatically. A device fulfilling these requirements is shown in Figures 78 and 79.

The basic structure of the device consists of a nine foot diameter metal base or floor which provides support for the structure. The base has a pattern of holes and slots to which a seat, couch, or harness can be fastened. Around the periphery of the metal base is a moveable ring. The ring, which rotates around the base at constant angular velocity, is powered by the Θ mode drive motor. When rotating in this manner, the z axis is defined as the axis of rotation of the moveable ring. The angular position Θ of the moveable ring with respect to the base is measured with a potentiometer. Erected on the moveable ring is a nine foot vertical column which is the guide and constraint for the power driven z mode carriage. The vertical position z of the carriage with respect to the base is measured with a potentiometer. Also shown in Figure 78 is the controller for the Θ mode drive motor and the vertical column stabilizing tubes. The reach data can be obtained either at incremental values of Θ or at constant angular velocity. The latter method appears most satisfactory because subject fatigue is minimized and the subject is less able to influence the test by his subconscious preconception of the results. The radial position of the subject's limb is measured by a space-saving pantograph-like mechanism attached to the z mode carriage. Magnetically attached to the protruding end of the pantograph is the finger ring designed to reference the subject's thumb tip. The magnetic attachment is fail safe in that the subject is never mechanically fastened to the moving apparatus. The pantograph also contains elements with which to measure the extent of reach r and to control the Θ mode drive motor.

The Θ mode drive is actuated by exerting a slight side force on the pantograph, thereby permitting the subject to sweep out his reach. When, at the limit of his reach, the subject's ability to supply the threshold force to the apparatus decreases, the apparatus stops rotating about the z axis. The subject may sweep his reach back to the starting position, or any intermediate position, by exerting a slight side force in the opposite direction. The apparatus can also be indexed remotely by the test observer. All the data for one reach envelope could be gathered in less than ten minutes including resting between sweeps. Data acquired during reach envelope evaluation is presented in three ways.

1. Normal evaluation will always require a certain amount of quick-look decision making. This is certainly desirable in suit fitting and adjusting procedures. For the display of this type of information, the parameters r and Θ would be plotted continuously in polar coordinates on the plotter located in the functional mechanics control console of the data acquisition system. (See Section VIII). This analog display has great merit for

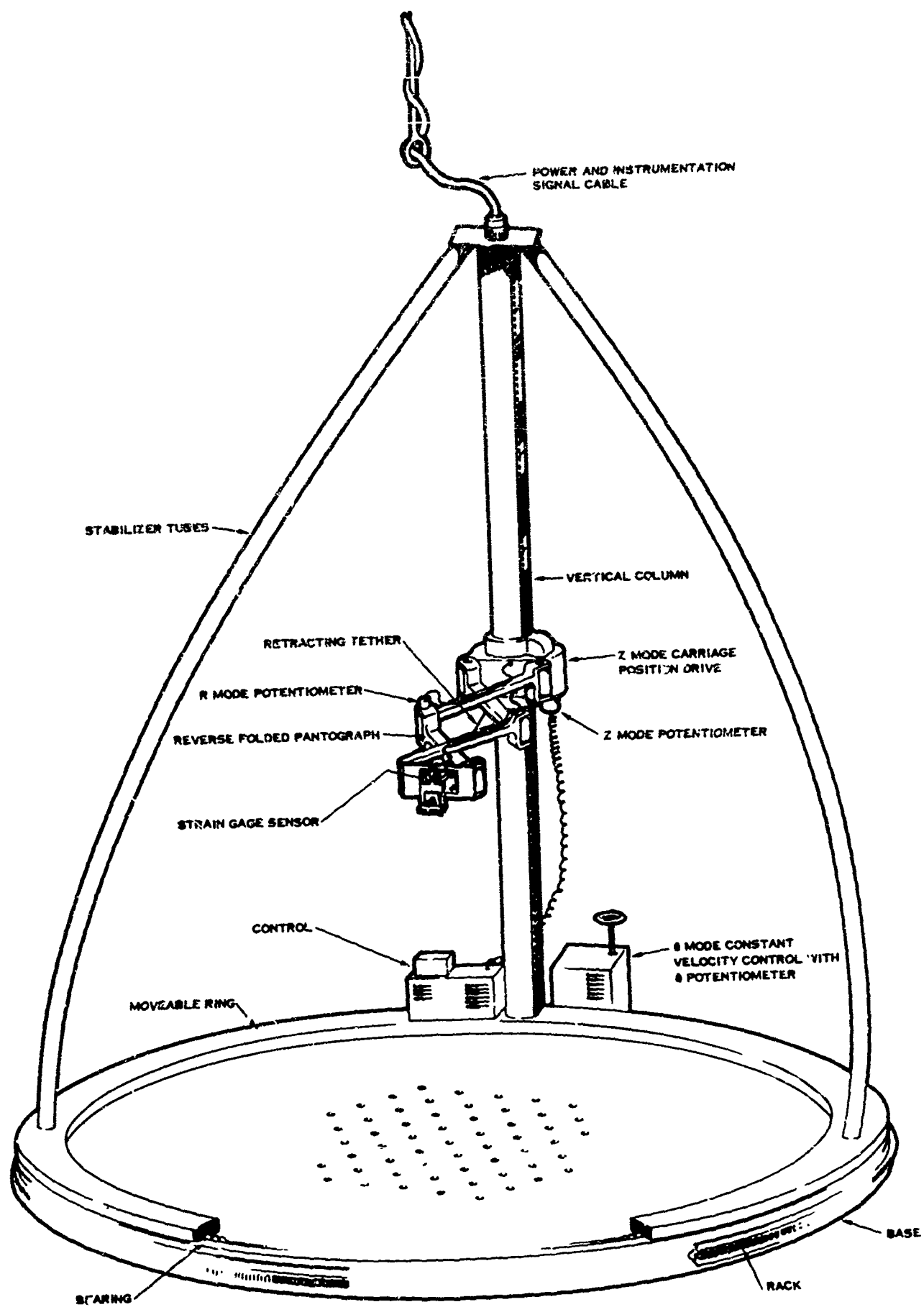


FIGURE 78. AUTOMATED REACH ENVELOPE APPARATUS

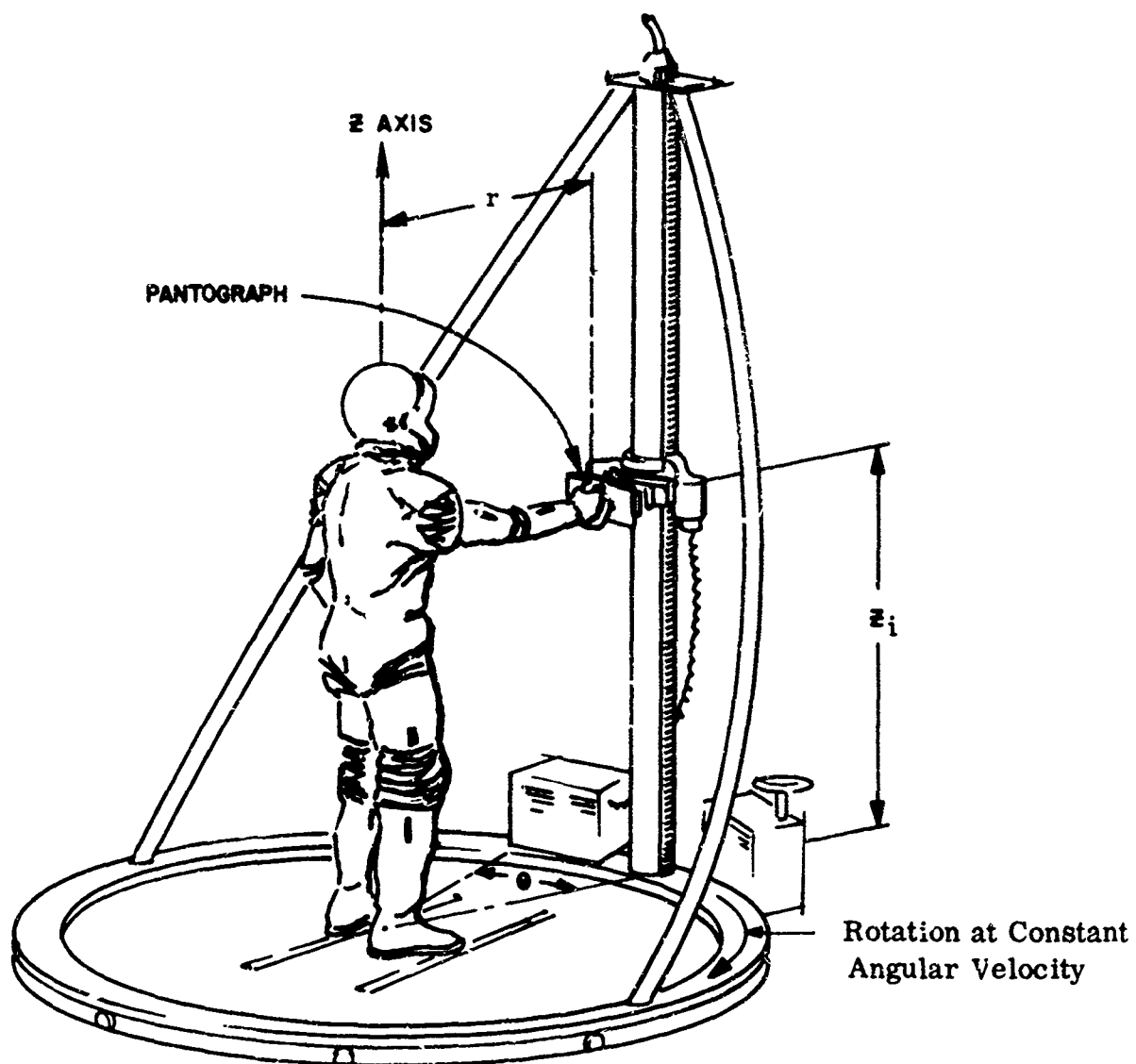


FIGURE 79. PICTORIAL VIEW OF REACH APPARATUS IN USE

visualization in the cylindrical system. By overlaying plots of a subject's performance in various horizontal planes, a picture of the total reach envelope can be obtained.

2. For motivational purposes, the test subject should be given some indication of his performance. This display, on a meter visible to the test subject, will tend to encourage the subject to concentrate upon achieving maximum reach but will not provide sufficient data for comparison with past performance. This approach should result in more uniform and repeatable data.
3. For rigorous dimensional and statistical analysis of steady state, time dependent, and test control data, the outputs of the transducers would be conditioned and recorded by the digital data acquisition system.

The several forms of data accumulation are an integral part of the functional mechanics control console discussed in detail in Section VIII. The console embodies various meters to display time-independent parameters, a plotter for on-line analysis of time-dependent information, and a digital magnetic tape data recording system.

CALCULATIONS -- Once digitized, the data can be used for off-line computation in several ways. Isometric drawings of the three dimensional reach envelopes can be compared with the nude values or with the available workspace. Without plotting, the computer can pick out inaccessible points on the control panels. Finally, appropriate figures of merit can be calculated. In terms of the data gathered on nude reach $r_n(\theta, z_i)$, suited reach $r_s(\theta, z_i)$, weighting factor $W(r, \theta, z_i)$, and elevation increments $(\Delta z)_i$, the figure of merit would be

$$R = \left(\frac{V_s}{V_n} \right)^{1/3} = \left\{ \frac{\sum_i \left[(\Delta z)_i \int_0^{2\pi} \int_0^{r_s(\theta, z_i)} W(r, \theta, z_i) r dr d\theta \right]}{\sum_i \left[(\Delta z)_i \int_0^{2\pi} \int_0^{r_n(\theta, z_i)} W(r, \theta, z_i) r dr d\theta \right]} \right\}^{1/3} \quad (116)$$

In actual practice these integrations would be performed numerically and a more accurate approximation, such as Simpson's rule, would be used for the z sum.

For recording of the suit area accessible to the subject and display of the data, two dimensional maps should be prepared of the back and front of a typical space suit. The maps would be produced in quantity like graph paper and would show grid lines around the limbs and torso intersected by vertical lines for surface coordinates. When a suit is being tested, its landmarks and controls would be drawn on the map. The subject would sweep the extent of his reach on his legs, helmet, and torso section while an observer marks the locus on the suit map. If the map is roughly an equal area projection, then planimeter integration of areas would yield the desired figure of merit $(A_s/A)^{1/2}$. The maps themselves would also be invaluable in evaluating suit performance.

Conclusions On Reach Measurements

Based on the foregoing discussion it is clear that reach envelope measurement is necessary for assessment of overall suit performance. With automated data acquisition and computation, reach measurement would become a powerful and frequently used tool. Some applications of the data are:

1. Suit evaluation and acceptance testing.
2. Cockpit design data.
3. Auxiliary equipment design and evaluation including couches, seat belts, and harnesses.
4. Determination of accessibility of suit components such as the emergency oxygen supply.
5. Suit fitting and adjustment and development of adjustment procedures.
6. Suit joint development testing.

The current techniques and equipment for reach measurement, while sufficiently accurate, lack versatility for the measurement of full body reach and the convenience that can be provided through computerized data processing. Therefore, the following additional hardware and techniques should be incorporated into the current AMRL reach testing facilities.

1. A cylindrical reach apparatus of the type shown in Figure 78 is needed together with a central data handling system to define full body reach for various body positions under various conditions of restraint and at several angular velocities.
2. A computer should be used to process data from the current AMRL reach device to eliminate the time consuming processes of coordinate transformation and reach volume calculation. Manual entry to the computer should be replaced by transducers for automatic handling as soon as a data system is available.
3. Improved reach criteria are needed to define better individual suit performance. The approaches discussed in this section can form the basis for the development of these criteria.

CONCLUSIONS ON FUNCTIONAL SUIT MECHANICS

Based on the study of functional suit mechanics, the following is concluded:

1. Four separate testing areas are required in the evaluation of functional suit performance.
 - a. Torque and angle measurements.
 - b. Mechanical load distribution measurements.
 - c. Dexterity measurements.
 - d. Reach measurements.

Although the complete mechanical interface between man and the suit to describe the suit torques, ranges of motion, total reach, and distribution of pressure over the skin surface can be conceptually described by the transduction of surface forces, practical limitations in transducer design and inaccuracy due to tissue compliance make this approach unfeasible.

2. Torque and angle measurements can be accomplished through a methodology that involves a powered articulated dummy and an exoskeletal electrogoniometer which together transduce data to be computer-processed for accurate, objective torque vector measurements and useful figures of merit.
3. Mechanical load distribution measurements can be of substantial value for evaluation of the skin pressure - comfort problem; however, the development of a transduction technique which meets the requirements for flexible mounting surface, low force levels, thinness, and low cost appears formidable.
4. New, relatively simple devices will improve the objective evaluation of glove performance by eliminating extraneous glove and arm motions which reduce the specificity of current measurements.
5. New reach apparatus are needed to supplement current apparatus in the definition of full body reach both inward and outward, and both new and current apparatus could benefit substantially from the accuracy, convenience, and speed of computer-based data reduction.
6. An analog/digital data system as described in Section VIII is needed in conjunction with the several test apparatus for suit functional testing to acquire, condition, edit, record, and display suit test data and to make this data available in a computer-compatible form for computation and final presentation.

7. Current criteria in all areas of functional suit mechanics are insufficient for adequate evaluation of suit performance. New criteria based on fundamental physical and physiological measures and adaptable to various mission goals can be of significant benefit in establishing the requirements and assessing the performance of both specific joints and the overall pressure garment. In particular, a better understanding is needed of the relationships between the mechanical measures of torque and work and metabolic cost; between off-axis torque and coordination (the tracking problem); between skin pressure and comfort; and between glove restraint and dexterity.

SECTION IV

METHODOLOGY FOR LIFE SUPPORT EVALUATION

INTRODUCTION

An adequate extravehicular protective garment must maintain an environment within the suit which can sustain life and assure a reasonable degree of comfort. This requires systems that will remove excess heat, provide a breathable atmosphere, remove contaminants and noxious odors, prevent excessive dehydration, and limit skin temperature extremes. Space suits are designed with cooling and gas control systems which are intended to perform these functions.

Historically, suit life support systems have been evaluated primarily through duplication of the expected environment and measurement of the resultant physiological stress on the test subject. Although this is necessary and, indeed, essential for the final overall assessment of suit performance, it seldom provides the detailed engineering data required to improve a suit design. In this section, test concepts and simulation techniques are discussed which attempt to make more objective the evaluation of suit life support performance, yet reproduce the complex interrelationships between the physiological needs and responses of the man and the physical provisions and limitations of the suit.

The section begins with a review of man's physiological needs in each of the fundamental areas of life support and establishes some of the basic suit requirements. Techniques for implementing the requirements are then discussed since the development of a sound methodology and a convenient, accurate, and objective test system depend upon a full understanding of the basic mechanisms of suit performance. Test concepts for both gas and liquid cooled suits are considered and, in particular, the problems of environment simulation are treated in detail. From this is developed an integrated test methodology to evaluate suit cooling performance, assess the effectiveness of respiratory exchange, and determine metabolic cost. Various specific measurement techniques particularly suited to an automatic data acquisition system are described, and an overall test system is recommended. The details of the data acquisition system are presented in Section VIII.

PHYSIOLOGICAL CONSIDERATIONS

The ultimate objective of the space suit engineer is to provide the astronaut with a life supporting environment in the hostile environment of space. To achieve this goal the engineer must understand the basic physiological requirements for life support. Man has evolved in an earth environment and can tolerate only small deviations in atmospheric temperature, pressure, and composition. Prolonged

adaptation permits greater departure from the normal environment, but the permissible departure is small, not well defined, and is of little value at this time for space suit design.

The basic physiological factors for the design and testing of the life support features of a space suit ensemble are the metabolic, thermoregulatory, and respiratory processes. These closely interrelated processes are discussed in the following paragraphs.

The Metabolic Process

Fundamentally, metabolism is a complex biochemical reaction in which foodstuffs are continually converted to heat, energy for useful work, needed compounds, and waste products. The heat produced must be rejected continuously by the body to maintain a constant body core temperature. Studies indicate that the combustion of foodstuffs is the sole source of energy within the body, convertible to useful work. Fortunately (for the mechanism is extremely complex), it is not necessary in space suit evaluation to consider the metabolic process at the detailed cellular level. Instead, the body may be viewed as a thermodynamic machine and only the energies and masses crossing the boundaries of the machine need be considered for steady state analysis.

In essence, steady state energy balance for man requires that the mechanical work performed on the environment plus the net heat rejected equal the total metabolic energy produced. Expressed algebraically:

$$Q_M = Q_R + W_O \quad (117)$$

where

Q_M = total metabolic energy expended
 Q_R = net heat rejected
 W_O = outside mechanical work

The rate of metabolic energy production depends, of course, upon the activity level of the total body. For healthy male adults from the astronaut population, the energy rate varies from about 80 kcal/hr during sleep, to 500 kcal/hr at peak sustained activity. During a typical space flight the rate during waking hours will probably range from 130 kcal/hr to 400 kcal/hr with an average activity level of 210 kcal/hr. During extravehicular operation, the average metabolic level will be about 300 kcal/hr.

The metabolic energy expended Q_M is normally measured by indirect calorimetry, which is measurement of oxygen consumption and carbon dioxide production and calculation of the heats of reaction, making certain assumptions about the types of foodstuffs oxidized and the physiological status of the test subject.

The volume ratio of carbon dioxide produced to oxygen consumed is known as the respiratory quotient (RQ). Classic experiments by Lusk and others have shown that the heat of combustion per liter of oxygen consumed is almost linearly related to RQ. The caloric equivalent, or metabolic energy per liter of oxygen consumed, varies from 5.05 kcal/liter for an RQ of 1.00 to 4.69 kcal/liter at an RQ of 0.70 corresponding to all-carbohydrate and all-fat diets respectively. A linear interpolation of caloric equivalent is assumed by Lusk between these RQ limits (ref. 70).

Thus, by measuring oxygen consumption and carbon dioxide production, the total metabolic heat production can be calculated.

Like all body processes, the metabolic process has a definite time delay. Instantaneous demands for muscular effort are met by a rapid increase in cardiac output and ventilation rate. The arterial blood begins to surrender a greater percentage of its oxygen supply and the body begins to switch a greater proportion of the total blood flow to the muscles, the site of heat production, and to the skin for heat rejection. Normally, about two minutes are required for this process to stabilize. Meanwhile the muscles incur an oxygen debt which will increase if the activity exceeds the oxygen capacity of the system. This oxygen debt is normally not repaid until the recovery period following the activity. Although the metabolic heat is produced within the muscles, the muscle temperature increase is extremely small due to the constant removal of heat by the blood stream which redistributes the heat throughout the entire body.

The net heat rejected by the body, Q_R , is the algebraic sum of all the heats transferred across the body surface. Heat can be transferred simultaneously by conduction through direct contact with hot or cold surfaces, by convection to or from the surrounding atmosphere, by radiation to hot or cold surfaces, and by phase change and mass transfer. The body has regulatory and compensatory mechanisms to aid in maintaining the net heat rejection rate at the proper level to maintain a constant body core temperature. If the body is unable to maintain thermal balance, that is, if heat is rejected either too slowly or too rapidly, the core temperature will rise or fall. Physiological stress and eventual collapse and death will occur. During a rise in body temperature, heat is stored. This heat storage is a transient term which does not enter the steady state heat balance equation.

The mechanical work output W_O is the actual mechanical work done on the environment (see Appendix II). Man's efficiency as a work-producing machine is relatively poor. Less than one fifth of his total metabolic energy can be converted to work. For very short periods, however, very high work levels can be achieved primarily through the mechanism of oxygen debt. It should be noted that the mechanical work done by the internal organs of the body, such as the heart pumping against the resistance of the vascular system, is converted to heat within the body system and, therefore, the heart does no useful work in the thermodynamic sense. Conversely, as shown by Otis, Fenn, and Rahn, the lungs perform work in pumping air in and out of the body system. (ref. 82).

The metabolic energy associated with breathing is not a significant factor in space suit design; however, it must be considered during space suit testing. Lung energy requirements become important when either pressure or resistance breathing is required.

Pressure breathing, a condition where the average intrapulmonary pressure is greater than the ambient pressure on the chest, does not occur in current suit concepts, and therefore is not considered.

Resistance breathing, that is, breathing against a resistance proportional to the respiratory flow rate, can occur during suit testing. Spirometry equipment used to measure oxygen consumption can add resistance to the breathing circuit and therefore raise the metabolic rate above that for normal breathing. Gainsler (ref. 39) indicates that a resistance of 0.65 centimeters of water per liter per minute causes an increase in the relative cost of breathing of about 10% of the total basal metabolic requirement or about 8 kcal/hr. Normally, spirometry equipment is used intermittently and normal breathing is permitted during the balance of the test. Therefore, an increase in metabolism caused by inadequate spirometry equipment will indicate a higher average metabolic rate than was actually developed, thus causing an error in the test results. In the interests of accurate measurements, the resistance of spirometry equipment must be kept to an absolute minimum.

The Thermoregulatory Process

For survival, the temperature of the human body must be controlled within narrow limits. The core temperature of a resting man has a mean value of 37.1°C (98.6°F). A decrease of 10°C in core temperature may be survived but an increase of 5°C is fatal. Within the body, complex physiological mechanisms act to prevent an increase or decrease in core temperature in spite of wide changes in internal heat production and variations in the temperature and humidity of the environment. The most obvious environmental limits are the onset of pain above 45°C and frostbite below 0°C. Between these limits thermoregulation permits reasonably wide ambient variations, but the normal comfort range lies within 17°C (62°F) to 24°C (75°F). Below the comfort range, regulatory control increases metabolic heat generation by involuntary shivering. Above the comfort zone the body becomes increasingly heat stressed, sweating begins, heart rate increases, and the body core temperature rises. As the total stress accumulates to the point of impending collapse, subjective reactions of fatigue, headache, nausea, faintness on exertion, and weakness are apparent.

Various measures of physiological heat stress have been used by thermophysiologicals. Craig (ref. 24) has shown that strain I may be indicated by the following expression

$$I = 0.01 H + \Delta T_r + S_n \quad (118)$$

In this expression I is the index of physiological strain, H is the heart rate in beats per minute at end of second half hour or at the end of the experiment if it is prematurely terminated. ΔT_r is the rise in rectal temperature in $^{\circ}\text{C/hr}$, and S_n is the sweat production (nude weight loss in kg/hr).

The above expression is of course essentially time dependent and does not indicate total physiological strain accumulation. Arbitrary levels of acceptable strain rates have been established but accumulated strain does not correlate well with physiological degradation. Kaufman has reported that as an index in full-pressure suit tests, heat storage per unit body weight correlates closely with the syndromes of imminent collapse. Neither index, however, is known to have been applied to exercising subjects; thus, an effective well substantiated index of physiological strain is not available for direct application to the space suit test problem. (ref. 57). Extensive testing will, undoubtedly, be required to establish an agreeable index.

Since close regulation of body core temperature is essential for survival, it is important to discuss some of the heat rejection mechanisms that the body has available. Basically, the body may reject heat by convection, conduction, radiation, and by evaporative cooling. While resting, convection and radiation are the principle heat rejection mechanisms. However, during intense activity, these mechanisms are seldom adequate to reject the entire metabolic heat energy produced and therefore sweating occurs. Through sweating, the body is able to reject large quantities of heat and to maintain core temperature even in an otherwise adverse environment. Heat can only be rejected, however, if the vapor pressure of water in the air which surrounds the man is lower than the saturation vapor pressure of sweat at the body skin temperature. When the cooling capacity of the environment is nonuniform over the body surface, the body has the capability to redistribute heat so as to take maximum advantage of the cooling available. This redistribution is carried out by the cardiovascular system.

At low heat rejection rates or in cold environments, the body controls heat rejection primarily by vascular dilation and increased blood flow through the subcutaneous capillaries. In effect, this results in a variable skin conductance. Table III shows the preferred skin temperatures, heat rejection, and apparent skin conductivity at resting conditions. A suggested heat rejection distribution is included which assumes that the heat distribution becomes more nearly proportional to the skin area at moderate exercise. Additional testing will be required to establish the comfort heat distribution over the expected range of activities. Not all of the heat, however, is carried away from the skin surface. A fairly substantial portion of the heat during resting, and a significant fraction during activity is carried away as both sensible and latent heat in the respiratory gas. Typically, the sensible and latent heat rejection by the respiratory system during rest and at moderate activity at 400 kcal/hr would be 12 kcal/hr and 65 kcal/hr, respectively.

TABLE III
SECTIONAL BODY HEAT TRANSFER*

SECTION	PREFERRED TEMPERATURE - °C	SKIN CONDUCTANCE kcal/m ² / hr / °C	AREA m ²	AREA FRACTION	RESTING HEAT LOSS kcal/hr	WORKING HEAT LOSS** kcal/hr
Head	34.6	7.55	0.20	0.111	4.0	44.4
Chest	34.6	18.20	0.17	0.095	8.2	37.7
Abdomen	34.6	14.16	0.12	0.067	4.5	26.6
Back	34.6	20.35	0.23	0.128	12.4	51.1
Buttocks	34.6	17.40	0.18	0.100	8.3	40.2
Thighs	33.0	8.55	0.33	0.184	12.0	73.4
Calves	30.8	11.30	0.20	0.111	14.6	44.4
Feet	28.6	9.65	0.12	0.067	10.0	26.4
Arms	33.0	19.80	0.10	0.056	8.4	22.4
Forearms	30.8	16.70	0.08	0.045	8.6	17.8
Hands	28.6	26.40	0.07	0.039	16.0	15.6
					<u>107.0</u>	<u>400.0</u>

* Modified from Kerslake (ref. 60) and Burton & Collier (ref. 15)

** Assuming Work Heat Loss proportioned to Area Fraction

Although the evaporative mechanism is an effective method for the removal of body heat, continued high activity and continued sweating for long periods of time result in excessive body dehydration and consequent physiological stress. In a gas ventilated space suit system which relies on sweat evaporation to reject heat, serious dehydration, that is, in excess of 2% of body weight, can occur during relatively short missions. On the other hand, in a liquid cooled suit which relies on conductive heat transfer, little dehydration will occur.

For comfort conditions and extended missions, heat storage must be minimized. Both heat storage capacity and distribution depend on whether the body is being cooled or heated. The thermal defenses of the body during cooling act to maintain the heart-lung-brain complex within narrow thermal limits at the expense of the extremities which can be cooled significantly. During heating of the body, large temperature differences do not occur. Heat storage is usually determined from both skin and core temperatures. Skin temperatures from a varying number of body locations are combined with the rectal temperature to approximate the mean body temperature T_m as follows

$$T_m = \frac{2}{3} T_r + \frac{1}{3} \sum_{j=1}^N \frac{T_{sj}}{N} \quad (119)$$

where T_r = rectal temperature
 T_{sj} = j th skin temperature
 N = number of skin temperature measurements

The body heat storage is then computed from Equation 120, assuming an average specific heat c_{pb} of the body of $0.83 \frac{\text{kcal}}{\text{kg } ^\circ\text{C}}$.

$$Q_S = 0.83 M_b \Delta T_m \quad (120)$$

where Q_S = Heat storage, kcal
 ΔT_m = Rise in T_m during the test, $^\circ\text{C}$
 M_b = Body mass, kg

N in the above expression normally takes on values from three to seventeen depending upon the particular experimenter and the nature of the test in progress. In general, however, for the heat stress condition, N can be relatively low, while for studies of cold exposure, the value of N must be rather high. The particular value of N that is chosen for any given experiment is determined by the actual variation in skin temperature which is measured on the subjects during the test.

The Respiratory Process

OXYGEN REQUIREMENTS -- Fundamentally, respiration may be defined as the gas exchange between cells and their environment. From the external environment to the cellular level, the numerous processes have a single essential purpose -- to supply living cells with required oxygen and to remove the carbon dioxide produced by combustion to prevent autointoxication. Few of the human tissues can survive direct extended exposure to the normal levels of atmospheric constituent gases. The evolved pulmonary structure provides a gaseous environment which differs considerably from ambient. A multitude of small sacs (alveoli) within the lungs provides the large surface for contact of the external environment with the blood. Within the lung structure, the alveolar gas environment provides the actual interface for exchange with body fluids. In addition to the oxygen and carbon dioxide exchange across this interface the respiration process also removes other products of combustion, determines the environment of the cells, and eliminates a limited amount of heat.

To supply the requirements for metabolism, approximately 20.8 standard liters of oxygen are consumed per 100 kcal of energy expended. Thus, the oxygen requirements range from about 16.6 liters/hr at rest to 104 liters/hr at maximum sustained activity. Not all the oxygen inspired, however, is actually absorbed by the blood stream. The total volume of air inspired per minute, the minute volume, varies from about 10 liters to 120 liters. The actual volume inspired per breath, the tidal volume, varies from about 0.6 to 3.5 liters/breath and less than 3% of the inspired volume is actually absorbed. (ref. 65).

The normal pressure of sea level atmospheric air is 760 mm Hg (14.7 psia), which contains an oxygen concentration of 160 mm Hg. The balance is primarily nitrogen. As the atmospheric air pressure decreases with increasing altitude, arterial oxygen saturation diminishes and functional impairment begins at altitudes between 10,000 and 13,000 feet ($pO_2 = 100$ mm Hg). At 25,000 feet and above, unconsciousness and eventual death occur. Progressive exposure to oxygen pressures at less than sea level equivalent results in adaptive changes which extend tolerance limits to altitudes in excess of 15,000 feet. Because adaptation is slowly acquired, quickly lost, and of limited magnitude, altitude adaptation can only be considered of supplemental value to suit design.

Although the oxygen partial pressure in normal sea level air is approximately 160 mm Hg, the equilibrium pressure of oxygen in the lungs is only about 100 mm Hg because of the presence of carbon dioxide and water vapor. For a pure oxygen environment, as is customary in current space suit design, the 100 mm Hg requirement is satisfied by an oxygen total pressure in the suit system of approximately 180 mm Hg.

Although atmospheric air contains a large percentage of nitrogen, the physiology of the body does not require nitrogen, at least for modest periods. As the oxygen partial pressure increases above the normal 100 mm Hg level, other

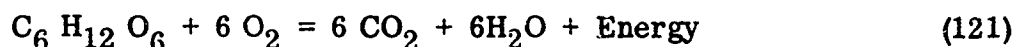
physiological effects can be encountered. Present information indicates that long-term exposure toxicity effects begin at about 425 mm Hg; however, exposure to pure oxygen at 760 mm Hg for two hours during denitrogenization procedures produces no evidence of permanent damage (ref. 104).

CARBON DIOXIDE REQUIREMENTS -- During the respiratory gas exchange, carbon dioxide is continuously evolved in the alveoli. Although the carbon dioxide partial pressure ($p\text{CO}_2$) varies considerably in the upper respiratory tract, the normal alveolar partial pressure is essentially constant at about 40 mm Hg for a resting man. Inspiration of carbon dioxide rich air results in increased arterial $p\text{CO}_2$ and a consequent increase in depth and rate of respiration. In his review on carbon dioxide tolerance limits, Schaeffer (ref. 100) indicates the following: In air at sea level pressure, 1% carbon dioxide (7.6 mm Hg) will probably cause no significant physiological, or adaptive changes; however, at 3% (22.8 mm Hg) and above, performance degrades and changes in pulse rate, blood pressure, metabolism, and respiratory function indicate significant alteration of the physiological process. Recent tests by Morgan, et al seem to indicate that carbon dioxide tolerance levels may be somewhat greater when breathing oxygen rather than air (ref. 77).

In the metabolic process carbon dioxide is evolved at a rate which depends primarily upon the quantity of oxygen consumed and the foodstuffs oxidized. The volume ratio of the carbon dioxide produced to the oxygen consumed is known as the respiration quotient RQ and forms the basis for the calculation of metabolic energy expenditure by indirect calorimetry.

RQ expressed in volume rates at standard conditions (i. e., 0°C , 760 mm Hg) can also be calculated from an assumed diet. The calculation of RQ for simple foodstuffs is illustrated in the following examples.

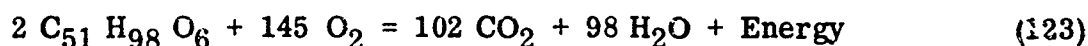
For a carbohydrate such as glucose, Equation 121 describes the combustion process.



and

$$\text{RQ} = 6/6 = 1.0 \quad (122)$$

For a fat such as tripalmitin the equation is:



and

$$\text{RQ} = \frac{102}{145} = 0.703 \quad (124)$$

For proteins, RQ is more difficult to calculate because some of the protein is converted to products which may be excreted without combustion; however, the combustion of protein is commonly ignored because the RQ is close to that of a mixed diet and normally constitutes less than 10% of metabolism. Only small errors are introduced and the simplification conveniently permits linear interpolation between the extremes of pure fat and pure carbohydrate combustion (ref. 43).

Pressure Requirements

Conventional suits operate at 180 mm Hg (3.5 psia), which is the minimum respiratory requirement. It is possible, however, in some suit concepts that lower pressures may be used to increase mobility of the body extremities. In these lower pressure regions, the actual physiological tolerance limits are uncertain; however, at an ambient pressure of 47 mm Hg, water will boil at body temperatures. The protein content of the body water increases the boiling temperature somewhat; however, excessive dehydration will probably occur in a normal atmosphere. Even if the lungs are protected from overdistention, the lower pressures will cause pooling of blood in the pulmonary capillaries and the great vessels of the torso and extremities. Over-distention can result in rupture while the blood pooling reduces venous return and, consequently, cardiac output.

In air containing as little as 4% nitrogen, decompression sickness (the bends) may occur if the astronaut is subjected to an abrupt pressure decrease.

Physiological Measurements

In this section the major physiological factors involved in the design and testing of space suit life support systems have been discussed. During testing of these systems, certain physiological measurements are required to evaluate the man/suit performance. The following list of parameters represents the significant measurements required.

Body Core Temperature

Skin Temperature Distribution

Oxygen Consumption

Carbon Dioxide Production

Respiratory Carbon Dioxide Partial Pressure

Oxygen Inlet Partial Pressure

Humidity of the Respiratory Air

Body Weight

Body Water Loss

Heart Rate

Respiratory Rate

This list does not include the ECG, visual observation, and voice communication required to monitor the medical status of a test subject.

SUIT SYSTEM DESIGN CONSIDERATIONS

Basically, the suit life support system must (1) provide adequate thermal control to maintain body core temperature and comfort and (2) provide a suitable atmosphere for respiration. Consider now some of the suit and helmet considerations in achieving these goals in current space protective garment designs.

Suit Considerations

ENERGY BALANCE

To maintain body core temperature, the suit must provide a medium by which metabolic heat may be rejected and heat leakage through the suit may be either absorbed or rejected. The suit need not provide an ideal environment but it must provide sufficient thermal control to remain within the control limits of the body thermoregulatory system. The degree to which this is achieved determines the physiological stress and thermal comfort limits of the suit. Consider the steady state energy balance equation for a suit system.

$$Q_M + Q_I = Q_O + Q_C + W_S \quad (125)$$

where

Q_M = metabolic heat

Q_I = inward heat leakage

Q_O = outward heat leakage

Q_C = heat removed by cooling flow

W_S = work done by suit

Energy enters the system in the form of metabolic heat and inward heat leakage through the suit and leaves the system in the cooling stream, through outward leakage, and as mechanical work done by the suit on the environment.

The entire steady state heat of metabolism Q_M including both rejected heat Q_R and work W_O (see Equation 117) is rejected to the suit. This is true since the useful work that the man performs W_O is performed entirely upon the suit rather than upon the external environment.

The heat leakage into the suit Q_I arises from either conduction or radiation through the suit wall. (In the space environment no convection will occur.) The conducted heat, transferred through direct contact with hot or cold spacecraft or extravehicular equipment surfaces, can be assumed negligibly small, although it may produce significant hot or cold spots on the suit surface for short times. Solar radiation is the principal heat leak into the suit and is discussed in detail in Section V. Heat leakage is kept to tolerable levels by an insulating meteoroid protecting coverall, which can reduce the inward heat leak to about 50 kcal/hr. The outward heat leak, due to radiation to the 4°K temperature of deep space will not normally exceed 40 kcal/hr.

The work W_g is the actual mechanical work done by the suit on the external environment. Considering the present tasks planned for the extravehicular astronaut, the external useful work done by the suit will be small and can generally be considered negligible. Thus from the sum of these effects, the suit cooling system must have the capacity to remove continuously up to 550 kcal/hr. This heat is normally removed by either a gas ventilating stream or a combined gas ventilation - liquid cooling system as described in Section II. Since the change in potential and kinetic energies of these fluids is normally negligible, net energy removed by the cooling stream is simply the change in total enthalpy between inlet and outlet. Thus, for most cases, the general energy equation may be simplified to the following form.

$$q_M = w \Delta h + q_L \quad (126)$$

where

- q_M = metabolic energy rate
- w = coolant flow rate
- Δh = change in coolant enthalpy
- q_L = net heat flow rate inward through the suit

In the next sections the mechanism of heat removal within both gas ventilated and liquid cooled suits is considered in more detail.

HEAT REMOVAL IN A GAS VENTILATED SUIT

In the conventional gas ventilated suit, gas enters at the torso umbilical and is distributed by ducts to the oral-nasal region and to the extremities. From these points the flow returns over the body surface to a torso plenum and outlet umbilical. Typically, saturated gas enters the suit at about 8°C. During passage through

the distribution ducts, some sensible heat is transferred to the gas thus raising its temperature and decreasing its relative humidity. As the gas issues from the distribution ducts it continues to pick up sensible heat from the skin surface and from heat leakage. As the temperature rises and the relative humidity falls, evaporation of perspiration and consequent cooling by latent heat transfer can begin. The gas exhausts from the suit at about 30°C. These values are typical and will vary considerably depending on the specific suit design and the activity level. Obviously, the ultimate capacity of the ventilating stream is reached when the gas exits from the suit saturated at the body core temperature. Since the gas has no further cooling capacity, increased activity can only result in body heat storage and eventual thermal collapse. The expression for the total energy removal rate of the gas ventilating stream is approximately:

$$w_g \Delta h = w_g c_p \Delta T + w_g h_{fg} \Delta \gamma \quad (127)$$

where

c_p = average specific heat of gas

ΔT = rise in gas temperature from inlet to outlet

$\Delta \gamma$ = rise in specific humidity

Δh = increase in enthalpy of gas

h_{fg} = latent heat of vaporization

w_g = mass flow rate of gas

Because in the respiratory process oxygen is consumed and carbon dioxide is produced, the calculation of the exact energy exchange is somewhat more complicated. The exact expression for the total energy removed by the cooling stream is given on page 214.

The relative magnitudes of the sensible and latent cooling capacities of the ventilation stream are seen by substituting typical inlet and outlet conditions into the simplified expression above or referring to the performance values in Figure 6.

Although the calculation of the total heat removed by the suit coolant stream is relatively straightforward, the determination, either analytically or experimentally, of the cooling at any local point in the suit is an extremely complex problem. Consider the small typical cross section of the ventilating passage shown in Figure 80.

On this elemental area of the suit, the heat rejected to the coolant stream depends on the suit wall conductivity, the outside surface temperature, the duct heat transfer coefficients, the duct wall conductivity, the skin temperature, the sweat rate, and the velocity, temperature, and humidity of the stream. Obviously, a great many factors must be known about the local conditions within the suit to

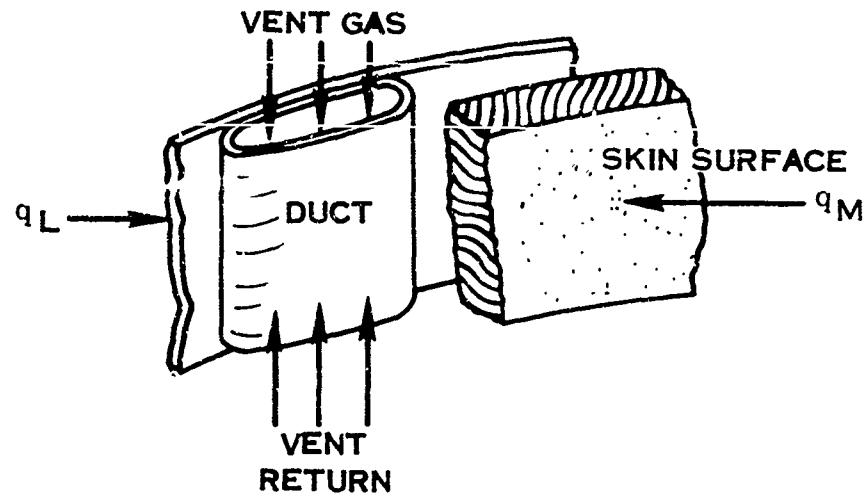


FIGURE 80. CROSS SECTION OF VENTILATING PASSAGE

analyze the local distribution of flow, temperature, and humidity. In suit design, therefore, the problem of ventilation distribution is normally solved empirically based upon the subjective impressions of the test subject and a relatively few temperature and perhaps humidity measurements.

To optimize suit design, the ventilation cooling flow must be as low as possible to minimize pressure drop and pneumatic power. Since unlimited cooling capacity is not available, some measure of the success of the cooling system in removing the total heat load is useful. One such measure is the ventilation effectiveness which is defined in Equation 126.

$$\text{Ventilation Effectiveness} = \eta_v = \frac{q_C}{q_{C \max}} \quad (128)$$

where

q_C = actual heat removal rate of coolant stream

$q_{C \max}$ = maximum possible heat removal rate of coolant at T_b

T_b = maximum possible suit outlet temperature, 37°C (98.6°F)

Ventilation effectiveness, however, does not indicate the actual capacity of the stream. Rather, it expresses the degree to which the capacity of the stream at the temperature T_b has been used.

Another measure of value in evaluating a ventilation system is the evaporated sweat ratio, defined in Equation 129.

$$SR = \frac{S_e}{S_n} \quad (129)$$

where

SR = sweat ratio

S_e = sweat evaporated

S_n = sweat produced

The sweat ratio is, in effect, a measure of the unnecessary dehydration and physiological strain of the test subject due to ineffective ventilation. Neither of these measures is sufficient as a single criterion or figure of merit of ventilation system performance. An overall figure of merit would include these measures and also the pneumatic power, maximum stream capacity, and ventilation distribution. To optimize ventilation performance one must determine how heavily to weight each of the many factors based on the intended mission. At present no universally acceptable weighting factors can be assigned because of inadequate theory and lack of experience in evaluation of ventilation systems.

Of particular interest in the problem of suit testing is the effect of suit pressure on stream cooling capacity (ref. 113), since tests are often conducted at sea level pressure and the results extrapolated to the actual suit operating pressure.

Sea level tests are simple and inexpensive to conduct and therefore present a very desirable approach to the evaluation of suit cooling provided the results are meaningful. Ideally, the test at sea level would be conducted so that both the latent and sensible heat rejected to the gas stream are independent of the suit pressure. Consider the effect on gas cooled suit performance of operation at 181 mm Hg and at 760 mm Hg at the same suit inlet temperature, humidity, and volume flow rate. The sensible heat capacity of the gas stream, q_s , is given in Equation 130.

$$q_s = \rho_g V_g c_{pg} (T_o - T_i) \quad (130)$$

where

ρ_g = gas density

V_g = volume flow rate

c_{pg} = specific heat of gas

T_o = outlet temperature

T_i = inlet temperature

If initially T_o is assumed independent of pressure, then q_s will vary in proportion to the change in density. Using the performance values from Figure 6, q_s will increase from 42 kcal/hr to about 176 kcal/hr. Heat leakage requires 38 kcal/hr of this capacity and, since the metabolic heat q_m is constant, the latent heat must decrease from 349 kcal/hr to 215 kcal/hr. Thus, the ratio of sensible to latent heat removed from the body varies with pressure as shown in Table IV.

TABLE IV

GAS COOLED SUIT

APPROXIMATE PERFORMANCE VALUES FOR
ALTITUDE AND SEA LEVEL OPERATIONS
 (REFERENCE FIGURE 6)

SUIT PRESSURE	181 mm Hg	760 mm Hg
Metabolic Heat	353 kcal/hr	353 kcal/hr
Sensible Heat	42 kcal/hr	176 kcal/hr
Heat Leakage	38 kcal/hr	38 kcal/hr
Body Heat	4 kcal/hr	138 kcal/hr
Latent Heat	349 kcal/hr	215 kcal/hr
Inlet Temperature	8°C	8°C
Outlet Temperature	31°C	31°C
Sensible-Latent Ratio	1:86	1:1.5
Evaporated Water Loss	0.60 kg/hr	0.37 kg/hr

If this were the only effect, then it might be possible to keep the ratio constant through control of the ventilation flow; however, there are other problems. Fundamentally, an accurate simulation requires that the local film coefficient, skin surface temperature, and mass transfer be duplicated. This is the ventilation distribution problem which is analytically so complex. Therefore, it is concluded that pressure changes will alter the local heat transfer conditions within the suit and variations in flow rate or inlet conditions cannot entirely negate these effects. This problem of cooling simulation at other than normal suit pressures can be an important factor in gas cooled suit evaluation. A better definition of the mechanism of local heat transfer within suits will require careful analytical study based on the results of controlled tests.

HEAT REMOVAL IN A LIQUID COOLED SUIT

In a combined gas-liquid cooled suit the liquid is the principal cooling medium. Gas ventilation is provided for respiration and removes both sensible and latent heat from the lungs. The gas flow rate is lower than in the gas cooled suit;

however, since the gas flow removes insensible perspiration and some sensible heat from the body, the analysis of the heat rejection to the gas cooling stream is identical to that in the previous discussion. Only the magnitudes of the sensible and latent heat are changed.

In current liquid cooling systems, the liquid, normally water, enters the suit at a torso umbilical and is distributed through major distribution tubes to an array of equi-resistant tubes which distribute the coolant over the body surface. The return flow is collected at a central manifold and exits through the umbilical. The direction of flow is usually from the extremities to the torso. Body heat is transferred directly to the coolant stream by conduction from the skin through the tube walls. The rate of heat removed by the liquid stream q_L is simply the product of the liquid flow rate, the specific heat of the cooling fluid, and the temperature rise as in Equation 131.

$$q_L = w_L c_{pL} \Delta T \quad (131)$$

where

w_L = liquid flow rate

c_{pL} = specific heat of the liquid

ΔT = temperature rise of the liquid

For instance, in a current suit operating at 402 kcal/hr, the total liquid cooling heat rejection is about 395 kcal/hr as shown on the chart of performance values in Figure 8. The analysis of the heat transferred to any individual tube within the system is very complex. All of the heat flow paths of the previous example must be considered and, in addition, there is the heat exchange between the skin and the cooling liquid and between the liquid and the gas stream.

Like the gas cooled suit, the sensible-latent heat ratio will vary as a function of suit operating pressure; however, since the heat rejected by the gas stream is only a fraction of the total heat, the pressure effect is proportionately reduced and is probably negligible. The approximate performance values for a typical gas-liquid cooled suit at a pressure of 181 mm Hg and 760 mm Hg are shown in Table V where the outlet temperature is assumed constant as in the previous example for the gas cooled suit. Again, the ratio of sensible to latent heat in the table refers to metabolic heat.

Helmet Considerations

Within the helmet, the ventilation flow must provide sufficient oxygen to meet metabolic needs, remove expired air to prevent rebreathing, provide visor defogging, remove that part of the energy of metabolism rejected as heat by the head surface area and the lungs, and remove the heat leaked into the helmet. In general, the ventilation air enters the helmet through ducts in the neck ring and is distributed over the top of the head and downward across the visor warming the inner surface

TABLE V

LIQUID COOLED SUIT

APPROXIMATE PERFORMANCE VALUES FOR
ALTITUDE AND SEA LEVEL OPERATIONS
 (REFERENCE FIGURE 8)

SUIT PRESSURE	181 mm Hg	760 mm Hg
Metabolic Heat	402 kcal/hr	402 kcal/hr
Heat Leakage	38 kcal/hr	38 kcal/hr
Sensible Heat - Gas	15 kcal/hr	63 kcal/hr
- Liquid	395 kcal/hr	307 kcal/hr
Latent Heat - Gas	30 kcal/hr	70 kcal/hr
Inlet Temperature - Gas	7°C	7°C
- Liquid	19°C	19°C
Outlet Temperature - Gas	31°C	31°C
- Liquid	24°C	24°C
Sensible-Latent Ratio	12:1	4.8:1
Evaporated Water Loss	0.05 kg/hr	0.12 kg/hr

to prevent fogging, deflecting the expired air away from the visor, and simultaneously flushing the oral-nasal region of carbon dioxide. From an engineering point of view, all of these functions must be provided at a minimum ventilation flow rate to minimize pneumatic power and maximize system efficiency. From a physiological point of view, minimum flow is also desirable to prevent drying of the eyes and eyelid flutter. The total oxygen flow to the helmet is typically about 170 liter/min (6 cfm).

Helmet geometry is normally designed to maximize the flow velocity through the oral-nasal region to sweep away the expired gas so that the quantity of carbon dioxide re-inspired is no greater than would be inspired in a sea level atmosphere enriched with, say 1% carbon dioxide. Whereas helmet vent flow is essentially steady state, respiration is not. Inspired and expired volumes and velocities are time variant as is the concentration of carbon dioxide. Consequently, a theoretical

evaluation of the mechanics of the turbulent mixing and diffusion in the oral-nasal region would be extremely difficult. Therefore, the volume flow rate to a helmet is normally established using an empirical measure of physiological performance rather than a theoretical determination of carbon dioxide concentration. Techniques for the measurement of these physiological factors are discussed in a subsequent section.

SUIT EVALUATION MEASUREMENTS

In this section the major suit factors involved in the design and testing of life support aspects of space protective garments have been discussed. During testing of these garments certain physical measurements are required to evaluate suit performance. These measurements are as follows

- Coolant inlet temperature
- Coolant outlet temperature
- Coolant inlet humidity
- Coolant outlet humidity
- Coolant flow rate
- Distribution of coolant temperature
- Inlet gas concentration
- Outlet gas concentration
- Helmet gas flow rate
- Defogging flow rate

This list does not include those measurements required to define heat leakage. The requirements for these leakage measurements and for the determination of the external environment depend on the nature of the testing being performed and are specific to the thermal protective quality of the suit. They, therefore, are deferred until Section V.

SUIT EVALUATION CONCEPTS

Now that the major physiological and suit life support requirements have been defined, consider the test methodology for the evaluation and further development of the life support features of a space protective ensemble. The basic life support

properties of the suit which must be evaluated are (1) the capacity of the suit to provide an adequate thermal environment for the astronaut and (2) the effectiveness of the helmet in supplying uncontaminated respiratory gas to the astronaut. In addition, a means must be available for the measurement of the metabolism so that the metabolic cost associated with the performance of any defined task may be determined and energy balances may be obtained. How can this evaluation best be performed? First consider the evaluation of the suit cooling system.

Cooling System Evaluation

During the development of full-pressure suits and currently in the development and testing of space suit assemblies, several different techniques have been employed to evaluate suit cooling systems. These have included both manned and unmanned testing. Ideally, the technique chosen should provide information relating body heat storage, skin temperature distribution, and the dehydration that will result for a particular environment and a specific mission. Obviously, this could be most realistically accomplished by a manned test in a thermal-vacuum simulator in which the environment and tasks for the complete mission profile are duplicated. The objective, however, is to develop a test methodology which will provide similar information without the physiological variability, hazard, time, and expense of such a program. Since we are seeking objectivity consistent with a realistic assessment of the true suit performance, several test concepts will be examined.

Consider first, however, the primary heat sources within the suit. Basically, the cooling stream absorbs (or rejects) heat from the body surface and the suit inner wall. Since the metabolic heat is the predominant heat load and the coolant is relatively uniform in temperature, the suit inner surface temperature is essentially independent of the rate of heat leakage through the suit. Therefore, at least to a first approximation, heat leakage and metabolic heat may be considered separately and their effects assumed additive. Obviously, this is not entirely true since the suit inner wall temperature will vary slightly and the increase in coolant enthalpy as it absorbs the heat leaking through the suit will alter skin temperature distributions and the relative proportion of sensible and latent heat rejected by the body. Although the effect of heat leakage separation appears small, no controlled tests have been conducted to determine the actual magnitude of the effect on body heat storage and skin temperature distribution. However, this separation of heat is of significant value in simplifying the thermal tests and, therefore, the heats will be considered independently. Only the effects of metabolic heat are considered in the following discussion.

UNMANNED TEST CONCEPTS

Since the distribution of cooling within a suit depends upon the geometry of the flow passages between the undergarment and the suit, it is readily apparent that realistic unmanned tests require, as a minimum, an anthropomorphic dummy which

will fill the suit. In the following discussion, consideration is given primarily to the liquid cooling system since thermodynamically this system is more amenable to objective dummy testing. Where pertinent, factors associated with the more complex gas ventilated system will be discussed. The several dummy concepts considered are the following.

1. Single-section Dummy, Temperature Controlled
2. Multi-section Dummy, Temperature Controlled
3. Multi-section Dummy, Heat Controlled
4. Multi-section Dummy, Thermoregulatory Simulator

SINGLE-SECTION DUMMY, TEMPERATURE CONTROLLED -- This dummy is a highly conductive "copper man" whose temperature is uniform and can be regulated. With the dummy wearing the liquid cooled garment and the pressure suit, the environment is adjusted to minimize or eliminate heat leakage through the suit. Water flow is circulated through the cooling system and the inlet and outlet temperatures of the flow are measured. Once thermal equilibrium has been reached, the heat rejected from the suit is identically equal to the electrical power dissipated within the dummy and the temperature over the dummy is uniform by definition. Say the dummy's skin temperature is maintained at 34°C and the total power to the dummy is monitored. Liquid water enters at 110 kg/hr at 8°C. Now the exit temperature of the water and the total heat supplied to the dummy will depend upon the thermal interface conductance between the tubes and the dummy. If the conductance is high, the water temperature will quickly rise to near 34°C and will remain at 34°C until it exits from the undergarment. The rate of heat transfer is simply, $q_L = w_L c_{pL} \Delta T$; for the assumed values, q_L is 2850 kcal/hr or an equivalent electrical power of 3310 watts. If the interface conductance is decreased, no apparent change will occur until the thermal capacity of the coolant stream exceeds the rate of heat transfer through the interface, at which time the exit temperature will begin to decrease. Since there is no assurance that the fit and, therefore, the conduction between the liquid cooling garment and the dummy will be similar to the fit with the man, there is no simulation in total metabolic heat. Since neither the local temperature of the water nor the dummy surface temperature simulates that of the man, the test is of no significant value for an assessment of the cooling capability of the suit system.

MULTI-SECTION DUMMY, TEMPERATURE CONTROLLED -- Consider a dummy similar to the single-section dummy; however, now the dummy is divided into a finite number of sections as shown in Figure 81, each of which is individually temperature controlled. The power supplied to each section is individually measured. As in the single-section dummy, the temperature rise of the water in each section will depend upon the interface conductance in each section. Consider, for example, the water entering the right lower leg section. Assume that the interface conductance is high; therefore, considerable heat will be picked up as the water

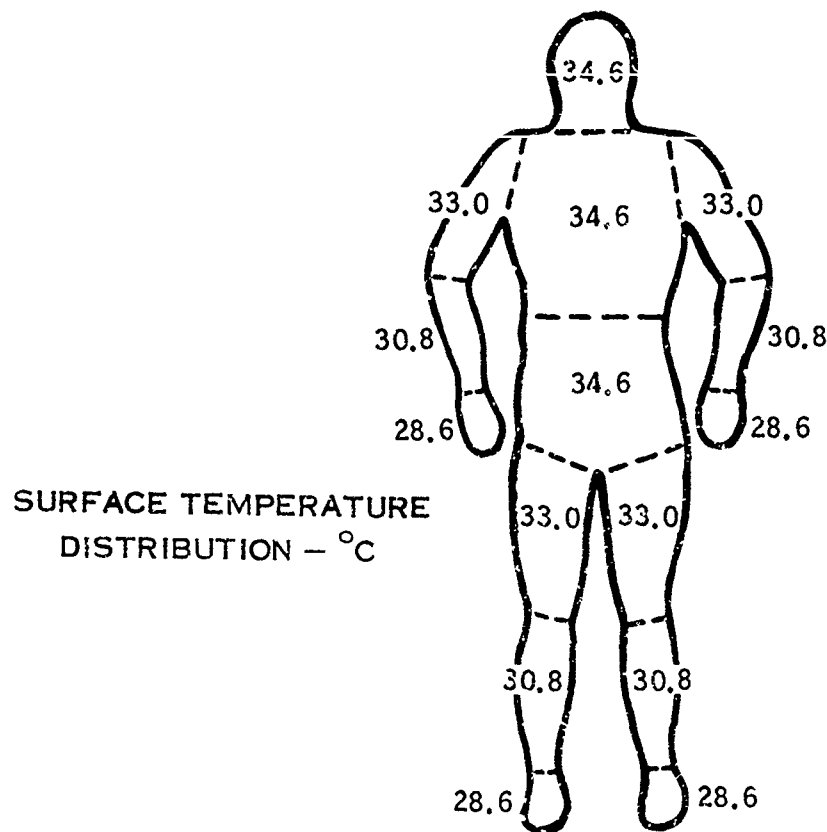


FIGURE 81. MULTI-SECTION DUMMY, TEMPERATURE CONTROLLED
(REFERENCE TABLE III)

cools this section and a large water temperature rise will occur. Therefore, when the water reaches the upper leg section, it no longer has the capacity to absorb as much heat because of the small temperature difference between the water and the section surface even though the interface conductance on the upper leg section may be large. The power supplied to the two sections will, therefore, differ. In man, however, the skin conductance is finite and the skin temperature in the lower leg section would fall. The body would sense this fall and vary the effective conductivity of the skin. Thus, in man the heat rejected in the lower leg would be less than that of the temperature controlled dummy, while the heat rejected in the upper leg would be greater than that in the dummy.

By observing the power supplied to each section of the dummy, some information can be gained as to the relative fit of the liquid undergarment on the dummy but little benefit beyond this is gained. The total heat (the sum of all the section heats) supplied to the dummy does not simulate the metabolic heat but depends only on interface conductance and coolant stream capacity. The simulation is still not sufficient to be useful.

MULTI-SECTION DUMMY, HEAT CONTROLLED -- Consider the same multi-section dummy; however, now a fixed amount of electrical power is supplied to each section and the section temperature is measured. Figure 82 shows this dummy with

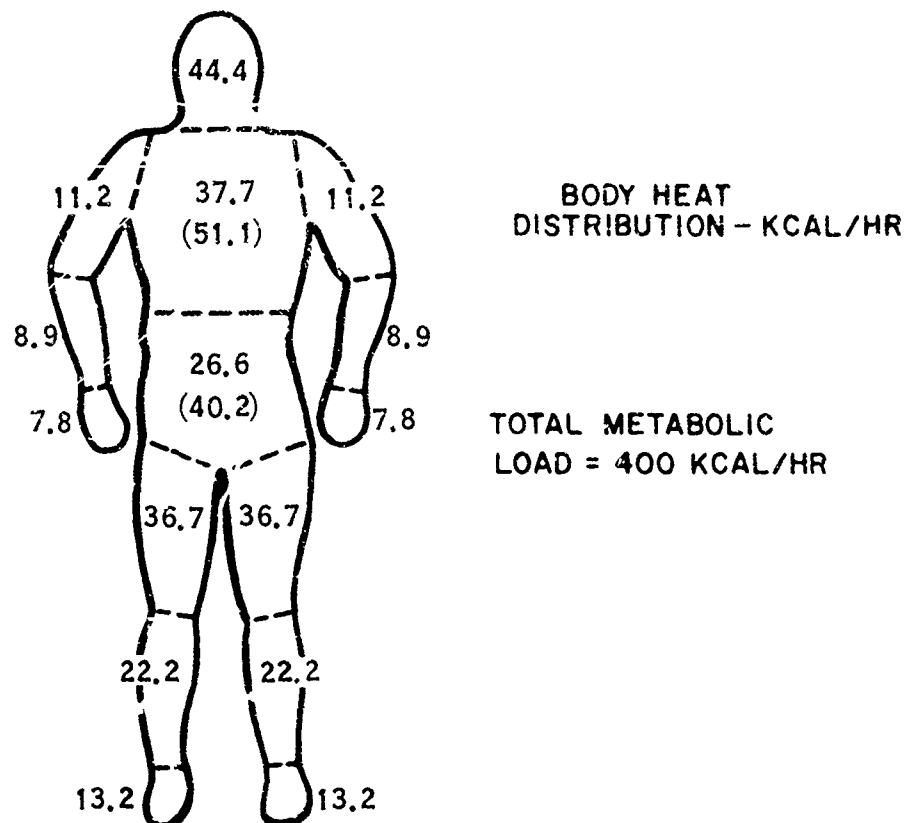


FIGURE 82. MULTI-SECTION DUMMY, HEAT CONTROLLED
(REFERENCE TABLE III)

equivalent metabolic heats assigned to each of the sections of the dummy, assuming that the regional heat rejection during work is nearly proportional to the regional skin area. The liquid cooling fluid enters the suit, circulates around each of the heated sections in turn and exits from the suit. Assume that the interface conductance and the dummy skin conductivity are constant. Again consider the case in which liquid enters the first section, the lower right leg. The heat transferred is again simply $q_L = w_L c_{pL} \Delta T_L$. Since q_L and c_{pL} are constant and q_L is controlled, ΔT_L is defined and thus the water temperature entering the second section is established. As this process is repeated over the entire dummy surface, the average skin temperature of each section will be uniquely defined by the prior section and the heat load q_L assigned to the section being considered. Clearly the dummy skin temperature will be defined by the arbitrary distribution of sectional loads and by the conductances.

Unlike a man whose skin conductivity can vary and whose circulatory system can carry heat internally between sections, an unnatural temperature distribution has been forced. Extreme variation in dummy section temperature may indicate a poor fit between the liquid cooling garment and the dummy surface.

It is apparent from the consideration of these three dummy concepts that the principal limitation of the thermal dummy is the failure to simulate adequately the thermoregulatory and compensatory mechanisms of the human. The regulatory

mechanisms which control the distribution of heat to optimize heat rejection, discussed briefly in Section II, are extremely complex and, in fact, are not well understood. Consider, however, the possibility of constructing a dummy which has some of the human regulatory mechanisms built into its heat control system.

MULTI-SECTION DUMMY WITH THERMOREGULATORY SIMULATION --
Clifford has shown by heat rejection measurements on various portions of the body that the effective conductivity of the skin of a resting man decreases as skin temperature decreases (ref. 21). This effect is illustrated in Figure 83. Note that the extrapolated curves intersect the temperature axis at about 39°C. Since 39°C is greater than any body temperature, the curves can, with caution, be explained by a variable skin conductivity.

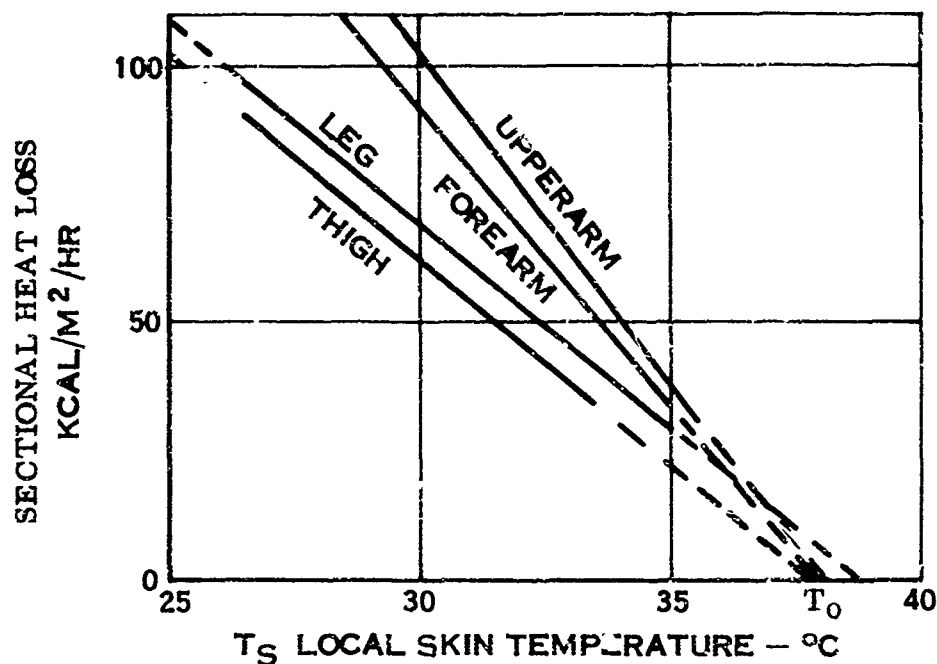
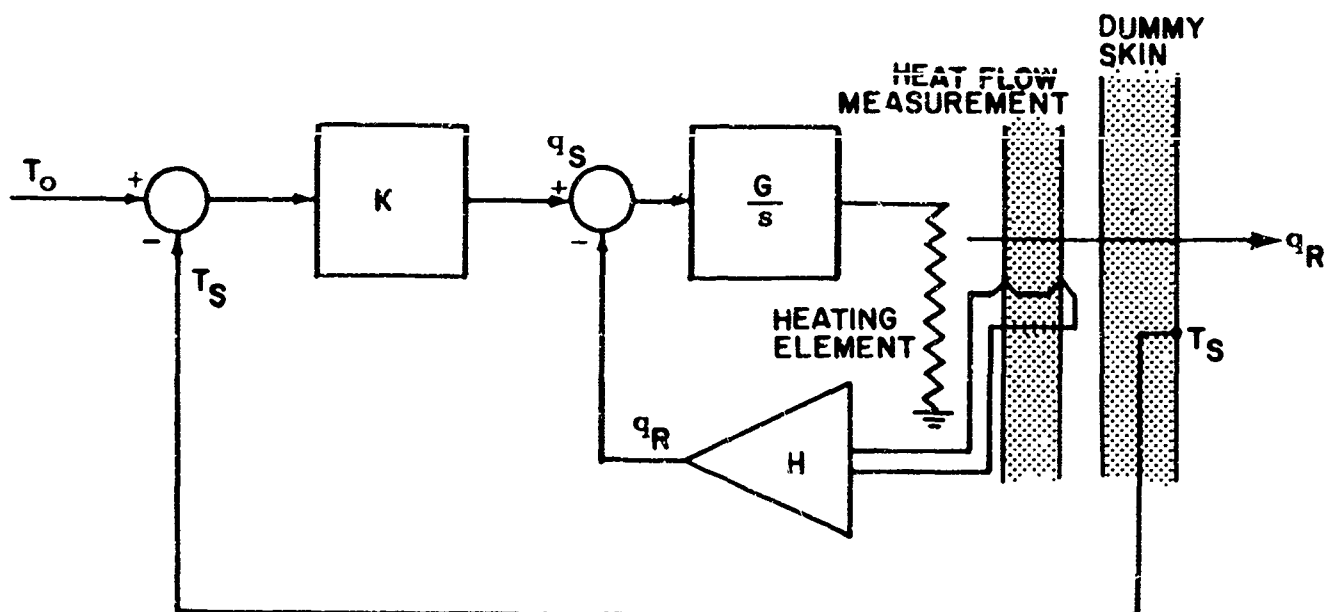


FIGURE 83. SECTIONAL HEAT LOSS VARIATION
(FROM CLIFFORD, REF. 21)

Consider now the same multi-section dummy programmed to follow these curves using a relatively simple operational amplifier technique which varies the electrical power supplied to any section as a function of temperature, as shown in Figure 84. In this circuit for a typical section, the heat rejection rate q_R is found by measuring the temperature drop across a thermal resistor between the heating element and the dummy skin. In steady state, q_R is controlled to the desired sectional heat q_S by the integrating amplifier $\frac{G}{s}$. q_S in turn is controlled according to a curve like Figure 83 by setting the gain K and the reference temperature T_0 .

For the test previously described, the temperature distribution on the dummy will now more closely approach that of the human. This is best seen by considering



LEGEND

- q_R = Heat Rejected
- q_S = Desired Sectional Heat
- T_o = Reference Temperature
- T_s = Skin Temperature

FIGURE 84. CONTROL CONCEPT FOR DUMMY THERMOREGULATORY SIMULATION

a hypothetical example. Water enters the right lower leg section as before where we assume there is high conductance between the liquid cooling garment and the dummy. This means that the surface temperature of the dummy in this region will fall. The control system will sense the temperature decrease and increase the sectional input power according to the programmed curve. The total heat supplied to the dummy is the sum of the heats to each individual section; the heat in each section in turn depends upon the skin temperature of that section. Therefore, a complex analog control system is required if each section is to assume a correct proportion of the total heat while maintaining total heat at the desired rate.

Testing with this dummy then yields results which are perhaps more valid than with any other dummy; however, the simulation is based on the extremely limited data of Clifford which thus far has been published only for the resting man. The major interest, of course, is in the active exercising man. Thus, dummy testing may be of some value in assessing the problem of temperature distribution within the suit; however, three major problems remain: (1) the thermoregulatory system of the dummy, although complex, hardly begins to simulate the thermoregulatory and compensatory mechanisms of the human, (2) skin temperature

simulation is critically dependent upon the fit of the cooling garment and the interface conductance and (3) even if the skin temperature distribution on the dummy simulated that of the human exactly, the data could not be easily interpreted because there is little information on the optimum surface temperature distribution.

A multi-section dummy of the type discussed is currently being designed and fabricated by the A. D. Little Company under contract to NASA/MSC. It is understood that this dummy will have 17 individually heated sections, the heat input to each section being controlled as a linear function of skin temperature. It is also understood that physiological tests are planned at NASA to establish more complete empirical relationships between heat flow and mean skin temperature to substantiate and extend the work of Clifford, particularly into the areas of the conduction cooled, exercising man. The results of these tests and the degree to which the A. D. Little dummy can simulate these processes should clarify the role of the thermal dummy in the testing of liquid cooled space suit systems.

Thus far, the discussion has been restricted to a liquid cooling system. If the problems of simulating the latent cooling of the gas ventilated system are also considered, the complexity becomes awesome because the dummy should sweat. It is clear that dummy testing cannot replace manned testing in the thermal evaluation of suits.

MANNED TEST CONCEPTS

Having been led ultimately to the conclusion that suit cooling systems must be evaluated through manned testing, consider now the possible approaches to this testing. These may be classified by the degree to which they duplicate the extravehicular environment and mission. The thermal tests may be transient or steady, with heat leakage or without, and at space vacuum or not.

Historically, transient thermal testing has been employed to evaluate full pressure suits. Kaufman has determined the ventilating capacity of various suits by measuring the rate of heat storage and the "unimpaired performance time" of test subjects in an intolerable thermal environment. (ref. 57) The suits being considered, however, were primarily emergency protective garments. The limits of unimpaired performance time are related to the maximum survival capability of the man under thermal emergency conditions. This type of testing will be valuable for testing of space suits to simulate emergency conditions such as failure of the vehicle thermal control system or during re-entry. However, for the testing of space garments under normal conditions, thermal steady state must be assumed. Therefore, steady state testing is not only preferred, but is essential for an accurate assessment of physiological strain.

Heat leakage will be kept to a minimum during the testing. As was shown earlier, heat leakage has only a small effect on the ability of the suit cooling system to absorb metabolic heat. Because it is normally low, its effect on stream capacity is small, and it is almost impossible to measure and control accurately.

Altitude affects the absolute pressure in the suit and, therefore, the cooling capacity of the gas system. Testing at other than normal suit pressure must be approached with caution. Consider first a simple sea level, steady state, zero heat leakage, manned test. The accuracy of this technique will first be explored and more complex tests then considered.

SEA LEVEL MANNED TEST -- The suit is pressurized to 180 mm Hg above ambient. The subject performs a task which produces the metabolic rate desired for the test. The nature of the task is unimportant provided the test subject can perform the task repeatably for a sufficient period of time to reach thermal stability. The test setup is shown in Figure 85.

The test subject walks on a level treadmill at a steady rate to develop a constant rate of metabolic energy expenditure, say 400 kcal/hr. The cooling system of the suit is supplied from the oxygen and liquid cooling systems shown on the schematic. Zero heat leak through suit is maintained by air conditioning and by providing sufficient insulation over the suit. Work done upon the environment is essentially zero since the subject walks on a level treadmill. The energy balance then reduces to Equation 132 which states that the metabolic heat equals the sum of the heat rejected and the heat stored.

$$Q_M = Q_R + Q_S \quad (132)$$

The right hand side of this equation can readily be evaluated since Q_S can be determined by measuring the rise of the mean body temperature, measuring body weight, and assuming a specific heat. Q_R is evaluated without spirometry by measuring the coolant weight flow and enthalpy change. This test, then, provides information concerning heat storage, dehydration, temperature distribution, heat removal, and, by summation, metabolic energy expenditure. Thus, a relatively simple test can yield much of the data required for an evaluation of the suit cooling system.

Now, however, examine the problems associated with this type of testing. First, the test is conducted at 940 mm Hg rather than the actual suit operating pressure. There is no evidence that the thermoregulatory process is pressure dependent, but the cooling capacity of the gas stream varies with specific volume as discussed on page 165. Second, the control of heat leak with air conditioning is inaccurate. Third, metabolic rate is not directly measured so there is not enough data for a heat balance to check for gross errors. However, in this test we are concerned with the way in which heat is distributed through the body and the skin temperature resulting from the combined effects of thermoregulation and ventilation distribution.

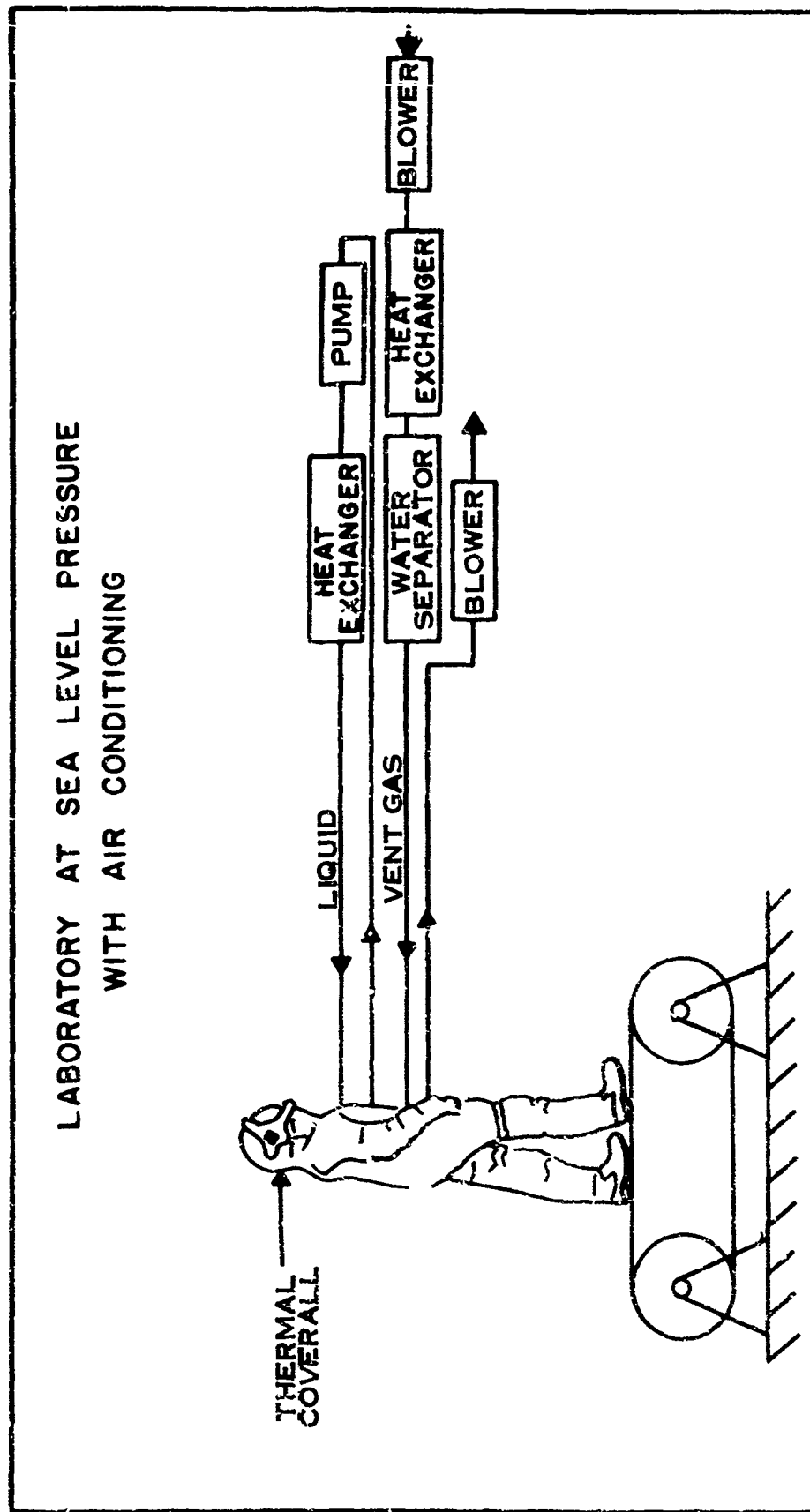


FIGURE 85. TYPICAL SEA LEVEL TEST SETUP

It is concluded that tests at other than normal suit pressure are useful, particularly in view of their simplicity and convenience, but the data must be interpreted with caution and in the final analysis cannot replace data from tests at the normal suit pressure. The error sources are now discussed in more detail.

Accuracy depends on the degree to which the useful work and heat leakage can be maintained zero. The goal of zero useful work is relatively easy to achieve by walking on a constant speed horizontal treadmill. All of the man's work is expended in moving the suit and is, therefore, converted to heat within the suit. (The suit does work in moving the air within the room, but the magnitude is insignificant). A zero heat leak is more difficult to achieve. Either the suit external surface temperatures must be maintained at the same temperatures as suit internal surface, or the conductivity of the suit must be near zero. The degree to which these goals can be achieved has not been accurately determined; however, limited data from testing at Hamilton Standard indicate that heat leakage in controlled tests has been kept below 10 kcal/hr. Heat leakage also affects metabolic cooling capacity and, therefore, must be considered in assessing cooling performance. Assume in the sea level zero heat test that a gas cooled suit is to be evaluated at about 350 kcal/hr (See Table IV and Figure 6). The actual heat leakage is 38 kcal/hr but in this test q_L is zero. Therefore, the gas stream has 38 kcal/hr of additional sensible capacity with which to remove metabolic heat. This will further alter the sensible-latent ratio. To avoid this, the sensible capacity of the inlet air can be decreased by adding 38 kcal/hr to the inlet stream before it enters the suit. The dew point of inlet stream must be maintained at 8°C if the latent capacity is to remain unchanged. Obviously this technique is effective only for the simulation of inward heat leakage. Since the local conditions within the suit are not entirely simulated, this method does not duplicate the actual extravehicular situation; however, it should improve the simulation without the attendant disadvantages of actually attempting to duplicate the heat leakage distribution through the suit.

In the simple sea level test the metabolic heat was not measured; therefore, no check is possible on the thermal balance of the suit system and measurement inaccuracies may go unnoticed. To develop further confidence in the validity of the data, the total metabolic heat produced must be measured by alternate methods. Since the pressure within the suit is 180 mm Hg above the ambient pressure, the gas analysis equipment normally used to determine metabolic energy expenditure cannot be used directly. Instead, three other approaches may be taken:

1. To measure the heart rate and rectal temperature rise of the nude test subject as a function of metabolic rate and then use these secondary measures to determine metabolic rate when suited and pressurized.
2. To redesign the gas analysis equipment for operation at other ambient pressures.
3. To conduct the test at reduced pressure (7300 ft pressure altitude) so that the suit internal pressure is at sea level pressure.

The first of these is indirect and variable. Although it is simple and requires no special equipment or suit penetrations, it is not sufficiently accurate to lend confidence to the thermal balance data, the principal purpose of its measurement. The two remaining techniques are equally valid and are discussed in greater detail later.

MANNED TESTS AT ALTITUDE -- Since the principal inaccuracy in the previous testing results from not simulating the heat removal capacity of the cooling stream, the obvious approach to the reduction in this error is lowering the suit internal pressure. An added benefit is the reduction in the error due to heat leakage that accompanies ambient pressure reduction. However, as the pressure is reduced, the hazard to the test subject, the number of test personnel required, and the time and difficulty associated with the testing increase disproportionately. A reduction in pressure to 60,000 feet in a conventional aircraft high-altitude chamber would reduce the suit internal pressure to 236 mm Hg. The error in total sensible heat capacity of the previous example is then only 12 kcal/hr, so small that any further decrease in pressure, say in a space simulator, is unjustified for zero heat leakage testing.

An even closer simulation is possible by reducing the suit differential pressure. If the internal pressure is reduced to 180 mm Hg absolute and the chamber pressure to about 140 mm Hg, then the cooling capacity is duplicated and only simple chamber facilities are required. However, the suit inflation pressure is only 40 mm Hg and, therefore, is considerably less encumbering. Thus, to develop a metabolic rate of, say 350 kcal/hr, the subject must walk faster than he would have at normal suit pressure.

In a liquid cooled suit, the liquid cooling capacity is unaltered by internal pressure except, possibly, for a very minor change in thermal conductance between the skin surface and tubes due to tube-wall distension as the external pressure is decreased. No measure of this change in conductivity is known, but, with adequate strength, the distension and, therefore, the conductance change must be very small.

In summary, sea level manned testing for the evaluation of the cooling performance of space suit garments can be of value in determining body heat storage, dehydration, and skin temperature distribution but must be approached with caution. To perform these measurements with confidence, a direct measure of metabolic heat production is required. Testing at lower suit pressures and higher altitudes will improve the accuracy of the data, but will involve increases in cost, time, and facilities. This method is recommended and discussed in detail in the integrated test system presented at the end of Section IV.

Helmet Flushing Evaluation

A complete evaluation of the helmet ventilation system requires the measurement and assessment of each of its several functions, i.e., oxygen transport, oral-nasal flushing, visor defogging, lung and head surface heat removal, and helmet heat removal. All of these functions can be separately evaluated. Oxygen transport is evaluated simply by an unmanned test in which the helmet ventilation flow rate is measured. Helmet heat leakage and visor defogging tests are discussed in Sections V and VI respectively and metabolic heat removal tests are an integral part of the cooling tests discussed earlier. In this section, test concepts for oral-nasal flushing are discussed.

The prime function of the ventilation flow to the helmet is to sweep away exhaled carbon dioxide-rich gas before the next inhalation. This oral-nasal flushing depends on the volume flow through the helmet and upon the head, oral-nasal, and helmet geometry. Test concepts for evaluating oral-nasal flushing include both dummy and manned tests.

UNMANNED TEST CONCEPTS

A breathing head replica could be fabricated which approximates the facial dimensions, tidal volume, respiration rate, and nasal discharge pattern of a human subject. On each inhalation, the gas inspired by the dummy would be injected with a contaminating tracer gas such as carbon dioxide in the same concentration as the human carbon dioxide production. This gas would then be expired and reinhaled. Upon reinhalation, the carbon dioxide level would be determined, this level being a measure of the effectiveness of the oral-nasal flushing. The approach is objective, would eliminate uncertainties due to the variations in the facial dimensions of different test subjects, and could probably simulate the human sufficiently well to be of value. However, the approach is initially expensive and does not eliminate the need to monitor carbon dioxide concentration for safety reasons in each new helmet design. A variation of this technique has been used for the analysis of respired gas in manned enclosures (ref. 58) and for the evaluation of face seal leakage in gas masks*.

MANNED TEST CONCEPTS

The principal difficulty with human test subjects appears to involve facial geometry rather than the respiratory or metabolic process itself. Careful selection of test subjects is required to insure that the range of the astronaut population

* Personal communication with Samuel Alderson, Alderson Research Laboratories, Long Island City, New York

has been covered. Two techniques using human test subjects in current use for the evaluation of the helmet oral-nasal flushing will be considered. These are known as the dead-space and end-tidal techniques. Also to be considered is a total inspired technique.

In the dead-space technique as reported by Comfort (ref. 22), a two-way valve is installed at the mouth of the test subject. Depth and rate of respiration at a particular activity level are measured. The two-way valve is then attached to a known volume so that the test subject must now rebreathe a given volume of expired gas before obtaining pure oxygen. Depth and rate of respiration are again measured and the test is repeated with increasingly larger volumes between the mouth and the breathing valve. As shown in Figure 86, a curve is obtained of dead-space volume, that is, the attached volume, plotted versus the depth and rate of respiration which depend in part on the partial pressure of CO_2 in the lungs. Now with the test helmet in place, and again performing the same activity, the depth and rate of respiration of the test subject are again measured. From the curve (Figure 86), an equivalent dead-space volume may be obtained. This technique requires several test subjects and several tests of each test subject for a statistical determination of the variability in the data.

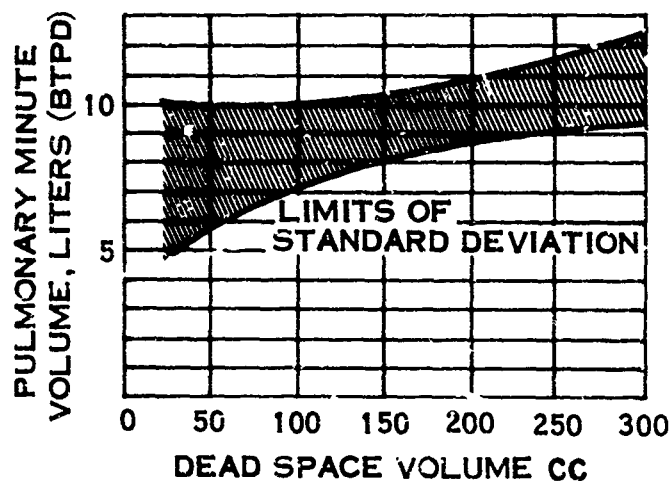


FIGURE 86. EFFECT OF REBREATHING THROUGH KNOWN DEAD SPACE VOLUMES (ADAPTED FROM COMFORT, REFERENCE 22)

In the end-tidal technique, as developed by Hardy and Lang (ref. 47), the end-tidal alveolar gas is sampled with a small capillary probe behind the incisors and carbon dioxide partial pressure is measured with a gas analyzer. Lambertsen (ref. 65) has shown that the alveolar partial pressure varies as a function of mean inspired carbon dioxide partial pressure, as shown in Figure 87. In an open room the alveolar CO_2 partial pressure of the test subject is measured as a function of the mean carbon dioxide partial pressure in the room. The subject then dons the helmet and as the ventilation flow rate is varied his end-tidal alveolar CO_2 partial pressure is measured. The results of this test are then compared with the open-room alveolar pressures, and thus a direct correlation between mean-inspired

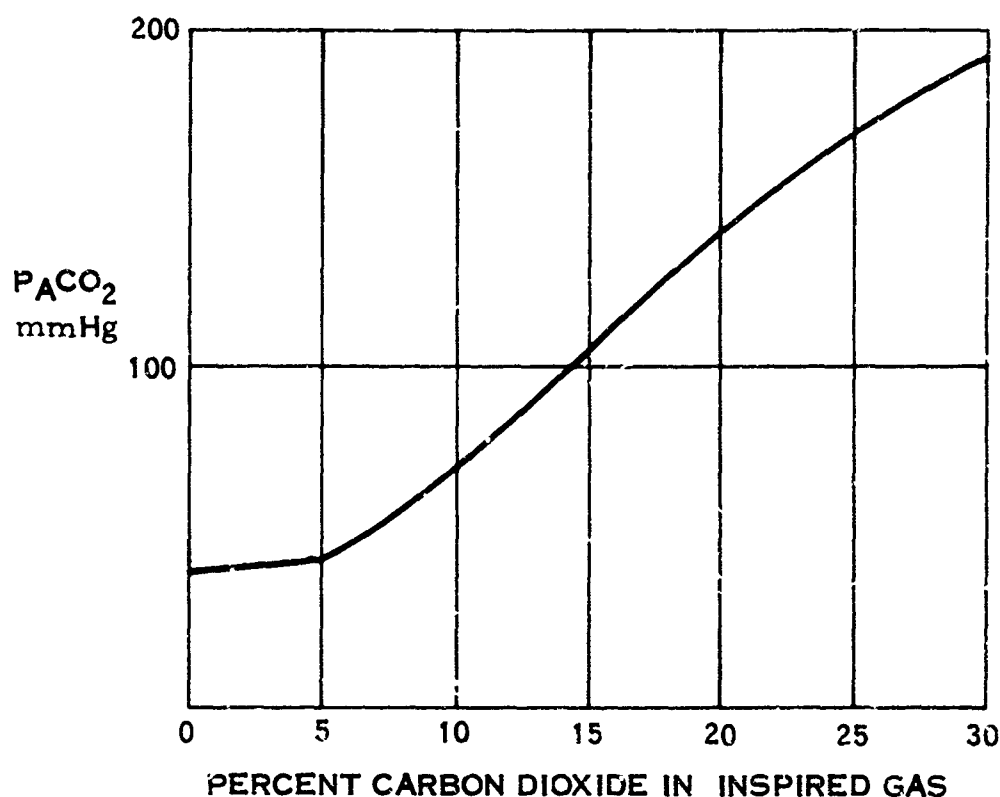


FIGURE 87. VARIATION OF ALVEOLAR PARTIAL PRESSURE WITH INSPIRED CARBON DIOXIDE (ADAPTED FROM LAMBERTSEN, REF. 65)

carbon dioxide and ventilation flow rate can be obtained. The end-tidal carbon dioxide partial pressure is somewhat less repeatable than the Haldane-Priestly forced exhalation carbon dioxide partial pressure, but it does not require trained test subjects. Either partial pressure could be used. This technique, used extensively at Hamilton Standard, has proved entirely satisfactory.

In the total inspired technique the quantity of inspired carbon dioxide is calculated. This quantity is the integral of the instantaneous volume flow rate times the carbon dioxide partial pressure level and could be obtained by electronic phase shifting, multiplication, and integration of the two measurements, sample traces of which are shown in Figure 88. The quantity of carbon dioxide inspired while wearing the helmet could then be compared to the quantity of carbon dioxide inspired by a test subject in a normal 7.6 mm Hg carbon dioxide environment. This provides an objective measure of the quantity of carbon dioxide inspired; however, the accuracy of the technique is uncertain because of the sample tube delay time and response time at the carbon dioxide analyzer. This technique is the most complex of the three discussed, has not been evaluated physiologically, and probably holds little, if any, benefit over the end-tidal method.

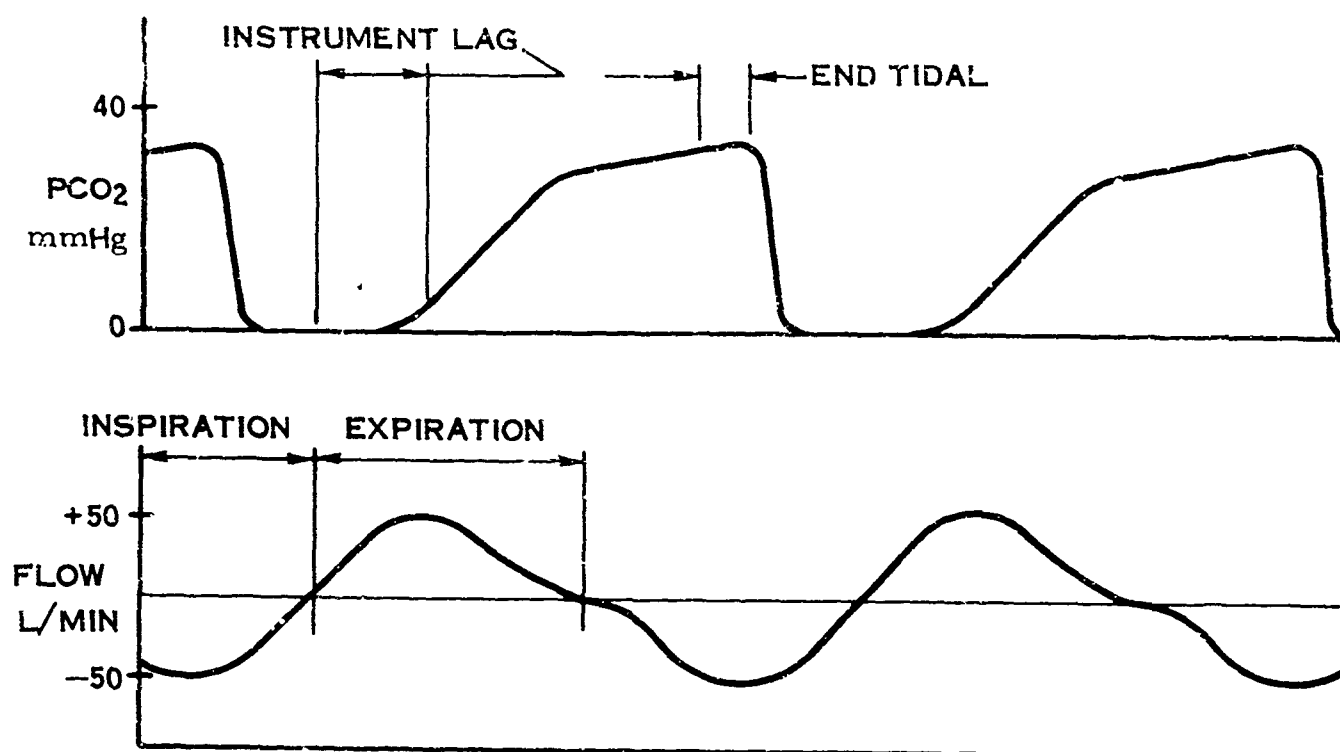


FIGURE 88. TYPICAL RESPIRATION RATE AND ALVEOLAR CARBON DIOXIDE CONCENTRATION

At the volume flow rates normally used for helmet ventilation, turbulent mixing and flow velocity rather than diffusion reduce the oral-nasal carbon dioxide concentration. Therefore, as the pressure of the ventilation gas in the helmet is varied from sea level to the actual suit operating condition, constant volume flow rates should be maintained for a more accurate simulation of the actual operating condition.

Metabolic Cost Evaluation

The determination of metabolic cost is not directly related to the evaluation of the life support system; however, it is discussed here because of its traditional association with thermal testing and because of the overlap in equipment requirements. First, methods of calculating metabolic cost from metabolic rate measurements will be discussed. Then various techniques for metabolic rate determination will be explored.

TEST CONDITIONS

The determination of the metabolic cost of a suit requires performance of a task; it is obvious that no dummy can replace the man for this testing. Metabolic cost is defined in Equation 35 as the difference between the nude and pressurized

metabolic energy rates for a specific task. To measure the metabolic cost of a suit, those variables which involve encumbrance must be simulated. It is shown in Section III that the mobility of a joint is primarily a function of the differential pressure across the joint and depends upon the angles through which the joints are moved and the rates at which they are moved. Therefore, a pattern of motion must be established and repeated uniformly, both nude and in a pressurized suit.

Except insofar as the cooling system influences the encumbrance of the astronaut, adequate cooling during the test is only of importance to the medical monitor. Inadequate cooling and body heat storage, although they may influence motivation and comfort, are not important unless they prevent completion of the testing. Since encumbrance is essentially independent of absolute pressure, all tests can be conducted at or near sea level pressure. The rate of metabolic energy production stabilizes for a given task within a few minutes; therefore, the testing need not be long nor must thermal equilibrium be reached. Consider first the performance of the task nude. Assume that the task to be evaluated involves full-body motion, for example rowing. The nude subject starts the rowing task, paced by a metronome to maintain repeatable performance. His oxygen consumption is monitored. It approaches a steady value in several minutes and the metabolic measurement is begun. Respiratory gas is collected over a sufficient period of time to obtain adequate accuracy and the subject is then allowed to stop and recover. This is repeated several times to obtain a good statistical sample.

The test subject now dons the suit to be tested and the suit is pressurized. If the gas analysis equipment can be operated at an elevated suit pressure, then the test is repeated in the sea level environment. If, however, the gas analysis equipment can be operated only at ambient pressure, the test is repeated in a chamber at a simulated 7300 foot altitude to obtain the desired 180 mm Hg pressure differential. The testing could also be carried out at higher altitudes, but since suit encumbrance is essentially independent of absolute pressure, there is no advantage to doing so. (The effect of absolute pressure depends on suit volume; but this and the effect of pressure regulation will normally represent less than 1% change in the work of joint motion. See Appendix III.)

Obviously, this technique is satisfactory only for tasks which can be performed for a sufficient period of time to obtain the required measurement accuracy. However, there are few tasks in this category which involve the motion of only a single joint and, therefore, the metabolic cost measurement, while useful in defining the overall encumbrance of the suit, is of little value in defining the encumbrance of a particular joint. The accuracy with which metabolic cost can be determined depends entirely on the ability to maintain a repeatable task for a sufficient period of time and the accuracy of the indirect determination of metabolic energy production. For well trained, conditioned test subjects in a post absorptive state, accuracies of metabolic measurement approaching 1% can be achieved.

MEASUREMENT TECHNIQUES FOR METABOLIC RATE

There are several methods of metabolic measurement that have been established as the classical basis for human energy studies. None of these techniques, however, is entirely satisfactory for use within a pressurized space suit. Therefore, before the discussion of an integrated test system for life support evaluation is begun, some of these metabolic measurement techniques will be considered briefly. Ideally, what is needed is a single instrument whose output is a direct measure of instantaneous metabolic energy production rate. None of the current techniques approaches this goal -- all depend on a number of external measurements taken over a finite period of time from which metabolic energy production rate can be computed.

The several traditional methods of metabolic determination may be classified as being either direct or indirect. The indirect techniques are further broken down into those techniques which involve the measurement of foodstuffs consumed and those which measure the oxygen required to oxidize those foodstuffs. Although these techniques are fully detailed in the literature, they are reviewed briefly here for purposes of completeness.

DIRECT CALORIMETRY -- In the measurement of metabolism by direct calorimetry, the subject occupies a thermally stabilized chamber with controlled wall temperatures to reduce heat leakage to zero. All of the heat and work produced within the chamber is directly measured as a rise in chamber temperature. Usually the food intake and waste products are also measured and an energy balance is computed. As early as 1892 Rubner was able to obtain balances within 0.5%. Even closer agreement has been obtained by Benedict and his associates. These results have confirmed that the combustion of foodstuffs is the sole source of energy in the body. (ref. 6).

Direct calorimetry forms the basis of comparison for all other calorimetric techniques. It is the fundamental and most accurate method; however, it is clearly unsuited for space suit testing. Although measurement of the heat rejection to the cooling stream of a space suit in a zero heat leak environment is in effect a direct calorimetry measurement, it does not compare in accuracy to the chamber-type direct calorimetry methods because of the zero heat leak assumption.

INDIRECT CALORIMETRY - DIET -- Metabolic expenditure may be determined from analysis of the dietary intake over an extended period of time. Since the energy of metabolism is derived from a mixed fuel composed of fats, carbohydrates, and proteins, it is necessary to determine the proportion of these substances in the mixture being oxidized. Further, the energy of foodstuffs have a lower physiological heating value than their equivalent physical heating value because of incomplete oxidation or absorption by the body. While this technique serves to evaluate long term metabolic energy production, it is unsuited for thermal evaluation of extravehicular space suits.

INDIRECT CALORIMETRY - RESPIRATION -- Metabolic energy production is most commonly determined from measurements of respiratory exchange. As discussed on page 153, the heating value of oxygen, that is, the kilocalories of heat produced per liter of oxygen consumed, is very nearly a linear function of respiration quotient. Experimental evidence (ref. 70) indicates that RQ tends to remain within narrow limits which may vary somewhat with hyperventilation, exercise, and other factors. Repeatable output requires that the test subject be in excellent physical condition on a plateau of physiological efficiency. This is assured by careful selection of test subjects and by a sustained program of physical training.

The accuracy of determination depends on the extent to which indirect calorimetry compares with direct calorimetry. Atwater has shown extremely small differences in long term tests, while the data of Merlin and Rusk show an average difference between direct and indirect calorimetry of about 1% with two-thirds of the experiments falling within 2%. The best agreement between direct and indirect calorimetry has been shown to lie in the intermediate range of RQ, about 0.8, which is a typical value for a well trained subject with a conventional diet. Tests must be conducted with the subject in a post-absorptive state performing a steady submaximal task (ref. 6).

In the following paragraphs the techniques for the determination of respiratory exchange are discussed. Traditionally the techniques have been classified as either closed or open circuit.

The Closed Circuit Method -- Closed circuit spirometry is the simplest means of measuring oxygen consumption accurately. In this method, the subject rebreathes pure oxygen from a spirometer, which is a variable volume container and carbon dioxide scrubber. The container may be an inverted, water sealed bell, counterbalanced over a pulley or it may be a wedged shaped bellows-like box pivoted and counterweighted over knife edges. The breathing circuit is shown in Figure 89. The test subject breathes through a two-way valve inhaling oxygen from the bell and exhaling carbon dioxide enriched oxygen to the bell. Carbon dioxide is prevented from accumulating in the bell by passing the expired gases through the carbon dioxide scrubber, normally a soda lime canister. A water absorber is normally installed upstream of the canister to prevent condensed water from entering the soda lime bed, thereby inhibiting carbon dioxide removal. The progressive decrease in spirometer volume indicates the consumption of oxygen. Added dead space of respiration is prevented by the two-way valve mouthpiece which effectively separates the inspiratory from the expiratory circuit. Resistance breathing can be minimized by a motor driven blower.

For accurate measurements, the bell should be sufficiently large to supply oxygen for a ten to twenty minute test period. As oxygen is inspired from the spirometer, the level of the bell drops and when oxygen is expired, the bell rises. The difference between the amount of oxygen removed and that returned to the

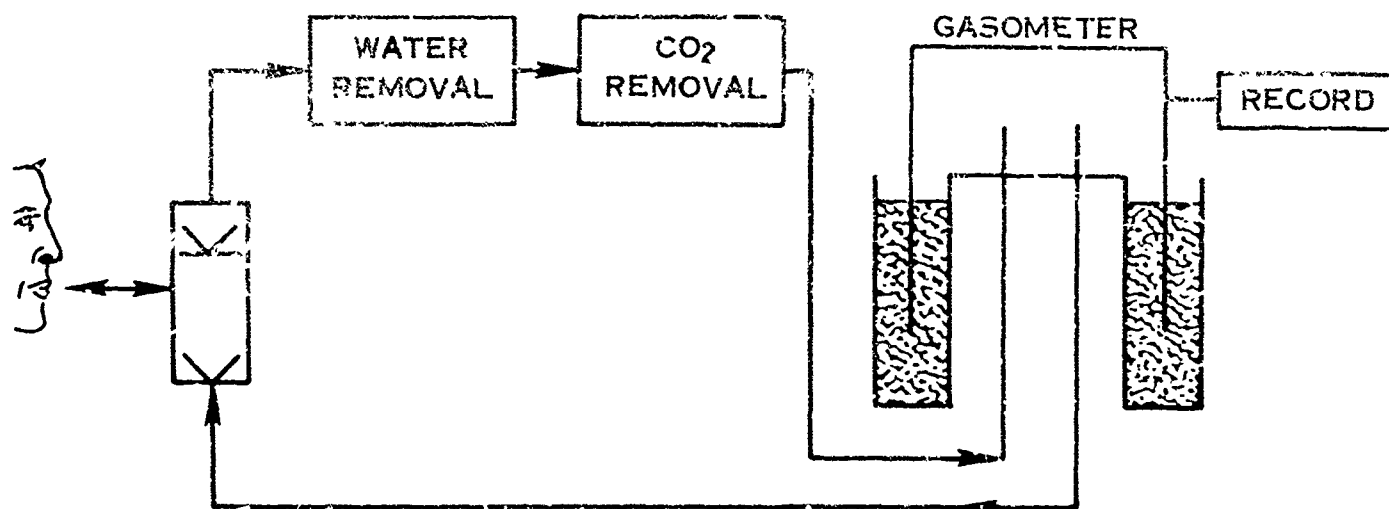


FIGURE 89. CLOSED CIRCUIT SPIROMETRY SCHEMATIC

spirometer is the amount consumed by the subject. The bell movement is recorded as a function of time. A typical time volume trace is shown in Figure 90.

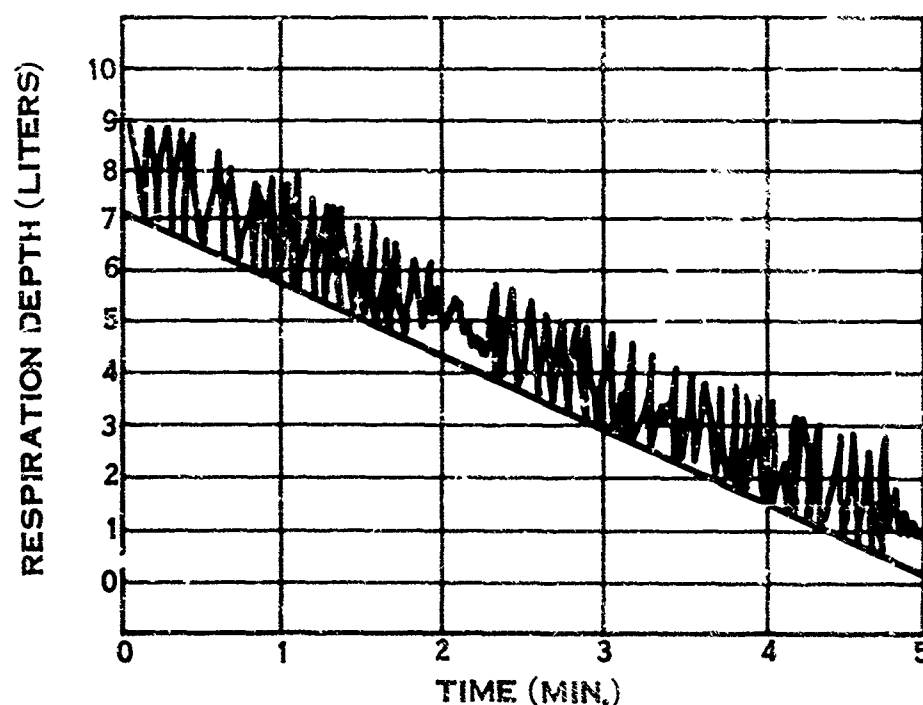


FIGURE 90. TYPICAL TIME-VOLUME SPIROMETRY TRACE
(ADAPTED FROM HARDY AND LANG, REF. 47)

The volume of each inspiration is the product of the spirometer calibration constant and the vertical projection of the inspiration trace. The progressive decrease in spirometer volume is determined from the slope of the spirometry trace. The minimum points of the trace correspond to expiration and the maximum points correspond to the full lung condition. The minima are more even because

the lung volume in the expired condition is determined by elasticity while the maxima depend on variable muscular contraction. Thus, the rate of oxygen consumption can best be obtained from the slope of the line connecting the minimum points on the spirometry trace.

In this method, respiration quotient is not determined and therefore must be assumed. Based on this assumed RQ, a caloric value for oxygen is selected and multiplied by the total volume of oxygen consumed. This number is a measure of total metabolic energy production during the period of oxygen measurement. The technique is very simple and provides a rather accurate measure of oxygen consumption. It also presents a permanent record of tidal volume, respiration rate, vital capacity, and other measures of pulmonary function. It is a standard, well developed technique; however, some problems remain. The failure to measure respiration quotient represents a potential error in metabolic energy production determination. The magnitude of this error depends upon how well the test subject's normal RQ can be inferred. Since this technique necessarily requires pure oxygen breathing, nitrogen will be evolved by the body during the test period unless the subject has been breathing pure oxygen for some time. This nitrogen will accumulate in the spirometer, and unless the gas within the bell is analyzed before and after the test, an error in oxygen consumption determination can occur. Likewise, failure of the canister to remove all of the carbon dioxide can result in a rise in carbon dioxide partial pressure in the spirometer producing an error in oxygen determination (ref. 39).

The Open Circuit Method is shown schematically in Figure 91.

The open circuit method is shown schematically in Figure 91.

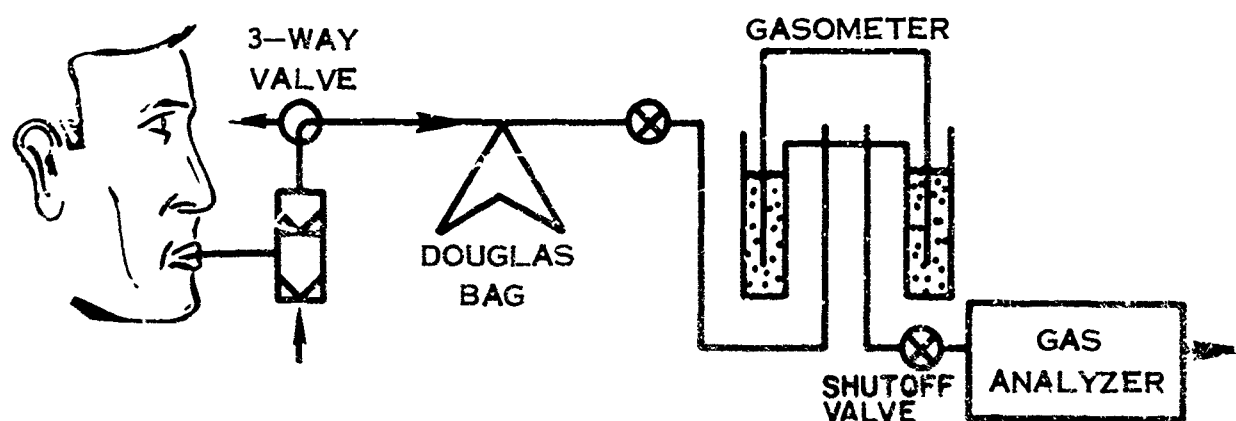


FIGURE 91. OPEN CIRCUIT SPIROMETRY SCHEMATIC

The subject breathes through a mouthpiece or mask with a valve arrangement to separate the inspired from expired air. The test subject breathes room air and exhales into a Douglas bag. The exact time required to fill the bag is recorded. During the test, the partial pressures of oxygen, carbon dioxide, and nitrogen in the inspired air are measured. At the end of the collection period, the corresponding pressures in the expired air are determined from analysis of the contents

of the Douglas bag. The volume of expired gas is determined by transferring the gas from the Douglas bag to a gasometer. By suitable calculation, the total respiratory exchange is obtained. From the respiratory exchange measurements, both RQ and the metabolic energy production can be calculated.

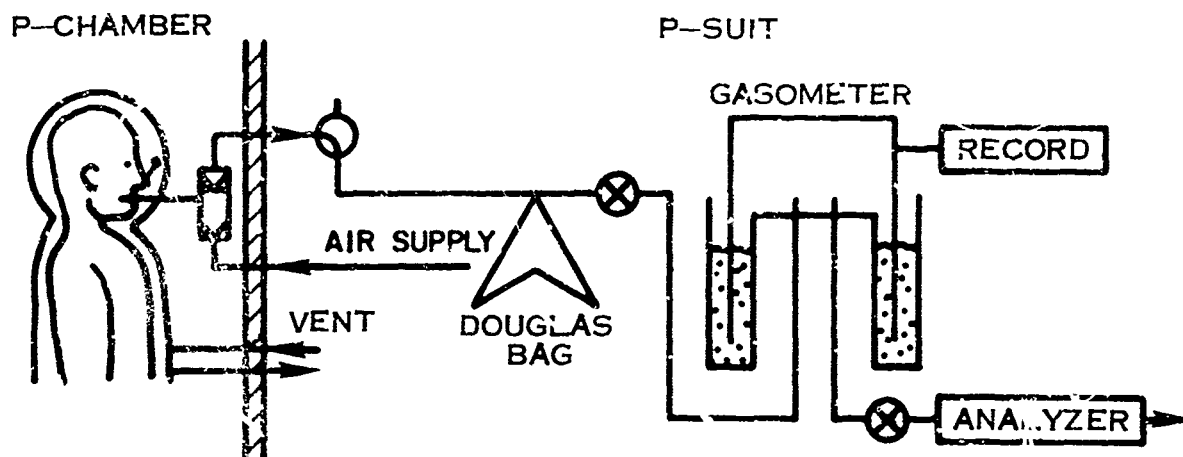
This technique has been used extensively and provides an accurate measure of total expired volume. It presents less breathing resistance than the closed circuit method and permits air rather than pure oxygen breathing; however, the determination of oxygen consumption rate depends on volume determination and in general is less accurate than in the closed circuit technique (refs. 23 and 39).

Neither the open nor closed circuit method can provide an instantaneous measure of metabolic energy production rate because of the time lags and volumes involved. They both necessarily add some breathing resistance and neither is without difficulty when applied within a pressurized space suit.

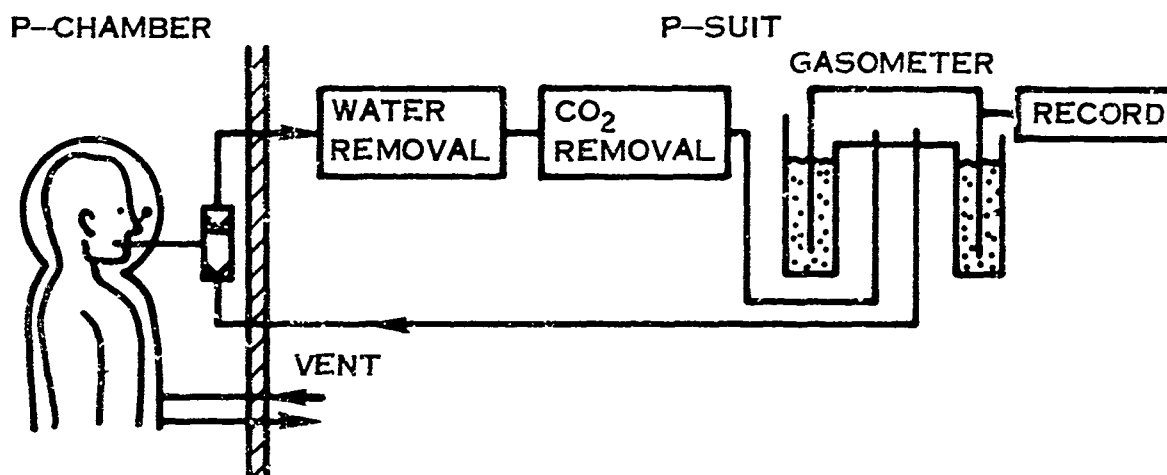
METABOLIC MEASUREMENT IN A PRESSURIZED SUIT

During a test in a normal laboratory environment, either the open circuit or closed circuit metabolic measurement method can be easily applied and presents no new or unusual measurement problems. In a space suit, however, the test subject is pressurized to a level above the laboratory ambient pressure, is enclosed within a helmet and face plate, and receives both cooling and breathing air from the same source. Under these restrictions, metabolic measurements are difficult to carry out and, in addition, are likely to defeat any attempts at cooling system or helmet flushing evaluation. The introduction of a mouthpiece into the helmet face plate system will alter the oral-nasal geometry and therefore influence the flushing system within the helmet. If a mouthpiece is not used, then oxygen is lost from the suit through leakage as well as being consumed in respiration. Further, if the breathing circuit and the suit ventilation circuit are separated, then the quantity of the heat given up by the lungs to the breathing circuit may be different from what the lungs would have given up had the test subject been breathing from the normal suit ventilation circuit. This will alter the results of the cooling system evaluation.

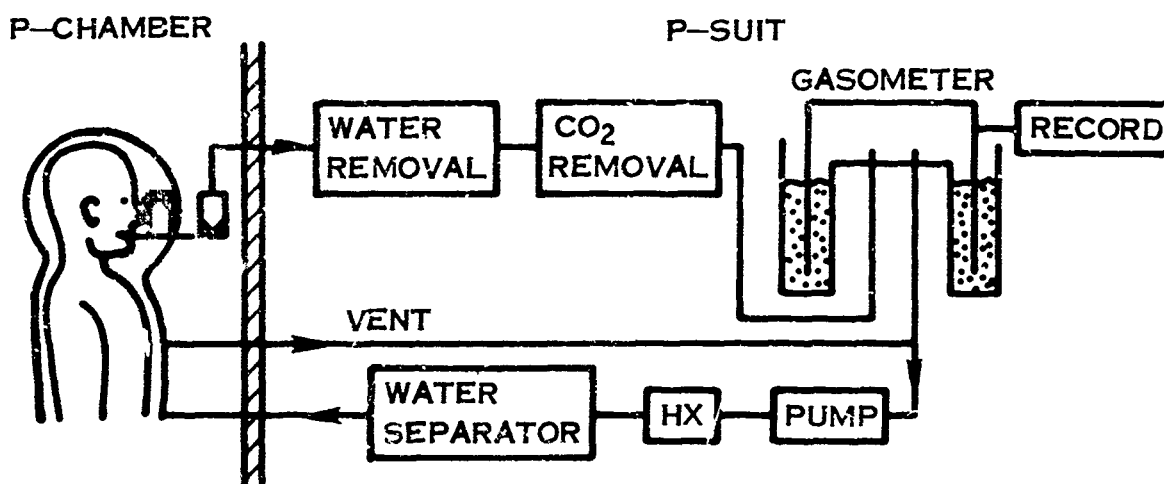
Consider now several possible methods for respiratory exchange measurements within a pressurized suit. These concepts are illustrated in Figure 92. Methods 1 and 2 are the classical open and closed circuit techniques. Method 3 is a modified closed circuit technique in which the test subject inhales from the suit ventilation system and exhales to the spirometer bell. A fan and heat exchanger are used to provide continuous suit ventilation. Method 4 is a conventional open circuit technique in which the subject inhales from the suit ventilation system instead of an external air supply and exhales to a Douglas bag. Method 5 is a modified box-ballon technique and Method 6 is a closed circuit technique similar to the oxygen supply of a suit portable life support system. Some of the features of these concepts are compared in Table VI.



METHOD 1

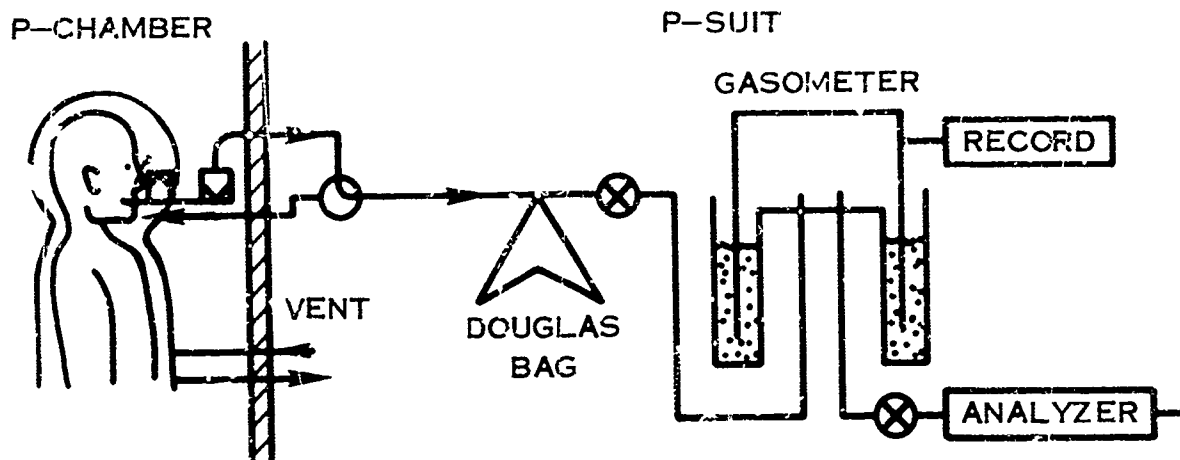


METHOD 2

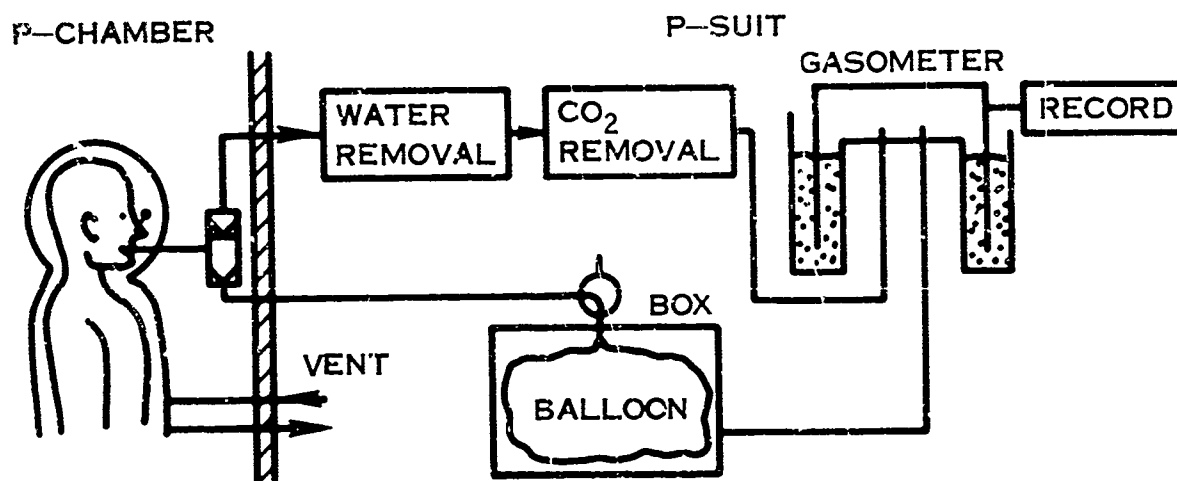


METHOD 3

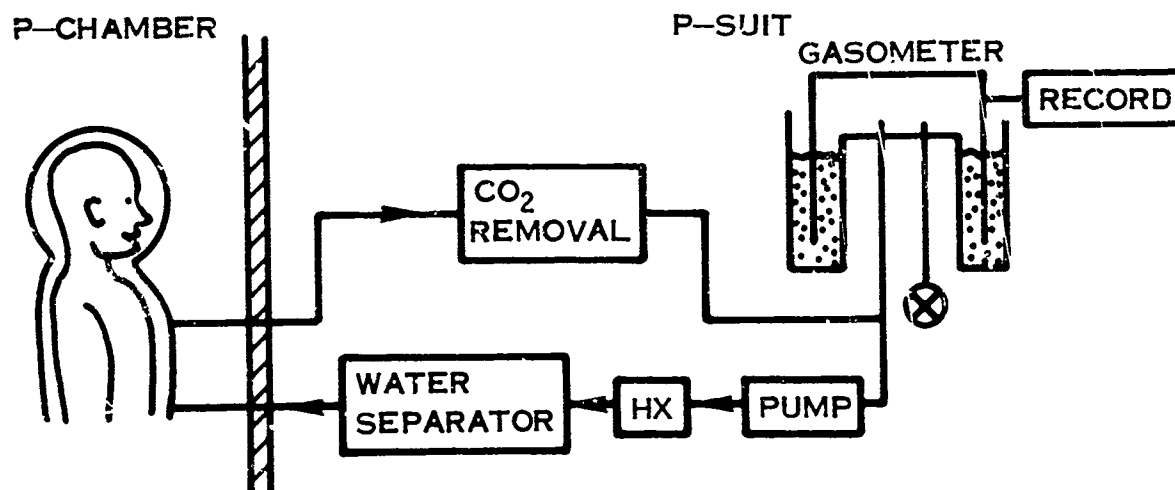
FIGURE 92. SPIROMETRY CONCEPTS FOR PRESSURIZED SUITS



METHOD 4



METHOD 5



METHOD 6

FIGURE 92. (CONTINUED)

TABLE VI
COMPARISON OF SPIROMETRY CONCEPTS

FEATURE	METHOD					
	1	2	3	4	5	6
Air breathing	yes	no	no	yes	yes	no
Oxygen breathing	no	yes	yes	no	yes	yes
Subject to suit gas leakage errors	no	no	yes	no	no	yes
High breathing resistance	no	yes	no	no	yes	no
Requires mouthpiece	yes	yes	yes	yes	yes	no

Consider first Method 6. Since the test subject inspires from the helmet without a mouthpiece, no modification of the helmet or visor is required and the heat removal from the head and body is unaltered by the metabolic measurement. This technique would be ideal were it not for the suit leakage problem. Suit leakage is a variable depending upon the particular suit design, the sealing of the closures, and to some extent the motion of the test subject. Since suit leakage cannot be well controlled and since the suit leakage in many suits is a substantial fraction of the total oxygen consumed, any technique which does not use a mouthpiece appears unsatisfactory. If, however, prior measurements of a particular suit show that the leakage rate is a negligible percentage of the oxygen consumption rate, then the no mouthpiece method should be strongly considered. Techniques using no mouthpiece are not known to have been tried previously and, therefore, the magnitude of the measurement errors and the ultimate success of these techniques cannot be assessed.

If Method 6 must be rejected because of suit leakage, then by the same token Method 3 must also be rejected. Methods 4 and 1 are essentially identical; only the design of the two-way valve differs. Method 4 simulates the ventilation cooling better but makes the inspired gas analysis measurements more difficult. Method 5 permits air breathing but complicates the hardware and measurement technique. Thus, only the original classical techniques of open circuit and closed circuit respiratory exchange measurements remain. It turns out that accurate measurements of metabolism can best be obtained by a combination of these techniques. This combined technique is discussed in greater detail in the following paragraphs.

Metabolic measurements in a pressurized suit require a modified helmet. Modifications should include a high velocity, low resistance, two-way breathing mouthpiece, preferably designed so that it can be easily moved into or away from the mouth with the teeth or by external actuation. A suggested helmet mouthpiece is shown in Figure 93.

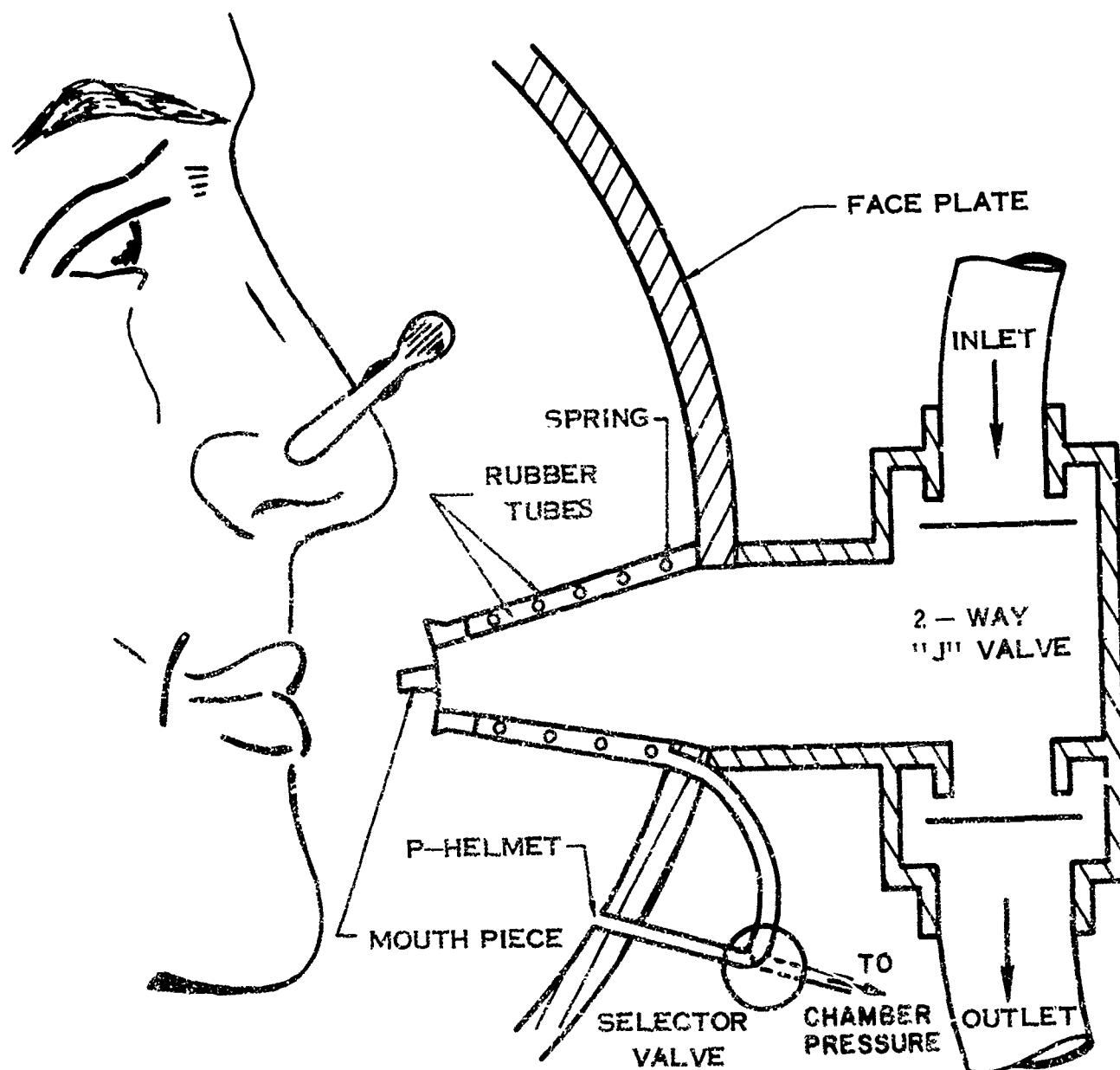


FIGURE 93. RETRACTABLE HELMET MOUTHPIECE FOR SPIROMETRY

Since a pressure differential must exist between the inside and the outside of the suit, tests should be conducted in an altitude chamber (approximately 7,300 feet) with the gas analysis equipment external to the chamber so that the suit may be maintained at laboratory ambient pressure. Alternatively, the gas analysis equipment could be enclosed in a pressure vessel so that the ambient pressure about the equipment is the same as the suit internal pressure. With this arrangement, the respiratory exchange equipment can be used at any suit operating pressure. For metabolic cost measurements, this technique should present few problems other than hardware complexity. Since thermal stability is not required, the tests are relatively short and pure oxygen breathing should be fully acceptable.

During evaluation of the suit cooling system, however, the technique may present some problems, principal of which are lung cooling and the discomfort associated with wearing a nose clip continuously. To insure that the heat removed from the body through respiration is the same as that which would have been removed by the suit ventilation air itself, the inspired air in the respiratory circuit must be temperature and humidity controlled so that its capacity for heat removal is the same as the ventilation air within the suit. Since the test must be run to thermal stability, any stop during the testing to remove or install a nose clip would change the thermal balance of the test subject. It is imperative that the nose clip or cover be worn continuously during the several hour test unless some technique could be devised to block the nose by the manipulation of an external device on the helmet. Any compromises which degrade the thermal stability of the test subject during the testing defeat the basic purpose of the metabolic measurement which is to add confidence and improve the accuracy of the basic data acquired. Thus, the cooling system evaluation should be performed separately from metabolic cost measurements.

Concerning the accuracy of the metabolic measurement technique, two questions remain. What is the effect of altitude and what is the effect of pure oxygen breathing on the caloric value of oxygen at a measured RQ? The literature seems agreed that there is little physiological basis for a variation in caloric value with altitude or with pure oxygen breathing, however, recent attempts at Hamilton Standard to substantiate this have produced unexplained discrepancies.

TRANSDUCTION TECHNIQUES

Numerous measurements are required to obtain the test data needed to control and monitor the test environment, monitor the physiological performance of the man, and accurately assess the life support performance and capability of the manned suit. Many techniques are possible for each measurement, but for the specialized requirements of manned suit testing, certain techniques are considered optimum for integrated test facilities. These selected techniques are described below and, where necessary for clarity, alternate methods are discussed. In general, the measurements are obtained from transducers which are directly connected to the signal conditioning and power supply equipment of the data acquisition system as described in Section VIII. Gas analysis requires individual instruments each of which is also connected directly to the system. A few intermittent measurements such as subject weight, spirometry information, and barometric pressure are entered into the recording system manually. In the following discussion of transduction techniques, various commercially available transducers and instruments are recommended based on their satisfactory performance during space suit tests at Hamilton Standard. This is not intended to imply that a thorough evaluation of these instruments has been conducted or that other instruments might not serve equally well.

The basic quantities which must be determined for life support testing may be categorized as follows

1. Temperature

- a) absolute
- b) differential

2. Pressure

- a) absolute
- b) differential

3. Flow

- a) mass
- b) volume

4. Gas Analysis

- a) oxygen
- b) carbon dioxide
- c) nitrogen
- d) water vapor

5. Task Magnitude

6. Physiological

- a) performance
- b) monitoring

Temperature

Measurements must be made of suit inlet and outlet coolant temperatures, suit surface temperatures, and test chamber environment temperature. Skin and core temperatures are needed to complete the thermal balance of the suit system, determine distribution of cooling capacity, and monitor the physiological performance of the man. The temperatures at gas-flow instruments and certain of the gas-analysis instruments must be determined to obtain corrections for standardization.

Either thermistors or thermocouples provide compatibility with the test and data handling facilities. However, in view of the large number of suit and chamber penetrations, each of which is a potential source for spurious thermal EMF's, thermocouples should be avoided where possible. In the temperature range from -80° to $+150^{\circ}\text{C}$, thermistors generally provide the greatest accuracy with the least difficulty. Thermistors manufactured by Yellow Springs Instruments (Series "400") or equivalent have proved convenient and assure interchangeability of probes without recalibration.

The accuracy of thermistor temperature measurements will depend primarily on the effectiveness of probe installation. Improper installation can result in large errors due to poor thermal contact with the point of interest, excessive lead wire conductance, or local temperature variations caused by mechanical geometry, flow distribution, self-heating, and probe radiation characteristics. Proper installation procedures are described in numerous references (refs. 5, 27, 108). The accuracy of thermistor probes is approximately 0.5°C neglecting installation errors. No generalizations of total system accuracy can be made without a consideration of each probe installation.

Where precision differential temperature measurements are needed such as those required to determine liquid coolant temperature rise, thermistors may be readily adapted to bridge circuitry. Extreme sensitivity can be achieved but, again, the absolute accuracy depends primarily on probe installation. For such measurements care must be exercised to measure the temperature corresponding to the average thermal content of the flow since across the flow there are gradients in both the temperature and velocity.

Pressure

Pressure measurements include suit coolant pressures, chamber pressures, and local environment pressure. In addition, sensor pressures are required for standardization of certain gas analysis instruments.

Various pressure transduction techniques are available; however, the technique embodied in the International Resistor Corporation's Low Pressure Cells is particularly adaptable to suit test requirements. This transducer consists of a bellows or a bourdon tube which deflects as pressure is applied. This deflection is transmitted directly without springs or linkages to the core of a differential transformer excited by an internal oscillator. The resulting AC output from the transducer secondary is demodulated within the transducer and the high-level DC signal is routed to the data handling system. Accuracies of calibrated pressure transducers are typically about 0.25% of full scale, assuming the temperature of the transducer does not exceed a specified range which is normally -18°C to 65°C.

Flow

Liquid and gaseous mass and/or volume flow must be measured at several locations. These measurements include suit inlet and outlet ventilation flow, helmet flow, and, when a liquid cooled undergarment is used, liquid coolant flow. Volume flow indicators are required to regulate sample flows to gas analyzers.

Various techniques are available for flow indication and transduction. For compatibility with the data handling system, suit ventilation and liquid flows are measured with thermal mass flowmeters. Presuming constant constituents, these instruments produce an output voltage proportional to mass flow rate without need of temperature and pressure compensation. The flowmeters do not actually measure true mass flow of the fluid because indicated mass flows vary with concentration of stream constituents and must be corrected using gas analysis test results.

The basic accuracy of the single gas mass flowmeter is 2% of full scale but improved accuracy may be obtained using calibration corrections. No generalizations of the accuracy of mixed gas mass flow can be made since this depends on concentration levels and thus on the accuracy of gas analysis.

The preceding discussion also applies in essence to the liquid thermal mass flowmeter. But the problem is less severe because the concentrations of constituent liquids are predictable and invariant for a particular liquid coolant system.

Volume flow indicators needed to set sample flows to gas analyzers require repeatability rather than accuracy. These set point flows will constitute a part of the calibration procedure and will not normally be entered in the data handling

system. Thus, the flow indicators used for gas sampling are inexpensive variable area flowmeters. In fact, simple purgemeters have been used with satisfactory results.

Gas Analysis

Gaseous constituents in the suit ventilation gas circuit must be measured to control, monitor, and evaluate suit thermal performance. In addition, gaseous constituents of respiratory air must be measured to monitor the physiological response of the man and to determine the respiratory effectiveness of helmet flushing.

AVAILABLE TECHNIQUES

There are many approaches to the problems of gas analysis, none of which is entirely satisfactory from both an economic and technical point of view. The more obvious means of gas analysis include

Emission spectroscopy

Absorption spectroscopy

microwave

infrared

ultraviolet

Mass spectroscopy

Polarography

Paramagnetism

Thermal conductivity

Dew point

Gas chromatography

Sonic velocity

All spectroscopic techniques involve atomic and molecular structure and thus are universal in that exact identification and measurement of every elemental constituent is in theory possible. These instruments are usually the most costly and provide more information than necessary for suit evaluation. Often the results are difficult to interpret.

Polarography involves the reaction between the gas of interest and an electrolyte at selected polarized electrodes separated from the gas stream by a permeable membrane. In general, these instruments are unstable, have slow response, and require frequent calibration. With a few notable exceptions, they are not specific and special techniques are required for constituent identification.

Paramagnetism is a property of few gases. This property is of significant advantage for accurate determination of oxygen concentration as it is the only gas in the suit environment which is strongly paramagnetic.

Thermal conductivity meters which are neither specific nor universal, determine only the thermal characteristics of the sample gas. Where two known gases are present, varying conductivity indicates the relative proportions of these gases. If more than two gases are present, conductivity can neither identify the gases nor relate constituent concentrations so that thermal conductivity meters are not useful for suit work. Similarly, sonic velocity instruments may be eliminated because of limitations which are similar to those of the conductivity meter.

Dew point indicators measure the temperature at which vapor condenses and from this the saturation pressure can be determined. Where only water vapor is present, this device is specific and highly accurate for determining water concentration. Moreover, this instrument more closely approaches a primary standard than do relative humidity instruments which exhibit appreciable drift and are difficult to calibrate.

Gas chromatographs may be highly selective and can produce exact constituent identification, provided that the gases to be analyzed are known beforehand and suitable columns selected. Difficulties include problems in gas sampling technique, lengthy analysis, slow response, and complicated calibration. In addition, it is difficult to evaluate low-level gas concentration in the presence of other gases at high concentration levels.

RECOMMENDED TECHNIQUES

A number of techniques have been described for the determination of gaseous constituents. Clearly, the choice of instruments depends on many factors including the gases to be measured. In suit thermal and respiratory evaluation, the primary gases which must be measured are oxygen, carbon dioxide, water, and nitrogen. Examining the practicality, expense, accuracy, response, and compatibility with data handling dictates the use of separate instruments with high specificity for each of the suit ventilation gases. Chosen measurement techniques are:

Oxygen - Paramagnetism

Carbon Dioxide - Infrared absorption

Water Vapor - Dew point hygrometry

Nitrogen - Ultraviolet emission

OXYGEN -- Since oxygen is strongly paramagnetic while the other gases of interest are not, analysis of oxygen concentration is based on its magnetic susceptibility. The susceptibility measurement is made in an analysis cell where a dumbbell shaped detector is suspended on quartz fiber in a nonuniform magnetic field. As the oxygen concentration in the gas sample surrounding the dumbbell changes, the magnetic field changes, causing the dumbbell to rotate through an angle proportional to oxygen concentration.

The instrument used for determination of oxygen partial pressure is the Beckman Type F-3 paramagnetic oxygen analyzer. The output of this instrument is not only dependent on the partial pressure of oxygen, but is also significantly effected by total pressure and volume flow. Thus, when using this paramagnetic analyzer, a sampling system is required to maintain constant pressure and flow. Gas temperature must also be held constant but this control is internal by controlling flow rates through the heated sample chamber.

CARBON DIOXIDE -- Two instruments are used for the determination of the partial pressure of carbon dioxide. Both are nondispersive infrared analyzers with carbon dioxide specific detectors. The analysis of the carbon dioxide is based on the infrared energy absorption of the sample gas compared with a standard reference gas containing a known concentration of carbon dioxide. For this application the reference gas contains zero percent carbon dioxide. A dual beam infrared source is directed through the reference and sample gases to opposite sides of a carbon dioxide filled detector. Both gases absorb some of the infrared but the reference gas passes essentially all of the energy in the carbon dioxide absorption band which is then absorbed in the detector. The sample gas absorbs in the carbon dioxide band in proportion to the carbon dioxide concentration and less infrared is transmitted to the detector. The resulting heat differential in the detector causes a pressure difference which moves a capacitive diaphragm. This is detected and indicates carbon dioxide concentration. Both instruments are total pressure and flow sensitive but these effects may be compensated by calibration at sampling conditions.

The Lira 300 made by Mine Safety Appliances is used for the essentially steady state carbon dioxide concentrations at suit inlet and outlet. This instrument has a poor response time (about 5 seconds), but is reasonably stable, insensitive to vibration, and is panel-mounted. A typical calibration of the Lira 300 is shown in Figure 94.

Instrument output is not linear with carbon dioxide partial pressure but, with zero and span adjusted, the transfer function is repeatable and is determined from an initial multipoint calibration. Because of instability, zero, span, and mid-point

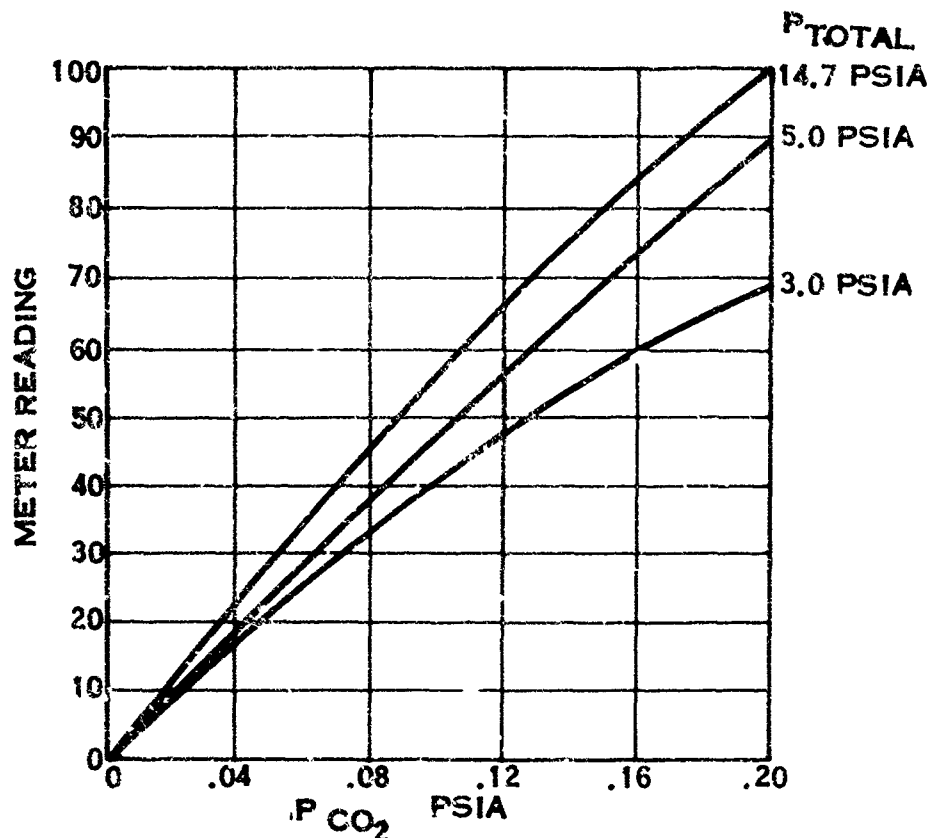


FIGURE 94. SAMPLE CALIBRATION CURVES - MSA LIRA 300

calibration gases are used at least every four hours to assure accuracy. Calibration gases are analyzed using a microschollander volumetric analyzer which, in turn, is checked against sample gases traceable to NBS.

The Beckman-Spinco LB-1 is used to determine the instantaneous carbon dioxide concentrations in respiratory samples. This instrument has a rapid response (about 0.1 second) for samples at the sensor. The instrument lacks stability and is calibrated frequently. Three mixtures at zero, span, and mid-point are normally used for calibration to assure that instrument accuracy remains within specified limits. The LB-1 consists of two separate components: the sensor and the amplifier. The amplifier is panel-mounted, but the sensor, which is extremely sensitive to vibration, is shock-mounted and is located as close as possible to the test subject to minimize sample transport delay time. The sample flow rate through this instrument is relatively small and long lines from the sampling point to the sensor result in prohibitive delay time. Furthermore, long lines, especially those containing cross sectional variations, permit diffusion of carbon dioxide from high concentration regions to adjacent low concentration regions. The result is much like a filter and degrades the inherent response of the sensor.

NITROGEN -- Nitrogen concentration is measured with a Med-Science Model 300AR Nitralizer. The instrument is panel-mounted with the sensing device located inside the console. The Nitralizer has an accuracy of 1% of full scale with ranges

of 0 - 20% to 0 - 100% nitrogen concentration. An extremely fine needle valve is used to meter the sample gas into a chamber where it is ionized. Light emitted by the ionized gas falls on a filter which passes only the spectral region in the range of the intense nitrogen band. The light passed by the filter is detected by a photocell whose output is amplified and indicated on a meter calibrated in percent nitrogen.

WATER VAPOR -- Water vapor concentrations are measured with Cambridge Systems Model 108 dew point hygrometers. This instrument consists of three major components: the sensor, control power supply, and indicator. The dew point sensor contains a thermoelectrically cooled mirror with an internal platinum resistance thermometer and an optical bridge consisting of two photocells and light source. The mirror is located in the flow of the gas sample and is cooled until dew forms. The formation of dew is sensed by the photocells in an optical bridge which senses the ratio change between specular and diffuse reflection. The output of the bridge is amplified and used to control the power supply output to the mirror cooler. The temperature at which dew forms on the mirror is sensed by the resistance thermometer, displayed on the null balance indicator, and routed to the data system. The input sample lines are heated by means of parallel hot water lines to prevent condensation of water in the sample prior to measurement. The sampling system is considered separately in the following section.

Water vapor concentration and absolute humidity are calculated from dew point temperature by the standard psychrometric relations. Accuracy in dew point temperature is approximately $\pm 0.3^{\circ}\text{C}$ over the range of -30°C to 82°C .

SAMPLING SYSTEMS -- A complex system carries the gaseous samples from the point of interest to the gas analysis instruments. Oxygen sampling and suit carbon dioxide sampling are relatively simple by themselves but are complicated by the presence of water vapor. The dew point at the suit exit is generally above ambient and the sample lines are heated to prevent condensation with consequent error in absolute humidity and possible error in oxygen and carbon dioxide partial pressure determinations. To maximize response, helmet respiratory gases are sampled through a minimum diameter short line which is free from valving and any other increases in cross section area or dead space. The sampling rate required for this instrument is low and a bypass system is provided in order to decrease delay time, improve response, and minimize line contamination. Delay is particularly critical with the nitrogen analyzer which requires only a minute sample for the ionization chamber. The sampling system requires leakproof valves, lines, and fittings to minimize contamination of the sample from ambient air. Normally, a simple vacuum pump is used to withdraw the sample which is dumped to ambient after analysis. However, if the sample is returned to the system, a special diaphragm (or equivalent) pump with back pressure compensation is needed.

With the exception of the dew point hygrometer, all analyzers are intermittently calibrated using calibration gases. Provisions are included in the sampling system to permit calibration at measurement flow and pressure conditions. Dew

point determinations are corrected to sample point conditions by providing sensor pressure information to the data handling system. A typical sampling system is shown in Figure 95.

Task Magnitude

In general, the task is defined by the test procedure. Numerous tasks may be proposed, but the treadmill walking task is best defined and most repeatable. The required measurements are simply treadmill speed and angle which are read from conventional instrumentation supplied with the treadmill unit and are manually entered in the data system.

Physiological

To evaluate the physiological performance of the test subject, measures are required of skin and core temperatures, respiratory gas analysis, and heart rate. Temperatures and gas analysis have been discussed in preceding sections. Heart rate is obtained from conventional ECG signals measured by a conventional instrument such as the Waters Cardiotachometer. Additional physiological measurements may be required by the medical monitor. In general, the monitor desires ECG, heart rate, respiration rate and depth, and body core temperature as a minimum. Heart rate and core temperature are supplied as part of the performance measurement. Techniques for ECG and respiration rate are well established and are discussed briefly in Section VIII in connection with the data system for monitoring or analog recording of the various medical variables.

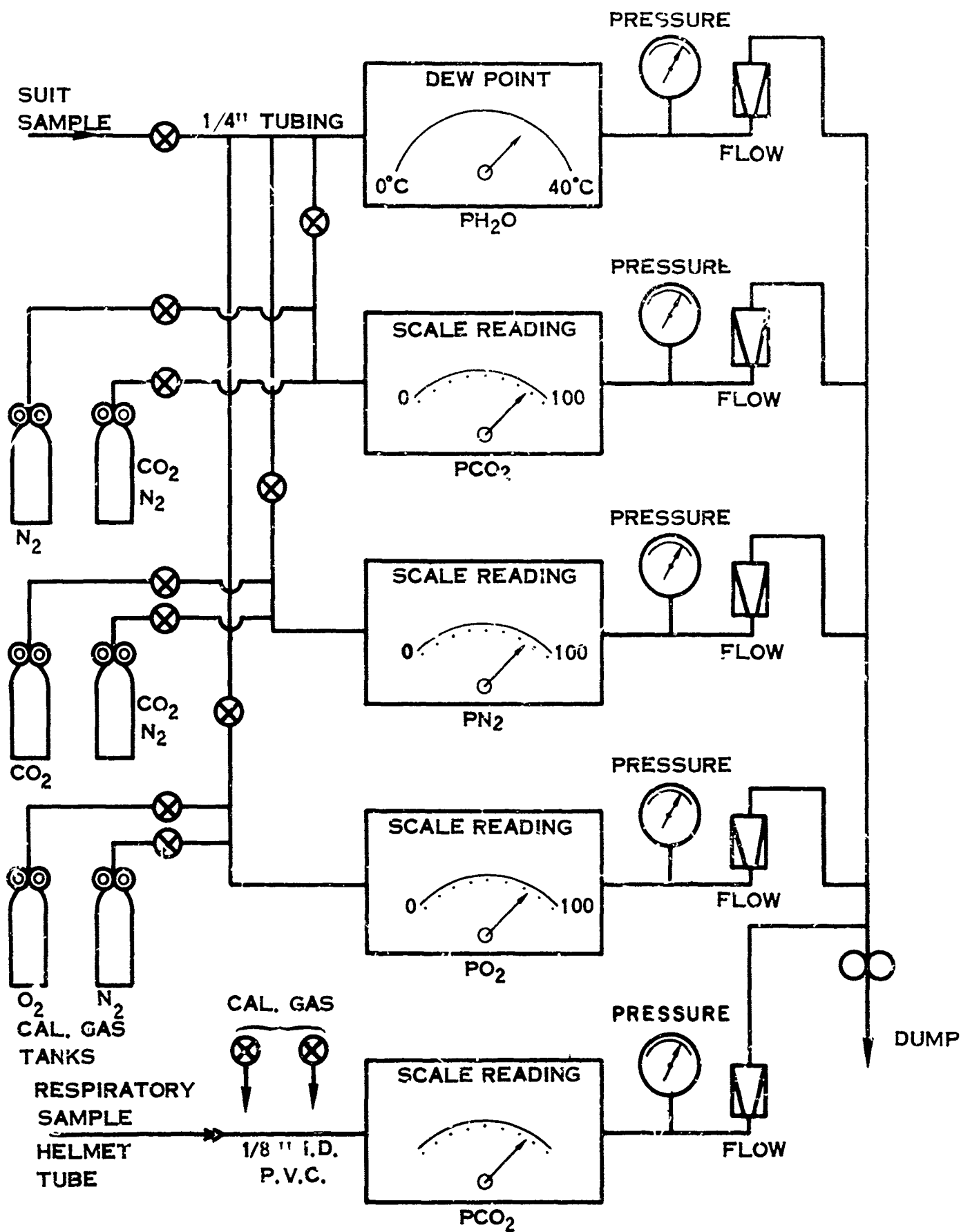


FIGURE 95. SIMPLE GAS ANALYSIS SAMPLING SYSTEM

AN INTEGRATED LIFE SUPPORT TEST SYSTEM

It has been shown that life support testing breaks down logically into three test areas: cooling system evaluation, helmet flushing evaluation, and metabolic cost evaluation. Similar equipment is required for each of these test areas but, because of test interactions and constraints, the tests must be executed at separate times. Also, the different evaluation areas require transducers with different accuracies, time responses, etc. In the remainder of this section, an integrated facility is recommended for all areas of life support testing. The choices were made on the basis of an optimum compromise between accuracy, convenience, and cost.

Description Of Test System

Consider the facility in Figure 96 which consists of an air-conditioned altitude chamber and antechamber for testing a suited subject walking on a treadmill. Ancillary systems include a suit ventilation supply, conventional equipment for respiratory determination of metabolism, and required instrumentation integrated into a complete data system.

The required chamber pressure is about 140 mm Hg or an equivalent pressure altitude of about 40,000 ft. The interior of the chamber is lined with fabric to equalize the thermal radiation exchange. Through the plenum volume formed between the fabric and the chamber wall, the air conditioning system for the chamber distributes the air from behind the fabric to minimize temperature differences. The suited astronaut is enclosed in a thermal garment which contains temperature sensors on the interior surface. The air temperature of the room is controlled to the average reading of these sensors. Suit ventilation air is taken from outside the chamber, conditioned and delivered to the suit through insulated ducts saturated at about 8°C. The helmet pressure is equalized with antechamber pressure to permit spirometry techniques using conventional equipment without requiring pressure breathing by the test subject. Flow capacity of the ventilation system is about 550 liter/min.

Conventional spirometry techniques are used for determination of metabolic energy expenditure. A special helmet face plate is used, containing a mouthpiece with check valves. Inlet and outlet of the mouthpiece communicate through a sealed pass-through in the face plate and thence to pass-throughs in the chamber wall to the spirometry measuring system in an external hyperbaric chamber. A typical spirometry setup is shown in Figure 97. Both direct and indirect spirometry techniques are employed to achieve confidence in the measures of oxygen consumption, carbon dioxide production, respiration rate, tidal volume, and minute volume.

Other than the special requirement for helmet compatibility, insulated lines, and pass-throughs, no special techniques are required for these measurements.

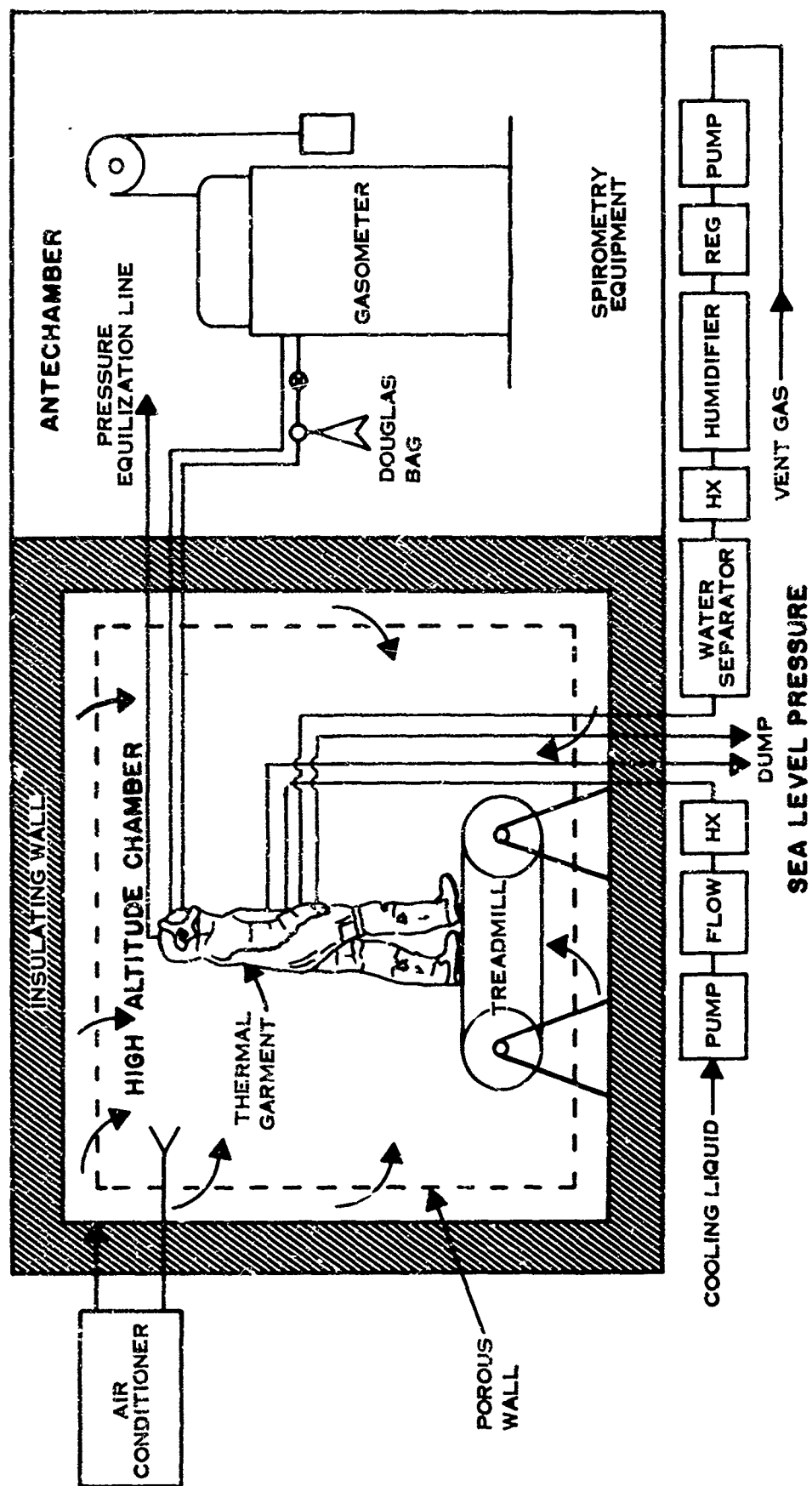


FIGURE 96. SCHEMATIC REPRESENTATION OF INTEGRATED TEST FACILITY

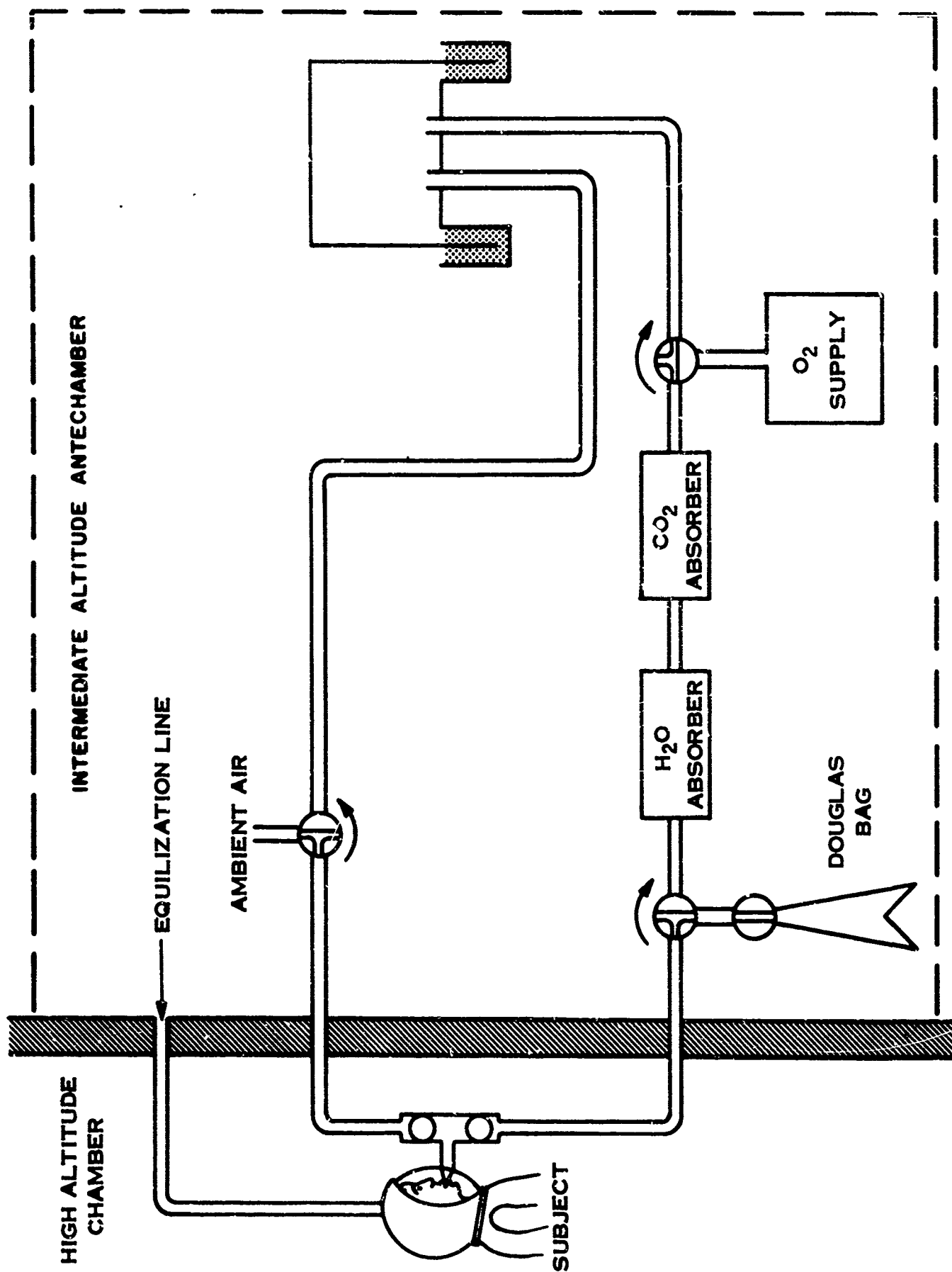


FIGURE 97. SCHEMATIC OF SPIROMETRY SETUP

The data system includes all of the instruments which are required for the evaluation integrated into a complete package which provides for instrument power, calibration and checkout, analog display (including meter and recorder readout), digitizing, recording, and ultimately computer input for data reduction as described in Section VIII.

Test System Operation

PRETEST PROCEDURES

To obtain reliable metabolic data, the test subject must maintain a plateau of physiological efficiency by a continuous program of physical training and should not deviate from his normal diet. He must obtain a minimum of eight hours of sleep on the night previous to the test and abstain from eating prior to the test for a sufficient time to reach a post-absorptive state.

Approximately one half hour before the start of the test, the subject is given a pretest physical. Immediately before being suited for the test, the subject is weighed nude and each article of the clothing configuration is weighed separately. Biosensors are installed and the suit is donned. Thus attired, the subject is weighed immediately with no umbilicals attached. Precision scales are used and the data manually entered in a digital/analog recorder.

An auxiliary umbilical from the suit ventilation supply is immediately attached to assure comfort with minimal sweating prior to exercise. The outputs from the man-suit instrumentation are continuously recorded by the data acquisition system whenever the umbilicals are attached. Immediately before mounting the treadmill, the suited subject is weighed with all umbilicals momentarily detached.

During the time that the test subject is being prepared, the test facilities are also being prepared. The chamber air conditioning system is placed in operation with a set point temperature approximating that expected with the controlling sensors on the interior of the insulating coverall (about 33°C). Vacuum pumps and treadmill are operated to assure that all is in readiness to begin testing with a minimum of delay. The suit ventilation supply system is placed in operation at the test inlet conditions to the suit with a simulated ventilation pressure load.

Before the start of testing all instruments are calibrated, where required, and all data system channels are standardized. Identification and pretest weight information are manually entered on the digital/analog recorder.

TEST PROCEDURE

The test procedure will follow, in general, this order.

1. Determine the adequacy of the helmet respiratory flow.
2. Determine the metabolic cost of various tasks.
3. Determine the suit cooling capabilities.

The test subject, fully attired and ventilated at outside ambient pressure, walks on the treadmill at a speed estimated to produce the desired metabolic rate. Chamber pressure is reduced 180 mm Hg below outside ambient.

Saturated air at 8°C is supplied to the suit inlet at design flow rate. Pressure is controlled to outside ambient in the helmet with the suit outlet air being dumped through an external blower. Initially, the helmet is identical to that of the suit system to be evaluated except for a tiny flexible probe to be taken up by the subject and held just inside of the oral cavity to determine respiratory effectiveness. It must be demonstrated that any rebreathing is insufficient to raise the end tidal $p\text{CO}_2$ above normal conditions.

Once this has been demonstrated, the chamber is immediately repressurized, and a spirometry face plate and nose clip or cover is substituted for the normal face plate to begin the metabolic cost evaluation. The subject then breathes external air while the suit is ventilated conventionally. Again the chamber is depressurized to 180 mm Hg below outside ambient and the helmet pressure adjusted to spirometry ambient.

The subject begins the desired task, the metabolic cost of which is to be determined, such as walking, rowing, climbing, etc. After two minutes to establish respiratory exchange at this exercise level, spirometry measurements begin.

An initial sample is taken with the Douglas bag in the open circuit mode. The spirometer circuit is then changed to closed circuit to determine oxygen uptake. Normally, a 10 to 20 minute trace is taken to assure stable, accurate measurements. The subject is then returned to open circuit and, after an adequate period to re-establish nitrogen balance, a second Douglas bag is taken. From the data obtained from spirometry measurements, the metabolic energy expenditure for the pressurized task can be determined. If the nude or unencumbered energy expenditure rate for the task has been determined previously, the two sets of measurements may be subtracted to determine the metabolic cost of the suit for the task performed. This portion of the test may be repeated for as many different tasks as required within the limits of test subject fatigue.

The test would normally end at this time due to subject fatigue. However, if the test is to continue for cooling system evaluation, then either water balance measurements should not be attempted or the subject and his clothing should be reweighed to determine initial moisture conditions.

For the evaluation of suit cooling performance the subject is placed on pure oxygen, the chamber pressure is decreased to 140 mm Hg, and the suit pressure and the antechamber containing the gasometer are adjusted to 180 mm Hg absolute. The subject walks on the treadmill at the speed estimated to produce the desired metabolic rate; since encumbrance is reduced by low suit differential pressure, the subject must walk faster than he did during the metabolic cost testing. After respiratory exchange levels have stabilized, the spirometry measurements are repeated. Immediately thereafter, if the helmet is so designed, the breathing mouthpiece is moved out of the immediate oral-nasal area to insure adequate flushing.

During these procedures, all measurements have been continually monitored and recorded to determine when the man-suit system has achieved thermal equilibrium. If it is apparent that thermal equilibrium will be achieved without undue physiological stress, the subject continues walking until the body core temperature reaches stability. The total period from start of treadmill activity to thermal stabilization should not exceed one hour. If cooling is inadequate, suit ventilation flow is increased (within the limits of suit design parameters) until thermal equilibrium is obtained. Steady state conditions are assumed to exist when all flows and temperatures, including the rectal temperature, have reached equilibrium. At steady state, the spirometry measurements are repeated to add confidence to the validity of the thermal measurements.

Throughout the test, the following measurements are made either continuously or at appropriate intervals depending upon the mode of data acquisition selected.

Flow

- Suit inlet
- Suit outlet

Pressure

- Suit inlet
- Suit outlet
- Suit differential
- Inlet flowmeter
- Outlet flowmeter
- Helmet
- Chamber
- Ambient
- Hyperbaric chamber

Temperature

- Suit inlet
- Suit outlet
- Inlet flowmeter
- Outlet flowmeter
- Chamber
- Ambient
- Skin
- Rectal

Physiological

- Heart rate
- Respiratory rate
- End tidal carbon dioxide partial pressure

Metabolic

- Oxygen uptake
- Carbon dioxide production
- Minute volume
- Tidal volume

Task

- Treadmill speed
- Rowing rate
- Other definitions of task performance
to define rate and external work

POST-TEST PROCEDURES

Immediately after completion of the test, the chamber is repressurized and the subject is disconnected from all umbilicals and weighed fully attired. Then he removes all garments and biosensors as quickly as possible. All residual sweat is wiped off with the undergarment, the weight of each article and of the subject is determined separately, and the data manually entered in the recording system.

Data Reduction

All pertinent data acquired during this test together with the necessary calibrations, correction factors, and identification are entered into the data handling system. As previously noted, some information is manually entered, while the remainder is automatically entered either continuously or at appropriate intervals, depending on the parameters measured.

For setting test conditions and monitoring the test subject, data is displayed on meters or digital readout. Analog data is recorded where necessary on strip chart recorders. Raw digital recorded data is retrieved on printout command for quick-look capability. The recorded digital data is computer-processed to obtain corrected data and simultaneously to produce the programmed evaluation criteria.

Evaluation Of Suit System

The criteria which are used to evaluate the suit at the test conditions are respiratory effectiveness, metabolic cost, and cooling capacity of the suit. Clearly, the evaluation of respiration efficiency in this procedure is either go or no-go. Under the conditions of the test, there can be no mechanism for lower than normal alveolar $p\text{CO}_2$. Higher than normal $p\text{CO}_2$ as indicated by end tidal measurements will cause physiological stress. By varying helmet flow the knee of the end tidal $p\text{CO}_2$ curve Figure 98 can be determined (ref. 47).

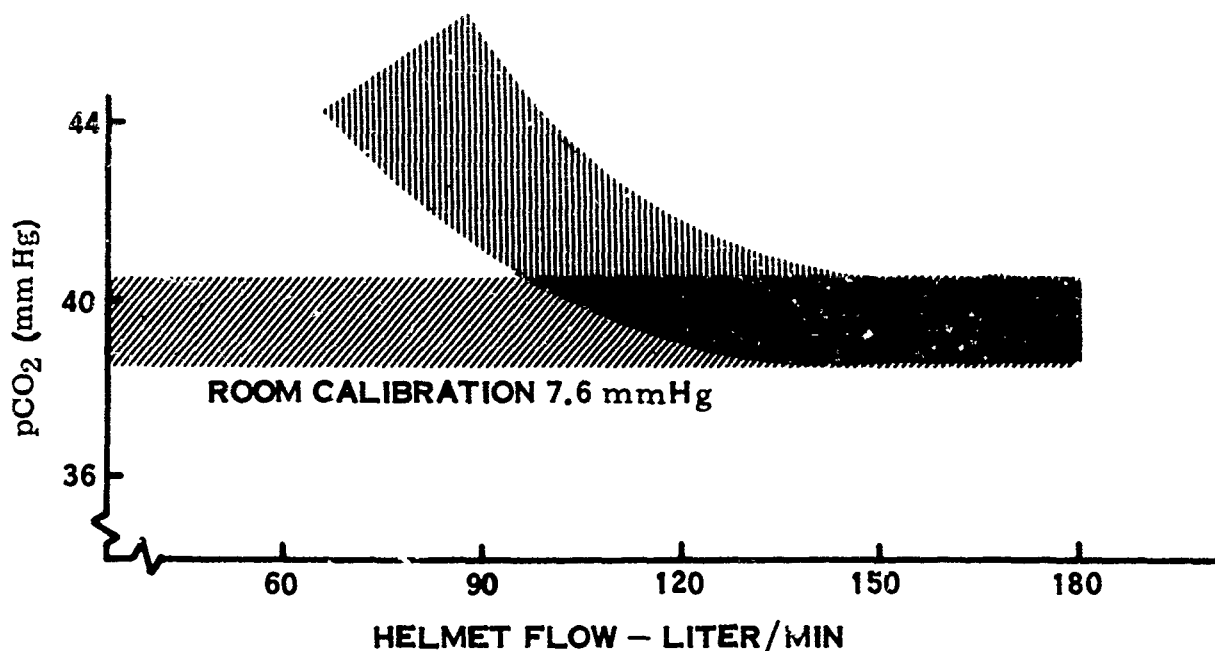


FIGURE 98. TYPICAL END TIDAL $p\text{CO}_2$ VS. HELMET FLOW

Metabolic cost evaluation is the determination of the incremental rate required to do a specific task while encumbered with the pressurized space suit. This requires that the subject has previously been calibrated at this task to determine his unencumbered metabolic rate. The metabolic expenditure is determined by spirometry and cross checked with the heat balance discussed below.

Evaluation of the cooling capacity of the suit ventilation system requires, first, that an energy balance be achieved within the suit-man system considered as a thermodynamic machine.

In addition to the required criteria, a water balance is made to determine the validity of measured data and enhance confidence in the suitability of test procedure. The ventilation effectiveness and sweat ratio are also computed to assist in the examination of coolant distribution and efficiency.

ENERGY BALANCE

The complete energy balance for the suit system is shown in Figure 99.

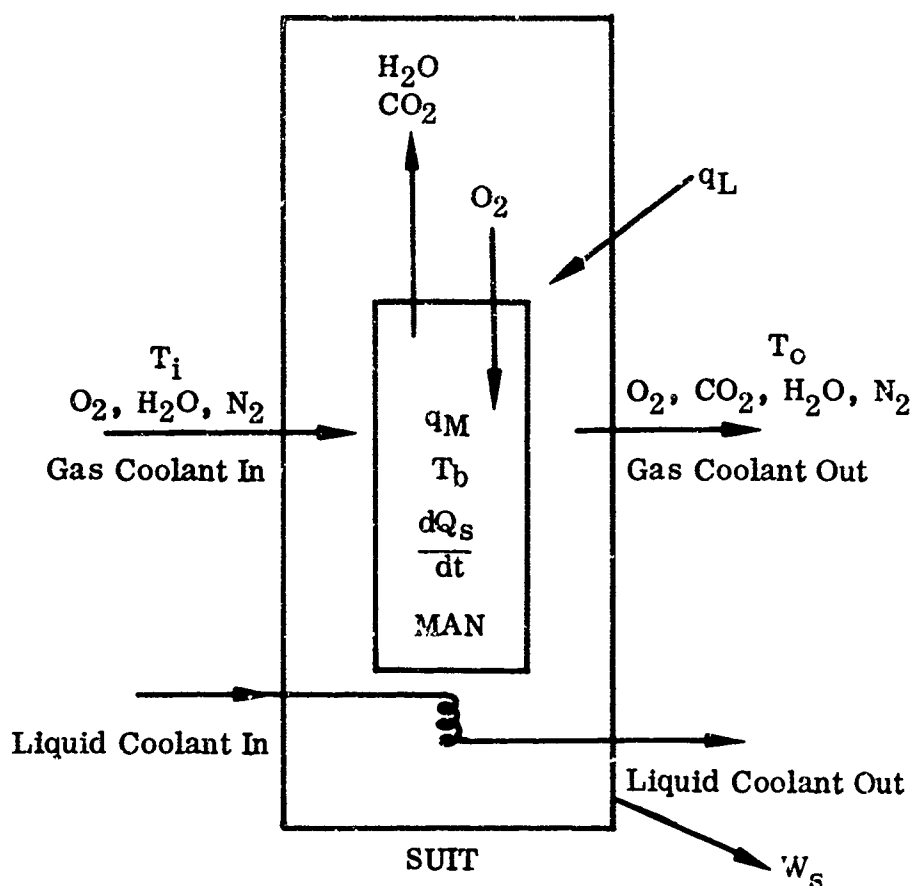


FIGURE 99. MODEL FOR ENERGY BALANCE

$$q_M = \text{Heat flow out of system} - \text{Heat flow into system} + \\ + \text{Work rate} - \text{Net heat leakage} - \text{Heat storage rate}$$

or

$$q_M = w^o \Delta h_{oi}^o + w^w \Delta h_{oi}^w + w^e (h_{fg} + \Delta h_{ob}^w) + w^c \Delta h_{ob}^c + \\ - w^{xo} \Delta h_{ob}^o + w^n \Delta h_{oi}^n + w^l \Delta h_{oi}^l + \frac{dW_s}{dt} - q_L - \frac{dQ_s}{dt} \quad (133)$$

where

q_M = metabolic energy rate

w = mass flow rate

Δh = enthalpy change

h_{fg} = latent heat of vaporization of water

W_s = work done by the suit

q_L = net inward heat leakage

Q_s = body heat storage

t = time

Superscripts

o = oxygen

ro = consumed oxygen

w = water vapor

e = evaporated water

c = expired carbon dioxide

n = nitrogen

l = liquid coolant

Subscripts

o = outlet conditions of temperature and pressure

i = inlet conditions of temperature and pressure

b = body conditions or temperature and pressure

Each of the quantities in the expression may be calculated from the measured flows, temperatures, pressures, gas compositions, work rates, and known constants for the system.

WATER BALANCE

The water balance calculation assumes that all of the weight change during the test is due to transfer of body water. That is

Sweat produced - Sweat evaporated = Sweat accumulated

Sweat produced = Nude weight before - Nude weight after = S_n

Sweat evaporated = Suited weight before - Suited weight after = S_e

Sweat accumulated = Apparel weight before - Apparel weight after = S_a

$$S_n - S_e = S_a \quad (134)$$

This balance is further checked by assuming that the water continuously carried off by the coolant stream, $w^e dt$, must equal the sweat evaporated.

VENTILATION EFFECTIVENESS

Ventilation effectiveness η_v is defined in Equation 135 as the ratio of the total heat removed by the ventilation stream q_c to the ultimate capacity of the stream $q_{c \max}$ that is

$$\eta_v = \frac{q_c}{q_{c \max}} \quad (135)$$

or

$$\eta_v = \frac{q_M}{w^o \Delta h_{oi}^o + w^e \Delta h_{fr}} \quad (136)$$

SWEAT RATIO

Sweat ratio defined in Equation 137 is the ratio of sweat evaporated to sweat produced.

$$SR = \frac{S_e}{S_n} \quad (137)$$

Sweat evaporated and sweat produced are defined and obtained as shown in the calculation for water balance. The ratio serves as a second measure of the effectiveness of the ventilation distribution and is used to indicate whether the subject is being exposed to unnecessary thermal stress.

SKIN TEMPERATURE DISTRIBUTION

Skin temperature distribution serves as a measure of cooling adequacy and comfort. Preferred skin temperatures for the resting man are shown in Table III on page 156. No published data have been located which establish preferred skin temperatures for the exercising man, nor have comfort limits been established for departures of the local skin temperature from the mean. Skin temperature distribution is evaluated by subjective reaction excepting that, if large or unsymmetrical variations are recorded, improper cooling distribution is indicated.

MEAN BODY TEMPERATURE AND HEAT STORAGE

The mean body temperature T_m is used to determine the body heat storage, which is an indication of physiological strain. T_m is calculated from Equation 138 in which the core temperature is weighted twice as heavily as the average skin temperature.

$$T_m = 2/3 T_r + 1/3 \sum_{j=1}^N \frac{T_{sj}}{N} \quad (138)$$

where T_r = rectal temperature
 T_{sj} = skin temperature of jth region
 N = number of regions measured

The stored heat is simply the product of body weight, specific heat of body tissue, and the change in mean body temperature.

Thus

$$Q_s = W_b c_{pb} \Delta T_m \quad (139)$$

where Q_s = stored heat
 W_b = body mass
 c_{pb} = body average specific heat, 0.83 kcal/kg/°C
 ΔT_m = rise in mean body temperature

CONCLUSIONS

In this section, techniques for the evaluation and development of suit thermal and respiratory control systems have been discussed in detail, general test methodology has been discussed, and a specific test and data acquisition system is described. Based on this study the following is concluded.

Until a more complete and detailed understanding of man's local heat rejection and thermoregulatory mechanism is developed, no manikin can replace manned testing for the quantitative evaluation of suit thermal performance.

The complex interrelationships between the physiological needs and responses of man and the physical provisions and limitations of the suit are not understood sufficiently well to define a specific test methodology which can be universally applied. Much testing, both physical and physiological, must be accomplished before this methodology can be established.

However,

1. Manned tests, using conventional high altitude facilities and relatively unsophisticated, traditional techniques, can provide much of the thermal, respiratory, and metabolic cost data needed for the development of improved life support systems in current suits.
2. A centralized automatic digital data acquisition system as described in Section VIII can be of significant value in fast and accurate processing of life support test data.
3. Simple thermal tests which do not duplicate the extravehicular heat leakage or altitude can be useful, but the results must be interpreted with care.
4. Better physical and physiological criteria are needed to assess and optimize ventilation distribution, dehydration, skin temperature distribution, and heat storage.

SECTION V

EXTRAVEHICULAR ENVIRONMENTAL HAZARDS

INTRODUCTION

Without protection from the space environment, the body fluids can boil, and the body can freeze, burn, absorb lethal radiation, or be impacted by hypervelocity particles. In this section, the nature of these hazards, their influence on protective garments, and techniques for quantifying the protective capability of the garments are discussed.

Many governmental agencies, research groups, and industrial organizations are currently investigating the multi-faceted problems of the space environment. More precise description of the environment, improved simulation techniques, and new protective mechanisms are constantly being developed. However, with existing knowledge, it is possible to estimate with reasonable surety the magnitude of the principal hazards. The hazards are:

Vacuum

Thermal Radiation

Meteoroids

Space Radiation

Each of these hazards, which are discussed individually in the following sections, represents a broad field of study. This report does not present original work in these fields, but attempts instead to bring into perspective the factors which are significant to extravehicular operations, to define the current achievements in the technology of space hazard simulation, and to point the direction for further test efforts with fully protective garments as the goal.

THE VACUUM ENVIRONMENT

Man must be protected from the ultralow pressures of space to prevent vaporization of the body fluids and to sustain the metabolic process. The vacuum of space can also have a significant effect on the materials and on the heat transfer properties of the suit that provides this protection. It is these effects which are considered in this discussion of the vacuum environment.

Description Of The Environment

The pressure in space is about 10^{-6} mm Hg at an orbital altitude of 160 km and is estimated to be 10^{-13} mm Hg in interplanetary space and 10^{-16} mm Hg in

interstellar space (ref. 45). Although measurement of the low pressure in space is complicated by the lack of a standard reference below 1 mm Hg, reasonable agreement and repeatability have been obtained with various types of sensors such as thermal conductivity and ionization gauges. The decrease in ambient pressure with altitude is shown in Figure 100.

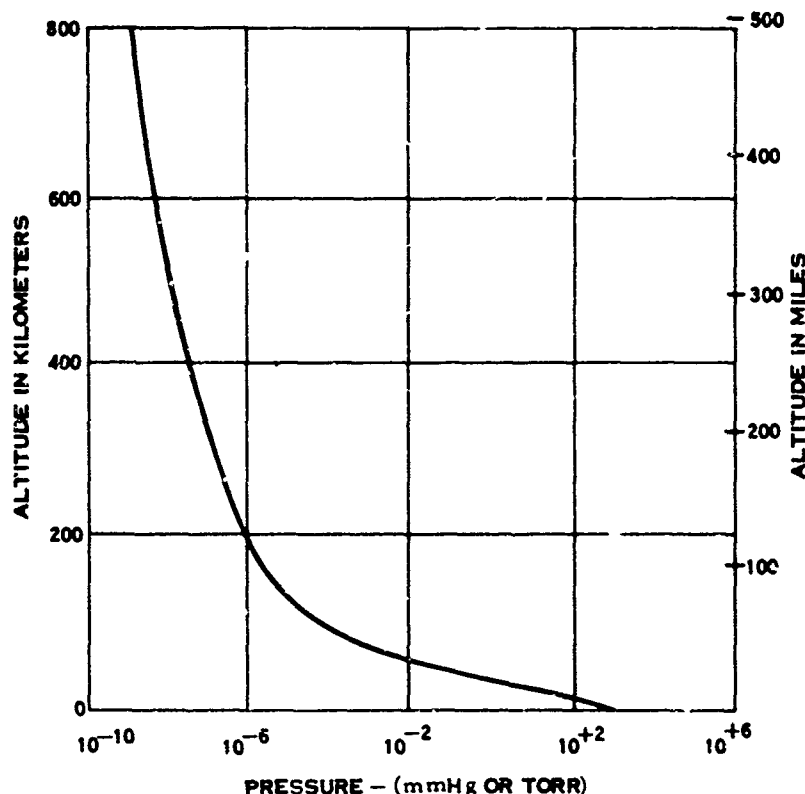


FIGURE 100. ALTITUDE versus AMBIENT PRESSURE

At altitudes greater than 22,000 km (14,000 mi) the gas is composed of about 85% hydrogen nuclei and 15% helium nuclei (ref. 54). Although the gas temperature is estimated to be on the order of 10^3°C to 10^5°C , the chemical composition and temperature of the gas is of small consequence since the concentration is only 10 to 100 ions/cm³ (ref. 45).

Effects Of The Environment On The Suit

The vacuum of space poses both material and functional problem in space suit design. While some of the material effects of space vacuum have been tolerable on rigid spacecraft, they may become intolerable on flexible space suit materials. Effects of the vacuum environment on the suit materials include evaporation or sublimation of material, friction, wear, and fatigue (refs. 17, 45, 87). Structural

properties of a material can be altered by vacuum accelerated evaporation or sublimation. Although structural weakening due to this weight loss is possible, embrittlement is more significant. Some of the organic materials used in present suits are long chain polymeric compounds which do not evaporate or sublime directly but break down into more volatile components, thus altering the composition of the material. Some plastics and elastomers embrittle significantly with less than 10% loss of volatile plasticizers. Evaporation of lubricants creates friction and wear problems in restraint cables, cable guides, bearings, and closures.

The surface characteristics of some materials are altered by hard vacuum. Below 10^{-5} mm Hg, evaporation of the adsorbed gas layer increases the problems of friction, wear, and cold welding and becomes especially severe near 10^{-9} mm Hg (refs. 17, 101). Evaporation or sublimation and/or recondensation of surface materials or adsorbed gases can alter absorptance and emittance characteristics thereby altering the thermal balance of a suit.

Space vacuum will alter the external heat transfer of a suit. At atmospheric conditions, external heat transfer is principally convection with some conduction and radiation. As pressure is decreased, convection disappears and heat transfer depends primarily on gas conduction and on radiation. At pressures below 10^{-3} mm Hg, thermal conduction of the ambient gas becomes negligible and heat transfer is then dependent only on the thermal radiation between the suit and the environment (ref. 101).

Simulation Of The Vacuum Environment

Space vacuums are simulated in vacuum chambers which range in size from small bell jars to huge 11 meter diameter by 20 meter high chambers with widely varying vacuum capabilities. The extremely low pressures can be produced most economically in small chambers. In two reported space suit materials evaluations (refs. 17, 56), the vacuum vessels used had volumes of 0.05 to 0.09 cubic meters (about 2 to 3 cubic feet). These studies involved both static and dynamic testing of the materials in vacuums from 10^{-6} to 10^{-9} mm Hg.

Simulation of the vacuum environment for thermal testing requires chambers in the order of 30 cubic meters (about 1,000 cubic feet). These larger chambers are welded of special stainless steels, polished to reduce outgassing, and usually employ mechanical roughing pumps to reduce the pressure to the 10^{-3} mm Hg range, below which cryopumps and diffusion pumps are used. The limit of these pumps is determined by the leakage through chamber penetrations and internal devices such as suits and cold shrouds and by the outgassing of all materials in the chamber. For manned suit evaluation, these chambers must include biomedical, suit pressurization, and communication systems and must have provisions for emergency repressurization and retrieval in the event of suit failure. Facilities of this type are described in detail in Section VII. In current chambers, with the

magnitude of leakage typical of current suits, duplication of the deep space vacuum is economically and technically impractical. Current chambers are capable of 10^{-8} mm Hg empty, but are estimated to be limited by suit leakage to pressures in the 10^{-6} mm Hg range (ref. 41).

Vacuum measurement is a fundamental problem of high vacuum simulation. Although a variety of vacuum measuring gauges are available, most of them work over only a portion of the vacuum range, do not read pressure directly, and cannot be calibrated with suitable standard gauges traceable to the National Bureau of Standards. Usually a combination of gauges is used in high vacuum simulation to cover the range adequately and to provide a cross check since a standard reference is lacking.

In general, these gauges include static pressure, thermal conductivity, and ionization gauges. One static pressure gauge, the McLeod Gauge, is used as a calibrating standard for the other gauges down to its lower limit of 10^{-5} mm Hg. In this gauge a known volume of gas is compressed to a known smaller volume to determine the pressure more accurately. Since this gauge cannot be operated continuously, it is normally used for calibration. Thermal conductivity gauges are usually employed in the 1 mm Hg to 10^{-3} mm Hg range where the conductivity of gases is strongly pressure dependent. These gauges measure the heat loss from a heated element due to the conductivity of the gas. The gauges must be calibrated for the particular gas in the system. Ionization gauges operate on the principle that below pressures of 10^{-3} mm Hg, the formation of ions resulting from the collisions of electrons with molecules varies linearly with pressure. The ambient pressure is then determined by measurement of the ion and electron currents of these gauges. A mass spectrometer must be used to determine the composition of the ambient gas since the ionization gauges are sensitive to gas composition. The lower limit of these gauges is about 10^{-10} mm Hg although some specialized gauges are claimed to measure pressures as low as 10^{-15} mm Hg.

Experience has generally shown that reasonable repeatability is obtained with the various gauges and that combinations of the gauges can be employed to provide additional confidence in the vacuum measurement. In the absence of a certified reference, there is no alternative.

Conclusions

The unpredictable effects of space vacuum on the structural and thermal properties of suit materials must be investigated by exposure to a simulated vacuum environment. Technically and economically the structural effects of vacuum can best be evaluated on the candidate material samples and components in small vacuum vessels at pressures from 10^{-10} mm Hg to 10^{-12} mm Hg. The evaluation must include static and flexural strength properties, surface characteristics, and frictional characteristics investigated under the state-of-the-art vacuum simulation.

Evaluation of the effects of space vacuum on the manned performance of current pressure suits does not require duplication of deep space vacuum. Heat transfer is predominantly radiative at pressures below 10^{-3} mm Hg and the adsorbed surface gas layer begins to disappear at pressures below 10^{-5} mm Hg, hence a vacuum of about 10^{-6} mm Hg is adequate for evaluating current pressure suits when the results are interpreted in conjunction with the results of materials investigations. At this vacuum any serious friction problems can be identified and meaningful investigation of the heat transfer characteristics can be conducted.

It is important to note that when suits are enclosed by an outer thermal protective garment, leakage gases which must escape from between the suit and the thermal garment prevent the suit surface from being exposed to the full space vacuum. For example, a minimum suit surface pressure of 10^{-4} mm Hg is anticipated with the current Apollo suit design.

Future suits, such as the diffusion cooled suits, may require closer simulation of space vacuum at levels where the mean free path of the sublimated molecules becomes sufficient to result in free molecular flow. The evaluation of portable life support equipment which uses fluid vaporization as a heat rejection mechanism may also require actual space vacuum simulation.

THERMAL ENVIRONMENT

Since the thermal conductivity of air begins to vanish at pressures below 10^{-3} mm Hg, (altitudes greater than about 100 km), radiation is the primary heat transfer mechanism during extravehicular operations. Outside the space vehicle a spacesuit may radiantly exchange heat with many sources including direct emission from the sun; reflected emission from the moon, earth, other planets, and the spacecraft; and direct infrared emission from all these sources. The net rate of radiation transfer is dependent on the intensity and spectral distribution of the sources, the effective areas, and the spectral absorptance and emittance properties of the suit materials. This net thermal radiation is a heat leak through the suit, adding to or subtracting from the heat load that must be rejected by the suit thermal control system. It can also produce hot or cold spots locally due to high conductivity or absorptances. A second thermal mechanism, that of thermal conductivity resulting from direct contact with hot or cold surfaces such as the spacecraft, extravehicular equipment, or planetary surfaces is discussed on page 270.

Nature Of The Environment

THE SOLAR SOURCE

The primary source of electromagnetic radiation is the sun. The intensity of the solar radiation varies inversely as the square of the distance from the sun. The electromagnetic energy flux density at the earth's mean distance from the sun is

called the solar constant and is equal to 1200 kcal/hr/m² (442 BTU/hr ft²) (ref. 6). The energy flux density would be 1.9 times as great at the orbit of Venus and 0.4 times as great at the orbit of Mars (ref. 54). The sun's radiation spectrum approximates that of a 5800 °K black body radiator and includes wavelengths in the X-ray, ultraviolet, visible, and infrared portions of the electromagnetic spectrum. The energy distribution of the solar radiation in space is presented in Table VII. The incident flux per unit area per unit wavelength at the earth's distance from the sun is shown in Figure 102 based on the data of Johnson (ref. 55). About 98% of the total solar energy is at wavelengths between 0.3 and 4.0 microns. At the earth's distance from the sun, this radiation is well collimated and contained within a field angle of 32 minutes of arc (ref. 66).

TABLE VII
SOLAR ENERGY DISTRIBUTION*

RADIATION TYPE	WAVELENGTH (MICRONS)	PORTION OF TOTAL (%)
X-Ray	10 ⁻⁵ - 10 ⁻⁴	10 ⁻⁹
Far Ultraviolet	10 ⁻⁴ - 0.25	1.3
Middle and Near Ultraviolet	0.25 - 0.4	7.7
Visible	0.4 - 0.7	40
Infrared	0.7 - 4.0	50
Infrared and Radio Frequency	above 4.0	1

The field angle (decollimation angle) is defined as the angle subtended by the source as viewed from the receiver while the collimation angle is defined as the angle subtended by the receiver as viewed from the source. For a spacecraft at the earth's distance from the sun, both angles are very small. Thus, the solar flux may be considered parallel, so that the energy absorbed by a body subjected to this radiation is:

$$q_a = \alpha S A_p \quad (139)$$

where α = absorptance based on solar spectrum
 S = solar constant at the location of the body (kcal/hr/m²)
 A_p = area of body projected onto plane normal to the flux (m²)

*Reference 55

OTHER THERMAL SOURCES

In the proximity of the planets and in view of their daylight hemispheres, reflected sunshine may add considerably to the electromagnetic radiation intensity. The ratio of this diffuse reflected radiation to the incident radiation is defined as the albedo of that planet. The albedos of some planets are shown in Table VIII. The earth albedo may vary considerably depending on the location of bodies of water and on the cloud cover. Any other objects such as spacecraft and space suits at close distances also are sources of reflected radiation. In addition, the planetary bodies will emit some electromagnetic radiation in the infrared wavelengths. Aside from the solar, albedo, and planetary infrared sources, the space environment is a cold radiative heat sink equivalent to about 4°K (ref. 101).

TABLE VIII

ESTIMATED PLANETARY ALBEDOS*

BODY	ALBEDO
Mercury	0.058
Venus	0.76
Earth	0.39
Mars	0.15
Jupiter	0.51
Saturn	0.50
Uranus	0.66
Neptune	0.62
Pluto	0.16
Moon	0.07

Effect Of The Environment On The Suit

The primary effect of the thermal environment on a space suit is the heat flow into or out of the suit. The magnitude of this heat flow depends on many environ-

*Reference 45

mental factors and suit material properties. The space garments must simultaneously provide the wearer with protection from various combinations of black space, solar irradiance, planetary albedo, and reflections from other space suits and spacecraft.

In addition, the thermal environment may affect the flexibility of a suit, and the X-ray and ultraviolet radiation of the solar spectrum below 0.3 microns may cause radiation damage and embrittlement as discussed on page 256.

Thermal analysis to establish the magnitude of the suit heat leak is fraught with difficulties and assumptions; however, reasonable estimates for current suit ensembles range from about 40 kcal/hr (160 BTU/hr) into the suit during lunar day to about 100 kcal/hr out of the suit during lunar night. This heat leak is only a moderate fraction of the total heat load on the life support system compared to the metabolic heat produced (130 kcal/hr to 400 kcal/hr).

Although the total heat leak through the suit represents the greatest possibility for physiological stress, local hot or cold spots due to high conductivity near suit folds, due to tears, or due to points of intense radiation could conceivably cause extreme discomfort. Likewise, cold spots may occur near locations which radiate directly to deep space. There is little data available on the actual temperature of hot and cold spots that may be experienced during extravehicular operations; however, the temperature of these spots should be within the limits of comfort as defined in the life support requirements section.

Simulation Criteria And Techniques

The primary purposes of thermal simulation are to determine the suit heat leak and the presence of hot spots. Simulation of the space thermal environment requires a chamber in which the ambient pressure can be reduced below 10^{-3} mm Hg, preferably in the 10^{-6} mm Hg range to eliminate the gas thermal conductivity.

Relatively poor thermal simulators have been used with reasonable success to test spacecraft by compensating for their limitations with calibration and analytical corrections (ref. 53). However, it should be realized that the variable geometry of the space suit presents quite a different problem from the rigid spacecraft since (1) the astronaut may move about and rotate to maintain an optimized heat exchange with the environment and (2) the flexibility of the suit surface will result in continually changing absorptance and emittance characteristics due to changing folds.

That folds are important can be seen by referring to Figure 101. Assuming that the transmission of the space suit material is negligible, a portion of the incident energy will be absorbed and the remainder reflected. The multiple reflections in a fold result in the absorption of a much larger portion of the incident radiation than adjacent unfolded surfaces. This is equivalent to a variation in the absorptance coefficient. Thus, folds are potential hot spots. As a consequence of

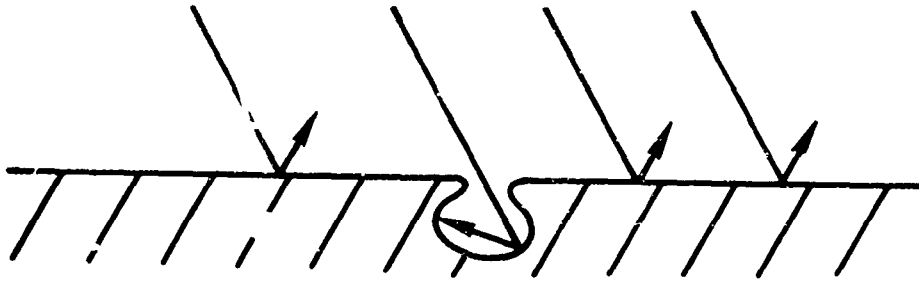


FIGURE 101. EFFECT OF FOLDS ON LOCAL ABSORPTANCE

the locally varying absorptance and the variable geometry of the suit, accurate simulation of the space environment is required to determine the total heat absorbed and emitted as functions of suit position and the number and intensity of hot spots.

SOLAR SIMULATION

In solar simulation the suit should absorb the same thermal energy from an artificial source as it would from the sun. The properties which affect the energy absorbed by the suit include:

1. Spectral content of radiation and spectral absorptance of the suit surface
2. Intensity of irradiation
3. Decollimation angle of radiation

Considering the problem of spectral match with various types of solar simulators, the question of how much error in absorbed energy will result from imperfect solar matches must be answered. Although accurate thermal data on current suit surface materials is either unavailable or classified, the nature of the problem can be explored by working through sample calculations for two candidate suit materials, Type 1 and Type 2. These materials have spectral absorptances as shown in Table IX. The heat absorbed per unit area by either of these materials when irradiated is:

$$q_a = \sum_i \alpha(\lambda_i) I(\lambda_i) (\Delta\lambda)_i \quad (140)$$

where $I(\lambda_i)$ = the incident intensity per unit wavelength in the wavelength band $(\Delta\lambda)_i$
 $\alpha(\lambda_i)$ = the absorptance of the material at the wavelength λ_i
 $(\Delta\lambda)_i$ = an incremental wavelength about the wavelength λ_i

TABLE IX

SPECTRAL ABSORPTANCE OF CANDIDATE MATERIALS

WAVELENGTH (MICRONS)	SPECTRAL EMITTANCE $\epsilon(\lambda)$		SPECTRAL ABSORPTANCE $\alpha(\lambda)$	
	TYPE 1	TYPE 2	TYPE 1	TYPE 2
0.32			0.95	0.24
0.50			0.22	0.21
0.75			0.20	0.31
1.00			0.16	0.26
1.25			0.15	0.24
1.50			0.15	0.19
1.75			0.20	0.24
2.00	0.29	0.03	0.29	0.02
2.50		0.03		0.03
3.00	0.69	0.04	0.69	0.04
3.5		0.04		
4.0	0.68	0.03		
4.5		0.03		
5.0	0.81	0.04		
5.5		0.05		
6.0	0.88	0.06		
6.5		0.04		
7.0	0.89	0.05		
7.5		0.05		
8.0	0.81	0.05		
8.5		0.06		
9.0	0.86	0.05		
9.5		0.06		
10.0	0.84	0.05		
10.5		0.05		
11.0	0.83	0.05		
11.5		0.05		
12.0	0.86	0.06		
12.5		0.05		
13.0	0.81	0.06		
13.5		0.06		
14.0	0.80	0.04		

In this manner, the energy that would be absorbed by each of these materials when irradiated by either the sun, a carbon arc, or a tungsten lamp was computed. The spectral distributions of these sources are shown in Figure 102. In each case, the intensity of the source was normalized to one solar constant. The estimated energy absorbed based on the spectral distribution of the source and the spectral absorptance of each of the two materials is shown in Table X.

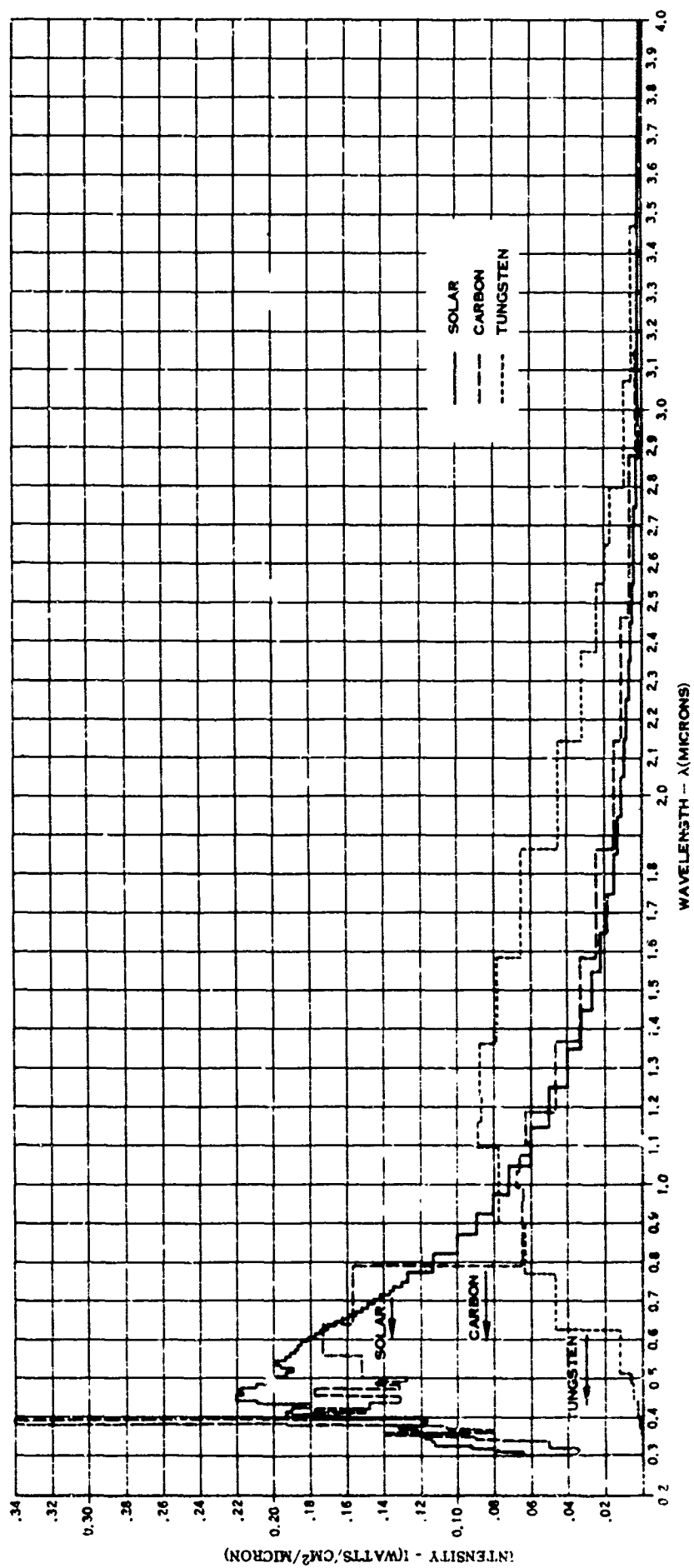


FIGURE 102. SPECTRAL INTENSITY DISTRIBUTION OF CARBON ARC, TUNGSTEN SOURCE, AND THE SUN

TABLE X

SPECTRAL ENERGY ABSORBED

SOURCE	TYPE 1 MATERIAL		TYPE 2 MATERIAL	
	kcal/hr	BTU/hr	kcal/hr	BTU/hr
Sun	29	116	24	97
Carbon	30	118	24	94
Tungsten	24	96	20	80

As shown, an accurate simulation can be expected with the carbon arc which closely approximates the solar spectrum. Combinations of short arc sources with appropriate filters also can provide a fair approximation to the solar spectrum. Although difficulties have been encountered with the stability of the filters, the short arc sources have an advantage over the carbon arc in ease and reliability of operation.

Correcting for spectral mismatch by adjusting the source intensity has been a frequently used technique in evaluating the thermal characteristics of rigid objects such as spacecraft. Infrared sources with the intensity adjusted are used to make the absorbed energy (q_a infrared) equivalent to that which would be absorbed from the sun (q_a solar). While this technique has been reasonably successful with rigid spacecraft, it may result in appreciable error when evaluating the flexible space suit. Consider again the fold shown in Figure 101. If the average absorptance of the suit for infrared radiation is much less than that for solar radiation, it would be desirable to make the intensity of the source some multiple of the solar constant to make q_a infrared = q_a solar. While this may result in equivalent energy absorption on the smooth surface, the folds act more like black body absorbers and as a consequence would absorb more energy from the infrared source than from the sun. With the flexibility of a space suit, it would be impossible to correct for these rapidly changing folds. Thus, intensity correction for spectral mismatch is unsatisfactory.

Intensity variations in the simulated solar radiation throughout the test volume can cause local variations in absorbed heat. However, current suits will only absorb about 40 kcal/hr under worst-case irradiation. At a metabolic load of 120 kcal/hr, the absorbed heat is 25% of the total heat load to be removed. A 10% variation in incident radiation would only provide a 2.5% variation in the total heat load. Intensity uniformity of $\pm 10\%$ throughout the test volume appears to be a reasonable requirement at the present state-of-the-art.

The simulator decollimation angle may cause irradiation of surfaces which would have been dark under exposure to the sun and may also cause partial shadowing (penumbral) regions. Bobco shows (ref. 9) that a conical simulator beam with a 5° decollimation half angle which irradiates a test plane at one solar constant (1200 kcal/hr/m²) would irradiate a plane normal to the test plane with a flux of 24 kcal/hr/m². This decollimation flux is only about 2% of the simulated solar flux, which would not be expected to cause significant error in heat leak.

In summary, space suit testing will require the spectral match of a carbon arc or short arc solar simulator. Infrared solar simulation is unacceptable even with attempted correction for the spectral mismatch. Intensity variations of ± 10% in the test volume can be tolerated as can a decollimation angle of ±10 degrees.

OTHER THERMAL SIMULATION

Evaluation of the thermal characteristics of a space suit may also require simulation of planetary albedo and infrared radiation. The planetary radiation incident on the space suit is dependent on the intensity of the albedo and infrared radiation emitted, the proximity of the space suit to the planet, and the orientation of the suit.

Currently there is no precise method of reproducing the albedo. The earth's albedo, for example, is a diffuse radiation spectrally similar to the solar radiation with the exception of gaps due to the selective absorptance of the earth's atmosphere. As a consequence, the albedo can only be approximated by reflecting radiation of a solar simulator from a diffuse reflector. The locations and orientations of the reflecting surfaces are chosen to effect simulation of the field angle. Frequently, only infrared sources are employed in the simulator.

Variable intensity infrared sources and reflectors are also employed to simulate the planetary emissions. The positioning of the sources and reflectors is normally variable to allow some adjustment in simulated field angle. For the actual suit with its changing positions and variable geometry, simulation of albedo and infrared radiation, at best, can only be approximated.

BLACK SPACE SIMULATION -- Current techniques for simulating the black space environment usually employ an optically dense shroud inside a vacuum chamber. The shroud is normally cooled with liquid nitrogen at 77°K or with liquid helium at 20°K. Auxier (ref. 4) shows from Christiansen's equation that the net rate of heat transfer by radiation from an enclosed grey body to its grey enclosure is:

$$q_{\text{net}} = \frac{\epsilon_s \sigma A_s (T_s^4 - T_w^4)}{1 + \epsilon_s \left(\frac{1}{\epsilon_w} - 1 \right) \frac{A_s}{A_w}} = F \epsilon_s \sigma A_s (T_s^4 - T_w^4) \quad (141)$$

where

ϵ_s = emissivity of enclosed body
 A_s = surface area of enclosed body
 T_s = temperature of enclosed body
 ϵ_w = emissivity of enclosure
 A_w = surface area of enclosure
 T_w = temperature of enclosure
 F = shape factor
 σ = Stefan-Boltzmann constant

As shown in Table IX, ϵ_s for a typical space suit material is about 0.85 at infrared wavelengths. For the suit in deep space the enclosure is considered a black body with $\epsilon_w = 1$, so that the shape factor $F = 1$. Then for radiation to deep space

$$q_{\text{net space}} = \epsilon_s \sigma A_s (T_s^4 - T_w^4) \approx 0.85 \sigma A_s T_s^4 \quad (142)$$

To see how closely the shape factor of a simulator approaches the desired $F = 1$, consider a 3 m diameter by 3 m long cylindrical chamber at 10^{-6} mm Hg containing a liquid nitrogen cooled shroud with $\epsilon_w = 0.94$. $A_w = 43.6 \text{ m}^2$ and $A_s = 1.8 \text{ m}^2$ so that

$$F = \frac{1}{1 + (0.85) \left(\frac{1}{0.94} - 1 \right) \left(\frac{1.8}{43.6} \right)} = 0.997 \quad (143)$$

Thus, because of the high emissivity of the chamber walls, the shape factor is essentially unity and the heat radiated to the walls is

$$q_{\text{net simulator}} = \epsilon_s \sigma A_s (T_s^4 - T_w^4) \quad (144)$$

a good simulation of the black space environment if T_w is sufficiently low.

To find how the wall temperature affects the heat leak, an iterative calculation must be performed because T_s is unknown. Assume that a given suit with $\epsilon_s = 0.85$ leaks 27.6 kcal/hr/m^2 to black space at an internal wall temperature T_{si} of 27°C . Then from Equation 142 the external wall temperature T_{so} would be:

$$T_{so} = \left(\frac{q_L}{\epsilon_s \sigma A_s} \right)^{1/4} = 160^\circ\text{K} \quad (145)$$

and the effective conductivity k of the suit would be:

$$k = \frac{q_L}{A_s (T_{si} - T_{so})} = 0.2 \text{ kcal/hr/m}^2/\text{°K} \quad (146)$$

Assuming k remains constant, the suit surface temperature T_{so} for an internal wall temperature T_{si} is determined by iterating Equation 147.

$$k (T_{si} - T_{so}) = \epsilon_s \sigma (T_{so}^4 - T_w^4) \quad (147)$$

Then $\frac{q_L}{A_s}$ is found from Equation 146. With the suit under consideration, heat leak through the suit at $T_{si} = 27^\circ\text{C}$ would be about 27.4 kcal/hr/m^2 with the chamber wall at liquid nitrogen temperature, 77°K . Thus good heat leak simulation is achieved with a relatively high wall temperature because of the fourth power dependence.

ROLE OF THE THERMAL DUMMY -- The hazards of manned testing in a simulated space environment and the difficulties of obtaining accurate heat balances with human test subjects make the use of dummies desirable for evaluation of the thermal properties of a space suit. Several dummy concepts were considered for evaluating (1) hot spots and (2) total heat leak.

1. A simple stick dummy which would merely support a space suit in a fixed position.
2. A simple anthropomorphic dummy which would provide the proper contour of man inside the suit and thus simulate flow paths for the gas or liquid cooling system.
3. A heated anthropomorphic dummy which could maintain fixed surface temperatures or a constant metabolic equivalent power.

It will be shown that none of these dummies is practical for evaluating the problem of hot spots but that a simple anthropomorphic dummy may provide an acceptable simulation for determining suit heat leak. The final decision on dummy testing for determining suit heat leak, however, requires data from actual test results.

Hot (or cold) spots may result from either locally high suit conductivity or locally high absorptance. High conductivity can result from increased body contact pressure as in the compression of the superinsulation layers in the suit at the palm, elbow, or knee. Locally high absorptance can result from folds. A dummy, therefore, would have to duplicate man's ability to turn and flex and also duplicate the pressure exerted by a man at a contact point. Such a dummy is not practical considering the relative importance of the problem and the ease with which human test subjects can identify the problem. However, additional instrumentation and possibly detailed testing may be desirable once the location and nature of any particular hot spot has been identified.

The total heat leak through a suit is dependent on the temperature differential across the suit wall and the effective conductivity of the wall. It is also dependent on the fourth power of the external surface temperature and the surface properties. Therefore, in a radiative environment, the heat leak will increase or decrease as the internal wall temperature varies. Further, for a typical coolant flow and heat leak, the local internal wall temperature nearly equals the local temperature of the coolant stream. Thus, at equilibrium, the heat leak through a manned suit can be duplicated in an unmanned suit if the internal wall temperature distribution is duplicated.

Consider a suited dummy positioned in a controlled radiation environment. A measured flow of gas or liquid through the normal suit coolant system is used to control the internal wall temperature. For simplicity assume that the heat leak is negative, that is, outward. Since the suit coolant will have to provide the heat flowing through the suit wall, the coolant temperature will drop from inlet to outlet; thus, the local internal wall temperature and consequently the local heat leak will decrease from near the inlet to the outlet. By regulating coolant flow, almost any desired temperature differential of the coolant system can be maintained. The internal wall temperature distribution, however, cannot be duplicated because the distribution in a manned suit is not known nor is calculation practical. If it were known from actual measurements there would be little need for dummy tests (except perhaps for the evaluation of minor suit improvements).

The local wall temperature lies between the coolant inlet and outlet temperatures, but is otherwise unknown. The maximum error in local heat leak, therefore, can be minimized by maintaining a small coolant temperature differential from inlet to outlet and by adjusting the inlet temperature to the average manned suit temperature.

On the basis of this reasoning, the major requirement placed on a dummy is that it must present the proper flow path for the coolant. The simple stick dummy would neither give the proper shape and flow distribution to a liquid cooled garment nor the proper flow path for gas ventilation. The simple anthropomorphic dummy would provide nearly correct coolant flow distribution. Although the heated anthropomorphic dummy might more nearly approximate the manned condition, particularly for a liquid cooled system, the simulated metabolic heat must be subtracted from the total load on the coolant system to determine suit heat leak. This subtraction introduces errors which negate any advantages of the heated dummy.

In view of the fact that the complex human thermoregulatory system cannot be simulated by dummies, the thermal performance of a suit must ultimately be demonstrated by manned testing as discussed in Section IV. Since simple anthropomorphic dummies can probably be used to determine heat leakage within 10%, their use is justified both in engineering studies of development suits and in predicting the safety of a subsequent manned test.

SPECIAL MEASUREMENT TECHNIQUES

In general, testing in a thermal vacuum simulator requires a great many specialized measurement techniques, most of which are incorporated in the existing facility. However, there are certain measurement capabilities which are necessary for suit testing but not necessarily common to the existing facilities. These are discussed below.

SUIT HEAT FLUX -- During thermal environmental testing it is of interest to know the total and local heat flow crossing the suit boundary. The total heat crossing the boundary can be measured rather simply with the thermal dummy by measuring the change in enthalpy of the ventilation gas stream, that is, by conventional heat exchanger thermal balance techniques. However, the local heat flow through the suit is a much more complex problem. To some extent this problem can be handled by individual temperature measurements on the internal and external surfaces of the suit. Some of the problems associated with these temperature measurements are discussed in the following paragraphs. Another approach is to use one of the various kinds of heat transducers that are available. These transducers normally consist of a pair of thermocouple junctions or a similar temperature measuring device installed on opposite sides of a thin thermally conductive wafer. The conductivity of the wafer is accurately known so that, with the measurement of temperature differential, the heat flux through the wafer can be easily computed. These heat flux transducers are installed either on the surface of or within the material through which the heat flow is of interest. The accuracy with which these transducers measure the true heat flow through the suit depends on how much they change the local flux. Because of the thinness of the suit fabric, the complexity of heat exchange mechanism, and the variability in conductance of the multi-layered superinsulation, heat flux transducers do not appear useful.

INTERNAL WALL TEMPERATURE -- When hot spots have been located in manned testing, it is of interest to measure the internal suit surface temperatures. Measurements can be made satisfactorily with either small thermocouples or bead type thermistors attached to the inner surface of the suit wall. Satisfactory results should be achieved provided the usual safeguards to prevent unnecessary lead conduction or convection errors are observed. Attaching the thermistor bead with conductive epoxy cement or the thermocouple junction with solder to a small metal tab about 5 mm square by 0.2 mm thick and securing this to the suit surface with a suitable adhesive should prove entirely satisfactory.

EXTERNAL SUIT SURFACE TEMPERATURE -- The measurement of suit external surface temperature may prove very difficult, primarily because of the problems associated with the emissivity and/or absorptance of the temperature sensing materials. A preferable, but not entirely satisfactory, procedure might be achieved by installing the temperature sensors on one of the inner surface layers of the outer garment. In this case, the multiple reflections that occur on the inner layers of the superinsulation will tend to reduce the emissivity error. Actual

attachment could be similar to the attachment of the internal temperature sensors. In this case, thermocouples are probably preferable due to the wider range of temperature over which they may be used.

CHAMBER WALL TEMPERATURE -- The measurement of chamber wall temperature is relatively straightforward. Although thermistors ease the problem of chamber penetration, thermocouples are probably more convenient for chamber wall installation. The error due to sensor emissivity should prove negligibly low due to the high conductivity of the chamber wall. Adequate precautions to reduce the lead conduction and the addition of flat black paint to the thermocouple surface to improve the absorptivity should eliminate any significant thermal error.

The measurement of ambient temperature in the chamber, however, should be approached with the greatest caution. At low pressures, radiation errors from the temperature sensor and the low convective or conductive heat input to the probe can produce very substantial thermal errors as has been reported many times in the literature.

SOLAR SIMULATION MEASUREMENT -- Major solar simulation facilities have instrumentation systems and specialized measurement techniques for defining the thermal environment during any test series. Measurements of the radiation field include (1) uniformity, (2) flux density, (3) temporal stability of the source, (4) field angle or decollimation angle, (5) collimation, and (6) spectral distribution. The first five of these measurements are performed with commercially available heat flux transducers such as pyroheliometers or thermopiles. The spectral distribution is usually measured either with a filter type radiometer, which divides the spectrum into multiple energy bands, or with a spectrophotometer, which sweeps the spectrum continuously. However, in this rapidly advancing field, new instrumentation techniques are constantly being developed and the choice of instrumentation will depend on the available measurement techniques at the time of testing.

Conclusions

Simulation of the thermal space environment should be performed in a vacuum chamber with pressure reduced below 10^{-6} mm Hg. This chamber should contain an optically dense cold shroud with the highest emissivity obtainable.

Solar simulation should employ sources with a minimum decollimation angle since shadowing on a suit is extensive. Good spectral match is required so that folds do not introduce significant errors in the absorbed energy. Either carbon or short arc sources can provide acceptable simulation with the ultimate source selection based on trade-offs in spectral match, ease and reliability of operation, and the optical transmission system requirements. In general, decollimation angles of $\pm 10\%$ in the test volume are within the state-of-the-art in solar simulators.

Simulation of planetary albedo is beyond the state-of-the-art. A solar simulator can be employed with a diffuse reflector to provide gross simulation of albedo, the shape of the reflector being adjusted to approximate the correct field angle. Infrared sources and reflectors can be employed to approximate planetary infrared emission. Although spectral contents of these simulators may be appreciably different from the actual sources, reasonable results can be expected if the spectral absorptances of the suits are relatively constant over the spectrum of the emitted radiation.

The simplification and expediency of thermal testing that would result from the employment of anthropomorphic dummies warrant further investigation into their possible use. Comparative tests of suits employing dummies and human test subjects are needed.

The complex and continuously varying geometry of a space suit assembly makes analysis of thermal radiation parameters virtually impossible. The uncertainties introduced by the gross assumptions required for analysis could easily result in errors approaching the magnitude of the parameter under consideration. Fortunately, however, heat leaks through current space suits are at most about 20 or 25 percent of the maximum suit heat removal capability, which reduces the effect of the simulation error in the evaluation of the total thermal performance of the suit.

METEOROID ENVIRONMENT

The extravehicular astronaut is continually exposed to the danger of impact and penetration by meteoroid material. The safety of the astronaut depends upon statistical factors. The probability of encounter with micrometeoroid material is very large; however, only a minimum protective cover is needed to prevent penetration of the suit surface. Encounter with larger particles at higher energies is less likely and depending upon the duration of the mission, the reliability desired, and the meteoroid environment which is likely to be encountered, an adequate protective garment can be provided. At the present time, any penetration of the suit is considered lethal. Not only would the pressure integrity of the suit be destroyed but, in a pure oxygen environment, flash burns and extensive tissue damage could result.

Description Of The Environment

Meteoroids are high velocity particles which are believed to have originated from both cometary disintegration and asteroid fragmentation. The presence of this space debris within the solar system has been indicated by light phenomena, ground observations, and direct measurement. The solar corona and zodiacal light are the results of the reflection and refraction of light by small particles. Larger particles have been detected by ground observation which has included

visual and radar detection as well as actual recovery of meteorite material. In recent years the availability of sounding rockets and satellites has led to direct measurements of the meteoroid environment using a variety of sensors (refs. 28, 29, 30, 84).

METEOROID CLASSIFICATIONS

Upon interaction with the earth's atmosphere, meteoroids are redesignated as meteors and/or meteorites (refs. 111, 115). A meteor is the visual or electromagnetic phenomenon associated with the interaction of a meteoroid with the earth's atmosphere. A meteorite is a particle that has reached the earth's surface. Meteoroids that are too small to produce either visual or radar meteors are by definition micrometeoroids. Micrometeoroid diameters are less than 1 mm (ref. 111).

Meteoroids are further classified as either sporadic or shower. Sporadic meteoroids are individual particles with random direction and occurrence, while shower or stream meteoroids are streams of particles traveling in similar orbits about the sun and occurring at predictable intervals. Meteoroids are either primary or secondary, the latter being ejecta from impacts by primary meteoroids.

PHYSICAL CHARACTERISTICS

Because meteoroids are very irregular in shape and originate from many sources, their physical characteristics vary widely. Meteoroid sizes range from particles of less than one micron diameter to several meters in diameter and larger. The velocity of meteoroids relative to the earth varies from 11 km/sec to 72 km/sec (36,000 ft/sec to 236,000 ft/sec). The density of meteoroid material is estimated to be from 0.01 g/cc to 9 g/cc (refs. 14, 45, 114). Asteroidal meteoroids are believed to be high density metallic materials while cometary meteoroids are believed to be mineral particles bound together by a low density, high porosity material. About 90% of the meteoroids are of the low density cometary type (refs. 14, 29).

Model Meteoroid Environment

The task of accurately defining the meteoroid environment is currently receiving considerable attention. Consequently, any models of the environment are subject to frequent revision as information continues to be compiled. The most recent model of the environment has been proposed by NASA-MSFC (ref. 36). This model was constructed from several trial models that were assessed and modified by spacecraft manufacturers, scientists, and engineers associated with the space environment.

Although near earth (≤ 70 km) and cislunar space are of primary interest here, the model includes the near lunar environment (≤ 30 km lunar altitude) as an indication of the hazards of secondary meteoroids near other bodies such as the moon or spacecraft. In near earth and cislunar space, the flux is composed of primary sporadic and primary shower meteoroids. Near the lunar surface, the flux is composed of both primary and secondary sporadic and shower meteoroids. The average density and velocity of primary meteoroids are taken as 0.5 g/cc and 30 km/sec (98,000 ft/sec) respectively. For secondary meteoroids (lunar ejecta) the respective values are 3.5 g/cc and 0.2 km/sec.

The more prominent meteoroid showers are predictable and the increase in meteoroid activity resulting from these showers has been determined (ref. 17). The increase in activity is known as the magnification factor F which is defined as the ratio of the shower to sporadic hourly rate of influx. The stream velocities of the showers are tabulated in Table XI. The current best estimate of the near earth, cislunar, and near lunar meteoroid flux is shown as a function of mass in Figure 103. These curves were determined from the following flux formulas (refs. 14, 36).

Primary Sporadic Meteoroid Flux

$$\log N = -1.34 \log M - 10.423 \quad (148)$$

Primary Shower Meteoroid Flux

$$\log N = -1.34 \log M - 2.68 \log V_s - 6.465 + \log F \quad (149)$$

Secondary Sporadic Meteoroid Flux

$$\log N = -1.34 \log M - 6.58 \quad (150)$$

Secondary Shower Meteoroid Flux

$$\log N = -1.34 \log M - 2.68 \log V_s - 2.635 + \log F \quad (151)$$

where the logs are to the base ten and

N = flux density (number of particles/ft²/day)

M = mass of meteoroids (grams)

V_s = velocity of meteoroid stream (km/sec)

F = magnification factor (ratio of shower flux to sporadic flux)

In these formulas N is interpreted to be the flux of particles with mass greater than or equal to M .

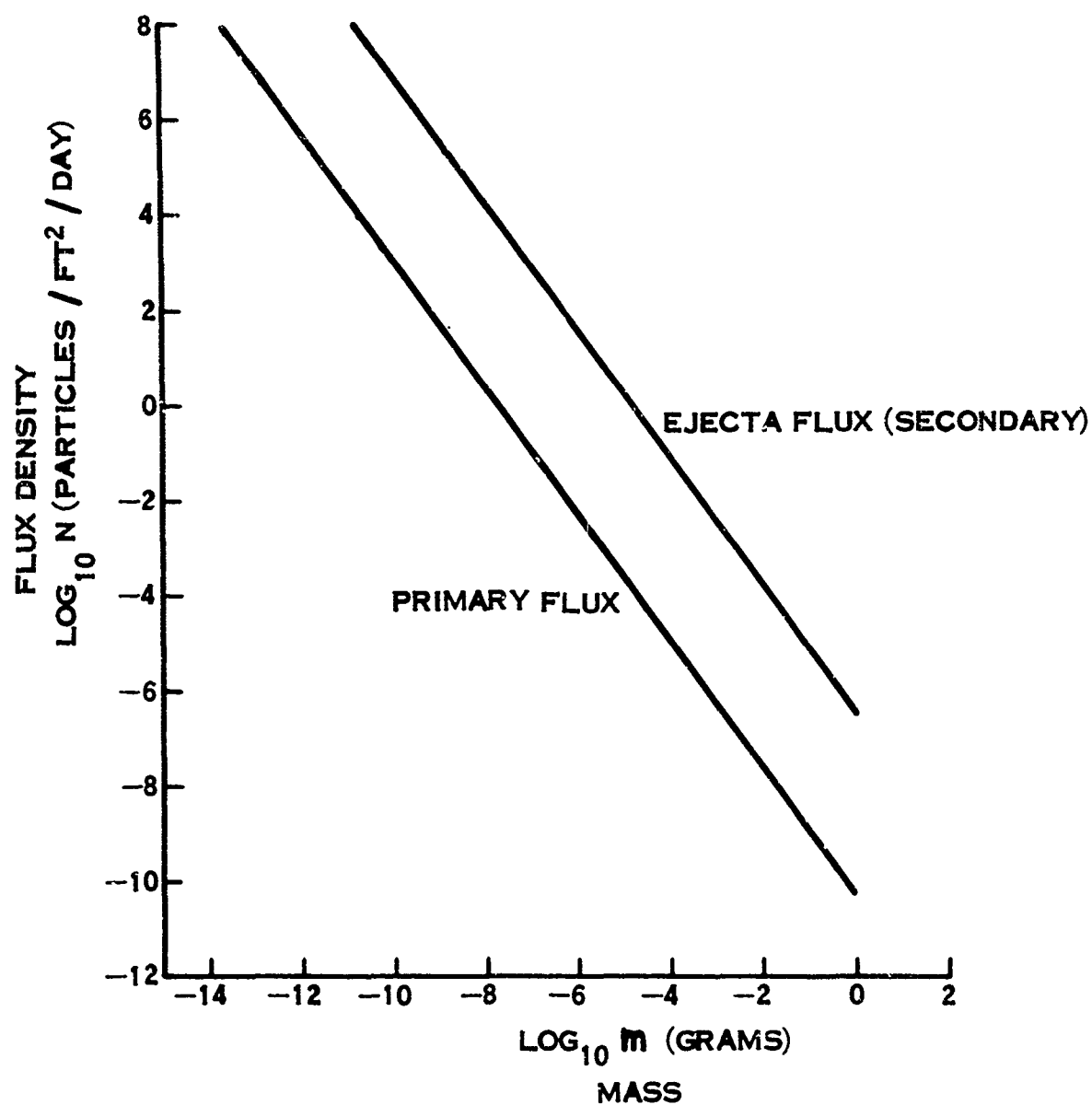


FIGURE 103. EARTH, CISLUNAR, AND NEAR LUNAR METEOROID ENVIRONMENT (REFERENCE 14)

TABLE XI

METEOROID SHOWER STREAM VELOCITIES*

SHOWER	DATE OF ACTIVITY	VELOCITY (km/sec)
Quadrantids	Jan 2 - 4	42
Lyrid	April 19 - 22	48
- Aquarid	May 1 - 8	61
O-Cetid	May 14 - 23	37
Arietid	May 29 - June 19	38
- Perseid	June 1 - 16	29
- Taurids	June 24 - July 5	31
- Aquarid	July 26 - Aug 5	40
Perseid	July 15 - Aug 18	60
Giacobinid	Oct 9 - 10	23
Orionid	Oct 15 - 25	66
Arietid, Southern	Oct - Nov	28
Taurids, Northern	Oct 26 - Nov 22	29
Taurids, Night	Nov	37
Taurids, Southern	Oct 26 - Nov 22	28
Leonid	Nov 15 - 20	72
Bielids	Nov 15 - Dec 6	16
Geminid	Nov 25 - Dec 17	35
Ursids	Dec 20 - 24	37

*Reference 14

EXPOSURE AND SHIELDING

The indicated fluxes were averaged over long periods of time because the occurrence of meteoroids is of a statistical nature. The total number of impacts on an object exposed to this environment is the sum of the impacts due to sporadic and shower meteoroids. The total surface area of the object is subject to impacts from the randomly oriented sporadic flux. Only the cross sectional area is exposed, however, to the unidirectional shower meteoroids.

The sporadic flux impacting an object will be reduced if the object is located in the vicinity of another body such as the earth, moon, or spacecraft. Equation 152 gives the shielding factor ξ which is defined as the fraction of total flux incident on object.

$$\xi = \frac{(1 + \cos \Phi_0)}{2} \quad (152)$$

where $\Phi_0 = \sin^{-1} \frac{R}{R+U}$

R = Radius of shielding body

H = Altitude from shielding body

The Equation 152 is derived in Appendix VIII.

Impact Phenomena And Consequences

In addition to the uncertainties in the meteoroid mass, velocity, and density distributions, the impact phenomena and the damage resulting from meteoroid impact are not well defined. Attempts are currently being made to assess the meteoroid hazard by impacting selected materials with particles accelerated to meteoroid velocities. However, acceleration of particles of proper mass to meteoroid velocities has proven extremely difficult. The best velocities attainable have been near the lower limit of meteoroid velocities (11 km/sec) and it has been necessary to predict meteoroid penetration and damage by extrapolating the results of the low velocity tests. Variations in the extrapolations and empirical relationships have resulted in postulation of various mathematical impact models, each of which may apply for some portion of the impact process.

IMPACT CLASSIFICATIONS

Dependent on the velocity of the projectile, impact processes are divided into four regions: (1) low velocity, (2) high velocity or transition, (3) hypervelocity, and (4) explosive. A given impact may involve combinations of these processes. The low velocity region includes projectile velocities up to about 0.9 km/sec

(3000 ft/sec). This is the region of conventional armor penetration where the projectile remains relatively undeformed and penetration is dependent primarily on the strengths of the projectile and target materials. The target will have plugging, petalling and/or ductile failures dependent on the relative magnitudes of the induced in-plane radial stresses and the elastic limit of the target material. In plugging, only elastic deformation occurs in the plane of the target plate and a plug is sheared out. If the target stretches and fails in tension, petalling will occur whereby a series of petals are formed around the penetration. Ductile penetration occurs when the induced stresses exceed the elastic limit of the target causing in-plane motion of the target material. The motion of the target material is evidenced by a thickening of the target around the penetration (ref. 29).

As the projectile velocity is increased above 0.9 km/sec the high velocity or transition region is entered. (Here the radial stresses induced in the projectile by the stress wave front are sufficient to cause flow of the material so that it deforms or fragments.) The transition region is relatively small for particular projectile and target materials and will generally occur at velocities somewhere between 0.9 and 4.5 km/sec. In this region the depth of penetration may actually decrease with increased velocity due to the fragmentation or deformation of the projectile which increases the area of impact. (If the projectile is brittle, it fractures; if ductile, it deforms.)

In the hypervelocity region the stress waves are initially many orders of magnitude higher than the strength of the material and the material flows like liquid. Hypervelocity impacts are characterized by this fluidlike flow of the material and a resultant hemispherical crater. In this region the penetration is dependent on the density rather than the strength of the projectiles being fired into ductile targets. The hypervelocity region begins at about .5 km/sec (ref. 62).

Although no experimental data exists, the explosive impact region is assumed to begin at velocities higher than 12 km/sec. In this region it is hypothesized that the impact energy is sufficient to vaporize both the projectile and a small volume of the target.

HYPERVELOCITY IMPACTS

The explosive and hypervelocity regions are the primary regions of concern in meteoroid impacts on spacecraft and/or space suits. Because of the difficulty of producing these velocities in the laboratory, the impact processes are not completely understood and extrapolation of results is not reliable. However, a current explanation of the phenomena of explosive and hypervelocity impacts will be presented. The target will first be considered infinite in thickness after which the effects of thinning the target will be discussed.

Consider an infinitely thick target being approached by a projectile at a velocity much greater than the velocity of sound in the target material. At impact, the energy imparted to the local area is so great that some of the projectile and target materials are vaporized, accompanied by a characteristic bright flash of light. At impact, a strong spherical shock wave emanates from the projectile-target interface and propagates into the target. Initially, the pressure increase across the wave is so much greater than the shear strength of the projectile and target materials that they flow like fluid, creating a hemispherical crater. The fluidlike material flows along the walls of the crater and is ejected at very high velocity.

As the projectile energy is dissipated, the cratering velocity decreases rapidly and the target strength properties begin to control the penetration. The shock wave separates from the crater surface and decays into an elastic wave. If this elastic compression wave encounters a free surface, it is reflected as a tensile wave although some of the energy of the compression wave may be transmitted into the media beyond the free surface.

As the target thickness is reduced, the tensile wave dissipates less energy before being reflected and the remaining energy becomes sufficient to induce stresses greater than the ultimate strength of the target material. Fractures then occur in the target near this free surface. With further reduction in target thickness, these fractures result in a shrapnel-like detachment of material known as spalling.

With continued reduction of target thickness a condition of threshold penetration will be reached. Here the penetration will start with the vaporization stage and progress through the fluid stage until energy dissipation allows material strength control of the process. Spalling will occur at the rear surface and the final stages of penetration will likely involve some combination of plugging, petaling, and ductile penetration.

Ultimately, thinning of the target will result in a penetration that involves only the vaporization and early fluid stages. When the target is a thin shield, the projectile and target are vaporized and fragmented with the debris being ejected as spray in the shape of diverging cones from both the front and rear of the target. The diverging of the projectile and target materials spreads the projectile energy over a larger area reducing penetration power in subsequent impacts. This phenomenon is employed in the design of meteoroid bumpers where thin shields are used to fragment the projectile and spread the energy over a larger area. Currently, considerable attention is being focused on composite bumpers consisting of a thin shield with an energy absorbing media filling the space between the shield and the final layer.

Accelerators

The problem of simulating primary meteoroid impacts has taxed the capability of existing accelerators. In the attempt to achieve meteoroid velocities, the numerous types of accelerators listed in Table XII have been used. An extensive listing of hypervelocity test laboratories including the type of accelerator available may be found in reference 29. The most successful accelerators to date have been the light gas gun, the exploding foil gun, and the Rhodes and Bloxson high temperature hypersonic hydrogen gun.

The underlying principle of the light gas gun is the acceleration of a projectile by the expansion of a compressed gas reservoir as shown in Figure 104. The piston is accelerated by the explosive charge, compressing the reservoir of driving gas in the pump tube. The model base is restrained with a shear disc while the driving gas is compressed. When the driving gas pressure is sufficient, the shear disc separates and the model base (projectile) is accelerated by the expansion of the driving gas trapped between the piston face and the model base. Three types of light gas guns are currently employed: the free piston, the caught piston, and the accelerated reservoir. In the free piston gun the piston is stopped by the gas pressure in the pump tube. In the caught piston version the piston is stopped by a taper at the end of the pump tube. The accelerated reservoir light gas gun uses a deformable but relatively incompressible piston and an end-tapered pump tube (ref. 25). The face velocity of the deformable piston is increased as it travels into the taper. The piston may actually travel partially into the launch tube, accelerating the gas reservoir with a subsequent increase in projectile velocity. Polyethylene models weighing 0.1 gram with 0.56 cm diameters have been accelerated to 9 km/sec.

In the exploding foil gun a storage capacitor system is discharged through a thin conducting foil placed back to back with a sheet of plastic in a breech barrel arrangement. The plasma generated by the foil explosion shears the plastic disc across the end of the barrel and accelerates it down an evacuated tube. Copper and aluminum discs have been accelerated by letting the plastic sheet act as a buffer between the exploding foil and the metallic discs. These guns are relatively small facilities compared to light gas guns. Particle sizes range from 0.16 cm to 0.32 cm diameter and maximum velocity is about 12 km/sec (refs. 26, 52).

A second type of exploding foil gun uses a capacitor discharge to generate a lithium plasma that flows through a nozzle to an evacuated flight range. The plasma drag accelerates a large number of spherical projectiles which are passed through a series of baffles for collimation. This gun was reported to have accelerated 50 micron particles of boron silicate glass to 18 km/sec (ref. 88).

The high temperature hypersonic hydrogen accelerator uses an electrical arc discharge to heat hydrogen gas to a high temperature and pressure in a closed chamber (refs. 8, 94). The gas is then accelerated through a diverging conical nozzle. Small particles are injected into the flow and drag accelerated as the gas

TABLE XII
HYPERVELOCITY ACCELERATORS

TYPE	PRINCIPLE	VELOCITY (km/sec)	PROJECTILE
A-C Solenoid Gun	Conductive projectile accelerated through coils	1.2	
D-C Rail Gun	Conductive projectile accelerated by current as it shorts two conducting rails	1.2	
Electrostatic Gun	Acceleration of charged particles with high voltage	14	Sub-micron
Light Gas Guns	Projectile accelerated by pressure of driving gas		
A. Adiabatic-Isentropic	Piston compression of driving gas		
1. Free Piston	Piston stopped by gas pressure in pump tube	7.6	0.04 cm
2. Caught Piston	Piston stopped by taper at end of tube (No buffer)	9.5	0.04 cm
3. Accelerated Reservoir	Piston stopped by taper, but partially extrudes into lower tube	9.5	0.04 cm
B. Adiabatic-Nonisentropic	Driving gas compressed by reflections of shock wave		
1. Shock - 2 stage	May use a piston between powder and light gas		
2. Shock - 3 stage	Light gas fires a light gas gun		
3. Explosive	Gas compressed by shaped explosive charge	7.6	
C. Non-Adiabatic	Heat constant volume gas to high temperature and pressure		
1. Arc-Discharge	Electrical energy to heat gas	9.2	Micron
2. Exploding Wire	Electrical energy to heat gas		
3. Steam Heated	O ₂ mixed with H ₂ burns to provide heated propellant gas	6.1	

TABLE XII
(Continued)

D. Combination	Various augmentation devices added to basic guns		
Traveling Charge Gun	Essentially a rocket - Propellant on base of projectile	2.5	
Explosive Devices			
A. Simple			
1. Explosive Charge	Pellet placed on end of charge	6.7	0.1 to 7g
2. Air Cavity Charge	Pellet placed in air cavity at base of charge	6.7	0.1 to 7g
3. Fragment	Self-forging fragment imbedded in end of charge	6.7	0.1 to 7g
B. Shaped-Charge	Shaped charge produces a jet that is elongated in flight, breaking up into discrete particles at pre-determined distance from the explosive charge	8.2	
C. Ballistic-Projection	Accelerates clusters of micron size particles using specially designed lined cavity charges		
	20° cone	10.7	
	0° cone (cylinder)	15	
	(Cluster of particles has a preferred particle size depending on grain size of the original liner material. Explosive actuated cut-off device can stop the heavier slug and residue.)		
D. Exploding Foil	Capacitor discharge explodes foil producing high temperature plasma accelerating plastic disc	9.1 12.2	0.16 - 0.32 cm
Hypersonic Hydrogen Gun	Electrical arc discharge heats hydrogen gas to a high temperature and pressure in closed chamber. Gas is then accelerated through nozzle, drag accelerating injected particles.	30	500 micron

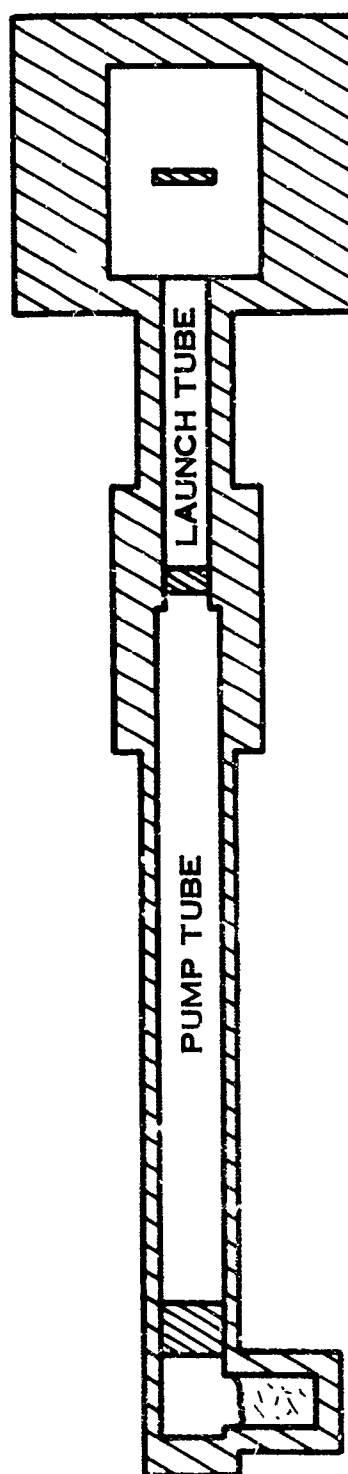
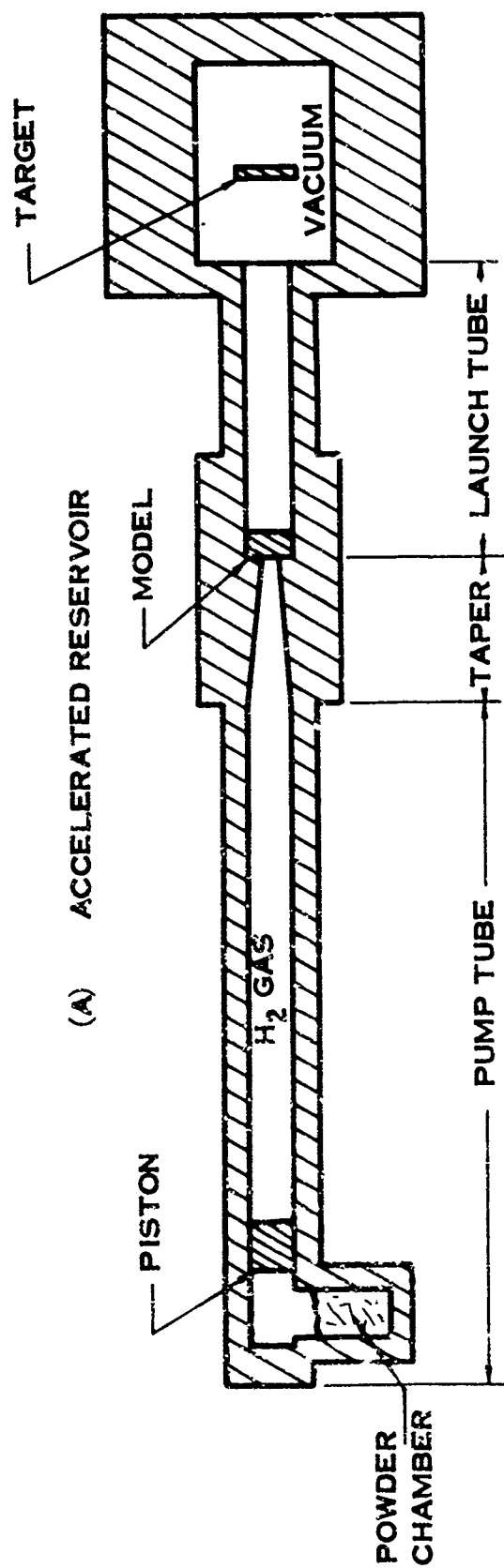


FIGURE 104. LIGHT GAS GUN HYPERVELOCITY ACCELERATORS

expands into a vacuum. Particle density and size are variable over wide ranges. The limit of this accelerator, which has recently become operational, is reported to be 500 micron diameter particles of 0.5 g/cm³ density accelerated to 30 km/sec (98,000 ft/sec).

Criteria And Results

The significant hypervelocity penetration parameters are not clearly defined, even for quasi-infinite homogeneous targets. Numerous investigations of hypervelocity impacts into such targets have resulted in an abundance of penetration formulae (refs. 16, 29, 36, 61, 81, 88, 105). Each empirical formula applies to some small range of velocities and/or specific projectile and target materials. There is very little agreement on significant parameters in these formulas and the list includes projectile dimensions, density, and velocity as well as target density, sonic velocity, strength, and hardness.

The situation degenerates even more when composite targets such as space suit garment materials are involved. Such targets require empirical evaluation of penetrability. With the restrictions imposed by current hypervelocity accelerators, space suits can be evaluated only by impacting targets that duplicate the suit structure. The penetrability of each variation in cross sectional structure of a given suit must be evaluated separately.

Since the meteoroid environment cannot be duplicated in the laboratory, experimenters have been forced to operate under some fairly broad assumptions in evaluating the penetrability of a space suit. Meteoroid flux density and velocity are assumed constant and penetrability is assumed to be energy dependent for particles of "reasonable size and velocity." With these assumptions, the penetrability of current space suits is determined through hypervelocity impact experiments based on a statistical prediction of the flux density of meteoroid energies probable for a given exposure.

For a random distribution of meteoroids in the space environment, penetrations are expected to be discrete, independent events in time. The probability distribution for random events such as penetrations of meteoroids is Poisson in nature (ref. 79). Equation 153 is the Poisson distribution which gives the probability P of exactly X events occurring in the interval of time t.

$$P(X, t) = \frac{(\lambda t)^X}{X!} e^{-\lambda t} \quad (153)$$

The constant λ is the average rate at which the random events occur and λt is the expected number of events in the interval t.

The probability that the number of events in the interval t is equal to or less than some number K is:

$$P(X \leq K, t) = P(0, t) + P(1, t) + \dots + P(K, t) \quad (154)$$

Reliability R is just a special case of the Poisson distribution, namely, the probability of having no events in the interval t .

$$R = P(0, t) = \frac{(\lambda t)^0}{0!} e^{-\lambda t} = e^{-\lambda t} \quad (155)$$

Space suit meteoroid penetrability evaluations are based on the assumptions that meteoroid flux is constant and the penetration depends on particle energy. With these assumptions, the reliability of a suit is evaluated as in the following example of current techniques for verifying space suit reliability in the meteoroid environment*.

Assume that a reliability of $R = 0.9995$ is required for a 0.5 hour exposure in a cislunar environment. Further assume a suit area of 24 square feet and an average meteoroid velocity of 30 km/sec. Then λ , the maximum allowable penetration rate, is found from Equation 155 as follows

$$R = 0.9995 = e^{-\lambda(0.5 \text{ hr})} \quad (156)$$

Taking logs of both sides of Equation 156 gives $\lambda = 10^{-3}$ penetrations per hour. The penetration rate per unit surface area is:

$$\gamma = \lambda \frac{24 \text{ hr}}{\text{day}} \frac{1}{24 \text{ sq ft}} \quad (157)$$

$$\gamma = \lambda 10^{-3} \text{ penetrations/sq ft/day} \quad (158)$$

Referring to Figure 103, we find that the flux density of particles with masses of 3.5×10^{-6} grams or greater is 10^{-3} particles/sq ft/day. Using this mass and the assumed average velocity of 30 km/sec, the threshold penetration energy E_0 is calculated from Equation 159 to be 1.57 joules.

$$E_0 = \frac{1}{2} m v^2 \quad (159)$$

Since penetrability is most closely related to energy, the threshold energy should be reproduced by the accelerator with the smallest projectiles possible. A light gas gun firing 1/64 inch diameter glass pellets (8.5×10^{-5} gram) should achieve velocities of 6 km/sec as calculated from Equation 159.

*Personal communication with P. B. Burbank, NASA-MSC, 1965.

The above calculation was based on some rather questionable assumptions but it illustrates current calculation techniques and also points out the need for better data.

Based on the test technique described, a suit was recently evaluated by impacts of 350 ± 50 micron particles of 0.5 g/cm^3 density, accelerated to velocities as high as 27 km/sec. The realistic velocity, density, and size of these simulated meteoroids provided a good empirical evaluation of the penetrability of the suit. Prior to this evaluation, the best simulated impacts on suits had been with 400 micron particles at about 2.6 g/cm^3 density, accelerated to a maximum velocity of 6.5 km/sec.

The criteria by which the penetration of a space suit structure is judged must be clearly defined. In past space suit penetrability tests, the targets have been monitored by means of witness plates and by visual inspection of the target. There has been some ambiguity in the determination of whether penetration has occurred when the rear of the target was charred but the witness plate indicated no penetration. Obviously, complete physical penetration of a suit will result in loss of pressure integrity and possibly in direct physiological damage to the astronaut. The primary hazard in the oxygen atmosphere of current suits, however, is a lethal flash explosion that will be touched off by the penetration of a hypervelocity particle. In fact, this flash explosion may occur with less than complete penetration due to the local heat liberated by the impact processes. For purposes of space suit evaluation, penetration must by definition include those cases where

1. The rear of the target is discolored or charred, indicating a flash explosion hazard.
2. The target is completely penetrated as evidenced by the witness plate.

Conclusions

The limited knowledge of the meteoroid environment, the lack of understanding of the hypervelocity penetration phenomenon, and the varied space suit constructions all dictate empirical space suit penetration studies. The model meteoroid environment is still somewhat indeterminate and additional information is constantly being compiled; consequently, the model needs revision frequently to include up to date velocity, density, and flux distributions. These criteria are essential in determining reliability and any assumptions made in regard to these distributions should be carefully observed in reliability estimates.

Hypervelocity penetration processes are not clearly understood, particularly for targets of suitlike construction. Consequently, the evaluation of the penetrability of development suits should be on a comparative basis. This comparison can probably be best performed by fixing the particle size and density and varying velocity to obtain threshold penetration. Based on current knowledge of the

meteoroid environment, particles of 0.5 g/cm^3 and 3.5 g/cm^3 densities would be appropriate. Particle size will usually be defined by the accelerator but can be selected by the method explained in the previous example. The tests should include the low velocity impacts (velocities below that at which the projectile fragments) as the penetration process is quite different from hypervelocity penetration. The evaluation should include impacts on targets composed of each variation in the suit cross sectional structure such as boots, gloves, joints, torso, helmet, closures, visors, etc. The targets should be pressurized with the normal ventilation gas to the operating suit differential pressure. The impacts should be monitored by a high response flash detector to indicate ignition of the gas, a witness plate, and visual inspection of the target. Penetration should be as defined on page 251.

Theoretical prediction of suit reliability depends on an accurate definition of the meteoroid velocity, density, and flux distributions as well as a definition of the hypervelocity penetration processes. Consequently, studies of the meteoroid environment should be continued and studies of hypervelocity penetration processes should be expanded to include impacts of typical suit cross sections. Until such data are available, current reliability estimates should be used with caution.

SPACE RADIATION ENVIRONMENT

The space environment can present a serious radiation hazard to both man and materials. The degree to which the space suit can protect the man from this environment depends largely on the actual construction of the suit. Since the radiobiological effect of the radiation environment is a problem of considerable scope and has received a great deal of attention elsewhere, in this study the radiation hazard has been restricted to an analysis of its effect on space suit materials. Current simulation techniques are quite limited and evaluation of the hazard is restricted to material studies. Although simulation techniques are restricted to materials irradiation, the biological dose that would be received through a particular suit can be predicted by monitoring the intensity of simulated radiation through samples of the various sections of the suit wall.

Description Of Environment

The space radiation environment consists of both particle radiation (ions and electrons) and electromagnetic (photon) radiation. There are three primary sources of particle radiation, geomagnetically trapped radiation belts, cosmic rays, and solar flare protons and one primary source of electromagnetic radiation, the sun. The electromagnetic radiation has a substantial thermal influence on the suit system and was therefore treated in the thermal environment section. However, it is the influence of the radiation on the suit materials that is discussed in this section.

GEOMAGNETICALLY TRAPPED RADIATION

The geomagnetically trapped radiation known as the Van Allen belt consists of a doughnut shaped radiation region encircling the earth at the equator. This region starts at altitudes between 400 and 1200 km (250 and 750 miles), depending on longitude. The outer edge varies between 40,000 and 72,000 km (25,000 and 45,000 miles), depending upon solar activity. The maximum flux density of protons of energy greater than 40 mev is about 30,000 protons/cm²/sec occurring at about 3900 km altitude (ref. 45). The maximum electron flux depends on the energy range considered. The peak flux of electrons having energy greater than 20 kev occurs at the equator at altitudes between 16,000 km and 22,500 km (ref. 54). An estimate of the electron and proton flux densities as a function of equatorial altitude is shown in Figure 105.

COSMIC RADIATION

Cosmic rays are high velocity atomic nuclei stripped of their electrons, originating from outside the solar system or from the sun during large solar flares. The omnidirectional intragalactic rays are very high energy particles of which about 80% are protons, 15% are alpha particles, and the remainder are nuclei of higher atomic numbers. The average particle energy is about 4×10^3 mev/nucleon. The peak intensity near the earth's orbit of the rays from solar flares is higher than the intensity of the primary rays, but the energy is lower (ref. 98).

SOLAR FLARES

Some investigators believe there is a steady solar output of protons (frequently called "solar wind") with a flux density less than 10^9 proton/cm²/sec, and energies less than 3 kev. The proton flux density and energy increases by many orders of magnitude during solar flares. The protons are accompanied by energetic electrons and electromagnetic radiation including solar X-rays. Radiation damage from the electrons and X-rays, however, is considered secondary to that from the protons. These flares occur at the rate of about one per month during the peak of the 11 year solar period and about one or two per year during the solar minimum. Proton flux near the earth is typically 10^4 proton/cm²/sec for energies above 20 mev, 10^2 proton/cm²/sec above 100 mev and 1 proton/cm²/sec above 500 mev. Record flares have had fluxes 10 times as great (ref. 54). The proton flux accompanying a solar storm usually lasts about a day.

OTHER SOURCES OF PARTICLE RADIATION

The high altitude nuclear explosions of the U. S. and U. S. S. R. have increased the depth of geomagnetically trapped radiation by adding a new shell of

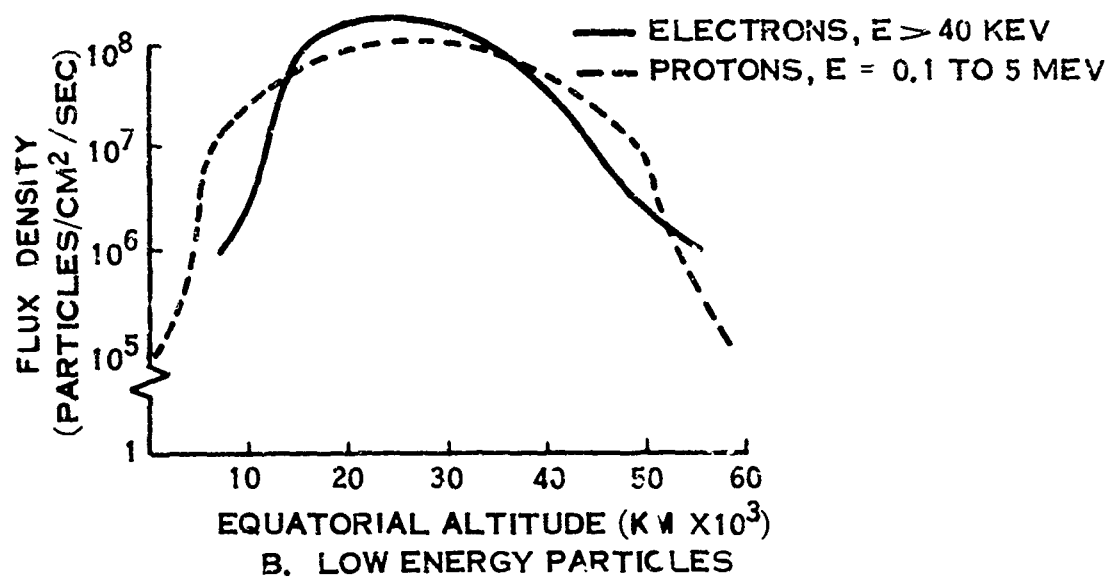
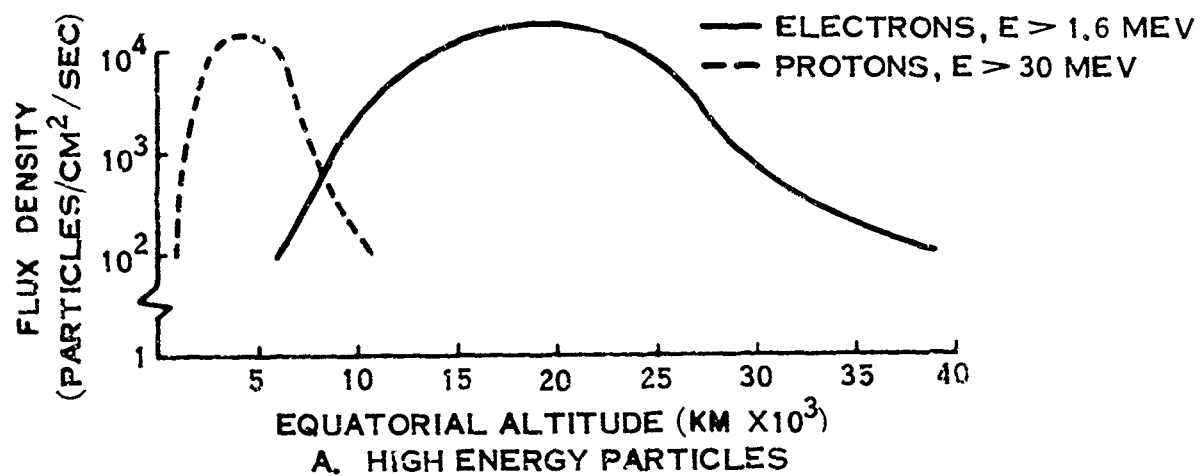


FIGURE 105. ELECTRON AND PROTON FLUX DENSITIES VERSUS EQUATORIAL ALTITUDE (REFERENCE 45)

trapped electrons and by intensifying the regions between former belts. Nuclear reactor powerplants aboard spacecraft are another possible source of man made radiation in space. However, for purposes of this study, these reactors are considered to be adequately shielded and to present no problem to the space suit or occupant.

Neutrons in space are not considered a significant radiation hazard because of their low flux density. Auroral fluxes resemble polar caps and have electron flux densities as high as 10^{11} electrons/cm²/sec during auroral storms. Due to the spatial distribution and the relatively low energy of the electrons (less than 50 kev), this radiation is significant only in polar orbits.

SOURCES OF ELECTROMAGNETIC RADIATION

The primary source of electromagnetic radiation is the sun. The bremsstrahlung process (X-rays produced by interaction of fast electrons with matter) also is a source of electromagnetic radiation. Of primary engineering interest for materials evaluation are the shorter wavelengths of the sun's electromagnetic spectrum since the energy of a photon is inversely proportional to its wavelength. The Duane-Hunt relation, Equation 160, relates the energy E in electron volts to the wavelength in Angstrom units.

$$\lambda = \frac{1.24 \times 10^4 \text{ \AA ev}}{E} \quad (160)$$

The threshold energy for ionization is around 20 ev (ref. 54), which corresponds to a wavelength of about 600 Å. Hence, sunlight with wavelengths less than 500 Å to 1000 Å would be ionizing radiation. Although other planetary bodies will contribute electromagnetic radiation, this radiation will be at the longer wavelengths and hence not of primary interest as a materials problem.

Effect Of Radiation On The Suit

SPUTTERING

Sputtering occurs when atoms or ions with energy from 10 ev to about 1 mev knock atoms off a surface. Although the particle radiation flux density that will be encountered by an object in space is uncertain, order of magnitude estimates of the sputtering damage have been made for exposure to the various sources of particle radiation. These estimates indicate that the effects of sputtering due to collisions with atoms of the upper atmosphere, protons and heavier ions in the radiation belts, solar flare protons, steady solar proton emission, and cosmic rays would be negligible.

EFFECT OF PENETRATING PARTICLE RADIATION

Protons and electrons of sufficient energy will penetrate a material causing internal damage. For a given particle energy, an electron will penetrate deeper than a proton. Fast electrons can produce photons during penetration by bremsstrahlung. Their range in matter is much greater than the electron range and they may also cause radiation damage.

Radiation damage occurs primarily through ionization and atomic displacement. Ionization is the primary damage resulting from interaction of electrons, protons, and photons with inorganic insulators and organic materials. Included in this class of material are the plastics and elastomers employed in current space suits. Atomic displacement, the dislocation of atoms from their normal lattice position, is the primary radiation damage in metals and some inorganic insulators such as glasses and ceramics.

Estimates of radiation damage for materials exposed to the various radiation sources in space have been made on the basis of what is known about the environment (ref. 54). Exposed surfaces of most materials would undergo major changes in engineering properties such as surface fatigue strength and emissivity within a year in the peak intensity locations of the Van Allen radiation region. Polymers and optical materials would probably be quite sensitive to this radiation. The optical transmission of some glasses and sensitive polymers may be damaged by the solar protons, especially in large solar flares. The other space particle radiations are not expected to cause severe damage, but may result in some alteration of surface characteristics. Consequently, it appears that the most serious particle radiation damage to space suits would result from the solar flares or from sustained exposure to the radiation of the Van Allen region. For this reason current missions require that man be within the space vehicle during passage through the Van Allen regions and during solar flares. Many uncertainties in the definition of the radiation environment remain to be clarified as well as the uncertainties in the manner in which these radiations effect the space suit materials.

EFFECT OF ELECTROMAGNETIC RADIATION

Metals and alloys are unaffected by ionization but atomic displacement can be caused by radiation at wavelengths below 0.1 \AA . However, electromagnetic radiation in this range amounts to only 10^2 to $10^3 \text{ erg/cm}^2/\text{yr}$ which is insufficient to alter the engineering properties of these materials. Hence, solar photons will not be detrimental to metals and alloys. Ionization in the inorganic insulating materials is more important. Sunlight at wavelengths below 500 \AA to 1000 \AA provides an ionization dose that is sufficient to increase optical absorption. The electronic excitation (electrons raised to higher energy states) caused by wavelengths up to 3000 \AA results in color centers (electrons trapped out of their normal equilibrium lattice position) which usually absorb light in the visible or ultraviolet region. This results in a general darkening of the material, a serious problem on temperature control surfaces.

Organic materials are especially subject to changes in reflectivity, absorptivity, and transmissivity due to sunlight of the 100 Å to 1000 Å wavelengths. Two general types of chemical change occur in polymers subjected to ultraviolet radiation in air: decomposition of polymer chains into smaller fragments and crosslinking of the chains. Fragmentation causes structural weakening and embrittlement, but it is severely retarded in vacuum. Crosslinking, however, is not retarded and also results in embrittlement and structural weakening. In the limited experiments performed in vacuum, unvulcanized natural rubber irradiated with wavelengths of 1000 Å to 3000 Å underwent considerable crosslinking when exposed to the equivalent of only a few days of sunlight. Polyethylene, mylar, and other polymers were discolored, mechanically weakened, and embrittled. These mechanical effects at 1000 Å to 3000 Å are not as pronounced as in air, but are still significant changes in material properties (ref. 54). The effect of exposure to radiation from 100 Å to 1000 Å is not known.

Simulation Techniques

PARTICLE RADIATION SIMULATION

Due to the interaction of various aspects of the environment, particle irradiation should be performed under a combined environment. This environment should include high vacuum, black body heat sinks, and temperature control of the test specimen. In addition, the radiation simulator should provide a uniform flux density with the specimen shielded from secondary radiation. Accelerated testing at increased flux density should be avoided until the effects of flux density have been determined for the specific material under test.

Cyclotrons and other high energy accelerators have been used to irradiate materials but they work in the 10^{12} particle/cm²/sec range for heavy particles and in the 10^{15} particle/cm²/sec range for electrons, which are very flux densities for simulation testing. Present DC accelerators permit proton and electron flux simulation more economically at realistic flux densities for energies under 4 mev, while nuclear reactions can be used to provide useful proton and electron fluxes in the 14 mev region (ref. 78).

ELECTROMAGNETIC RADIATION SIMULATION

The simulation of the ultraviolet wavelengths (below 3000 Å) is a formidable task further complicated by the fact that the distribution of energy in this portion of the solar spectrum is not well defined. The evaluation of the effect on polymers at wavelengths below 1000 Å, an area of prime interest, is particularly difficult because all solids are opaque at wavelengths below 1000 Å (ref. 54), hence the radiation source cannot be external to the wall of a test fixture. Again, the irradiation of candidate suit materials should be performed in a combined environment

that includes vacuum, black body heat sink, and thermal control of the test specimen. Some fixturing to permit high speed flexing of the test specimen during irradiation is desirable for the evaluation of embrittlement.

A suggested laboratory approach to circumvent the opaqueness of all solids for the shorter wavelengths involves testing the material specimen in what is essentially an X-ray tube (ref. 54). A suggested alternative is to use electron irradiation to produce ionization equivalent to that of the solar photons. It is clear, however, that state-of-the-art simulators cannot provide a simultaneous simulation of the entire electromagnetic radiation spectrum. The effects of the space radiation on the material must be extracted from integrated doses in each applicable portion of the spectrum using simulators of several types. One recent test of a candidate space suit material employed a water cooled, high pressure mercury argon lamp as the ultraviolet source (ref. 56). The source was located inside a small vacuum chamber which provided a combined vacuum-radiation environment for the materials testing. This lamp approximated the spectrum from 2200 Å to 4000 Å.

Conclusions

In summary, the effects of the space nuclear radiation environment on space suit materials can be significant. There are major uncertainties both in the flux and energy spectra of the radiation and in the effects of the radiation on candidate materials. Simulation of the environment is difficult and is currently limited to materials studies over restricted regions of the energy spectra. Although there is an abundance of literature available on the effect of material irradiation, most of this work was done in conjunction with nuclear reactor studies. Limited radiation damage studies have been performed on candidate suit materials, however, considerable work is planned (refs. 17, 56).

Also underway is work to define more accurately the flux, energy spectra, and time variation of the space radiation environment. This work should continue. Even with the uncertainties in the radiation environment and the limitations of current simulators, gross estimates can and should be made of the radiation damage to space suits. Specifically, each candidate material should be evaluated for both particle and electromagnetic irradiation and these materials should be evaluated in combination to investigate the interaction due to the various layers of the composite structure of a space suit. The simulation must be performed in a combined environment which includes vacuum and thermal simulation and pressurization with oxygen to include the ozone effect.

SUMMARY OF EXTRAVEHICULAR ENVIRONMENTAL HAZARDS

In this section the vacuum, thermal, meteoroid, and radiation environments have been discussed in separate subsections. In each case the environment was

described, the effects on the suit enumerated, and techniques for simulation of the environment were discussed. The simulation requirements are essentially distinct and thus require separate tests for different aspects of the environment.

METHODOLOGY FOR THE EVALUATION OF SUIT COMPONENTSINTRODUCTION

Thus far, this report has been directed toward the development of a test methodology for evaluating the functional performance, life support, and protective characteristics of a space suit as a complete assembly. However, there are many evaluation requirements that are pertinent only to components of a space suit assembly such as the pressure garment, helmet, boots, and gloves. For the sake of clarity, discussions of these component evaluation procedures have purposely been omitted from the previous sections. Although these procedures in many cases are simple, they are by no means trivial and their evaluation is an important part of the overall evaluation of any space suit. It is to the methodology for evaluating the properties of these components that this section is directed. Naturally, some aspects of each specific suit design will require specialized evaluation and it is beyond the scope of this study to include all these possibilities. Included, instead, are certain fundamental evaluation requirements that are common to nearly all designs. Tests for the pressure garment are presented first followed by tests for the helmet, boots, and gloves.

PRESSURE GARMENT

The primary function of the pressure garment assembly is to provide protection from the ultra-low pressures of space. The vital nature of this function places severe requirements on the quality and reliability of the pressure garment assembly to insure structural integrity when subjected to the tensile stresses imposed by the pressure differential across the garment and the forces exerted against the garment by the occupant. Numerous strength tests such as tensile strength, abrasion resistance, and grab tear can be conducted on the basic materials, and it is assumed that these tests have been performed prior to the selection of the garment materials. However, the evaluation of the structural integrity of the completed garment must be determined statistically due to the uncertainties in the interaction of the layers in the multilayered garment, the many modes of material failure, and the interaction of the garment with the occupant. Unfortunately, no data are available from which a reliability figure for the pressure garment can be estimated and until such data are available, a valid reliability model cannot be developed.

In this section, pressure garment properties such as fatigue life, burst pressure, incremental inflation, coolant flow distribution, thermal conductivity, and leakage rate may be evaluated.

A fatigue failure is a crack or separation in a substance due to repeated application of stress in a direction normal to the failure. The exact mechanism of fatigue is unknown although much is known about factors that affect it. The fatigue life of a material is normally defined in terms of the number of stress cycles that the material will withstand before failure.

Generally, the material in a piece of operational hardware is subjected to a cyclic stress load superimposed on a fixed stress load. With a homogeneous material such as a metal under atmospheric conditions, the number of stress cycles which will cause fatigue of the metal is fairly predictable for a given metal, heat treatment, surface conditions, cyclic stress amplitude, and steady stress amplitude. This fatigue life can be predicted on the basis of the stress load from a family of curves constructed from experimental fatigue tests of the metal.

By applying a steady stress level to several identical metal specimens and then cycling at a fixed stress amplitude, the fatigue life of the metal can be demonstrated. By taking several sets of identical samples and subjecting the samples to different steady stress and cyclic stress amplitudes, a family of curves can be constructed which relates the fatigue life to both steady stress amplitude and cyclic stress amplitude for a particular metal.

The primary sources of stress in the pressure garment are the inflation pressure and the joint flexure. Since these stresses act along different axes, both sources must be considered when evaluating the fatigue life of a suit. The fatigue life of a fabric cannot readily be determined by the method used to evaluate the homogeneous materials, however. There are many modes of failure in the multi-layered structure of a space suit such as fiber tensile failure, fiber shear, shear of rubber sealer, shear of sealer-fabric interface, and abrasive effect of relative motion between layers. Therefore, it appears that a more meaningful approach to the evaluation of the fatigue life of the pressure garment would be a determination of fatigue life as a function of cyclic load for built up components of the garment such as a complete joint. The validity of this approach depends on the interaction of the components being negligible.

Although the evaluation of the fatigue life of the pressure garment could probably be best performed on the garment as a whole, it is shown in Appendix IX that the required test duration is unacceptable. In the face of pressing space program schedules, determination of fatigue life will probably have to be accomplished as a combination of unmanned component tests and manned suit tests. It is expected that a correlation can be established between fatigue life predictions from tests of components and those from tests of the garment as a whole, although it is emphasized that no such correlation presently exists. From the component testing it is expected that a relationship between the life and the subjected load could be established which would resemble Figure 106. This information could

then be compared to fatigue failures experienced during manned testing with development and training suits to predict the fatigue life of the pressure garment.

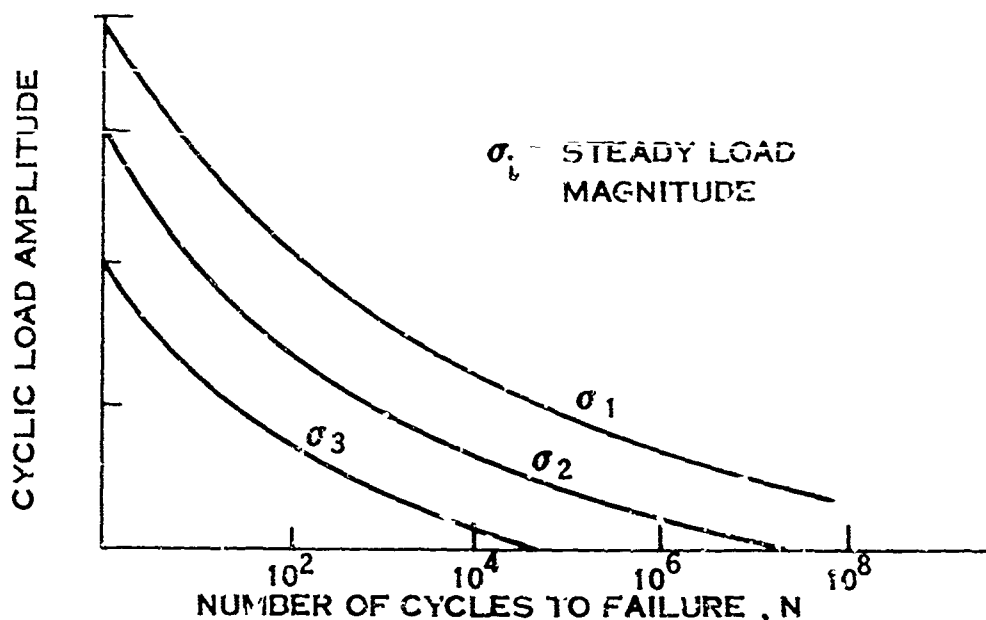


FIGURE 106. FATIGUE LIFE AS A FUNCTION OF LOAD

To evaluate the flexure induced fatigue, the joints should be subjected to the normal differential pressure during the cycling since this would induce more severe stresses than vent pressure would. A possible form for a cycling fixture is shown in Figure 107. Several of these fixtures could be ganged and driven by one source to accumulate the desired statistical data. The statistical data could then be used for reliability calculations as discussed in Appendix IX.

In a similar manner, the pressure induced fatigue of the pressure garment could be evaluated by pressure cycling either the components or the entire garment. A dry, oil-free air supply would be required. Again a family of curves relating the cyclic load amplitude to the number of cycles to failure could be constructed at various pressure levels.

It has been found that many materials are adversely affected by environmental conditions of space and furthermore that these effects cannot be extrapolated from the current knowledge of atmospheric properties and behavior. For example, ozone, which reacts severely with materials such as rubber compounds, is formed by the action of ultraviolet light and other space radiations on O_2 . The effect of ozone on rubber compounds is to form surface cracks normal to the direction of stress in the material. These surface cracks may alter the fatigue life of the material appreciably. Leakage through a pressure garment would make oxygen concentration on the garment surface possible. Since both the ultraviolet content of the solar radiation and the intensity of space radiation are greater in space, the fatigue life of a pressure garment may be shortened appreciably by the resulting ozone concentration. The effects of other space environmental conditions on the

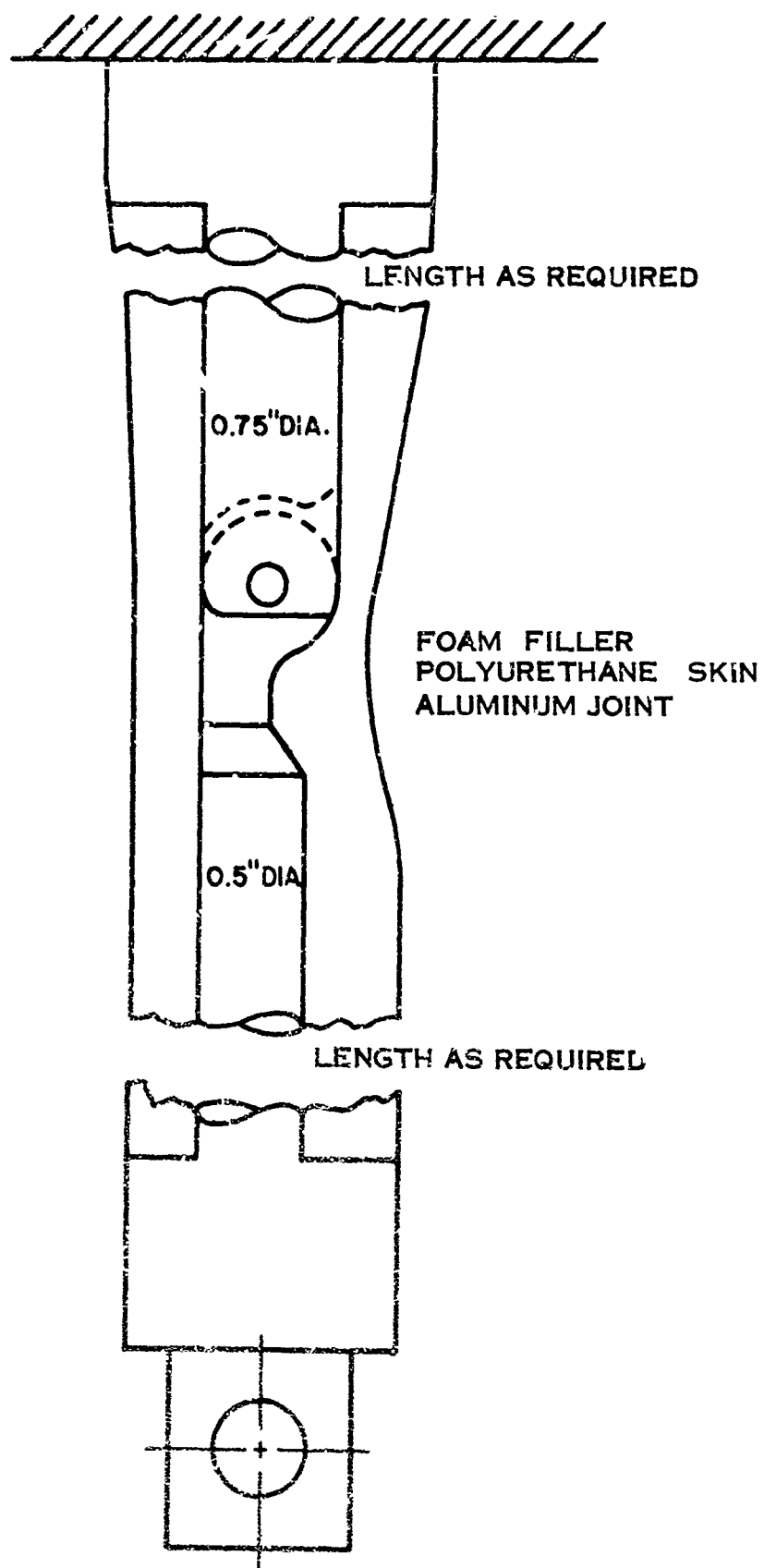


FIGURE 107. ELBOW OR KNEE JOINT CYCLING FIXTURE

suit materials are discussed in Section V. Since interaction of the space conditions on the garment materials may be severe, the fatigue testing of the garment must be conducted in an environment in which the radiation, vacuum, and thermal properties of space are simulated.

Again it is emphasized that no correlation has yet been established between fatigue life as based on component testing and that based on testing of the garment as a whole. However, the economic and technical test advantages realized through component testing make this approach desirable if the correlation can be established.

Burst Pressure

To insure the structural integrity of a pressure garment when subjected to the tensile stresses induced by the pressure differential across it, a considerable margin of safety must be allowed in the garment design. The design burst pressure of the garment, therefore, is usually much higher than the normal operating pressure. Normally, the integrity of each pressure garment is assured by testing to an intermediate proof pressure to avoid destruction of the garment. However, to be assured that the integrity of the garment is not marginal at the proof pressure and that the burst pressure meets the minimum design specifications, the burst pressure test should be performed once on each pressure garment design. In effect the burst pressure test is the same as that for proof pressure: the pressure is increased slowly to the specified level and the suit is inspected for failure.

Since the tensile stresses induced in the garment depend on the differential pressure, this test can be performed under room ambient conditions. A dry, oil free air supply with a closely controlled pressure regulator will be required to pressurize the garment. Depending on the physical construction of the test garment, a shield may be required for the safety of test personnel. In performing the test, the pressure should be increased slowly to avoid any pressure gradients in the garment. Furthermore, once the test has started, pressure should be increased continuously (no pressure cycling is permissible).

The only measurement required is that of garment pressure. Due to the non-repeatability of the test, the garment pressure should be measured at the garment with a continuous electrical output pressure transducer and recorded on a continuous recorder such as an oscillograph, a pen type recorder, or the tape in the data acquisition system. The response time of the transducer-recorder system is not critical provided this response is considered in determining the rate at which pressure is increased in the garment. With the high response systems normally available, the rate of pressure change would probably be restricted by the requirement for no internal pressure gradients in the garment rather than the measurement system response.

Incremental Inflation

To provide the required mobility, current pressure garments have some elasticity which allows growth or incremental inflation when the garment is pressurized. The primary consequences of this incremental inflation are reduction in mobility and increase in overall size. Since the effects on mobility and techniques for evaluating these effects without measuring the actual growth are discussed in Section III, the discussion of incremental inflation is restricted here to anthropometric dimensions of the astronaut and the physical dimensions of spacecraft such as seats, hatches, and control panels. Since the tensile stresses and hence the growth depend only on the differential pressure across the garment, the measurements can be made under room ambient conditions. Adequate basic incremental inflation measurements are currently made on full pressure suits at AMRL. The measurements include the following

1. Axillary chest circumference
2. Waist circumference
3. Axillary arm circumference
4. Forearm circumference
5. Thigh circumference
6. Calf circumference
7. Shoulder breadth
8. Elbow - elbow breadth
9. Hip breadth
10. Posterior body plane - anterior knee area
11. Thigh clearance from floor

The measurements are made at the same locations on (1) the nude subject and (2) the suited subject with the measurements repeated at various suit pressure levels. Of course, measurement of local incremental inflation could also be made at any location where the growth appears excessive on a particular suit or where the measurement is of interest for design purposes.

The measurements are currently made with calipers and measuring tapes. Although schemes have been proposed in which the calipers and tapes would be modified to provide electrical outputs, the current techniques appear adequate.

Cable Tension

Cable restraints may be employed in a pressure garment design to suppress incremental inflation, to control the location of joints, and to restrict helmet rise. Since the life of these cables depends on their tensile load, measurement of the load is desirable. A device which will measure the cable tension is shown in Figure 108. As shown, the device consists of a frame which provides two reference points a known distance apart. A movable hook which slides in the frame deflects the cable a fixed distance as determined by a limit switch and indicated by a light. The indicator measures the deflection of the spring and thus the force on the cable. The force is nearly proportional to cable tension as determined by calibration with dead weights on the cable.

The cable tensiometer could be used to measure the cable loads of a particular garment design under operating conditions. With this information, the same type cables with their appropriate cable guides could be load cycled with identical loads until they failed. From these results, the life of the cables in the garments could be predicted. Measurement of cable tension is also useful when making adjustments on development suits, particularly when redundant cables are used.

Coolant Flow Distribution

Current pressure garment assemblies provide either liquid or gas type coolants to remove the metabolic and leakage heat loads. Techniques by which the coolant flow distribution can be studied are basically the same for either type coolant. In both cases, the required tests can be conducted under room ambient conditions.

The liquid cooled garment distributes the coolant flow through a network of small flexible tubing. To measure the flow in any portion of the garment, the unmanned garment is connected to the coolant supply and the normal operating pressures and weight flow are established. One tube is clamped off and the coolant inlet pressure and pressure drop are adjusted to the previous values. The change in weight flow is the normal flow through the clamped off tube.

Pressure garments employing gas coolants depend on the clearance between the man and the garment wall to establish the proper flow path resistance. Evaluation of the gas coolant flow distribution, then, must be performed with a manned garment. The manned garment is connected to the applicable portion of the environmental control system stand as shown in Figure 109. After establishing the normal operating garment inlet pressure, pressure drop, and weight flow, the ventilation duct in the desired portion of the garment, such as one of the limbs, is clamped off. By readjusting the operating pressures to their previous values and determining the change in weight flow, the normal flow in the clamped off portion is found.

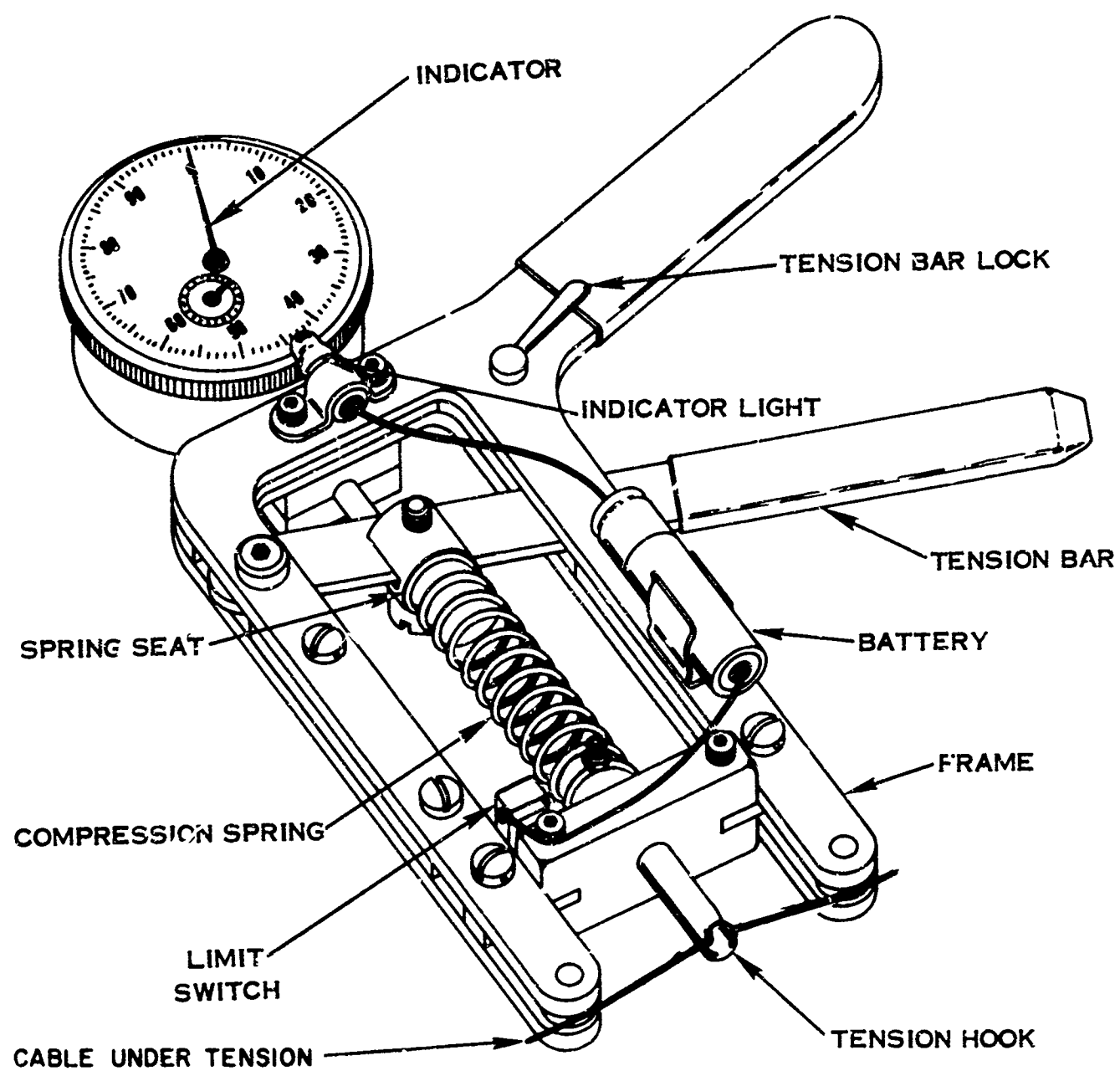


FIGURE 108. CABLE TENSIO METER

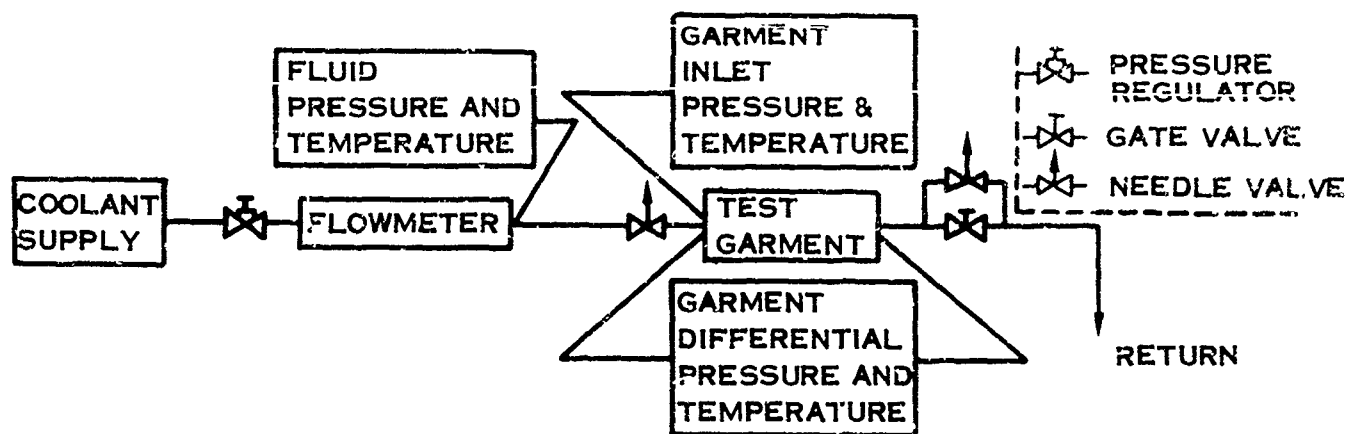


FIGURE 109. COOLANT FLOW DISTRIBUTION TEST SETUP

The coolant flow pressure drop across the garment and the volumetric flow rate represent the power required to sustain that flow. That is

$$\text{Power} = (\text{Volume Flow Rate}) \times (\text{Pressure Drop}) \quad (161)$$

Since this power requirement in turn defines the weight, size, and power requirements of the flow source, measurement of the pressure drop as a function of flow is essential in evaluating a pressure garment assembly. This test series could be performed with the test setup shown in Figure 109 and the results could be plotted to show the power requirements of the flow source as a function of volumetric flow rate. Knowing the flow rate required to remove a given heat load, these curves could be used to compare the power requirements for various suit designs.

For best accuracy, the required pressure measurements should be made with manometers. Since substantial pressure drop is normally encountered in the lines connecting the coolant supply to the garment, inlet and differential pressures should be measured as close to the garment as possible. With current facilities, the location of the pressure ports is required to be within 6 inches or less of the connections to the garment. The required flowmeter is discussed in Section IV.

In connection with studies of the pressure garment ventilation distribution, local measurement of the critical ventilation variables can be of significant value in developing optimized ventilation systems. Local measurement of the micro-climate, that is flow, temperature, and humidity, is needed to design a distribution system that will provide maximum ventilation efficiency. With the normally small body - suit clearance, low stream velocities, and in the presence of extensive sweating, the development of a system for accurate measurement of the micro-climate without altering the climate is a formidable task. However, one such micro-environment analyzer is currently being developed by Parametrics, Inc. for

the Army Natick Laboratories and should be followed closely for possible applications in space suit testing.

Thermal Conductivity

Current thermal garments rely on spacing between the layers of the garment to provide an effective thermal barrier to the extreme temperatures of the space environment. Heat is transferred through the layers primarily by radiation and a thermal barrier is provided by selecting materials with suitable surface radiation characteristics. While performing assigned tasks, however, an astronaut is likely to come into contact with hot or cold surfaces. The spacing between the layers of the thermal garment would be reduced by the contact pressure, altering the effective thermal conductance of the garment appreciably. Due to the suit surface temperature extremes possible in space, the thermal conductivity of a suit pressure garment and/or thermal garment requires evaluation. The thermal conductivity of the pressure garment alone is also of interest in determining allowable temperature limits of the spacecraft structure such as seat arm rests, walls, structural members, etc.

A device which could be used to measure the thermal conductivity of the garments is shown in Figure 110. As shown, the device consists of a counterbalanced fixture which holds a cross sectional sample of the pressure garment and/or thermal garment. The sample is thermally insulated from the fixture. A material of known thermal conductivity, preferably approximating the conductivity of human skin would be bonded to a metal plate containing coiled tubing. This assembly would be placed over the test sample and locked in place. A port would be provided as shown to allow desired pressure on the inside of the test sample. The coiled tubing would provide a means of controlling the surface temperature of the intermediate skin simulating material. The counterbalanced fixture would then be installed in a small vacuum chamber which contains a temperature controlled test plate. This device would allow control of internal and external surface temperatures and pressures as well as contact pressure.

Two temperature sensors (T_1 and T_2) would be installed a known distance apart d_1 in the material simulating the human skin. At equilibrium, the local heat flow through this material would be:

$$q = \frac{k_1}{d_1} (T_1 - T_2) \quad (162)$$

where q = local heat flow, kcal/cm²/hr
 k_1 = thermal conductivity of the material, kcal/cm/°C/hr
 d_1 = distance between temperature sensors, cm
 $T_1 - T_2$ = temperature differential in the material, °C

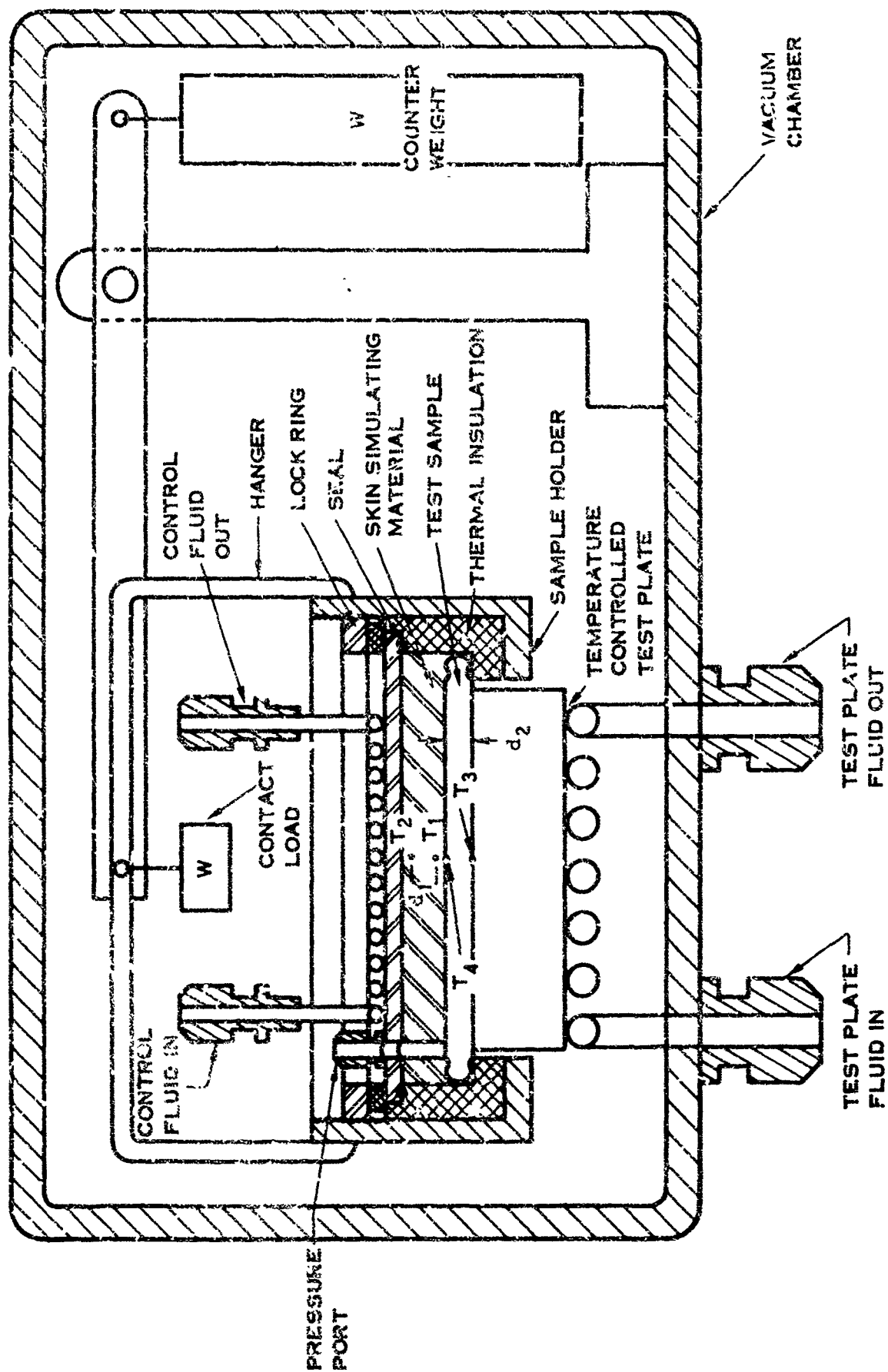


FIGURE 110. GARMENT THERMAL CONDUCTIVITY TEST FIXTURE

Likewise, two temperature sensors (T_3 and T_4) would be installed at the surfaces of the test sample. At equilibrium, then, the effective thermal conductivity of the test sample would be:

$$k_2 = \frac{q d_2}{(T_3 - T_4)} \quad (162)$$

where k_2 = thermal conductivity of the test sample, kcal/cm/°C/hr

q = local heat flow as measured above, kcal/hr

d_2 = thickness of the test sample, cm

$T_3 - T_4$ = temperature differential across the test sample, °C

The chamber pressure and the pressure on the internal wall of the test sample could be varied to simulate either intravehicular or extravehicular operating conditions. Likewise, the test plate temperature could be varied as desired. For a given operating condition, the dependence of thermal conductivity on contact pressure could be determined by varying the weights placed on the sample holding fixture.

Either small thermocouples or bead type thermistors could be used as the temperature sensors, observing the usual safeguard to prevent lead conduction or convection errors. The sensors could be attached to the test sample surfaces by the method described for the internal wall temperature measurement on page 235.

A somewhat similar technique has been employed to measure the effective thermal conductivity of cross sectional samples of early Apollo space suit designs. Although some difficulty was experienced with the test fixturing in these tests, the test technique was satisfactory. The fixture described herein should overcome the difficulties experienced in the earlier tests.

Leakage

Although every effort is made to minimize leakage through the pressure garment, leakage rates are still somewhat formidable. Since weight is at a premium on space missions, the leakage rate of the pressure garment is an important parameter in the evaluation of any space suit. The primary sources of leakage are the garment closures and the component interface seals. The leakage rates are directly dependent on pressure and on the size of leakage openings which vary with the stress on the garment. This stress is a function of both the differential pressure across the garment wall and the exertion of man against the suit. Consequently, leakage rate should be measured as a function of differential pressure, both manned and unmanned. Since the pressure induced stresses depend on the differential pressure across the wall and not on the absolute pressures, this test can be conducted at room ambient conditions.

Leakage rates can be measured by either of two methods with the environmental control system stand discussed in Section VII. For convenience, the applicable portion of the stand is shown in block diagram form in Figure 111. To measure the leakage flow directly, the garment outlet shutoff valve is closed, the reference tank valve opened, and the garment pressurized to the desired pressure. The reference tank valve then is closed to provide a stable reference and the inlet flow adjusted to keep the ΔP indicator nulled. The leakage flow is then read directly from the flowmeter.

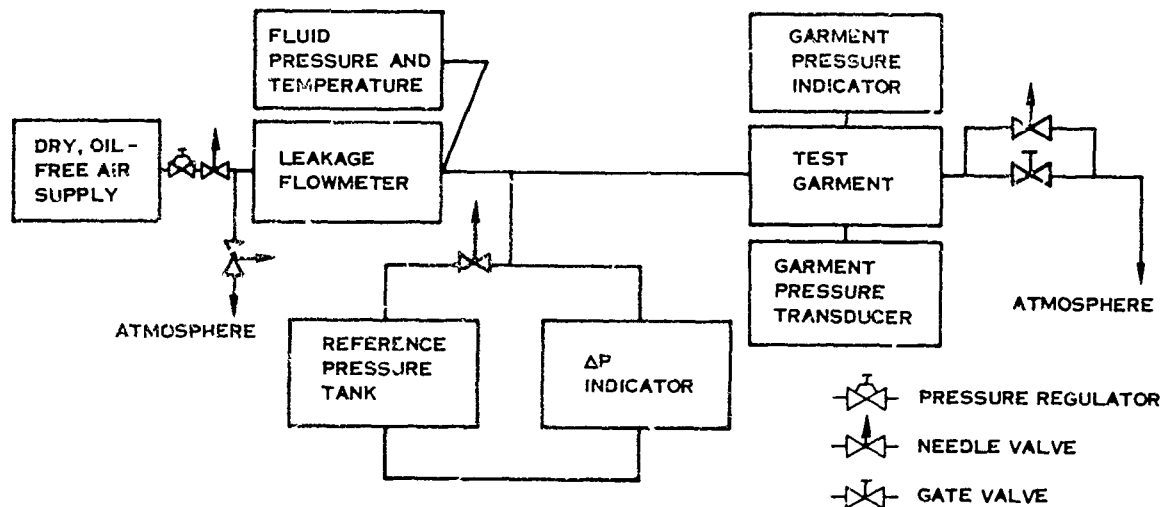


FIGURE 111. LEAKAGE RATE TEST SETUP

Current leakage rates are sufficiently high to permit direct flow measurement. Leakage rates of future suits, however, may be reduced to the point where direct flow measurement cannot be made accurately and the pressure decay method will be required. In the pressure decay method, the garment outlet is again blocked, the reference tank opened, the garment pressurized to the desired pressure, and the inlet shut off. The garment pressure is then recorded as a function of time. The slope of the pressure decay can then be related to the mass flow from either theoretical considerations or by direct calibration.

HELMET, BOOTS, AND GLOVES

Several isolated test techniques for component evaluation are described in the following subsections.

Visor Optics and Defogging

Ideally, the space suit helmet visor should provide man with his normal visual capabilities while simultaneously protecting him from the effects of intense direct and reflected sunlight. The visor design must be evaluated to determine how

well it meets these requirements. Evaluation of the visual degradation caused by a visor requires measurement of the following.

1. Refractive power
2. Prismatic power
3. Luminous transmittance
4. Distortion
5. Field of vision
6. Defogging

Evaluation of the visor protective capability requires these measurements:

1. Luminous transmittance
2. Phototropic response

The first four measurements can be accomplished with standard test techniques which appear entirely adequate when used with care. References to the techniques for measuring refractive power, prismatic power, luminous transmittance, and distortion are given in the general specification for helmet visor optical characteristics, MIL-L-38169 (USAF). There also seems to be no problem in evaluating the field of vision with an apparatus such as the visual field apparatus at AMRL, which has been used successfully with full pressure suits (refs. 11, 95). Although numerous schemes could be devised to "take the man out of the measurement," the present technique provides a direct and meaningful evaluation. Since pressure suits normally experience some degree of helmet rise with pressurization and posture changes, the field-of-vision test should be performed both unpressurized and pressurized, standing and sitting.

Visor fogging causes a reduction in visual acuity. Several techniques have been proposed for objectively evaluating the effectiveness of defogging, such as photoelectrically measuring transmitted or scattered light, however, the technique currently employed by the Biophysics Section at AMRL is more direct and meaningful. In this technique, the reduction in visual acuity of a test subject is measured during tests in which an initially clean visor becomes progressively more fogged in an altitude chamber. The required visual image for the acuity test is projected onto a screen mounted in the chamber window. During space suit testing in a chamber with walls which simulate the heat sink of space, all the windows will probably be required for test monitoring, therefore the present window projection technique may be unacceptable. However, the projection apparatus shown in Figure 112 can be located inside the chamber for the defogging tests. The apparatus is in essence a commercially available zoom lens slide projector which projects the desired

SUBJECT TO PROJECTOR DISTANCE , 3-6 FT

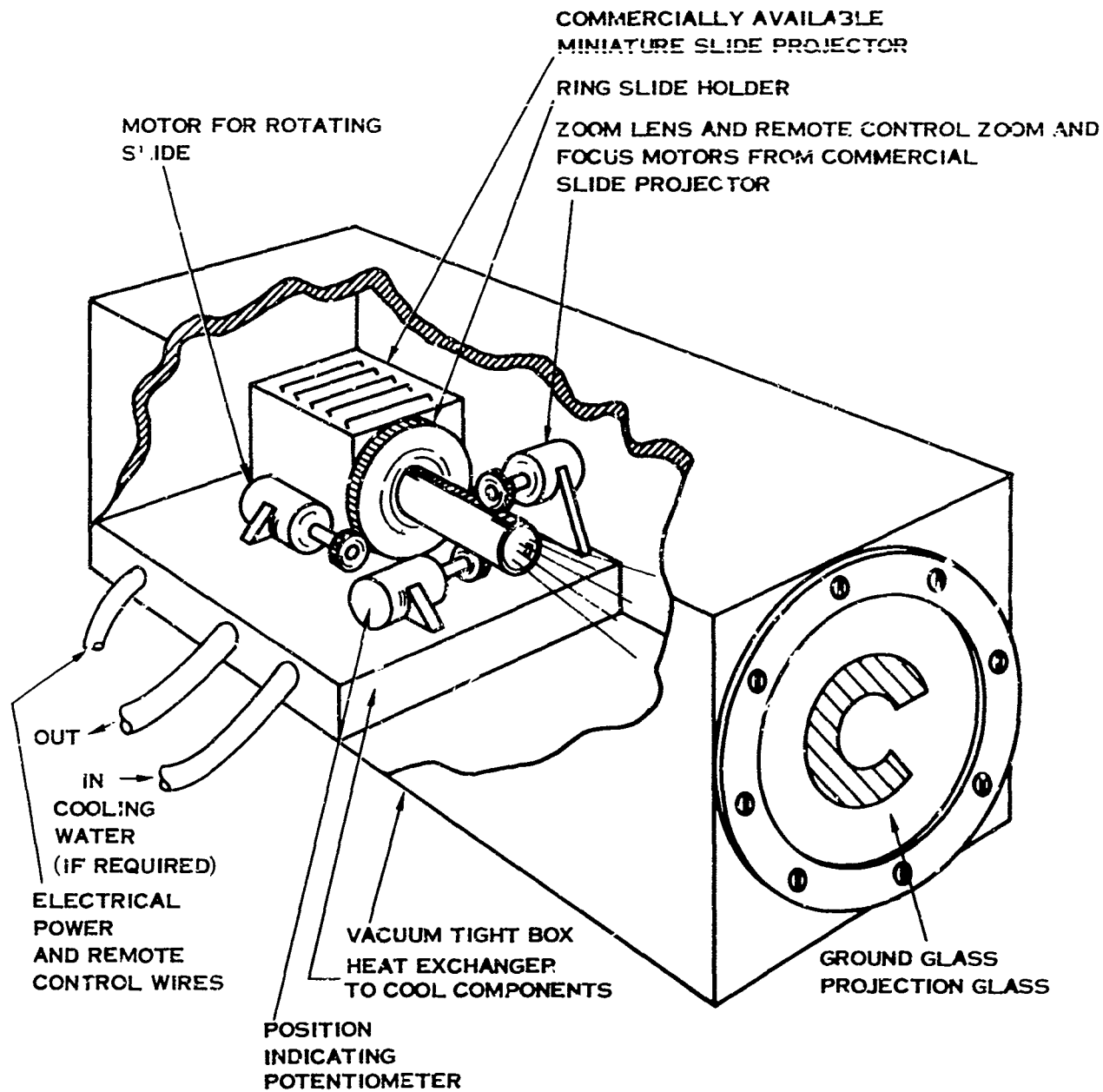


FIGURE 112. REMOTE CONTROLLED VISUAL ACUITY PROJECTOR
FOR HELMET DEFOG TESTING

image on a ground glass end plate in the enclosing vacuum tight box. The projector zoom lens, focus, and rotary drive motors are remotely controlled. Feedback potentiometers on the rotary and lens position drives provide remote indications of the image angular position and size. The projector lamp is ventilated and remotely shuttered, if necessary, to provide cooling.

To protect retinas from radiation damage, visors are treated to decrease transmittance when subjected to high intensity light. This phototropic response can be evaluated with current techniques employing high response photocells and a millisecond shuttered source to provide an adequate measure of the rise time, intensity, and decay time of the transmitted radiation.

Helmet Impact

It seems inevitable that the space suit helmet will eventually be impacted during extravehicular operations. The astronaut may accidentally impact the helmet against the spacecraft, for example, or he may fall while traversing an unfamiliar planetary surface.

An experimental investigation of the ability of space suit helmets to withstand damage by impact loads was performed at Hamilton Standard. For this series of tests, any loss of helmet pressure integrity was considered evidence of helmet damage. This test program employs the impact test fixture shown in Figure 113.

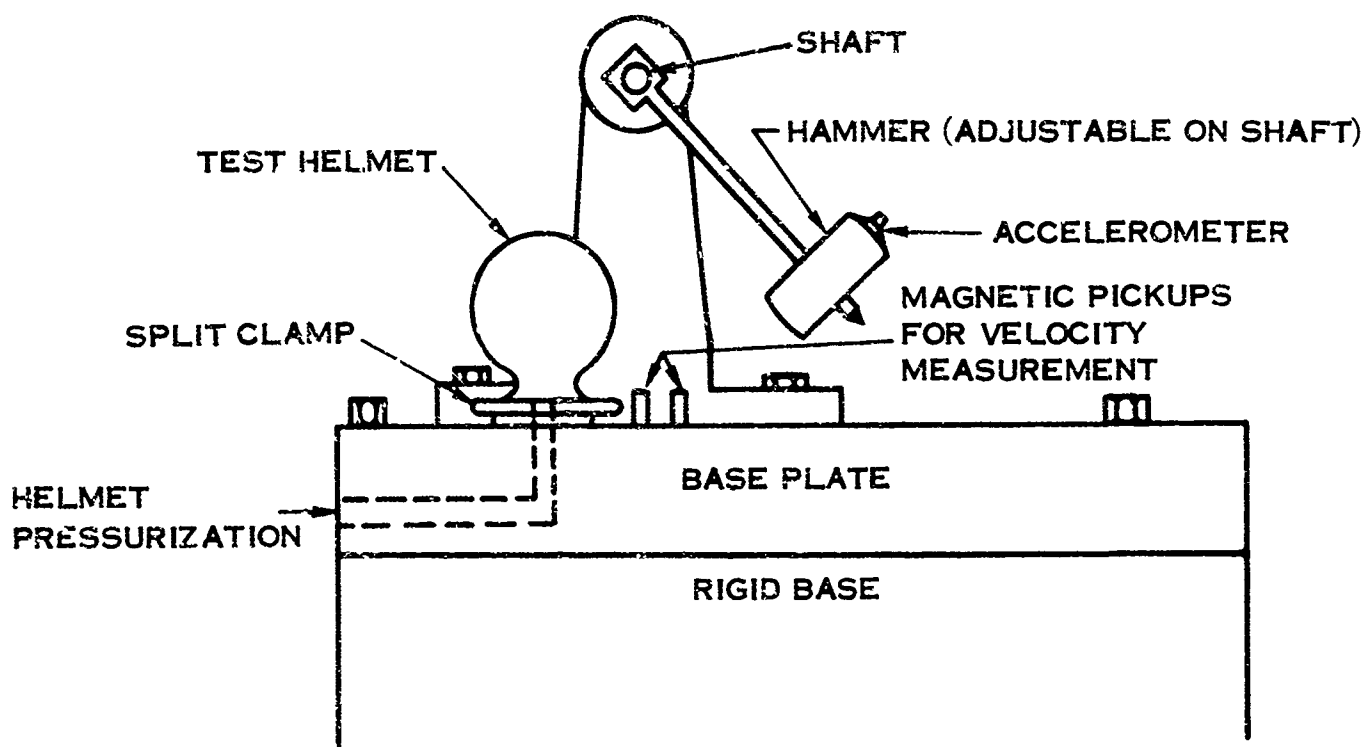


FIGURE 113. HELMET IMPACT TEST FIXTURE

The impact machine consists of a 24 pound hammer mounted on a 2 foot shaft. The hammer can be positioned on the shaft to line up with the desired point of impact and the impacting face plate is removable to provide either a flat or a 2 inch diameter spherical surface. The incident kinetic energy on impact can be varied from 2 to 80 foot pounds. The helmet is secured to a base plate weighing approximately 1600 pounds by means of a split clamp which allows for various orientations of the helmet with respect to the hammer. An adapter plate provides for vertical impacts. The helmet is pressurized by nitrogen gas supplied through the base plate.

The variables measured are the incident and rebound velocities, the helmet and visor strain, the hammer acceleration on impact, the height of the free fall, and the helmet internal pressure. The velocities are measured with the two magnetic pickups pulsed by the passing hammer. The interval between the pulses is accurately subdivided by the time base of the recorder. The acceleration is measured by a commercial crystal accelerometer mounted on the hammer while helmet and visor strains are measured by strain gages which have been applied in the areas which are to be impacted. The height of the free fall is measured statically by the angular displacement. The internal pressure is measured statically by a gage and dynamically by a strain gage type pressure transducer. The measurements are recorded on a continuous type recorder such as an oscillograph.

The energy absorbed in this system is the difference in the incident and rebound energies except for the energy dissipated by the test fixture and the base. Fortunately, these energy losses can be made negligible by proper fixture design and by using a rigid heavy base that will neither deform nor move during the impact process.

Thermal Conductivity Of Boots And Gloves

The boots and gloves, more than any other part of a space suit, are likely to come into contact with other objects during extravehicular activities, such as walking and working with tools. Since the temperatures of objects in the space thermal environment can range between very wide extremes, evaluation of the thermal conductivity of the boots and gloves is an important part of suit evaluation. The lunar surface, for example, can have temperatures ranging from about plus 135°C to minus 150°C (ref. 7). The boots and gloves must have adequate thermal insulation to protect an astronaut from such extreme temperatures while he is performing the assigned tasks.

A device which could be used to measure thermal conductivity of the boots is shown in Figure 114. It consists of a dummy foot on which the boot can be mounted. This assembly is then placed on what is, in essence, a hot (or cold) plate. Since the overall conductivity of the boot depends somewhat on the pressure with which the boot is pressed against the plate, the assembly is counterbalanced and weights can be added to obtain the desired pressure. As shown, the dummy foot contains coiled tubing. By pumping fluids through this tubing at appropriate temperatures

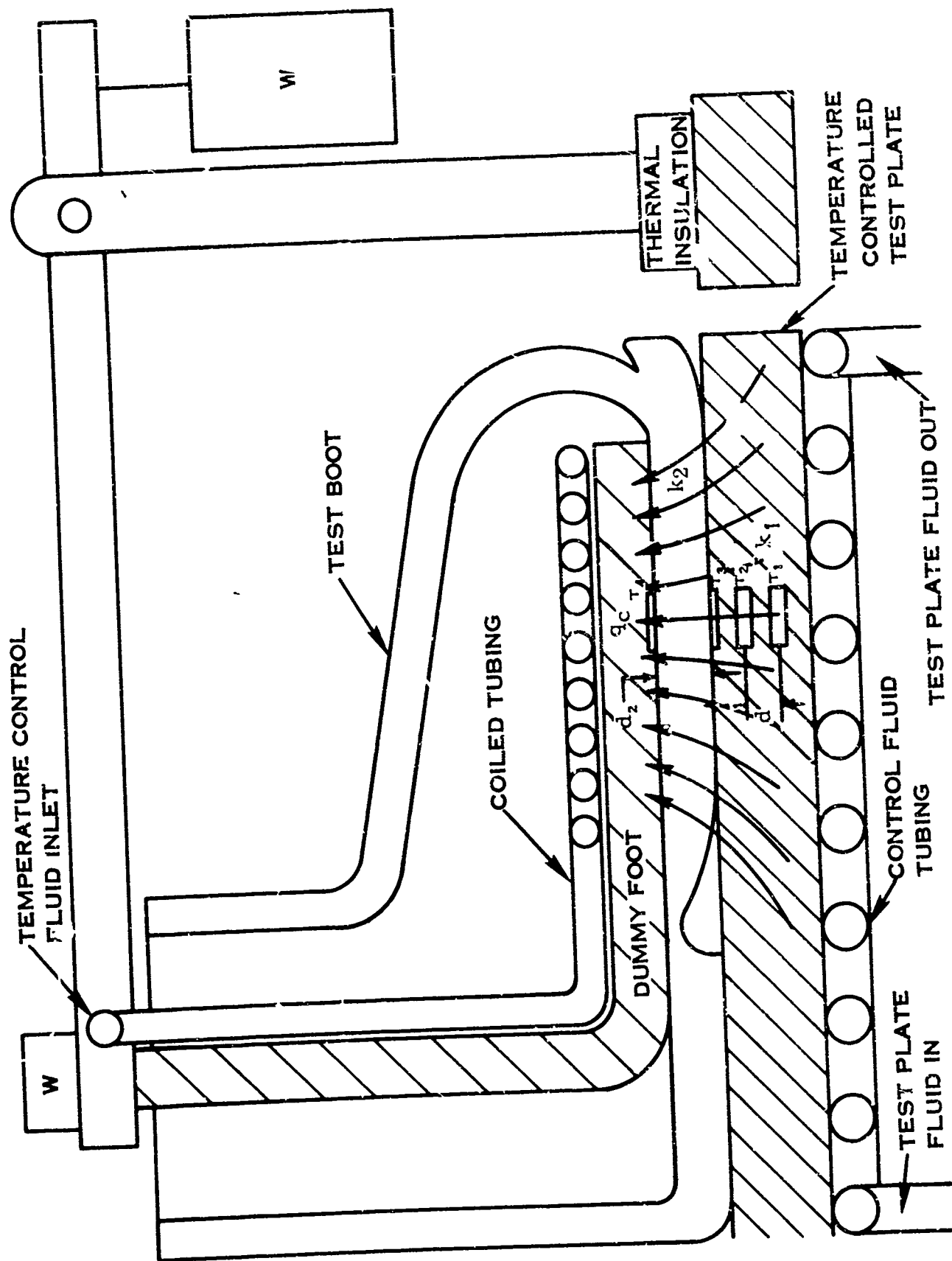


FIGURE 114. BOOT THERMAL CONDUCTIVITY TEST FIXTURE

and flow rates, the internal temperature of the boot sole can be controlled. The combined internal-external temperature control of the boot will permit determination of the boot thermal conductivity as a function of mean temperature.

The temperature controlled plate is constructed of a material whose thermal conductivity is accurately known. By installing two temperature sensors (T_1 and T_2) a known distance apart, the local heat flow through the plate can be determined from Equation 164.

$$q = \frac{k_1}{d_1} (T_1 - T_2) \quad (164)$$

where q = heat flow, kcal/cm²/hr
 k_1 = thermal conductivity of the plate, kcal/cm/°C/hr
 d_1 = distance between temperature sensors, cm
 $T_1 - T_2$ = temperature differential in the plate, °C

At equilibrium, the local heat flow through the boot is the same as the local heat flow through the plate. Thus, if two temperature sensors (T_3 and T_4) are installed on the surfaces of the plate and the dummy boot, the heat flow through the boot is given by Equation 165.

$$q = \frac{k_2}{d_2} (T_3 - T_4) \quad (165)$$

where k_2 = thermal conductivity of the boot, kcal/cm/°C/hr
 d_2 = thickness of boot, cm
 $T_3 - T_4$ = temperature differential across the boot, °C

Then the conductance per unit area can be calculated from Equation 166.

$$\frac{k_2}{d_2} = \frac{T_1 - T_2}{T_3 - T_4} \cdot \frac{k_1}{d_1} \quad (166)$$

where $\frac{k_2}{d_2}$ has the units kcal/cm²/°C.

A similar fixture could be constructed to measure the thermal conductivity of the glove. Either thermistors or thermocouples could be used as the temperature sensors. Caution should be exercised to keep enough of the boot area surrounding the temperature sensors in contact with the plate to minimize transverse temperature gradients. This would keep the local heat flow through the boot and plate normal to the base of the boot as desired.

SUMMARY

In this section has been presented a number of isolated test techniques for the evaluation of the pressure garment and the helmet, boots, and gloves. Some of the techniques such as those for coolant flow distribution, and helmet impact are well established; whereas others such as thermal conductivity will require hardware development. All the tests are necessary for the characterization of any suit design.

SECTION VII

TEST PLANNING, PROGRAMS, AND FACILITIES

INTRODUCTION

Thus far in the development of the test methodology for the testing of extra-vehicular protective assemblies, each of the significant factors in space suit evaluation has been discussed independently. Now these factors must be reviewed to determine how to integrate them into an overall test program and to determine the requirements for the test facilities. When the facility requirements have been established, these requirements are compared to the capabilities of available facilities. These facilities include an integral data acquisition system, the description of which is deferred until the following section.

The purpose of this section is not to establish a definite test order, but instead to offer guide lines to effective test planning -- planning which will yield objective and economic tests, provide valid data, and establish confidence in the reliability of a basic suit design.

TEST PLANNING

Needless to say, a great many tests are required for proper evaluation of an extravehicular protective assembly and only through careful test planning can the benefits from these tests be maximized. The guide lines to effective test planning are test subject safety, validity and applicability of the test data, and operational cost of the required facilities. Many of the simple tests require little or no facilities, whereas the final evaluation of any space protective garment requires a full duplication of the space environment. Between these extremes there are many possible compromises, which depend upon economic and convenience factors as well as the technical problems associated with the individual test programs. Trade-offs between component and suit system testing can frequently be made. The possibility of conducting multiple tests simultaneously in a simulated environment also required consideration as a means of reducing cost. Particularly, when using a complex data acquisition system, careful planning of the data system format can both improve the accuracy of the basic data acquired and minimize the acquisition time. In addition, since the data system is designed for computer entry, many of the test points that might normally be determined redundantly to facilitate manual calculation of the test results can be eliminated. Likewise, careful test planning and computer programming can help minimize the delays in data processing and provide the greatest benefit in data display.

The primary suit characteristics to be evaluated are its functional, life support, and protective capabilities. A broad test program outline to evaluate these capabilities is presented in Table XIII. As shown, the evaluation of each of a

TABLE XIII
BROAD TEST PROGRAM OUTLINE

SUIT CHARACTERISTIC	REQUIRED EVALUATION
Functional Performance	Mobility Coordination Sensory Deprivation Physiological Energy Cost
Life Support	Respiratory Supply Pressure Regulation Heat Removal Toxic Gas Control Moisture Control Skin Temperature Regulation
Environmental Protection	Thermal Insulation Structural Integrity Environmental Reliability

suit's major characteristics breaks down into the evaluation of numerous suit parameters. These individual tests may be assembled into an effective test program for the evaluation of a suit as illustrated by the test program given in Table XIV. Naturally, this program is an idealization. It is only intended to point out some of the organizational possibilities that exist. For the purposes of this illustration, it is assumed that a typical state-of-the-art gas ventilated suit is to be evaluated. It is further assumed that the necessary atmospheric, altitude chamber, and space chamber facilities are all available at one central location. With these assumptions, the suit test program is determined by considering all the quantitative tests that are required, the complexity of these tests, the safety of the test subject, and the nature of the test facilities required. Within these planning guide lines, the detailed test procedure of Table XIV was established.

The table also shows the necessary major test facilities, test hardware, and biomedical and test instrumentation required to implement the test program. Examining the table, it can be seen that all the required tests can be performed in three major test facilities: (1) static, actuation, and functional suit mechanics tests in an atmospheric facility, (2) life support tests in an altitude chamber facility, and (3) environmental protection tests and performance demonstrations in a space

chamber facility. A discussion of these facilities begins on page 288. The instrumentation is discussed in Section VIII.

As shown in the table, the suit test program progresses sequentially from short static and actuation tests requiring simple facilities into the extensive quantitative tests and concludes with a subjective demonstration of environmental task performance. With this arrangement, both the testing and the necessary facilities become successively more complex with the exception of the preliminary life support tests. Although these preliminary tests require a more complex facility than some of the subsequent tests, they assure the well-being of the test subject during the prolonged subsequent tests.

The static and actuation tests form an effective suit acceptance test which will determine the worthiness of the suit for the more extensive tests. The static tests are primarily a subjective evaluation of suit performance. The subjective observations will indicate any gross deficiencies before proceeding with the more complex tests. The functional and life support tests provide the detailed, objective data required for suit development and improvement. The environmental performance demonstration is a final "Can he do it?" type of suit evaluation.

There are many important suit properties which are best evaluated on suit components or materials rather than during suit system tests. The tests for these properties include the following.

1. Helmet impact
2. Boot and glove properties
3. Visor optical characteristics
4. Meteoroid penetrability
5. Ozone evaluation
6. Space radiation evaluation
7. Fatigue and reliability
8. Destructive tests

These tests can be conducted at any time provided data for the safety and well-being of the test subjects are available before exposure to the hazard. Naturally, each particular suit design must be approached independently and the numerous quantitative evaluation tests assembled into the most efficient and meaningful test procedure for that design.

DETAILED TEST PROCEDURE

284

TABLE XIV (CONTINUED)

[illegible]

TABLE XIV (CONTINUED)

	INSPECTION	STATIC TESTS	SUIT ACTUATION	EXTENSIVE MANNED TESTS	FINAL SUIT DEMONSTRATION
ENVIRONMENT PARAMETERS					
CHAMBER PRESSURE					
AIR TEMPERATURE					
WALL TEMPERATURE					
SOLAR SIMULATOR INTENSITY					
ALBEDO SIMULATOR INTENSITY					
INFRARED SIMULATOR INTENSITY					
GAS ANALYSIS					
PCO ₂ SUIT-IN					
SENSOR PRESSURE					
SENSOR FLOW					
PCO ₂ SUIT-OUT					
SENSOR PRESSURE					
SENSOR FLOW					
PCO ₂ HELMET					
SENSOR PRESSURE					
SENSOR FLOW					
PO ₂ SUIT-IN					
SENSOR PRESSURE					
PO ₂ SUIT-OUT					
SENSOR PRESSURE					
PH ₂ SUIT-IN					
DEWPOINT SUIT-IN					
SENSOR PRESSURE					
SENSOR FLOW					
DEWPOINT SUIT-OUT					
SENSOR PRESSURE					
SENSOR FLOW					
CO ₂ BREATH ANALYZER					
SPIROMETRY					
SPIROMETER ROOM TEMPERATURE					
SPIROMETER TEMPERATURE					
DOUGLAS BAGS					
CO ₂ ANALYSIS					
O ₂ ANALYSIS					
N ₂ ANALYSIS					
O ₂ UPTAKE TISSOT SPIROK ETRY GASOMETER					

TABLE XIV (CONTINUED)

	STATIC TESTS										SUIT ACTUATION										EXTENSIVE MANNED TESTS										FINAL SUIT DEMONSTRATION																																																																																																																																																																																																																																																																																																																																																																																																																																																																																																																																																																																																																																																																																																																																																																																																																																																																																																																																																																																																																																																																																																																																																																																																																																																																																												
	INSPECTION	COMPATIBILITY OF DESIGN AND OBJECTIVES	FABRICATION QUALITY	MATERIAL COMPATIBILITY	COMPONENT WEIGHTS	INTEGRATION OF HARDWARE	COMMUNICATIONS	FUNCTIONAL	PROOF PRESSURE	LEAKAGE RATE	SUBJECTIVE OBSERVATIONS	DONNING AND DOFFING EASE	FITTING EASE	PRESSURE POINTS (COMFORT)	VENTILATION (COMFORT)	MOBILITY	DISTORTION	SUIT HARDWARE FUNCTION	SUBJECTIVE OBSERVATIONS	RANGE OF FIT AND BALLOONING	FIELD OF VISION	PRESSURE DROP-FLOW	LEAKAGE RATE	PRELIMINARY LIFE SUPPORT	HELMET VENTILATION	THERMAL EFFECTIVENESS	FUNCTIONAL SUIT MECHANICS	REACH CAPABILITY	DEXTERITY	LOAD DISTRIBUTION	JOINT TORQUES	LIFE SUPPORT	THERMAL STRESS	PHYSIOLOGICAL ENERGY COST	VENTILATION EFFECTIVENESS	SWEAT RATIO (REMOVED/PRODUCED)	ENVIRONMENTAL PROTECTION	PRESSURE INTEGRITY	HEAT LEAK AND TEMP DISTRIBUTION	ENVIRONMENTAL TASK PERFORMANCE																																																																																																																																																																																																																																																																																																																																																																																																																																																																																																																																																																																																																																																																																																																																																																																																																																																																																																																																																																																																																																																																																																																																																																																																																																																																																			
SUIT TEMPERATURES																																																																																																																																																																																																																																																																																																																																																																																																																																																																																																																																																																																																																																																																																																																																																																																																																																																																																																																																																																																																																																																																																																																																																																																																																																																																																																																											</

FACILITIES

The required test environments fall into three categories: normal atmospheric ambient, high altitude, and space thermal-vacuum duplication. In general, atmospheric facilities are required for evaluation of suit functional performance, an altitude chamber for evaluation of life support system performance, and a space chamber for evaluation of the overall thermal-protective performance. All of the major facility requirements could be fulfilled, however, by a properly designed space chamber.

Facilities Requirements

The cost and operational complexity of a facility grow very fast with increasing size and degree of simulation. Therefore, in determining the requirements of major environmental test facilities, the nature of the environment necessary for the proposed testing in the facility must be firmly established. Tests should be conducted in facilities having the minimum simulation consistent with allowable error and component tests should be employed instead whenever possible. The criteria for specifying facilities then are:

1. Minimum environmental simulation for proposed testing
2. Minimum size and complexity
3. Maximum utilization
4. Component versus total suit tests

Suit functional performance can be evaluated at atmospheric pressure and life support characteristics can be evaluated in an altitude chamber with a 12,500 meter (40,000 foot) capability. Many of the protective characteristics can best be evaluated on test samples in small relatively inexpensive space simulators. A large man-rated space chamber facility is required for determining total suit heat leaks and demonstrating task performance and reliability of the suit in a space environment.

Atmospheric Facility

This facility consists of two large clean rooms, the suit donning and check-out room, and the functional performance test room. A single large room would also be acceptable. The suit checkout room is used for suit inspection, donning, and actuation tests and would contain the field of vision apparatus, a treadmill, and an environmental control system (ECS) stand. The purpose of this stand is to provide suit gas ventilation and/or liquid circulation and communications. A block diagram of one such ECS stand is shown in Figure 115. The ventilation supply

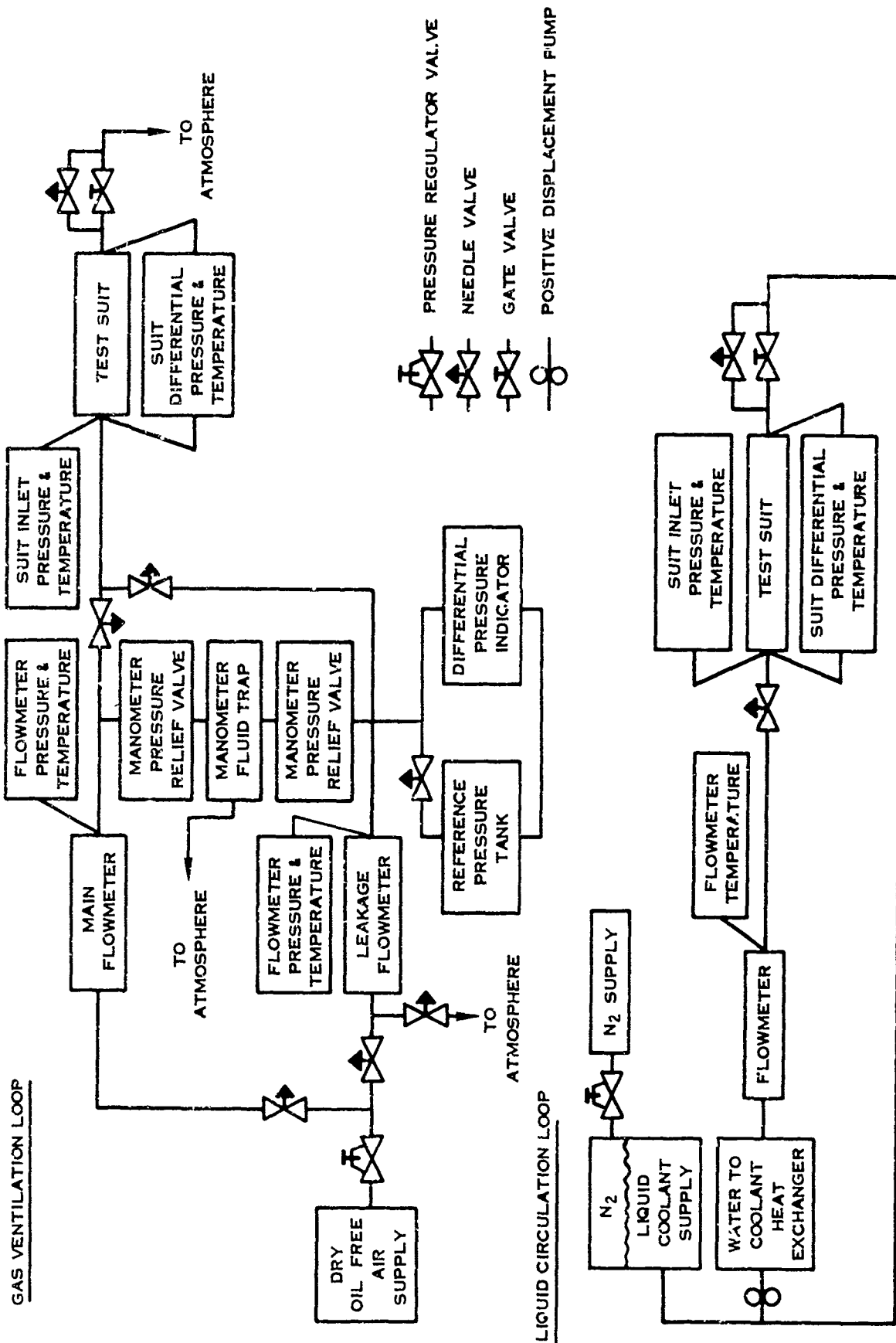


FIGURE 115. ENVIRONMENTAL CONTROL SYSTEM STAND

should be capable of providing 1100 liters/min (40 CFM) at 950 mm Hg (18.4 psia) to accommodate two suits or 550 liter/min (20 CFM) at 950 mm Hg to accommodate one suit. For the atmospheric tests the stand supplies dry air rather than oxygen. To measure leakage flow, as described on page 272, the ventilation system contains the separate subloop shown.

The functional performance test room would contain ECS provisions, a reach apparatus, an articulated anthropomorphic dummy, and the other equipment for functional mechanical testing as described in Section III including the control console of the data acquisition system described in Section VIII.

Altitude Chamber Facility

This facility consists of a suit donning and checkout room and an altitude chamber. The only major apparatus required in the suit checkout room is an ECS stand such as the one employed in the atmospheric facility. In fact, if the atmospheric and altitude chamber facilities were adjacent, the same suit checkout room could be used for both.

The altitude chamber should have a minimum capability of about 12,500 meters (40,000 feet) although most tests can be conducted at 2500 meters (8000 feet). To provide a minimum heat leak environment the interior of the chamber should be lined with a fabric material. Temperature controlled air would then be distributed from behind the liner. Temperature sensors on the test suit could be used to control the temperature of the inlet chamber air. The chamber should contain a treadmill and an integral environmental control system for controlling the internal environment of the suit. This ECS system includes the features of the stand in the atmospheric facility and, in addition, controls the temperature and relative humidity of the gas inlet flow, controls the temperature of the liquid inlet flow, and provides for the safe introduction of contaminants such as carbon dioxide to the helmet ventilation flow. The chamber should also have integrated spirometry capabilities with insulated gas sample lines extending through the chamber wall to an external hyperbaric chamber containing the spirometry measuring system.

The life support control console of the data acquisition system will be located in the control room of the chamber. Also, in the room will be analog recording equipment which displays, when required, the medical status of the test subject.

Space Chamber Facility

The space chamber facility includes a suit donning and checkout room as in the altitude chamber facility, a man-rated space chamber, and a medical treatment room. The primary purposes of the facility are (1) to determine suit heat

leak and hot spots in the space thermal radiation environment and (2) to demonstrate task performance and establish reliability under space conditions.

CHAMBER REQUIREMENTS

Consider first the basic chamber requirements and then the man-rating requirements. The basic chamber must be large enough for a man to stand erect, move several feet in any direction, lie down, and perform simple repetitive tasks. The walls must be sufficiently distant to prevent accidental contact. Thus, a spherical chamber about 3.5 to 4.5 meters (12 to 15 feet) in diameter or a cylindrical chamber of similar dimensions would suffice. A vacuum capability to 10^{-6} mm Hg eliminates the thermal conductance of air, permitting a realistic evaluation of the thermal properties of a suit. The chamber should contain an optically dense, liquid nitrogen cooled shroud with an emissivity of at least 0.9 to simulate the radiative heat sink of space. The chamber should also have carbon arc or short arc solar simulators plus infrared sources and reflectors for simulating planetary infrared and albedo radiation.

To man-rate the chamber and employ it as a space suit testing facility imposes the following additional requirements.

1. Emergency repressurization capability to pressures above 180 mm Hg (3.5 psia) within a few seconds
2. A biomedical safety lock with an inside observer for quick rescue of a test subject
3. An oxygen supply for both the test subject and the observer in the safety lock
4. An extensive automatic control system on the chamber with interlocks to insure proper operation
5. An automatic emergency power system to sustain operation of the chamber and essential biomedical monitoring equipment long enough to return to atmospheric conditions in the event of primary power failure
6. A treadmill, rowing machine, or other devices in the chamber to establish metabolic rates
7. Adequate penetrations for biomedical monitoring and test instrumentation electrical leads
8. Heated gas sample lines for gas analysis

The major problems in repressurization are fogging, noise level, and extremely low chamber air temperature after repressurization. Experience has shown that fogging can be reduced by using sufficiently dry air either from high pressure storage tanks or from humidity controlled room air. The noise level can be reduced through the use of commercially available air compressor exhaust silencers. The extremely low temperature chamber air may necessitate protective thermal garments for rescue personnel depending on the size of the chamber.

The versatility and safety features that can be built into the oxygen supply system are exemplified by the suit test system employed in the Hamilton Standard man-rated space chamber. This oxygen supply system is shown in block diagram form in Figure 116. The system is capable of supplying 0-550 liters/min (0-20 CFM) at 190 to 950 mm Hg (3.7 to 18.4 psia), controlling the inlet flow temperature of the suit between 10 and 32°C (50 and 90°F), and inlet flow dewpoint between -18 and 32°C (0 and 90°F). The temperature is controlled by the glycol heat exchanger while dewpoint is controlled by the steam heat exchanger and steam injector. There are provisions for introducing a regulated flow of a contaminant such as carbon dioxide into the oxygen supply system. Reliability is provided by using redundant high pressure oxygen sources through parallel check valves and a pressure sensitive alarm switch. As shown, the redundant supply would automatically provide the necessary oxygen flow and an alarm would automatically be sounded in the event of failure of the main oxygen supply. The redundant supply is sufficient to operate for 30 to 60 minutes, allowing a safe termination of the test. The system can also be operated with air from 0 to 550 liters/min at 950 mm Hg at temperatures between 10 and 32°C and dewpoints between -18 and 32°C. The life support console of the data acquisition system could be intimately tied to the space chamber and its control systems; however, since the console is also needed for the altitude facility, it must be designed either for portability or for a hard wire data link to the other facility or else two separate systems must be procured.

The biomedical monitoring instrumentation and medical personnel requirements for the space chamber facility are more extensive than those required for the altitude chamber facility.

The medical treatment room is located in the immediate vicinity of the chamber. Normally, the minimum equipment requirements for this room would be as follows.

1. Standard medical equipment such as a medical bed, plasma stand, blood plasma, etc.
2. X-ray apparatus
3. Mechanical resuscitator
4. Electrical pacemaker - defibrillator

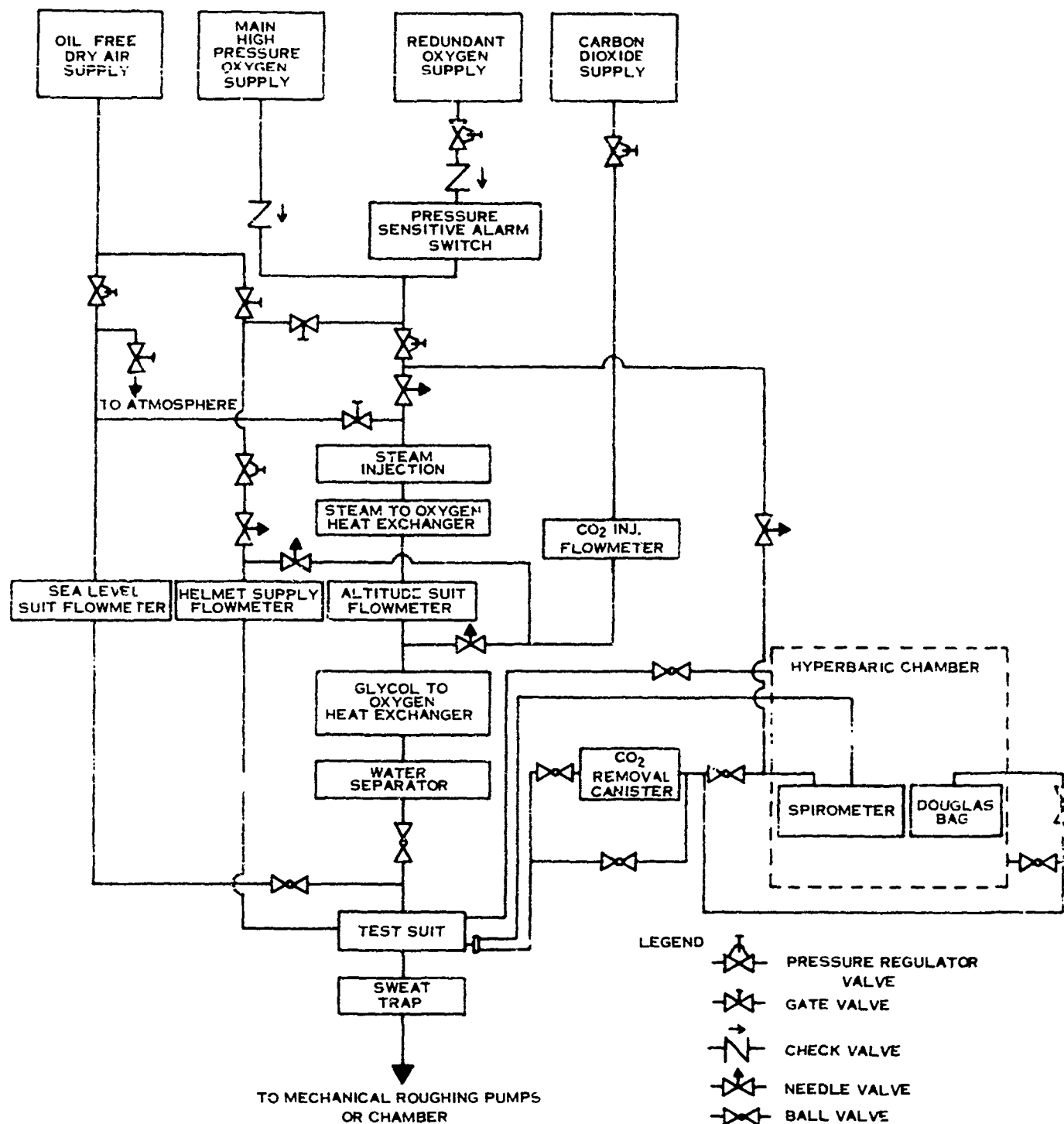


FIGURE 116. SPACE CHAMBER OXYGEN SUPPLY SYSTEM

5. Sterile surgical instruments

6. Electrocardiograph

AN IDEAL FACILITY

Ideally, the three facilities should be combined into one central space suit testing facility with integrated data acquisition system. By adding accurate altitude control and chamber wall temperature control, the space chamber could also serve as the altitude chamber.

The central facility would then include the space chamber, the functional performance test room, the suit donning and checkout room, and the medical treatment room. The physical requirements for these rooms are so general that they could easily be located adjacent to existing space chambers. Figure 117 is a schematic presentation of this ideal facility.

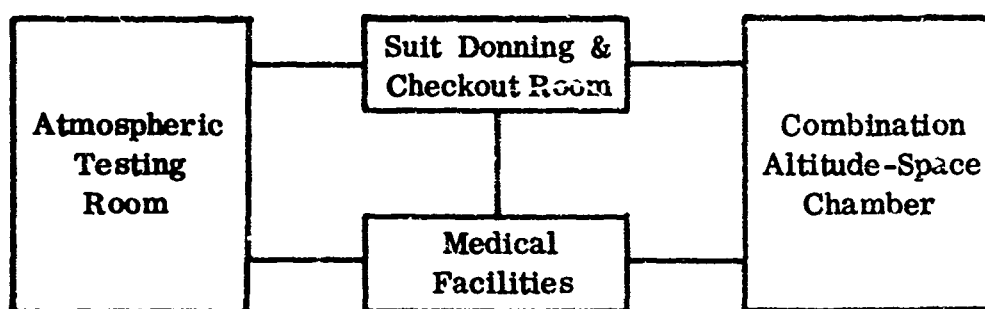


FIGURE 117. IDEAL SPACE SUIT TEST FACILITY

AVAILABLE CHAMBERS AND CONCLUSIONS

There are currently available many space chambers of sufficient size for testing; however, only one of these is currently man-rated and fulfills both the altitude and the space chamber requirements. Several of the others are currently scheduled to be man-rated. In general, these chambers may be classified as small chambers for space suit and spacecraft subsystem testing, medium sized chambers for tests of satellites, and large chambers for manned spacecraft systems performance evaluations. Respective chamber volumes are roughly 10 - 10^2 , 10^2 - 10^3 , and 10^3 - 10^4 cubic meters. Three specific chambers which meet the basic chamber requirements are compared in Table XV. Some typical operating costs of space chambers are plotted in Figure 118 as a function of chamber volume. The figure shows the economic advantage of keeping the size of required facilities at a minimum.

TABLE XV

CLASSIFICATION OF OPERATIONAL CHAMBERS

CLASS	SHAPE	INTERIOR SIZE	VOLUME CUBIC METERS	MAN RATED
1	cylindrical (horizontal)	4.0 meters diameter 3.5 meters long	45	yes
2	spherical	11.9 meters diameter	880	to be
3	cylindrical (vertical)	10.7 meters diameter 19.8 meters high	1780	to be

There are three cylindrical space chambers currently available at the Arnold Engineering Development Center, Tullahoma, Tennessee. The largest is the Mark I facility which is 10.7 meters in diameter by 19.8 meters high (35 by 65 ft). The other two are supporting facilities measuring 2.1 meters by 3.7 meters long (7 by 12 ft) and 3.7 meters by 3.7 meters high (12 by 12 ft), respectively. The Mark I facility is intended to provide environmental simulation for testing of integrated manned spacecraft systems and for mission training. High operating cost (estimated to be \$1400 per hour), possible test system damage during any necessary emergency depressurization, and rapid personnel retrieval make it essential that the reliability of the space suits be proven elsewhere in advance. Neither of the remaining two chambers is currently suitable for space suit evaluation testing.

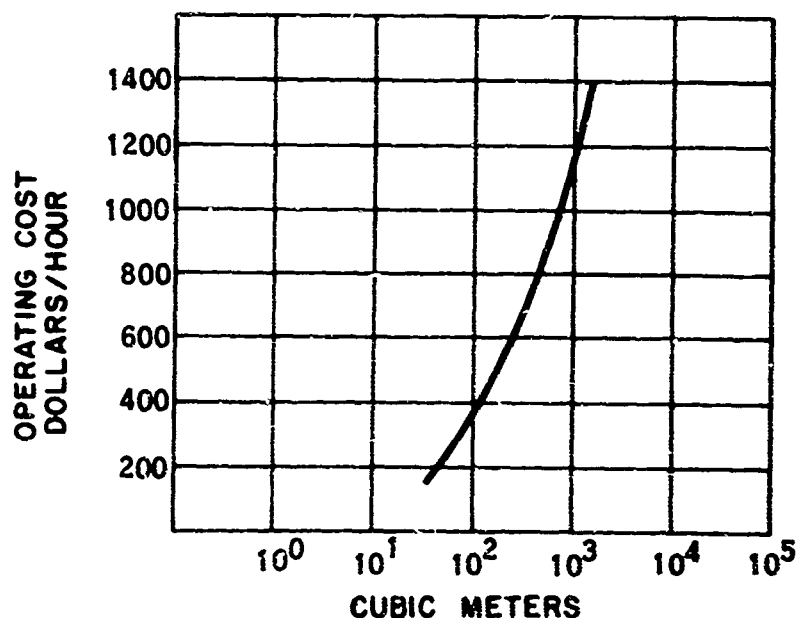


FIGURE 118. SPACE CHAMBER OPERATING COST versus VOLUME

The 2.1 x 3.7 chamber is too small and the 3.7 x 3.7 chamber has neither solar simulation nor man-rating. Furthermore, both of these chambers are required in support of the Mark I chamber and may not be available for the extensive space suit evaluation tests required.

At the present time there seems to be no fully acceptable space chamber facilities available within the Air Force complex for extravehicular space suit development. Consideration should be given to either the construction of such facilities or the renting of existing facilities. Obviously, there are many economic and technical factors in a decision of this nature and it is not the intent of this report to recommend either approach. It is pointed out, however, that by proper test planning the use of space chamber facilities can be minimized and an extensive program of space suit development in leased facilities could be carried out before the economic "break even point" is reached.

SUMMARY OF CONCLUSIONS

1. Before any testing is performed, a precise plan of test must be established by integrating the type of suit, applicable tests, and available test facilities.
2. With such a plan it is possible to implement the testing in one central space suit testing facility.
3. The central facility, although extensive, does not have to be large and, in fact, should be kept small for test subject safety and economy.

SECTION VIII

DATA ACQUISITION AND PROCESSING SYSTEM

INTRODUCTION

As shown in the preceding sections, extravehicular suit testing is a complex process involving many different kinds of tests and test procedures. In studying these test procedures, it is apparent that large volumes of both quasi-steady state and time variant test data are produced and that substantial computation is required to convert these data to useful quantities. The data acquisition system required for suit testing, therefore, must be sufficiently flexible to handle these large volumes of data rapidly and accurately and must provide an efficient link to the computation equipment.

The purposes of a generalized data system are to measure test variables, display these variables so that the test personnel may monitor the progress of the test, and provide a means of making permanent test records. These basic tasks have many technical approaches. For small quantities of steady state data, measurements can be made using simple instruments such as pressure gages and manometers, the test data can be hand logged, and the desired output quantities can be manually computed. For small quantities of time variant data, measurements can be made with simple transducers, recorded on an analog recorder such as an oscillograph, and manually computed from the oscillograph. Large steady state tests in which substantial quantities of data are expected may be successfully approached using automatic data loggers with typewriter or punch card output for computer entry. When large volumes of data or faithful reproduction of rapidly varying data is required, magnetic tape data systems are normally employed. These systems may be either analog or digital in character. Analog tape is best suited for multi-channel time variant applications such as vibration data where direct computer entry is not required. Digital tape is best suited for direct computer entry of large quantities of steady state data or a moderate number of time variant channels. Many hybrids of these basic systems are used to meet specific requirements.

Considering the many areas of suit testing discussed in the preceding sections, it is apparent that a multiplicity of data systems is required to handle all the testing. Many of the more specialized facilities for testing in such areas as micrometeoroid penetration, vacuum embrittlement, and solar-thermal heat balance are already fully instrumented with versatile data systems uniquely adapted to the specific requirements of that facility. Other areas of testing, particularly of components such as boot conductivity measurement, suit restraint cable tensions, and visor optics, require only the most rudimentary data systems by virtue of the relatively small quantities of data involved. Two test areas, however, clearly require a versatile, accurate, high speed data system. These test areas are functional suit mechanics and life support. The test methodology and techniques required to evaluate these areas are discussed in detail in Sections III and

IV respectively. As is discussed in Section VII, the facilities and data system for this testing should be closely integrated to realize substantial economies in time and equipment.

This section describes a centralized data acquisition system which will satisfy the long range requirements for mechanical and life support evaluation of space suit assemblies. For complete suit evaluation, this system must be augmented by other test equipment and procedures as discussed in the preceding sections.

DATA SYSTEM CONCEPTUAL DESIGN

In developing a satisfactory concept for data acquisition, it is advantageous to review briefly the data handling requirements for each of the two major test areas, functional suit mechanics and life support.

Data Requirements For Functional Suit Mechanics

The evaluation and testing of the functional mechanics of a suit require the acquisition and processing of data from the major test apparatus described in Section III. These apparatus which determine the suit torques, reach, and mechanical load distribution need not be used simultaneously so that time sharing is possible.

During suit torque testing, the outputs of approximately 25 force or torque transducers on an articulated dummy must be continuously recorded. Simultaneously, the angles of several of the dummy's joints, measured by potentiometers, must be recorded. At other times, the dummy joint angles and the outputs of an electro-skeletal goniometer must be recorded for calibration of the goniometer. To be useful, the outputs of the force and torque transducers must be entered in a computer to determine the net suit torque vector at the joint of interest. Plots of joint torque versus joint angle, angular velocity, and angular acceleration are desired as well as more sophisticated calculations of suit joint figures of merit.

During pressurized suit reach testing, the outputs of three reach coordinate potentiometers must be monitored, recorded, and plotted. Concurrently, it may prove desirable to record the outputs of several load transducers and certain thermodynamic data. Computer analysis of the reach data makes possible useful coordinate transformations and the calculation of reach volume criteria.

During mechanical load distribution measurements, as many as 140 mechanical pressure transducers must be monitored, displayed, and recorded. Again computation is required to reduce the data to useful contour plots of suit loading.

Since time sharing of functional tests is possible, the total data recording capacity required is 140 quasi-steady state channels and approximately 40 channels of time variant data with frequency components up to 30 cycles per second.

Data Requirements For Life Support

The evaluation and testing of the life support characteristics of the suit require the acquisition and processing of data principally from the integrated chamber facility described in Section IV. In this facility, suit thermal, respiratory, and pressure control systems are tested. During the chamber testing, quasi-steady state data from up to 150 transducers measuring suit and chamber pressures, temperatures, flows, and gas compositions must be monitored, recorded, and stored for calculation of the engineering and physiological parameters of interest. Additionally, steady state and time variant inputs from biomedical transducers must be recorded to monitor continuously the status of the test subject.

Since it is assumed that the basic data handling system can be time shared between the mechanical and life support testing, a total data recording capacity of about 170 channels is required. Of this, approximately 40 channels must handle frequency components up to 30 cycles per second. Adding some spare channel capacity, a data recording capacity of 200 channels was established.

Data System Concept

The purpose of the data acquisition system is to accept the outputs of the many transducers, drive steady state displays for on-line test monitoring, drive analog displays for biomedical monitoring, digitize transducer outputs, and format them for computer entry. In general, a system accuracy, not including transduction, of about 0.25% for recorded data and 2% to 5% for monitored data is readily achievable. Because transduction accuracies can vary considerably, they are discussed separately.

The equipment required to digitize the transducer output and format it for the computer varies with the data origination rate and the input characteristics of the computer. If all data were quasi-steady state, they could be handled using punched or incremental tape equipment. Since conversion equipment is required to handle punched card inputs on a high speed computer like the IBM 7090 at ASD, the incremental tape is preferred. However, both the punched cards and the incremental tape equipment are too slow for the time variant mechanical data which requires continuous recording magnetic tape. Since continuous magnetic tape is required to handle the time variant data, economies in cost and complexity of the data acquisition system can be achieved through the exclusive use of continuous recording, digital magnetic tape and, therefore, this tape based system is recommended.

In the digital tape system the transducer outputs are multiplexed into PAM (pulse amplitude modulated) pulse trains, converted to digital code, formatted for the computer, and recorded on magnetic tape. To provide the test director with sufficient on-line data to conduct the test, analog displays of significant test parameters are provided. Thus a secondary data path provides sufficient data to conduct the test but the primary data path is automatic. This relieves test personnel of the task of hand-logging, reducing, editing, and plotting data. At the end of the test, the magnetic tape may be edited using a direct writing oscillograph. In the editing process, the digital magnetic tape information is converted back to analog and displayed at reduced accuracy on an oscillograph. In this manner, the significant data records, which will be computer-reduced, are segregated from the data of less interest. The editing function gives the test director an opportunity to examine the results of the test immediately and to decide which data are pertinent, thus minimizing computer time and cost. After editing, the data are sent to the computing center for processing. The computer performs the calculations directed by the program and outputs the calculated data to a printer, plotter, or other suitable output device.

In concept, the data system would be packaged for easy transport from one test site to another without damage or undue effort and would withstand the usual test site environmental conditions; however, like all systems of this size, maximum versatility and minimum maintenance are derived when the system is semi-permanently installed in a central facility.

A preliminary system block diagram has been evolved and is described below. This system will perform the basic functions intended but it has not been optimized, nor does it necessarily include all of the features that a detailed system design might show desirable. Standard, commercially available components are used wherever possible. In several instances, specific manufacturer's equipment have been recommended. These recommendations are made where it is known from experience that this equipment will perform the intended task. This is not intended to imply that a complete evaluation has been made, nor that this is the only equipment that will meet the requirements, nor that design trade-offs could not be made which would make other types of equipment preferable.

DATA SYSTEM DESCRIPTION AND OPERATION

The basic data acquisition system, which is shown in Figure 119 consists of a control console for the testing of functional suit mechanics, a multicabinet control console for life support and biomedical testing, a digital/analog recording system, and suitable test monitoring displays. For convenience, the following discussion of the system has been divided into descriptions of the systems for mechanical and life support testing and is followed by a detailed description of the recording system.

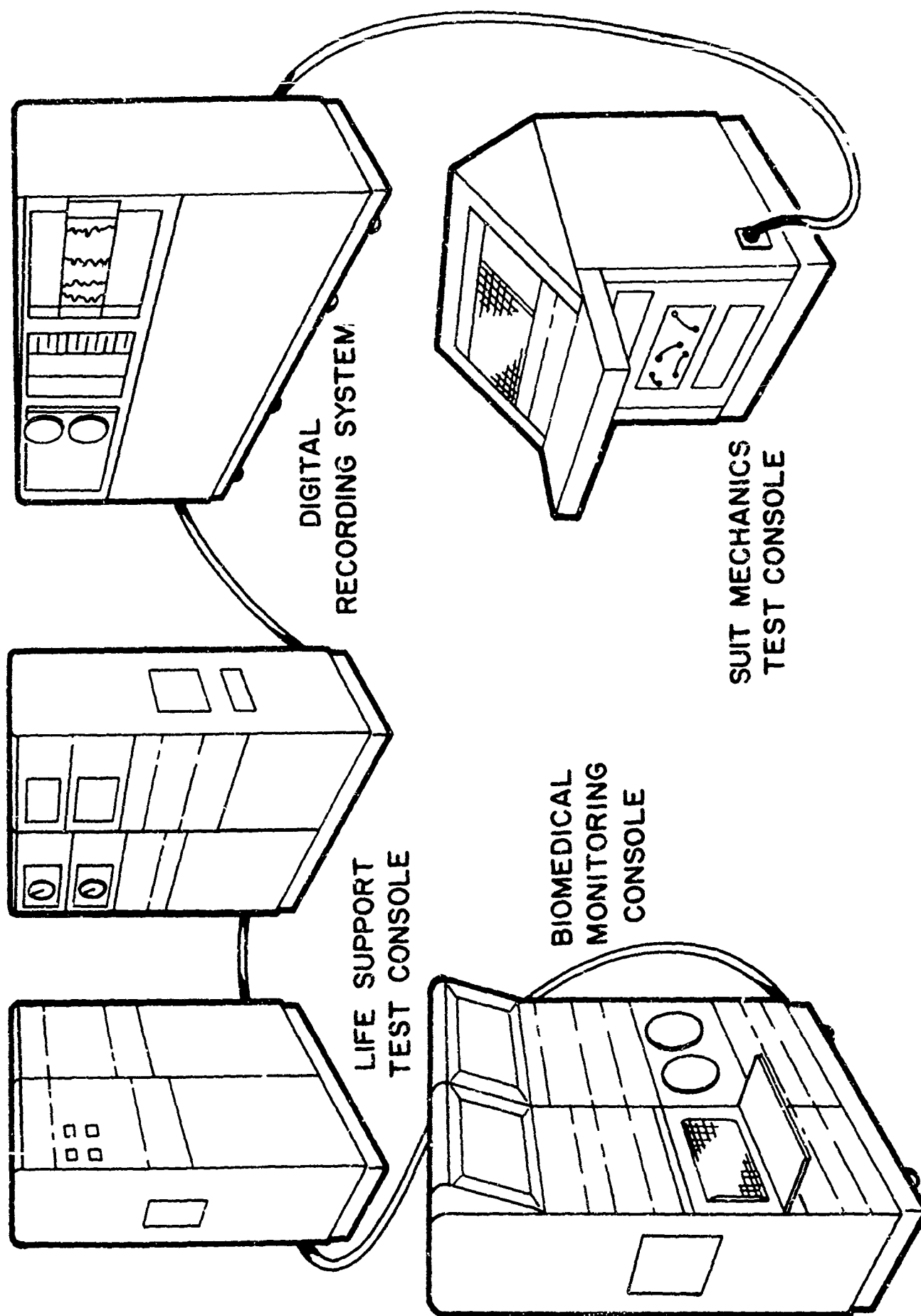


FIGURE 119. THE DATA ACQUISITION SYSTEM

Functional Suit Mechanics Test System

The data acquisition system required for mechanical testing must be sufficiently flexible to handle measurements of exoskeletal position, dummy torque and position, reach, and mechanical load distribution as discussed in Section III. During torque testing, the data system excites the transducers for torque and angle measurement, accepts the transducer outputs, and records them on either digital magnetic tape or a direct writing oscillograph at speeds capable of faithful reproduction of the test subject's or dummy's maximum limb velocities. During reach testing, the position transducers on the reach apparatus are recorded on digital tape and simultaneously displayed on a monitoring plotter. During mechanical load distribution testing, the suit mechanical pressures exerted on the test subject's skin surface are transduced and displayed on a manikin covered with luminescent segments or, on command, the data system will record their outputs on tape or oscillograph. Thus, the data system, in conjunction with specialized test facilities, can be used to evaluate suit encumbrance, measure localized forces, determine limb position, ensure proper suit fitting, and aid in joint and suit geometry design problems.

SYSTEM DESCRIPTION

The data acquisition system for functional suit mechanics test is composed of three units: a control console (Figure 120), a manikin covered with light segments (Figure 121), and a digital/analog recording system (Figure 122).

The control console contains signal conditioning for 140 strain gage force transducers and 40 position potentiometers, 180 sample and hold devices, transducer excitation and standardization sources, 140 amplifiers for driving the light segments, an output patchboard permitting connection of the force transducers to any of the 1000 display light segments, and a plotter for display of reach and torque measurements.

The manikin, used as a display for mechanical load distribution measurements, is a commercial clothiers manikin covered with approximately 1000 electroluminescent segments whose light intensity will vary in proportion to the force transducer outputs. The segments will be from one to three square inches in area.

The digital/analog recording system is used to record the mechanical data in digital form for computer entry and in analog form for quick-look and editing as described on page 326.

A block diagram of the data system is shown in Figure 123. Typically, both force and position transducer outputs are routed to signal conditioners where the transducer excitation is provided along with zero and span control capability. The conditioned transducer output is then routed to a sample and hold device. This device samples the output of the transducer at any desired time as commanded by

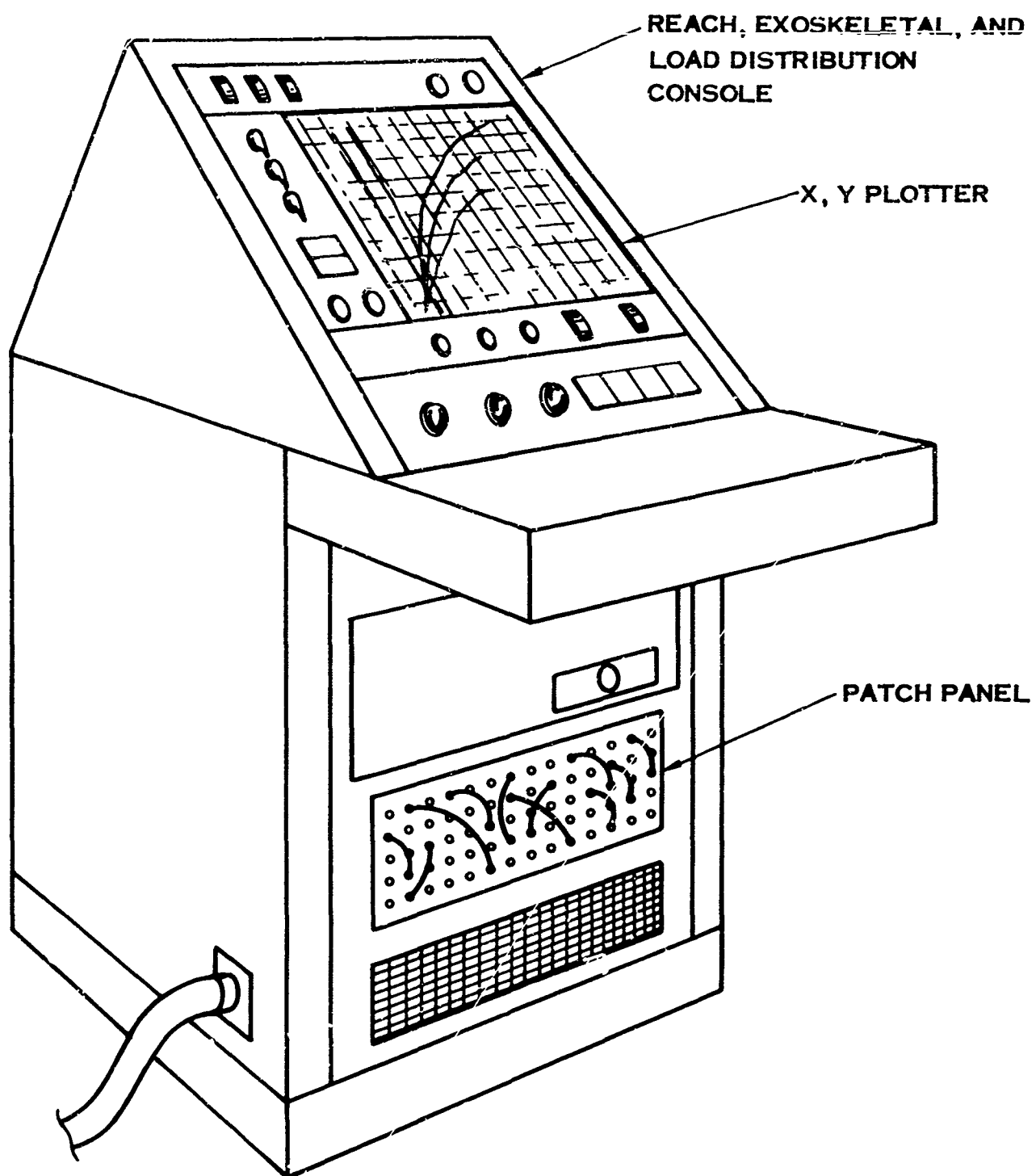


FIGURE 120. SUIT MECHANICS TEST CONSOLE

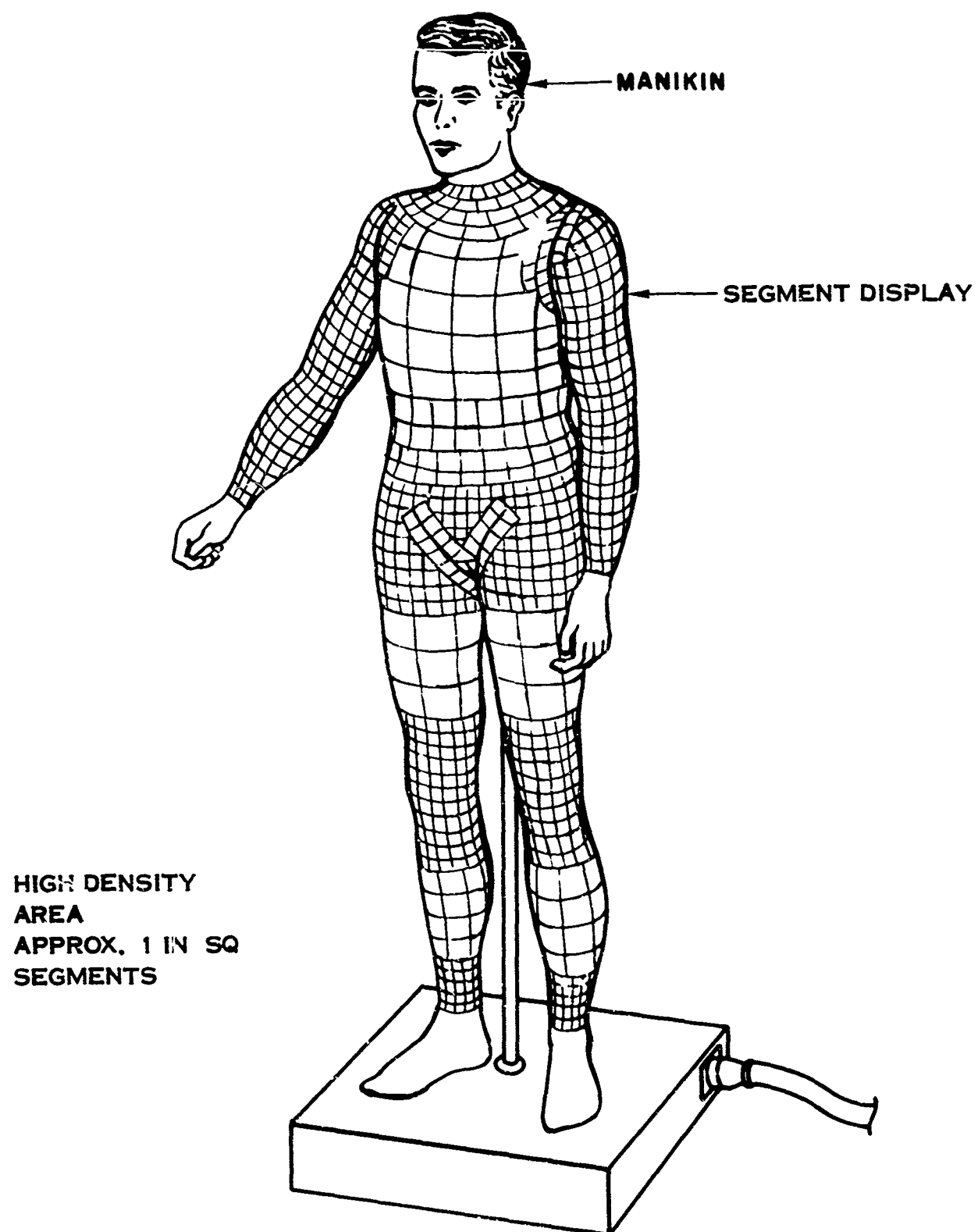


FIGURE 121. LOAD DISTRIBUTION DISPLAY MANIKIN

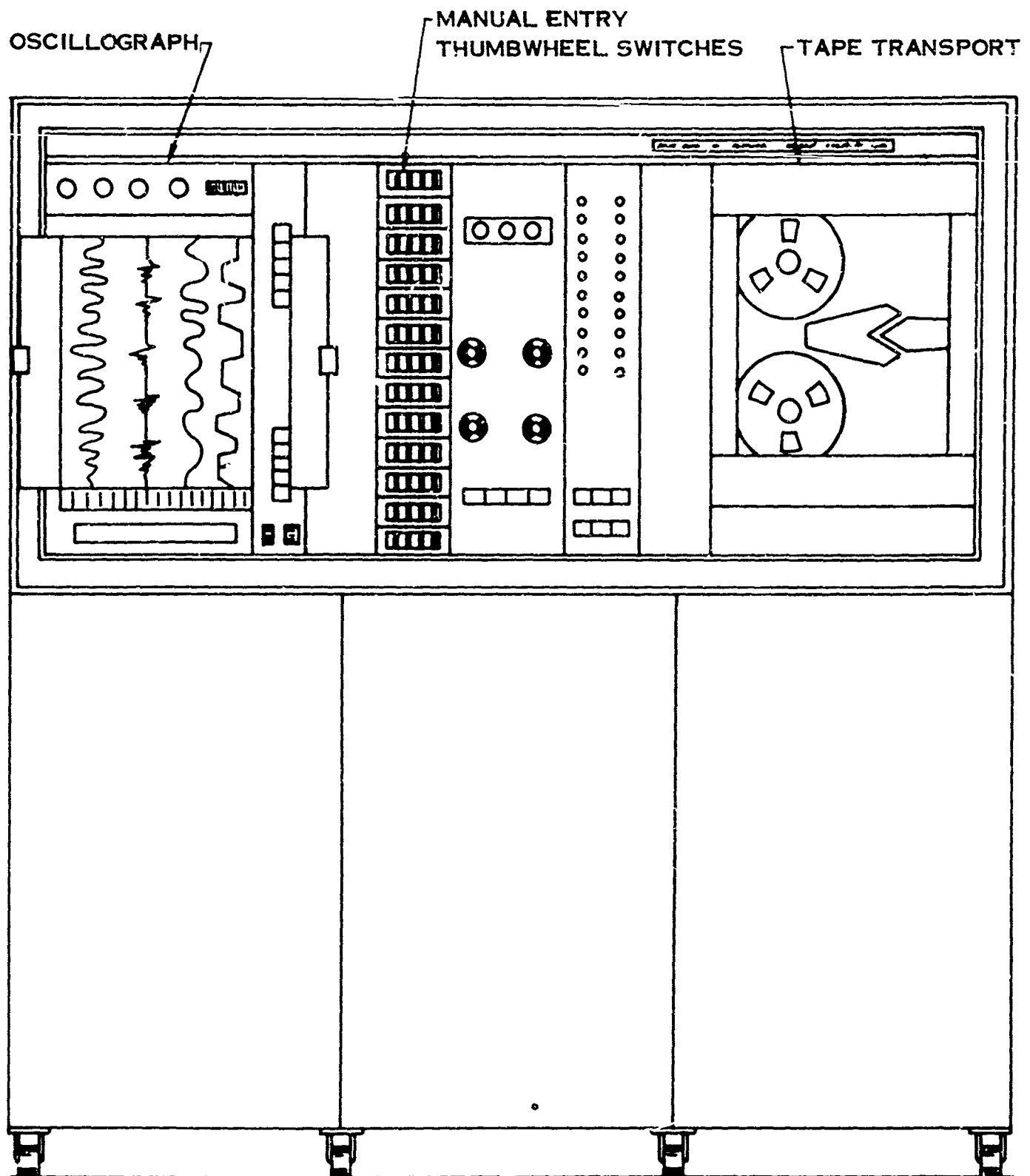


FIGURE 122. RECORDING SYSTEM DIGITAL/ANALOG

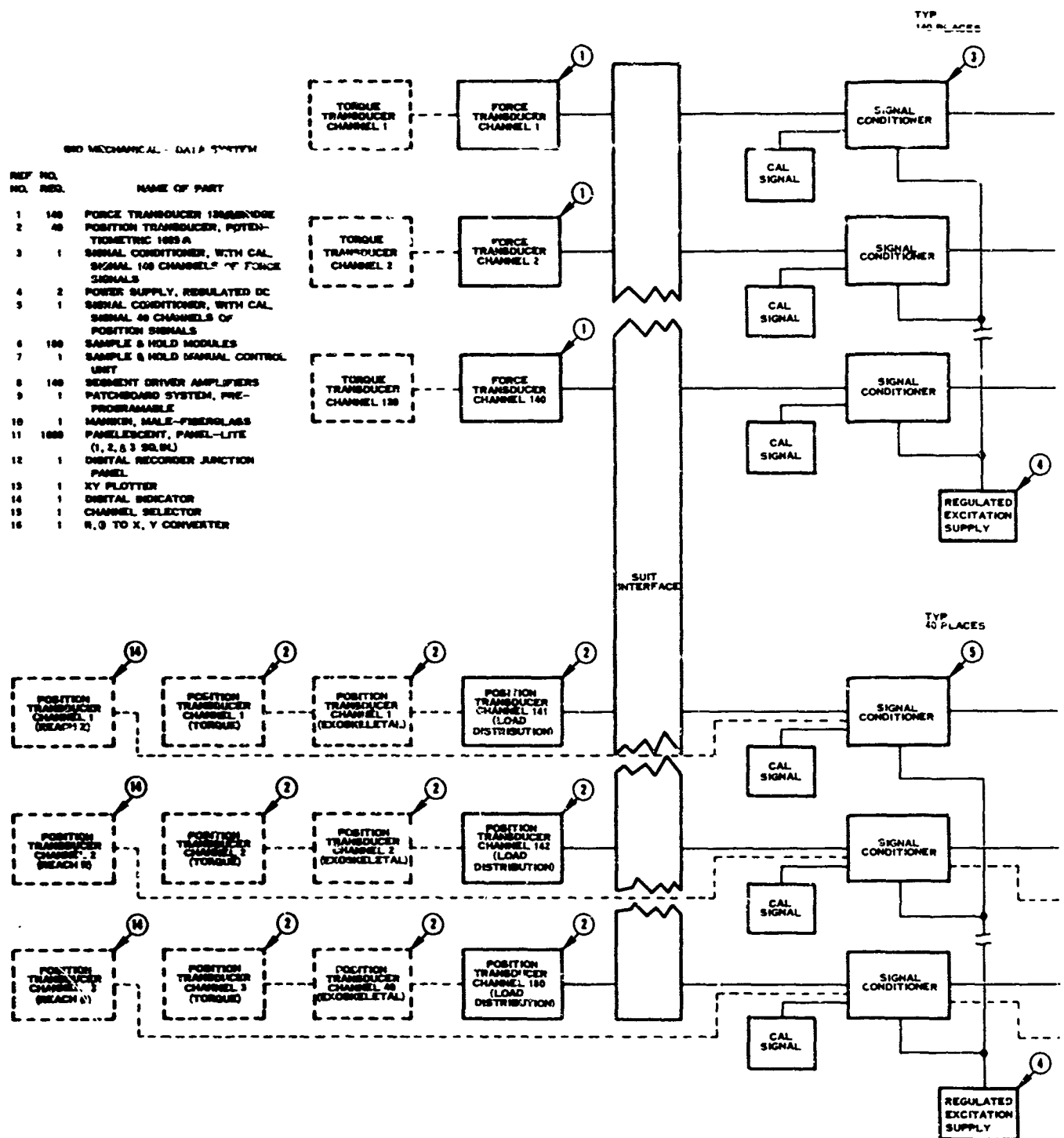


FIGURE 123. SUIT MECHANICS DATA SYSTEM BLOCK DIAGRAM

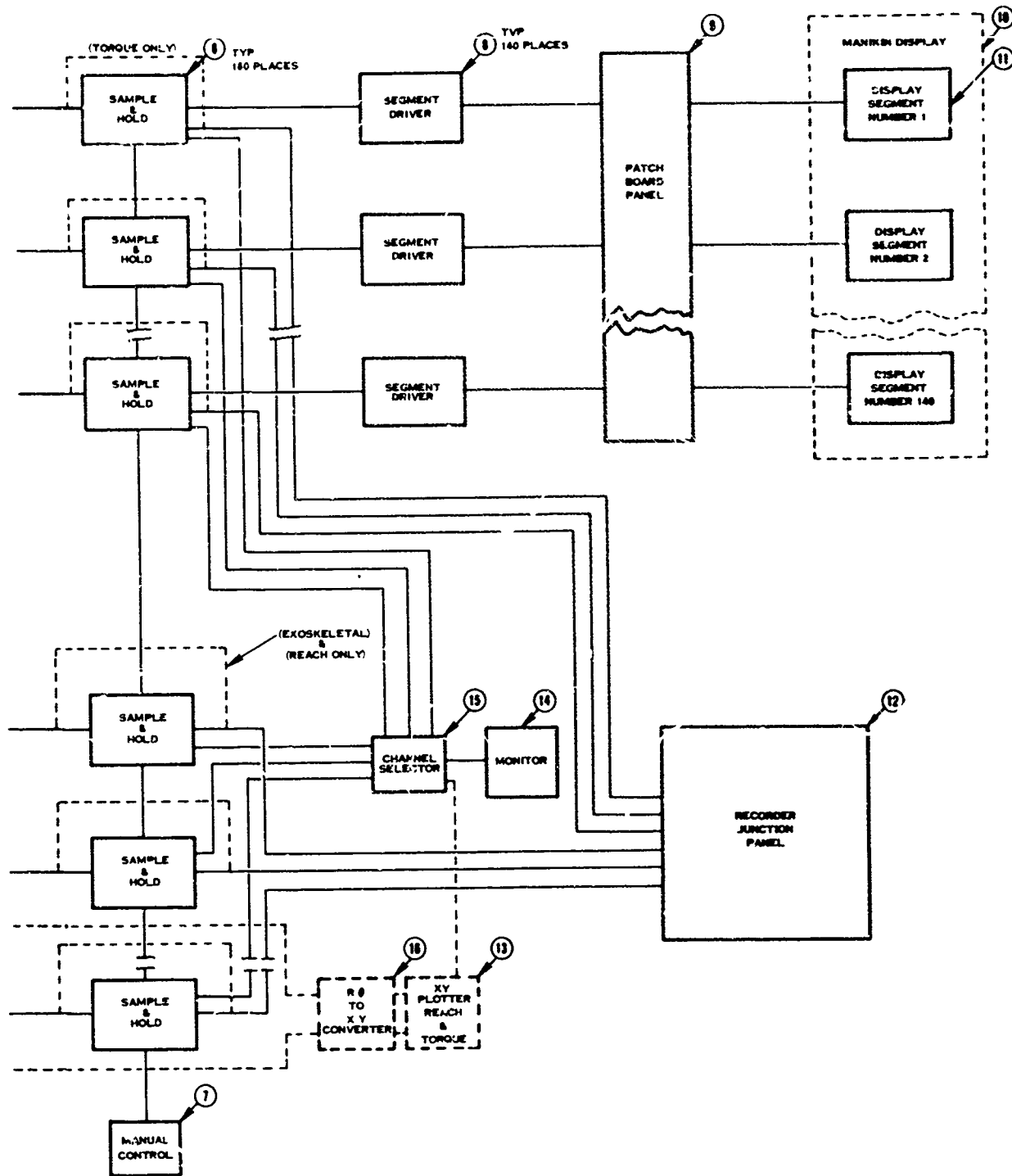


FIGURE 123. (CONTINUED)

a central control and stores the voltage value on a capacitor. This technique of stopping the time variant signals is of particular value when evaluating the mechanical load distribution on a test subject and also serves to store the position transducer outputs temporarily so that, when recorded, the force and position data represent the same point in time. On command, the sample and hold output can be directed to the digital/analog recording system. A selectable monitor is also provided as an on-line display of the actual physical value of any transducer output.

During suit reach testing, the outputs of the radial and angular potentiometers on the reach apparatus may be simultaneously plotted on-line and entered into the digital/analog recording system.

The transducers used to measure force and torque on the articulated powered dummy and for mechanical load distribution measurements are discussed in detail in Section III. For purposes of data system design, these transducers are all assumed to be 350 ohm, full bridge, strain gage type devices. If another type of transducer proves more suitable, only minor system changes would be required which would probably involve only signal conditioners and transducer power supplies. The transducers to measure dummy position, exoskeleton position, and reach coordinates are assumed to be 1000 ohm wire wound or film-type linear and angular potentiometers. Likewise, changes in this type of transducer will present only minor system design changes.

A typical signal conditioning circuit is shown in Figure 124. This is a 350 ohm, full bridge, strain gage signal conditioner channel with zero and standardizing control typical of that required for force and torque transduction. A similar conditioner would be used to provide zero and span control and the sample and hold feature for a potentiometric transducer.

The sample and hold device will be similar to the one shown in Figure 125. Relays K_1 and K_2 are common to all channels and provide complete control of the sample and hold functions. If contact bounce problems become excessive, a solid state circuit may be substituted.

SYSTEM OPERATION

For suit torque testing the operation of the data acquisition system is quite simple. The two units needed are the control console and the digital/analog recording system. After the two consoles are cabled together and the dummy force, torque, and position transducers are connected, the system is ready for calibration. This is accomplished by setting the calibration signal dial in the signal conditioner on each channel to the calibration constant previously determined by direct physical calibration of the transducer. The constant is in the form of E_o/E_{in} for full scale. Next, the residual output of each transducer is balanced out using the signal conditioner zero balance control. The function switch is then positioned to standardize, generating a voltage representing 80% of full scale for each transducer

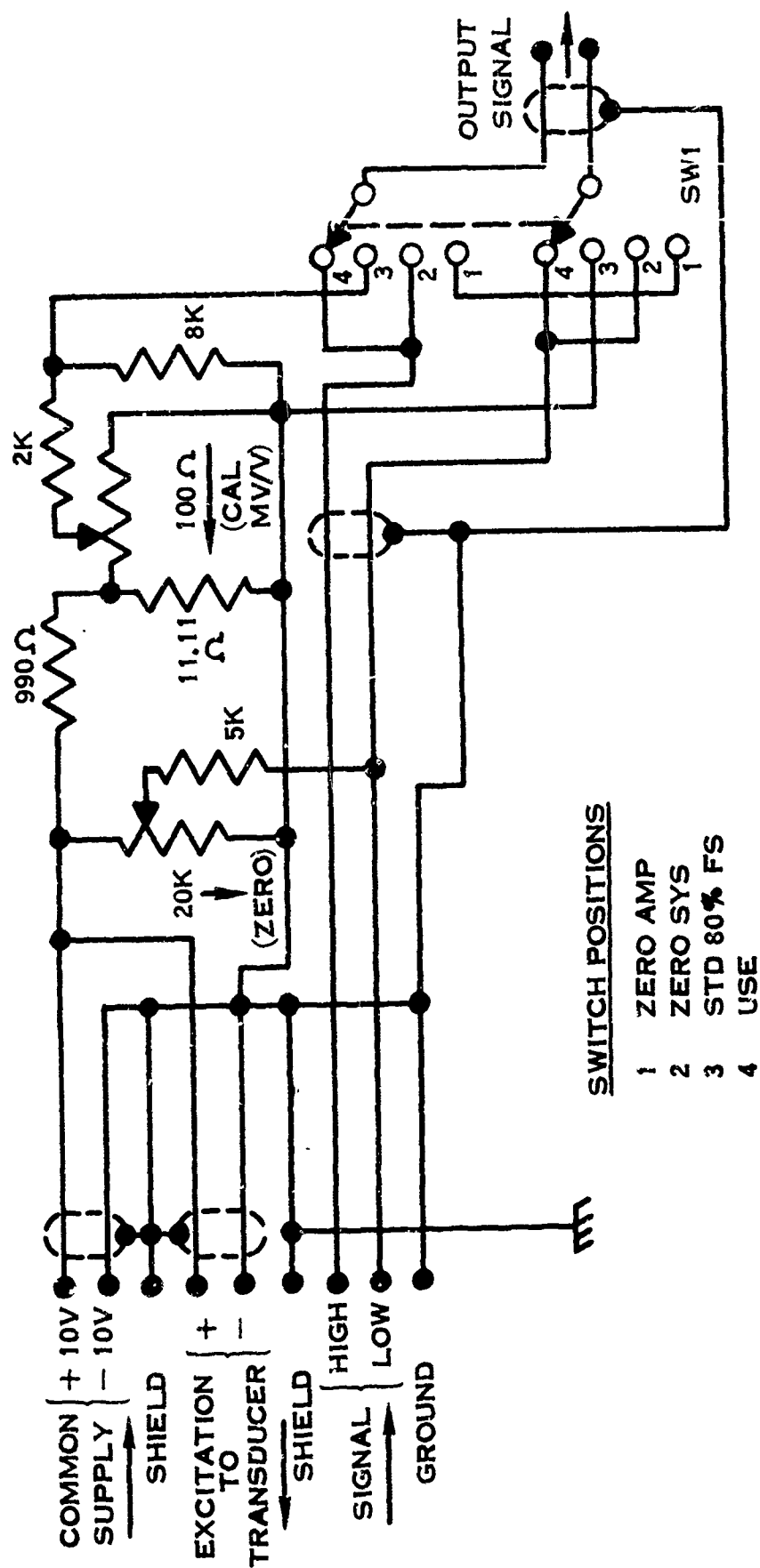


FIGURE 124. 350 Ω FULL BRIDGE SIGNAL CONDITIONER

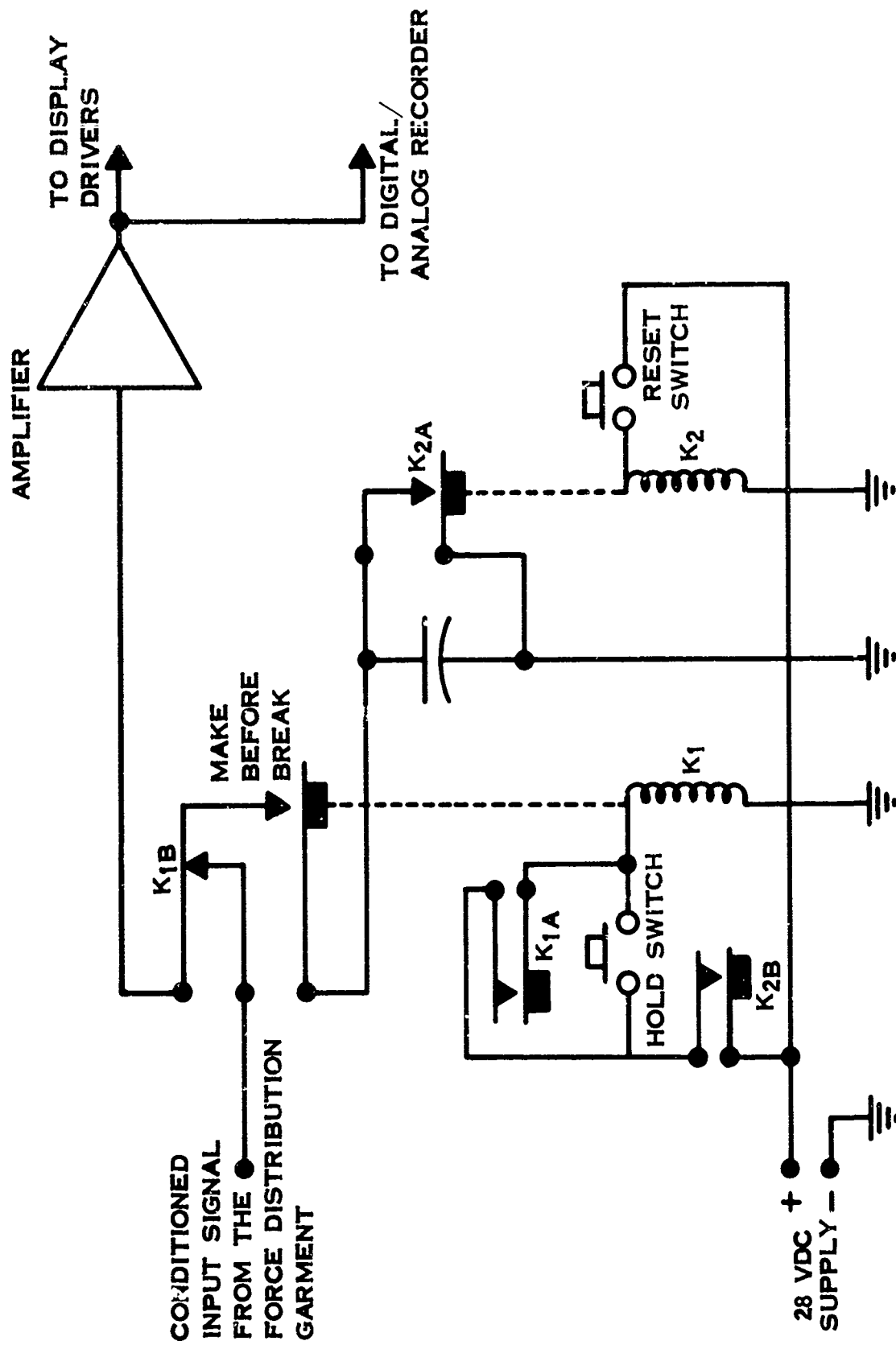


FIGURE 125. SAMPLE AND HOLD DEVICE

based on the calibration signal dial setting. This signal is used to set the analog recorder amplifier gain and to check the digital recording system, thus completing calibration.

When the limbs of the dummy start to perform the specified limb motion routine, the outputs of the load and position transducers are monitored on the oscillograph. When the test director is satisfied that the dummy is performing the motion correctly and repetitively, the director presses the digital record button and starts recording. The digital data representing the measured values are later reduced by the computer to values of suit torques, dummy velocities, and accelerations. By recording only selected portions of the data, the computation burden is reduced. Before the digital data are sent to the computation lab, the data may be played back through digital to analog converters and recorded on the oscillograph. This feature permits additional editing and also serves to check the performance of the digital system, thus ensuring a valid test and further reducing expensive computer time.

Operation of the data system for exoskeletal position and reach testing is similar to suit torque test operation. The sample and hold feature is valuable in reducing the total data recorded during exoskeletal testing since the test subject wearing the exoskeleton may require some practice before he can perform the desired exercise repeatably. In reach testing, it is possible to obtain on-line plots of the reach envelope at constant elevation using a conventional plotter.

For mechanical load distribution testing, the three units needed are the control console, the display manikin, and the digital/analog recording system. After the units are connected together and a selected group of skin force transducers and exoskeleton potentiometers are connected, the system is ready for calibration. This is accomplished by setting the calibration signal dial on each channel of the signal conditioner to the calibration constant previously determined in the laboratory. Next, the residual output of each force transducer is balanced out by dialing into the signal conditioner the zero force output determined in the laboratory. The signal conditioner function switch is moved to the standardize position, generating a voltage representing 80% of full scale for each transducer. This signal is used to set the analog recorder amplifier gain and to check the digital recorder. Additional signals are used to standardize the light segments on the manikin by adjusting the gain of the light segment driver amplifier until an amplitude comparator lamp glows. This technique standardizes the display system without dependence upon visual observation, thus completing calibration.

When the test subject starts to perform the specified exercise routine, the outputs of the force transducers are indicated on the display manikin as intensity modulated light. Concurrently, the output of the force transducers and the exoskeleton position transducers may be monitored on the oscillograph. While the test subject is exercising, the test director observes the display looking for brightly illuminated areas indicating high skin pressure. For example, if when the test subject moves his arm back and forth, the lights in the shoulder area of the manikin change intensity, the test director would note that at some angle the light intensity

distribution maximizes. With the arm at this angle, the data are arrested through the sample and hold circuitry. It is now possible to study the force distribution at leisure and in detail by reading the numerical values of the forces and angles using the steady state monitor. The test director can decide to record the stored information on magnetic tape or free the data sample and continue observing the time variant force patterns on the manikin. At the completion of the test, the recorded digital data may be played back for additional editing and study. The edited digital tape is then sent to the computation center for final data reduction.

When adjusting the suit, the manikin display can be used to correlate the test subject's comments with the indicated forces, thus expediting and quantifying the fitting procedure. These data may also be recorded if a permanent record is desired.

Life Support And Biomedical Test System

The primary objective of manned extravehicular suit testing is to ensure the integration of the life support and functional characteristics of the man-suit system. The principle test objectives for the evaluation of life support are the following.

1. Evaluation of the space suit as a heat and mass exchanger
2. Evaluation of the space suit respiratory exchange environment
3. Evaluation of the physiological performance of man within the system
4. Evaluation of metabolic expenditure in the determination of suit encumbrance

The system required to acquire and process data for these evaluations must be sufficiently versatile to handle the inputs from many types of transducers and instruments as discussed in Section IV and must form an integral part of a complete test facility as described in Section VII.

During the suit testing the data system must not only record the outputs of the many transducers but must also provide on-line displays to monitor the status of the test, the safe condition of the facilities, and the well being of the test subject. In addition, many of the significant parameters for the assessment of suit and subject performance must be calculated from the measured variables, therefore, for speed, accuracy, and convenience the system must be capable of computer entry.

SYSTEM DESCRIPTION

The data acquisition system for life support testing consists of a multicabinet control unit with integral displays and the digital/analog recording system. The

control unit is divided into two major subsystems: the thermal instrumentation and the biomedical monitoring equipment. The block diagram of the complete data system is shown in Figures 126 and 127.

If for some reason it is desired to operate the system without the digital/analog recorder no modification is necessary. All test data required are provided with on-line displays at reduced accuracies. The same data system can be used for all thermal tests whether performed in a space-vacuum chamber, constant temperature enclosure, or at ambient, sea-level conditions.

THERMAL INSTRUMENTATION -- Figure 128 shows the thermal instrumentation housed in two double modular enclosures. These heavy duty mobile enclosures are equipped with casters for moving ease. The racks are completely independent of one another and can be used separately for other testing if desired. Rack 1 contains all thermocouple and thermistor signal conditioning, selector switches, and temperature readouts, while Rack 2 contains all pressure and flow signal conditioning and monitoring. A thermocouple reference junction unit, excitation power supply, and other associated equipment are located inside the cabinets. Input electrical signal connectors and a digital/analog recorder junction panel are located on the sides of the racks in recessed panels. The remaining double rack of the thermal instrumentation contains all of the gas analysis instruments. Rack 3 houses two dew point indicators, a nitrogen analyzer, two oxygen analyzers, their gas sampling systems, and the gas analyzer signal conditioner. Inside this dual cabinet are gas sampling pumps, the dew point, nitrogen, and oxygen sensors, and all the pressure transducers. Both electrical and pneumatic input connections are made through the recessed input side panel, while digital/analog recorder outputs are located on a similar recessed panel. A multiconductor cable connects the two dual enclosures.

For convenience, accurate data storage provisions are made on the digital/analog recorder for manually entering information that will remain constant during the test but appear in data calculations. This is accomplished using the twenty manual entry stations shown as thumbwheel switches on the digital/analog recorder in Figure 122. The input information dialed on these manual stations is recorded each time a data scan is taken. Parameters such as nude and suited test subject weight before and after the test, spirometry information, test suit weight, barometric pressure and other pertinent information can be entered in this manner.

The transducers and instruments used to measure the many variables such as temperature, flow pressure, and gas composition are discussed in detail in Section IV. In general, each different type of transducer is wired to an appropriate signal conditioner which excites, standardizes and zeros the transducers, and provides two output signals for each channel for on-line monitoring and recording.

Temperatures are measured with either thermistors or thermocouples depending upon the temperature range and probe location. Each thermistor probe is wired to a 95 channel signal conditioner for monitoring and recording. All channels are

REF NO	NO.	REQ	NAME OF PART
1	32		THERMISTOR PROBE SURFACE TEMP
2	22		THERMISTOR PROBE SKIN TEMP
3	1		THERMISTOR PROBE RECTAL
4	12		THERMISTOR PROBE 1/2" LENGTH
5	8		THERMISTOR PROBE AIR TEMP
6	12		THERMOCOUPLES CUC SURFACE
7	1		SIGNAL CONDITIONER 16 CHANNELS WITH CAL SIGNAL
8	3		PUSH BUTTON CHANNEL SELECTOR 4 PTS
9	1		PUSH BUTTON CHANNEL SELECTOR 8 PTS
10	2		PUSH BUTTON CHANNEL SELECTOR 2 PTS
11	1		PUSH BUTTON CHANNEL SELECTOR 3 PTS WITH RECORDER SWITCH-ING CONTROL
12	27		METER P.M.S. TYPE
13	1		DIGITAL TEMPERATURE INDICATOR CUC
14	1		POWER SUPPLY 5 VOLTS
15	1		COLD JUNCTION 100 THERMOCOUPLE 12 PTS
16	1		POWER SUPPLY 10 VDC EXCITATION
17	2		SAMPLING SYSTEM CO ₂
18	2		CO ₂ ANALYZER LWA
19	1 SET		CALIBRATION GASES CO ₂ ZERO 8 SPAN
20			SAMPLING SYSTEM HELMET CO ₂
21	1		ANALYZER CO ₂
22	2		SAMPLING SYSTEM O ₂
23	1 SET		SAMPLING SYSTEM O ₂ SPAN, ZERO
24	2		ANALYZER OXYGEN
25	1 SET		CALIBRATION GAS, H ₂ ZERO, SPAN
26	1		SAMPLING SYSTEM N ₂
27	1		ANALYZER NITROGEN
28	2		FLOWMETER ELEMENT GAS
28A	2		FLOWMETER ELEMENT GAS
28B	1		FLOWMETER ELEMENT WATER
29	3		POWER SUPPLY CAL SIGNAL
30	3		PURGE METER
31	2		ZCO ELECTRODES SERIES 130
32	1		ECG CAL. SIGNAL GENERATOR
33	1		AUDIO MONITOR & ALARM
34	1		SIGNAL CONDITIONER BIO MEDICAL, 5 CHANNELS
35	1		OSCILLOSCOPE, 2 CHANNEL FUNCTION SELECTOR
36	1		HEART RATE CAL. SIGNAL GENERATOR
37	1		HEART RATE SELECTOR
38	1		HEART RATE MONITOR
39	1		RESP RATE MONITOR
40	1		RESP RATE RATE TRANSDUCER
41	1		RESP RATE RATE CAL. SIGNAL GENERATOR
42	1		RESP RATE RATE MONITOR
43	1		BLOOD PRESSURE TRANSDUCER
44	1		BLOOD PRESSURE CUFFING SYSTEM
45	1		BLOOD PRESSURE MONITOR
46	10		MOBIDAC IV MANUAL ENTRY STATION
47	1		DIGITAL RECORDER JUNCTION PANEL
48	1		ANALOG RECORDER 8 CHANNEL
49	1		PRESSURE TRANSDUCER LVDT
50	1		DIFFERENTIAL PRESSURE TRANSDUCER LVDT
51	1		PRESSURE SIGNAL CONDITIONER 14 CHANNELS
52	2		POWER SUPPLY 25 VDC EXCITATION
53	1		DEW POINT MEASURING SYSTEM
54	2		SAMPLING SYSTEMS DEW POINT
55	2		SIGNAL CONDITIONER GAS ANALYSIS 8 CHANNELS
56	1		1/2" TAPE RECORDER 4 CHANNEL
57	1		TONE CODE-AUDIC CONVERTER
58	1		TV CAMERA
59	1		ZOOM, PAN-TILT UNIT
60	1		CAMERA CONTROL
61	1		ZOOM CONTROL
62	1		PAN-TILT CONTROL
63	1		TV MONITOR
64	1		EMERGENCY RECORDER CONTROL UNIT
65	1		DIGITAL DATA RECORDER 200 CHANNELS

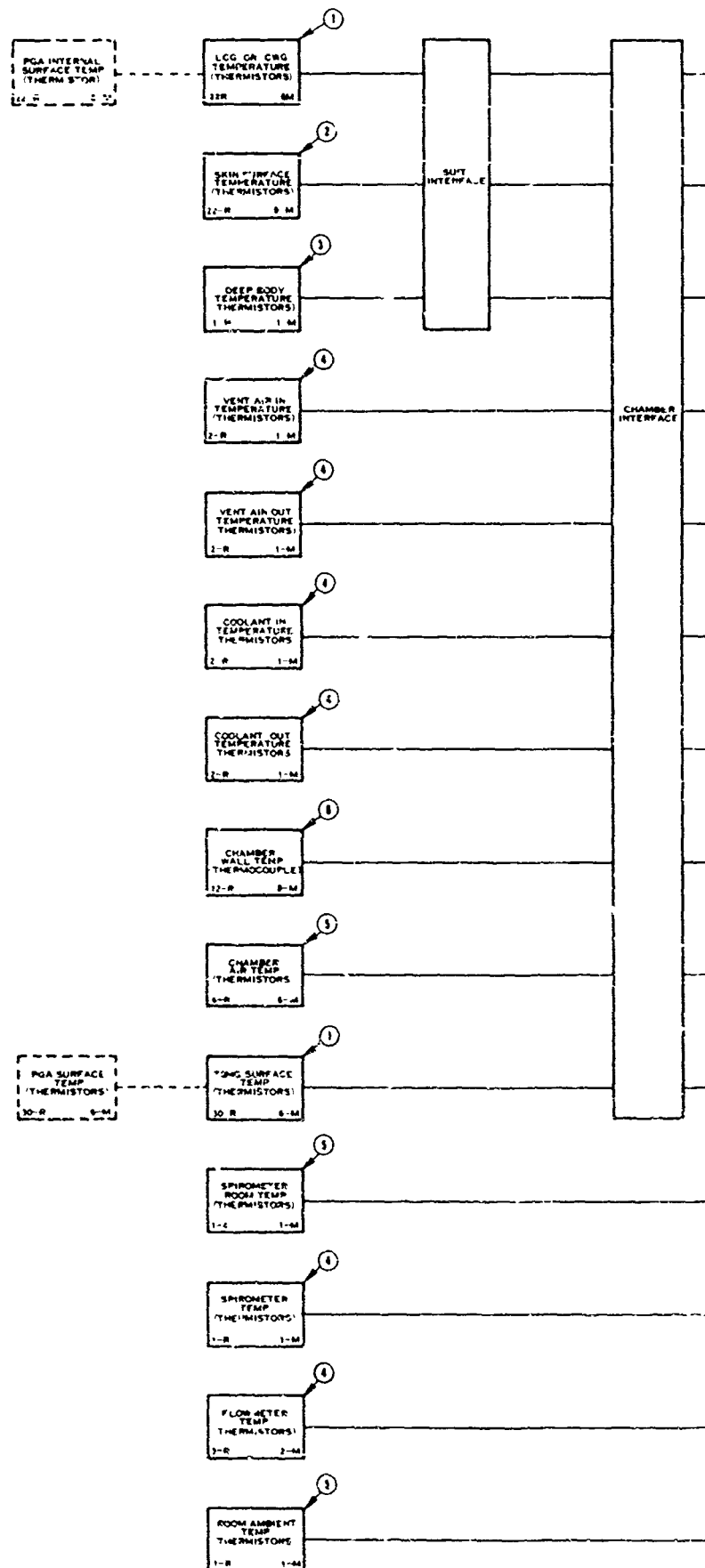
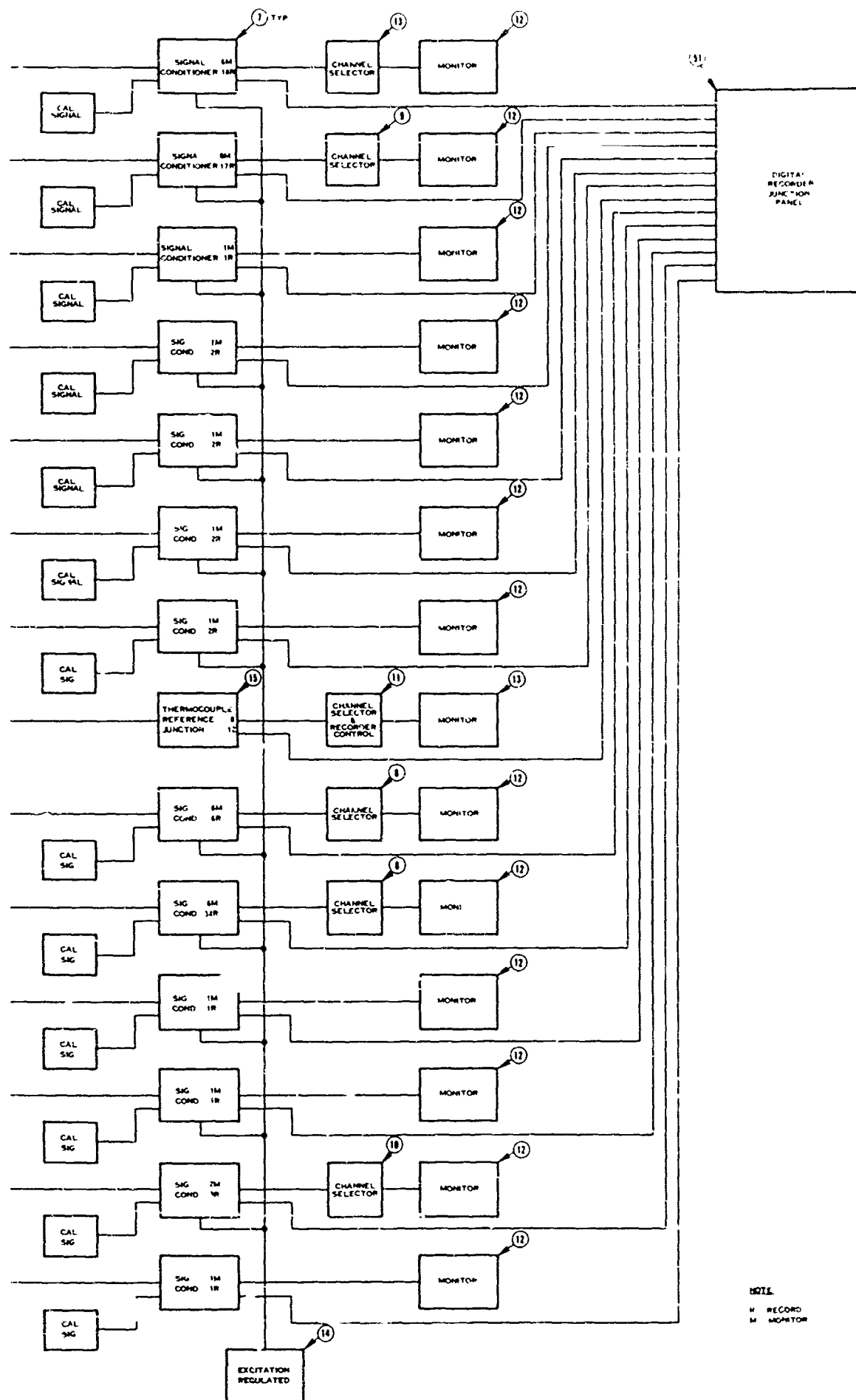


FIGURE 126. LIFE SUPPORT DATA SYSTEM BLOCK DIAGRAM, PART I



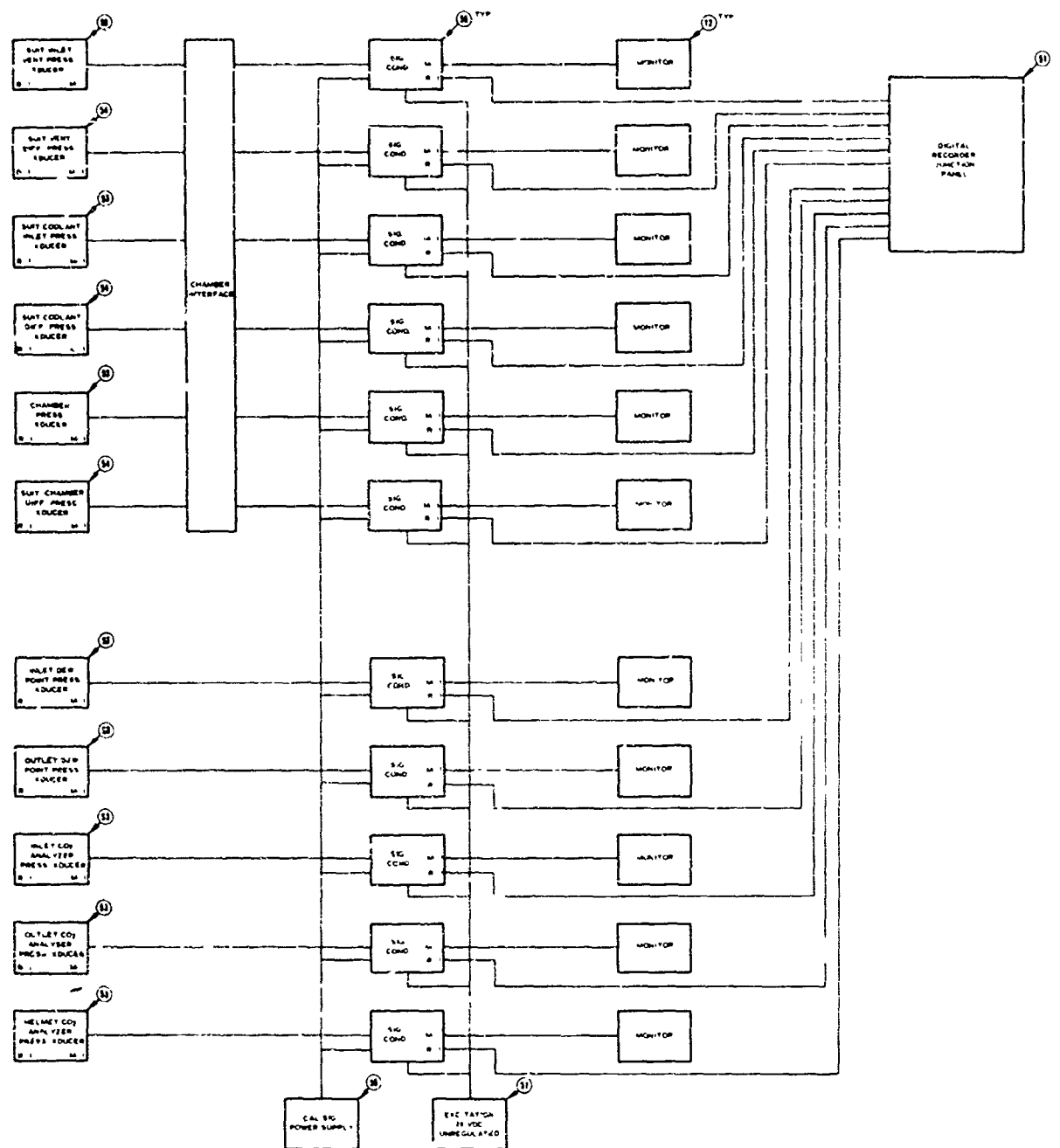
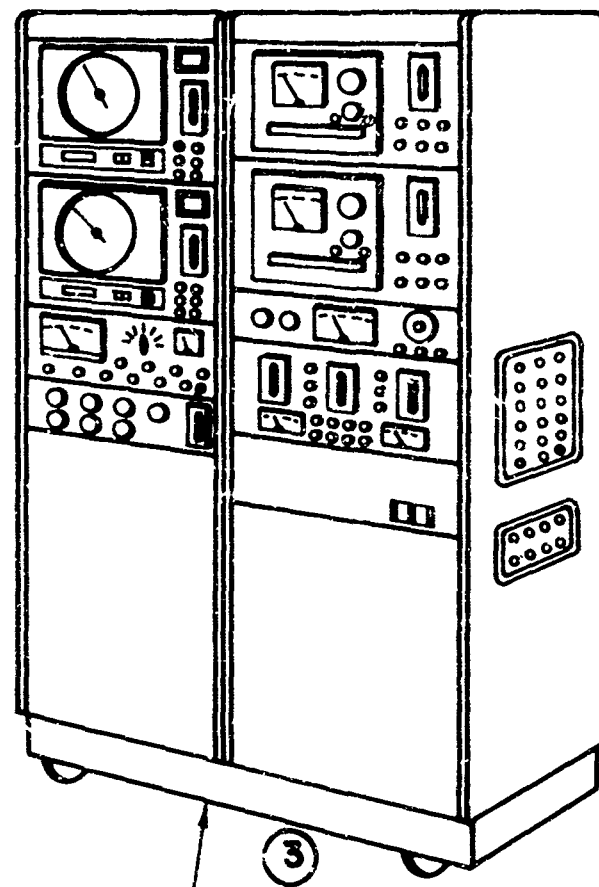
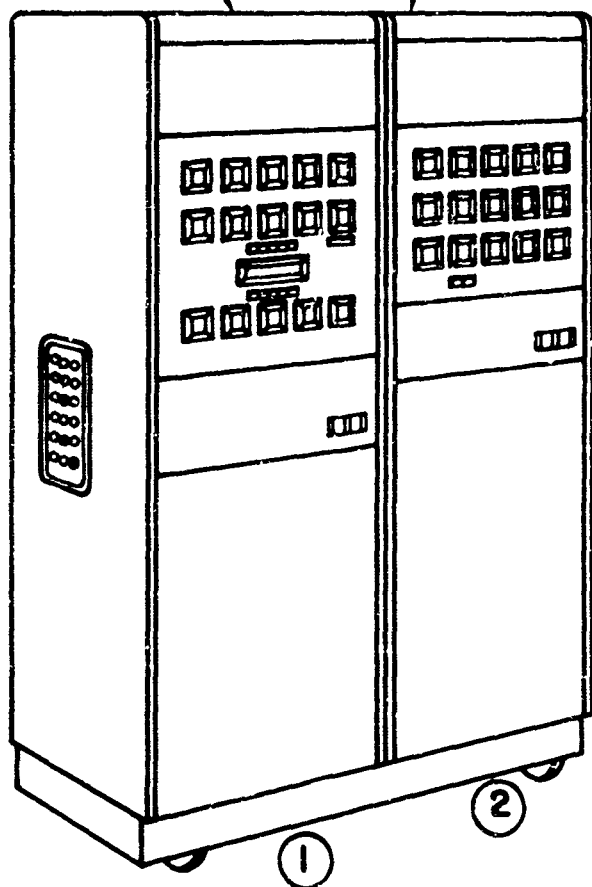


FIGURE 127. LIFE SUPPORT DATA SYSTEM BLOCK DIAGRAM, PART II

TEMPERATURE
READOUTS

FLOW & PRESSURE
MONITORS



GAS ANALYZERS
AND SAMPLE PANELS

FIGURE 128. THERMAL INSTRUMENTATION

standardized simultaneously by resistance substitution and all probes may be interchanged without loss of accuracy. The thermocouples are wired to a copper-constantan reference junction unit which maintains the reference junctions at 0°C. The outputs of the junction unit are routed to the recording system or may be individually selected for display on a null balance indicator.

Pressures are measured with differential transformer type bourdon tube or bellows transducers, depending upon the pressure range. The output of each transducer is routed to the multichannel pressure and flow signal conditioner as a high level DC signal. The signal conditioner supplies unregulated DC transducer excitation and directs the conditioned signal to the recorder and a panel display meter.

Flow is measured with thermal anemometer-type transducers. As with the pressure transducers, the conditioned output signals are directed to the recorder and to panel displays. These outputs can also be recorded on the oscillograph to observe the waveform of respiratory flow when the transducer is so installed.

Water, oxygen, carbon dioxide, and nitrogen partial pressures are measured with individual instruments each of which has a self contained meter display. Outputs from each instrument are routed to signal conditioners for recording. Several of these instruments have an internal null balance control loop. When this loop is unbalanced, the output signal does not represent the input quantity; therefore, the system includes a blanking circuit which blocks the signal to the recorder when the analysis instrument is unbalanced beyond a specific tolerance band.

BIOMEDICAL MONITORING EQUIPMENT -- The biomedical monitoring system is used by the medical monitor to observe the physiological status of the test subject during suit testing to ensure that the subject is not stressed beyond safe limits.

There is considerable controversy concerning the number and type of physiological measures necessary to monitor the test subject adequately. It is not the intent of this report to recommend which measures are of most value, but instead, to present techniques for their measurement. Even in this area, there is debate concerning the best biomedical transduction techniques. Rather than discuss all possible techniques, only those techniques which have been used with some success for space suit testing are presented. The measures that all agree are required for adequate monitoring are heart rate, deep body temperature, visual observation of the subject, and voice communication with him. The measures on which there is a controversy include electrocardiography, pneumography, and blood pressure; it is these which are the most difficult to measure accurately and consistently.

The biomedical monitoring equipment is designed to indicate and/or record all of these measures at the biomedical console. The system consists of signal conditioners, a closed circuit television monitor and its controls, an emergency control panel, a four channel tape recorder, two channel oscilloscope, eight channel direct writing analog recorder, and miscellaneous power supplies.

The block diagram of the medical monitoring system is shown in Figure 129. The instruments are housed in a dual rack as shown in Figure 130. One rack contains the television monitor and controls, emergency control panel, and tape recorder. The remaining cabinet houses the oscilloscope with gating amplifiers; a programming pin board; separate modular signal conditioners for ECG, blood pressure, heart rate, respiration rate, and deep body temperature; a direct writing eight channel analog recorder; a writing surface; and miscellaneous power supplies. The medical monitoring enclosures are equipped with cooling blowers and recessed, side mounted, connector panels.

The accuracy of the various meter read-outs located on the biomedical console is $\pm 2\%$ while all channels being recorded on the direct writing recorder are $\pm 3\%$ of full scale.

Heart Rate -- The heart rate signal is derived from the output of an ECG channel, either axillary or sternal. This signal is conditioned and displayed on a meter located on the front of the conditioner. The meter has high and low limit controls to actuate a visual and audio alarm and start the analog recorder. The signal conditioner also has an output to be used by the digital/analog recorder. Front panel controls are available to adjust trigger level and damping.

Deep Body Temperature -- Deep body temperature will be read out on the biomedical monitoring equipment console. This is in addition to the readout on the thermal instrumentation console. It is also equipped with high and low limit control to actuate an audio and visual alarm. A probe similar to Yellow Springs Instruments Model 401 is used.

Closed Circuit TV -- The closed circuit television system consists of a conventional hermetically sealed camera complete with zoom lens, pan and tilt motors, a camera control panel, and a 17 inch rack-mounted TV monitor. The system is a 20 MC bandwidth type with 800 x 700 lines resolution. The zoom lens has a range of 15 to 150 mm at f2.8. All camera controls are arranged within convenient reach of the medical monitor. The 17 inch rack-mounted monitor will be located at the top of the medical monitoring console as shown in Figure 130 at an angle of approximately 20 degrees.

The communications system used during testing is provided by the test facility. Connection to the system is possible through a side panel-mounted connector with outlets available on each console for headset plug-in.

Electrocardiography -- The ECG probes used on the test subject are of silver/silver chloride construction with reusable "floating" electrodes which are capable of being processed to ensure that no more than 1 millivolt differential between electrodes can be measured in a normal NaCl solution (ref. 31). Six Space Lab Model 101 electrodes or equivalent are used. One set (two probes) will be attached to the subject as axillary leads, while the other is used as sternal leads with dual back-of-neck ground electrodes. The signals obtained are to be condi-

tioned in a module where calibration and simulation signals are available for read-out on the various indicators and recorders used. These devices have two channels of the direct writing analog recorder, two channels of the oscilloscope, and two channels of the tape recorder. The simulation signal mentioned above is of the heart waveform type equivalent to that incorporated in the Sanborn Model 116E signal generator.

Blood Pressure -- Blood pressure is measured using an automated occluding cuff with built in microphone. Oxygen is used for cuff pressurization to eliminate the possibility of other gases leaking into the suit. Both cuff pressure and the microphone output signals are connected to the blood pressure signal conditioning module. The output recorded signal of the system is a DC voltage ramp corresponding to cuff pressure with the "Korotkoff" sound signals superimposed on the ramp. The composite signal is recorded by the analog recorder. A pair of meters is located on the conditioner to indicate systolic and diastolic levels. A cuff pressure control system is located in a separate module and contains all necessary pneumatics for automatic operation of the system on a manual or timed basis.

Respiration Rate -- Respiration rate is measured with an impedance pneumograph using two or three standard ECG electrodes. This system uses a high frequency, low voltage excitation source to measure changes in thoracic impedance during a respiratory cycle. The respiration signal is conditioned and the rate is indicated on a meter provided with limit controls. These limit controls, both high and low, are used to actuate an audio and visual alarm when preset points are exceeded. The signal conditioner also provides an output signal in the form of an undistorted respiratory pulse to be recorded by the analog recorder.

Analog Recorder -- The analog direct writing recorder is a basic eight channel, solid state, direct writing, hot stylus recorder with added marker pens to display digital time code and one second timing pulses. The paper drive is capable of being operated manually, by a timed program, or by remote control. The drive system is mounted vertically and able to operate at speeds from 0.25 mm/sec to 100 mm/sec. The driver amplifiers are the solid state, plug-in type with frequency response of DC to 100 cps and enough sensitivity to drive the galvanometer to full deflection with 0.1 volts at the input.

Monitoring Oscilloscope -- The two channel oscilloscope will display both channels of ECG continuously. It will use a 17 inch cathode ray tube with a polaroid safety filter to minimize glare. Linearity is 3% or better with sweep rates of 3, 6, and 12 seconds per cycle. The gating amplifiers have an input impedance of 500 kilohms or greater and may be driven either balanced or single ended. Front panel controls include an attenuator control, variable gain control, and position controls.

Biomedical Tape Recorder -- The biomedical monitoring tape recorder is a four channel, solid state recorder using standard 1/4" tape. Both the axillary and sternal ECG signals will be continuously recorded on two channels. The remaining channels will handle time code, and conversation between the test subject and test

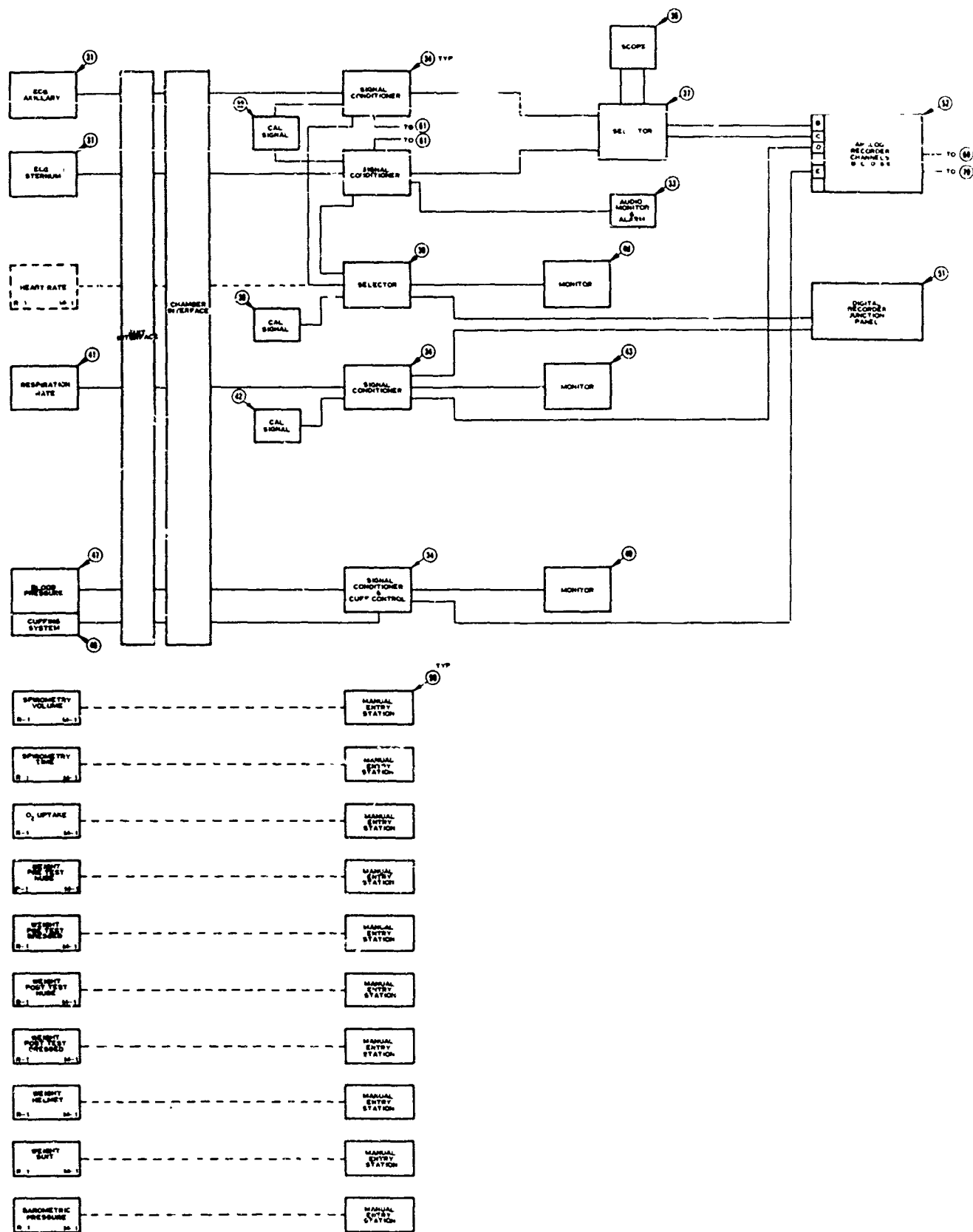


FIGURE 129. MEDICAL SYSTEM BLOCK DIAGRAM

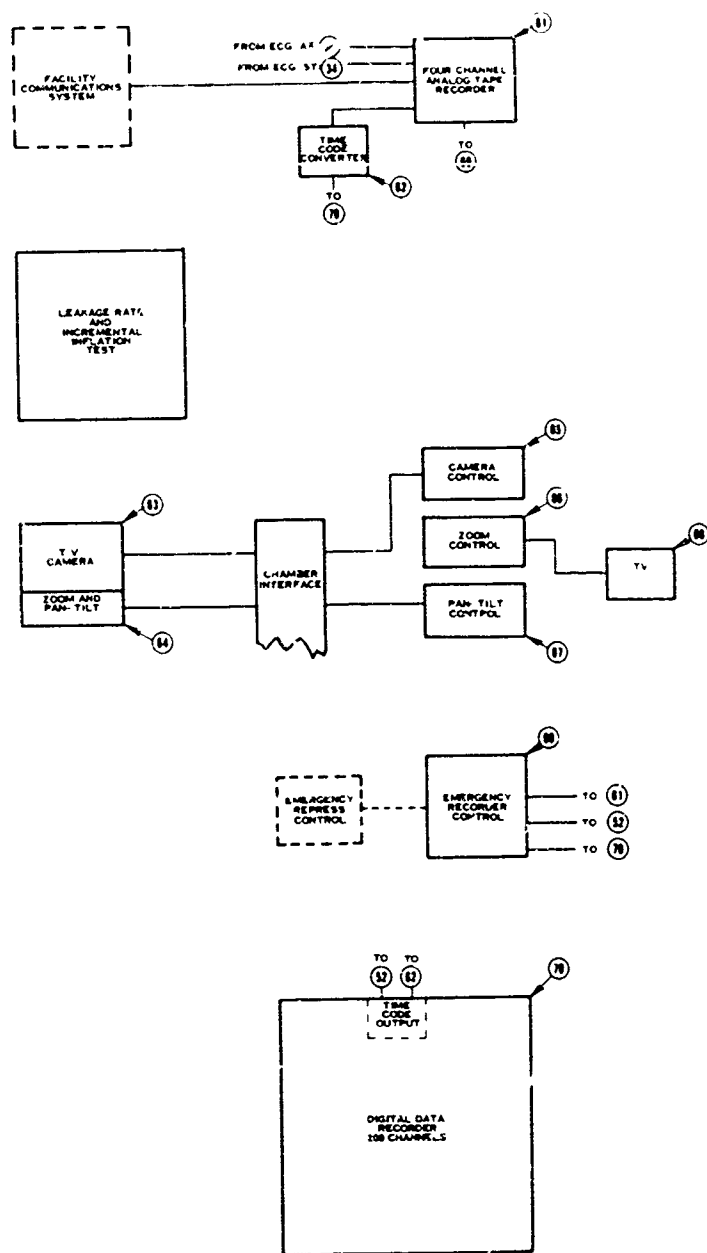


FIGURE 129. (CONTINUED)

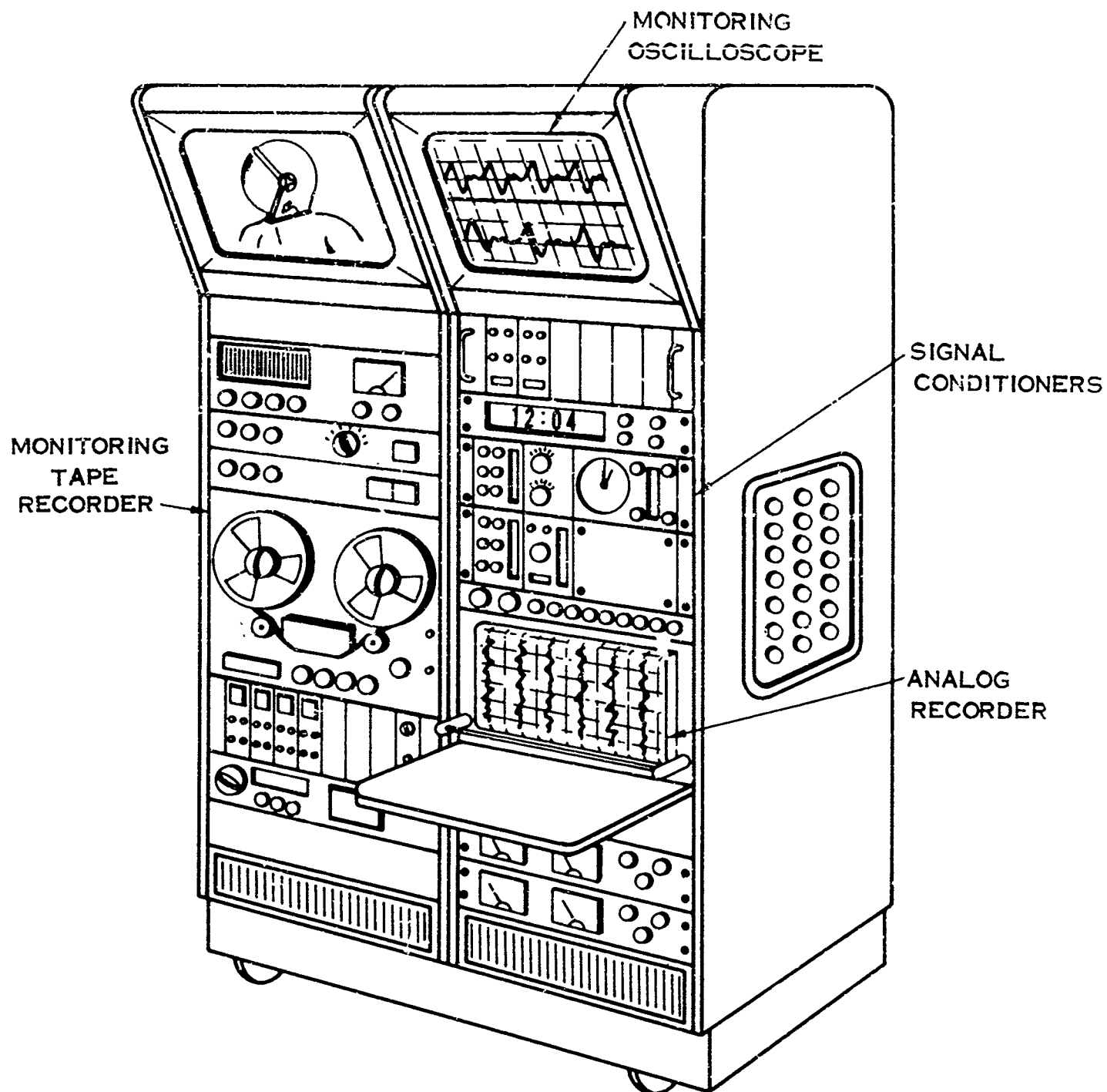


FIGURE 130. MEDICAL MONITORING INSTRUMENTATION

personnel. The FM frequency response will be at least 0 to 300 cps, adequate for faithful ECG reproduction, while the AM response is 50 to 5000 cps at a tape speed of 1 7/8 ips. Total harmonic distortion should not exceed 1.5%.

Emergency Control Panel -- An emergency control panel is located on the medical monitoring console. The function of this panel is to provide emergency repressurization and record control. A red illuminated recessed button with safety pin interlock and emergency communications system switch will be provided on this panel. This panel also affords automatic analog, digital, and voice recorder starting in the event of an emergency.

SYSTEM OPERATION

Prior to the start of thermal testing, the test subject undergoes the normal pretest physical check as deemed necessary by the medical monitor. Certain parameters such as suit and helmet weights, barometric pressure, date, etc., should be entered in the digital/analog recording system with the manual entry stations. The various gas analyzers are aligned and calibrated. Medical monitoring and test transducers are applied to the test subject and the entire instrumentation system is standardized. The pretest preparation of the test subject and suit is one of the most important phases of the test. Without proper transducer installation and suit adjustment the test may be aborted. The deep body thermistor probe should be well lubricated and firmly taped in place after insertion. To avoid spurious signals, the ECG and pneumograph probes must be carefully applied by mildly abrading the skin to achieve lower surface resistance and installing the electrodes using a sufficient amount of ECG paste similar to that manufactured by the Burton Parsons Company. Skin temperature probes should next be applied followed by the undergarment with its necessary temperature measuring probes (ref. 107).

During the actual testing, the instrumentation will be standardized at least every four hours and necessary corrections made by the realignment of instruments and/or signal conditioners at that time. Most of the test data displayed may be monitored during the test, while all of the pertinent data will be recorded on the digital/analog recording system. Following the test, post-test weights must be taken and the complete instrument system again standardized. All transducers should be carefully removed, inspected, and cleaned for future use.

All transducers, indicators, recorders, and analyzers should be provided with a laboratory calibration at a period of not more than 60 days. Transducers should be removed and calibrated using secondary standards when possible. Indicators and recorders require calibration using signal sources of at least ten times the accuracy of the instrument. All gas analyzers require a multipoint system calibration in place, using special calibration gas directly traceable to the National Bureau of Standards.

Biomedical monitoring equipment used in this installation should also be calibrated and its performance observed using simulated signals to duplicate actual test conditions.

Digital/Analog Recording System

The digital/analog recording system is used with both the mechanical control console and the thermal and medical monitoring consoles. This system provides the link between the analog transducer output and the computer and also permits quick-look editing of the data using an oscillograph.

BASIC SYSTEM DESCRIPTION

The digital/analog recording system will accept either 40 channels of high level (0 - 5 volts) or 200 channels of low level information (± 5 millivolts to ± 100 millivolts). The 40 channel high level system is used for moderate frequency time variant data like the exoskeletal data with a sampling rate of 375 samples/sec/channel. The 200 channel low level system is used for quasi-steady state data like the thermal data with a sampling rate of 75 samples/sec/channel.

A block diagram of the digital/analog recording system is shown in Figure 131 and a pictorial sketch in Figure 122. The system contains the following sub-units

1. High Level Multiplexer
2. Low Level Multiplexer
3. Analog to Digital Converter
4. Data Format Unit
5. Magnetic Core Memory
6. Tape Format Unit & Write Amplifiers
7. Magnetic Tape Transport
8. Tape Error Analyzer
9. Digital to Analog Converter
10. Oscillograph

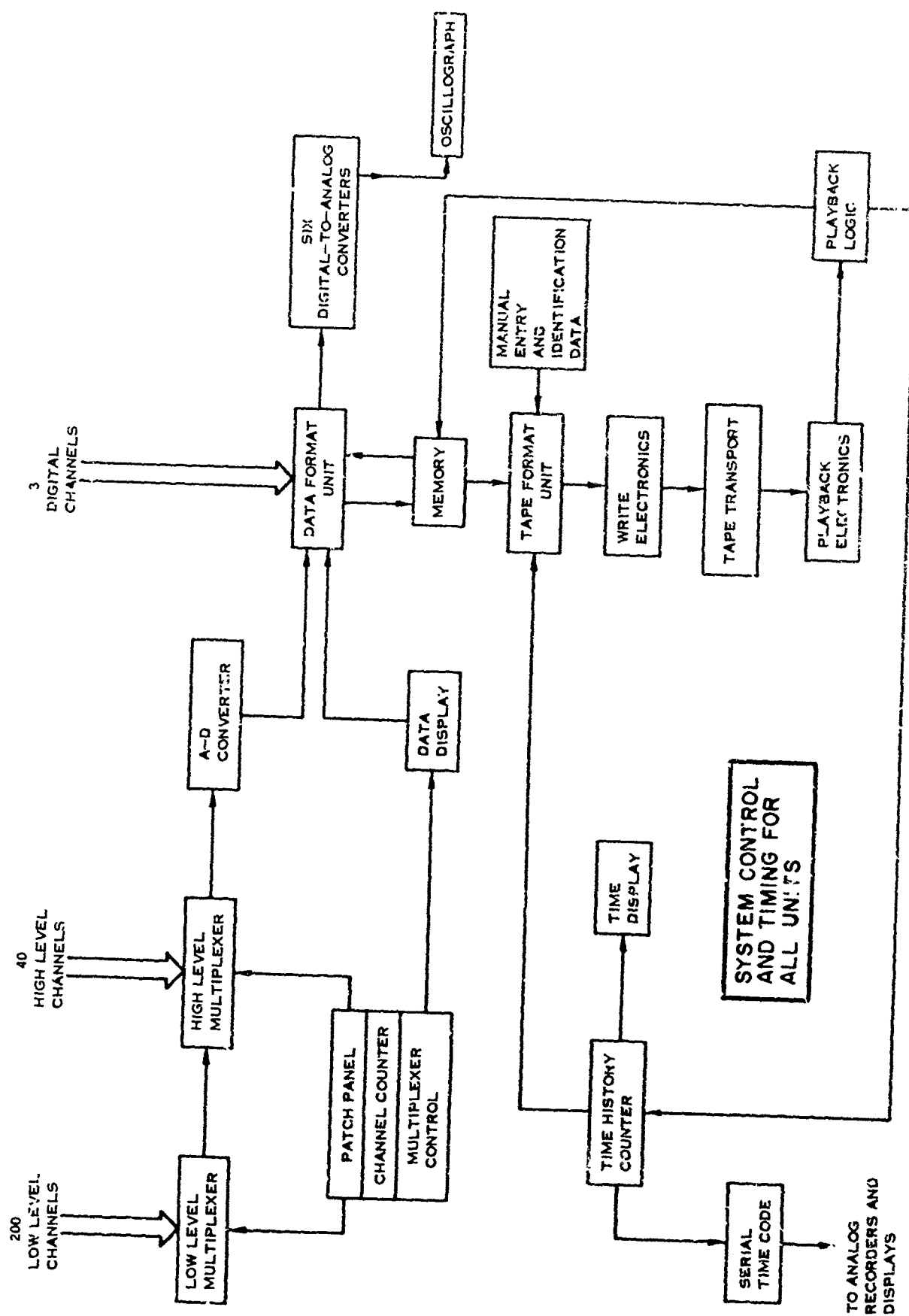


FIGURE 131. DIGITAL/ANALOG RECORDING SYSTEM BLOCK DIAGRAM

In the recording system the analog data is multiplexed, amplified, and presented to the analog to digital converter for coding to an eleven bit and one sign binary code and is presented to the data format unit with the digital inputs. The data format unit contains a binary to decimal converter to drive a nixie display and a secondary output to the six digital to analog converters that drive six oscillograph channels. The primary data path transfers the data to memory in serial form where it is stored for formatting by the tape format unit. The tape format unit accepts inputs from memory, the time history counter, and the manual entry stations and formats them for recording on the magnetic tape transport in gapped form.

A read-after-write tape analyzer checks all tapes being recorded or played back for lateral parity error, longitudinal parity errors, characters per record, and packing density.

In the playback mode the data coming off the tape is loaded into memory and unloaded at approximately the same rate at which it was sampled. The time at the beginning of each record will be decoded and displayed. A BCD serial time code will be provided for the oscillograph.

BASIC SYSTEM SPECIFICATION

Number of Channels (depending on sampling rate)

Low Level Analog	200, 100, 50
High Level Analog	40, 20, 10, 5
Manual Entry	20
Digital	3

Input Voltage

Low Level Analog	± 5 , ± 10 , ± 50 , ± 100 millivolt ranges
High Level Analog	0 - 5 volts
Digital	0 or 6 volts (1-2-4-8 BCD)

Input Impedance

Low Level Analog	greater than 1 megohm
High Level Analog	greater than 1 megohm
Digital	1 kilohm

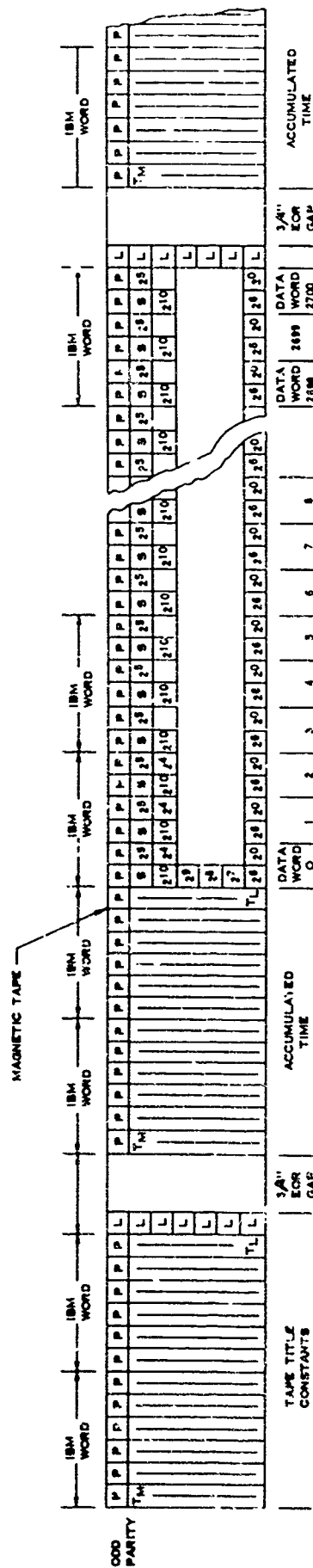
Sampling Rates

Low Level	See Multiplexer Specification
High Level	Maximum of 15 kc

Sampling Program	For normal configuration: 1 bit plus sign binary, 450 characters per record, 556 bits per inch on 1/2 inch 7 track IBM compatible tape
Data Display	A nixie display will display any input channel in decimal form while data is being acquired
Time History Counter	A time history of milliseconds, seconds, minutes, and hours will be provided. Time will be inserted at the beginning of each record
Identification Data and Manual Entry	Twenty thumb wheel switches will be provided for manual data entry
Quick-Look	Six digital to analog registers will be provided for quick-look capability. The accuracy will be 1% of full scale driving optical oscillograph galvanometers. Provisions for zero adjustment 0 - 90% full scale and gain adjustment 10 to 1 will be provided. The data playback will be ungapped and within 3% of real time
System Accuracy	
Short Term	0.12% full scale $\pm 1/2$ least significant bit
Long Term	0.22% full scale $\pm 1/2$ least significant bit

DIGITAL TAPE FORMAT

Before presenting a detailed discussion of the major system components, it is well to review certain characteristics and definitions of digital systems. Data is recorded on digital tape in the form of bits (a contraction of the term binary digit). A binary digit is represented as either 0 or 1. One or the other number is represented by the magnetic condition of a small area on the tape. The recording areas across the width of the tape are located on seven parallel tracks as shown in Figure 132. Each strip across the tape therefore consists of seven bits and is called a character. Six bits hold data, while the seventh is a parity check bit. A parity bit is added, if necessary, to keep the number of bits written in any character an odd integer. By continuously monitoring the number of bits per character, the parity check circuit can identify flaws, "drop-outs," on the tape. Recording density in the longitudinal direction (along the length of the tape) is determined by the bit packing density. A typical bit packing density is 800 bits per inch (bpi). The standard IBM word uses six characters. However, the proposed system would use



CONSTANTS ARE BINARY CODE
PACKING DENSITY 800 BITS INCH

P - PARITY
T - TIME
S - SIGN
L - LONGITUDINAL REDUNDANCY CHECK
TM - MOST SIGNIFICANT BIT
TL - LEAST SIGNIFICANT BIT
EOR - END OF RECORD

TAPE DIMENSIONS:
1/2 INCH WIDE, CONTAINING SEVEN PARALLEL TRACKS
2400 FEET LONG
1.5 MIL BASE THICKNESS (1 MIL EQUALS 1/1000 INCH)

FIGURE 132. BINARY FORMAT - DATA WORDS OF 11 BIT PLUS SIGN

two characters or twelve bits per data word, that is 11 bits and a plus or minus sign. This data word would represent one transducer's output at one instant of time. The generated tape is gapped to facilitate computer handling of the data. This gap is a 3/4 inch dataless piece of tape used to allow the tape transport time to start and stop without loss of data.

MAJOR COMPONENT DESCRIPTIONS

MULTIPLEXERS -- Multiplexing is defined as the sharing of a single information handling facility by several information channels. In this case we are concerned with time division multiplexing or sampling. The multiplexer serially samples the analog outputs of many transducers creating a serial pulse train representing the outputs of the transducers.

The errors associated with multiplexing center about the sampling rate. Both theoretical and empirical studies of optimum sampling rate have been made (refs. 40, 73, 72) which have yielded general guide lines for selection of the sampling rates required to achieve specified accuracies. The reduced data accuracy of a sampled data system is primarily affected by the three error sources described below.

The first error is that of omission where the incoming data is truncated or desired information is omitted. The second error is that of commission where the sampling rate is too low and the sampled data spectrum and the original data spectrum overlap. This error source is also called aliasing error or foldover error. If the sampling rate is adequate, a large guard or vacant band will exist between the original data spectrum and the sampling generated spectra. This guard band permits utilization of realizable filters to separate the desired spectrum from the other spectra present after sampling. This guard band must be sufficiently wide to permit the actual filter used to reject all but a negligible fraction of the undesired signal. The third error is that of interpolation. Since each data point is sampled sequentially, no two data points are taken at the same time. For accurate computation all the parameters must be referenced to the same point in time. Thus the system must interpolate between sequential data points. The error associated with interpolation is a function of the sampling rate (samples/cycle) and the method of interpolation.

To utilize the sample rate selection techniques that have been developed, the cut off rate of the sampled data source must be known. This rate is described in 6 db/octave units with each unit called an order. For example, 6 db/octave is called first order data and 12 db/octave is called second order data. For $\pm 0.2\%$ composite sampling rate error, first order data requires a rate in excess of 10,000 samples/cycle of the highest frequency of interest. Thus for frequency components of 30 cps a sampling rate of 300 kc is required. This fantastically high sampling rate is due mostly to the restraints needed to avoid foldover or commission error. To reach a reasonable sampling rate the incoming data to the multiplexer or

sampler must be of fourth or higher order. To change the first order data of a thermocouple or the second order data of a strain gage pressure transducer to fourth order, presampling filters must be used. By proper choice of presampling filter cut off frequency, no data of interest is lost. The sampling rate is then selected to reduce errors of commission and interpolation to the levels required to achieve the specified accuracy. Two types of multiplexers to perform this time shared sampling of the data are required: one for low level signals and one for high level signals.

Low Level Multiplexer -- The low level multiplexer is designed to accept signals from transducers such as strain gages and thermocouples. These low level signals are scanned at a rate determined by the programming patch panel. The same digital patch panel allows the operator to program both the number of channels to be sampled and the sequence in which they are sampled. The specifications for the low level multiplexer are as follows

Number of Channels	200, 100, 50 (depending on sampling rate)
Channel Sampling Rate	75, 150, 300 samples/sec
Input Voltage Levels	± 5 , ± 10 , ± 20 , ± 50 , ± 100 millivolt ranges
Input Impedance	greater than 1 megohm
Linearity	$\pm 0.035\%$ full scale
Temperature Coefficient	± 2 microvolts/degree F or less between 65°F and 95°F
Crosstalk	0.02% full scale or less
Noise	5 microvolts or less when referred to the input on the highest gain setting
Zero Drift	± 1 microvolt/degree F referred to the input

High Level Multiplexer -- The high level multiplexer is designed to accept signals from high level transducers such as potentiometers. Patch capability is similar to the low level multiplexer. The specifications are as follows

Number of Channels	40, 20, 10, 5 (depending on sampling rate)
Channel Sampling Rate	375, 750, 1500, 3000 samples/sec
Input Voltage Level	0 - 5 volts
Input Impedance	1 megohm

Linearity	0.0125% full scale
Crosstalk	±1 millivolt peak to peak
Noise	±1 millivolt peak to peak
Zero Drift	0.0175% full scale/degree F

ANALOG TO DIGITAL CONVERTER -- The analog to digital converter accepts the sequentially sampled analog signals from the high and low level multiplexers and converts them to an 11 bit plus sign digital code. The encoder operates on a successive approximation principle. The input analog signal is compared to an internal voltage reference which is equal to one half of full scale. If the input analog signal is greater than one half of full scale, an additional comparison is made at one half plus one fourth full scale, and at this point another decision is made. If the comparison indicates that the analog signal is less than the three fourths full scale value previously compared, the one fourth reference value is removed and another decision made at one half plus one eighth full scale. This process of comparing the input analog signal against internal references is used to generate a binary code which represents the amplitude of the analog input sample. This code is transmitted from the analog to digital converter to a data format unit which arranges the data into computer format.

The analog to digital converter meets the following specifications

Bit Rate	Up to 249 kc
Word Rate	Up to 15 kc
Channel Input Impedance	100,000 ohms or greater
Output Impedance	1 ohm or less
Gain	Fifty front panel, 6-position gain switches are provided. Each switch will control the gain on four low-level channels. Each switch will have ±5, ±10, ±20, ±30, ±50, and ±100 millivolt positions. Gain trimmers are provided for each channel to adjust the absolute gain accuracy
Linearity	±0.0125% ± least significant bit
Stability	±0.025% per day
Temperature Coefficient	±0.005%/degree from 65°F to 95°F

Chopper Intermodulation	0.02% or less
Common Mode Rejection	$10^7:1$ or greater at DC, $10^6:1$ at 60 cps with a 120 ohm unbalanced input and 1.2×10^{-5} at 60 cps with a 1000 ohm unbalanced input. Common mode rejection shall be independent of the gain setting
Common Mode Voltage	300 volts DC or peak volts AC
Feedback Current	10 nanoamperes or less and adjustable to zero
Channel Offset	An individual adjustment shall be provided for each channel to compensate for 200 microvolt offset referred to input
Overload Current	± 50 ma at the multiplexer input without permanent damage

DATA FORMAT UNIT -- The data format unit receives digital data from the analog to digital converter, external digital inputs, and playback logic. The digital input words are parallel gated to a parallel to serial converter by gate commands from the multiplexer unit.

All data are shifted into a binary storage register and through a binary to digital converter to a BCD storage register. Either of these registers may be gated from a character counter for loading the magnetic core memory. The data display register and the digital to analog converter receive their data from the BCD storage register.

MAGNETIC CORE MEMORY -- The data from the data format unit is presented to a 8 x 2048 magnetic core memory. The purpose of the magnetic core memory is to allow the system to acquire data at a continuous rate while at the same time generating a magnetic tape which is compatible with an IBM computer. The IBM 7090 and similar computers require a minimum gap of 3/4 inch between computer records of data. This inter-record gap is generated by storing the continuous data in a memory, but inhibiting the readout of the memory to the magnetic recorder while the tape recorder itself continues to run at a constant speed.

Data enters the memory at a continuous rate determined by the system configuration which has been programmed into the individual patch program of the format unit. The system output rate is determined by the bit packing density multiplied by the tape speed. A tape transport has been chosen which operates at 75 inches per second. If the data is formatted at 200 bits per inch, the overall character rate on to magnetic tape is 15,000 characters per second. Likewise, if a bit

packing density of 556 bits per inch has been chosen, then a transfer rate of 41.66 kc exists. However, due to the fact that an inter-record gap must exist for computer compatibility, the time allotted for the gap is time in which data may not be recorded onto the output tape. This implies that the rate into the magnetic core memory is less than the data rate out of the memory. However, the average rates of input and output data are equal.

TAPE FORMAT LOGIC AND WRITE AMPLIFIERS -- The output of memory is unloaded and presented to the write amplifier for recording on magnetic tape in computer compatible records. At the beginning of each record, the clock time and data from the identification data are inserted. The characters are presented to the write amplifiers and the magnetic tape recorder.

MAGNETIC TAPE TRANSPORT -- The outputs of the write amplifiers are used to drive the tape transport recording heads. An Ampex TM-4 tape transport is well suited to the data system. This tape transport will operate at 75 ips or 37 1/2 ips as determined by the overall system sampling rate. The specifications are as follows

Speed	37.5 or 75 in/sec
Stop Time	1.8 milliseconds maximum
Start Distance	0.162 to 0.203 inches at 75 ips
Stop Distance	0.03 to 0.10 inches at 75 ips

TAPE ERROR ANALYZER -- The data from the playback electronics are checked for lateral and longitudinal parity errors. A 4 bit error counter checks the number of characters per second and bit packing density. This logic performs all checks during recording and playback modes, thus providing assurance that the system is operating properly.

Occasionally dust particles on the magnetic tape will cause bit drop-outs which will be indicated by the parity check circuit. Generally speaking, only one parity error in 10^6 bits is experienced when using a high quality instrumentation tape. Parity errors may be indicated by the parity check circuit and yet these errors may not be indicated when the tape is read by the computer because the computer may be programmed to re-read each tape when a parity error is indicated. Thus, the computer is able to read tapes to a higher degree of accuracy than most analog data systems.

DIGITAL TO ANALOG CONVERTERS -- Six digital to analog converters are provided for quick-look outputs in both real time and during tape playback. The data from the tape is ungapped to provide a time base with a maximum error of 3 percent. The output signal level is ± 1.5 volts at 100 milliamps. A serial time code is available for time correlation in real time and playback.

OSCILLOGRAPH -- The outputs of the digital to analog converters are routed to a direct writing optical oscillograph such as the Minneapolis Honeywell 1612. This provides quick-look editing of the data. The basic specifications are as follows

Basic Recording Speeds	1, 2, 4, 8, 16 in/sec
Speed Multipliers	0.1, 1, 10
Writing Speed	25,000 in/sec
Frequency	0 - 5,000 cps
Number of Channels	6
Operating Temperature	20°F to 125°F

SYSTEM CHARACTERISTICS

As described in the preceding sections, the data system is composed of the control console for functional suit mechanics tests, display manikin, life support and biomedical control console, and digital/analog recording system. The system is modular in nature and easily connected for the different types of tests. Additionally, being modular in nature, it is readily transportable from one test site to another.

Controls and adjustments have been minimized for convenient set up and operation permitting the test personnel to spend most of their time monitoring the test. The system is designed so that measurements may be added or deleted easily.

The accuracy of the data system is primarily limited by the transducer accuracy. Digitizing the data at the test site helps to preserve system accuracy by preventing the degradation that occurs with analog systems.

The data system should prove highly reliable. It is composed of conservatively designed solid state electronics similar to well proven systems. Generation of computer compatible tapes at the test site tends to increase system reliability further by reducing the total amount of equipment involved, resulting in procurement and maintenance economies.

The digital/analog recording system is a flexible recording system that may be used for other purposes than extravehicular suit testing. By designing new signal conditioning consoles and displays, it can accommodate almost any new task. The digital tape format may also be changed using the output format patch board so that the recorder tape may be used with different computers. Thus, this equipment has the flexibility to perform many data gathering tasks.

Although AMRL does not have a system of this type, several of the system components may be available. Before finalizing a data system design, this possibility should be explored. Current equipment which might be incorporated include an analog skin and mean body temperature recorder, an optical oscillograph, a 14 channel Ampex analog FM tape recording system, and a Bendix time-of-flight mass spectrometer gas analyzer.

CONCLUSIONS ON DATA ACQUISITION SYSTEM

Based on the foregoing study of data acquisition requirements and the system evolved, the following is concluded

1. The detailed specification and procurement of an integrated magnetic tape digital data system should be undertaken to encompass the test needs at AMRL for functional suit mechanical and life support system evaluation.
2. Serious consideration should be given to the expansion of the recommended system to encompass other areas of testing at AMRL.
3. Prior to completion of the final design, instrumentation which may be currently available at AMRL should be studied to determine the extent to which it can be incorporated into the final system.

SECTION IX

CONCLUSIONS AND RECOMMENDATIONS

CONCLUSIONS

The basic objectives of this study were to delineate those critical areas of suit test technology where improved evaluation methods are required; to develop a test methodology for each of these areas; to define and bring into focus vague or misleading concepts in the current methodology of suit testing; to study methods, equipment, facility requirements, and data handling techniques for the implementation of the methodology; and to recommend an overall approach to suit evaluation based on modern instrumentation techniques and facilities which maximize objectivity, accuracy, and convenience. It is well now to review these objectives to determine to what extent they have been achieved.

The study was divided into three broad areas of investigation: functional suit mechanics, life support, and environmental protection. Each of these was further divided to encompass the major performance characteristics of suits. There are an indefinitely large number of tests that could conceivably be conducted on suit materials, components, and systems. These tests can be placed in categories ranging from completely quantitative but unrealistic at one extreme to completely subjective but realistic at the other. In this study, the emphasis has been to fill the current gap which exists between these two extremes with techniques which are accurate and objective but which retain sufficient realism to be of value for the development of improved protective garments.

In each of the areas studied, a test methodology has been conceived and brought to varying states of development and levels of confidence.

Of the three basic areas, functional suit mechanics presents the most formidable problem in the development and implementation of a logical, effective methodology. It is perhaps to be expected since this is the area of suit design that is least understood and in which current suits are most deficient. Much has been accomplished here to define clearly in mathematical form the fundamental nature of the mechanical interface between man and suit. The methodology suffers, however, from a lack of basic, quantitative physiological and engineering data on which to construct effective criteria and judge the soundness of the concepts evolved. Nevertheless, the quantities which must be measured are clear. In all but one case, these measurements are realizable with well developed transduction techniques; however, the implementation of the overall methodology remains a formidable task. New test apparatus are needed, of which some will require considerable effort to obtain the full potential of the methodology. Basic studies are needed to define relationships of measurable mechanical quantities such as torque, angle, and work to physiological needs and limitations. By implementing this methodology, however, a substantial step forward will have been made in suit test technology.

The second basic area, suit life support, presents relatively few equipment problems. All of the required measures can be defined with considerable surety and the techniques of measurement are known. The methodology of suit thermal evaluation, however, is less clear. An objective test procedure necessarily requires compromises in simulation. However, the effects of these compromises are difficult to assess with confidence because the complex thermal interrelationships between man and suit are not well understood and lack quantitative definition. A methodology is, therefore, proposed which attempts to minimize these uncertainties consistent with the requirements for objectivity and convenience and which makes possible through digital data handling techniques the acquisition of accurate, timely, computer-processed test data. Test experience will in time demonstrate the acceptability of this approach and determine what modifications may be required.

In the third basic area, environmental protection, the four principal hazards of space were studied, not to develop a new methodology, but to determine to what extent the current techniques of simulation and testing are applicable to the evaluation of extravehicular garments. Current knowledge of the space environment is fraught with many uncertainties, and with the extensive exploratory programs in progress, environmental models are subject to frequent refinement. The protective capabilities of current suits, however, are such that precise definition and duplication of the environment is in general not required. Evaluation of suit protective capability can be accomplished through combined materials studies and suit tests conducted in specialized test facilities which, with few exceptions, are within the state-of-the-art. Only in the area of meteoroid penetration are more extensive studies needed to establish the degree of simulation required.

In addition to the three basic areas of study, certain suit component test techniques were investigated. It may be generally concluded that the methodology and equipment for these tests present no intrinsic problems. Specific conclusions on each of the component tests are presented in Section VI. Likewise, specific conclusions in each basic study area are presented at the end of each major section or subsection.

Study of the overall facility and data acquisition requirements indicates that an integration of functional and life support testing into a central facility could result in substantial cost and time savings. Centralization of the data acquisition system is particularly desirable.

Versatility, accuracy, convenience, and computer compatibility are the essential features of the proposed digital/analog data recording system which will acquire, condition, monitor, record, and display for editing all of the required basic engineering and physiological measures.

RECOMMENDATIONS

The implementation of the basic torque measurement methodology requires the fabrication of an instrumented articulated dummy and an intra-suit exoskeletal goniometer. Both of these devices will require careful design study. The dummy, in particular, presents many developmental problems in the integration of the actuators, controls, and instrumentation into an anthropomorphic package. It is, therefore, recommended that the dummy development be undertaken in at least two phases. In the first phase a dummy shoulder-arm-hand complex would be fabricated to isolate and solve the basic design integration and development problems. This arm complex could be more than a working model. If successful, it could be of considerable value for the testing and development of actual suit arms. The second phase, of course, would be the fabrication of a complete dummy system.

Concurrently with the first phase, the development of an exoskeletal goniometer is recommended. This would then be available for the programming of the dummy arm and the study of more fundamental torque criteria.

It is strongly suggested that the study of criteria be continued to realize the full potential of the test data that will be acquired.

The methodology for skin pressure distribution testing cannot be implemented until a satisfactory skin pressure transducer is developed. This development should be pursued since a technique for measuring the dynamic interface between man and his environment has application not only to space suit technology but to many other areas as well. It is recommended that the development of other aspects of this methodology be deferred pending the successful outcome of the transducer development.

Basic study of the local microclimate within the suit is needed to understand the relationship between the suit cooling potential and the human heat rejection mechanism. It is recommended that studies in this area, particularly at moderate work levels, be expanded to assess with more confidence the value of the thermal test methodology. These studies could be of even more significance for the optimization of suit cooling systems.

The proposed digital/analog data acquisition system has great flexibility and may be used as a data gathering tool for many purposes. Therefore, it is recommended that the possibility of its more general use be explored before finalizing the data system design.

APPENDIX I

SOME MATHEMATICS OF PIN JOINTED LINKAGE SYSTEMS FOR APPLICATIONS TO EXOSKELETONS AND DUMMIES

INTRODUCTION

In this appendix the basic mathematics required for multiple pin jointed linkage applications is presented. The subjects treated include coordinate systems, vectors, matrices, and applications of these tools to coordinate transformation. Finally, a step-by-step procedure is presented for setting up the transformation equations in a generalized pin jointed linkage system. The treatments are meant for review and to define notation and conventions.

BASICS

Coordinate Systems

To describe the mechanics of a physical linkage system, a coordinate system must be defined in which to represent the properties of the system. The physical properties of the system such as velocities and moments of inertia are unaffected by the choice of coordinates; however, the representations of these quantities are affected. This distinction is essential when operating with vector and matrix components.

The basic coordinate system used in this report is the right handed Cartesian (or rectangular) coordinate system (CS) as shown in Figure 133.

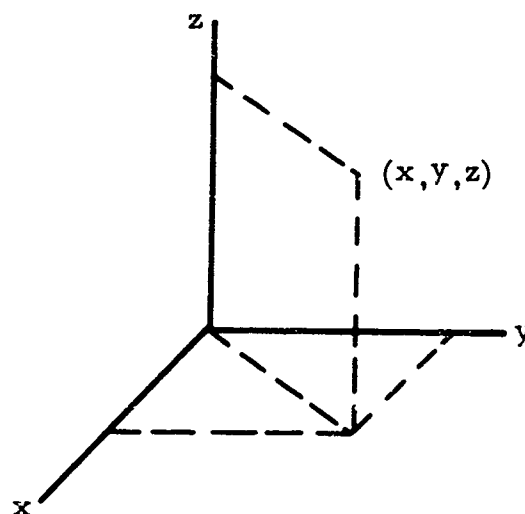


FIGURE 133. CARTESIAN COORDINATES

In a right handed CS a screw with its axis on the z axis will advance in the positive z direction when the positive x axis is rotated into the positive y axis. The location of a point in space is specified by the coordinates of the point (x, y, z) . Depending on the geometry of the linkage problem, the cylindrical or spherical coordinate systems may be more useful. In the cylindrical coordinate system shown in Figure 134 the location of a point is specified by the coordinates (r, θ, z) .

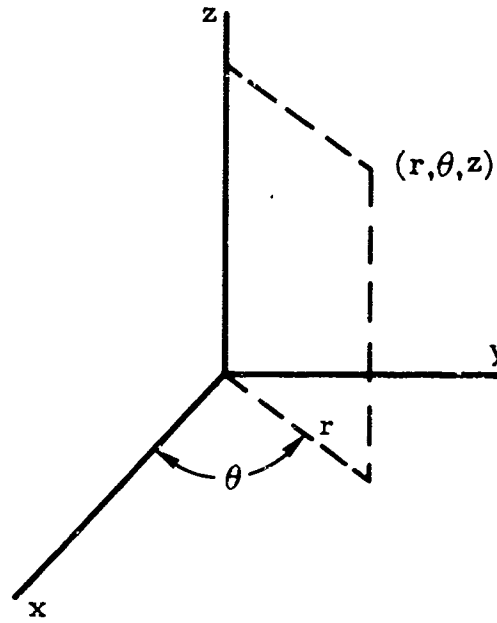


FIGURE 134. CYLINDRICAL COORDINATES

Similarly in a spherical CS, the location of a point is specified by the coordinates (ρ, θ, ϕ) as shown in Figure 135.

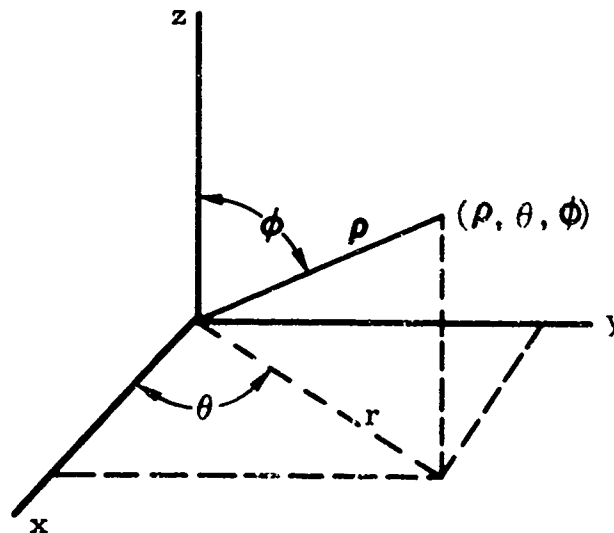


FIGURE 135. SPHERICAL COORDINATES

The coordinates of the point P in the cylindrical, spherical, and Cartesian CS, when erected as in Figure 136, are related by Equations 167, 168 and 169.

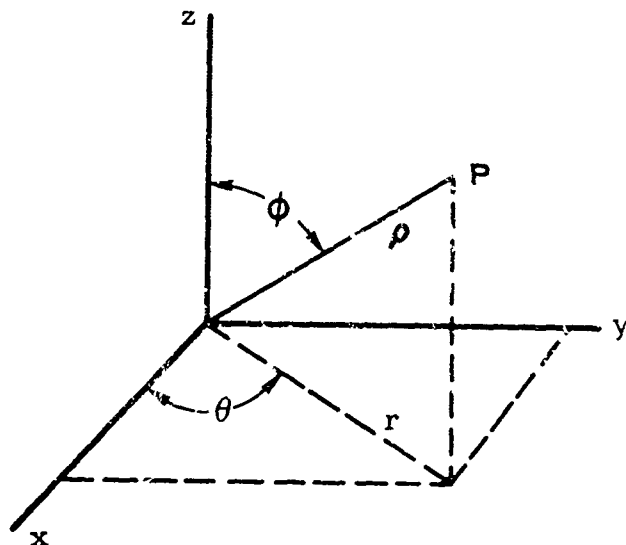


FIGURE 136. RELATIONS BETWEEN COORDINATES

Rectangular - Cylindrical - Rectangular

$$\begin{aligned} x &= r \cos \Theta & r &= \sqrt{x^2 + y^2} \\ y &= r \sin \Theta & \Theta &= \arctan \left(\frac{y}{x} \right) \\ z &= z & z &= z \end{aligned} \quad (167)$$

Cylindrical - Spherical - Cylindrical

$$\begin{aligned} r &= \rho \sin \Phi & \rho &= \sqrt{r^2 + z^2} \\ \Theta &= \Theta & \Theta &= \Theta \\ z &= \rho \cos \Phi & \Phi &= \arctan \frac{r}{z} \end{aligned} \quad (168)$$

Rectangular - Spherical - Rectangular

$$\begin{aligned} x &= \rho \cos \Theta \sin \Phi & \rho &= \sqrt{x^2 + y^2 + z^2} \\ y &= \rho \sin \Theta \sin \Phi & \Theta &= \arctan \left(\frac{y}{x} \right) \\ z &= \rho \cos \Phi & \Phi &= \arctan \frac{\sqrt{x^2 + y^2}}{z} \end{aligned} \quad (169)$$

These are the basic coordinate systems and conventions used in this report. It is emphasized that, to describe the location of a point, a coordinate system must be clearly defined and the coordinates of that point in the coordinate system must be specified.

Vectors

Vectors can be defined in several ways and many notational systems are in use. In this report, the vector, \vec{A} , is defined to be an ordered set of three numbers (A_1, A_2, A_3) which obeys the rules for the algebraic operations listed below, and which can be represented in any way which presents the three components and their ordering. Equation 170 shows four notations for the same vector.

$$\vec{A} = (A_1, A_2, A_3) = \begin{bmatrix} A_1 \\ A_2 \\ A_3 \end{bmatrix} = A_1 \hat{i}_1 + A_2 \hat{i}_2 + A_3 \hat{i}_3 \quad (170)$$

Two vectors are said to be equal if all corresponding components are equal, i.e., if $A_i = B_i$ for $i = 1, 2, 3$, then $\vec{A} = \vec{B}$.

The sum or difference of two vectors $\vec{A} \pm \vec{B}$ is another vector \vec{C} where $\vec{C} = \vec{A} \pm \vec{B} = (A_1 \pm B_1, A_2 \pm B_2, A_3 \pm B_3)$. That is

$$C_i = A_i \pm B_i \quad i = 1, 2, 3 \quad (171)$$

The scalar product or dot product of two vectors $\vec{A} \cdot \vec{B}$ is a scalar.

$$\vec{A} \cdot \vec{B} = A_1 B_1 + A_2 B_2 + A_3 B_3 = \sum_{i=1}^3 A_i B_i \quad (172)$$

Note that the dot product commutes: $\vec{A} \cdot \vec{B} = \vec{B} \cdot \vec{A}$.

The vector product or cross product of two vectors $\vec{A} \times \vec{B}$ is another vector \vec{C} .

$$\vec{C} = \vec{A} \times \vec{B} = (A_2 B_3 - A_3 B_2, A_3 B_1 - A_1 B_3, A_1 B_2 - A_2 B_1) \quad (173)$$

The cross product is anticommutative: $\vec{A} \times \vec{B} = -\vec{B} \times \vec{A}$.

The length or magnitude A of the vector \vec{A} is defined by Equation 174.

$$A = |\vec{A}| = \sqrt{A_1^2 + A_2^2 + A_3^2} = \left[\sum_{i=1}^3 A_i^2 \right]^{\frac{1}{2}} \quad (174)$$

Finally, the angle Θ between two vectors is defined by Equation 175.

$$\cos \Theta = \frac{\vec{A} \cdot \vec{B}}{AB} \quad (175)$$

This completes the definition of vectors and their operations. What follows is some additional notation and a few of the consequences of the algebra above.

A unit vector \hat{A} is a vector in any direction with magnitude equal to unity, e. g., $\hat{A} = \frac{\vec{A}}{A}$. The unit basis vectors are:

$$\hat{i} = \hat{i}_1 = (1, 0, 0) = \begin{bmatrix} 1 \\ 0 \\ 0 \end{bmatrix}; \hat{j} = \hat{i}_2 = (0, 1, 0) = \begin{bmatrix} 0 \\ 1 \\ 0 \end{bmatrix}; \hat{k} = \hat{i}_3 = (0, 0, 1) = \begin{bmatrix} 0 \\ 0 \\ 1 \end{bmatrix} \quad (176)$$

The unit vectors \hat{i}_1 , \hat{i}_2 , and \hat{i}_3 are called the basis set because any vector can be written as a linear combination of them as in the following equivalent notations:

$$\begin{aligned} \vec{A} = (A_1, A_2, A_3) &= A_1 \hat{i}_1 + A_2 \hat{i}_2 + A_3 \hat{i}_3 = \sum_{m=1}^3 A_m \hat{i}_m = A_x \hat{i} + A_y \hat{j} + A_z \hat{k} \\ &= A_1 \begin{bmatrix} 1 \\ 0 \\ 0 \end{bmatrix} + A_2 \begin{bmatrix} 0 \\ 1 \\ 0 \end{bmatrix} + A_3 \begin{bmatrix} 0 \\ 0 \\ 1 \end{bmatrix} = \begin{bmatrix} A_1 \\ 0 \\ 0 \end{bmatrix} + \begin{bmatrix} 0 \\ A_2 \\ 0 \end{bmatrix} + \begin{bmatrix} 0 \\ 0 \\ A_3 \end{bmatrix} = \begin{bmatrix} A_1 \\ A_2 \\ A_3 \end{bmatrix} \end{aligned} \quad (177)$$

Note also that $\hat{i}_1 \times \hat{i}_2 = \hat{i}_3$, $\hat{i}_2 \times \hat{i}_3 = \hat{i}_1$, and $\hat{i}_3 \times \hat{i}_1 = \hat{i}_2$. The circumflex (\wedge) is used exclusively to denote unit vectors.

The Kronecker delta, δ_{ij} , is defined to be unity when $i = j$ and zero when $i \neq j$. That is $\delta_{11} = \delta_{22} = \delta_{33} = 1$; $\delta_{12} = \delta_{23} = \delta_{31}$; etc. = 0. From this definition it is apparent that $\hat{i}_m \cdot \hat{i}_n = \delta_{mn}$.

The alternating symbol, ϵ_{ijk} , is defined to be unity if the subscripts i, j, k are cyclic as 1, 2, 3; minus unity if the subscripts are anticyclic as 3, 2, 1; and zero if any two of i, j , and k are equal.

$$\begin{aligned} \epsilon_{123} &= \epsilon_{231} = \epsilon_{312} = 1 \\ \epsilon_{213} &= \epsilon_{132} = \epsilon_{321} = -1 \\ \epsilon_{223} &= \epsilon_{112} = \epsilon_{121}, \text{ etc.} = 0 \end{aligned} \quad (178)$$

In this notation, if $\vec{C} = \vec{A} \times \vec{B}$, then

$$C_i = \sum_{j=1}^3 \sum_{k=1}^3 \epsilon_{ijk} A_j B_k \quad (179)$$

The form of the cross product can be remembered from the following determinant,

$$\vec{A} \times \vec{B} = \begin{vmatrix} \hat{i}_1 & \hat{i}_2 & \hat{i}_3 \\ A_1 & A_2 & A_3 \\ B_1 & B_2 & B_3 \end{vmatrix} \quad (180)$$

The relation between vectors as defined above and actual physical quantities is now apparent. The position of an object in a rectangular coordinate system is specified by its coordinates (x, y, z) . Thus position is a vector quantity, \vec{R} , and can be represented by an arrow from the origin to the point.

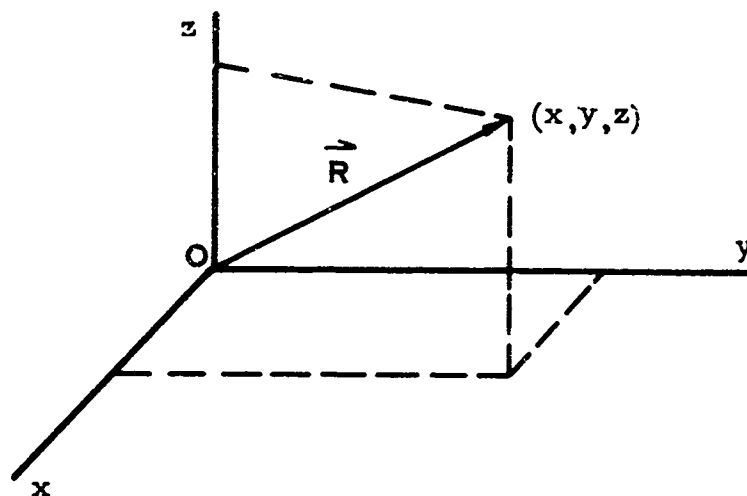


FIGURE 137. POSITION OF AN OBJECT

From the equivalent notations in Equation 177, $\vec{R} = (x, y, z) = x\hat{i} + y\hat{j} + z\hat{k}$.

Any vector quantity such as force, velocity, or torque can be written as a sum of components times directions. For example, the force \vec{F} is the sum of the component F_x of \vec{F} in the x direction times \hat{i} plus the component F_y of \vec{F} in the y direction times \hat{j} plus the component F_z of \vec{F} in the z direction times \hat{k} . That is

$$\vec{F} = F_x \hat{i} + F_y \hat{j} + F_z \hat{k} \quad (181)$$

or

$$\vec{F} = \sum_{m=1}^3 F_m \hat{i}_m \quad (182)$$

The directional properties of vectors can be illustrated with this vector \vec{F} . Rewrite \vec{F} as follows.

$$\vec{F} = F \left(\frac{F_x}{F} \hat{i} + \frac{F_y}{F} \hat{j} + \frac{F_z}{F} \hat{k} \right) \quad (183)$$

Then define the following direction cosines.

$$b_x = \cos \alpha = \frac{F_x}{F}; b_y = \cos \beta = \frac{F_y}{F}; b_z = \cos \gamma = \frac{F_z}{F} \quad (184)$$

Then $\vec{F} = F (b_x \hat{i} + b_y \hat{j} + b_z \hat{k})$. The b_j 's are direction cosines and α , β , and γ are direction angles of a line through the origin in the direction of \vec{F} .

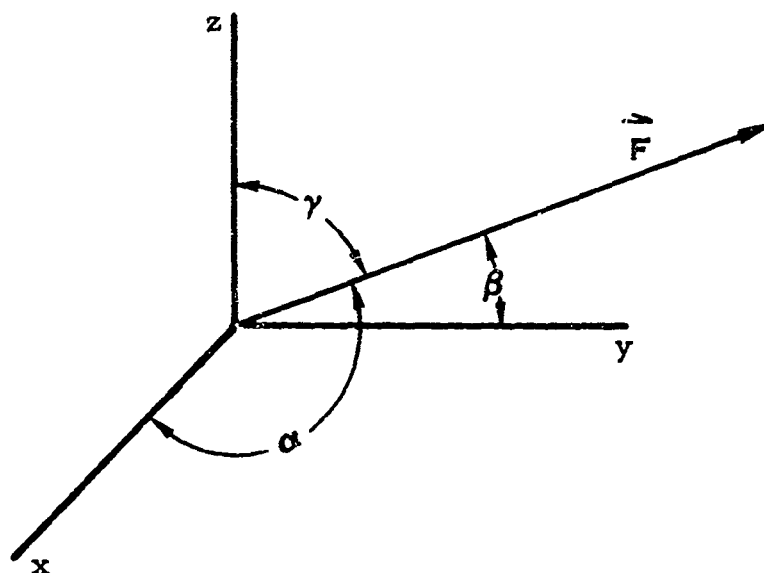


FIGURE 138. DIRECTION ANGLES

The concept of a vector as a directed magnitude has followed from the mathematical definition of vector because the b_j 's define a direction and F is by definition the magnitude of \vec{F} . When the vector is expressed this way, four numbers are used but only three are independent because $\sum_{j=1}^3 b_j^2 = 1$.

For this report the only vector calculus required is the differentiation and integration of vectors. The derivative of a vector is the sum of the derivatives of its components. Similarly, the integral of a vector is the sum of the integrals of the components. That is, if

$$\vec{A} = (A_x, A_y, A_z) = A_x \hat{i} + A_y \hat{j} + A_z \hat{k} \quad (185)$$

then

$$\frac{d\vec{A}}{dt} = \left(\frac{dA_x}{dt}, \frac{dA_y}{dt}, \frac{dA_z}{dt} \right) = \frac{dA_x}{dt} \hat{i} + \frac{dA_y}{dt} \hat{j} + \frac{dA_z}{dt} \hat{k} \quad (186)$$

and

$$\int \vec{A} dt = \left(\int A_x dt, \int A_y dt, \int A_z dt \right) = \hat{i} \int A_x dt + \hat{j} \int A_y dt + \hat{k} \int A_z dt \quad (187)$$

Matrices

Matrix algebra is a powerful tool in the solution of linkage problems by virtue of the simplicity it affords in coordinate transformations. A matrix is defined to be an array of numbers which satisfies the rules for algebraic operations enumerated below.

The matrix A is written as follows.

$$A = \begin{bmatrix} a_{11} & a_{12} & a_{13} \\ a_{21} & a_{22} & a_{23} \\ a_{31} & a_{32} & a_{33} \end{bmatrix} \quad (188)$$

where the a_{ij} 's are called the elements of the matrix A. The groups of elements a_{ij} with the same first subscripts i are called rows; the groups with the same second subscripts j are called columns. The number of rows and the number of columns define the size of a matrix. This discussion is confined to 3 x 3 matrices.

The group of elements with equal subscripts a_{ii} is called the principle diagonal.

Two matrices A and B are said to be equal if all corresponding elements are equal. That is $A = B$ if $a_{ij} = b_{ij}$ for all i and j.

The sum or difference of two matrices is another matrix obtained by adding or subtracting corresponding elements. That is, $A \pm B = C$ if $c_{ij} = a_{ij} \pm b_{ij}$ for all i and j.

Matrix addition obeys the commutative and associative laws:

$$A + B = B + A \quad (189)$$

and

$$A + (B + C) = (A + B) + C \quad (190)$$

The product of a matrix A and a scalar b is simply a matrix in which each element is multiplied by the scalar.

$$bA = \begin{bmatrix} ba_{11} & ba_{12} & ba_{13} \\ ba_{21} & ba_{22} & ba_{23} \\ ba_{31} & ba_{32} & ba_{33} \end{bmatrix} \quad (191)$$

The product C of two matrices A and B is obtained as follows.

$$c_{ij} = \sum_{k=1}^3 a_{ik} b_{kj} \quad \text{for } C = AB \quad (192)$$

Writing out the components,

$$\begin{bmatrix} c_{11} & c_{12} & c_{13} \\ c_{21} & c_{22} & c_{23} \\ c_{31} & c_{32} & c_{33} \end{bmatrix} = \begin{bmatrix} a_{11} & a_{12} & a_{13} \\ a_{21} & a_{22} & a_{23} \\ a_{31} & a_{32} & a_{33} \end{bmatrix} \begin{bmatrix} b_{11} & b_{12} & b_{13} \\ b_{21} & b_{22} & b_{23} \\ b_{31} & b_{32} & b_{33} \end{bmatrix} =$$

$$\begin{bmatrix} a_{11}b_{11} + a_{12}b_{21} + a_{13}b_{31} & a_{11}b_{12} + a_{12}b_{22} + a_{13}b_{32} & a_{11}b_{13} + a_{12}b_{23} + a_{13}b_{33} \\ a_{21}b_{11} + a_{22}b_{21} + a_{23}b_{31} & a_{21}b_{12} + a_{22}b_{22} + a_{23}b_{32} & a_{21}b_{13} + a_{22}b_{23} + a_{23}b_{33} \\ a_{31}b_{11} + a_{32}b_{21} + a_{33}b_{31} & a_{31}b_{12} + a_{32}b_{22} + a_{33}b_{32} & a_{31}b_{13} + a_{32}b_{23} + a_{33}b_{33} \end{bmatrix} \quad (193)$$

It follows that

$$x_{ij} = \sum_{k=1}^3 \sum_{p=1}^3 \dots \sum_{m=1}^3 a_{ik} b_{kp} \dots k_{mj} \quad \text{for } X = AB \dots D \quad (194)$$

From this it can be seen that the associative law holds for matrix multiplication. That is, $A(BC) = (AB)C$. However, matrix multiplication in general is not commutative. That is, $AB \neq BA$. For instance, consider $C = AB$ and $C' = BA$.

From the definition, $c_{ij} = \sum_{k=1}^3 a_{ik} b_{kj}$; $c'_{ij} = \sum_{k=1}^3 b_{ik} a_{kj} = \sum_{k=1}^3 a_{kj} b_{ik}$. By writing out a typical pair of elements, it can be seen that $c_{ij} \neq c'_{ij}$. This noncommutative property of matrices is most important because they can represent noncommutative rotation operators.

A vector can be written as a matrix with one column. The product of a column vector and a square matrix is another column vector. If A is a square matrix with elements a_{ij} and B is a vector with elements b_j , then

$$(AB)_i = \sum_{j=1}^3 a_{ij} b_j \quad (195)$$

That is,

$$\begin{bmatrix} a_{11} & a_{12} & a_{13} \\ a_{21} & a_{22} & a_{23} \\ a_{31} & a_{32} & a_{33} \end{bmatrix} \begin{bmatrix} b_1 \\ b_2 \\ b_3 \end{bmatrix} = \begin{bmatrix} a_{11} b_1 + a_{12} b_2 + a_{13} b_3 \\ a_{21} b_1 + a_{22} b_2 + a_{23} b_3 \\ a_{31} b_1 + a_{32} b_2 + a_{33} b_3 \end{bmatrix} \quad (196)$$

Multiplication in the reverse order, BA , is undefined.

The transpose \tilde{A} of a matrix A with elements a_{ij} is the matrix made up of elements a_{ji} . This is equivalent to "reflecting" the elements in the principle diagonal of the matrix.

The determinant of a matrix is made up of the elements of the matrix.

$$|A| = \det A = \begin{vmatrix} a_{11} & a_{12} & a_{13} \\ a_{21} & a_{22} & a_{23} \\ a_{31} & a_{32} & a_{33} \end{vmatrix} \quad (197)$$

The inverse A^{-1} of a matrix has the property that $A A^{-1} = A^{-1} A = 1$, where 1 is the unit matrix $\begin{bmatrix} 1 & 0 & 0 \\ 0 & 1 & 0 \\ 0 & 0 & 1 \end{bmatrix}$. The elements $(A^{-1})_{ij}$ of the inverse A^{-1} of the matrix A are given by Equation 198.

$$(A^{-1})_{ij} = \frac{\text{cofactor of } (A)_{ji} \text{ in } A}{\det A}$$

for matrices with $\det A \neq 0$. The cofactor of A_{ji} is the product of $(-1)^{i+j}$ and the determinant obtained by striking the row and column of A_{ji} . For example, if

$$A = \begin{bmatrix} a_{11} & a_{12} & a_{13} \\ a_{21} & a_{22} & a_{23} \\ a_{31} & a_{32} & a_{33} \end{bmatrix} \text{ and } A^{-1} = \begin{bmatrix} a'_{11} & a'_{12} & a'_{13} \\ a'_{21} & a'_{22} & a'_{23} \\ a'_{31} & a'_{32} & a'_{33} \end{bmatrix}, \text{ then}$$

$$a'_{12} = \frac{(-1)^{2+1} (a_{12} a_{33} - a_{13} a_{32})}{\det A} = - \frac{a_{12} a_{33} + a_{13} a_{32}}{\det A} \quad (199)$$

The inverse of a product of matrices is the product of the inverses in the reverse order. For proof, write $AB (AB)^{-1} = 1$ and multiply from the left by A^{-1} then B^{-1} : $B (AB)^{-1} = A^{-1}$; $(AB)^{-1} = B^{-1} A^{-1}$. This proof generalizes immediately to any number of matrices.

$$(ABC \dots D)^{-1} = D^{-1} \dots C^{-1} B^{-1} A^{-1} \quad (200)$$

An orthogonal matrix by definition has the property $A^{-1} = \tilde{A}$. Thus to find the inverse of an orthogonal matrix, simply interchange the subscripts of the elements. Orthogonal matrices represent rotations of Cartesian coordinate systems and are therefore fundamental to the study of jointed linkage systems.

Positions And Orientations Of Rigid Objects

A mathematical description of the location and orientation of one rigid object with respect to another requires, in general, a minimum of six numbers; that is, a rigid body has six degrees of freedom. These can be broken down into three numbers (a vector) which describe the position of some point in one body with respect to the coordinates of the other and three numbers which describe the orientation of one body with respect to the other. The vector description has been discussed in detail. The orientation problem will be discussed here; then the steps in the complete description will be enumerated.

Consider two coordinate systems, CS and CS' in Figure 139, with coincident origins but rotated with respect to one another.

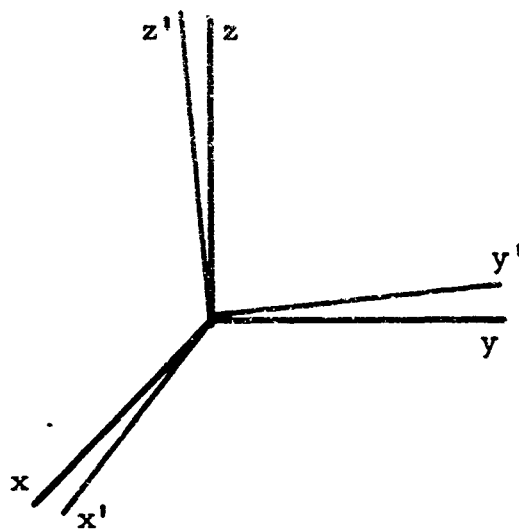


FIGURE 139. ROTATED COORDINATE SYSTEMS

The problem is to describe the orientation of the primed coordinate system (CS') with respect to the unprimed coordinate system (CS). Each axis of CS' can be oriented by the three direction angles between it and the axes of CS. Since there are three axes in CS', the nine direction angles or their cosines completely define the orientation of CS' with respect to CS and vice versa. If only right handed rectangular coordinate systems are considered, the nine direction cosines overspecify the orientation. Nevertheless, the matrix of direction cosines is a very useful representation of this orientation.

The orientation of CS' with respect to CS can be defined to be the matrix D of direction cosines written as follows.

$$D = \begin{bmatrix} d_{11} & d_{12} & d_{13} \\ d_{21} & d_{22} & d_{23} \\ d_{31} & d_{32} & d_{33} \end{bmatrix} \quad (201)$$

where d_{mn} is the cosine of the angle between the m th primed and the n th unprimed axis. Or using unit basis vectors, $d_{mn} = \hat{i}_m \cdot \hat{i}_n$. Note that $\hat{i}_m \cdot \hat{i}_n = \hat{i}_n \cdot \hat{i}_m$; that is, $d_{mn} = d_{nm}$. Since the orientation is overspecified, there must be conditions on the d_{mn} 's. These are six equations, called the orthogonality conditions, and are written:

$$\sum_{p=1}^3 d_{mp} d_{np} = \delta_{mn} \quad (202)$$

Another useful description of the relative orientation of two bodies is the set of Eulerian angles. The Eulerian angles with their convention are a set of instructions which tell how to rotate one set of axes (CS') to become parallel to another (CS) by a series of three single-axis rotations. Several different conventions in the definition of Eulerian angles exist but in this report the roll-pitch-yaw convention commonly used in flight dynamics was arbitrarily chosen. Since Eulerian angles are particularly useful in gyroscopic problems, x' , y' , and z' will be called the space-fixed axes and x , y , and z will be called the body-fixed axes. Starting with the space-fixed axes, successive rotations to two intermediate sets of axes (X , Y , Z) and (X' , Y' , Z') and finally to the body-fixed axes (x , y , z) are performed as in Figures 140, 141, and 142.

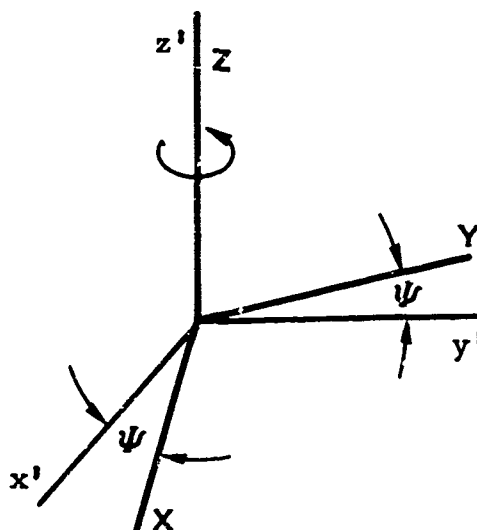


FIGURE 140. ROTATION OF THE SPACE AXES THROUGH ψ ABOUT z' TO FORM THE INTERMEDIATE AXES (X , Y , Z)

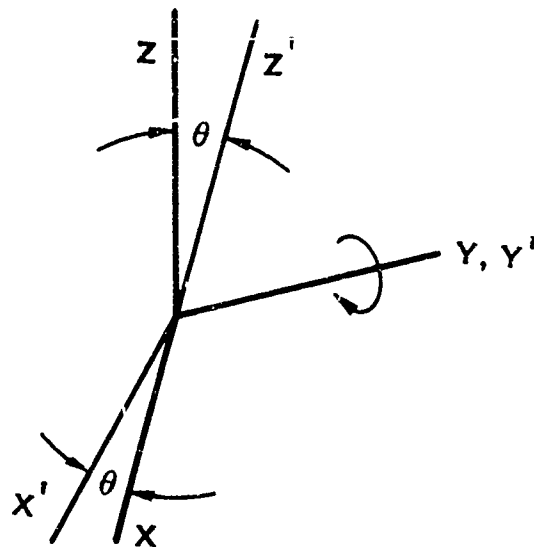


FIGURE 141. ROTATION OF THE (X, Y, Z) AXES THROUGH THE ANGLE Θ ABOUT Y TO FORM THE SECOND SET OF INTERMEDIATE AXES (X', Y', Z')

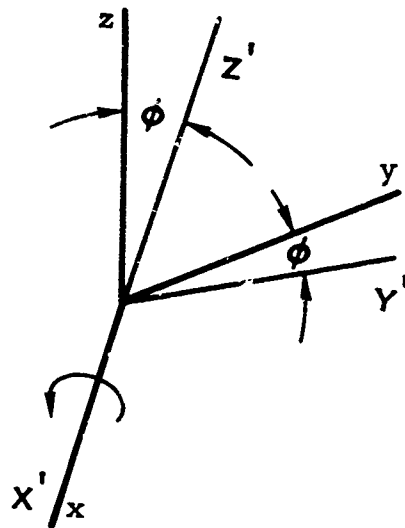


FIGURE 142. ROTATION OF THE (X', Y', Z') AXES THROUGH THE ANGLE Φ ABOUT X' TO FORM THE FINAL OR BODY-FIXED AXES (x, y, z)

All rotations are positive, which means that a right hand screw would advance in the positive direction along the axis of rotation. Now the set of three angles (Ψ, Θ, Φ) and their convention uniquely define the orientation of CS with respect to CS' .

The meaning of Eulerian angles can be made clearer if they are given the hardware interpretation of Figure 143. Four links are joined by three pin joints which represent the angles.

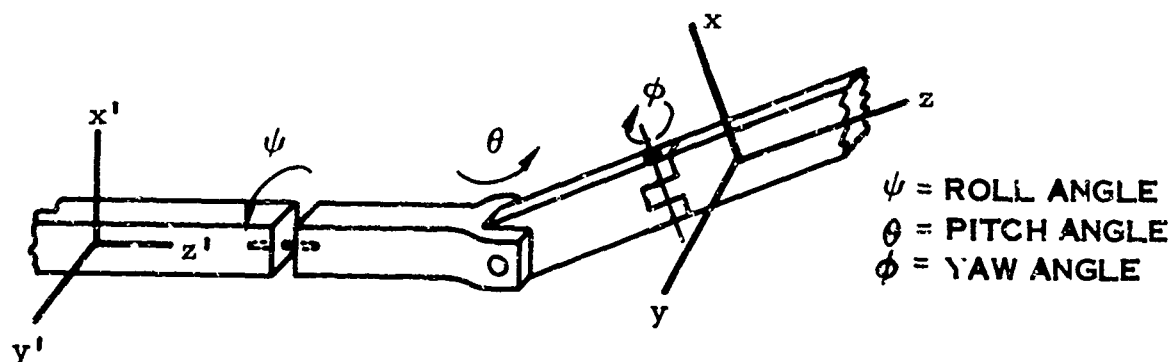


FIGURE 143. HARDWARE INTERPRETATION OF EULERIAN ANGLES

Note that more than one set of angles (all less than 360°) can specify the same orientation. For example $(180^\circ, 180^\circ, 180^\circ)$ is equivalent to $(0, 0, 0)$. Note also that the order of the rotations is important. If the last two rotations were interchanged, Figure 144 would represent the model.

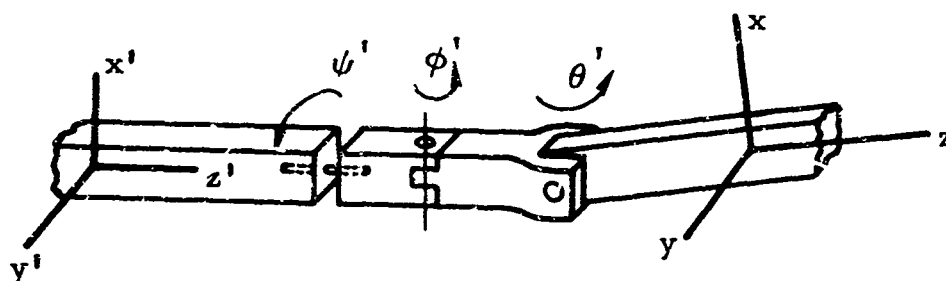


FIGURE 144. INTERPRETATION WITH ORDER OF ROTATIONS INTERCHANGED

Consider these two rotations: $(\Psi = 0, \Theta = 90^\circ, \Phi = 90^\circ)$ and $(\Psi' = 0, \Phi' = 90^\circ, \Theta' = 90^\circ)$. In the first, the z axis ends up parallel to the y' axis; in the second, the z axis ends up parallel to the x' axis. This illustrates the noncommutative property of rotation operators.

Since Eulerian angles and direction cosines are equivalent representations, the direction cosines can be written as functions of the Eulerian angles. Equations 203, 204, and 205 are derived later in this appendix.

$$\left. \begin{aligned} d_{11} &= \cos \Theta \cos \Psi \\ d_{12} &= \sin \Phi \sin \Theta \cos \Psi - \cos \Phi \sin \Psi \\ d_{13} &= \cos \Phi \sin \Theta \cos \Psi + \sin \Phi \sin \Psi \end{aligned} \right\} \quad (203)$$

$$\left. \begin{aligned} d_{21} &= \cos \Theta \sin \Psi \\ d_{22} &= \sin \Phi \sin \Theta \sin \Psi + \cos \Phi \cos \Psi \\ d_{23} &= \cos \Phi \sin \Theta \sin \Psi - \sin \Phi \cos \Psi \end{aligned} \right\} \quad (204)$$

$$\left. \begin{aligned} d_{31} &= -\sin \Theta \\ d_{32} &= \sin \Phi \cos \Theta \\ d_{33} &= \cos \Phi \cos \Theta \end{aligned} \right\} \quad (205)$$

In summary, all the tools have been presented for the description of the position and orientation of one rigid body with respect to another. The steps in this description are as follows.

1. Erect a Cartesian coordinate system in each of the two bodies. Choice of the location is arbitrary, but problems are usually simplified if the locations are chosen from symmetry considerations.
2. Describe the position of body #2 with respect to body #1 by giving the location of the origin of coordinates of body #2 in body #1's coordinates. That is, give the vector from origin #1 to origin #2.
3. Describe the orientation of body #2 with respect to body #1, by giving either of the following.
 - a. The cosines of the angles between the axes of body #1 and those of body #2 and array them as a matrix D with components d_{mn} . As explained above, d_{mn} is the cosine of the angle between the m th axis of body #1 and the n th axis of body #2.
 - b. The three Eulerian angles (with a statement of convention) which rotate body #1 so that its axes are parallel to those of body #2.

COORDINATE TRANSFORMATION

Frequently, it is necessary to add vector quantities which have been measured in coordinate systems which move relative to one another. Then the vectors must be transformed to the same CS before the simple definitions of vector algebra apply. In this section, transformations will be performed between coordinate systems which have been rotated, translated, and both translated and rotated. Then some examples will be given.

Rotation

Consider Figure 145 showing a primed and an unprimed coordinate system and a vector \vec{A} .

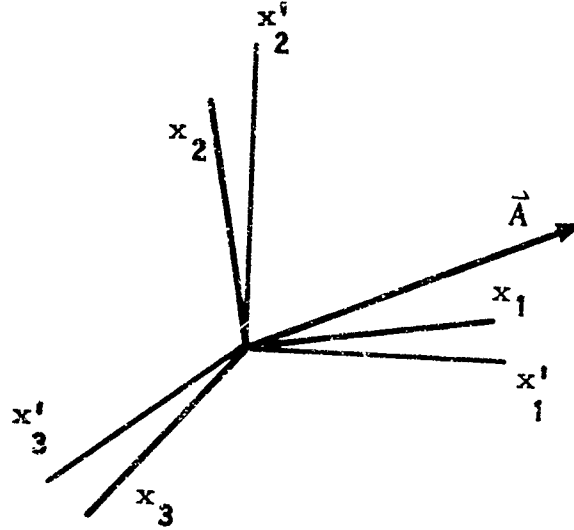


FIGURE 145. ROTATED COORDINATE SYSTEM

The components of \vec{A} are known in the unprimed coordinate system: $\vec{A} = A_1 \hat{i}_1 + A_2 \hat{i}_2 + A_3 \hat{i}_3$; and the representation of \vec{A} in the primed CS is desired: $\vec{A}' = A'_1 \hat{i}'_1 + A'_2 \hat{i}'_2 + A'_3 \hat{i}'_3$. The two representations are related by the matrix of direction cosines as follows.

$$\begin{bmatrix} A'_1 \\ A'_2 \\ A'_3 \end{bmatrix} = \begin{bmatrix} d_{11} & d_{12} & d_{13} \\ d_{21} & d_{22} & d_{23} \\ d_{31} & d_{32} & d_{33} \end{bmatrix} \begin{bmatrix} A_1 \\ A_2 \\ A_3 \end{bmatrix} \quad (206)$$

And conversely,

$$\begin{bmatrix} A_1 \\ A_2 \\ A_3 \end{bmatrix} = \begin{bmatrix} d_{11} & d_{21} & d_{31} \\ d_{12} & d_{22} & d_{32} \\ d_{13} & d_{23} & d_{33} \end{bmatrix} \begin{bmatrix} A'_1 \\ A'_2 \\ A'_3 \end{bmatrix} \quad (207)$$

To show this, write $\sum_n A'_n \hat{i}'_n = \sum_n A_n \hat{i}_n$ and multiply both sides by \hat{i}'_m .

$$\sum_n A'_n \hat{i}'_m \cdot \hat{i}'_n = \sum_n A_n \hat{i}'_m \cdot \hat{i}_n \quad (208)$$

$$\sum_n A'_n \delta_{mn} = A'_m = \sum_n d_{mn} A_n \quad (209)$$

In pure matrix notation $A' = DA$ and $A = D^{-1} A'$. Thus a rotational transformation is represented by matrix multiplication. The d_{mn} 's could be written in terms of Eulerian angles.

Translation

Consider two coordinate systems with parallel axes but with origins separated by the vector \vec{R} .

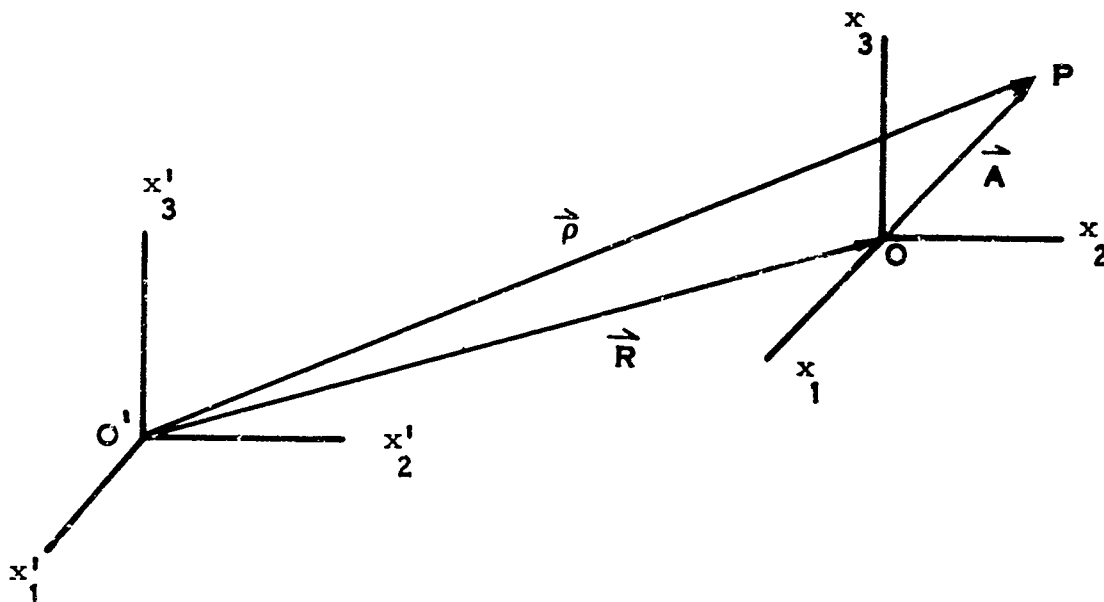


FIGURE 146. TRANSLATED COORDINATE SYSTEM

\vec{A} is the vector from O to P and may be written in either coordinate system:

$\vec{A} = \sum A'_m \hat{i}'_m = \sum A_m \hat{i}_m$. Since, in this case, $\hat{i}_m = \hat{i}'_m$, it follows that $A_m = A'_m$. That is, the vector has the same components in either system.

This important point is true of all vectors in translated systems. Simple vector quantities which do not contain position implicitly such as force and velocity transform simply. That is, the components of the force vector \vec{F} are the same in either coordinate system, $F_m = F'_m$.

When position is implicit, however, confusion can result. If \vec{A} is the vector defining the position of the point P with respect to O, represented in the unprimed CS, then \vec{A}' is the vector defining the position of the point P with respect to O' represented in the primed CS. \vec{A}' is not the same vector as $\vec{\rho}$ which defines the position of the point P with respect to O'. \vec{A} and $\vec{\rho}$ are related by \vec{R} , the vector defining the relative positions of the two CS's.

$$\vec{\rho} = \vec{R} + \vec{A} \quad (210)$$

Although this operation is usually called a transformation of a position vector, analytically, it is not a vector transformation.

Similarly, other vectors which include position implicitly such as torque or angular velocity can easily be confused. Consider a torque \vec{T} about O, represented in the unprimed CS as $\vec{T} = \sum T_m \hat{i}_m$. The same vector represented in the primed CS is $\vec{T} = \sum T'_m \hat{i}'_m = \sum T'_m \hat{i}_m$. \vec{T} in either representation is still the torque about O; representing it in CS' does not make it the torque about O'. This important point will be brought out further in the next section.

Rotation And Translation

Consider Figure 147 which illustrates the general case. As before, the vector \vec{A} transforms under the matrix of direction cosines as $A'_m = \sum_n d_{mn} A_n$ and back by $A_m = \sum_n d_{nm} A'_n$. And as before, $\vec{\rho} = \vec{R} + \vec{A}$, but now, to add components of \vec{R} and \vec{A} , they must be represented in the same coordinate system. Thus

$$\rho'_m = R'_m + A'_m = R'_m + \sum_n d_{mn} A_n \quad (211)$$

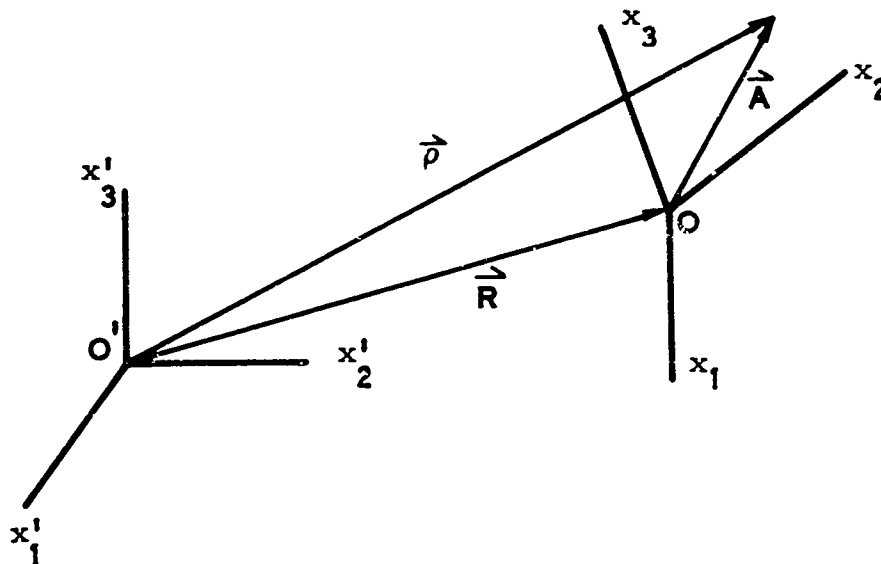


FIGURE 147. TRANSLATED AND ROTATED COORDINATE SYSTEM

Fundamental to the study of linkage systems is the description of the effects on the system of torques due to forces acting at different points in the linkage. Consider the torque \vec{T}_O about O due to a force \vec{F} acting at \vec{r} as shown in Figure 148. By definition, $\vec{T}_O = \vec{r} \times \vec{F}$.

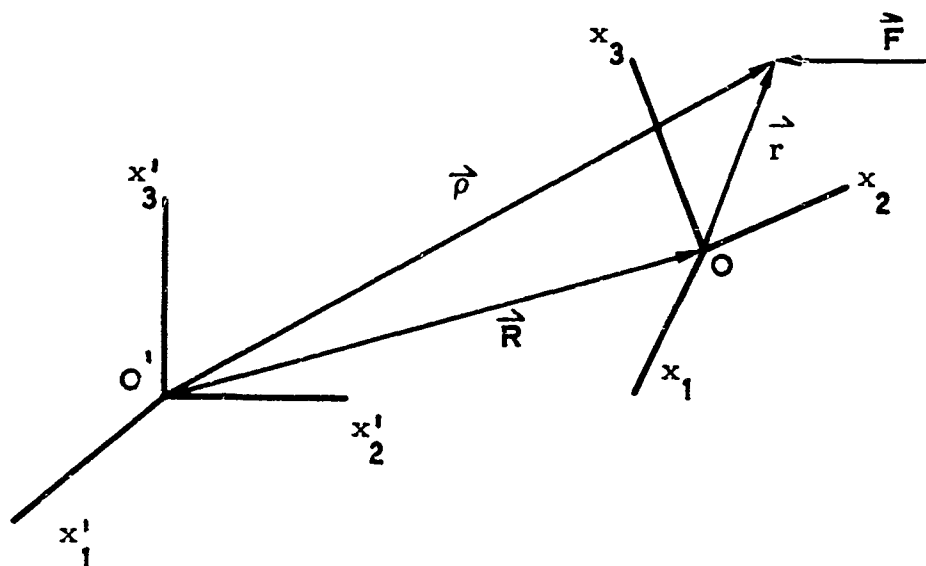


FIGURE 148. MODEL FOR TORQUE DISCUSSION

The torque about O' due to \vec{F} is defined similarly. $\vec{T}_{O'} = \vec{\rho} \times \vec{F}$. Equation 212 shown the relation between the torques \vec{T}_O and $\vec{T}_{O'}$ due to the same force \vec{F} .

$$\vec{T}_{O'} = \vec{\rho} \times \vec{F} = (\vec{R} + \vec{r}) \times \vec{F} = \vec{R} \times \vec{F} + \vec{r} \times \vec{F} \quad (212)$$

But since $\vec{T}_O = \vec{r} \times \vec{F}$,

$$\vec{T}_{O'} = (\vec{R} \times \vec{F}) + \vec{T}_O \quad (213)$$

Say the components of \vec{T}_O and \vec{F} are known (measured) in CS and \vec{R} is known in CS'; that is, $\vec{R} = R'_1 \hat{i}'_1 + R'_2 \hat{i}'_2 + R'_3 \hat{i}'_3$, $\vec{F} = F_1 \hat{i}_1 + F_2 \hat{i}_2 + F_3 \hat{i}_3$, and $\vec{T}_O = T_{O1} \hat{i}_1 + T_{O2} \hat{i}_2 + T_{O3} \hat{i}_3$. The torque about O' due to \vec{T}_O is desired, i.e., $T'_{O'1} \hat{i}'_1 + T'_{O'2} \hat{i}'_2 + T'_{O'3} \hat{i}'_3$. Since the cross product and the adding operations must be performed in the same coordinate system, F'_n and T'_{om} must be transformed to CS'.

$$F'_n = \sum_s d_{ns} F_s \quad (214)$$

and similarly,

$$T'_{om} = \sum_s d_{ms} T_{os} \quad (215)$$

All in the same coordinate system,

$$\begin{aligned}
 \vec{T}'_{O'm} &= (\vec{R} \times \vec{F})_m + T'_{om} \\
 &= \sum_{p,n}^3 \epsilon_{mpn} R'_p F'_n + \sum_s^3 d_{ms} T_{os} \\
 &= \sum_{p,n,s}^3 \epsilon_{mpn} R'_p d_{ns} F_s + \sum_s^3 d_{ms} T_{os}
 \end{aligned} \tag{216}$$

or

$$\vec{T}'_{O'} = \sum_{m,s}^3 \hat{i}'_m \left[\sum_{p,n}^3 \epsilon_{mpn} d_{ns} R'_p F_s + d_{ms} T_{os} \right] \tag{217}$$

This is the torque about O' expressed as a function of the force and torque represented (measured) in another coordinate system located at \vec{R} with respect to O' . Equation 218 expresses $\vec{T}'_{O'}$ in terms of forces, distances, and direction cosines alone. This particular example was chosen because it arises in a pin jointed linkage system with force transducers on the various links when the torque about a point due to the external forces is desired. Transformations in a generalized pin jointed linkage system are treated in the next section.

$$\vec{T}'_{O'} = \sum_{m,s}^3 \hat{i}'_m \left[\sum_{p,n}^3 \epsilon_{mpn} d_{ns} R'_p F_s + d_{ms} \sum_{a,b}^3 \epsilon_{sab} r_a F_b \right] \tag{218}$$

TRANSFORMATIONS FOR A GENERALIZED PIN JOINTED LINKAGE SYSTEM

In this section working equations will be developed for the coordinate transformation of vector quantities measured in actual linkage systems composed of any number of pin joints and sliding joints. Ball joints can be handled by this technique also, but are not treated explicitly here. This analysis is fundamental to an understanding of the mechanics of anthropomorphic dummies and exoskeletons as applied to the generalized evaluation of torques in space suits.

In the exoskeleton, joint angles and varying link lengths are transduced with potentiometers and recorded as functions of time. For the dummy, the joint angles and suit imposed forces are transduced and recorded also as functions of time. From these recorded values the torque about any desired joint may be computed. To accomplish this, however, the measured values must be operated upon to transform them from their original CS to the CS of the joint about which the torque is desired.

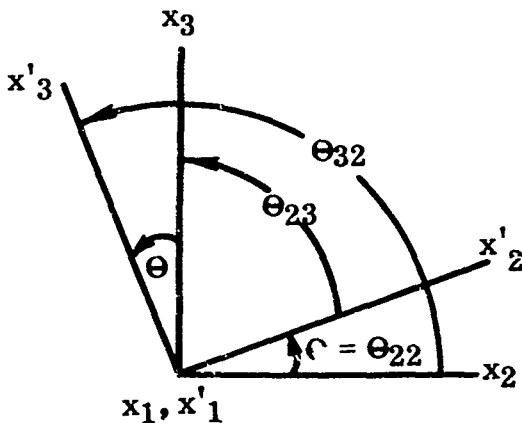
Any pin jointed linkage system can be represented by an ordered sequence of pure rotations and translations. In fact the only rotations needed are the three single degree of freedom rotations about coordinate axes. That is, the most general transformation can be made up of four basic transformations, each of which has a particularly simple form. The coordinate axes are chosen so that each pin joint falls on an axis and each sliding joint falls along a translation vector. In this way all transduced quantities appear in the transformation equations and the equations are directly adaptable to computer programming. First, the four basic transformations will be explained; then the method of combining them will be explained and illustrated.

Rotations About Coordinate Axes

The problem here is to transform a vector \vec{A} represented in an unprimed coordinate system to its representation in a primed system. This amounts to finding the d_{mn} 's in Equation 219.

$$\begin{bmatrix} A'_1 \\ A'_2 \\ A'_3 \end{bmatrix} = \begin{bmatrix} d_{11} & d_{12} & d_{13} \\ d_{21} & d_{22} & d_{23} \\ d_{31} & d_{32} & d_{33} \end{bmatrix} \begin{bmatrix} A_1 \\ A_2 \\ A_3 \end{bmatrix} \quad (219)$$

In pure matrix notation, Equation 219 would be written: $A' = DA$. Rotations about an axis are considered positive if a right hand screw on the axis would advance in the positive direction under rotation of the unprimed axes into the primed axes. Figure 149 illustrates the direction cosines for the x axis rotation.



$$\begin{aligned} d_{11} &= \cos \Theta_{11} = \cos 0^\circ = 1 \\ d_{21} &= \cos \Theta_{21} = \cos 90^\circ = 0 \end{aligned} \quad (220)$$

$$\begin{aligned} d_{31} &= \cos \Theta_{31} = \cos 90^\circ = 0 \\ d_{12} &= \cos \Theta_{12} = \cos 90^\circ = 0 \\ d_{22} &= \cos \Theta_{22} = \cos \Theta \\ d_{32} &= \cos \Theta_{32} = \cos (90^\circ + \Theta) = -\sin \Theta \end{aligned} \quad (221)$$

$$\begin{aligned} d_{13} &= \cos \Theta_{13} = \cos 90^\circ = 0 \\ d_{23} &= \cos \Theta_{23} = \cos (90^\circ - \Theta) = \sin \Theta \\ d_{33} &= \cos \Theta_{33} = \cos \Theta \end{aligned} \quad (222)$$

FIGURE 149. THE x AXIS ROTATION

Thus,

$$D_x = \begin{bmatrix} 1 & 0 & 0 \\ 0 & \cos \Theta_x & \sin \Theta_x \\ 0 & -\sin \Theta_x & \cos \Theta_x \end{bmatrix} \quad (223)$$

Rotation matrices for the other axes (Equations 224 and 225) are found similarly.

$$D_y = \begin{bmatrix} \cos \Theta_y & 0 & -\sin \Theta_y \\ 0 & 1 & 0 \\ \sin \Theta_y & 0 & \cos \Theta_y \end{bmatrix} \quad (224)$$

$$D_z = \begin{bmatrix} \cos \Theta_z & \sin \Theta_z & 0 \\ -\sin \Theta_z & \cos \Theta_z & 0 \\ 0 & 0 & 1 \end{bmatrix} \quad (225)$$

Note that each matrix is a function of one variable only. Note also that the form of the y rotation is different from the other two by the sign of the sine.

Consider Figure 150 showing the z rotation.

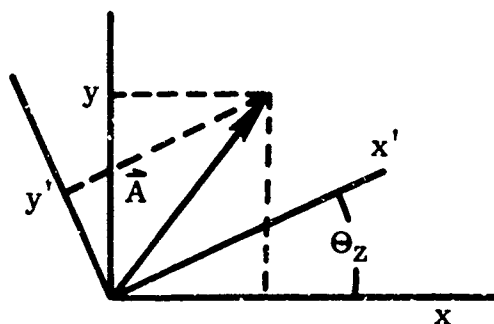


FIGURE 150. THE z AXIS ROTATION

$$\begin{bmatrix} x' \\ y' \\ z' \end{bmatrix} = \begin{bmatrix} \cos \Theta_z & \sin \Theta_z & 0 \\ -\sin \Theta_z & \cos \Theta_z & 0 \\ 0 & 0 & 1 \end{bmatrix} \begin{bmatrix} x \\ y \\ z \end{bmatrix} \quad (226)$$

This reduces to the familiar transformation equations:

$$\begin{aligned} x' &= x \cos \Theta_z + y \sin \Theta_z \\ y' &= -x \sin \Theta_z + y \cos \Theta_z \\ z' &= z \end{aligned} \quad (227)$$

Any number of these single axis rotations can be performed in succession and the product of the matrices of the individual rotations will represent the total rotation. For example, consider the representation of the vector \vec{A} in the double primed system

$$\vec{A} = \begin{bmatrix} A''_1 \\ A''_2 \\ A''_3 \end{bmatrix} \quad (228)$$

where the axes of CS'' are related to those of CS' by the matrix D' of direction cosines d'_{mn} :

$$A'' = D'A' \quad (229)$$

But from above $A' = DA$, therefore, $A'' = D'DA$. Thus the matrix $D'D$ represents the compound rotation from the unprimed CS to CS'' . The inverse transformation is performed with the inverse matrix. $A = (D'D)^{-1} A''$. But $(D'D)^{-1} = D^{-1} (D')^{-1} = \tilde{D} \tilde{D}'$ so that $A = \tilde{D} \tilde{D}' A''$. These properties generalize immediately to any number of rotations.

For a specific example, the equations for the direction cosines as functions of the Eulerian angles will be derived. These equations and the definition of the angles in the roll-pitch-yaw convention were presented earlier on page 354. The matrix D is the rotation from the body-fixed axes to the space axes but the Eulerian angles were defined as rotations from the space axes so that D^{-1} will be the product of the rotations in the order Ψ, Θ, Φ ; that is, $D^{-1} = D_X(\Phi) D_Y(\Theta) D_Z(\Psi)$. Note that $D_Z(\Psi)$ was written last because it operates on a vector in the space axes first:

$$A_{\text{body}} = D^{-1} A_{\text{space}} = D_X(\Phi) D_Y(\Theta) D_Z(\Psi) A_{\text{space}} \quad (230)$$

Inverting,

$$D = [D_X(\Phi) D_Y(\Theta) D_Z(\Psi)]^{-1} = \tilde{D}_Z(\Psi) \tilde{D}_Y(\Theta) \tilde{D}_X(\Phi) \quad (231)$$

And multiplying out the components,

$$\begin{aligned} D &= \begin{bmatrix} d_{11} & d_{12} & d_{13} \\ d_{21} & d_{22} & d_{23} \\ d_{31} & d_{32} & d_{33} \end{bmatrix} = \begin{bmatrix} \cos \Psi & -\sin \Psi & 0 \\ \sin \Psi & \cos \Psi & 0 \\ 0 & 0 & 1 \end{bmatrix} \begin{bmatrix} \cos \Theta & 0 & \sin \Theta \\ 0 & 1 & 0 \\ -\sin \Theta & 0 & \cos \Theta \end{bmatrix} \begin{bmatrix} 1 & 0 & 0 \\ 0 & \cos \Phi & -\sin \Phi \\ 0 & \sin \Phi & \cos \Phi \end{bmatrix} \\ &= \begin{bmatrix} \cos \Psi & -\sin \Psi & 0 \\ \sin \Psi & \cos \Psi & 0 \\ 0 & 0 & 1 \end{bmatrix} \begin{bmatrix} \cos \Theta & \sin \Theta \sin \Phi & \sin \Theta \cos \Phi \\ 0 & \cos \Phi & -\sin \Phi \\ -\sin \Theta & \cos \Theta \sin \Phi & \cos \Theta \cos \Phi \end{bmatrix} \end{aligned} \quad (232)$$

$$D = \begin{bmatrix} \cos \Psi \cos \Theta & \cos \Psi \sin \Theta \sin \Phi - \sin \Psi \cos \Phi & \cos \Psi \sin \Theta \cos \Phi + \sin \Psi \sin \Phi \\ \sin \Psi \cos \Theta & \sin \Psi \sin \Theta \sin \Phi + \cos \Psi \cos \Phi & \sin \Psi \sin \Theta \cos \Phi - \cos \Psi \sin \Phi \\ -\sin \Theta & \cos \Theta \sin \Phi & \cos \Theta \cos \Phi \end{bmatrix} \quad (233)$$

This is the same as Equations 203, 204, and 205. The same equation would have been obtained if the rotations were performed through negative angles from the body axes to the space axes as follows.

$$D = D_z (-\Psi) D_y (-\Theta) D_x (-\Phi) \quad (234)$$

But for these particular matrices, $D_x (-\Phi) = \tilde{D}_x (\Phi)$, etc. because $\sin (-\Phi) = -\sin \Phi$ and $\cos (-\Phi) = \cos \Phi$. Therefore as before, $D = \tilde{D}_z (\Psi) \tilde{D}_y (\Theta) \tilde{D}_x (\Phi)$.

The set of Eulerian angles is just one set of successive single axis rotations. In general any rotation can be represented by a matrix which is a product of D_x 's, D_y 's, and D_z 's. Given this matrix, vectors such as force and velocity can be transformed readily.

Translations and Rotations

Consider the geometry in Figure 151 which might represent any system consisting of links and pin joints. Note that from origin to origin, pure translations are performed before any rotations. Some of the angles and link lengths will represent constants and some of them variables of the linkage system. The subjects discussed here are the orientation of the last CS with respect to the first, the transformation of the vector \vec{A} from the last CS to the first, and the locations of points P and o_n in terms of rotation matrices and link lengths.

Note how the transformations are performed one at a time. The steps are these:

- CS (1) is rotated through Θ_1 about x_1 to form CS (1')
- CS (1') is translated by \vec{R}_{12} to form CS (2)
- CS (2) is rotated through Θ_2 about z_2 to form CS (2')
- CS (2') is translated by \vec{R}_{23} to form CS (3)
- CS (3) is rotated through Θ_3 about x_3 to form CS (3')
- CS (3') is rotated through Θ'_3 about z'_3 to form CS (3'')
- CS (3'') is rotated through Θ''_3 about x''_3 to form CS (3''')
- CS (3''') is translated by \vec{R}_{34} to form CS (4)
- CS (4) is translated by \vec{R}_{45} to form CS (5)
- CS (5) is rotated through Θ_5 about y_5 to form CS (5')

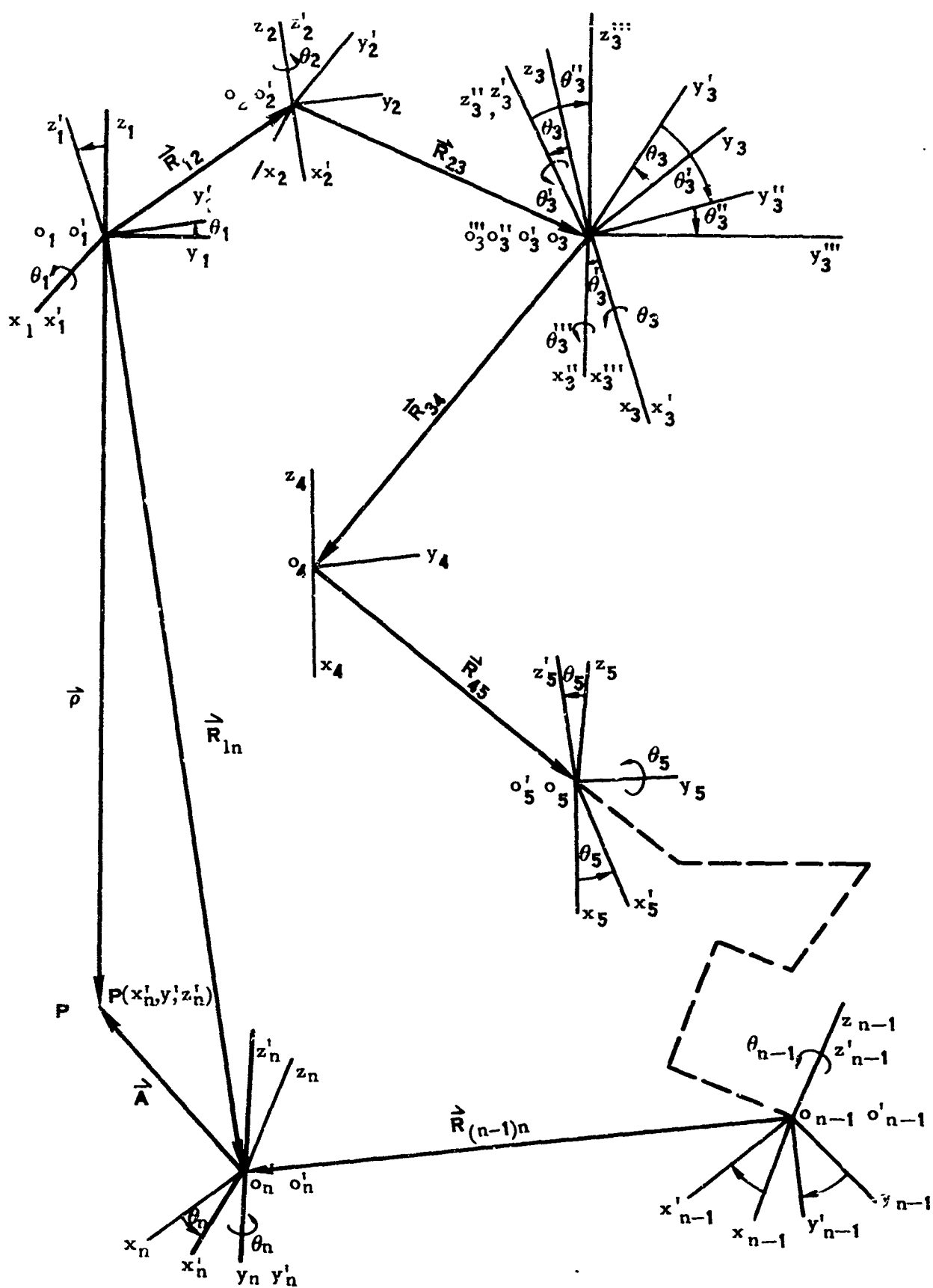


FIGURE 151.

GENERALIZED MODEL ILLUSTRATING
SUCCESSIVE TRANSFORMATIONS

More rotations and translations to CS (n-1).

CS (n-1) is rotated through Θ_{n-1} about z_{n-1} to form CS [(n-1)']

CS [(n-1)'] is translated by $\vec{R}_{(n-1)n}$ to form CS (n)

CS (n) is rotated through Θ_n about y_n to form CS (n')

\vec{A} is a vector represented in the nth coordinate system, $\vec{R}_{1n} = \vec{R}_{12} + \vec{R}_{23} + \vec{R}_{34} + \dots + \vec{R}_{(n-1)n}$ and $\vec{\rho} = \vec{R}_{1n} + \vec{A}$. The components of each of the $\vec{R}_{m(m+1)}$'s are considered known in the preceding coordinate system; that is, in CS (m) with the highest number of primes. For instance,

$$\vec{R}_{23} = \begin{bmatrix} x'_2 \\ y'_2 \\ z'_2 \end{bmatrix} \quad ; \quad \vec{A} = \begin{bmatrix} A_{x'n} \\ A_{y'n} \\ A_{z'n} \end{bmatrix} \quad (235)$$

$$(236)$$

Several quantities are of interest and will be written out here.

1. Orientation of the last CS with respect to the first. This is the matrix of direction cosines which transforms a vector represented in CS (n') to its representation in CS (1). Call this matrix D. In a continuation of the process used above to derive the Eulerian angle equations, the transposes of the rotation matrices are simply multiplied in order:

$$D = \tilde{D}_x(\Theta_1) \tilde{D}_z(\Theta_2) \tilde{D}_x(\Theta_3) \tilde{D}_z(\Theta_3') \tilde{D}_x(\Theta_3'') \tilde{D}_y(\Theta_5) \dots \tilde{D}_z(\Theta_{n-1}) \tilde{D}_y(\Theta_n) \quad (237)$$

The \tilde{D}_x 's etc. are the transposes of the single axis rotations given in Equations 223, 224, 225.

2. Representation of the vector \vec{A} in CS (1) in terms of its components in CS (n'):

$$\begin{bmatrix} A_{x1} \\ A_{y1} \\ A_{z1} \end{bmatrix} = D \begin{bmatrix} A_{x'n} \\ A_{y'n} \\ A_{z'n} \end{bmatrix} \quad (238)$$

3. The vector $\vec{\rho}$ represented in CS (1) in terms of the rotation matrices, the components of the $\vec{R}_{m(m+1)}$'s in the CS's in which they are known, and the components of \vec{A} in CS (n'):

$$\vec{\rho} = \tilde{D}_x(\Theta_1) \left\{ \vec{R}_{12} + \tilde{D}_z(\Theta_2) \left[\vec{R}_{23} + \tilde{D}_x(\Theta_3) \tilde{D}_z(\Theta_3') \tilde{D}_x(\Theta_3'') \left(\vec{R}_{34} + \vec{R}_{45} + \dots + \tilde{D}_y(\Theta_5) \left[\vec{R}_{56} + \dots + \tilde{D}_z(\Theta_{n-1}) \left\{ \vec{R}_{(n-1)n} + \tilde{D}_y(\Theta_n) \begin{bmatrix} A_{x'n} \\ A_{y'n} \\ A_{z'n} \end{bmatrix} \right\} \right] \right) \right] \right\} \right\} \quad (239)$$

4. The vector $\vec{R}_{1n} = \vec{\rho} - \vec{A}$:

$$\begin{aligned} & \tilde{D}_x(\Theta_1) \left\{ \vec{R}_{12} + \tilde{D}_z(\Theta_2) \left[\vec{R}_{23} + \tilde{D}_x(\Theta_3) \tilde{D}_z(\Theta_3') \tilde{D}_x(\Theta_3'') \left(\vec{R}_{34} + \vec{R}_{45} + \right. \right. \right. \\ & \left. \left. + \tilde{D}_y(\Theta_5) \left[\vec{R}_{56} + \dots + \tilde{D}_z(\Theta_{n-1}) \vec{R}_{(n-1)n} \right] \right] \right\} \end{aligned} \quad (240)$$

A study of Equations 239 and 240 reveals a general method of writing down the position of a point P in terms of all the simple transformations used to get to P from the initial origin. Write down in order each matrix and each vector which is used to transform from CS (1) to the point P.

$$\begin{aligned} & \tilde{D}_x(\Theta_1) \vec{R}_{12} \tilde{D}_z(\Theta_2) \vec{R}_{23} \tilde{D}_x(\Theta_3) \tilde{D}_z(\Theta_3') \tilde{D}_x(\Theta_3'') \vec{R}_{34} \vec{R}_{45} \tilde{D}_y(\Theta_5) \vec{R}_{56} \dots \\ & \tilde{D}_z(\Theta_{n-1}) \vec{R}_{(n-1)} \tilde{D}_y(\Theta_n) \vec{A} \end{aligned} \quad (241)$$

Then consider adjacent pairs of operations, of which there are four possible types:

1. When a $\tilde{D} \vec{R}$ occurs, place a bracket between the two: $\tilde{D} [\vec{R}$
2. When an $\vec{R} \tilde{D}$ occurs, place a + sign between them: $\vec{R} + \tilde{D}$
3. When an $\vec{R} \vec{R}$ occurs, place a + sign between them: $\vec{R} + \vec{R}$
4. When a $\tilde{D} \tilde{D}$ occurs, leave it as the product: $\tilde{D} \tilde{D}$

Applying these rules to Equation 241 yields Equations 239 and 240.

These general methods have been obtained to find positions and orientations and to transform vectors through a series of transformations. The equations are particularly applicable to computer language.

Application

How is this transformation theory applied to an actual physical system? For these equations to be useful, all quantities on the right hand sides must be either fixed lengths or angles, measured lengths or angles which can be set, or transduced lengths or angles. Consider for example the Cornell Aeronautical Laboratories exoskeleton in Figures 65 and 66. It has adjustable link lengths, transduced angles, and fixed geometry and is therefore susceptible to the treatment developed above. To determine the location and orientation of any link, say the hand link, with respect to another, say the spine link, place a coordinate axis along each pin joint axis and mark an origin at a convenient place on the link. Draw vectors from origin to origin starting at the first origin. Put in extra origins if necessary so that each sliding or adjustable link has a vector along its length. Erect a rectangular coordinate system, x_1 , y_1 , and z_1 wherever desired in link

number one. This is the "bench mark" or starting point. Number the origins from 1 to n. Extend the linkage to the position which will be called the neutral or zero position. Starting with CS (1), transform this set of axes out along the linkage in successive steps each one of which is either a rotation about an x, y, or z axis or a pure translation. For each, write down the matrix $D_x(\Theta_m)$ etc. or vector $\vec{R}_{m(m+1)}$. Then build up the desired transformations as shown in the preceding section.

Comments

No more than three successive rotations will be required after a vector translation. If three are required, this amounts to an Eulerian triad and Equations 203, 204, and 205 may have to be solved to find the angles if they are not obvious from symmetry. At any rate, the last rotation before each translation should be the transduced angle. If it is desirable to shift the nominal zero of this angle, use the two trigonometric identities given in Equations 242 and 243 where the matrix

$$\sin(\Theta_{on} + \Theta_n) = \sin \Theta_{on} \cos \Theta_n + \cos \Theta_{on} \sin \Theta_n \quad (242)$$

$$\cos(\Theta_{on} + \Theta_n) = \cos \Theta_{on} \cos \Theta_n - \sin \Theta_{on} \sin \Theta_n \quad (243)$$

components are written out. Sometimes an origin will not be in the hardware as in the arm rotation joints in the CAL exoskeleton. Since there are many ways to solve each problem, care and experience in setting up the coordinate systems can make the resultant expressions much simpler.

Once the equations have been set up, and the fixed angles and lengths calculated, the resulting expression can be multiplied out leaving only the transduced and adjustable quantities as unknowns. When that is done, the working equations will have been derived for transforming any vector quantity measured in the nth coordinate system to its representation in the original coordinate system and for finding the position of a point in the nth link with respect to the original system in terms of transduced quantities.

APPENDIX II

MECHANICAL WORK AND ITS RELATION TO SUIT JOINT MOTION

The concept of mechanical work is essential to an understanding of suit mechanics. Consider a force \vec{F} acting at a point \vec{r} . The point \vec{r} moves in time and its path is described by the function $\vec{r}(t)$.

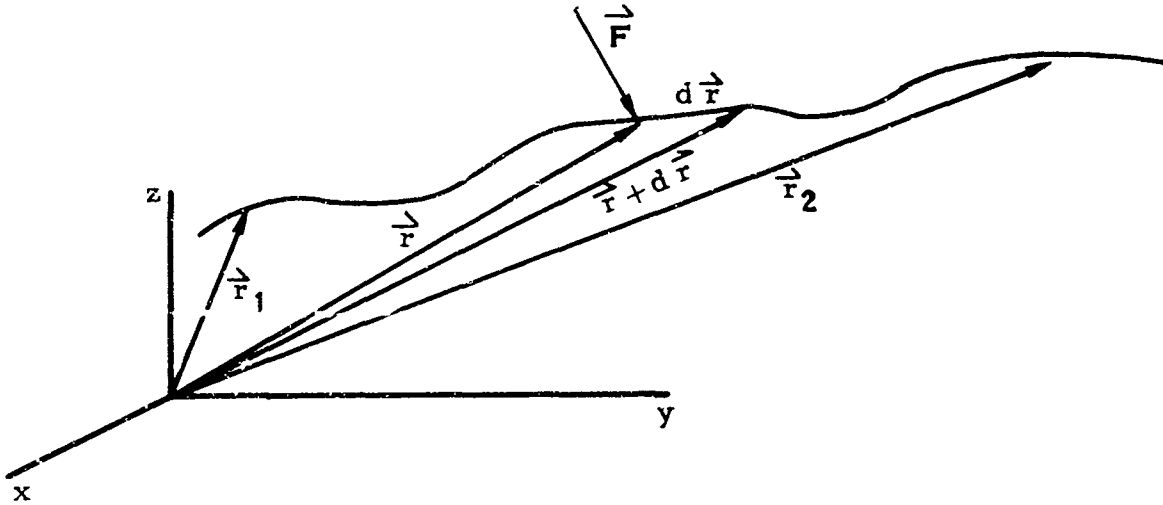


FIGURE 152. MODEL FOR DEFINITION OF MECHANICAL WORK

The work done by the force \vec{F} acting at \vec{r} as \vec{r} moves from \vec{r}_1 to \vec{r}_2 is defined by Equation 244.

$$W_{12} = \int_{\vec{r}_1}^{\vec{r}_2} \vec{F}(\vec{r}) \cdot d\vec{r} \quad (244)$$

Since the special case of rotational motion and torque is of primary interest here, the expression for work will be written in terms of these quantities. Referring to Figure 153, the velocity \vec{V} of the point is related to the angular velocity $\vec{\omega}$ of the point about the origin by Equation 245.

$$\vec{V} = \frac{d\vec{r}}{dt} = \vec{\omega} \times \vec{r} \quad (245)$$

If $d\vec{\theta}$ is defined by $\frac{d\vec{\theta}}{dt} = \vec{\omega}$, then $d\vec{r} = d\vec{\theta} \times \vec{r}$ and from Equation 244, $W_{12} = \int_{\vec{r}_1}^{\vec{r}_2} \vec{F} \cdot (d\vec{\theta} \times \vec{r})$. But recall the vector identity: $\vec{A} \cdot (\vec{B} \times \vec{C}) = (\vec{C} \times \vec{A}) \cdot \vec{B}$

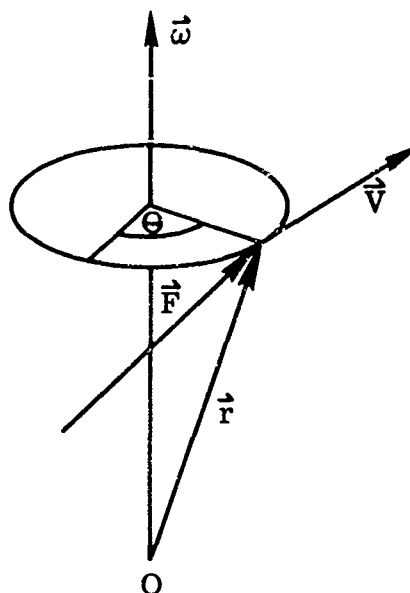


FIGURE 153. FORCES AND ROTARY MOTION

and the definition of torque \vec{T} about the origin due to the force \vec{F} acting at \vec{r} :
 $\vec{T} = \vec{r} \times \vec{F}$. Substituting in the last expression for W_{12} ,

$$W_{12} = \int_{\vec{r}_1}^{\vec{r}_2} (\vec{r} \times \vec{F}) \cdot d\vec{\Theta} \quad (246)$$

or

$$W_{12} = \int_{\vec{r}_1}^{\vec{r}_2} \vec{T} \cdot d\vec{\Theta} \quad (247)$$

This is the expression for the work done by the torque in moving the point from Θ_1 to Θ_2 . But for pure rotational motion, $\vec{T} \cdot d\vec{\Theta} = T d\Theta$, so that

$$W_{12} = \int_{\Theta_1}^{\Theta_2} T d\Theta \quad (248)$$

If there is no motion, i.e., if $d\vec{r}$ or $d\vec{\Theta}$ equals zero, then there is no work done. Furthermore, in a conservative force field (no dissipative forces such as friction acting), the work done in moving a body from \vec{r}_1 to \vec{r}_2 is a function of \vec{r}_1 and \vec{r}_2 and is independent of the path traveled or the time taken. A consequence of this is that, when the body is returned to its starting position at its initial speed, the work done on it from start to finish is zero.

Thus, when a body with mass m is raised a distance h , the work done on it is given by Equation 249.

$$W_{12} = \int_{x_1}^{x_2} F \, dx = \int_{x_1}^{x_2} (ma + mg) \, dx \quad (249)$$

where g is the acceleration of gravity and $a = \frac{dv}{dt}$ is the acceleration imparted by F .

Integrating,

$$W_{12} = \int_{x_1}^{x_2} m \frac{dv}{dt} dx + \int_{x_1}^{x_2} mg dx = m \int_{v_1}^{v_2} v dv + mg \int_{x_1}^{x_2} dx \quad (250)$$

$$W_{12} = \frac{1}{2} m (v_2^2 - v_1^2) + mg (x_2 - x_1) \quad (251)$$

$$W_{12} = \frac{1}{2} m \Delta (v^2) + mgh \quad (252)$$

In words, the work equals the sum of the increases in kinetic and potential energies. If the body is returned to its starting point at zero velocity, the work done on it is zero because $\Delta (v^2) = 0$ and $x_1 = x_2$. Similarly, when a suit joint is flexed through a cycle and frictional forces are negligible or not considered, the work done is zero.

For some time, several experimenters in human engineering have been measuring motion, forces, and torques involved in raising and lowering weights repetitively in flexing and extending suit joints, etc. They calculate a quantity which they report as work which seems to treat all displacements as positive. This quantity is not work nor is it the metabolic energy expended. It does not appear to bear any useful theoretical relationship to metabolic energy expenditure. It is, nevertheless, reported as work, usually without definition.

Other experimenters have chosen "correction factors" to account for negative work terms (ref. 95). To compute metabolic energy expenditure, they add some fraction of the absolute value of the negative work terms to the positive work terms. The fraction varies from 0.4 to 0.7 and is appropriate only for a specific motion. This "rule of thumb" approach does not appear to be based on fundamental physiological considerations and is therefore unsatisfactory for general motions. A more fundamental approach is presented on pages 57 through 61.

APPENDIX III

CALCULATION SHOWING NEAR EQUIVALENCE OF TORQUE TESTING AT SEA LEVEL PRESSURE TO TESTING AT SPACE PRESSURE

It is generally assumed that torque testing at 3.5 psi above sea level pressure is equivalent to testing at 3.5 psia. This appendix shows that, while this is not strictly true, the difference is negligible. It is shown that the mechanical work to flex a joint to a given angle depends not only on the differential pressure but also on the absolute pressure.

MODEL

If, when a suit joint is flexed, the gas is compressed due to a volume change, mechanical work must be done. Figure 154 is adequate for discussion of the pressure dependence of this work.

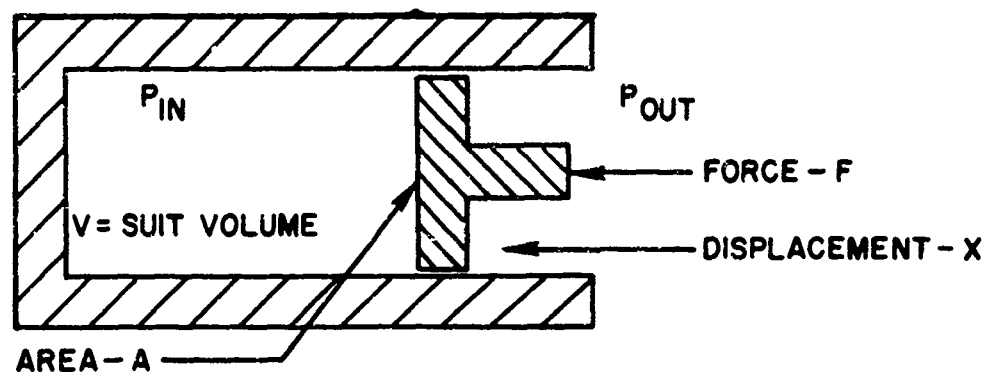


FIGURE 154. MODEL FOR DISCUSSION OF THERMODYNAMIC WORK

An actual suit has a pressure regulator but a man can flex the joint much faster than the regulator can follow.

DERIVATION OF WORK EQUATION

To eliminate the dynamics of the regulator from the discussion, a "worst case" calculation is made. We assume an adiabatic compression and no pressure regulation. For an adiabatic compression,

$$P_{in} V^{\gamma} = P_{in1} V_1^{\gamma} \quad (253)$$

where P_{in1} and V_1 are the initial absolute pressure and volume and γ is the ratio of specific heats, which is taken to be 1.4. Equation 254 gives the work done on the gas.

$$W = \int_{V_1}^{V_1 + \Delta V} F dx = \int_{V_1}^{V_1 + \Delta V} (P_{in} - P_{out}) A dx \quad (254)$$

or

$$W = - \int_{V_1}^{V_1 + \Delta V} (P_{in} - P_{out}) dV \quad (255)$$

The minus sign indicates that a positive displacement decreases the volume. When Equation 255 is integrated using the expression in Equation 253 for P_{in} , we find

$$W = - \frac{P_{in1} V_1^\gamma}{1-\gamma} \left[(V_1 + \Delta V)^{1-\gamma} - V_1^{1-\gamma} \right] + P_{out} \Delta V \quad (256)$$

Equation 256 can be expanded in powers of ΔV .

$$W = - \frac{P_{in1} V_1^\gamma}{1-\gamma} \left[V_1^{1-\gamma} + (1-\gamma) V_1^{-\gamma} \Delta V + \frac{1}{2} (1-\gamma) (-\gamma) V_1^{-1-\gamma} (\Delta V)^2 + \dots - V_1^{1-\gamma} \right] + P_{out} \Delta V \quad (257)$$

If terms of order $(\Delta V)^3$ and higher are neglected, Equation 258 results.

$$W = - (P_{in1} - P_{out}) \Delta V + \frac{\gamma P_{in1} V_1}{2} \left(\frac{\Delta V}{V_1} \right)^2 \quad (258)$$

where $(P_{in1} - P_{out})$ is the initial differential pressure and P_{in1} is the initial absolute pressure.

CALCULATIONS

To find the relative sizes of the two terms in Equation 258, some values are assumed for ΔV and V_1 . It was shown in the test that a joint with torque which increases linearly from 0 at 20° to 4 ft lb at 100° changes volume by 9.5 cubic inches over that range. The gas volume in a manned suit is about 1.8 cubic feet. Using the following values

$$\begin{aligned} P_{in1} - P_{out} &= 3.5 \text{ psi} \\ \Delta V &= 9.5 \text{ cubic inches} \\ \gamma &= 1.4 \\ V_1 &= 1.8 \text{ cubic feet} \approx 3100 \text{ cubic inches} \end{aligned}$$

in Equation 258, we find that

$$W = 33.3 \text{ in lb} + 0.020 P_{in1} \text{ in}^3 \quad (259)$$

At space condition $P_{in1} = 3.5$ psia; in the laboratory $P_{in1} = (14.7 + 3.5)$ psia = 18.2 psia. Under these two conditions, the second term in equation 259 takes on the values 0.070 in lb and 0.36 in lb respectively. The ratio of the difference of these numbers to the first term in Equation 259 is 0.8%.

COMMENTS

This was a "worst case" calculation. A more realistic case would involve some pressure regulation and would not be perfectly adiabatic. Both of these facts tend to make the 0.8% figure conservatively high. Thus, torque testing at sea level outside pressure is entirely adequate.

APPENDIX IV

CALCULATION OF THE TORQUE ABOUT ANY JOINT OF A GENERALIZED DUMMY LINKAGE SYSTEM FROM THE READOUTS OF FORCE TRANSDUCERS ON THE LINKS AND THE INTERLINK ANGLE TRANSDUCERS

In this appendix expressions are derived for the torque at any dummy joint due to the forces acting on the dummy surface. The derivation applies to a general linkage geometry with an array of force transducers on the links. It is assumed that the orientation of the sensitive axis and the location of the loading point of each transducer are fixed and known within each link. The expressions are presented in a form for computer programming in terms of fixed dummy geometry with force and interlink angle transducer readouts as input data.

The expressions to be derived are valid for any array of force transducers on each link, such as (1) a two dimensional array completely covering the skin surface, (2) a series of load supporting rings surrounding the dummy link, or (3) the four or six transducers supporting a light weight shell over the link. The transduction errors in the first and the last cases are treated in Appendixes V and VI.

MODEL

For the dummy linkage, consider the general linkage system presented in Figure 151. We will calculate the torque at any origin O_j due to the forces on the n th link. Then the torques on each of the links will be summed to give the total torque at O_j due to all the outboard suit forces. For example, O_j may be the origin of the shoulder elevation joint. The torque about O_j is due to all the forces acting on the upper arm, forearm, and hand. The j th and the n th links are shown in Figure 155 for definition of notation. The interlink angles and link lengths are defined in Appendix I. O_j and O_n are the origins of link j and link n . \vec{F}_{ni} is the i th force on the n th link. F_{ni} (a transducer readout) is the magnitude of \vec{F}_{ni} . $\hat{C}_{ni} = \frac{\vec{F}_{ni}}{F_{ni}}$ is a unit vector fixed in link n which defines the sensitive axis of the transducer. \vec{A}_{ni} is the position vector fixed with respect to O_n which defines the loading point of the i th transducer. $\vec{B}_{ni} = \vec{A}_{ni} \times \hat{C}_{ni}$ is a vector fixed in link n .

CALCULATION

The torque at O_j due to the i th force on the n th link is \vec{T}_{jni} . By definition,

$$\vec{T}_{jni} = \vec{\rho}_{jni} \times \vec{F}_{ni} \quad (260)$$

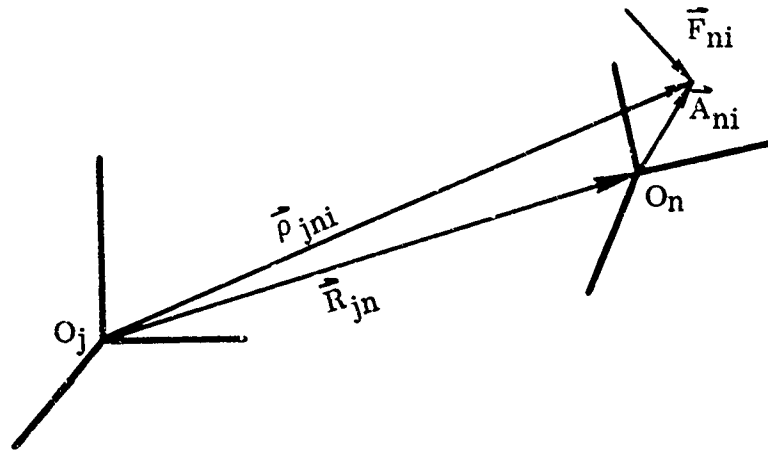


FIGURE 155. MODEL FOR DEFINITION OF NOTATION

But, from Figure 155, $\vec{\rho}_{jni} = \vec{R}_{jn} + \vec{A}_{ni}$, so that

$$\begin{aligned}\vec{T}_{jni} &= \vec{R}_{jn} \times \vec{F}_{ni} + \vec{A}_{ni} \times \vec{F}_{ni} \\ &= (\vec{R}_{jn} \times \hat{C}_{ni} + \vec{B}_{ni}) F_{ni}\end{aligned}\quad (261)$$

\hat{C}_{ni} and \vec{B}_{ni} are considered to be fixed in link n. To represent these vectors in the coordinate system of link j, they are multiplied by the matrix rotation operator D^{jn} . \vec{R}_{jn} must also be represented in link j. A straightforward method for writing D^{jn} and \vec{R}_{jn} is presented at the end of Appendix I. These expressions represent the orientation and position of link n with respect to link j and contain dummy geometry and the transduced interlink angles. Thus, \vec{T}_{jni} is represented in link j as follows.

$$\vec{T}'_{jni} = \left[\vec{R}_{jn} \times (D^{jn} \hat{C}_{ni}) + D^{jn} \vec{B}_{ni} \right] F_{ni} \quad (262)$$

Say there are N_n transducers on the nth link and M links altogether. Then the total torque at O_j due to all forces on the outboard links is obtained by summing over i and n.

$$\vec{T}'_j = \sum_{n=j}^M \left\{ \sum_{i=1}^{N_n} \left[\vec{R}_{jn} \times (D^{jn} \hat{C}_{ni}) + D^{jn} \vec{B}_{ni} \right] F_{ni} \right\} \quad (263)$$

All the transduced angles, Θ_j through Θ_{n-1} , are contained in \vec{R}_{jn} and the matrix D^{jn} which are set up as shown in Appendix I. The F_{ni} 's are the force transducer readouts. The \hat{C}_{ni} 's and \vec{B}_{ni} 's are fixed vectors which can be determined from geometrical calculations or by calibration.

APPENDIX V

ERROR ANALYSIS FOR SUIT TORQUE AS CALCULATED FROM THE OUTPUTS OF A BLANKET OF FORCE TRANSDUCERS COMPLETELY COVERING A DUMMY ARM IN AN OPTIMAL ARRAY

In this appendix the probable error in suit torque determination from measurements of mechanical pressure distribution over the surface of the body is treated. The error is assumed to be due to instrument error and geometrical considerations. The layout of the transducers is optimized for minimum error. If sufficiently accurate, the mechanical pressure distribution technique would be an excellent method for determining suit imposed torques since it fully defines the mechanical interface between man and the suit.

The transducers considered completely cover the dummy surface and are assumed to support only normal forces. Because of the finite size of the sensitive face of the transducers, the exact point of loading is not known. The transducer faces are expected to be between 1 cm and 5 cm on the sides.

MODEL

For error analysis, the transducers are assumed to lie on a right circular cylinder. This model should have very nearly the same error as a dummy forearm of the same length.

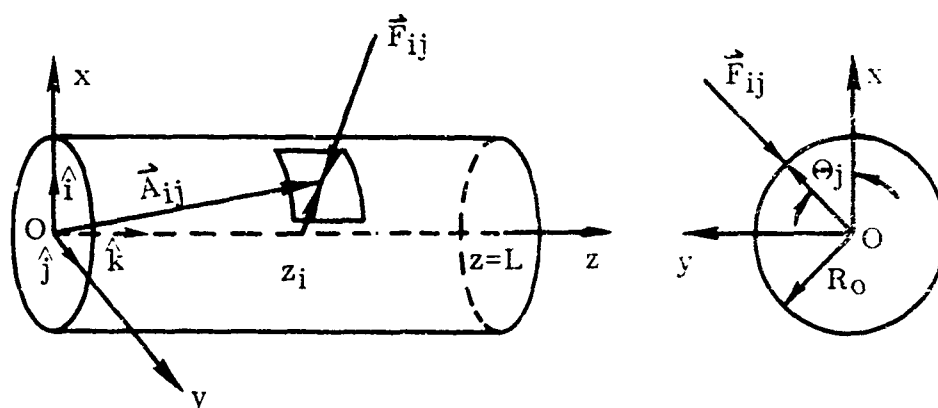


FIGURE 156. MODEL FOR ERROR ANALYSIS

\vec{F}_{ij} is the force acting on the surface at z_i and θ_j . $|\vec{F}_{ij}| = F_{ij}$ is the transducer readout. (Note that the notation has been changed from that of Appendix IV for convenience.)

DERIVATION OF ERROR EQUATION

The error in torque \vec{T} about O is the rms sum of the errors of its components; however, for purposes of illustration, only the error in the x component T_x is considered here. By the procedures of Appendix IV,

$$\vec{T} = \sum_{i=1}^M \sum_{j=1}^N \vec{A}_{ij} \times \vec{F}_{ij} \quad (264)$$

$$\vec{T} = \sum_{i=1}^M \sum_{j=1}^N (\hat{i} R_0 \cos \Theta_j + \hat{j} R_0 \sin \Theta_j + z_i \hat{k}) \times (\hat{i} \cos \Theta_j + \hat{j} \sin \Theta_j) F_{ij} \quad (265)$$

So that T_x , hereafter written simply T, is

$$T = - \sum_{i=1}^M \sum_{j=1}^N z_i \sin \Theta_j F_{ij} \quad (266)$$

The transducers are abutting on all sides to cover the entire cylinder. There are M rings of transducers along the z axis and N columns around the cylinder. MN is the total number of transducers. In practice, $-z_i \sin \Theta_j$ could be written B_{ij} and would be determined by calibration. However, for the error calculation, the explicit form is used.

From random error theory (ref. 99), if a quantity Q is calculated from the measured independent quantities q_1, q_2, \dots, q_n , then the probable error in Q can be written in terms of the probable errors in the q_i 's as follows.

$$\Delta Q = \left[\sum_{i=1}^N \left(\frac{\partial Q}{\partial q_i} \right)^2 (\Delta q_i)^2 \right]^{1/2} \quad (267)$$

By definition, the probable error band contains 50% of the experimental points for a large sample of points. When Equation 267 is applied to Equation 266, the expression for probable error in torque results.

$$(\Delta T)^2 = \sum_{i,j}^{M,N} (z_i \sin \Theta_j \Delta F_{ij})^2 + \sum_{i,j}^{M,N} (F_{ij} \sin \Theta_j \Delta z_i)^2 + \sum_{i,j}^{M,N} (F_{ij} z_i \cos \Theta_j \Delta \Theta_j)^2 \quad (268)$$

The sums will be calculated separately and will be referred to by Roman numerals:

$$I = \sum_{i,j} (z_i \sin \Theta_j \Delta F_{ij})^2 \quad (269)$$

$$II = \sum_{i,j} (F_{ij} \sin \Theta_j \Delta z_i)^2 \quad (270)$$

$$III = \sum_{i,j} (F_{ij} z_i \cos \Theta_j \Delta \Theta_j)^2 \quad (271)$$

Thus

$$(\Delta T)^2 = I + II + III \quad (272)$$

The errors $\Delta \Theta_j$ and Δz_i come not from manufacturing or calibration errors but from the finite size of the transducing area. That is, $B_{ij} = -z_i \sin \Theta_j$ is determined with high accuracy by calibrating with a known force at the center of the transducer. However, the actual suit loading forces will not, in general, fall at the center of each transducer. ΔF_{ij} is the instrument error.

ASSUMPTIONS

1. The instrument error ΔF_{ij} is independent of location (i and j), transducer area (M and N), and instantaneous load F_{ij} . Thus, the transducers are "percent of full scale" devices
2. Δz_i is independent of i, j, and N but dependent on M
3. $\Delta \Theta_j$ is independent of i, j, and M but dependent on N

CALCULATIONS

The sums I, II, and III will be calculated one at a time, by removing the dependence of the sums on M, N, and ΔF_{ij} and then approximating the sums by area integrals involving functions of the mechanical pressure distribution $P(z, \Theta)$. Then the error is minimized by optimum choices of the total number of transducers MN and the ratio of rings to columns $R = M/N$. Pressure distributions are assumed so the necessary instrument error (or accuracy) ΔF_{ij} can be calculated as a function of allowable torque error ΔT .

Consider the first term in Equation 272.

$$I = \sum_{i=1}^M \sum_{j=1}^N (z_i \sin \Theta_j \Delta F_{ij})^2 \quad (273)$$

By Assumption (1) ΔF_{ij} is independent of everything under the sum so that

$$I = (\Delta F)^2 \sum_{i=1}^M \sum_{j=1}^N (z_i \sin \Theta_j)^2 \quad (274)$$

I increases indefinitely with M or N , as expected with an infinite number of transducers each with finite error. To approximate I by an integral, consider the following. $(\Delta z)_i = \frac{L}{M}$ = length of i th transducer. Similarly, $(\Delta \Theta)_j = \frac{2\pi}{N}$ = angular width of j th transducer. Note that $(\Delta z)_i \neq \Delta z_i$ and $(\Delta \Theta)_j \neq \Delta \Theta_j$. Then I can be written:

$$I = (\Delta F)^2 \frac{M}{\tau} \frac{N}{2\pi} \sum_{i=1}^M \sum_{j=1}^N (\Delta z)_i (\Delta \Theta)_j z_i^2 \sin^2 \Theta_j \quad (275)$$

Now, as M and N become large, the sum approaches a constant, finite integral.

$$I \approx (\Delta F)^2 \frac{MN}{2\pi L} \int_0^L \int_0^{2\pi} dz d\Theta z^2 \sin^2 \Theta \quad (276)$$

This can be integrated immediately to give

$$I = \frac{MNL^2}{6} (\Delta F)^2 \quad (277)$$

Consider next Π .

$$\Pi = \sum_{i=1}^M \sum_{j=1}^N (F_{ij} \sin \Theta_j \Delta z_i)^2 \quad (278)$$

This sum is treated similarly but depends on the pressure distribution. Here we must find Δz_i as a function of M and L . The length of the transducer is L/M . Since the loading point has equal probability of falling anywhere along the length of the transducer, half the loading points will fall within a length $L/2M$. Thus the probable error band $2\Delta z_i = \frac{L}{2M}$ or

$$\Delta z_i = \frac{L}{4M} \quad (279)$$

Thus

$$\Pi = \left(\frac{L}{4M}\right)^2 \sum_{i=1}^M \sum_{j=1}^N F_{ij}^2 \sin^2 \Theta_j \quad (280)$$

Dividing the force F_{ij} by the transducer area

$$R_o (\Delta\theta)_j (\Delta z)_i = \frac{2\pi R_o L}{MN} \quad (281)$$

will yield the mechanical pressure when the sum is written as an integral.

$$\Pi = \left(\frac{L}{4M}\right)^2 \sum_{i=1} \sum_{j=1} \left(\frac{F_{ij}}{R_o (\Delta\theta)_j (\Delta z)_i}\right)^2 \sin^2 \theta_j \frac{2\pi R_o L}{MN} R_o (\Delta\theta)_j (\Delta z)_i \quad (282)$$

$$\Pi = \frac{\pi R_o^2 L^3}{8M^3 N} \sum_{i=1} \sum_{j=1} P^2(z_i, \theta_j) \sin^2 \theta_j (\Delta\theta)_j (\Delta z)_i \quad (283)$$

$$\Pi = \frac{\pi R_o^2 L^3}{8M^3 N} \int_0^L \int_0^{2\pi} \sin^2 \theta P^2(z, \theta) dz d\theta \quad (284)$$

$P(z, \theta)$ is the mechanical pressure distribution.

By similar treatment,

$$\text{III} = \frac{\pi^3 L R_o^2}{2N^3 M} \int_0^L \int_0^{2\pi} z^2 \cos^2 \theta P^2(z, \theta) d\theta dz \quad (285)$$

The torque T can also be written in terms of $P(z, \theta)$. Recall from Equation 266 that

$$T = - \sum_{i=1}^M \sum_{j=1}^N z_i \sin \theta_j F_{ij} \quad (286)$$

By the same arguments used above,

$$T = R_o \int_0^L \int_0^{2\pi} z \sin \theta P(z, \theta) d\theta dz \quad (287)$$

We define some new quantities to write the expression for $\frac{\Delta T}{T}$:

$$S \equiv MN = \text{number of transducers} \quad (288)$$

$$R \equiv M/N = \text{transducer "aspect ratio"} \quad (289)$$

$$E \equiv \frac{\Delta T}{T} = \frac{\sqrt{I + \Pi + \text{III}}}{T} \quad (290)$$

$$A = \int_0^L \int_0^{2\pi} \sin^2 \Theta P^2(z, \Theta) dz d\Theta \quad (291)$$

$$B = \int_0^L \int_0^{2\pi} z^2 \cos^2 \Theta P^2(z, \Theta) dz d\Theta \quad (292)$$

$$C = \int_0^L \int_0^{2\pi} [P(z, \Theta) z \sin \Theta dz d\Theta]^2 = \left(\frac{T}{R_0}\right)^2 \quad (293)$$

Recall that

R_0 = Cylinder radius

L = Cylinder length

ΔF = Probable error of each force transducer

$P(z, \Theta)$ = Normal mechanical pressure distribution

Then

$$E^2 = \frac{S}{6} \left(\frac{L \Delta F}{T}\right)^2 + \frac{\pi L^3}{8 S^2 R} \frac{A}{C} + \frac{\pi^3 L R}{2 S^2} \frac{B}{C} \quad (294)$$

Now the optimal number S and layout R of the transducers will be found by minimizing E with respect to S and R in Equation 294. This is equivalent to minimizing E^2 .

$$\frac{\partial E^2}{\partial R} = -\frac{\pi L^3}{8 S^2 R^2} \frac{A}{C} + \frac{\pi^3 L}{2 S^2} \frac{B}{C} \quad (295)$$

Equating $\frac{\partial E^2}{\partial R}$ to zero gives the optimal R .

$$R_{opt} = \frac{L}{2\pi} \sqrt{\frac{A}{B}} \quad (296)$$

Substituting this into Equation 294 yields for $R = R_{opt}$

$$E^2 = \frac{S}{6} \left(\frac{L \Delta F}{T}\right)^2 + \frac{\pi^2 L^2}{2 S^2} \frac{\sqrt{AB}}{C} \quad (297)$$

Now E is minimized with respect to S .

$$\frac{\partial E^2}{\partial S} = \frac{1}{6} \left(\frac{L \Delta F}{T}\right)^2 - \frac{\pi^2 L^2}{S^3} \frac{\sqrt{AB}}{C} = 0 \quad (298)$$

Solving for optimal S with R_{opt} gives

$$S_{opt} = \left(\frac{6\pi^2 L^2 \sqrt{AB}}{C} \right)^{1/3} \left(\frac{T}{L \Delta F} \right)^{2/3} \quad (299)$$

Substituting Equation 299 into Equation 297 gives the equation for optimal E.

$$E_{opt} = \frac{1}{2} \left(\frac{6\pi^2 L^2 \sqrt{AB}}{C} \right)^{1/6} \left(\frac{L \Delta F}{T} \right)^{2/3} \quad (300)$$

This is the expression for the fractional error $\frac{\Delta T}{T}$ in torque as a function of instrument error ΔF . The transducer layout is to be chosen optimally on the basis of an assumed pressure distribution. Numbers can be obtained for E_{opt} , S_{opt} , and R_{opt} if a pressure distribution is chosen and the instrument error is given. To gain an understanding of these functions, several pressure distributions are assumed and $\frac{\sqrt{AB}}{C}$ is calculated from the defining integrals for A, B, and C.

Let

$$\begin{aligned} P_a(z, \Theta) &= P_0, & 0 \leq \Theta \leq \pi \\ P_b(z, \Theta) &= P_0 \sin \Theta, & 0 \leq \Theta \leq \pi \\ P_c(z, \Theta) &= P_0 z/L, & 0 \leq \Theta \leq \pi \\ P_d(z, \Theta) &= (P_0 z/L) \sin \Theta, & 0 \leq \Theta \leq \pi \\ P_e(z, \Theta) &= P_0, & 0 \leq \Theta \leq 3\pi/2 \\ P_f(z, \Theta) &= P_0, & 0 \leq \Theta \leq 3\pi/4 \\ & & 0 \leq z \leq L/4 \end{aligned}$$

P_a through $P_f = 0$ elsewhere

Consider P_d for example. Here the loading is all on the top half of the arm and increases linearly with z .

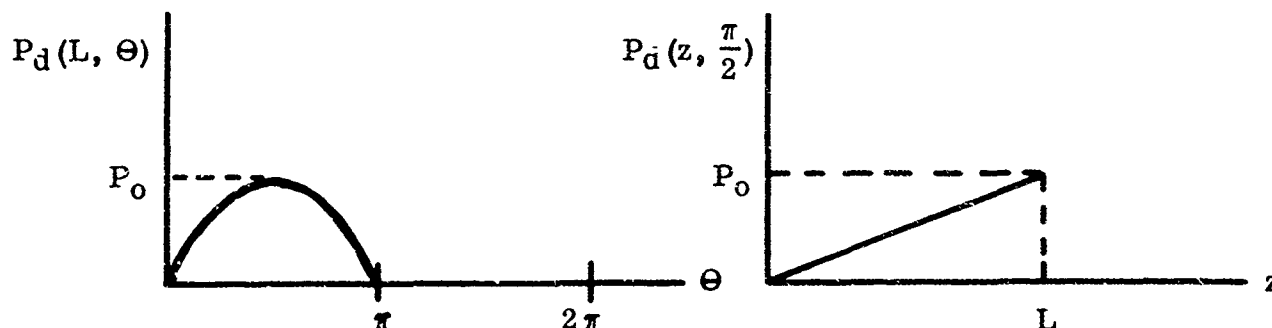


FIGURE 157. SAMPLE PRESSURE DISTRIBUTION

In all cases (a through f) the results are independent of P_0 . The results are summarized below.

TABLE XVI

VALUES FOR CALCULATING OPTIMAL R, S, AND E
BASED ON ASSUMED PRESSURE DISTRIBUTIONS

$P_x (z, \Theta)$	R_{opt}	$S_{opt} \left(\frac{L \Delta F}{T} \right)^{2/3}$	$E_{opt} \left(\frac{T}{L \Delta F} \right)^{2/3}$
x = a	0.28	3.8	0.97
b	0.48	3.4	0.92
c	0.21	3.8	0.97
d	0.36	3.4	0.92
e	0.31	6.9	1.31
f	2.34	8.1	1.46

R_{opt} is only weakly dependent on pressure distribution while S_{opt} and E_{opt} are slightly more dependent.

P_d and a typical L and T are used to find the instrument accuracy, ΔF , necessary to give a 5% torque measurement. A typical forearm link length L is 0.40 meter and a typical suit elbow torque is 0.80 kg meter. Then from Table XVI above,

$$\begin{aligned} \Delta F &= \left(\frac{(E_{opt})_d}{0.92} \right)^{\frac{3}{2}} \times \frac{T}{L} \\ &= \left(\frac{0.05}{0.92} \right)^{\frac{3}{2}} \times \frac{0.80 \text{ kg meter}}{0.40 \text{ meter}} \end{aligned} \quad (301)$$

$$\Delta F = 0.025 \text{ kg (0.055 lb)} \quad (302)$$

Each transducer would have to be rated for at least 10 kg (22 lb) which means that the transducers must be accurate to 0.25% of full scale.

The number of transducers calculated using the same figures is

$$S_{opt} = 70 \text{ transducers}$$

COMMENTS

It is interesting to note that $R_{opt} \approx 0.3$ calls for long thin transducers aligned with the z axis. However, the error in the torque determination is not strongly dependent on S or R. Therefore, other considerations can be included in their choice.

It should be noted that the figure of 0.25% accuracy for the force transducers to give a 5% torque determination is optimistic. Only instrument error and the finite size of the transducer were considered in the error calculation. Temperature and other sources of systematic error would make the situation worse. If, in addition, the transducers were mounted on the compliant human skin, then the uncertainty in the orientations of their sensitive axes would also contribute to error. Finally, it should be noted that only one link was considered. In a several link system, the error would increase considerably due to the large distances of some of the transducers from the origin.

Because of these considerations, it is apparent that 5% torque transduction using the technique of this appendix is beyond the foreseeable state of the art.

APPENDIX VI

ERROR ANALYSIS FOR SUIT TORQUE AS CALCULATED FROM THE OUTPUTS OF FORCE TRANSDUCERS SUPPORTING A LOAD BEARING SHELL ON A DUMMY LINKAGE SYSTEM

In this appendix, a treatment of the error in suit torque determination by the shell force transduction technique (see page 75) is presented. Because the technique is simpler and more accurate than the transduction technique using load distribution transducers, a larger portion of the dummy linkage is treated. The sources of error treated are the random instrument errors in the force transducers and angle transducers and the error due to inexact location of the force transducers. The notation is consistent with that of Appendix IV.

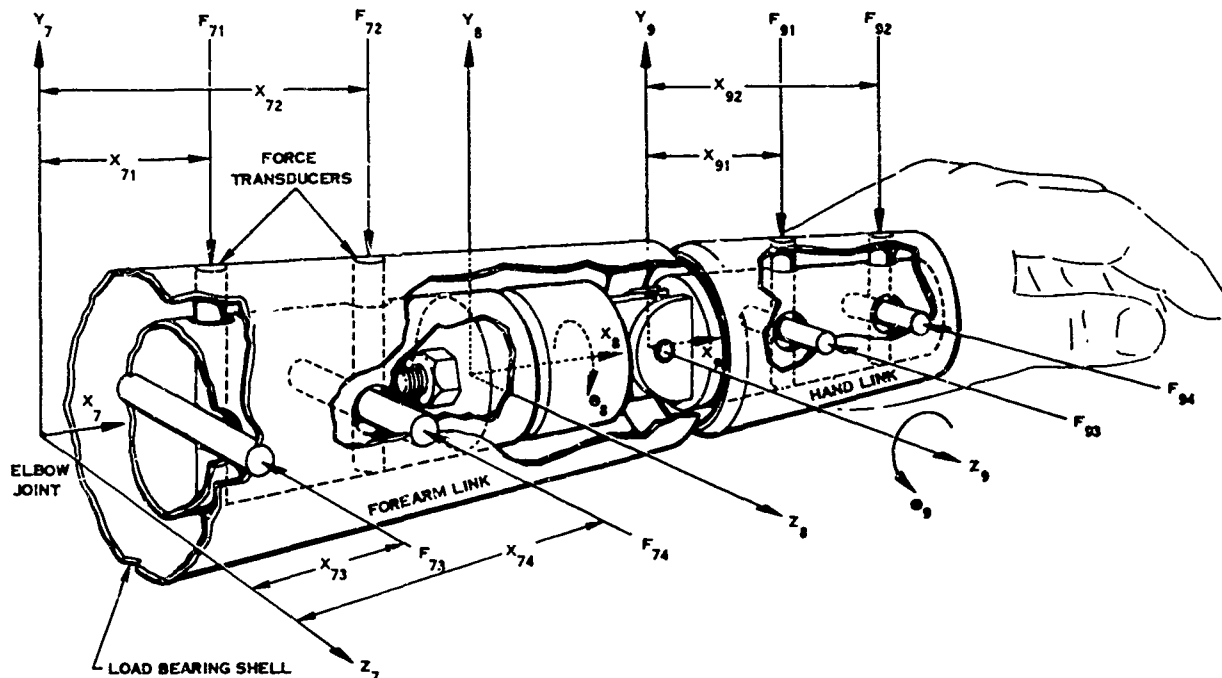


FIGURE 158. MODEL FOR ERROR CALCULATION

For error analysis purposes, this is an adequate model for the dummy forearm and hand. On the heavy underlying linkage are mounted force transducers which support lightweight load bearing shells. One shell is cantilevered from link 7 to carry the suit load of links 7 and 8. Another shell surrounds link 9. In this analysis, the weights and inertias of the shells are neglected. These effects would be included, if necessary, in a computer program for torque computation; but their neglect here has little effect on the accuracy of the error analysis.

The notation is as follows.

Θ_8 corresponds to forearm pronation

Θ_9 corresponds to wrist flexion

F_{ni} is the reading of the i th force transducer on the n th link

x_{ni} is the x coordinate of the sensing axis of the i th transducer on the n th link

X_{79} is the distance from the elbow joint to the wrist joint

From Equation 263, the expression for the torque at the elbow joint can be written down immediately.

$$\vec{T}_7 = \sum_{n=7}^9 \left\{ \sum_{i=1}^4 \left[\vec{R}_{7n} \times (D^{7n} \hat{C}_{ni}) + D^{7n} \vec{B}_{ni} \right] F_{ni} \right\} \quad (303)$$

And from notational definitions in Appendix IV, it follows that

$$\vec{R}_{77} = 0$$

$$\vec{R}_{79} = X_{79} \hat{i}_7$$

n takes on the values 7 and 9

$$D^{77} = \begin{bmatrix} 1 & 0 & 0 \\ 0 & 1 & 0 \\ 0 & 0 & 1 \end{bmatrix}$$

$$D^{79} = \begin{bmatrix} 1 & 0 & 0 \\ 0 & C_8 & -S_8 \\ 0 & S_8 & C_8 \end{bmatrix} \begin{bmatrix} C_9 & -S_9 & 0 \\ S_9 & C_9 & 0 \\ 0 & 0 & 1 \end{bmatrix} = \begin{bmatrix} C_9 & -S_9 & 0 \\ C_8 S_9 & C_8 C_9 & -S_8 \\ S_8 S_9 & S_8 C_9 & C_8 \end{bmatrix}$$

where $C_8 = \cos \Theta_8$, $S_8 = \sin \Theta_8$, etc. Also,

$$\begin{aligned} \hat{C}_{71} &= \hat{C}_{72} = \hat{j}_7 & \hat{C}_{91} &= \hat{C}_{92} = \hat{j}_9 \\ \hat{C}_{73} &= \hat{C}_{74} = \hat{k}_7 & \hat{C}_{93} &= \hat{C}_{94} = \hat{k}_9 \end{aligned}$$

$$\vec{B}_{ni} = \begin{cases} x_{ni} \hat{k}_n & \text{for } n = 1, 2 \\ -x_{ni} \hat{j}_n & \text{for } n = 3, 4 \end{cases}$$

When these are inserted into Equation 303 and terms are collected, the following expression is found for the z component of the torque vector at the elbow joint.

$$(\vec{T}_7)_z = - \left[x_{71} F_{71} + x_{72} F_{72} + (X_{79} C_9 + x_{91}) C_8 F_{91} + (X_{79} C_9 + x_{92}) C_8 F_{92} + \right. \\ \left. - (X_{79} + x_{93} C_9) S_8 F_{93} - (X_{79} + C_9 x_{94}) S_8 F_{94} \right] \quad (304)$$

ERROR EQUATION

The problem now is to calculate the probable error in $(\vec{T}_7)_z$ due to random error in the x's, Θ 's, and F's. From Equation 304, it is seen that $(\vec{T}_7)_z$, or simply T , is a function of 15 independently measured quantities. That is

$$T = T(x_{71}, x_{72}, x_{91}, x_{92}, x_{93}, x_{94}, X_{79}, F_{71}, F_{72}, F_{91}, F_{92}, F_{93}, F_{94}, \Theta_8, \Theta_9) \quad (305)$$

The x's are measured and the F's and Θ 's are transduced. Application of Equation 267 from Appendix V yields the equation for error in torque determination.

$$(\Delta T)^2 = (F_{71})^2 (\Delta x_{71})^2 + (F_{72})^2 (\Delta x_{72})^2 + (C_8 F_{91})^2 (\Delta x_{91})^2 + (C_8 F_{92})^2 (\Delta x_{92})^2 + \\ + (S_8 C_9 F_{93})^2 (\Delta x_{93})^2 + (S_8 C_9 F_{94})^2 (\Delta x_{94})^2 + \\ + (-C_8 C_9 F_{91} - C_8 C_9 F_{92} + S_8 F_{93} + S_8 F_{94})^2 (\Delta X_{79})^2 + (x_{71})^2 (\Delta F_{71})^2 + \\ + (x_{72})^2 (\Delta F_{72})^2 + (X_{79} C_9 + x_{91})^2 C_8^2 (\Delta F_{91})^2 + \\ + (X_{79} C_9 + x_{92})^2 C_8^2 (\Delta F_{92})^2 + (X_{79} + C_9 x_{93})^2 S_8^2 (\Delta F_{93})^2 + \\ + (X_{79} + C_9 x_{94})^2 S_8^2 (\Delta F_{94})^2 + \left[(X_{79} C_9 + x_{91}) S_8 F_{91} + \right. \\ + (X_{79} C_9 + x_{92}) S_8 F_{92} + (X_{79} + C_9 x_{93}) C_8 F_{93} + \\ \left. + (X_{79} + C_9 x_{94}) C_8 F_{94} \right]^2 (\Delta \Theta_8)^2 + (X_{79} C_8 S_9 F_{91} + \\ + X_{79} C_7 S_8 F_{92} - S_3 S_9 x_{93} F_{93} - S_8 S_9 x_{94} F_{94})^2 (\Delta \Theta_9)^2 \quad (306)$$

To evaluate Equation 306, the arm is arbitrarily assumed to be pronated with the wrist unflexed, i.e. $\Theta_8 = \pi$ and $\Theta_9 = 0$. Furthermore, it is assumed that all force transducers have the same probable error ΔF , that $x_{n1} = x_{n3}$ and $x_{n2} = x_{n4}$, and that all the length measurements have the same error Δx . Under these assumptions, the error equation reduces to the following form.

$$(\Delta T)^2 = \left[F_{71}^2 + F_{72}^2 + 2 (F_{91}^2 + F_{92}^2 + F_{91} F_{92}) \right] (\Delta x)^2 + \\ + \left[x_{71}^2 + x_{72}^2 + x_{91}^2 + x_{92}^2 + 2 X_{79} (x_{91} + x_{92} + X_{79}) \right] (\Delta F)^2 + \\ + \left[(X_{79} + x_{91}) (F_{93}) + (X_{79} + x_{92}) (F_{94}) \right]^2 (\Delta \Theta_8)^2 \quad (307)$$

CALCULATIONS

To evaluate Equation 307, assume the following lengths.

$$x_{71} = 0.10 \text{ meter}$$

$$x_{72} = 0.20$$

$$X_{79} = 0.25$$

$$x_{91} = 0.05$$

$$x_{92} = 0.15$$

Also, the instrument errors ΔF and $\Delta \Theta_8$ must be chosen and Δx must be estimated. For measurement of Θ_8 , film potentiometers are available with as little as 0.1% error including the effects of nonlinearity, hysteresis, and temperature. The loading points of the force transducers and X_{79} can be determined to within 0.5 mm (0.020"). The flexures supporting the shells can measure the forces to within 2% of full scale, including effects of cross-coupling, hysteresis, and temperature. As in Appendix V, we assume full scales for the force transducers of 10 kg. With these considerations,

$$\Delta \Theta_8 = 0.01 \text{ radian}$$

$$\Delta x = 5 \times 10^{-4} \text{ meter}$$

$$\Delta F = 0.2 \text{ kg}$$

The relative magnitudes of the terms in Equation 307 can be estimated by assuming the force levels F_{ni} . When all the F_{ni} 's are assumed equal, it is found that the term due to ΔF is two orders of magnitude larger than the $\Delta \Theta_8$ term and four orders of magnitude larger than the Δx term. Thus, Equation 308 gives the only error term which need be considered.

$$(\Delta T)^2 = [x_{71}^2 + x_{72}^2 + x_{91}^2 + x_{92}^2 + 2 X_{79} (x_{91} + x_{92} + X_{79})] (\Delta F)^2 \quad (308)$$

When the values assumed above are inserted in Equation 308, we find

$$T = 0.012 \text{ kg m} \quad (309)$$

For a typical suit elbow torque level of 0.80 kg m, the fractional error is

$$\frac{\Delta T}{T} = 1.5\% \quad (310)$$

COMMENTS

This error figure has been derived using state of the art values for the force flexures. However, the placement of the transducers is not necessarily optimal. The vast improvement in accuracy over the method of Appendix V is due primarily to the reduction in the number of transducers. Transduction of the entire upper extremity would involve larger error, but it is apparent that adequate accuracy can be achieved. In a design study for the transduction of a dummy shoulder and arm, a more complete error analysis should be performed optimizing all controllable factors subject to economy and other practical considerations.

APPENDIX VII

CALCULATION OF DUMMY SHOULDER INTERLINK ANGLES FROM EXOSKELETON DATA

In this appendix, expressions for the five angles (θ_2 , θ_3 , θ_4 , θ_5 , and θ_6) of the conceptual dummy shoulder and upper arm linkage are derived in terms of the vector \vec{R}_{16} and the matrix D , which describe the position and orientation of link 6 with respect to link 1. This derivation shows the feasibility of using an exoskeleton, attached to the body only at the spine and lower humerus, for unique determination of shoulder and upper arm position. \vec{R}_{16} and D are calculated by straightforward matrix and vector operations from exoskeleton transducer outputs.

Consider Figure 159 showing the dummy shoulder linkage geometry.

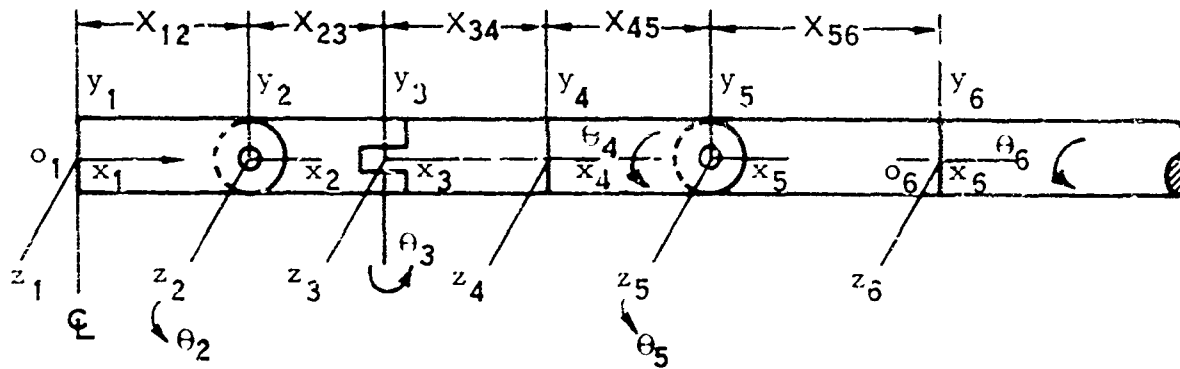


FIGURE 159. DUMMY SHOULDER LINKAGE GEOMETRY

NOTATION

$$\vec{R}_{16} = \begin{bmatrix} R_x \\ R_y \\ R_z \end{bmatrix} = \text{vector from } o_1 \text{ to } o_6$$

D = matrix of d_{ij} 's

d_{ij} = cosine of the angle between the i th axis of link 1
and the j th axis of link 6

\vec{X}_{mn} = vector from origin m to origin n

θ_i = positive angle between links i and $i + 1$

C_i = $\cos \theta_i$

S_i = $\sin \theta_i$

By the procedures of Appendix I, D and \vec{R}_{16} can be written down immediately.

$$D = \tilde{D}_z(\Theta_2) \tilde{D}_y(\Theta_3) \tilde{D}_x(\Theta_4) \tilde{D}_z(\Theta_5) \tilde{D}_x(\Theta_6) \quad (311)$$

$$\vec{R}_{16} = \vec{X}_{12} + \tilde{D}_z(\Theta_2) \left\{ \vec{X}_{23} + \tilde{D}_y(\Theta_3) \left[\vec{X}_{34} + \tilde{D}_x(\Theta_4) (\vec{X}_{45} + \tilde{D}_z(\Theta_5) \vec{X}_{56}) \right] \right\} \quad (312)$$

The $\vec{X}_{m(m+1)}$'s in their own coordinate systems all have the form

$$\vec{X}_{m(m+1)} = X_{m(m+1)} \begin{bmatrix} 1 \\ 0 \\ 0 \end{bmatrix} \quad (313)$$

The rotation matrices are

$$\tilde{D}_z(\Theta_2) = \begin{bmatrix} C_2 & -S_2 & 0 \\ S_2 & C_2 & 0 \\ 0 & 0 & 1 \end{bmatrix}; \quad \tilde{D}_y(\Theta_3) = \begin{bmatrix} C_3 & 0 & S_3 \\ 0 & 1 & 0 \\ -S_3 & 0 & C_3 \end{bmatrix} \quad (314)$$

$$\tilde{D}_x(\Theta_4) = \begin{bmatrix} 1 & 0 & 0 \\ 0 & C_4 & -S_4 \\ 0 & S_4 & C_4 \end{bmatrix}; \quad \tilde{D}_z(\Theta_5) = \begin{bmatrix} C_5 & -S_5 & 0 \\ S_5 & C_5 & 0 \\ 0 & 0 & 1 \end{bmatrix} \quad (315)$$

$$\tilde{D}_x(\Theta_6) = \begin{bmatrix} 1 & 0 & 0 \\ 0 & C_6 & -S_6 \\ 0 & S_6 & C_6 \end{bmatrix}; \quad D = \begin{bmatrix} d_{11} & d_{12} & d_{13} \\ d_{21} & d_{22} & d_{23} \\ d_{31} & d_{32} & d_{33} \end{bmatrix} \quad (316)$$

Multiplication of the matrices yields the components of D.

$$\begin{aligned} d_{11} &= C_2 C_3 C_5 - S_2 C_4 S_5 + C_2 S_3 S_4 S_5 \\ d_{12} &= -C_2 C_3 S_5 C_6 - S_2 C_4 C_5 C_6 + C_2 S_3 S_4 C_5 C_6 + S_2 S_4 S_6 + C_2 S_3 C_4 S_6 \\ d_{13} &= C_2 C_3 S_5 S_6 + S_2 C_4 C_5 S_6 - C_2 S_3 S_4 C_5 S_6 + S_2 S_4 C_6 + C_2 S_3 C_4 C_6 \end{aligned} \quad (317)$$

$$\begin{aligned} d_{21} &= S_2 C_3 C_5 + C_2 C_4 S_5 + S_2 S_3 S_4 S_5 \\ d_{22} &= -S_2 C_3 S_5 C_6 + C_2 C_4 C_5 C_6 + S_2 S_3 S_4 C_5 C_6 - C_2 S_4 S_6 + S_2 S_3 C_4 S_6 \\ d_{23} &= S_2 C_3 S_5 S_6 - C_2 C_4 C_5 S_6 - S_2 S_3 S_4 C_5 S_6 - C_2 S_4 C_6 + S_2 S_3 C_4 C_6 \end{aligned} \quad (318)$$

$$\begin{aligned} d_{31} &= -S_3 C_5 + C_3 S_4 S_5 \\ d_{32} &= S_3 S_5 C_6 + C_3 S_4 C_5 C_6 + C_3 C_4 S_6 \\ d_{33} &= -S_3 S_5 S_6 - C_3 S_4 C_5 S_6 + C_3 C_4 C_6 \end{aligned} \quad (319)$$

And by similar multiplication, the components of \vec{R}_{16} are

$$R_x = X_{12} + C_2 X_{23} + C_2 C_3 X_{35} + (C_2 C_3 C_5 + C_2 S_3 S_4 S_5 - S_2 C_4 S_5) X_{56}$$

$$R_y = S_2 X_{23} + S_2 C_3 X_{35} + (S_2 C_3 C_5 + S_2 S_3 S_4 S_5 + C_2 C_4 S_5) X_{56}$$

$$R_z = -S_3 X_{35} + (-S_3 C_5 + C_3 S_4 S_5) X_{56}$$

These are twelve transcendental equations in the unknowns $\Theta_2, \Theta_3, \Theta_4, \Theta_5$, and Θ_6 . The link lengths, X_{mn} , are fixed and the d_{ij} 's and R_x, R_y , and R_z are known from exoskeleton data. They are solved below.

$$R_z = -S_3 X_{35} + (-S_3 C_5 + C_3 S_4 S_5) X_{56} \quad (321)$$

$$= -S_3 X_{35} + d_{31} X_{56} \quad (322)$$

$$\therefore \sin \Theta_3 = \frac{d_{31} X_{56} - R_z}{X_{35}} \quad (323)$$

$$R_y = S_2 X_{23} + S_2 C_3 X_{35} + (S_2 C_3 C_5 + S_2 S_3 S_4 S_5 + C_2 C_4 S_5) X_{56} \quad (324)$$

$$= S_2 (X_{23} + C_3 X_{35}) + d_{21} X_{56} \quad (325)$$

$$\therefore \sin \Theta_2 = \frac{R_y - d_{21} X_{56}}{X_{23}} \quad (326)$$

To use Equation 326, C_3 is obtained from $\sin \Theta_3$ in Equation 323.

Eliminate C_5 from the equations for d_{11} and d_{21} .

$$\frac{d_{11} + S_2 C_4 S_5 - C_2 S_3 S_4 S_5}{C_2 C_3} = C_5 = \frac{d_{21} - C_2 C_4 S_5 - S_2 S_3 S_4 S_5}{S_2 C_3} \quad (327)$$

Then

$$d_{11} S_2 + S_2^2 C_4 S_5 - S_2 C_2 S_3 S_4 S_5 - d_{21} C_2 + C_2^2 C_4 S_5 + S_2 C_2 S_3 S_4 S_5 = 0 \quad (328)$$

$$d_{11} S_2 - d_{21} C_2 + C_4 S_5 = 0 \quad (329)$$

$$\therefore C_4 S_5 = d_{21} C_2 - d_{11} S_2 \quad (330)$$

Equation 330 is used to eliminate S_4 from the equation for d_{31} .

$$d_{31} + S_3 C_5 = C_3 S_5 \sqrt{1 - \left(\frac{d_{21} C_2 - d_{11} S_2}{S_5} \right)^2} \quad (331)$$

Squaring gives

$$d_{31}^2 + 2 d_{31} S_3 C_5 + S_3^2 C_5^2 = C_3^2 S_5^2 - C_3^2 (d_{21} C_2 - d_{11} S_2)^2 \quad (332)$$

$(1-C_5^2)$ is substituted for S_5^2 in Equation 332 and the binominal theorem is applied.

$$\cos \Theta_5 = d_{31} S_3 \pm C_3 \sqrt{1 - d_{31}^2 - (d_{21} C_2 - d_{11} S_2)^2} \quad (333)$$

Then from the Equation 330,

$$\cos \Theta_4 = \frac{d_{21} C_2 - d_{11} S_2}{S_5} \quad (334)$$

The equations for d_{12} and d_{13} are multiplied by S_6 and C_6 and added to give Equation 337.

$$d_{12} S_6 = - C_2 C_3 S_5 S_6 C_6 - S_2 C_4 C_5 S_6 C_6 + C_2 S_3 S_4 C_5 S_6 C_6 + S_2 S_4 S_6^2 + C_2 S_3 C_4 S_6^2 \quad (335)$$

$$d_{13} C_6 = C_2 C_3 S_5 S_6 C_6 + S_2 C_4 C_5 S_6 C_6 - C_2 S_3 S_4 C_5 S_6 C_6 + S_2 S_4 C_6^2 + C_2 S_3 C_4 C_6^2 \quad (336)$$

$$d_{12} S_6 + d_{13} C_6 = S_2 S_4 + C_2 S_3 C_4 \quad (337)$$

Similar treatment of the equations for d_{22} and d_{23} yields Equation 340.

$$d_{22} S_6 = - S_2 C_3 S_5 S_6 C_6 + C_2 C_4 C_5 S_6 C_6 + S_2 S_3 S_4 C_5 S_6 C_6 - C_2 S_4 S_6^2 + S_2 S_3 C_4 S_6^2 \quad (338)$$

$$d_{23} C_6 = S_2 C_3 S_5 S_6 C_6 - C_2 C_4 C_5 S_6 C_6 - S_2 S_3 S_4 C_5 S_6 C_6 - C_2 S_4 C_6^2 + S_2 S_3 C_4 C_6^2 \quad (339)$$

$$d_{22} S_6 + d_{23} C_6 = - C_2 S_4 + S_2 S_3 C_4 \quad (340)$$

Then Equations 337 and 340 are multiplied by d_{23} and d_{13} , giving Equation 343.

$$d_{12} d_{23} S_6 + d_{13} d_{23} C_6 = S_2 S_4 d_{23} + C_2 S_3 C_4 d_{23} \quad (341)$$

$$d_{13} d_{22} S_6 + d_{13} d_{23} C_6 = - C_2 S_4 d_{13} + S_2 S_3 C_4 d_{13} \quad (342)$$

$$S_6 (d_{12} d_{23} - d_{13} d_{22}) = S_4 (S_2 d_{23} - C_2 d_{13}) + S_3 C_4 (C_2 d_{23} - S_2 d_{13}) \quad (343)$$

Thus,

$$\sin \Theta_6 = \frac{S_4 (S_2 d_{23} + C_2 d_{13}) + S_3 C_4 (C_2 d_{23} - S_2 d_{13})}{d_{12} d_{23} - d_{13} d_{22}} \quad (344)$$

Thus, Equations 323, 326, 333, 334, and 344 define the Θ_i 's in terms of known quantities. As written, these equations must be solved in order because they contain functions of the previous angles. The multivaluedness of the trigonometric functions provides some of the equations with more than one solution. In some cases, and perhaps all, this corresponds to valid different discrete positions for the linkage as shown in Appendix I. The physical significance of the \pm sign choice in Equation 333 has not been explained, but it appears that acceptable physical constraints on the dummy angular excursions will eliminate ambiguity due to this sign choice and the multivaluedness of the inverse trigonometric functions.

APPENDIX VIII

METEOROID SHIELDING

Planetary bodies can provide some meteoroid shielding for a nearby astronaut. Consider the situation shown in Figure 160. Here the astronaut is at the point O, which is located at an altitude H above the planetary body of radius R. Construct an imaginary sphere of radius $R_0 = R + H$ about the point O. The fractional reduction in the omnidirectional meteoroid flux crossing this imaginary boundary will be the ratio of the area A_1 of the constructed sphere intercepted by the cone tangent to the planet to the total area of the constructed sphere.

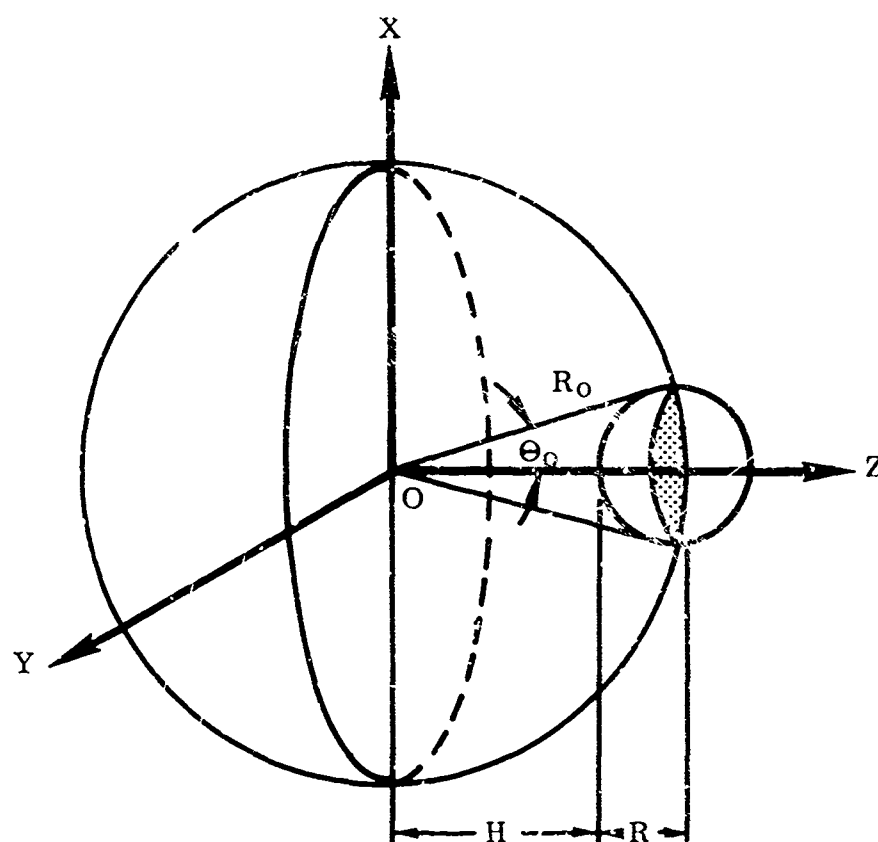


FIGURE 160. METEOROID SHIELDING

The fraction of incident meteoroids that remains unobstructed is called the shielding factor, ξ . Thus,

$$\xi = 1 - \frac{A_1}{4\pi R_0^2} \quad (345)$$

As shown in Figure 161, an element of the imaginary shielded surface is

$$dA_i = 2\pi R_o^2 \sin \Phi d\Phi \quad (346)$$

Then

$$\begin{aligned} A_i &= 2\pi R_o^2 \int_0^{\Phi_o} \sin \Phi d\Phi \\ &= 2\pi R_o^2 (1 - \cos \Phi_o) \end{aligned} \quad (347)$$

Substituting this value for A_i into Equation 345 gives the shielding factor ξ .

$$\xi = \frac{(1 + \cos \Phi_o)}{2} \quad (348)$$

where $\Phi_o = \arcsin \frac{R}{R + H}$.

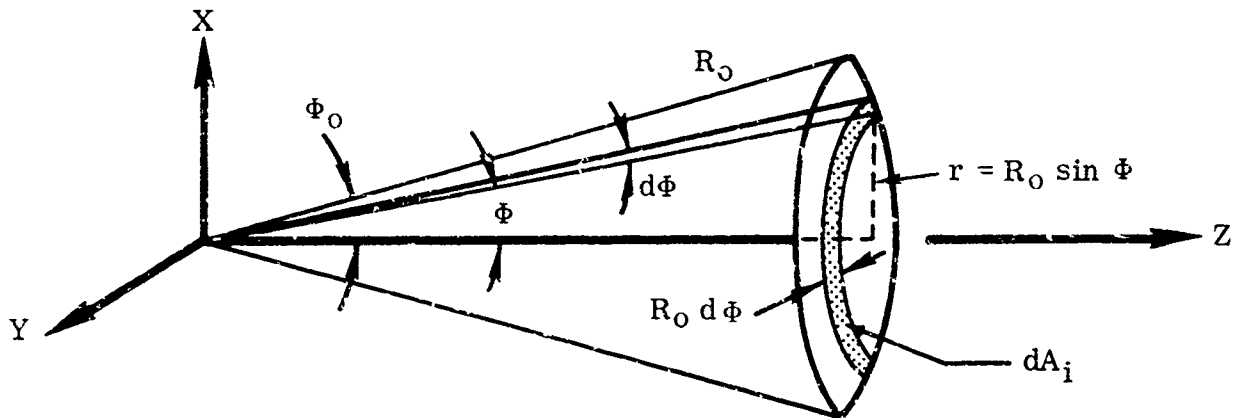


FIGURE 161. SHIELDED AREA

APPENDIX IX

SPACE SUIT RELIABILITY EVALUATION

This appendix contains a brief outline of a methodology for estimating the reliability of a space suit. The reliability of a space suit is defined as the probability that the suit system will maintain a life supporting environment plus the required operational characteristics for the astronaut to accomplish his mission. In brief, reliability is the probability of success. Like all probability figures, reliability is expressed in terms of numbers ranging from 0 to 1. These numbers are derived by various statistical techniques involving the manipulation of measured quantities. The word "statistical" means the making of valid inferences from limited but accurate data.

Ultimately the suit reliability will depend upon:

1. The quality of the research which went into its conception
2. The strength and performance margins built into its design
3. The quality control employed in its manufacture
4. The adequacy of the maintenance employed
5. The actual environmental conditions under which it is used

Assessment of reliability, however, is normally based on tests conducted on production items. It is assumed that these production items have been "debugged," manufactured with good quality control, and adequately maintained after assembly and check out. It is also assumed that failures occurring in the useful life or characteristic operation period of the suit can be distinguished from failures occurring during the wear out period.

For reliability purposes, the suit is defined as a "series" system; that is, if any component fails, the system is considered to have failed. This concept is significant in that it means that the reliability of the suit as a whole is the product of the individual reliabilities of its component parts.

In detailing the procedure to be followed in a reliability evaluation, it is assumed that two or more complete suit systems (pressure garment, back pack, etc.) and a number of critical component items are available for testing. Before defining the actual tests it is necessary to:

1. Review the reliability goals which were established at the design stage. It should be remembered that there is always some risk and that establishing a reliability figure of 0.9999 normally involves a length of test which is quite beyond practicality.

2. Define an acceptable confidence level and confidence limits. The confidence level is the probability that the true value of the reliability lies within specified upper and lower bounds (the confidence limits). In applying statistical concepts to any set of measurements, there are two sources of uncertainty. The first lies in the assumption that the distribution of the data fits a prescribed mathematical model and the second in the assumption that the magnitude of the parameters of the parent (population) distribution are the same as those calculated from the sample. Confidence levels for the former can be established by means of the so called "Chi Square Distribution" and for the latter by means of the "Normal Distribution" for large sample size and by the "t Distribution" for small sample size.
3. Define the suit mission. This is one of the main factors in specifying the required sample size, the extent of testing, etc.
4. Define suit systems, assemblies, components, and interfaces as in Figure 162. The test data will pertain to components but the final reliability is for the complete suit assembly.
5. Determine all possible failure modes. A failure mode is defined as any malfunction which could result in permanent injury to the astronaut or in any failure of his mission. Some obvious failure modes are:
 - a. Fatigue failure of pressure garment due to joint flexure or cyclic pressurizing; that is, fatigue failures which result in the loss of either environment or mobility
 - b. Grab tearing of the pressure garment
 - c. Malfunctioning of the ventilation system
 - d. Malfunctioning of the cooling system
 - e. Meteoroid penetration
 - f. Helmet failure due to impact
 - g. Excessive fogging of the visor
 - h. Interface connection malfunctioning such as the failure of the neck ring

The test program must be designed on the basis of the above factors and should include tests on complete suit systems in a simulated space environment with the astronaut simulating a mission. The complete suit system tests are aimed at covering the entire sequence of activities that the astronaut will perform

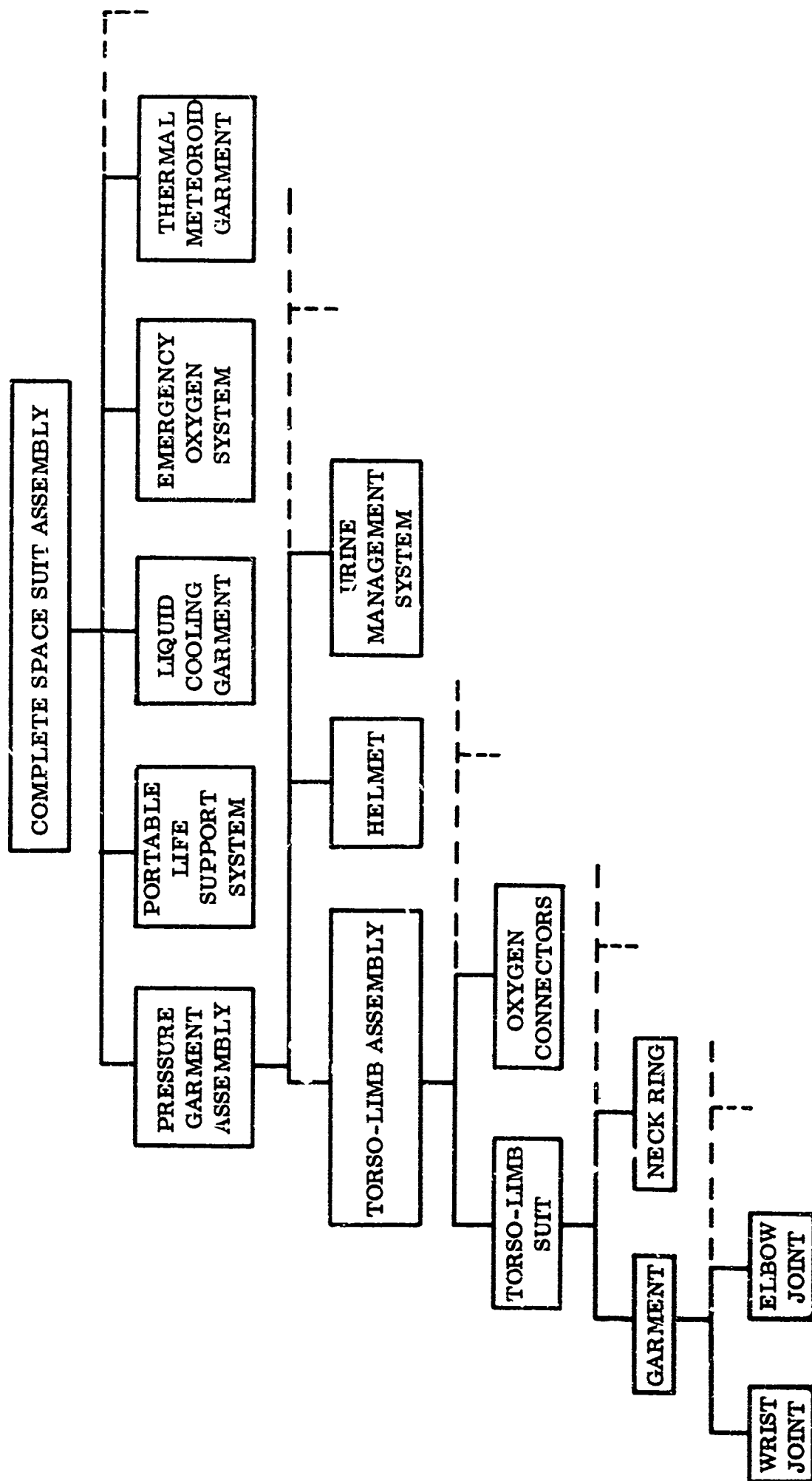


FIGURE 162. PARTIAL DEFINITION OF SUIT SYSTEMS, ASSEMBLIES, AND INTERFACES FOR RELIABILITY PROGRAM

during a mission. Items where interface problems would not invalidate the results should be tested as components. These would be accelerated tests of such items as zippers, valves, suit joints, helmet visor attachments.

Reliability tests are incorporated into the various testing discussed in this report. Except for the accelerated tests, they are not conducted as separate and distinct entities. The concept of integrated testing is useful here in that it includes all the conventional functional, endurance, and fatigue tests and then extends the test time to obtain additional data from which reliability predictions can be made.

The tests must generate data in the form of "times-to-failure." From these data it will be possible to calculate "mean-time-between-failures" and the "failure rates." The tests must also be directed toward distinguishing between wear out failures and chance failures. Wear out failures are not included in the analysis. Reliability analysis is normally carried out only on those failures which occur in the characteristic operation period. However, the lower limit of the wear out failures is used to establish the upper limit wherein chance failures may occur.

Reliability figures are derived from observations of failures. The frequency with which these occur is called the failure rate λ (the number of failures per hour). The failure rate will not be constant for the entire life of the suit but will follow the pattern shown in Figure 163.

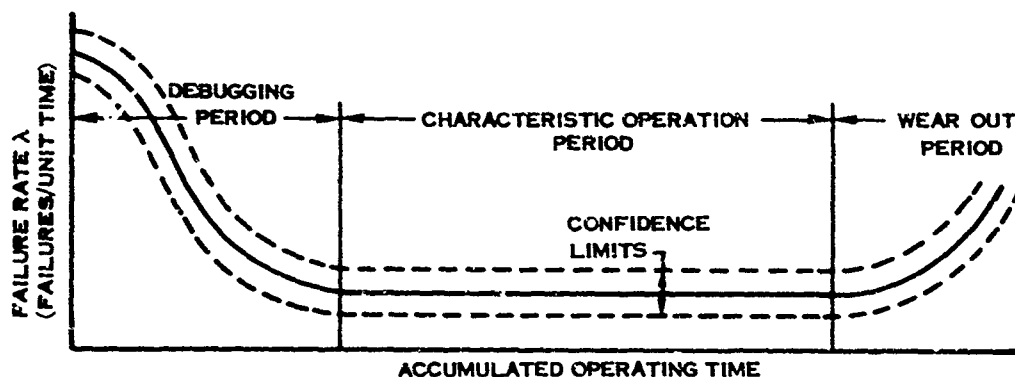


FIGURE 163. LIFETIME FAILURE RATE DISTRIBUTION

In the characteristic operation or useful life period, failures occur at random intervals, irregularly, and unexpectedly. However, if the failure rate is constant over the operation period as shown in Figure 163, then the so called "Poisson Probability Distribution" can be used as the mathematical model for studying the reliability during the useful life period.

Equation 349 is the Poisson distribution which gives the probability of having exactly X failures in the interval N (time, number of cycles, etc.).

$$P \{X, N\} = \frac{(\lambda N)^X (e^{-\lambda N})}{X!} \quad (349)$$

where λ is the constant failure rate and λN is the expected number of failures in the interval N . Reliability is just a special case of the Poisson distribution, namely the probability that no failures will occur in the interval N or

$$R(N) = P \{0, N\} = \frac{(\lambda N)^0 (e^{-\lambda N})}{0!} = e^{-\lambda N} \quad (350)$$

Reliability can also be expressed in terms of the reciprocal of the failure rate called the mean time between failures M . Thus

$$R(t) = e^{-\lambda t} = e^{-\frac{t}{M}} \quad (351)$$

where $R(t)$ is the reliability of the suit system for any given mission time t . A plot of Equation 351 for a constant failure rate is shown in Figure 164.

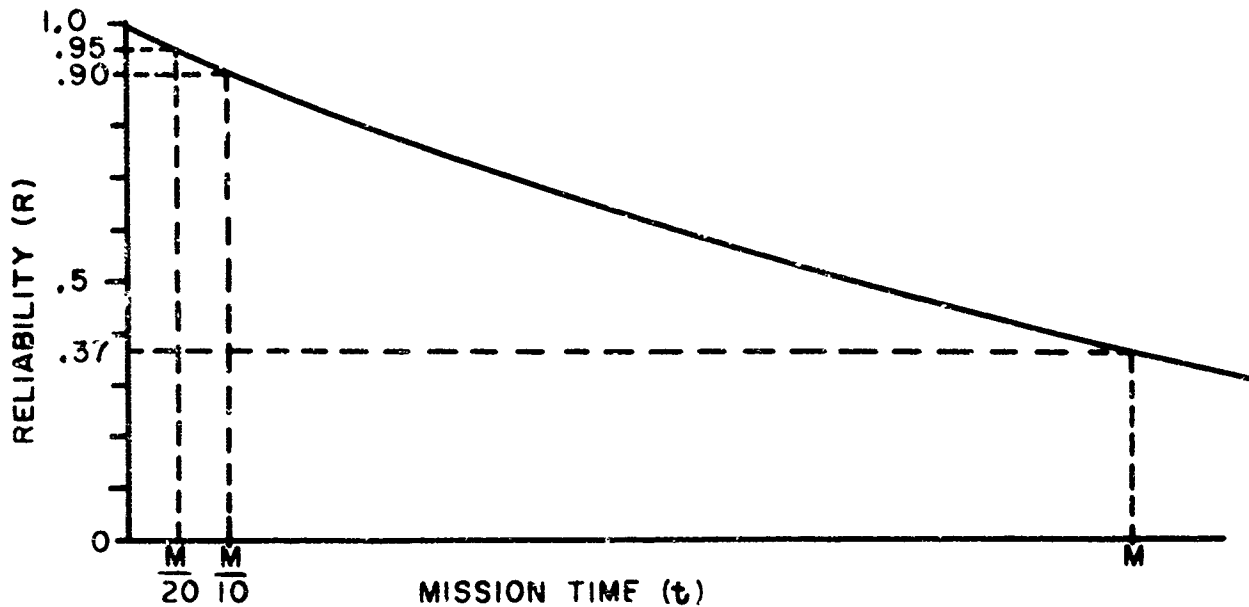


FIGURE 164. RELIABILITY versus MISSION TIME

When the operating time is equal to the mean time between failures, the reliability

is $R(t) = e^{-\frac{M}{M}} = 0.37$ which means that there is a 37% probability of failureless operation of the system. Thus if the mean-time-between-failures M were 100 hours, there would be only a 37% probability that the system will operate successfully for 100 hours. However, the probability for successful operation over a period of five hours would rise to 95% and for one hour to 99%.

The purpose of the reliability study is to gain information about the probability that the suit system will maintain the required life environment and mobility for a specific mission time. When the mean-time-between-failures is known with an acceptable accuracy, the reliability curve gives the probability value.

REFERENCES

1. Adrian, M., Tipton, C. M., and Karpovich, P. V., Electrogoniometry Manual, Physiological Research Lab., Springfield College, Springfield, Mass., 1965.
2. Anderson, J. R., Strain Gage Balances for Wind Tunnels: An Outline of Practice in the United Kingdom, North Atlantic Treaty Organization Advisory Group for Aeronautical Research and Development, Report #5, 64 Rue De Varenne, Paris, France, February, 1965.
3. Aronovitz, R., et al, A Pneumatic Cell Matrix to Measure the Distribution of Pressure Over the Human Body, 16th Annual Conference on Engineering in Medicine and Biology, Baltimore, Maryland, November 18-20, 1963.
4. Auxier, T. A., A Theoretical Study of Space Equivalent Thermal Conditions and Their Applicability, AMRL-TDR-64-20, AD 437-575, Aerospace Medical Research Laboratories, Wright Patterson Air Force Base, Ohio, March, 1964.
5. Baker, D. H., Ryder, E. A., and Baker, N. H., Temperature Measurement in Engineering, John Wiley and Sons, Inc., 1953.
6. Bard, Philip (Editor), Medical Physiology, (1961 Edition), C. V. Mosby, Co., St. Louis, Missouri.
7. Berner, F. W. and Schueller, O., Aerospace Environment Simulator, AMRL-TDR-64-6, AD 438-047, Aerospace Medical Research Laboratories, Wright-Patterson Air Force Base, Ohio, February, 1964.
8. Blossom, D. E., Jr., Experimental Equilibrium Conditions of Dissociated and Ionized Hydrogen Hypersonic Flows, Rhodes and Bloxsom, Canoga Park, California.
9. Bobco, R. P., Radiation from a Directional Source: Beam Divergence in Solar Simulation, ASME 64WA-SOL-3, American Society of Mechanical Engineers, Winter Annual Meeting, New York, N. Y., November 29, 1964.
10. Bomelburg, Herbert J., "Performance of Pressure Sensitive Materials", Review of Scientific Instruments, Vol 30, pp 43-44, 1959.
11. Bowen, J. D., X-20A Full Pressure Suit Quantitative Performance, AMRL-TDR-64-36, AD 602-701, Aerospace Medical Research Laboratories, Wright-Patterson Air Force Base, Ohio, May 1964.
12. Bradley, J. V., "A Methodology for Glove Evaluation", Perceptual and Motor Skills, 12, pp 373-374, 1961.

13. Bradley, J. V., Glove Characteristics Influencing Control Manipulability, WADC Tech. Rep. 57-389, AD 130-836, Wright Air Development Center, Wright-Patterson Air Force Base, Ohio, August, 1957.
14. Burbank, P. B., "A Meteoroid Environment for Near-Earth, Cislunar and Near-Lunar Operation", Engineering Design and Operation of Manned Spacecraft Seminar Series, Lecture 8a, 1964.
15. Burton, D. R. and Collier, L., The Development of Water Conditioned Suits, TN-Mech-Eng. 40, Royal Aircraft Establishment, Farnborough, England, April, 1964.
16. Collins, R. D., Sr. and Kinard, W. H., The Dependency of Penetration on the Momentum per Unit Area of the Impacting Projectile and the Resistance of Materials to Penetration, NASA TND-238, National Aeronautics and Space Administration, Langley Research Center, Langley Station, Hampton, Virginia, May, 1960.
17. Cardarelli, Nathan, "Space Suit Materials Testing Program," Institute of Environmental Sciences, 1962 Proceedings, Chicago, Illinois.
18. Chorafas, D. N., Statistical Processes and Reliability Engineering, D. Van Nostrand Co., Inc., Princeton, New Jersey, 1960.
19. Clark, D. B., "Rare-Earth Pressure Transducers", Instruments and Control Systems, February, 1963.
20. Clark, D. C., et al, Exploratory Investigation of the Man Amplifier Concept, AMRL-TDR-62-89, AD 290-070, Aerospace Medical Research Laboratories, Wright-Patterson Air Force Base, Ohio, August, 1962.
21. Clifford, J. M., "Requirements for the Thermal Control of a Manikin for Clothing Investigation", Industrial Medicine and Surgery, Royal Air Force Institute of Aviation Medicine, Farnborough, England, January, 1963.
22. Comfort, E., Effective Dead Space in the MA-3 Helmet, WADD 60-362, AD 243-298, Wright Air Development Division, Wright-Patterson Air Force Base, Ohio, May, 1960.
23. Consolazio, C. F., Johnson, R. E. and Pecora, L., Physiological Measurements of Metabolic Functions in Man, McGraw Hill, 1963.
24. Craig, F. N., Ventilation Requirements of an Impermeable Protective Suit, Medical Division Research Report No. 5, CMLEM-52, Publications Control No. 5030-5, Chemical Corps, Medical Division, Army Chemical Center, Maryland, April, 1950.

25. Curtis, J. S., An Accelerated Reservoir Light-Gas Gun, NASA TND-1144, National Aeronautics and Space Administration, Ames Research Center, Moffett Field, California, February, 1962.
26. Curtis, J. S. and Gehring, J. W., Projection Techniques - Proceedings of Symposium on Structural Dynamics Under High Impulse Loading, ADS-TDR-63-140, AD 408-777, Aeronautical Systems Division, Wright-Patterson Air Force Base, Ohio, 1963.
27. Dahl (Editor), "Temperature, Its Measurement and Control in Science and Industry", Applied Methods and Instruments, Vol III, Part 2, 1962.
28. D'Aiutolo, C. T., The Micrometeoroid Satellite Explorer XIII (1961 chi) Collected Papers on Design and Performance, NASA TND-2468, National Aeronautics and Space Administration, Langley Research Center, Langley Station, Hampton, Virginia, November, 1964.
29. Davidson, J. R. and Sandorf, P. E., Environmental Problems of Space Flight Structures II Meteoroid Hazard, NASA TND-1493, National Aeronautics and Space Administration, Langley Research Center, Langley Station, Hampton, Virginia, January, 1963.
30. Davidson, E. H. and Winslow, P. C., Jr., Micrometeoroid Satellite (Explorer XVI) Stainless Steel Penetration Rate Experiment, NASA TND-2445, National Aeronautics and Space Administration, Lewis Research Center, Cleveland, Ohio, August, 1964.
31. Day, J. L. and Lippitt, M. W., Improved Electrode Gives High-Quality Biological Recordings, NASA Tech Brief 64-10025, National Aeronautics and Space Administration, Technology Utilization Officer, Manned Spacecraft Center, Houston, Texas.
32. Deem, H. W., Lucks, O. F., and Wood, W. D., Emissivity and Emittance - What Are They, Defense Metals Information Center, Batelle Memorial Institute, Memorandum Number 72.
33. Dempster, W. T., Space Requirements of the Seated Operator, WADC TR 55-159, AD 878-92, Wright Air Development Center, Wright-Patterson Air Force Base, Ohio, July, 1955.
34. Eberhart, H. D. and Inman, V. T., "An Evaluation of Experimental Procedure Used in a Fundamental Study of Human Locomotion", Annals of New York Academy of Sciences, Vol 51, 1951.
35. Elftman, H., "The Basic Pattern of Human Locomotion, Human Engineering", Annals of the New York Academy of Sciences, Vol 51, 1951.

36. Faget, M. A., Meteoroid Environment and Penetration Mechanism, Memorandum for Apollo Spacecraft Project Office, September 10, 1963.
37. Fogel, L. J., Biotechnology, Concepts and Applications, Prentice-Hall, Inc., 1963.
38. Frank, W. E. and Gibson, R. J., "A New Pressure-Sensing Instrument", Journal of the Franklin Institute, Vol 258, No 1, pp 21-30, July, 1954.
39. Gaensler, E. W. USAF (M. C.) and Lindgren, I., "Open-Circuit Techniques for the Measurement of Ventilation", The Scandanavian Journal of Clinical and Laboratory Investigation, Vol 7, Supplementum 20, 1955.
40. Gardenhire, L. W., "Selecting Sample Rates", ISA Journal, April, 1964
41. Gauthier, P. R., Man Rated High Vacuum Space Simulator, HSIR 2263, Hamilton Standard Division, United Aircraft Corporation, Windsor Locks, Connecticut, December 17, 1964.
42. Gemini Space Suit Reliability Program Final Report, NASA T-23772-G, Advanced Project Laboratory, U. S. Army Natick Laboratory, Natick, Massachusetts, July 16, 1965.
43. Gemmell, C. L., Medical Physiology, (Editor: Bard), C. V. Mosby Co., St. Louis, Missouri, 1961.
44. Gurdjian, E. S., Lissner, H. R., and Patrick, L. M., "Protection of the Head and Neck in Sports", The Journal of the American Medical Association, Vol 182, No 5, 1962.
45. Hall, Eugene and Pitek, Martin, Space Simulation Testing, PWA-2277A, Pratt and Whitney Aircraft, Division of United Aircraft Corporation, East Hartford, Connecticut, July, 1962.
46. Hansen, R. M., Mechanical Design and Fabrication of Strain-Gage Balances, Report No 9, P 4, North Atlantic Treaty Organization, Advisory Group for Aeronautical Research and Development, 64 Rue De Verenne, Paris, France, February, 1956.
47. Hardy, J. C. and Lang, R., Techniques for Physiological Monitoring of Human Performance in a Pressurized Space Suit, TP 64-10, AIAA/NASA Third Manned Space Flight Meeting, Houston, Texas, November 4-6, 1964.
48. Hertzberg, H. T. E., "Some Contributions of Applied Physical Anthropology to Human Engineering", Annals of New York Academy of Sciences, Vol 64, 1955.
49. Hildebrand, F. B., Introduction to Numerical Analysis, McGraw Hill, 1956.

50. Hill, A. V., "The Heat of Shortening and the Dynamic Constants of Muscle", Procedures of the Royal Society, Vol 126B, pp 136-195, August 3, 1938.
51. Hill, A. V., "The Maximum Work and Mechanical Efficiency of Human Muscles and Their Most Economical Speed", Journal of Physiology, Vol 56, No 19, 1922.
52. Hopkins, A. K., "You Don't Worry About the Big Ones", Machine Design, Vol 34, No 23, September 27, 1962.
53. Hrycak, R., Ungei, B. A., and Wittenberg, A. M., "Thermal Testing of the Telstar Satellite", Institute of Environmental Sciences, 1963 Proceedings, Los Angeles, California.
54. Jaffee, L. D. and Rittenhouse, J. B., "Behavior of Materials in Space Environments", ARS Journal, March, 1962.
55. Johnson, F. S. (Editor), "Solar Radiation", Satellite Environment Handbook 2nd Edition, Stanford University Press, Stanford, California.
56. Juster, Allan, "The Evaluation of Candidate Space Suit Materials and Assemblies", Institute of Environmental Sciences, 1964 Proceedings, Institute of Environmental Sciences Mt. Prospect, Illinois.
57. Kaufman, W. C., "Human Tolerance Limits for Some Thermal Environments of Aerospace", Aerospace Medicine, Vol 34, No 10, October, 1963.
58. Keating, D. A., et al, "Movement of Respired Gas in a Manned Space Enclosure", Aerospace Medicine, Vol 36, No 3, p 206, March, 1965.
59. Kennedy, R. W., The Outer Boundaries of Grasping-Reach Envelopes for the Shirt-Sleeved, Seated Operator, Reach Capability of the USAF, Population, Phase I, AMRL-TDR-64-59, AD 608-59, Aerospace Medical Research Laboratories, Wright-Patterson Air Force Base, Ohio, September, 1964.
60. Kerslake, D. M., "Factors Concerning the Regulation of Sweat Production in Man", Journal of Physiology, Vol 127, pp 280-296, 1955.
61. Kinnard, W. H., Lambert, C. H., Jr., Scheyer, D. R., and Casey, F. W., Effect of Target Thickness on Cratering and Penetration of Projectiles Impacting at Velocities to 13,000 Feet per Second, National Aeronautics and Space Administration Memorandum 10-18-58L, 1958.
62. Kinslow, R., "Collisions at High Velocity", International Science and Technology, Vol 40, pp 38-47, April, 1965.
63. Kolk, R. W., Modern Flight Dynamics, Space Technology Series, Prentice-Hall, Inc., Englewood Cliffs, New Jersey, 1961.

64. Kreith, F., Radiation Heat Transfer for Spacecraft and Solar Power Plant Design, International Textbook Co., Scranton, Pa., 1962.
65. Lambertsen, C. J. in Medical Physiology (Editor: Bard), C. V. Mosby Co., St. Louis, Missouri, 1961.
66. Landau, A. and Roos, P. A., "Solar and Planet Radiation Simulation", Test Engineering and Management, November, 1964.
67. Lay, W. E. and Fisher, L. C., "Riding Comfort and Cushions", Society of Automotive Engineers Journal (Transactions), Vol 47, No 5, pp 482-496, 1940.
68. Lindan, Olgierd, and Hickman, K. E., Physiopathology of Decubitus Ulcers: An Experimental Study of Physical and Biological Responses of Tissues Subjected to External Pressure, Final Report, Vocational Rehabilitation Administration, Grant No RD-695, Highland View Hospital, Western Reserve University Medical School, Cleveland, Ohio, April, 1964.
69. Lindgren, B. W. and McElrath, G. W., Introduction to Probability and Statistics, MacMillan, New York, 1959.
70. Lusk, G., The Elements of the Science of Nutrition, W. B. Saunders Co., Philadelphia, Pa., 1928.
71. Matas, R. and Lecuyer, D. W., "Performance of Pressure-Sensitive Materials", Review of Scientific Instruments, Vol 30, p 750, 1959.
72. McRae, D., "Interpolation Errors", Advanced Telemetry Study, Technical Report 1, Parts 1 and 2, Radiation, Inc., Melbourne, Florida.
73. McRae, D. and Smith E., "Computer Interpolation", Advanced Telemetry Study, Technical Report 2, Parts 1 and 2, Radiation, Inc., Melbourne, Florida.
74. Metzger, F. B., Acoustic Attenuation of the Roanwell Stereo Hi-Fi Headset, Internal Memorandum MG 491, Hamilton Standard Division, United Aircraft Corporation, Windsor Locks, Connecticut, June 18, 1965.
75. Mizen, N., Design and Test of a Full-Scale, Wearable Exoskeletal Structure, CAL Report No VO-1692-V-3, Cornell Aeronautical Laboratory, Inc., Buffalo, New York, March, 1964.
76. Mizen, N. J., Feasibility of a Wearable Exoskeletal Structure, presented at American Society of Mechanical Engineers, Human Factors Section Meeting, New York, New York, December 3, 1964.

77. Morgan, T. E., Jr., et al, Physiological Effects of Exposure to Increased Oxygen Tension at 5 psia, SAM-TDR-63-64, N64-16640, School of Aviation Medicine, Brooks Air Force Base, Texas, October, 1964.
78. Nablo, S. V., and Beggs, W. C., "Simulation of the Near Terrestrial Space Radiation Environment", Test Engineering and Management, February, 1965.
79. Natural Environment for the Manned Orbiting Laboratory System Program (MOL), AFCRL-64-845, Air Force Cambridge Research Laboratories, Bedford, Massachusetts, October 25, 1964.
80. Nubar, Yves, "Energy of Contraction in Muscle", Human Factors, October, 1963.
81. Nysmith, R. C. and Summers, J. L., Preliminary Investigation of Impact on Multiple-Sheet Structures and an Evaluation of the Meteoroid Hazard to Space Vehicles, NASA TND-1039, National Aeronautics and Space Administration, Ames Research Center, Moffett Field, California, September, 1961.
82. Otis, A. B., Fenn, W. O., and Rahn, H., "Mechanics of Breathing in Man", Journal of Applied Physiology, Vol 2, pp 592-607, May, 1950.
83. Paton, W. D. M., (Scientific Editor), "Physiology of Voluntary Muscle", British Medical Bulletin, Vol 12, No 3, September, 1956.
84. "Pegasus Returning Meteoroid Flux Data", Aviation Week and Space Technology, p 28, New York, New York, February 23, 1965.
85. Pierce, B. F., "Effects of Wearing a Full-Pressure Suit on Manual Dexterity and Tool Manipulation", Human Factors, October, 1963.
86. Pierce, B. F., "Manual Capabilities of a Pilot in a Full Pressure Suit: Techniques of Measurement and Data Presentation", Engineering and Industrial Psychology, Vol 2, pp 27-33, 1960.
87. Podloseck, S. and Suhorsky, J., "The Stability of Organic Materials in Vacuum", Institute of Environmental Sciences, 1963 Proceedings, Los Angeles, California.
88. Posevers, F. G., Rish, F. L., and Scully, C. N., An Evaluation of Impact Effects on Meteoroid Shielding Configurations for Velocities up to 60,000 Feet per Second, presented at the American Institute of Aviation and Astronautics Fifth Annual Structures and Materials Conference, Palm Springs, California, April 1-3, 1964.
89. Proposed Space Suit Mobility Notation Standards, Grumman Document Number LED-480-13A, Grumman Aircraft Corporation, Long Island, New York, March 8, 1965.

90. Ramsey, R. W., "Muscle Physics", Medical Physics (Glasser: Editor), Chicago Year Book, Vol 1, pp 784-798, 1944.
91. Ramsey, R. W., "Muscle Physics", Medical Physics (Glasser: Editor), Chicago Year Book, Vol 3, pp 399-402, 1944.
92. Rebuffet, P., Some Strain Gage Balances Used in French Wind Tunnels, Report No 6-T, pp 2-4, North Atlantic Treaty Organization, Advisory Group for Aeronautical Research and Development, 64 Rue De Varenne, Paris, France, February, 1956.
93. Rebuffet, P., Some Strain Gage Balances Used in French Wind Tunnels, Report No 6-T, pp 31-32, North Atlantic Treaty Organization, Advisory Group for Aeronautical Research and Development, 64 Rue De Varenne, Paris, France, February, 1956.
94. Rhodes and Bloxsom, Micrometeoroid Accelerator, Caloga Park, California.
95. Rock, L. C., Performance Parameters of the X-20 Dyna-Soar Prototype Full Pressure Assembly, AMRL-TDR-64-27, AD 603-307, Aerospace Medical Research Laboratories, Wright-Patterson Air Force Base, Ohio, May, 1964.
96. Roth, Emanuel M., Bioenergetic Considerations in the Design of Space Suits for Lunar Exploration, Report II, National Aeronautics and Space Administration Contract No NASr-115, July, 1964.
97. Savet, Paul H. (Editor), Gyroscopes: Theory and Design, McGraw Hill, New York, New York, 1961.
98. Saylor, W. P., Winer, D. E., Eiwen, C. J., and Carriker, A. W., Space Radiation Guide, AMRL-TDR-62-86, AD 287-863, Aerospace Medical Research Laboratories, Wright-Patterson Air Force Base, Ohio, August, 1962.
99. Scarborough, J. B., Numerical Mathematical Analysis, The Johns-Hopkins Press, Baltimore, Maryland, 1930.
100. Schaeffer, E., Bioastronautics, MacMillan Company, New York, New York, 1964.
101. Schueller, Otto and Berner, Fred W., Aerospace Environment Simulator, AMRL-TDR-64-6, AD 430-047, Aerospace Medical Research Laboratories, Wright-Patterson Air Force Base, Ohio, February, 1964.
102. Sharp, Earl D. and Bowen, John H., An Exploratory Investigation of the Effects of Wearing Full-Pressure Suits on Control Operation Time, WADD TN 60-90, Wright Air Development Division, Wright-Patterson Air Force Base, Ohio, May, 1960.

103. Singh, Mohan, Isotonic and Isometric Forces of Forearm Extensors and Flexors, Abstract of a Dissertation Presented to the Faculty of Springfield College, Springfield, Massachusetts, April, 1965.
104. Slager, U. T., Space Medicine, Prentice-Hall, Inc., Englewood Cliffs, New Jersey, 1962.
105. Summers, James L., Investigation of High-Speed Impact: Regions of Impact and Impact at Oblique Angles, NASA TND-94, National Aeronautics and Space Administration, Ames Research Center, Moffett Field, California.
106. Swearingen, J. J., Wheelwright, C. D., and Garner, J. D., An Analysis of Sitting Areas and Pressures of Man, CARI 62-1, Civil Aeromedical Research Institute, Federal Aviation Agency, Aeronautical Center, Oklahoma City, Oklahoma, January, 1962.
107. Techniques of Physiological Monitoring, AMRL-TDR-62-98, AD 288-905, AD 426-816, AD 609-481, Aerospace Medical Research Laboratories, Wright-Patterson Air Force Base, Ohio.
108. Thermocouples and Thermocouple Extension Wire, ISA RP 1.1 to 1.7, Instrument Society of America, Pittsburgh, Pennsylvania, July, 1959.
109. Thompson, Noel P., "Implanted Periarterial Pressure Transducers", Medical Electronics and Biological Engineering, pp 387-390, October, 1964.
110. Ukrainetz, P. R. and Hertz, P. B., Pressure Sensitive Paint Force Transducers, Paper Presented at the Society for Experimental Stress Analysis Meeting at Denver, Colorado, May 6, 1965.
111. Vedder, James F., "Micrometeoroids", Satellite Environment Handbook (Second Edition), Stanford University, Stanford, California, 1965.
112. Webb, Paul (Editor), Bioastronautics Data Book, NASA SP-3006, Scientific and Technical Information Division, National Aeronautics and Space Administration, Washington, D. C., 1964.
113. Welch, B. E., et al, Effect of Ventilating Air Flow on Human Water Requirements, School of Aviation Medicine, USAF Aerospace Medical Center, Brooks Air Force Base, Texas, May, 1963.
114. Whipple, Fred L., "Dust and Meteorites", Astronautics, pp 40-42, August, 1962.

115. Whipple, Fred L., "Meteoritic Phenomena and Meteorites", Physics and Medicine of the Upper Atmosphere, University of New Mexico Press, Albuquerque, New Mexico, 1952.
116. Wright, Ian B., "Applications of a System of Functional Anthropometry in Pressure Suit Design", Journal of the British Interplanetary Society, Vol 19, pp 31-41, 1963-1964.

Security Classification

DOCUMENT CONTROL DATA - R&D

(Security classification of title, body of abstract and indexing annotation must be entered when the overall report is classified)

1 ORIGINATING ACTIVITY (Corporate author) Hamilton Standard Division of United Aircraft Corporation Windsor Locks, Connecticut 06096		2a REPORT SECURITY CLASSIFICATION UNCLASSIFIED	
		2b GROUP N/A	
3 REPORT TITLE A STUDY OF TECHNIQUES AND EQUIPMENT FOR THE EVALUATION OF EXTRAVEHICULAR PROTECTIVE GARMENTS			
4 DESCRIPTIVE NOTES (Type of report and inclusive dates) Final report, August 1964 - June 1965			
5 AUTHOR(S) (Last name, first name, initial) Parry, David G. Curry, LeRoy R., Jr Hanson, Donald B. Towle, George B.			
6. REPORT DATE February 1966		7a TOTAL NO. OF PAGES 425	7b NO. OF REFS 116
8a CONTRACT OR GRANT NO. AF 33(615)-1780 b. PROJECT NO. 6301 c. Task No. 630104 d		9a ORIGINATOR'S REPORT NUMBER(S) Hamilton Standard Report No. HSER 3671 9b. OTHER REPORT NO(S) (Any other numbers that may be assigned this report) AMRL-TR-66-4	
10. AVAILABILITY/LIMITATION NOTICES Distribution of this document is unlimited.			
11. SUPPLEMENTARY NOTES		12. SPONSORING MILITARY ACTIVITY Aerospace Medical Research Laboratories, Aerospace Medical Div, Air Force Systems Command, Wright-Patterson AFB, Ohio	
13 ABSTRACT The purpose of this study was to establish a test methodology and a test system for objective, quantitative, and accurate evaluation of extravehicular space protective garments. Areas of testing studied include functional performance, life support, and environmental protection. Emphasis is placed on the problem of suit torque restraints, i.e., mobility. Concepts for appropriate evaluation criteria are discussed. The information presented and conclusions reached are the results of experience in suit testing, technical analysis, search of the literature, and discussions with experts. The nature and causes of suit torque restraint are discussed and a pin jointed model is developed for precise description of suit torques and body interlink angles. Various techniques for torque vector and body angle measurement are explored and it is concluded that a powered articulated dummy and an intrasuit exoskeletal electrogoniometer with off-line computer coupling are required to produce accurate data and useful figures of merit. Measurement techniques for reach envelope, glove evaluation, and comfort are also discussed. Various approaches to thermal and respiratory system evaluation were studied and steady state manned tests at moderate altitudes with minimum suit-wall heat transfer are recommended. The meteoroid, vacuum, thermal, and radiation hazards of space are reviewed and direction for further study in these fields is suggested. Overall facility requirements for suit evaluation are discussed and a digital data acquisition system for conditioning, editing, recording, and processing of functional and life support data is described.			

DD FORM 1473

JAN 64

Security Classification

14 KEY WORDS	LINK A		LINK B		LINK C	
	ROLE	WT	ROLE	WT	ROLE	WT
Protective garments						
Life support						
Instrumentation						
Goniometers						
Space environmental conditions						
Altitude chambers						
Body temperature						
Metabolic testing						
Data acquisition systems						
Oxygen consumption						

INSTRUCTIONS

1. **ORIGINATING ACTIVITY:** Enter the name and address of the contractor, subcontractor, grantee, Department of Defense activity or other organization (*corporate author*) issuing the report.

2a. **REPORT SECURITY CLASSIFICATION:** Enter the overall security classification of the report. Indicate whether "Restricted Data" is included. Marking is to be in accordance with appropriate security regulations.

2b. **GROUP:** Automatic downgrading is specified in DoD Directive 5200.10 and Armed Forces Industrial Manual. Enter the group number. Also, when applicable, show that optional markings have been used for Group 3 and Group 4 as authorized.

3. **REPORT TITLE:** Enter the complete report title in all capital letters. Titles in all cases should be unclassified. If a meaningful title cannot be selected without classification, show title classification in all capitals in parenthesis immediately following the title.

4. **DESCRIPTIVE NOTES:** If appropriate, enter the type of report, e.g., interim, progress, summary, annual, or final. Give the inclusive dates when a specific reporting period is covered.

5. **AUTHOR(S):** Enter the name(s) of author(s) as shown on or in the report. Enter last name, first name, middle initial. If military, show rank and branch of service. The name of the principal author is an absolute minimum requirement.

6. **REPORT DATE:** Enter the date of the report as day, month, year, or month, year. If more than one date appears on the report, use date of publication.

7a. **TOTAL NUMBER OF PAGES:** The total page count should follow normal pagination procedures, i.e., enter the number of pages containing information.

7b. **NUMBER OF REFERENCES:** Enter the total number of references cited in the report.

8a. **CONTRACT OR GRANT NUMBER:** If appropriate, enter the applicable number of the contract or grant under which the report was written.

8b, 8c, & 8d. **PROJECT NUMBER:** Enter the appropriate military department identification, such as project number, subproject number, system numbers, task number, etc.

9a. **ORIGINATOR'S REPORT NUMBER(S):** Enter the official report number by which the document will be identified and controlled by the originating activity. This number must be unique to this report.

9b. **OTHER REPORT NUMBER(S):** If the report has been assigned any other report numbers (*either by the originator or by the sponsor*), also enter this number(s).

10. **AVAILABILITY/LIMITATION NOTICES:** Enter any limitations on further dissemination of the report, other than those

imposed by security classification, using standard statements such as:

- (1) "Qualified requesters may obtain copies of this report from DDC."
- (2) "Foreign announcement and dissemination of this report by DDC is not authorized."
- (3) "U. S. Government agencies may obtain copies of this report directly from DDC. Other qualified DDC users shall request through _____."
- (4) "U. S. military agencies may obtain copies of this report directly from DDC. Other qualified users shall request through _____."
- (5) "All distribution of this report is controlled. Qualified DDC users shall request through _____."

If the report has been furnished to the Office of Technical Services, Department of Commerce, for sale to the public, indicate this fact and enter the price, if known.

11. **SUPPLEMENTARY NOTES:** Use for additional explanatory notes.

12. **SPONSORING MILITARY ACTIVITY:** Enter the name of the departmental project office or laboratory sponsoring (paying for) the research and development. Include address.

13. **ABSTRACT:** Enter an abstract giving a brief and factual summary of the document indicative of the report, even though it may also appear elsewhere in the body of the technical report. If additional space is required, a continuation sheet shall be attached.

It is highly desirable that the abstract of classified reports be unclassified. Each paragraph of the abstract shall end with an indication of the military security classification of the information in the paragraph, represented as (TS), (S), (C), or (U).

There is no limitation on the length of the abstract. However, the suggested length is from 150 to 225 words.

14. **KEY WORDS:** Key words are technically meaningful terms or short phrases that characterize a report and may be used as index entries for cataloging the report. Key words must be selected so that no security classification is required. Identifiers, such as equipment model designation, trade name, military project code name, geographic location, may be used as key words but will be followed by an indication of technical content. The assignment of links, rules, and weights is optional.